Universidade do Minho
Escola de Engenharia

Emanuel Mouta Fernandes

New Functionalization / Reinforcement Strategies for Cork Plastics Composites: Opening a wide Range of Innovative Applications for Cork based Products

dezembro de 2013

New Functionalization / Reinforcement Strategies for Cork Plastics Composites: Opening a wide Range of Innovative Applications for Cork based Products

Emanuel Mouta Fernandes

UMinho | 2013

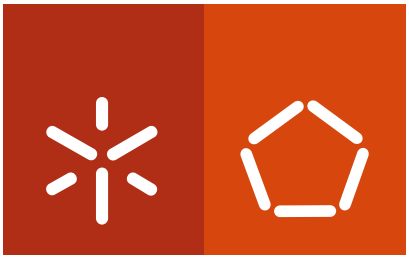

Universidade do Minho
Escola de Engenharia

Emanuel Mouta Fernandes

New Functionalization / Reinforcement Strategies for Cork Plastics Composites: Opening a wide Range of Innovative Applications for Cork based Products

Tese de Doutoramento em Engenharia de Materiais

Trabalho realizado sob a orientação do
Professor Doutor Rui Luís Gonçalves dos Reis
e do
Professor Doutor João Filipe Colardelle da Luz Mano

dezembro de 2013

Nome:

Emanuel Mouta Fernandes

Endereço electrónico: efernandes@dep.uminho.pt

Número do Bilhete de Identidade:10980762

Título da tese:

New Functionalization / Reinforcement Strategies for Cork Plastics Composites: Opening a wide Range of Innovative Applications for Cork based Products

Orientadores:

Professor Doutor Rui Luís Gonçalves dos Reis

Professor Doutor João Filipe Colardelle da Luz Mano

Ano de conclusão: 2013

Designação do Doutoramento:

Tese de Doutoramento em Engenharia de Materiais

Universidade do Minho, ___/___/_____

Assinatura: _____

Acknowledgements

I believe that my thesis would not have been completed without the support and concern of many people. I would like to express my extremely sincere acknowledge to my coach and scientific supervisor Professor Rui L. Reis for his guidance, encouragement, discussions and support in many processes during this years, for the opportunity to work with the Amorim Group integrating a team to develop new applications and products in/with cork (DNAPC), to be involved in the writing proposals, patents, manuscripts, lab responsible, passing my knowledge trough formations and for the challenge and his vision to perform a literature review in the bionanocomposites field. I am thankful to Professor João F. Mano, co-supervisor for the very valuable discussions, corrections in the last years which contributed to the coherence and added-value of this scientific research thesis.

I gratefully acknowledge the University of Minho for providing the conditions and financial support to perform the work presented in this thesis. Also, I would like to acknowledge Professor Ana Pinto, as a representative of the Doctoral Program in Materials Engineering, to be available to support the academic process related to the University of Minho.

A special thanks to the co-authors in the publications, not only for the few experimental tasks or support but mostly for the scientific and market ideas, discussions and corrections to improve the quality of the work. To P. Sol, for the several times that I needed support, "always for yesterday" in the several processing tasks in the laboratory. I am thankful to the 3B´s Group and mostly to the management team and to the support and Administration Staff of the Group.

A special thanks to the technical staff of the Department of Polymer Engineering (DEP), Campus de Azurém, almost since from the day that I start in 2004, always contributing with support and advises to fast learning to improve our knowledge.

To Professor A.P.O. Carvalho and colaborators, from the department of acoustics (FEUP), Porto, for the valuable support on the acoustic tests.

I would like to acknowledge the financial support of Portuguese Foundation for Science and Technology (FCT) for the doctoral grant (SFRH/BD/71561/2010) co-financed by the Operational Human Potential Program (POPH) developed under the scope of the National Strategic Reference Framework (QREN) from the European Social Fund (FSE). I acknowledge through the COMPETE/QREN/EU funding program in the project with acronym *NovelComp* (QREN FCOMP-01-0202-FEDER-003107) and to the

New Functionalization / Reinforcement Strategies for Cork Plastics Composites: Opening a wide Range of Innovative Applications for Cork based Products

Adi project (Programa IDEIA) with acronym *CompCork*. To the European project with acronym *Wacheup* (FP6-NMP 013896). To Corticeira Amorim S.G.P.S. on the development of new products based in/with cork, specially to Dr. António Amorim and to many other persons from the Holding Group that provided a unique experience during several brainstorming's and meetings, sharing knowledge and their entrepreneurial spirit and supporting the work on cork-polymer composites.

To my friends, that still contribute to the equilibrium of my life and my deepest apologies for the lack of space for so many names, they really deserve these lines. In special to Dr. T.Silva for the valuable help and for the advices in the difficult moments during this process and to Dr. H. Sousa for 90% of the Saturdays that we spent working in our scientific different domains.

I take this last paragraph to acknowledge my family and especially my parents that always prefer to teach me "how to fish" instead to provide "all the fish that I will need in my life". Their understanding and patience always gives constant encouragement and make me believe in myself.

Abstract

Advances on forest-based composites, shows a growing trend in the use of lignocellulosic materials as filler and/or reinforcement in plastic composites. Cork-Polymer Composites (CPC) is one of the most promising fields in cork technology to produce new materials based on sustainable development. Cork combined with polymer matrices, has the prospective of lead to composite materials with better properties. In this context, new fields of application where cork cannot compete alone might be reached.

The present thesis focuses on the investigation of engineering properties of the thermoplastic matrices, such as High Density Polyethylene (HDPE) and Polypropylene (PP), combined with cork trough melt based technologies, by taking advantage of their intrinsic properties to create cork-based composites. Towards to reach more bio-based composite materials, cork was combined with biodegradable aliphatic polyesters mainly, PolyhydroxyButyrate-co-HydroxyValerate (PHBV); Poly(L-Lactic Acid) (PLLA); Poly-ε-CaproLactone (PCL) and Starch-Poly-ε-CaproLactone (SPCL).

Cork and its by-products obtained from finishing industrial operations and end-of-life products were compounded, promoting added-value to cork based composites. The process methods used to create CPC were either pultrusion or twin-screw extrusion processes. Whereas, compression moulding and injection moulding were used to obtain the final composite product. During this process, the compatibility and adhesion between the polar cork and the non-polar polymer is one of the key challenges. Reinforcement strategies show that the lignocellulosic–matrix compatibility was improved by (i) via the structure of matrix, by employing coupling agents (CA) based on maleic anhydride, (ii) the use of natural fibre, or by modifying the fibre surface (i.e. hybrid composites). Indeed, all of them lead to cork based composites with considerably better mechanical properties. In addition, the interfacial adhesion of cork-polymer was also improved either using suberin or lignin isolated from cork by-products as bio-based coupling agents with significant benefits for the environment.

The findings presented in this thesis show that the general properties of CPC materials reveals the required: (i) dimension stability with reduced water absorption, (ii) homogeneous distribution and dispersion of the cork particles in the polymer matrix, (iii) improved fire resistance to the matix, good thermal and acoustic insulation properties and (iv) an interesting range of mechanical properties. As for as bio-based composite materials, it was engineering a class of cork biocomposites more sustainable with acceptable in-service performance and tendency for rapid out-of-service biodegradation.

New Functionalization / Reinforcement Strategies for Cork Plastics Composites: Opening a wide Range of Innovative Applications for Cork based Products

Lignocellulosic materials such as natural fibres and cork also offer economic and environmental advantages over traditional inorganic reinforcements and fillers. The work described in this thesis brings new knowledge and contribute to a deeper understanding in the promising cork-polymer composites (CPC) materials field. Overall, the findings presented in this thesis make a significant contribution to better understand the CPC materials. Therefore, the combination of cork with polymeric matrices reveals to be a significant added-value to cork based materials, with high potential for a wide range of innovative applications.

Resumo

Avanços em compósitos de base florestal, mostram uma tendência de crescimento no uso de materiais lenhoccelulósicos como carga e/ou reforço em compósitos de plástico. O campo dos materiais compósitos cortiça-polímero (CPC) é dos mais promissores da tecnologia cortiça para produzir novos materiais com base no desenvolvimento sustentável. A cortiça combinada com matrizes poliméricas, apresenta o potencial de obter materiais compósitos com melhores propriedades. Neste contexto, novos campos de aplicação onde a cortiça não pode competir por si só podem ser alcançados.

A presente tese centra-se na investigação das propriedades de engenharia das matrizes termoplásticas, como o polietileno de alta densidade (HDPE) e o polipropileno (PP), combinadas com a cortiça através de tecnologias baseadas na fusão, tirando proveito de suas propriedades intrínsecas, para criar compósitos à base de cortiça. No sentido de obter materiais compósitos de origem natural, a cortiça foi combinada com poliésteres alifáticos biodegradáveis principalmente, polihidroxibutirato-co-hidroxivalerato (PHBV), Poli(L-ácido láctico) (PLLA), poli-ε-caprolactona (PCL) e Amido poli-ε-caprolactona (SPCL).

A cortiça e os seus sub-produtos obtidos a partir de operações de acabamento industriais e produtos em fim de vida foram misturados, com o intuito de potenciar valor acrescentado aos diferentes compósitos com cortiça. Os métodos de processamento usados para criar CPC são processos de extrusão de duplo-fuso ou pultrusão. Tendo em consideração que a moldação por compressão e moldação por injecção foram usadas para obter o produto compósito final. Durante este processo, o grau de compatibilidade e de adesão entre a cortiça polar e o polímero não-polar é um dos principais desafios. Estratégias de reforço mostram que o grau de compatibilidade lenhocelulósico-matriz foi melhorado (i) através da estrutura de matriz, pelo emprego de agentes compatibilizandores (CA) com base no anidrido maleico, (ii) pela utilização de fibras naturais, ou modificando a superfície da fibra (isto é, compósitos híbridos). Na verdade, todos eles levam a compósitos de cortiça com consideravelmente melhores propriedades mecânicas. Além disso, a adesão interfacial da cortiça-polímero também foi melhorada quer utilizando suberina ou lenhina isolada a partir de sub-produtos da cortiça como agentes compatibilizantes de base florestal, com vantagens significativas para o ambiente.

Os resultados apresentados nesta tese mostram que as propriedades gerais dos materiais CPC revelam a necessária: (i) a estabilidade dimensional com reduzida absorção de água, (ii) distribuição homogénea e dispersão das partículas de cortiça na matriz polimérica, (iii) melhorada resistência ao

fogo da matriz, boas propriedades de isolamento térmico e acústico e (iv) e um conjunto interessante de propriedades mecânicas. Quanto aos materiais compósitos com bio-poliesters, foi desenvolvida uma classe de engenharia de biocompósitos de cortiça mais sustentáveis, com desempenho aceitável em serviço e tendência de rápida biodegradação fora-de-serviço.

Materiais lenhocelulósicos, como as fibras naturais e a cortiça também oferecem vantagens económicas e ambientais sobre os materiais de reforço ou de cargas inorgânicas tradicionais. O trabalho descrito nesta tese traz novos conhecimentos e contribui para uma compreensão mais profunda no campo dos promissores materiais compósitos de cortiça -polímero (CPC). No geral, os resultados apresentados nesta tese contribuiem significativamente para uma melhor compreenção dos materiais CPC. Portanto, a combinação de cortiça com matrizes poliméricas revela ser uma mais-valia significativa para materiais com base na cortiça, com alto potencial para uma ampla gama de aplicações inovadoras.

Table of Contents

List of Symbols and Abbreviations

α, scale parameter or denotes significance level

β, shape parameter

μ, mean

σ, variance

ρ, specific gravity of the solid

ρ (liq), density of the liquid

χ_c, degree of crystallinity

λ, thermal conductivity)

ΔH_m, melting enthalpy

$\Delta H'_m$, apparent enthalpy of fusion

ΔL_w, impact sound improvement index

ΔH_c, crystallization enthalpy

ΔH_{rec}, enthalpy of recrystallization

3D, three-dimensional

Acryst, crystalline area

Atotal, total area

CV, critical value (α')

d, density or denotes specific weight

D_n, maximum deviation

D_{nc}, critical value from K–S test table

F_0, Weibull cumulative distribution function

F_n, cumulative observed values

$F(x)$, probability of failure

h, thickness

L, span

L/D, extruder length-to-diameter ratio

n, denotes sample size or number of measurements

p, denotes probability

x, applied stress (strength)

w, weight fraction

A

ANOVA, analysis of variance

ALP, alkaline phosphatase

ATR, attenuated total reflectance

ASTM, International Standards Worldwide

B

BC, bacterial cellulose

BCP, biphasic calcium phosphate

BMPs, bone morphogenetic proteins

BNC, bacterial nanocellulose

BPO, benzoyl peroxide

BSA, bovine serum albumin

C

Ca, calcium

CA, cellulose acetate (chapter 1 - introduction)

CA, coupling agent (experimental section)

CaP, calcium phosphate

CdHA, calcium-deficient hydroxyapatite

CNC, computer numerical control

CNWs, cellulose nanowhiskers

CO_2, carbon dioxide

CP, cellulose phosphate

CPC, cork-polymer composite

% Cr, crystallinity percentage

D

DMAc, N,N-dimethylacetamide

DMSO, dimethylsulfoxide;

DN, double-network structure

DPPH, alpha,alpha-diphenyl-beta-picrylhydrazyl

DSC, Differential scanning calorimetry

E

ECM, extra cellular matrix

EDC, N-(3-dimethylaminopropyl)-N'-ethylcarbodiimide hydrochloride

EDS, energy dispersive X-ray analysis

F

FGF, fibroblast growth factor

FTIR, Fourier transform infrared spectroscopy

G

GGM, galactoglucomannan

H

HA, hydroxyapatite

hBMSC, human bone marrow stromal cells

HDF, high density fibreboard

HDPE, high density polyethylene

HEC, hydroxyethyl cellulose

HPC, hydroxypropyl cellulose

HPMC, hydroxypropylmethyl cellulose

I

ILs, ionic liquids

IPN, interpenetrating networks

PANI, polyaniline

K

K-S, Kolmogorov-Smirnov

K, coefficient of thermal conductivity

L

LbL, layer-by-layer

LCST, lower critical solution temperature

L/D, length to diameter ratio

LDPE, low density polyethylene

M

MA, maleic anhydride

MC, methylcellulose or denotes moisture content

MCC, microcrystalline cellulose

MBAAm, N,N'-Methylenebisacrylamide

MDF, medium density fibreboard

MFI, melt flow index

MSW, municipal solid waste

M_w, molecular weight

N

NaOH, sodium hydroxide

NIPAAm, N-isopropylacrylamide

NMMO, N-methylmorpholine-N-oxide

O

ORC, oxidized regenerated cellulose

PCL, Poly(ε-caprolactone)

PE, polyethylene

PEG, polyethylene glycol

PE-g-MA, polyethylene-graft-maleic anhydride

PGH, poly(L-glutamic acid-g-2-hydroxylethyl methacrylate)

PHA, polyhydroxyalkanoate

PHBV, poly(3-hydroxybutyrate-co-3-hydroxy-valerate

PHB, polyhydroxy butyrate

PLA, poly(lactic acid)

PLLA, poly(L-lactic acid)

PNIPAm, poly N-isopropylacrylamide

PP, polypropylene

PP-g-MA, polypropylene-graft-maleic anhydride

Ppy, polypyrrole

PS, polystyrene

PVA, polyvinyl alcohol

PVC, Polyvinyl chloride

S

SBF, simulated body fluid

SCA, starch cellulose acetate

SEM, scanning electron microscopy

PP-g-MA, polypropylene-graft-maleic anhydride

Ppy, polypyrrole

PS, polystyrene

PVA, polyvinyl alcohol

PVC, Polyvinyl chloride

TSE, twin-screw extruder

S

SBF, simulated body fluid

SCA, starch cellulose acetate

SEM, scanning electron microscopy

SEVA-C, corn starch-ethylene vinyl alcohol

SPCL, starch-polycaprolactone

T

TE, tissue engineering

TEM, transmission electron microscopy

TERM, tissue engineering and regenerative medicine

Tg, glass transition temperature

TGA, thermogravimetric analysis

TS, thickness swelling variation

V

VEGF, vascular endothelial growth factor

VOC, volatile organic compound

W

WA, water absorption

WL, weight loss

WPC, wood polymer composite

X

WAXRD, wide-angle X-ray diffraction

XRD, X-ray diffraction

List of Figures

SECTION I – GENERAL INTRODUCTION

Chapter 1. Bionanocomposites from lignocellulosic resources: properties, applications and future trends for their use in the biomedical field

SECTION II – EXPERIMENTAL SECTION

Chapter 2. Materials and methods

Chapter 5 – Polypropylene-based cork-polymer composites: Processing parameters and properties

Chapter 8. Hybrid cork-polymer composites containing sisal fibre: Morphology, effect of the fibre treatment on the mechanical properties and tensile failure prediction

Chapter 9. Cork-polymer biocomposites: assessment of biodegradability, mechanical, morphological and thermal properties

List of Tables

Chapter 6. Functionalized cork-polymer composites (CPC) by reactive extrusion using suberin and lignin from cork as coupling agents

Chapter 7. Novel cork-polymer composites reinforced with short natural coconut fibres: Effect of fibre loading and coupling agent addition

Chapter 8. Hybrid cork-polymer composites containing sisal fibre: Morphology, effect of the fibre treatment on the mechanical properties and tensile failure prediction

Chapter 9. Cork-polymer biocomposites: assessment of biodegradability, mechanical, morphological and thermal properties

List of Publications

The work performed under the scope of this PhD thesis resulted in the publications listed below:

Papers in international scientific journals with referees

1. **Fernandes EM**, Correlo VM, Chagas JA, Mano JF and Reis RL, 2010, Cork Based Composites using Polyolefin's as Matrix: Morphology and Mechanical Performance, Composites Science and Technology, 70: 2310-2318.
2. **Fernandes EM**, Correlo VM, Chagas JA, Mano JF and Reis RL, 2011, Properties of new cork-polymer composites: Advantages and drawbacks as compared with commercially available fibreboard materials, Composite Structures, 93: 3120-3129.
3. **Fernandes EM**, Correlo VM, Mano JF, Reis RL, 2013, "Novel cork-polymer composites reinforced with short natural coconut fibres: Effect of fibre loading and coupling agent addition", Composites Science and Technology, 78, 56–62.
4. **Fernandes EM**, Mano JF and Reis RL, 2013, Hybrid cork-polymer composites containing sisal fibre: Morphology, effect of the fibre treatment on the mechanical properties and tensile failure prediction, Composite Structures, 105: 153-162.
5. **Fernandes EM**, Pires RA, Mano JF and Reis RL, 2013, Bionanocomposites from lignocellulosic resources: properties, applications and future trends for their use in the biomedical field, Progress in Polymer Science, 38 (10-11): 1415-1441.
6. **Fernandes EM**, Aroso IM, Mano JF, Covas JA and Reis RL, 2013, Functionalized cork-polymer composites (CPC) by reactive extrusion using suberin and lignin from cork as coupling agents, *submitted.*
7. **Fernandes EM**, Correlo VM, Mano JF, Reis RL, 2013, Polypropylene-based cork-polymer composites: Processing parameters and properties, *submitted.*
8. **Fernandes EM**, Correlo VM, Mano JF, Reis RL, 2013, Cork-polymer biocomposites: assessment of biodegradability, mechanical, morphological and thermal properties, *submitted.*

New Functionalization / Reinforcement Strategies for Cork Plastics Composites: Opening a wide Range of Innovative Applications for Cork based Products

Patents

1. **Fernandes EM**, Correlo VM, Chagas JA, Reis RL, 2007, "Grânulos compósitos de cortiça com polímero (CPC) e processos para obtenção dos mesmos" PT 103898, Amorim Revestimentos S.A., Granted
2. **Fernandes EM**, Correlo VM, Chagas JA, Reis RL, 2009, "Cork-Polymer composite (CPC) materials and processes to obtain the same" WO2009072914 (A1), Amorim Revestimentos S.A., Patent Pending.
3. **Fernandes EM**, Correlo VM, Chagas JA, Reis RL, 2009, "Compósitos à base de cortiça reforçados com fibras" PT 104704, Amorim Revestimentos S.A., Granted
4. **Fernandes EM**, Correlo VM, Chagas JA, Reis RL, 2011, "Fibre-Reinforced cork-based composites" WO 2011014085 (A3), Amorim Revestimentos S.A., Patent Pending.

Conference papers:

1. **Fernandes EM**, Correlo VM, Mano JF and Reis RL, 2013, Natural fibres as reinforcement strategy on cork-polymer composites, Materials Science Forum, 730-732: 373-378.

Oral communications

1. **Fernandes EM**, Pires RA, Silva SP, Aroso IM, Correlo VM and Reis RL, Vencedores do Concurso Nacional do BES Inovação 2007 na área da Fileira Florestal - Novos Materiais Compósitos Cortiça-Polímero., 3º Fórum da educação, Penela, Portugal, September 2008.
2. **Fernandes EM**, Correlo VM, Chagas JA, Mano JF and Reis RL, Novos materiais compósitos cortiça-polímero: Optimização do processo e Efeito do agente compatibilizador nas propriedades mecânicas, ENMEC 2010, Encontro Nacional de Materiais e Estruturas Compósitas, Porto, Portugal, September 2010.
3. **Fernandes EM**, Correlo VM, Mano JF and Reis RL, Cork based composites as core in flooring applications: Characterization and optimization process using experimental design, 2nd IBB Scientific Meeting, Braga, Portugal, October 2010.
4. **Fernandes EM**, Correlo VM, Mano JF and Reis RL, Natural Fibres as Reinforcement Strategy on Cork-Polymer Composites, MATERIAIS 2011, VI International Materials Symposium and XV meeting of SPM - Sociedade Portuguesa de Materiais, Guimarães, Portugal, April 2011.

5. **Fernandes EM**, Aroso I, Pires RA, Correlo VM, Pitkänen P, Koskimies S, et al. Improvement on the mechanical properties of cork composites using suberin as coupling agent through a reactive extrusion process. 69th Annual Technical Conference of the Society of Plastics Engineers, ANTEC 2011. Boston, MA: Conference Proceedings; 2011. p. 611-5, May 2011.
6. **Fernandes EM**, Correlo VM, Mano JF and Reis RL, Innovative bio-based composites comprising cork and biodegradable polyester, 16th International Conference on Composite Structures (ICCS16), Porto, Portugal, June 2011.
7. **Fernandes EM**, Mano JF, and Reis RL, "Characteristics of fibre-reinforced cork-polymer composites and prediction of tensile failure using the Weibull distribution", Workshop on Bio-based material characterisation from full-field measurements, UTAD, Vila Real, 9 July 2013

Conference posters

1. Silva SP, Aroso IM, **Fernandes EM**, Pires RA, Correlo VM and Reis RL, New products and applications based on cork, 1st IBB Scientific Meeting, Faro, Portugal, May 2009.
2. **Fernandes EM**, Mano JF and Reis RL, Cork composites: Potential to be used as MDF substitute in flooring applications, Week of Engineering School at University of Minho. ISBN: 978-972-8692-59-9, Guimarães, Portugal, October 2010.

Introduction to the thesis format

The format of the thesis is divided into 4 main sections that are organized according with the defined aims, the nature of the work developed and the results achieved. The high potential of the cork-polymer composites (CPC) to obtain sustainable materials; the complexity to compound high volumes of cork through melt based technologies; the reinforcement strategies using hybrid systems (i.e. based on cork and natural fibres) to improve the mechanical response and the improvement of cork-polymer adhesion, were the key issues considered in this work to potentiate a wide range of innovative applications for cork based products. The thesis is sub-divided in 10 chapters, being 7 of them experimental work and 1 literature review that is based on peer-reviewed papers published / submitted for publication. All papers are identified in the front page of each chapter. In this sense, each thesis chapter is the published, submitted or an adapted version of these, in order to maintain the global structure of the work. Finally, and in appendix format, are provided 2 international patents developed during this thesis complementing in more detail some parts of the work. Figure A shows the structure of the thesis divided in the 4 main sections. The contents of each chapter are summarized below.

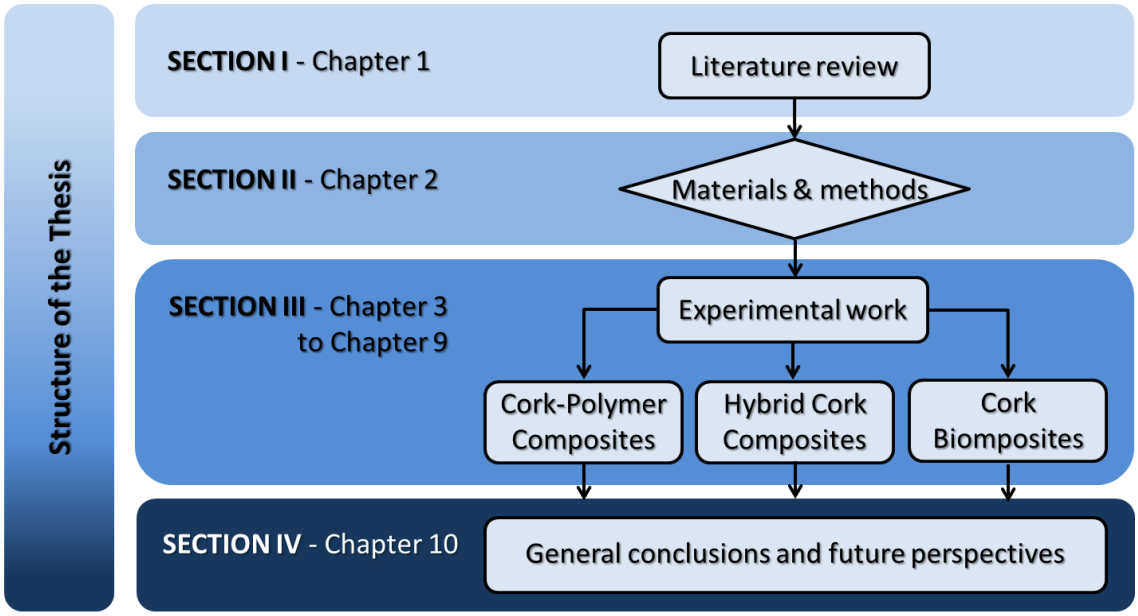

Figure A. Scheme representing the structure of the thesis.

SECTION I (Chapter 1): The first section consists of a comprehensive and detailed literature review about bionanocomposites from lignocellulosic resources and their potential uses particularly in the

biomedical field. The review highlights the potential of different lignocellulosic components as reinforcement at the nanometer level in different structures. This review combined with the introductions presented in the section III (i.e. chapter 3 up to chapter 9) aims to give a higher consciousness, the recent developments and potentialities of this technological area, where the main issue is the lack of knowledge on cork-polymer composites (CPC) through melt based technologies.

SECTION II (Chapter 2): The second section describes in detail the materials used, the processing techniques employed to develop the different CPC and the characterization techniques used to evaluate and understand the characteristics of the developed CPC. The objective was to complement the provided information in each of the following experimental chapters.

SECTION III (Chapter 3 to 9): The third section includes 7 chapters, corresponding to the results and discussion sections of 7 research papers. As previously pointed, the introduction of each chapter intends to support the reader on the subject, providing information of the state-of-art on the area and the central motivations of the work.

Chapter 3 and **Chapter 4**, are devoted to the development of cork based polyolefin composite pellets by pulltrusion process followed by compression moulding. In both chapters, high consumption thermoplastic materials (i.e. polypropylene (PP) and polyethylene (PE)) were tested to obtain cork-based composites (50-50) wt.% with a competitive cost. Moreover and accounting with the polar behaviour of cork and the non-polar behaviour of the polyolefin, a small amount of coupling agent (2 wt.%) based on maleic anhydride (i.e. PE-g-MA or PP-g-MA) was used to improve the adhesion.

Chapter 3 focuses on the potential of different cork by-products from the industrial process, creating added value to cork and a profitable alternative to storage or burn of cork powder to generate energy in industrial process.

Chapter 4 describes a comparative study between a selected cork-polymer composition previously developed in Chapter 3, with the well-established commercial products, namely high-density fibreboard (HDF) and medium density fibreboard (MDF) products. An extensive characterization of these systems

included water absorption and thickness swelling of the materials, warping and density, morphology, mechanical and thermal properties and other specific tests such as fire resistance and acoustic tests.

Chapter 5 focuses on the use of cork particles and cork powder compounded with polypropylene (PP) by co-rotating twin-screw extrusion and further processed by injection or compression moulding. Thus, a different technology to compound the CPC pellets was evaluated. The addition of polypropylene-graft-maleic anhydride (PP-g-MA) and stearic acid were also tested as coupling agents. The influence of cork on the melt viscosity, on morphological particle distribution, physical and thermal properties is described. The mechanical response before and after water immersion tests was also analysed to evaluate the potential of application. Moreover, the maximum incorporation of cork in the composite was also accessed.

Being the compatibility between cork-polyolefin one of the key issues, **Chapter 6** proposes the use of suberin and lignin isolated from cork powder as bio-based coupling agents through a reactive extrusion process, in order to overcome the insufficient adhesion between cork and a polyethylene matrix with environmental benefits. To evaluate their potential as an adhesion promoter, the properties of the new functionalized composites are compared with those of an equivalent system using a coupling agent PE-g-MA.

Chapter 7 and **Chapter 8** were devoted to reinforcement strategies using short natural fibres to improve the mechanical response of the cork based composites. It was developed and tested hybrid CPC systems using counter-rotating twin-screw extrusion followed by compression moulding, maintaining a high cork content. Special emphasis was given in both chapters to obtaining higher mechanical properties by increasing the amount of the natural component in the final composite. In addition, the need of low amount of coupling agent based on maleic anhydride (2 wt.%) was tested. In **Chapter 7** cork powder-polymer composites (50-50) wt.% reinforced with coconut fibre were evaluated.

Following a similar strategy, in **Chapter 8**, it was selected a fibre with higher mechanical performance to reinforce the developed composites. In this chapter, we investigated the use of short sisal fibres, with and without alkali treatment as a strategy to reinforce cork granules-polymer (40-60) wt.% composite

materials. Weibull cumulative distribution was employed to accurately predict the mechanical failure of the hybrid cork based materials.

Pursuing more sustainable materials and the constant concern as a research group that envisages the use polymers from natural resources in noble applications in the biomedical field, the natural evolution was to design cork biocomposites. **Chapter 9** addresses the preparation of biocomposites combining different biodegradable aliphatic polyesters with granulated cork 30 wt.%. Cork was compounded with poly(L-lactic acid), (PLLA); polyhydroxybutyrate-co-hydroxyvalerate, (PHBV); poly-ε-caprolactone (PCL) and starch-poly-ε-caprolactone (SPCL) using co-rotating twin-screw extruder followed by injection moulding. The contribution of cork to the composite density and mechanical performance was evaluated. Biodegradation of these cork biocomposites under water and soil conditions accessed by means of morphology and by the physico-mechanical behaviour was described.

SECTION IV (Chapter 10): This thesis ends with Chapter 10, which consists on the summary and the overall conclusions of the research work developed under the scope of this thesis with some recommendations and future perspectives on the cork-polymer composites (CPC) area.

SECTION I – GENERAL INTRODUCTION

Chapter 1. Bionanocomposites from lignocellulosic resources: properties, applications and future trends for their use in the biomedical field

Bionanocomposites from lignocellulosic resources: properties, applications and future trends for their use in the biomedical field[1]

Abstract

The selection, synthesis, modification and shaping of biomaterials are complex tasks within the biomedical field. Human and plant tissues, such as, wood, bone and cartilage are structured at the nanometer level and exhibit a hierarchical structure up to the macroscale. Their morphological similarities enable the exploitation of lignocellulosic materials in the development of nanostructured composites targeting tissue engineering and regeneration. In this review, lignocellulosic materials and their chemical constituents are highlighted as promising alternatives for the development of drug-delivery vehicles and for the engineering or regeneration of bone and cartilage. Special focus is given to the recent developments of lignocellulosic bionanocomposite supports that induce cell attachment and proliferation. Chemical modifications techniques as well as composite processing methodologies that enhance the biomaterial performance are reviewed. It is anticipated the increasing interest in nanocellulose, bacterial cellulose, hemicellulose and lignin from natural resources as added-value biomedical materials in the near future.

[1] This chapter is based on the following publication:

Fernandes EM, Pires RA, Mano JF and Reis RL, 2013, Bionanocomposites from lignocellulosic resources: properties, applications and future trends for their use in the biomedical field, Progress in Polymer Science, 38 (10-11): 1415-1441.

1.1 Introduction

The Bionanocomposites are usually defined as a combination of two or more materials or phases in which one of the phases has at least one dimension in the nanometer range (1–100 nm) [1-4]. The terminology usually refers to a matrix for the more concentrated component that enables a phase continuum, while reinforcements are components that induce an enhanced performance (e.g. mechanical, thermal, etc.) from the composite. Matrices may be biodegradable polymers (e.g. chemical modified cellulose systems), ideally derived from renewable resources (e.g. plants). In terms of reinforcements, they might include plant fibers and by-products from lignocellulosic renewable resources or synthetic inorganic materials, as well as natural or modified clays. Plant-based nanocellulose and bacterial cellulose [5] are included in this definition. Moreover, blended polymers that act as matrices in a composite perspective are also included. The reviewed constructs target the development of biocompatible medical devices, or biodegradable materials under a complete tissue regeneration approach. The interest in lignocellulosic polymers, in particular the cellulose-based ones, is due to their reinforcement capacity and biodegradability. Moreover, cellulose-based materials have proven to present excellent biocompatibility [6, 7]. Being the term biocompatibility defined as the ability of a material to perform with an appropriated host response in a specific biomedical application [8].This set of characteristics are the most relevant to consider these materials as good candidates for tissue engineering and regenerative medicine (TERM) applications, both as scaffolds or as drug-delivery carrier systems. Nanotechnology can be applied across different application areas, allowing the development of the so called enabling science. The ability to control the material features at the nanoscale and the evaluation of their influence in the micro and macroscopic properties provides the opportunity to develop new bionanocomposite systems in a previously unimaginable dimension. Bionanocomposites are attractive materials for biomedical applications due to the matching of the length scales of: their structure and the components of the extracellular matrix (ECM). Under these conditions, the development of nanostructured biomaterials for medical applications implies a multidisciplinary research approach that combines engineering, chemistry, physics, biology and life sciences.

In this review we have compiled the research executed with lignocellulosic materials in the biomedical field, with particular emphasis on drug-delivery systems and scaffolds relevant in the scope of TERM. The main focus will be on the development of bionanocomposite structures formulated with lignocellulosic components within the previously described fields of application. Nanostructured

pyrolyzed lignocellulosic structures will be also discussed as carbon templates for scaffold development. The addition of plant-based and bacterial-based cellulose (BC) to enhance thermal and mechanical properties, as well as the biodegradability of biomaterials is also analyzed. The use of cellulose, hemicellulose and lignin as components of bionanocomposite systems are described, with special focus on micro and nano-sized reinforcements. It is also highlighted the use of chemical modified lignocellulosic materials, focusing on the advantages of these modifications in order to promote biocompatibility. Moreover it is compiled the available processing methodologies and their impact in the properties of the bionanocomposites.

This review intends to show that biomaterials from lignocellulosic sources have potential to play an important role in human health. An overview of the current and potential applications of lignocellulosic-based bionanocomposites is performed and includes the research relevant mainly for bone and cartilage engineering and regeneration; although, their application as drug-delivery carriers and wound dressing systems are also described. Complementary information can be found in literature reviews that focus on the potential of cellulose-based nanocomposites in different areas such as: food packaging materials and films [2, 9, 10]; printing and paper industry [2, 3, 11]; optical, light-responsive composites and other electronic devices [3, 9, 12-14]; advanced composites manufacturing [10, 12]; pharmaceutical and medical applications [3, 5, 13]. Additionally it is also possible to find reviews on the properties and potential of cellulose nanofibers and its composites [10, 15]; on BC-based materials [11, 16-18], and methodologies to control their physical and chemical structure targeting their application as scaffolds and wound healing systems, as well as, within the scope of tissue engineering (TE) [19, 20]; and lignocellulosic-based hydrogels, including biodegradation of some cellulose derivatives [21-23].

1.2 Bone and cartilage tissue regeneration

1.2.1 Materials properties

The selection of biomaterials is particularly relevant within most of the TE strategies. Its main function is to act as a support for the colonization by cells in the intervened area, promoting the formation of new tissue. In this perspective, the biomaterial should present a set of adequate mechanical, thermal, morphological, chemical and biological characteristics [24-26].

In a mechanical point of view the support biomaterial should withstand the mechanical stresses within the tissue to be repaired. Most of the biomaterials (e.g. metals, high performance polymers, etc.) used

to substitute the bone/cartilage possess a higher stiffness than the tissue to be intervened. This usually imposes additional stresses to the surrounding biological tissue enhancing the probability of its mechanical failure [27]. There is thus the need for the development of materials that present mechanical performance similar to the tissue to be repaired enabling a better mechanical integration of the constructs in the biological tissue. The mechanical properties of different biological tissues are summarized in Table 1.1, including examples of references [28-33].

Table 1.1. List Mechanical properties of different human biological tissues. Compiled from Refs. [28-33].

Tissue	Compressive modulus (GPa)	Compressive strength (MPa)	Tensile modulus (GPa)	Tensile strength (MPa)	Elongation to failure (%)	(Refs.)
Bone (Cortical)	3 - 18	131 - 205	15 - 30	70 - 150	0 - 8	[28-31, 33]
Bone (Cancellous)	0.10 - 1.3	0.1 - 100	0.18 – 1.7	7.4	0.5 – 0.8	[28-31, 33]
Tendon	—	–	0.401	46.5	—	[30, 31]
Cartilage	0.51–15.3 × 10^{-3}	–	a	7 - 15	20	[30, 32]
Skin	—	–	0.1 – 0.2 × 10^{-3}	7.6	—	[30, 31]
Meniscus (Knee)	0.22 × 10^{-3}	—	0.2	—	—	[32]

[a] Strongly viscoelastic.

The cortical bone usually possesses a compressive strength between 131 and 205 MPa; typical values for its flexural and tensile strength is between 53 and 135 MPa and its modulus is between 3 and 18 GPa [28]. Although, it is relevant to notice that, *in vivo*, the performance of the biomaterial-based structure is not only derived from the mechanical resistance of the biomaterial itself, but from the complex mixture of biomaterial, ECM components (e.g. proteins) and cells [27].

In TE, it is common the use of a regenerative approach that intends to promote the formation of new tissue while the original biomaterial is being degraded. In this strategy, it is common the use of porous scaffolds that allow cell colonization in the bulk of the constructs [24]. Porosity is mandatory not only to

allow the accessibility of cells to the bulk but also to allow the exchange of nutrients and oxygen that are vital for cell survival under *in vivo* conditions [24, 34, 35].

Under this approach it is considered acceptable a lower mechanical performance than the original tissue, as long as, the scaffold itself will not be subject to loadings above is elastic regime. In fact, the mechanical performance of this type of scaffolds is significantly lower than the base biomaterial. It is common to occur a 10-fold reduction of different mechanical properties, e.g. modulus [36].

Other important factor in designing TE supports is its surface properties [37]. They are relevant to induce cellular attachment, differentiation and proliferation. The first response of the biological medium when in contact with the TE constructs is to coat the biomaterial with a layer of proteins. The composition of this layer is strongly affected by the biomaterial surface chemistry and energy [38]. This initial process is critical for the first steps of cell attachment. Although, it is often difficult to match the different bulk properties of the selected scaffold biomaterials with a surface chemistry/energy optimized to promote cell attachment.

In order to achieve an appropriate surface chemistry/energy, surface modification techniques are often used to confer specific chemical groups that are known to promote cell attachment [39-41]. These can range from chemical grafting, plasma modification, surface coating or patterning approaches [42-46].

1.2.2 Biological requirements

Depending on the target tissue there are a number of biological requirements that the support structure and the biomaterial should present. In the case of bone, the most relevant are related with [47, 48]: bioactivity; osteoproduction, osteoconduction and osteoinduction; angiogenic potential; and capacity to minimize the foreign body response.

Bioactivity is defined as the capacity of the biomaterial to form a biologically active apatite layer on its surface [47, 49]. The formation of these types of layers occurs by a complex set of chemical steps that promote the surface immobilization of calcium and phosphate ions [48] and their subsequent organization into calcium phosphate phases. These phases are one of the responsible for a series of properties that are relevant for bone TE, namely, bone-bonding properties of the implanted device. Supports/biomaterials can present different biological characteristics that define their classification in terms of bioactivity. Biomaterials that only possess osteoconduction (capacity to stimulate bone growth at the biomaterials' surface) are considered to be of class B. When a biomaterial possesses both osteoproduction (bone growth in the interior of the support) and osteoconduction it is said to present

class A bioactivity [47]. An additional advantage is the promotion of not only the proliferation, but also the differentiation of progenitor cells (osteoinduction) into osteoblasts [50]. This can be achieved with the incorporation of bone morphogenetic proteins (BMPs) into the biomaterials [51-53]. There are a series of different BMPs that are relevant at different stages of bone/cartilage formation, healing and remodeling [54, 55]. As an example, BMP-2 appear to peak at one day after fracture; BMP-14 has a maximum of activity at one week during cartilage formation; finally, BMP-3, -4, -7 and -8 are more relevant between the second and third week of bone repair [55, 56]. These observations motivated the development of a series of strategies to achieve BMP controlled delivery from the support structures to the biological medium, with a profile that match their biological relevance [55].

In a bone TE perspective, a complete bone remodeling and growth is better achieved by biomaterials and supports that present the whole set of the discussed biological characteristics: bioactivity, osteoconduction, osteoproduction and osteoinduction. A highly relevant part of new bone formation in the interior of the support is the existence of a vasculature that is able to transport nutrients essential to cellular development [57]. It is known that osteocytes (the most common type of cells present in bone) possess intact capillaries at a distance lower than 100 μm. Additionally, the nutrient transport from the blood vessels to the cells is mainly governed by diffusion. As an example, theoretical modeling reveals that non-vascularized support structures with 1 cm can hold 1000 times lesser cells than native cancelous bone [58]. In this perspective, it is clear that the importance of angiogenesis is increasing with the dimension of the intervened area [35, 59]. Different strategies can be applied to increment angiogenesis, namely: the tuning of the construct geometry; the inclusion of angiogenic growth factors (e.g. VEGF, FGF); and the culturing of the structures in the presence of stem cells, endothelial cells, as well as the use of co-culture systems [53, 60-65].

Finally, the implantation of a biomaterial in the biological tissue always generates an inflammatory response related with the surgical procedure. The use of degradable supports can also increase inflammation due to the degradation products that are leached from the biomaterial [66]. Initial foreign body response can be minimized by surface modification of the biomaterials (e.g. surface chemistry, topography, roughness) [67, 68] or the use of bioactive compounds (e.g. anti-inflammatory drugs, growth factors) in their formulation [69-71].

1.3 Sources of lignocellulosic materials

1.3.1 Plant based

The use of cellular materials has the advantage of possessing good mechanical properties while presenting low density [72]. In nature, several materials present a cellular anisotropic structure, e.g. bone, wood, cork, among others; although, while bone is ceramic-polymer composite, wood is mostly a polymer-based composite.

Wood is a natural composite material with a hierarchical architecture where biopolymers such as cellulose, hemicellulose and lignin form a highly porous anisotropic cellular microstructure, which exhibits unique combination of high strength, stiffness, toughness and low density [72, 73]. The chemical constituents of the wood cell wall, as well as other lignocellulosic-based materials are presented in Table 1.2, including their concentrations reported in the literature [73-80]. It's clear that the concentration of each component can significantly differ depending on the plant species. In general, the major organic constituents are [73, 74, 79, 81-83]:

- Cellulose is the most abundant biopolymer and presents a long-chain polysaccharide structure composed by repeated units of d-glucose building blocks [81] see Figure 1.1. The polymeric chains are packed through hydrogen bonds and van der Waals forces forming fibrous structures called microfibrils. As a structural component in plants, cellulose is arranged as a system of fibrils embedded in a lignin matrix. The microfibrils are a few nanometers of diameter presenting highly ordered regions (i.e. crystalline phases) alternated with disordered domains (i.e. amorphous phases) [81, 84, 85]. A single fibril has a diameter of *ca.* 5 nm and a length up to tens of micrometers [81]. These fibrils are comprised of different hierarchical microstructures commonly known as nano-sized microfibrils with high structural strength and stiffness, being the crystalline part named nanowhiskers [1], or nanocellulose crystals [10, 86]. Cellulose nanowhiskers are defined as elongated crystalline rod-like nanoparticles with a diameter ranging from 2 to 20 nm, typically obtained by acid hydrolysis of cellulose fibers [14, 15, 87]. The hydrolysis conditions and the type of acid affect the properties of the nanocrystals, such as a longer reaction time leads to shorter nanocrystals [88, 89]. Furthermore, the use of sulfuric acid for the preparation of cellulose whiskers leads to more stable aqueous suspensions than the ones prepared using hydrochloric acid [12, 89, 90]. It promotes a negatively charged surface resulting from the surface oxidation promoted by the sulfate ions, so that the cellulose suspension forms a stable colloidal system [89, 91].

Table 1.2. Chemical constituents from lignocellulosic biomass (wt%) with potential to be applied as biomedical composites. Compiled from Refs. [73-80].

Lignocellulosic material	Chemical composition (wt%)				(Refs.)
	cellulose	hemicellulose	lignin	suberin	
Hardwood					[76, 80]
Poplar/Aspen	50.8-53.3	26.2-28.7	15.5-16.3	–	
White Birch	41	36.2	18.9	–	
Eucalyptus	42.3-54	16-36.6	17.9-23.3	–	
Red Oak	39	24	22	–	
Softwood					[76, 78,
Pinus pinaster	42.9	17.6	30.2	–	80]
Pinus radiate	42-50	24-27	20	–	
Fir	43.9	26.5	28.4	–	
Bark					[73-75]
Birch bark	7.3-23.4	–	18.1-33.2	33-45	
Cork bark	12-25		21-29	33-45	
Agricultural Residues					[76]
Corn cob	33.7-41.2	31.9-36	6.1-15.9	–	
Sugar cane bagasse	32.9-50	24-35.5	8.9-17.3	–	
Natural Fibers					[77, 79]
Flax	71	18.6-20.6	2.2	–	
Cotton	82.7- 95	2-5.7	1	–	
Sisal	73	14	11	–	
Hemp	70.2-74.4	17.9-22.4	3.7-5.7	–	
Wheat straw	30	50	15	–	

Moreover, cellulosic materials exhibit poor degradation *in vivo* [6]. Strategies to overcome this drawback are: the enzymatic oxidation with peroxidase secreted by fungi as well as being degraded by bacteria, yielding non-toxic products [92]. The presence of amorphous regions can increase biodegradability.

Lowering the crystallinity and hydrophobicity of cellulose-based materials are known approaches to improve their biodegradability *in vivo* [6].

- Hemicelluloses, are located mainly in the secondary cell walls, and together with cellulose and lignin, they build up the structure of the plants in a fashion that generates the best combination of mechanical support and transport properties [82]. They are a group of branched polysaccharides (see Figure 1.1) that are characterized by being neither cellulose nor pectin and by presenting β-(1→4)-linked repeating units of glucose, mannose or xylose [23, 83]. Cellulose and hemicelluloses contain free hydroxyl groups that confer to the wood its inherent hygroscopic character [85]. Since hemicelluloses are responsible for the interactions with water in wood, hydrogels using these materials have applications within different fields [82, 93].

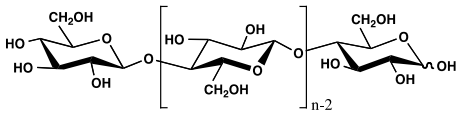

Cellulose

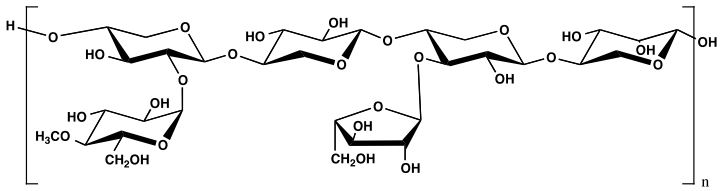

Hemicellulose

Figure 1.1. Chemical structure of cellulose and hemicellulose.

- Lignin, is an amorphous polymer and its main role is to act as a structural support in plants. Lignin has a phenolic-based chemical structure; its high carbon and low hydrogen content suggests that it has a highly unsaturated and aromatic character. Lignin is characterized by its hydroxyl and methoxy groups [79] as it is represented in Figure 1.2. The chemical structure of lignin in natural fibers has not been completely established, although, most of its functional groups and units which make up the molecule have been identified [73, 79]. More than its potential as biomaterial, lignin has demonstrated antioxidant capacity; strong antiviral activity against human immunodeficiency virus; and other anti-microbial activities [94, 95].

- Suberin, consists of a complex polyester structure composed by long chain fatty acids, hydroxy fatty and phenolic acids, linked by ester groups [73] present in the outer tissues of numerous vegetable species. It is mostly found in the cell walls of normal and wounded external tissues of aerial and/or subterranean parts of plants. It acts as a protective barrier between the organism and its environment

[74, 96]. The presence of terminal carboxylic and hydroxy groups and of side hydroxy and epoxy moieties on the long chains of suberin ''monomers'' makes them appropriate as building blocks for polymers with interesting properties. Suberin represents typically between 20 and 50% of the extractive-free bark weight [74].

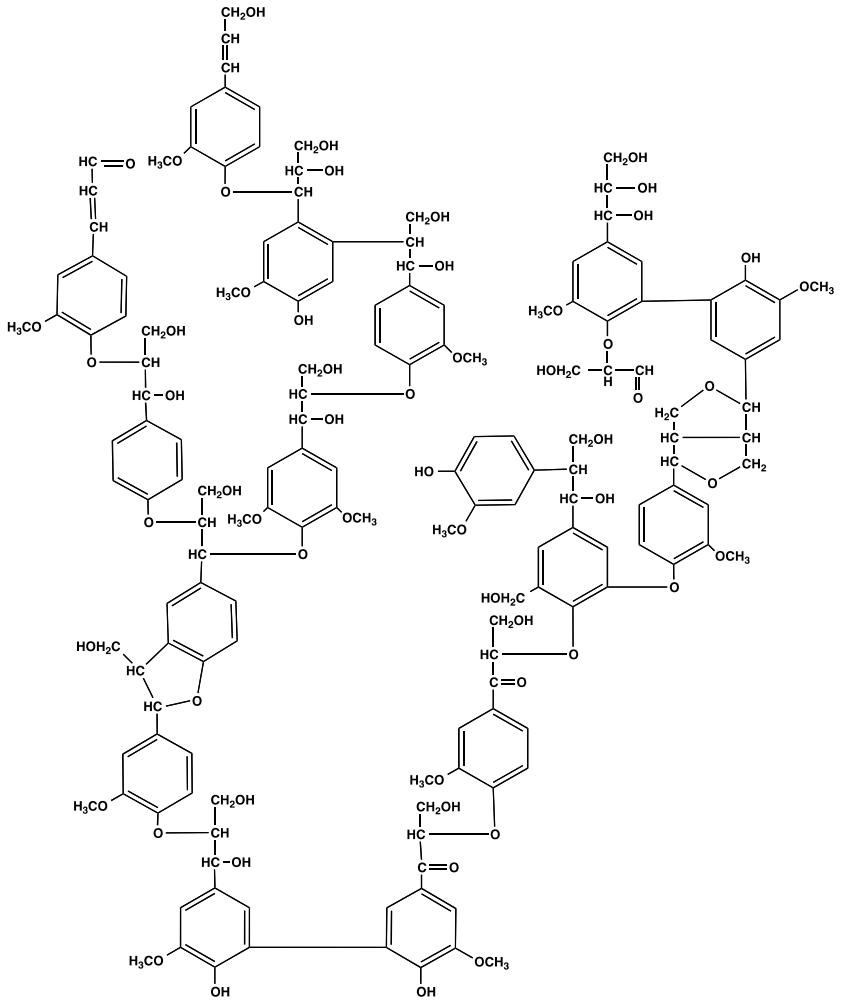

Figure 1.2. Chemical structure of a softwood lignin. Adapted from Adler [79].

Like bone, lignocellulosic materials exhibit pores for the transportation of nutrients. Bone and wood present similar hierarchical structure from the nano to the macro-scale, (see the structure of both types of materials in Figure 1.3. Collagen is a fibrous structural protein that can be found in all vertebrates. It is present in bone, cartilage, skin, tendons and other tissues [30, 97]. Collagen in combination with hydroxyapatite (HA) offers mechanical support in bone; similarly, cellulose has the same function in

wood. Lignocellulosic materials and bone present porous networks in both biological materials, although different in size and connectivity, they provide channels for nutrient transport and exchange [98].

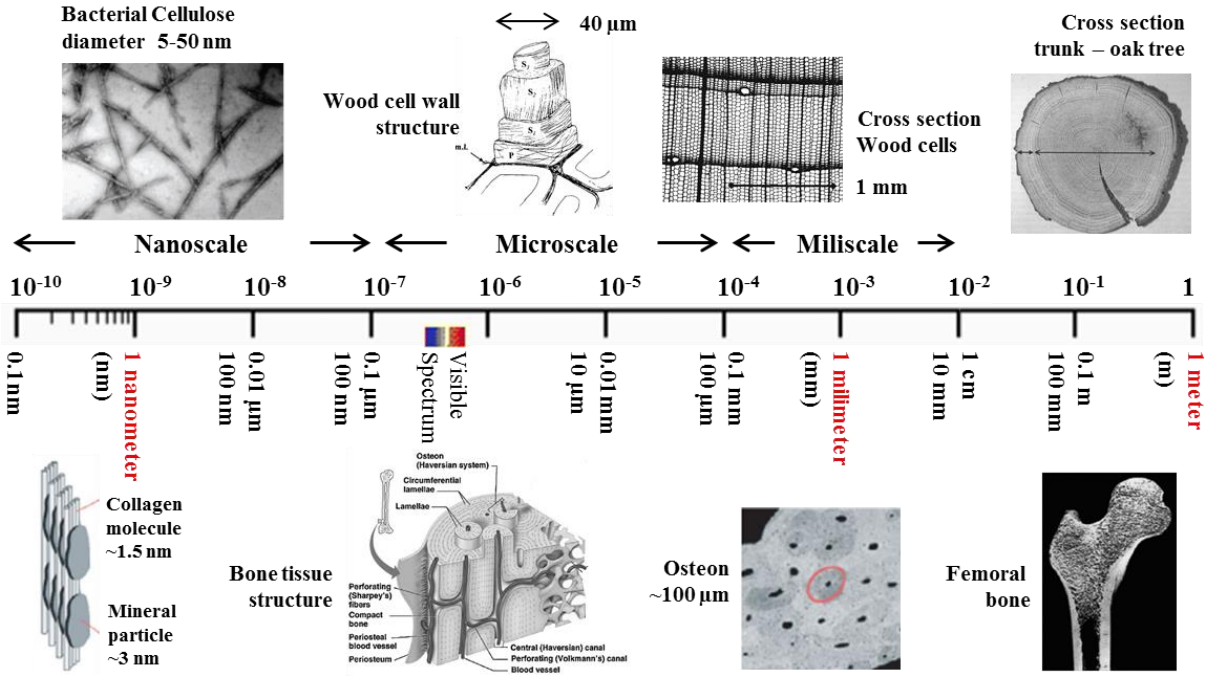

Figure 1.3. Schematic representation of hierarchical structure of lignocellulosic materials and bone from nano to the macro-scale. Reproduced from Stokke and Gardner [85] and Beniash [99] with permission. Copyright 2003 and 2011, Wiley. From Sprio et al. [100] with permission. Copyright 2011, Elsevier and from Grunert and Winter [101] with permission. Copyright 2002, Springer.

There are plant species that present similar chemical components in different sections of the tree, e.g. bark [75]. The extraction of bark, in some cases, can be executed without harvesting the whole tree, maintaining it alive. An example is the outer bark of *Quercus suber*, commonly known as cork. As wood, cork is a lignocellulosic material were suberin is the main chemical component, with concentrations between 30 and 50% [73]. Suberin is not present in the wood cell walls. This material presents a anisotropic closed cellular structure and a unique combination of properties, such as imperviousness to liquids, a high coefficient of friction, resilient, low density, viscoelastic, low thermal conductivity, fire resistance, high energy absorption and a near-zero Poisson coefficient [72, 73, 102]. The combination of these unique properties and the potential of the lignocellulosic chemical components has been issue of several studies for different purposes [74, 103-105].

Moreover, lignocellulosic materials from plant fibers such as bamboo, sisal, hemp, among others, also present an anisotropic structure and they are a relevant source of cellulose and hemicellulose derivatives in the biomedical field. Just as an example it can be referred the use of bioactive ceramic coatings on bamboo [106] generating a material that presents mechanical properties close to the modulus of human long bone [107]. Bamboo has been tested for its *in vitro* cytotoxicity before and after heat or chemical treatments [107]. The results showed that ethanol, methanol and toluene can remove toxic and some extend leachable components from bamboo. More recently, the preparation of cellulose nanofibers from bamboo with diameters of 30-80 nm was achieved by chemical pretreatment and ultrasonication, followed by freeze-drying [84]. These nanofibers presented an organized structure composed by millions of parallel nanofibrils of 1-5 nm and several microns of length. The main composition of the produced nanofibers was based in cellulose due to the removal of non-cellulosic polysaccharides via conventional chemical treatment.

The use of lignocellulosic structures and their components on the production of nanocomposites will open new opportunities for biomedical applications.

1.3.2 Bacterial cellulose

Bacterial Cellulose (BC) sometimes referred to as bacterial nanocellulose or microbial cellulose is a natural polymer whose properties are similar to the hydrogels produced from synthetic polymers; for example, it displays high water content (98-99%) and good sorption of liquids, it is non-allergenic, and can be safely sterilized. BC is synthesized by the acetic bacterium *Acetobacter xylinum* (or *Gluconacetobacter xylinus*), a gram-negative strain of acetic-acid-producing bacteria using a fermentation process [108, 109]. BC is a nanomaterial, having several characteristics that make it valuable for biomedical applications such as: a highly pure and crystalline structure, high mechanical properties, ultra-fine network, high hydrophilicity and biocompatibility and it has the advantage of *in situ* mouldability [81, 109-112]. The fibrous structure of BC consists of a 3D network of microfibrils containing glucan chains bounded together by hydrogen bonds. BC fibers of <100 nm in diameter have high mechanical properties, e.g. tensile strength and modulus. BC microfibrils have a density of 1600 kg m^{-3}, Young's modulus of 138 GPa, and tensile strength of at least 2 GPa, which are almost equal to those of aramid fibers [113]. Its unique network structure is the main responsible for the previously described characteristics. The potential applications of BC are quite vast; it can be used in the

preparation of materials targeting decellularised devices for wound healing or as scaffold for skin engineering after seeded with epithelial cells [19] or more recently in vascular grafts [114, 115].

In an *in vivo* study of subcutaneous BC implantation in rats [116] it was found that after 12 weeks, no fibrotic capsule or giant cells was detectable by microscopy, indicating that no foreign body reaction was occurring (see Figure 1.4). Furthermore, macroscopically, no redness, swelling, or exudate developed around the implantation sites was observed showing the biocompatibility and the potential of this nanomaterial.

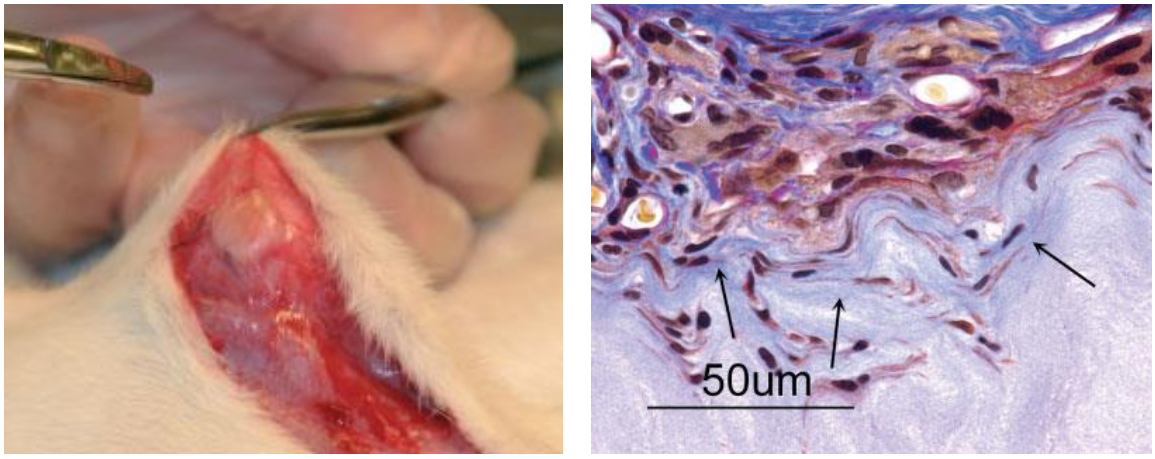

a) b)

Figure 1.4. BC after one week of subcutaneous implantation (a) and high magnification micrograph of the interface area at the porous side of BC, 12 weeks after implantation (b). Arrowheads show collagen synthesized by the fibroblasts. Reproduced from Helenius et al. [116] with permission. Copyright 2006, Wiley.

Another study performed by Klemm *et al.* [5, 16] evaluated the suitability of BC cylindrical conduits with an inner diameter of, approximately, 1 mm as artificial blood vessels. Bodin *et al.* [117] have also proposed BC as a potential meniscus implant being similar to human skin. BC can be produced in a meniscus shape and, through the promotion of cell migration, makes it an attractive material as a meniscus implant. BC can be also applied as skin substitute in treating extensive burns [118]. The nanostructured network and morphological similarities with collagen make BC very attractive for cell immobilization, cell migration, and the production of ECMs [5].

As reviewed by Klemm *et al.* [5, 81, 108], celluloses with different functionalities clearly open novel fields of application e.g., nanoporous hydrophilic membranes, nanoscaffold-based composite materials, and medical implants for repair of hard and soft tissue, as well as cardiovascular substitutes.

1.4 Reinforced nanocomposite structures

1.4.1 Cellulose-based materials

TE represents an emerging interdisciplinary field that combines biological, chemical, engineering and life sciences towards the goal of tissue regeneration [24, 119, 120]. Scaffolds with different architectures and pore sizes can be produced from synthetic or naturally occurring materials. BC and cellulosic nanofibers are widely used as biobased nanoreinforcements in several polymeric matrices owing to their superior mechanical properties [113, 121]. The high surface area to volume ratio of the nanofibers combined with their microporous structure favors cell adhesion, proliferation, migration, and differentiation, all of which are highly desired properties for TE applications [122]. The development of nanofibers can be used to formulate bionanocomposites that can potentially mimic the architecture of natural human tissue at the nanometer scale. On a composite perspective, one of the main reasons to use cellulose nanofibers is based on their high stiffness, being highly relevant as a reinforcement strategy. For example, this can be achieved by breaking down the hierarchical structure of the plant into individualized nanofibers of high crystallinity, with a reduction of amorphous parts [10]. Studies have been reported the use of BC alone or combined with HA, microcrystalline cellulose (MCC) or cellulose nanowhiskers (CNWs) as reinforcement strategies, to create bionanocomposites [112, 121, 123-126]. MCC consists generally of stiff rod-like particles called whiskers, obtained from different natural resources such as eucalyptus [127], sisal [87], cotton [86, 128], spruce [91, 129], ramine [130], tunicin [131, 132], among others. The morphology of CNWs from different sources is shown in Figure 1.5.

CNWs possesses: very large surface to volume ratio; good mechanical properties, including high modulus, high tensile strength; low coefficient of thermal expansion; and formation of highly porous meshes compared to the commercial fibers [2, 10, 128]. In cellulose, each microfibril can be considered as a string of polymer whiskers having a modulus close to that of the perfect crystal of native cellulose, which is estimated to be 150 GPa, and possessing a strength of about 10 GPa [136].

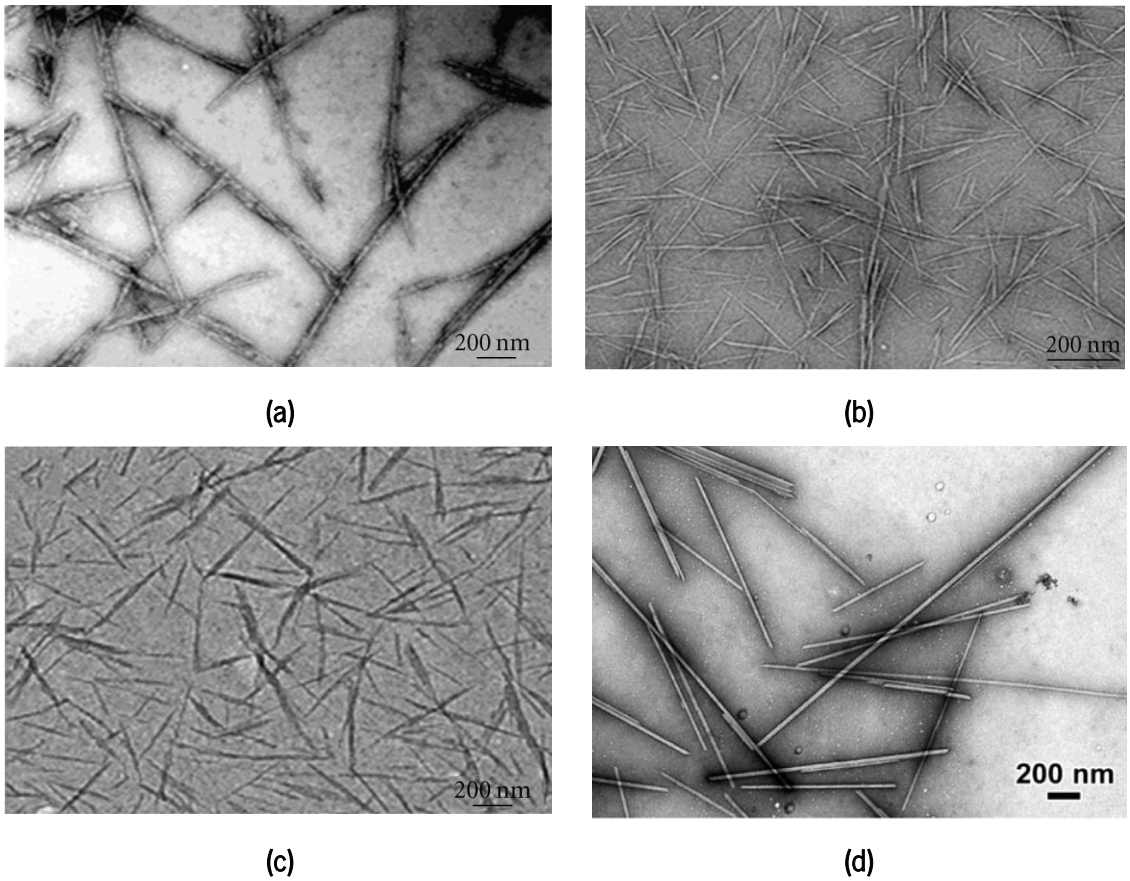

Figure 1.5. Transmission electron micrographs of dilute suspensions of nano-sized cellulose from a) bacterial [101]; b) sisal [133]; c) cotton [134] and d) CNWs [135]. Reproduced from a) Grunert et al. and b) Rodriguez et al. with permission. Copyright 2002 and 2006, Springer; c) Fleming et al. and d) Osorio-Madrazo et al. with permission. Copyright 2000 and 2012, ACS Publications.

General properties such as diameter, length and aspect ratio of various nanofiber types are presented in Table 1.3. Information related with the geometric characteristics of a specific fiber was recently reviewed by Kalia *et al.* [3].

BC fibrils are in the nanometer range and are microscopically similar to collagen fibers [138, 139]. Moreover, some studies [124, 140] point out the biological capacities of BC, which has shown, for example, osteoconduction properties. These characteristics make them particularly interesting to be used as a collagen-mimicking component in scaffolds. For example, HA with BC has been combined by Wan *et al.* [124, 141, 142] to prepared a novel class of bionanocomposites SEM observations demonstrated that HA crystals were uniformly distributed on the phosphorylated BC fibers after soaking

in 1.5 simulated body fluid (SBF) [124]. The 3D network structure revealed that the crystallite size of the HA crystals formed on the BC fibers after 7 and 14 days of soaking in 1.5 SBF are nano-sized, dimensions of 37 nm and 46 nm for 7 and 14 days, respectively [141].

Table 1.3. Chemical Typical geometrical sizes of nano-sized celluloses, in terms of length (L), cross section (D) and aspect ratio (L/d). Compiled from Refs [14] and [137].

Cellulose structure	Diameter (nm)	Length (nm)	Aspect ratio (L/d)
Microcrystalline cellulose (MCC)	>1000	>1 000	~1
Microfibril	2-10	>10 000	>1000
Microfibrillated cellulose (MFC)	10-40	>1 000	100-150
Cellulose whisker (CNWs)	2-20	100-600	10-100
Bacterial cellulose (BC)	5–10 × 30–50	100 to >1 000	—

Nanocomposites containing HA with structural features close to the biological apatites are attractive for applications as artificial bone supports within for TE [2, 141]. Research on BC-HA nanocomposites in the form of membranes demonstrated the potential application of these systems in TE and bone regeneration [123, 125, 143]. Fang *et al.* [123] showed that BC-HA nanocomposite scaffolds were biocompatible and could promote cell proliferation and differentiation *in vitro*. In this study the authors used stromal cells derived from human bone marrow (hBMSC), and real-time reverse transcription PCR results showed that their alkaline phosphatase (ALP) activity and the expression of osteopontin, osteocalcin, bone sialoprotein, and ALP mRNA were all higher for cells cultured for 7 days in the presence of the nanocomposites than for those cultured on pure BC with and without the presence of osteogenic supplements, such as, L-ascorbic acid, glycerophosphate, and dexamethasone. These results suggest that the developed scaffolds have potential for bone TE. Shaska *et al.* [125] also described the preparation of membranes composed by BC reinforced with HA and evaluated the biological behavior of these membranes for the regeneration of non-critical bone defects in rat tibiae, throughout a time period of 16 weeks. The nanocomposites were prepared from BC membranes and

incubated in solutions of $CaCl_2$ followed by Na_2HPO_4. The work revealed that the membranes are effective for bone regeneration since they accelerated new bone formation. Recently, bionanocomposites scaffolds based on BC were prepared in a collagen solution followed by freeze-drying. The resulted material presented biocompatibility [144]. Collagen was also combined with cellulose nanofibers to produce nanocomposites as implantable scaffolds in biomedical applications, more specifically, for ligament or tendon regeneration [126]. The methodology is based on gluteraldeyhyde crosslinking; the two composite phases (cellulose nanofibers and collagen) were prepared by solution casting followed by pH induced *in situ* partial fibrillation of the collagen phase. The collagen fibrils (50 nm of diameter) provided biocompatibility, fatigue resistance and elasticity while the cellulose nanofibers of 12-39 nm acted as a reinforcing phase. These composites, at room temperature, presented mechanical strength of 132–150 MPa and a modulus of 5–6 MPa, significantly higher than the collagen matrix. Moreover, biocompatibility studies indicated non-cytotoxicity for collagen-cellulose bionanocomposites and revealed that the composite surface is promising for cell adhesion. The main drawback of this methodology is the type of crosslinking agent due to its typical cytotoxicity. Additionally, collagen-cellulose ratio as well as crosslinking level for collagen phase needs to be further improved to match the mechanical performance of natural ligament or tendon.

Some studies on bionanocomposites have been reporting the use of clay or modified clay as reinforcements to promote the mechanical (e.g., toughness) and interfacial adhesion in matrices relevant for the biomedical field, namely: polylactic acid (PLA); poly(butylene succinate) (PBS); polycaprolactone (PCL); polyhydroxy butyrate (PHB); and aliphatic polyesters blends [145-147]. On the reinforcement side, few studies have been published concerning the processing of cellulose nanofibers reinforced nanocomposites by conventional melt compounding, such as extrusion [121, 126, 129]. Most of these studies were not executed for TE purposes. The use of cellulose whiskers in bionanocomposites has been mainly limited to hydrophilic matrices due to their surface chemistry [129] and to its limited production enabling only a lab scale usage. In this sense their exploitation on nanoreinforcement in biopolymers requires the scale-up of their production in order to achieve higher amounts at an appropriated time and yield [91].

Lignocellulosic materials are quite sensitive to thermal degradation and start to degrade near 230 °C, restricting the type of matrix that can be used in association with natural fillers [12, 148]. On the other hand, during processing, the hydrophilic nature of cellulose promotes the irreversible agglomeration and aggregation in nonpolar matrices. This is due to the formation of hydrogen bonding between the

amorphous parts of the nanofibers. Surface modification of the whiskers, have been able to improve their mixability with the hydrophobic matrices. The addition of coupling agents, such as, polyethylene glycol (PEG) grafting [121]; or polyvinyl alcohol (PVA) [129] improves the dispersion of the nanowiskers into the matrix. Other chemical treatments have been also reported, and will be discussed in the section dedicated to modified cellulose.

The preparation of CNWs reinforced PLA nanocomposites by melt extrusion was carried out by pumping a suspension of CNWs into the polymer melt during the extrusion process using a proper venting system, able to remove the solvent during extrusion [121]. MCC has been used and treated with N,N-dimethylacetamide (DMAc) containing lithium chloride (LiCl) to swell the MCC and partly separate the cellulose whiskers. After extrusion the composite structure presented a partial dispersion of the CNWs mostly when PEG and maleated PLA were used. The results showed that DMAc/LiCl is effective as swelling/separation agent for MCC, however it causes degradation of the composites at the high temperatures used during processing. The mechanical properties of the maleated PLA/PEG/CNWs bionanocomposites improved compared to PLA treated with DMAc. The elongation at break increased about 800%, the tensile strength 20% and the modulus decreased by 10%. An attempt to use PVA as a compatibilizer to promote the dispersion of CNWs within the PLA matrix has also been reported [129]. PVA is a water-soluble polymer with high tensile strength. The authors hypothesized that the hydroxyl groups of the partial hydrolyzed PVA interact with the hydrophilic surfaces of cellulose and the residual vinyl acetate groups with the hydrophobic PLA. A small improvement was observed in the tensile modulus, tensile strength, and elongation at break, indicating that the main responsible for the mechanical enhancement was derived from the PVA phase reinforced with CNWs and not from the PLA matrix. Although, microscopic analysis revealed inadequate dispersion of the CNWs in the PLA phase due to the immiscibility of the PLA and PVA. No relevant variation on the thermal performance was observed since the CNWs were more allocated to the PVA phase and only a negligible amount was located in the PLA phase.

Replacing the clay reinforcement by cellulose in the form of microfibrils, CNW, BC or MCC leads to fully natural-based and renewable bionanocomposite materials with higher mechanical properties and with potential to be applied in biomedical field.

CNWs from different plant species have been proposed as a reinforcement strategy in the development of bionanocomposites. Their combination with PVA nanofibers, starch/PVA sponges [128, 149], chitosan [127] and PLA [129, 150] has demonstrated potential to be used in the biomedical field. Not

all of these studies have produced relevant reinforcement improvements in terms of dimensional stability, mechanical or thermal properties. Enhanced results were obtained with the production of honeycomb structures of starch with PVA using freezing-thawing technique [128]. This methodology produced stable sponges that were reinforced with CNWs for wound dressing and TE purposes. The CNWs were homogeneously distributed and restricted the packaging of the starch/PVA sponges, leading to an improvement of dimensional stability, compression strength and storage modulus. These bionanocomposites presented biocompatibility and the presence of CNW induced a small reduction on the swelling. More recently, CNWs in the 5-10 nm range have demonstrated a more significant reinforcement effect on the aligned electrospun PVA fiber webs compared with the isotropic electrospun fiber webs. The modulus and tensile strength of the aligned webs obtained by electrospining increased 35% and 45%, respectively. The aligned fibers presented lower diameter when compared with the fibers produced with PVA alone. The addition of 15% of CNWs induced a 95% higher tensile strength and an increase of 118% in the modulus [149].

CNWs were recently used by Zhang *et al.* [151] to prepare a supramolecular hydrogel based on cyclodextrin/polymer inclusion. It was shown that the incorporation of 0.5 wt% of CNWs into the hydrogel enhances its gelation, mechanical strength and facilitates sustained release of drugs. The modulus of the bionanocomposite hydrogel was 50 times higher than that of the native hydrogel. Further evaluation of the bionanocomposite hydrogel, namely cell viability evaluation did not indicate any additional cytotoxicity. These results support their potential as smart drug delivery systems and as injectable biomaterial.

Biodegradable nanocomposites were also obtained with layer-by-layer (LbL) assembly technique [120] using chitosan and CNWs from eucalyptus wood. Chitosan is a biodegradable cationic aminopolysaccharide derived from its acetylated form, chitin. The interaction of chitosan and CNWs occurred due to the formation of hydrogen bonding and electrostatic interactions between the sulfate groups on the whisker surface and the amine groups of chitosan. SEM analysis indicated a dense and homogeneous distribution of the CNWs with a formation of a porous network structure that increases the contact area and the interfacial adhesion between the rigid polymer and the nanofillers. Moreover, the cross section of the assembled films showed a nanometric thickness of ~7 nm per bilayer [127]. The relevant contributions of chitosan are its biocompatibility, biodegradability, and antibacterial properties, making this polymer suitable for drug delivery, TE, wound healing applications, and as a tool to produce antimicrobial materials [152-154]. The authors of this study concluded that chitosan lacks

the flexibility necessary for strong adhesion and efficient load transfer between the organic matrix and the clay platelets. However, CNWs is reported as an alternative to clay platelets as nanofiller for the preparation of multilayered nanocomposite films [127].

The fabrication of nanoscale devices is currently the subject of a great deal of research; although, limited progress has been achieved. The nanoscale constructions using a bottom-up approach to build devices have many foreseeable applications in diverse areas, such as: miniaturized electronics; sensors; and biomedical devices [2, 10, 155]. CNWs are one of the most chemically versatile, abundant and inexpensive nanoparticles available for nanodevice development [10].

1.4.2 Modified celluloses and lignin-based materials

The biocompatibility of cellulose, hemicellulose and their derivatives confers to them biomedical relevance. Different chemical modifications have been reported to the cellulose and lignin structures. A resume of the most relevant ones is compiled in Table 1.4.

In relation to bone and cartilage TE, one of the most studied chemical modifications is the acetylation of cellulose hydroxyl moieties (Figure 1.6, Table 1.4), producing cellulose acetate (CA). CA has been used as isolated component or as part of composites or blends in the development of TE supports. Blending CA with starch produces starch cellulose acetate (SCA), a biocompatible material that exhibits biodegradability and biocompatibility [169]. A series of different CA combinations have been attempted to produce TE scaffolds [156-164], bone cements [165-168] and drug-delivery vehicles [170-172].

SCA and CA have been reinforced with HA and bioglasses in the perspective of generating composite structures with enhanced bioactivity [160, 161]. Moreover, the surface coating of SCA with a calcium phosphate (CaP) layer has been proposed as a surface modification technique to improve the surface bioactivity of SCA [159]. The compounding of SCA with nanosized HA, generates composite nanofibre meshes that improves the calcium deposition by the osteoblasts as demonstrated by Von Kossa staining and alkaline phosphatase (ALP) activity [160]. The microhardness of SCA immersed for 30 days in phosphate buffer saline (PBS) decreases to, approximately, 94% of its initial value [156]; this variation was accompanied by a weight loss of 16% and a water uptake of 50%, being the highest variations compared to the starch-polycaprolactone (SPCL) blend. It was reported by the authors that these variation has a more dramatic influence in the surface morphology and roughness, generating a negative impact in the osteoblast adhesion and proliferation.

Table 1.4. Chemical Modified cellulosic and lignin-based materials and references that exploit them in the biomedical field. Compiled from references [50, 156-193, 196, 255].

Modified Material	Processing strategy	Biomedical application	Refs.
Cellulose			
Cellulose acetate	Chemical substitution	Bone TE; Cartilage TE; Bone cements; Drug-delivery systems	[156-169]
Cellulose acetate phthalate	Chemical substitution	Drug-delivery systems	[170-172]
Hydroxypropyl cellulose	Chemical substitution	Drug-delivery systems; Periodontal TE; Bone cements	[173-176]
Hydroxyethyl cellulose	Chemical substitution	Bone TE	[177]
Silanized-hydroxyethyl cellulose	Chemical substitution	Bone TE	[178]
Hydroxypropylmethyl cellulose	Chemical substitution	Drug-delivery systems; Bone TE; Bone cements	[179, 180]
Silanized-hydroxypropylmethyl cellulose	Chemical substitution	Bone TE; Bone cement; Cartilage TE	[181-184]
Carboxymethyl cellulose	Chemical substitution	Bone TE	[50, 185-190]
Methylcellulose	Chemical substitution	Bone TE; Cartilage TE	[191, 192]
BSA modified or PEGylated cellulose	Click chemistry	—	[193]
Lignin			
Kraft lignin	Alkali treatment	Bone TE	[193]
Acid hydrolysis lignin	Acid hydrolysis	Bone TE; Drug-delivery systems	[255]

In vivo studies were performed on the developed composites/blends showing the suitability of SCA-based materials as TE scaffolds. SCA induced better biological response (through the formation of direct bone contact) than corn starch-ethylene vinyl alcohol (SEVA-C) blend and calcium phosphate (CaP) coated SEVA-C.

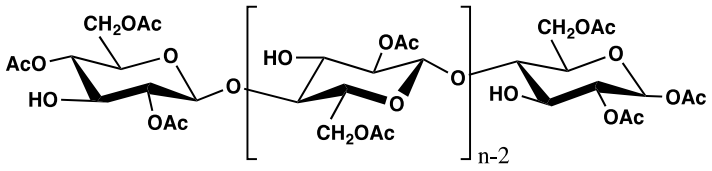

Cellulose acetate

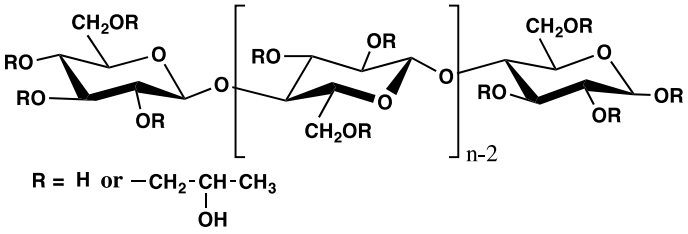

Hydroxypropylcellulose

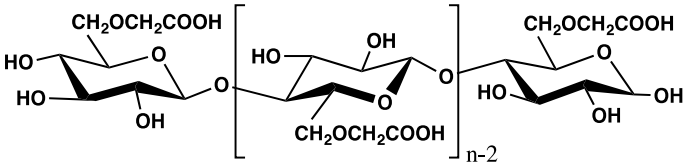

Carboxymethylcellulose

Figure 1.6. Chemical structure of some cellulose derivatives.

Boesel *et al.* [165-168] explored the use of SCA for the development of hydrophilic partially degradable bone cements. This set of studies used SCA has a filler of acrylic resins based on the combination of methylmethacrylate and acrylic acid. With the use of 55-60% of SCA the authors were able to produce a cement formulation that fulfills the requirements of the ASTM standard for acrylic bone cements [165]. The cement formulation was reinforced with bioactive glass compositions or HA and their mechanical behavior and bioactivity was significantly enhanced [166, 167].

CA phthalate-based formulations have been proposed as drug-delivery vehicles, for the controlled release of stimulants for bone formation (e.g. parathyroid hormone, simvastatin), and their efficiency has been proven both *in vitro* and *in vivo* [170-172].

Hydroxypropylmethyl cellulose (HPMC), hydroxypropyl cellulose (HPC), hydroxyethyl cellulose (HEC) and their silanized derivatives, has been proposed as a component for the preparation of injectable bone cements [174, 175, 177-181] and as 3D scaffolds for bone and cartilage regeneration [182-184]. In the bone cement formulations such materials are added at a percentage between 2 and 3% due to its gelification properties, being used as a carrier of the solid component, e.g. CaP phases. HPC has been reported to enhance bone formation when added to bone cement formulations [174]. HPMC is able to promote the formation of a crystalline CaP phase in the surface of biphasic CaP [179]. HPMC also proved to be non-cytotoxic in formulations of injectable hybrid bone cements, without altering the biological properties of the inorganic phase [180].

Carboxymethyl cellulose (CMC) reinforced with nano-sized HA has been tested as bionanocomposites [186] for bone regeneration in a TE approach. The addition of chitosan to these formulations was reported as a methodology to control the biodegradation rate of the composites [187]. Substitution materials for bone repair should have good biocompatibility and a suitable biodegradation rate, as well as higher mechanical properties to support the ingrowth of new bone tissue. Studies involving a tri-component polyelectrolyte composite structure of chitosan and CMC with nano HA have demonstrated potential for that purpose [187, 188, 194]. In a first case using a co-solution method to produce the composites was possible to obtain a morphology and size similar to natural bone with improved compressive strength when compared to HA/chitosan based composites [188]. Combining nano HA with chitosan and cross-linking with CMC in a weight ratio (40/30/30) it was obtained an organic network structure of polyelectrolyte complexes with nanometer crystals of HA uniformly distributed. These structures presented a high compressive strength, acceptable biodegradation and high bioactivity [187]. Self-assembly of static electricity methodology was used to create polyelectrolyte complex membranes with similar compositions obtaining the previously improved mechanical, degradation, swelling and bioactivity characteristics. The combination of chitosan/CMC previously ionic cross-linked with 40 wt.% of nano HA presents a compressive strength near 120MPa that meets the requirement for bone repair material and can be used as biomimetic bone repair material [194].

Within the context of bionanocomposites, CNW has a largely unexploited potential within the biomedical field. Their high surface area to volume ratio may change drastically the properties of CNW through the manipulation of its surface chemistry [10]. One of the drawbacks of the CNW is its poor compatibility with nonpolar solvents or resins due to its hydrophilic nature [2], and the thermal degradation of the cellulosic components at high temperatures [121]; although, the presence of reactive hydroxyl groups

enable a variety of chemical modifications mediated by organic solvents [130, 132], crosslinking agents [132, 195] or using surfactants [197].

The synthesis of BC in the presence of methylcellulose (MC) and CMC has been reported [191] to enhance the water adsorption capability of BC. MC was used in combination with the triblock co-polymers P123 and F127 to generate mesopores and macropores in bioglass formulations developed as scaffolds for bone TE [192].

Svensson *et al.* [112] tested native and chemically modified BC as supports structures for cartilage TE. Transmission electron microscopy (TEM) analysis, and RNA expression of the collagen II from human chondrocytes seeded on the BC-based supports, indicated that unmodified BC induces the proliferation of chondrocytes. Moreover, it was observed by TEM the ingrowth of chondrocytes into the bulk of the BC scaffold. This work showed that BC is a promising material for the development of cartilage TE scaffolds. BC has been also modified with xyloglucan and RGD aminoacid sequence as a tool to promote endothelial cell adhesion. This strategy is highly relevant for bone TE in an attempt to promote vascularization [198].

Recently, Fillponen *et al.* [196] proposed the functionalization of cellulose through the adsorption of a surface layer of CMC modified with azide or alkyne moieties followed by a "click" chemistry strategy to functionalize the CMC surface with bovine serum albumin (BSA) or PEG. The authors report that this strategy can be also employed with other molecules, such as fluorescent dyes or other types of proteins. This methodology can be exploited in the biomedical field through the decoration of the cellulose surface with biochemical cues to induce different types of cellular responses.

In contrast to cellulose-based materials, the lignin counterpart has not yet been significantly exploited in the biomedical field. However, its natural origin, and its abundance in renewable feedstocks motivated some attempts in recent years.

Several chemical modifications on lignins are reported in the literature [28, 48, 55, 60, 199]; although, very few of them were already been tested in the preparation of materials with biological relevance within the field of bone and cartilage TE. However, Kraft lignin has been reinforced with HA and beta-tricalcium phosphate (TCP) to produce composite structures for bone TE [193]. It was observed the formation of porosities between 50 and 100 μm upon sintering at 900 °C. These pores were derived from the positions that lignin occupied before the thermal treatment and occur due to its degradation.

The combination of conducting polymers with lignin can produce anti-oxidant materials capable of reducing the oxidative stress of the surrounding biological tissue. It has been shown that a combination

of polyanyline (PANI), poly(anilinesulfonic acid) or polypyrrole (Ppy) with lignin generate materials with anti-oxidant capacity. These results lead the authors to suggested that this type of materials are relevant coatings of different polymeric scaffolds or biomedical implants with the capacity to reduce the foreign body response [200].

1.4.3 Pyrolised lignocellulosic structures

Inspired by Nature and following a biomimetic approach, natural wood cellular structures have been selected to serve as a 3D porous scaffold for bone TE [98, 100, 201-203]. After appropriated material selection, including a characterization of the wood specie (balsa, oak, rattan, eucalyptus, pine, birch, among others), a development strategy was established through the controlled pyrolyzation (under inert atmosphere) of wood samples. This methodology produced a porous preform of carbon that is chemically infiltrated, generating a coated inner surface of the wood cell walls which gave rises to biomorphic oxides (Al_2O_3, SiO_2, TiO_2, MnO and ZrO_2) [204-208] or, alternatively, carbide phases (SiC, TiC and ZrC) [201, 209-211]. As an example, SiC structure is produced by the spontaneous reaction between molten infiltrated Si with the preform carbon to form SiC-based material. The result is a biomorphic SiC ceramic material (bioSiC) that replicates the highly interconnected microstructure of the wood cell wall [201, 203]. The biodiversity of natural wood offers a variety of morphologies and chemical compositions that can be exploited in the development of constructs relevant for the biomedical field. They have the potential to form structures with unique pore distributions, from the micro to nanometer scale. When developing this type of materials for biomedical applications it is relevant to analyze their osteointegration capacity and biocompatibility. *In vitro* bioactivity studies were performed by means of immersing these types of samples in SBF. Energy dispersive X-ray analysis (EDS) analysis confirmed the formation of a dense CaP layer, demonstrating that, coating the bioSiC with bioactive silicate glass it is possible to improve its osteoconducting properties [203]. Additionally, the culturing of human osteoblast-like cells in the presence of these materials demonstrated a cell proliferation rate similar to the positive controls without cytotoxicity response [212]. Additionally they have demonstrated good biomechanical performance [203, 213]. *In vivo* biocompatibility studies in the femur of rabbits were also performed. Histological results of a bioSiC construct after 12 weeks of implantation confirmed the existence of new bone within the bulk of the SiC porous matrix. Moreover, no tissue inflammation was detected in the surrounding tissue [213].

Recently it was proposed [202] a new process to transform the starting wood into a HA porous scaffold. After the decomposition of the wood organic components, the remaining structure was infiltrated with calcium vapor over the carbon structure to produce calcium carbide (CaC). Using a multi-step chemical and physical process, presented in the scheme of Figure 1.7, it was possible to convert the calcium carbide into a spongy carbonated HA scaffolds to act as artificial bone.

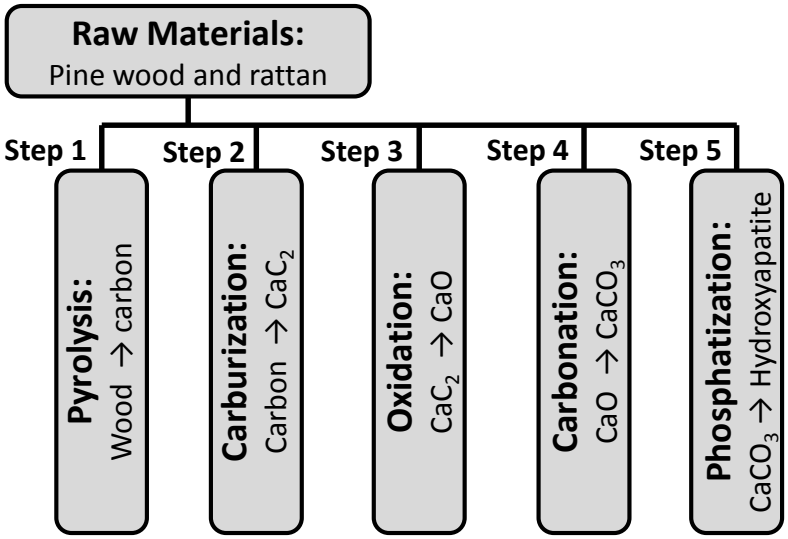

Figure 1.7. Processing steps to convert the wood hierarchical structure into a biomorphic bone scaffolds. Adapted from Sprio et al. [100] and Tampieri et al. [202].

Rattan wood has a strong morphological similarity with bone (see Figure 1.8). This observation promoted the testing of Rattan-based scaffolds targeting bone TE. The developed structures are characterized to present a porosity of 85% and large pore sizes, 250 ± 40 μm. The constructs present channel-like pore system interconnected with smaller pores [202].

In vivo tests carried out on skeletally mature, adult New Zealand White disease-free rabbits, confirmed the bioactivity and osteoconductivity of Rattan-derived biomorphic HA. Histological analysis confirmed the absence of inflammatory or histotoxic reactions. Additionally, the newly formed bone tissue (in the surface and bulk of the constructs) presented a regular architectural pattern surrounding the scaffolds without connective capsules or gaps [100].

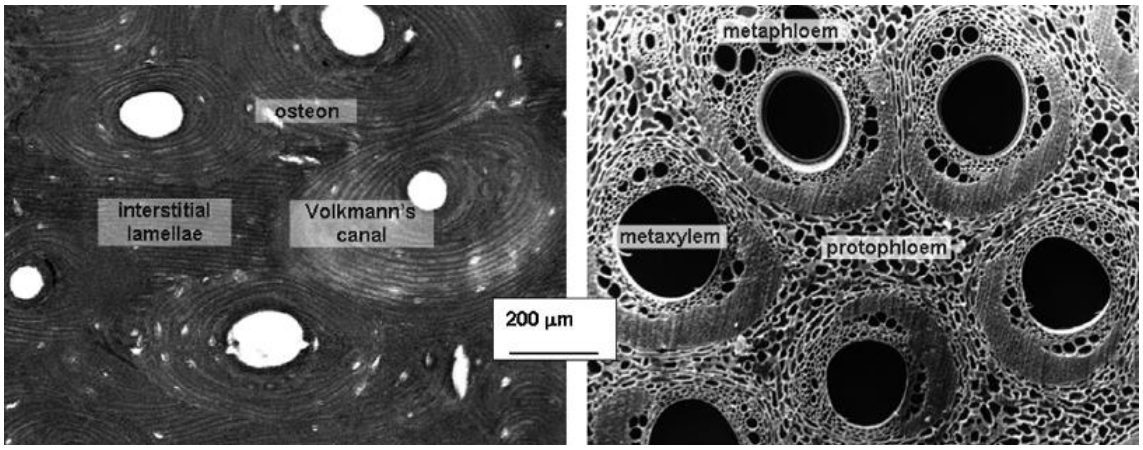

Bone Rattan wood

Figure 1.8. Morphological similarity between bone and Rattan wood structures. Reproduced from Sprio et al. [100] with permission. Copyright 2011, Elsevier.

1.5 Composite hydrogels from lignocellulosic materials

Hydrogels are three-dimensional networks (3D) formed from hydrophilic homopolymers, copolymers, or macromers (preformed macromolecular chains) crosslinked to form insoluble polymer matrices [214]. In terms of materials requirements for regenerative medicine, hydrogels have received attention due to their intrinsic structural and compositional similarities to the ECM and their extensive framework for cellular proliferation and survival. Hydrogels are a class of biomaterials that have demonstrated great potential for biological and medical applications [22, 215-217]. These structures can absorb from 20% up to thousands of times their dry weight [216, 218]. They are highly relevant and appealing for biomedical applications since they usually are biocompatible, the aqueous environment of the hydrogel can protect cells and fragile drugs (such as peptides, proteins, etc.), they present good transport of nutrient to cells and metabolic products from the cells, they may be easily modified with cell adhesion ligands, or they can be injected *in vivo* as a liquid that gelifies at body temperature [216]. Usually they do not dissolve in water due to its permanent cross-linked network (chemical or physical). Some hydrogel systems have attracted significant attention in the biomedical field due to their stimuli-responsive swelling-deswelling capabilities without disintegration, and their biocompatibility [23, 215, 219]. Polysaccharides are one class of polymers that are able to form hydrogels that are highly hydrated and porous, being similar to living tissue. When implanted, these hydrophilic materials allow the permeation of water, metabolic products and chemical signals in the aqueous physiological environment [140]. Polysaccharides such as chitosan [64, 118, 220, 221], starch-based [222, 223],

gellan gum [17, 224, 225], hyaluronic acid [226-228] and alginate [50, 229] have been widely used to prepare natural hydrogels. They present the advantages of being biocompatible, biodegradable, low toxicity, and high availability from renewable resources [120, 219, 220]. The main areas in which hydrogels are used as biomaterials are in contact lenses, synthetic wound coverings, drug-delivery systems, permselective membranes, and in organ and tissue replacements, such as, skin, tendon, cartilage, heart valve stents, and bone [109]. Examples of the use of lignocellulosic-based hydrogels in the biomedical field, during the last decade, are presented in Table 1.5.

Table 1.5. Overview of biomedical applications using hydrogels containing lignocellulosic constituents. Compiled from Refs. [17, 21, 50, 95, 109, 118, 124, 140-142, 181, 182, 189, 198, 217, 220, 226, 230-255].

Material type	Reinforced / with	Application	(Refs.)
Cellulose based			
Cellulose	Cellulose phosphates	Femoral implantation; bone regeneration;	[230-233]
	Calcium - containing solution	Orthopaedic.	[234]
	calcium-deficient hydroxyapatite	Orthopaedic.	[235]
Carboxymethyl cellulose	Calcium phosphates	Ectopic bone.	[50]
	Acrylic acid solution and gamma radiation	Drug carrier.	[236]
	Nanofibrillated cellulose powder	Human nucleus pulposus.	[217]
Hydroxyethylcellulose	Carboxymethylcellulose sodium Salt (NaCMC)	Bulking agent for stomach; Treatment of overweight; Drug delivery.	[21, 237, 238]
		Diuretic therapies for edemas.	[239]
	Hyaluronic acid	Postsurgical soft tissue adhesion.	[226]

Hydroxypropylcellulose	Acrylic acid and poly(L-glutamic acid-g-2-hydroxylethyl methacrylate)	Oral drug delivery.	[240]
Hydroxypropyl-methylcellulose	Silanol (Si) groups	Injectable hydrogel; Articular cartilage.	[182, 241, 242]
	Silanol (Si) groups and biphasic calcium phosphate	Orthopaedic; Bone filling and regenerative capacities; Crosslinkable bone substitute .	[181, 242, 243]
Methylcellulose	poly(N-isopropylacrylamide)	Articular cartilage.	[244]
Bacterial cellulose	Hydroxyapatite	Artificial bones, scaffolds and cardiovascular tissues.	[124, 141, 142]
	Xyloglucan	Vascular grafts.	[198]
	Calcium - deficient hydroxyapatite	Orthopaedic biomaterial; Bone substitution and regeneration.	[140, 189, 235]
	Polyvinyl alcohol	Bone substitution and regeneration; soft tissue; cardiovascular tissues;	[109, 245]
		Polymeric heart valves;	[246]
		Artificial cornea replacement.	[247]
	Gelatin, or sodium alginate, or gellan gum	Articular cartilage.	[17]
	Chitosan	Wounds; burns and ulcers.	[118]
	Polyaniline	Bio-sensors, cell function for Tissue Engineering (TE).	[248]
Hemicellulose based			
Hemicellulose galactogluco-mannan	Chemical; enzymatic modification	Drug delivery.	[249-251]
Hemicellulose	Chitosan	Drug delivery (gastric fluid).	[220]
Hemicellulose derivate	N - isopropylacryl-amide	Smart materials for medical applications.	[252]
Lignin based			
Lignin	Xanthan gum	Biodegradable hydrogel-films.	[95, 253]

Polyethylene glycol diglycidyl ether	Drug delivery.	[254]
N-isopropylacrylamide and N,N'-methylenebi-sacrylamide	Temperature sensitive.	

1.5.1 Cellulose-based materials

Cellulose-based hydrogels are biocompatible and its modified systems may be considered biodegradable. Several water-soluble cellulose derivatives can be used as mono-component of multi-component systems to form hydrogel networks possessing specific properties in terms of swelling capability and sensitivity to external stimuli [21]. They can be prepared from a cellulose solution through physical cross-linking. As it was pointed out before, cellulose has several hydroxyl moieties able to form an interlinked network stabilized by hydrogen bonding. However, it is usually difficult to dissolve cellulose in common solvents due to its highly extended hydrogen bonded structure, being one of the main challenges in the development of cellulose-based hydrogels. A recent work on cellulose hydrogels refers new solvents, such as N-methylmorpholine-N-oxide (NMMO), ionic liquids (ILs), and alkali/urea (or thiourea) aqueous systems that have been developed to dissolve cellulose, providing a set of new opportunities for the preparation of cellulose hydrogels [22]. The current trend in the design of cellulose-based hydrogels is associated to the use of non-toxic crosslinking agents or crosslinking chemical treatments, to further improve the safety of both the final product and the manufacturing process.

BC was also used to prepare a nanostructured hydrogels for TE. BC has more than 200 times higher surface area than isolated softwood cellulose. Compared with cellulose from plants, BC possesses higher water holding capacity, higher crystallinity, higher tensile strength, and a finer web-like network [141, 185].

Hutchens *et al.* [140] have used BC hydrogels as templates to form biomimetic calcium-deficient hydroxyapatite (CdHA). After the purification process, the cellulose was incubated in solutions of calcium chloride followed by dibasic sodium phosphate. An amount of apatite higher than 50% of total dry weight was incorporated throughout the hydrogel. Their results indicate that CdHA spherical clusters (1mm) are composed by nanosized crystallites that were formed inside the BC network. The formation of this bionanocomposite is similar to the physiological biomineralization of bone producing apatite

crystals of comparable shape and size. XRD analysis showed that the CdHA is comprised of anisotropic 10–50 nm elongated crystallites mimicking the geometry of bone apatite crystals. Combining the biocompatibility of BC with the bioactivity of CdHA, these bionanocomposites are promising materials to be used as scaffold for bone TE [235]. It was also observed that the CdHA implants are rapidly incorporated into the bone tissue due to its high biocompatibility and strong bioactivity [140].

Millon *et al*. [109, 245] have considered hydrophilic BC fibers combined with PVA to form a bionanocomposite that mimic the role of collagen and elastin, respectively. Their main objective was to evaluate its use as cardiovascular tissue replacements. More recently, Mohammadi [246] presented a novel technique to exploit the anisotropy and the non-linear mechanical properties of BC-PVA hydrogels in the development of heart valves. Hydrogels based on BC-PVA were prepared for cornea replacement, due to their high water content, high visible light transmittance, suitable UV absorbance, high mechanical strength and appropriated thermal properties [247]. However these systems require further improvements before being tested under clinical applications.

After the discovery that electrical signals can regulate cell attachment, proliferation and differentiation, researchers sought to incorporate conducting polymers into biomaterials to take advantage of the electrical stimuli [256]. Polyaniline (PAni) is a conductive electroactive polymer, where the reaction time of polymerization, the type and concentration of doping acids plays the main role in the electro-conductivity properties of the composites. BC-PAni nanofiber composite is an electro-conductive hydrogel that combines the properties of hydrogels and conductive systems [248]. The study showed that PAni could be synthesized on the surface of BC nanofibers and assembled into a novel 3D membrane structure, enhancing considerably the composite electroconductivity. The nanocomposites may potentially be used for flexible displays, biosensors, and platform substrates to study the effect of electrical signals on cell activity or to direct desirable cell function in TE applications.

Interpenetrating polymer networks (IPNs), consist of a combination of two or more polymer networks synthesized in juxtaposition, i.e. a blend of two or more cross-linked polymers, which may be incompatible, but are physically interlocked, forming a 3D structure between its constituent phases [257]. IPNs can be divided into two specific forms [17, 22]: sequential IPN and semi-IPN. In the case of sequential IPN, cellulose is used as the first network and the second network is synthesized by polymerization in the presence of the cellulose network. When cellulose or its derivative is linear or branched in a cross-linked network, it is called as semi-IPN hydrogel [22]. In the biomedical field, high mechanical strength double-network (DN) hydrogels, combining BC and gelatin, has been prepared by

Gong and coworkers [17]. Gelatin is a polypeptide derived from collagen, one of the main constituents of the ECM. A BC-gelatin system in the form of a gel can retain water and recover consecutively from compression [22]. The authors have prepared BC-gelatin hydrogels by immersing BC gel in aqueous gelatin solution, followed by cross-linking with N-(3-dimethylaminopropyl)-N'-ethylcarbodiimide hydrochloride (EDC), generating a sequential IPN hydrogel. The tensile strength of the DN hydrogel along the direction of the stratified layer and the compressive strength in the direction perpendicular to the stratified layer was about 112 times and 31 times higher than that of gelatin gels, respectively. A similar enhancement on the mechanical strength was reported for the combination of BC with other polysaccharides such as sodium alginate, gellan gum and carrageenan [17]. Moreover, these hydrogels present a low friction coefficient of the order of 10^{-3} and potential to be used as artificial cartilage.

1.5.2 Modified cellulose-based materials

Cellulose derivatives can be tuned to produce hydrogel structures, either reversible or stable, through their covalent cross-linking using aqueous solutions of cellulose ethers, such as, methylcellulose (MC), hydroxypropyl cellulose (HPC), hydroxypropyl methylcellulose (HPMC) and hydroxyethyl cellulose (HEC) [258].

HPC and its chemical derivatives have been proposed as smart responsive materials [29] for drug-delivery applications [29, 173]. Its use as an oral administration vehicle with thermo- and pH-responsive capacity has been reported, showing stability at acidic pH and enhanced degradation rate at neutral pH. Additionally, the HPC hydrogels reduce their swelling rate with increasing temperature [29]. HPC was recently tested in a phase II clinical trial for the controlled release of FGF-2 targeting periodontal bone regeneration in patients diagnosed with periodontitis. The results showed a significant increase in the alveolar bone height, which was used by the authors as an argument to prove that these delivery systems in combination with FGF-2 stimulate bone regeneration [174]. A delay in the delivery of gentamicin from CaP bone cements was proposed by the addition of HPC to the formulation [176].

The delivery of cells using a noninvasive surgery can be achieved using injectable scaffolds [183]; although, the desired cell-based construct has to be retained at the repair site after being injected. Considering these requirements, some strategies were developed using a hydrophilic polymer able to exhibit self-reticulation properties in order to promote the mechanical integrity of the gel phase.

HPMC grafted with silanol groups (Si-HPMC) is a self-hardening gel at the physiological pH and has been proposed to promote cartilage and bone regeneration [182, 183] also as injectable systems [184,

259]. Si-HPMC hydrogels have been also proposed as injectable bone cements for the treatment of periodontal defects, with the advantage of being able to promote new bone formation 3 months after *in vivo* implantation. Additionally, it was reported that Si-HPMC promotes the fixation of the inorganic phase in the intervention area [181]. Vinatier et al. [184], proposed Si-HPMC hydrogels as TE supports capable of promoting chondrocyte proliferation. The study reported that chondrocytes were metabolically active, and were able to produce glycosaminoglycans. Overall, it was concluded that Si-HPMC is a promising material for cartilage TE. More recently, it was proposed an injectable therapeutic strategy for the regeneration of articular cartilage using autologous rabbit nasal chondrocytes (RNC) with Si-HPMC hydrogel [241]. The use of nasal chondrocytes presents the advantages of reducing donor site morbidity while exhibiting greater chondrogenic potential than articular chondrocytes [260]. After 6 weeks of *in vitro* studies, histological analysis of autologous RNC transplanted in an articular cartilage defect revealed the formation of new cartilage tissue with a histological organization similar to that of healthy articular cartilage. Moreover, immunohistological analysis of type II collagen suggested that the new tissue was a hyaline-like cartilage [241].

Orthopedic devices made from biodegradable materials present advantages over metal or nondegradable materials since they can transfer stress over time to the damaged area as it heals, and there is no need of a second surgery to remove the implanted devices [256]. Cellulose phosphate (CP) has been investigated as a biomaterial for orthopedic applications to improve the osseointegration of cellulose. Granja *et al.* [231, 261] have studied the phosphorylation of regenerated cellulose hydrogels using MCC. Their work assessed the mineralization potential of CP, i.e. the ability of a material to induce the formation of an apatite layer in a SBF, revealing that only the Ca salt of CP promoted formation of apatite. It was reported that the interface between the polymer and the mineral layer was continuous [231]. Moreover, moderate degrees of surface phosphorylation were able to induce mineralization.

In a different work, the pre-incubation of unmodified regenerated cellulose hydrogels with Ca resulted in the formation of a homogeneous apatite layer. However, in this case, the interface between the polymer and the mineral layer was not continuous [234, 262].

Granja *et al.* [230, 232, 233] also studied the biocompatibility of CP under *in vitro* and *in vivo* conditions. Their *in vitro* biocompatibility was studied in cultures of human Bone Marrow Stromal Cells (hBMSC), showing that CP is not cytotoxic, independently of the phosphate content [233, 262]. In another *in vitro* study, it was reported that regenerated cellulose hydrogels showed good rates of

hBMSC proliferation after 22 days in culture and it was observed an homogeneous colonizatrion of the surface of the materials [232]. It is important to indicate that these structures without cells do not mineralize. Animal implantation studies were performed in rabbits and the results revealed that both unmodified and phosphorylated cellulose were biocompatible and reveal osteoconductive properties [230]. A complete osseointegration was not observed, although some remodeling activity of the bone tissue was referred when CP was used. These works showed that regenerated cellulose hydrogels presented potential to be applied in different orthopedic applications.

CMC hydrogels have been also tested for the containment of the inorganic phases in CaP bone cements. They presented degradation between 50 to 60% at the second week of experiment and no negative impact in the bioactivity of CaP. CMC-CaP formulations possess osteoinductive properties, allowing the formation of ectopic bone at the same level as the CMC-free CaP [50]. The coating of cellulose-based scaffolds with CMC induces the formation of CaP crystalline phases on their surface [162, 189], therefore promoting bioactivity. More recently, polyelectrolyte complexes composed by CMC, chitosan and polyglutamic acid presented significant antibacterial properties and limited *in vivo* foreign body response [190]. Additionally, polyelectrolyte hydrogels present a high sensitivity to their sorption capacity. This can be manipulated by varying the ionic strength and pH of the external solutions [21, 239].

The smart behavior of some cellulose derivatives, such as, NaCMC and HPMC, in response to physiologically variables (i.e., pH, temperature, ionic strength) makes the lignocellulosic-based hydrogels appealing for *in vivo* applications in the field of TERM. Recently, Eyholzer *et al.* [217] have demonstrated the potential of nanofibrillated CMC in the preparation of hydrogels for the replacement of nucleus pulposus in intervertebral discs. The methodology consisted in the UV polymerization of N-vinyl-2-pyrrolidone in a suspension of nanofibrillated CMC, using Tween 20 trimethacrylate as cross-linking agent. The results of the study showed that the developed hydrogels could successfully mimic the mechanical and swelling behavior of the nucleous pulposus.

1.5.3 Hemicellulose and modified hemicellulose-based materials

Hemicelluloses present sufficient hydrophilic functional groups (hydroxyl and carboxyl) on their backbones to act as reactive sites for chemical modification. They are widely available feedstocks and confer relevant properties to their corresponding hydrogels, e.g. renewability, biodegradability and biocompatibility [23]. Recently Albertsson *et al.* [251] presented a new method to prepare hydrogels

from chemically modified hemicelluloses. The procedure used a freeze-dried hemicellulose rich fraction and can be described as a three-step procedure: (1) the synthesis of cross-linkable precursors by activating 2-hydroxyethylmethacrylate (HEMA) with N,N-carbonyldiimidazole (CDI); (2) the covalent attachment of the cross-linkable precursor to the polysaccharide backbones (DMSO); and (3) cross-linking the hydrogels through the reaction between the HEMA-modified hemicellulose and free HEMA molecules. The developed hydrogels presented a swelling that is greatly dependent on the degree of HEMA substitution and the co-monomer to hemicellulose ratio. Swelling was found to reduce with increasing HEMA substitution degree [23]. The main drawback of this methodology is related to the high cost derived from the synthesis of the intermediate precursors.

Galactoglucomannan (GGM) is the main hemicellulose in Norway Spruce (*Picea abies*), the most common raw material used in the thermochemical mills in Scandinavia. It can be used isolated after an established procedure involving microfiltration [249]. O-acetyl-GGM (AcGGM) is the major softwood hemicellulose, and the synthesis of AcGGM hydrogels can be achieved by chemical grafting of acrylates and their subsequent cross-linking. BSA was encapsulated into HEMA-grafted AcGGM hydrogels, and its release was studied as a function of the HEMA grafting degree and of the addition β-mannanase to hydrolyze the hydrogel. The hydrogel preparation procedure involved the enzymatic modification of the AcGGM chains and synthetic coupling of HEMA. Two parameters were found to influence the release of BSA in water: the degree of substitution of HEMA and the presence of β-mannanase [250]. While lower release of BSA occurred for an HEMA grafting degree between 0.10 and 0.36, the presence of β-mannanase increased the BSA release. This study demonstrated the potential of HEMA grafted AcGGM hydrogels as drug delivery vehicles.

Hydrogels usually exhibits low mechanical resistance; therefore, a significant effort has been made to develop hydrogel reinforcement strategies that do not compromise their water absorption capacity. A type of strategy already mentioned for the cellulose-based hydrogels is the assembling of IPNs or semi-IPNs. These strategies can produce hydrogels with enhanced mechanical performance [23]. Hydrogels based on semi-IPN of hemicellulose and chitosan have been investigated [220]. A recent work [23] reviews two distinct routes to prepare hydrogels based on semi-IPN of hemicellulose and chitosan. The first method is based on the mixing of two different solutions, of hemicellulose and chitosan, and subsequent cross-linking with glutaraldehyde. The second method consists in mixing hemicellulose with chitosan in the dry form and then dissolving the mixture in acidified water. A recent work performed by Karaaslan *et al.*, [220] using the first method, produced hydrogel films based on semi-IPN with high

molecular weight hemicellulose and chitosan. The resulting hydrogel presented a pH-responsive drug delivery using riboflavin as a model active agent. These results demonstrated that hemicellulose-based hydrogels are capable to crystallize in the presence of 50 wt% of chitosan, acting as reinforcement component within the semi-IPN structure. Additionally higher swelling ratios were observed with the increase of hemicellulose content due to the lower degree of crosslinking and higher hydrophylicity [23, 220].

1.5.4 Lignin-based materials

The incorporation of lignin can lead to an increase on the thermal stability, hydrophilicity, biocompatibility and biodegradability of hydrogels [95]. Similar to the hemicellulose, lignin-based molecules can be used in semi-IPN hydrogels. A recent work [95] reports the development of superabsorbent hydrogels based on different types of lignin. These materials are semi-IPN hydrogels with structures between lignin and xanthan gum, an anionic extracellular bacterial polysaccharide known to be biocompatible, biodegradable and to exhibit gel-like properties. These lignin-based semi-IPN hydrogels are prepared by a crosslinking reaction with epichlorohydrin, followed by intensive washing to remove the unreacted crosslinking agent. The methodology leads to a biodegradable superabsorbent hydrogel with high swelling rate in aqueous media. The study revealed that the nature of lignin influences the thermo-oxidative stability and the swelling properties of the hydrogels.

The performance of the lignin based gels could be improved by means of a chemical modification of the starting lignin [23]. As an example lignin hydrogels can be prepared by crosslinking it with polyethylene glycol diglycidyl ether [254]. The lignin-based hydrogels swells in water: ethanol mixtures and in alkaline solutions, and they shrink upon heating. The swelling properties of such materials are attributable to lignin. This study was not developed in a biomedical perspective, although, the results confirm that lignin-based hydrogels have a large unexploited potential for the development of drug delivery systems.

Lignin has been also used in the development of a thermo-responsive hydrogel [255]. These “smart” materials have the ability to respond to temperature changes, modifying their gelling behavior [263]. Thermo-responsive lignin-based hydrogel were developed by Feng *et al.* [255]. This was achieved by reaction between acetic acid lignin with NIPA, generating NIPA-g-lignin. The developed material presented a lower critical solution temperature (LCST) of 31 °C with tunable pore sizes (between 20 and 100 μm) that is dependent on the percentage of lignin fraction.

1.6 Some recent applications in the biomedical field

With the rapid diminishment of oil resources and serious environmental pollution caused by the refining of petrochemical products, alternative and sustainable resources have attracted a growing interest among researchers. The increase of knowledge on the lignocellulosic components acted as a leverage on its use as composites in the biomedical field.

Wound dressing systems based on pure oxidized regenerated cellulose (ORC) have been developed such as Tabotamp® and as well as a mixture from collagen and ORC named Promogran®. Tabotamp® is a thin gauze layer from pure ORC that is used in acute wounds like trauma, surgical injuries and burns. It provides hemostatic and antimicrobial properties [264]. Collagen is recognized as the major component of the ECM and serves as a natural substrate for cell attachment, proliferation and differentiation. Collagen has been employed as a matrix material for TE and wound dressing [265]. Promogran®, is a commercial spongy collagen matrix (55%) containing ORC (45%) that has been recently introduced in the US and European markets for the treatment of exuding diabetic and ulcer wounds [265, 266]. This product is a dressing consisting of a sterile, freeze-dried matrix and combines the properties of its components, such as fluid absorption and haemostatic properties.

BC in the form of membranes has been applied for guided bone regeneration in: bone defects of critical and noncritical size [125]; in periodontal lesions [181]; and as a resorbable barrier membrane for preventing the invasion of fibroblast cells and fibrous connective tissue into the bone defects [123]. Results from the literature indicate that BC membranes promote effective bone formation at the site, besides being a low-cost treatment [125, 267, 268].

The current trend in the design of cellulose-based hydrogels is related to the use of non-toxic crosslinking agents or crosslinking treatments, to further improve the safety of both the final product and the manufacturing process [21]. Hydrogels are considered optimum candidates to be used in wound dressings. In this sense hydrogels should be designed to maintain the appropriated moisture in the wound; relieve the pain, not adhere to the wound; and conform to the body shape [269]. Several systems based on natural or synthetic solutions are patented [270-272] or on the market [273, 274] offering additional characteristics, including non-adherent dressings or systems comprising antimicrobial agents in their formulations. Several of the hydrogels applied on wound dressing present water content between 70 and 95%. The most cited commercially available hydrogels designed as

wound dressing systems are listed in Table 1.6, including examples from the literature [21, 139, 140, 269, 274, 275].

Table 1.6. Overview of Commercially available hydrogel wound dressings containing cellulose derivates, such as, BC, CMC or NaCMC. Compiled from Refs. [21, 139, 140, 247, 269, 275].

Producer	Local	Product Name (®, ™)	Cellulose polymer type / composition	(Ref.)
Xylos Corporation	United States	XCell	Water BC Polyhexamethylene biguanide (PHMB)	[140, 274]
Smith and Nephew	United States	IntraSite Gel	Water Propylene Glycol NaCMC	[21]
ConvaTec	United States	Aquacel Ag	NaCMC Silver ions (1.2%)	[21]
Johnson & Johnson	United States	Silvercel	Calcium alginate CMC Silver ions (8%)	[21]
ConvaTec	United States	GranuGel	Water NaCMC Propylene glycol Pectin	[21]
BMS/ ConvaTec	United States	DuoDERM Gel	Water 81.5% Sodium CMC Pectin Propylene glycol	[269]
Smith & Nephew Healthcare Limited	United Kingdom	IntraSite Gel	Water 78% Modified CMC 2.3% Propylene glycol 20%	[269]
Coloplast	Denmark	Purilon Gel	Water 90% CMC Calcium alginate	[269]
BioFill, Produtos Bioetecnologicos	Brazil	Biofill	Microbial cellulose	[139, 275]
BioFill, Produtos Bioetecnologicos	Brazil	Bioprocess	Microbial cellulose	[139, 275]

Several natural and synthetic wound dressings have been developed; however the search for an ideal wound dressing is still in progress. Some commercial products use silver particles on the hydrogel composition to confer antimicrobial activity. After approval from the Food and Drug Administration,

Xylos Corporation (USA) is commercializing a skin substitute based on BC (XCell). This material it referred to maintain the moisture balance in the wound and to speed up healing and epithelialization [140, 274]. BC has been widely investigated for wound healing due to its purity and high water retention capacity, and a series of BC-based wound dressings are currently on the market. Their potential as wound dressing has been reviewed by Czaja et al. [20, 139]. BC has been used in cartilage TE [112, 276], replacement of blood vessels in rats [16] and in wound healing processes [20, 139]. Hydrogels based on BNC mimic basic living processes and are of growing importance as bioactive scaffolds.

From the large number of different cellulose derivatives, HPMC is the one that has been more commercially exploited as a pharmaceutical excipient and as vehicle for controlled drug delivery. The polymer molecular weight (M_w) is of significant importance due to its intimate relation with the delivery profile of the loaded drug. In this sense, by controlling the polymer M_w it is possible to adapt the drug-release profile to the required timeframe and rate. This strategy has been recently reported in the new line of Benecel™ (Ashland Inc.) commercial HPMC excipients [273].

1.7 Concluding remarks and future trends

The development of scaffolds that mimic the architecture of tissue at the nanoscale is one of the major challenges in the field of TE in the last 15 years. The development of nanofibers, has greatly enhanced the scope for fabricating scaffolds that can potentially meet this challenge. Agricultural fibers represent an abundant, inexpensive, and readily available source of renewable lignocellulosic components that can be used integrated in a biorefinery process.

Cellulose is the most abundant natural polymer on Earth, which is an almost inexhaustible source of raw material for the increasing demand for environmentally friendly and biocompatible products. Therefore, cellulose based materials have become one of the most important bioresources in the 21st century. This increasing relevance induced the investment on bionanocomposites research targeting biomedical purposes. This also includes its purified, modified or biodegradable constituents that are used as matrix or nano-reinforcements.

A relevant, and still unexplored, component of plants is suberin. Its general chemical structure is polyester-based, one of the most common type of FDA-approved synthetic biomaterial, e.g. PLA, PLGA, etc. Usually, these FDA-approved synthetic polyesters used in the development of biomedical materials are hydrophobic. Additionally, the chemical characterization of suberin structure has shown the

presence of a high concentration of hydroxyl moieties [96]. This feature can be used as an added value due to the possibility of synthesizing suberin-based polyester structures with pendant hydroxyl groups that promotes some hydrophilicity [74]. Suberin or chemical modified suberin from bark was already applied in composites to promote adhesion between the phases and to enhance their mechanical performance [277]. It is envisaged a large spectrum of possible applications for these structures, although, polymerization studies need to be executed to understand the real potential of suberin-based polymeric structures in the biomedical area. Under the current environmental, societal and political status there is a pressing need for innovative, sustainable and recyclable materials. Figure 1.9 presents a schematic representation of possible future trends and effects on lignocellulosic-based bionanocomposites relevant for the biomedical field. There is a gradual tendency to move to greener materials made from renewable resources where the lignocellulosic components or templates have a relevant potential.

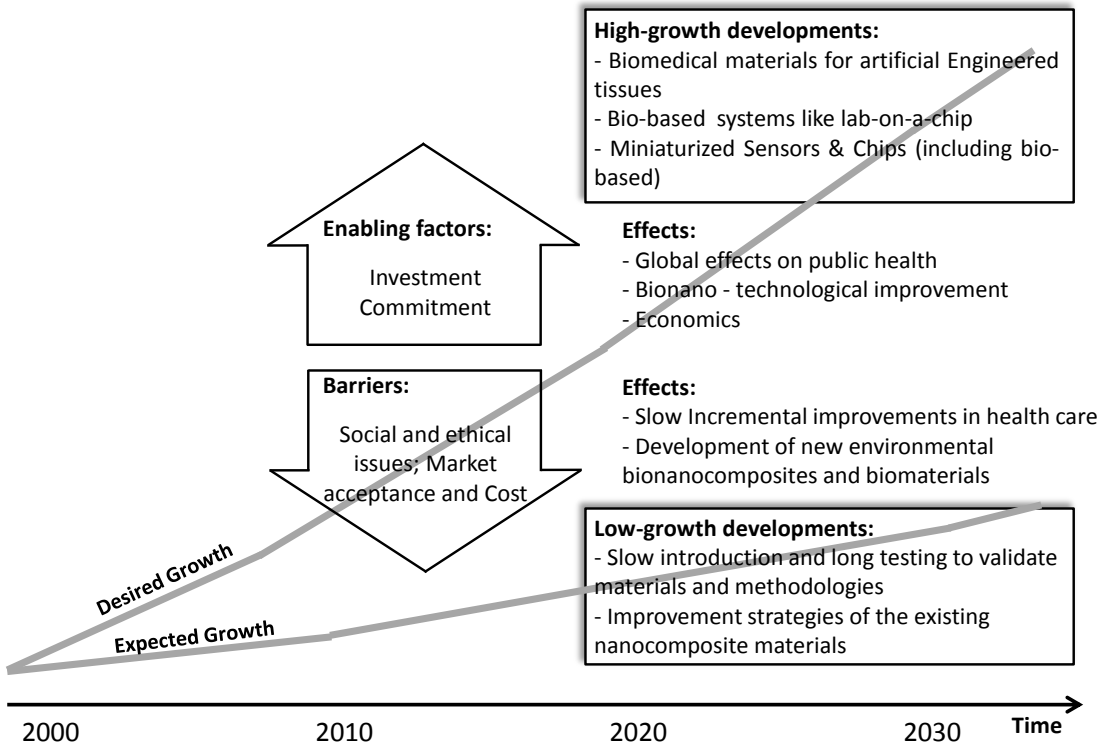

Figure 1.9. Range of possible future trends and effects on bionanocomposites using lignocellulosic components or nanofibers relevant for the biomedical field.

A significant effort is under way to match the properties of the lignocellulosic materials with the ones required for specific applications. In the field of TE it is relevant to mention that research is evolving by improving the mechanical resistance of the lignocellulosic-based constructs, namely, by applying different types of nano-reinforcements, e.g. HA or the different CaP phases; although, there are other properties that the materials should match, namely, biocompatibility, bioactivity, degradability (if a regenerative approach is targeted), among many others.

As it was pointed out in this review, materials with a hierarchical structure, such as wood, provide a design strategy within the development of biomaterials. This biomimetic approach exploits the micro to nanoscale organization of the wood porous structure to design nanostructured materials with enhanced mechanical, chemical and biological properties. Additionally, the alternation of fiber bundles and channel-like porous areas also makes wood a material of choice to be used as a template in starting the development of new bone substitutes. In particular, some of the wood-derived structures were already tested as bioinert bone scaffolds [100, 213]. In this area more biological knowledge in terms of *in vitro* studies will be required to understand the potential of these structures, as well as, more investment is needed for the *in vivo* tests involving large animals.

The current trend in the design of cellulose-based hydrogels is related to safety improvement issues, namely in the development of non-toxic crosslinking agents/treatments. It is expected that the origin of the lignocellulosic component will induce some differences in terms of swelling, chemistry, among others. These variations influence the behavior of the biomaterial. In this field it is expected the development of new approaches for modifying and crosslinking hemicellulose and lignin in order to improve the mechanical strength and adsorption capacity of their respective hydrogels.

These new formulations are expected to present controllable physical properties that can be matched to address the specific biological and medical challenges. These developments will allow the formulation of, for example, novel injectable materials for non-invasive surgical procedures, presenting suitability mechanical and biological properties. Hydrogels applied within TE should be capable to provide adequate mechanical properties, as well as the biochemical cues to promote tissue regeneration. The nanoscale structuring of these hydrogels, such as, pore size and controlled degradation rate must be optimized. In the future, the incorporation of modified functional hydrogels from plant-based polymers into micro-devices will contribute to improve and provide new routes for fabricating enhanced TE based systems with efficient *in vivo* performance.

In drug delivery, the development of "smart" responsive bionanocomposites that can respond to changes in their surrounding environments will provide for new and improved methods of delivering molecules for therapeutic applications. The use of lignocellulosic components in drug-delivery systems is studied for several years [175, 218, 220, 278]. Additionally, the use of cellulose derivatives as excipients in drug formulations is already a standard in the pharmaceutical industry [273]. In the future it is expectable the appearance of commercial formulations that are able to control the release rate and timeframe of different drugs. These systems can be combined with biomedical devices typically used for bone and cartilage TE (e.g. bone cements).

As schematically presented in Figure 1.9, it will be necessary to attract the industry to this growing market opportunity capable of creating sustainable technological improvements in bionanocomposites. The successful exploitation of these biomedical markets requires the commitment and interaction between industry and scientists.

It is expected a growing interest in the development of bionanocomposite structures based on lignocellulosic materials that target the biomedical field. The positive results obtained within the academic activity with the proposed strategies to enhance the performance of the bionanocomposites will contribute to sustain these market developments. In this sense, it is important to validate: the most sustainable supplies of lignocellulosic materials; and the origins that present a more stable composition, better properties and lower variability. In addition, it is also relevant to create mechanisms to conduct to the certification of these nanostructured biomaterials according to common methods and standards.

1.8 References

[1] Sain M, Oksman K. Introduction to cellulose nanocomposites. In: Oksman KSM, editor. Cellulose Nanocomposites: Processing, Characterization, and Properties. Washington, DC: American Chemical Society; 2006. p. 2-8.

[2] Kamel S. Nanotechnology and its applications in lignocellulosic composites, a mini review. Express Polym Lett. 2007;1:546-75.

[3] Kalia S, Dufresne A, Cherian BM, Kaith BS, Avérous L, Njuguna J, Nassiopoulos E. Cellulose-Based Bio- and Nanocomposites: A Review. Int J Polym Sci. 2011;2011:1-35.

[4] Darder M, Aranda P, Ruiz-Hitzky E. Bionanocomposites: A New Concept of Ecological, Bioinspired, and Functional Hybrid Materials. Adv Mater. 2007;19:1309-19.

[5] Klemm D, Kramer F, Moritz S, Lindstrom T, Ankerfors M, Gray D, Dorris A. Nanocelluloses: A New Family of Nature-Based Materials. Angew Chem-Int Ed. 2011;50:5438-66.

[6] Entcheva E, Bien H, Yin LH, Chung CY, Farrell M, Kostov Y. Functional cardiac cell constructs on cellulose-based scaffolding. Biomaterials. 2004;25:5753-62.

[7] Martson M, Viljanto J, Hurme T, Laippala P, Saukko P. Is cellulose sponge degradable or stable as implantation material? An in vivo subcutaneous study in the rat. Biomaterials. 1999;20:1989-95.

[8] Williams DF. On the mechanisms of biocompatibility. Biomaterials. 2008;29:2941-53.

[9] Siró I, Plackett D. Microfibrillated cellulose and new nanocomposite materials: a review. Cellulose. 2010;17:459-94.

[10] Eichhorn S, Dufresne A, Aranguren M, Marcovich N, Capadona J, Rowan S, Weder C, Thielemans W, Roman M, Renneckar S, Gindl W, Veigel S. Review: current international research into cellulose nanofibres and nanocomposites. J Mater Sci. 2010;45:1-33.

[11] El-Saied H, Basta AH, Gobran RH. Research progress in friendly environmental technology for the production of cellulose products (bacterial cellulose and its application). Polym-Plast Technol. 2004;43:797-820.

[12] Azizi Samir MAS, Alloin F, Dufresne A. Review of Recent Research into Cellulosic Whiskers, Their Properties and Their Application in Nanocomposite Field. Biomacromolecules. 2005;6:612-26.

[13] Zhang J, Zhang J. Advanced Functional Materials Based on Cellulose. Acta Polym Sin. 2010:1376-98.

[14] Abdul Khalil HPS, Bhat AH, Ireana Yusra AF. Green composites from sustainable cellulose nanofibrils: A review. Carbohydr Polym. 2012;87:963-79.

[15] Eichhorn SJ. Cellulose nanowhiskers: promising materials for advanced applications. Soft Matter. 2011;7:303-15.

[16] Klemm D, Schumann D, Udhardt U, Marsch S. Bacterial synthesized cellulose - artificial blood vessels for microsurgery. Prog Polym Sci. 2001;26:1561-603.

[17] Nakayama A, Kakugo A, Gong JP, Osada Y, Takai M, Erata T, Kawano S. High Mechanical Strength Double-Network Hydrogel with Bacterial Cellulose. Adv Funct Mater. 2004;14:1124-8.

[18] Gatenholm P, Klemm D. Bacterial Nanocellulose as a Renewable Material for Biomedical Applications. Mrs Bull. 2010;35:208-13.

[19] Petersen N, Gatenholm P. Bacterial cellulose-based materials and medical devices: current state and perspectives. Appl Microbiol Biotechnol. 2011;91:1277-86.

[20] Czaja WK, Young DJ, Kawecki M, Brown RM, Jr. The future prospects of microbial cellulose in biomedical applications. Biomacromolecules. 2007;8:1-12.

[21] Sannino A, Demitri C, Madaghiele M. Biodegradable Cellulose-based Hydrogels: Design and Applications. Materials. 2009;2:353-73.

[22] Chang C, Zhang L. Cellulose-based hydrogels: Present status and application prospects. Carbohydr Polym. 2011;84:40-53.

[23] Li X, Pan X. Hydrogels Based on Hemicellulose and Lignin from Lignocellulose Biorefinery: A Mini-Review. J Biobased Mater Bio. 2010;4:289-97.

[24] Langer R, Vacanti JP. Tissue Engineering. Science. 1993;260:920-6.

[25] Hutmacher DW. Scaffold design and fabrication technologies for engineering tissues - state of the art and future perspectives. J Biomat Sci-Polym E. 2001;12:107-24.

[26] Dvir T, Timko BP, Kohane DS, Langer R. Nanotechnological strategies for engineering complex tissues. Nature Nanotechnology. 2011;6:13-22.

[27] Luo Y, Engelmayr G, Auguste DT, Ferreira LS, Karp JM, Saigal R, Langer R. Three-Dimensional Scaffolds. In: Lanza R, Langer R, Vacanti JP, editors. Principles of Tissue Engineering. 3rd ed. Amsterdam: Elsevier; 2007. p. 359-73.

[28] Keaveny TM, Morgan EF, Yeh OC. Bone Mechanics. In: Kutz M, editor. Standard Handbook of Biomedical Engineering and Design. New York: Mc-Graw Hill; 2003. p. 8/1-22.

[29] Keaveny TM, Hayes WC. Mechanical Properties of Cortical and Trabecular Bone. In: Hall BK, editor. Bone. Boca Raton: CRC Press; 1992. p. 285-344.

[30] Ratner BD, Hoffman AS, Schoen FJ, Lemons JE. Biomaterials Science: An introduction to materials in medicine. San Diego, CA: Elsevier, Academic Press; 2004. p. 851.

[31] Mano JF, Neves NM, Reis RL. Mechanical characterization of biomaterials. In: Reis RL, Román JS, editors. Biodegradable systems in tissue engineering and regenerative medicine: CRC Press, Boca Raton; ISBN-0-8493-1936-6; 2005. p. 127-44.

[32] Almarza AJ, Athanasiou KA. Design characteristics for the tissue engineering of cartilaginous tissues. Ann Biomed Eng. 2004;32:2-17.

[33] Rho J-Y, Kuhn-Spearing L, Zioupos P. Mechanical properties and the hierarchical structure of bone. Med Eng Phys. 1998;20:92-102.

[34] Oh SH, Ward CL, Atala A, Yoo JJ, Harrison BS. Oxygen generating scaffolds for enhancing engineered tissue survival. Biomaterials. 2009;30:757-62.

[35] Sachlos E, Czernuszka JT. Making Tissue Engineering Scaffolds Work. Review on the Application of Solid Freeform Fabrication Technology to the Production of Tissue Engineering Scaffolds. Eur Cell Mater. 2003;5:29-40.

[36] Hollister SJ, Chu T-MG, Halloran JW, Feinberg SE. Design and Manufacture of Bone Replacement Scaffolds. In: Cowin SC, editor. Bone Mechanics Handboork. Boca Raton: CRC Press; 2001.

[37] Alves NM, Pashkuleva I, Reis RL, Mano JF. Controlling Cell Behavior Through the Design of Polymer Surfaces. Small. 2010;6:2208-20.

[38] Castner DG, Ratner BD. Biomedical surface science: Foundations to frontiers. Surf Sci. 2002;500:28-60.

[39] Falsey JR, Renil M, Park S, Li SJ, Lam KS. Peptide and small molecule microarray for high throughput cell adhesion and functional assays. Bioconjugate Chemistry. 2001;12:346-53.

[40] Lee JH, Lee JW, Khang G, Lee HB. Interaction of cells on chargeable functional group gradient surfaces. Biomaterials. 1997;18:351-8.

[41] Anselme K. Osteoblast adhesion on biomaterials. Biomaterials. 2000;21:667-81.

[42] Lutolf MP, Gilbert PM, Blau HM. Designing materials to direct stem-cell fate. Nature. 2009;462:433-41.

[43] Kingshott P, Andersson G, McArthur SL, Griesser HJ. Surface modification and chemical surface analysis of biomaterials. Curr Opin Chem Biol. 2011;15:667-76.

[44] Lopez-Perez PM, da Silva RMP, Sousa RA, Pashkuleva I, Reis RL. Plasma-induced polymerization as a tool for surface functionalization of polymer scaffolds for bone tissue engineering: An in vitro study. Acta Biomater. 2010;6:3704-12.

[45] Lopez-Perez PM, Marques AP, da Silva RMP, Pashkuleva I, Reis RL. Effect of chitosan membrane surface modification via plasma induced polymerization on the adhesion of osteoblast-like cells. J Mater Chem. 2007;17:4064-71.

[46] Pertile RAN, Andrade FK, Alves C, Gama M. Surface modification of bacterial cellulose by nitrogen-containing plasma for improved interaction with cells. Carbohydr Polym. 2010;82:692-8.

[47] Hench LL. Bioactive materials: The potential for tissue regeneration. J Biomed Mater Res. 1998;41:511-8.

[48] Hench LL, Jones JR, Sepulveda P. Bioactive Materials for Tissue Engineering Scaffolds. In: Polak JM, Hench LL, Kemp P, editors. Future Strategies for Tissue and Organ Replacement. London: Imperial College Press; 2002. p. 3-24.

[49] Alves NM, Leonor IB, Azevedo HS, Reis RL, Mano JF. Designing biomaterials based on biomineralization of bone. J Mater Chem. 2010;20:2911-21.

[50] Barbieri D, Yuan HP, de Groot F, Walsh WR, de Bruijn JD. Influence of different polymeric gels on the ectopic bone forming ability of an osteoinductive biphasic calcium phosphate ceramic. Acta Biomater. 2011;7:2007-14.

[51] Barradas AMC, Yuan H, van Blitterswijk CA, Habibovic P. Osteoinductive biomaterials: current knowledge of properties, experimental models and biological mechanisms. Eur Cell Mater. 2011;21:407-29.

[52] Peschel D, Zhang K, Fischer S, Groth T. Modulation of osteogenic activity of BMP-2 by cellulose and chitosan derivatives. Acta Biomater. 2012;8:183-93.

[53] Gomes S, Leonor IB, Mano JF, Reis RL, Kaplan DL. Natural and genetically engineered proteins for tissue engineering. Prog Polym Sci. 2012;37:1-17.

[54] Santo VE, Gomes ME, Mano JF, Reis RL. From nano- to macro-scale: nanotechnology approaches for spatially controlled delivery of bioactive factors for bone and cartilage engineering. Nanomedicine. 2012;7:1045-66.

[55] Bessa PC, Casal M, Reis RL. Bone morphogenetic proteins in tissue engineering: the road from laboratory to clinic, part II (BMP delivery). J Tissue Eng Regen M. 2008;2:81-96.

[56] Cho TJ, Gerstenfeld LC, Einhorn TA. Differential temporal expression of members of the transforming growth factor beta superfamily during murine fracture healing. J Bone Miner Res. 2002;17:513-20.

[57] Santos MI, Reis RL. Vascularization in Bone Tissue Engineering: Physiology, Current Strategies, Major Hurdles and Future Challenges. Macromol Biosci. 2010;10:12-27.

[58] Muschler GE, Nakamoto C, Griffith LG. Engineering principles of clinical cell-based tissue engineering. J Bone Joint Surg Am. 2004;86A:1541-58.

[59] Landman KA, Cai AQ. Cell proliferation and oxygen diffusion in a vascularising scaffold. B Math Biol. 2007;69:2405-28.

[60] Hofmann A, Ritz U, Verrier S, Eglin D, Alini M, Fuchs S, Kirkpatrick CJ, Rommens PM. The effect of human osteoblasts on proliferation and neo-vessel formation of human umbilical vein endothelial cells in a long-term 3D co-culture on polyurethane scaffolds. Biomaterials. 2008;29:4217-26.

[61] Santos MI, Unger RE, Sousa RA, Reis RL, Kirkpatrick CJ. Crosstalk between osteoblasts and endothelial cells co-cultured on a polycaprolactone-starch scaffold and the in vitro development of vascularization. Biomaterials. 2009;30:4407-15.

[62] Santos MI, Tuzlakoglu K, Fuchs S, Gomes ME, Peters K, Unger RE, Piskin E, Reis RL, Kirkpatrick CJ. Endothelial cell colonization and angiogenic potential of combined nano- and micro-fibrous scaffolds for bone tissue engineering. Biomaterials. 2008;29:4306-13.

[63] Santos MI, Pashkuleva I, Alves CM, Gomes ME, Fuchs S, Unger RE, Reis RL, Kirkpatrick CJ. Surface-modified 3D starch-based scaffold for improved endothelialization for bone tissue engineering. J Mater Chem. 2009;19:4091-101.

[64] Ahmadi R, Burns AJ, de Bruijn JD. Chitosan-based hydrogels do not induce angiogenesis. J Tissue Eng Regen M. 2010;4:309-15.

[65] Rubenstein DA, Venkitachalam SM, Zamfir D, Wang F, Lu HB, Frame MD, Yin W. In Vitro Biocompatibility of Sheath-Core Cellulose-Acetate-Based Electrospun Scaffolds Towards Endothelial Cells and Platelets. J Biomat Sci-Polym E. 2010;21:1713-36.

[66] Franz S, Rammelt S, Scharnweber D, Simon JC. Immune responses to implants - A review of the implications for the design of immunomodulatory biomaterials. Biomaterials. 2011;32:6692-709.

[67] Yim EKF, Darling EM, Kulangara K, Guilak F, Leong KW. Nanotopography-induced changes in focal adhesions, cytoskeletal organization, and mechanical properties of human mesenchymal stem cells. Biomaterials. 2010;31:1299-306.

[68] Fink J, Fuhrmann R, Scharnweber T, Franke RP. Stimulation of monocytes and macrophages: Possible influence of surface roughness. Clin Hemorheol Microcirc. 2008;39:205-12.

[69] Richardson TP, Peters MC, Ennett AB, Mooney DJ. Polymeric system for dual growth factor delivery. Nat Biotechnol. 2001;19:1029-34.

[70] Patil SD, Papadmitrakopoulos F, Burgess DJ. Concurrent delivery of dexamethasone and VEGF for localized inflammation control and angiogenesis. J Control Release. 2007;117:68-79.

[71] Li B, Davidson JM, Guelcher SA. The effect of the local delivery of platelet-derived growth factor from reactive two-component polyurethane scaffolds on the healing in rat skin excisional wounds. Biomaterials. 2009;30:3486-94.

[72] Gibson LJ. Cellular solids. Mrs Bull. 2003;28:270-1.

[73] Silva SP, Sabino MA, Fernandes EM, Correlo VM, Boesel LF, Reis RL. Cork: properties, capabilities and applications. Int Mater Rev. 2005;50:345-65.

[74] Gandini A, Pascoal Neto C, Silvestre AJD. Suberin: A promising renewable resource for novel macromolecular materials. Prog Polym Sci. 2006;31:878-92.

[75] Pinto PCRO, Sousa AF, Silvestre AJD, Neto CP, Gandini A, Eckerman C, Holmbom B. Quercus suber and Betula pendula outer barks as renewable sources of oleochemicals: A comparative study. Ind Crop Prod. 2009;29:126-32.

[76] Garrote G, Domínguez H, Parajó JC. Hydrothermal processing of lignocellulosic materials. Eur J Wood Wood Prod. 1999;57:191-202.

[77] Bledzki AK, Gassan J. Composites reinforced with cellulose based fibres. Prog Polym Sci. 1999;24:221-74.

[78] Adler E. Lignin Chemistry - Past, Present and Future. Wood Sci Technol. 1977;11(3):169-218.

[79] Mohanty AK, Misra M, Hinrichsen G. Biofibres, biodegradable polymers and biocomposites: An overview. Macromol Mater Eng. 2000;276-277:1-24.

[80] Bledzki AK, Letman M, Viksne A, Rence L. A comparison of compounding processes and wood type for wood fibre - PP composites. Composites Part A. 2005;36:789-97.

[81] Klemm D, Schumann D, Kramer F, Hessler N, Koth D, Sultanova B. Nanocellulose Materials - Different Cellulose, Different Functionality. Macromol Res. 2009;280:60-71.

[82] Gabrielii I, Gatenholm P, Glasser WG, Jain RK, Kenne L. Separation, characterization and hydrogel-formation of hemicellulose from aspen wood. Carbohydr Polym. 2000;43:367-74.

[83] Scheller HV, Ulvskov P. Hemicelluloses. In: Merchant SBWROD, editor. Annual Review of Plant Biology, Vol 612010. p. 263-89.

[84] Chen W, Yu H, Liu Y. Preparation of millimeter-long cellulose I nanofibers with diameters of 30-80 nm from bamboo fibers. Carbohydr Polym. 2011;86:453-61.

[85] Stokke DD, Gardner DJ. Fundamental aspects of wood as a component of thermoplastic composites. J Vinyl Addit Techn. 2003;9:96-104.

[86] Mangalam AP, Simonsen J, Benight AS. Cellulose/DNA Hybrid Nanomaterials. Biomacromolecules. 2009;10:497-504.

[87] Siqueira G, Bras J, Dufresne A. Cellulose Whiskers versus Microfibrils: Influence of the Nature of the Nanoparticle and its Surface Functionalization on the Thermal and Mechanical Properties of Nanocomposites. Biomacromolecules. 2009;10:425-32.

[88] Dong XM, Revol JF, Gray DG. Effect of microcrystallite preparation conditions on the formation of colloid crystals of cellulose. Cellulose. 1998;5:19-32.

[89] Beck-Candanedo S, Roman M, Gray DG. Effect of reaction conditions on the properties and behavior of wood cellulose nanocrystal suspensions. Biomacromolecules. 2005;6:1048-54.

[90] Araki J, Wada M, Kuga S, Okano T. Flow properties of microcrystalline cellulose suspension prepared by acid treatment of native cellulose. Colloids and Surfaces A: Physicochemical and Engineering Aspects. 1998;142:75-82.

[91] Bondeson D, Mathew A, Oksman K. Optimization of the isolation of nanocrystals from microcrystalline cellulose by acid hydrolysis. Cellulose. 2006;13:171-80.

[92] Vroman I, Tighzert L. Biodegradable Polymers. Materials. 2009;2:307-44.

[93] Karaaslan MA, Tshabalala MA, Yelle DJ, Buschle-Diller G. Nanoreinforced biocompatible hydrogels from wood hemicelluloses and cellulose whiskers. Carbohydr Polym. 2011;86:192-201.

[94] Cazacu G, Pascu MC, Profire L, Kowarski AI, Mihaes M, Vasile C. Lignin role in a complex polyolefin blend. Ind Crop Prod. 2004;20:261-73.

[95] Raschip IE, Hitruc EG, Vasile C. Semi-interpenetrating polymer networks containing polysaccharides. II. Xanthan/lignin networks: a spectral and thermal characterization. High Perform Polym. 2011;23:219-29.

[96] Kolattukudy PE. Bio-polyester membranes of plants - cutin and suberin. Science. 1980;208:990-1000.

[97] Cheng ZY, Teoh SH. Surface modification of ultra thin poly (epsilon-caprolactone) films using acrylic acid and collagen. Biomaterials. 2004;25:1991-2001.

[98] Gross KA, Ezerietis E. Juniper wood as a possible implant material. J Biomed Mater Res A. 2003;64A:672-83.

[99] Beniash E. Biominerals - hierarchical nanocomposites: the example of bone. Wiley Interdiscip Rev Nanomed Nanobiotechnol. 2011;3:47-69.

[100] Sprio S, Ruffini A, Valentini F, D'Alessandro T, Sandri M, Panseri S, Tampieri A. Biomimesis and biomorphic transformations: New concepts applied to bone regeneration. J Biotechnol. 2011;156:347-55.

[101] Grunert M, Winter WT. Nanocomposites of Cellulose Acetate Butyrate Reinforced with Cellulose Nanocrystals. J Polym Environ. 2002;10:27-30.

[102] Mano JF. The viscoelastic properties of cork. J Mater Sci. 2002;37:257-63.

[103] Fernandes EM, Correlo VM, Chagas JAM, Mano JF, Reis RL. Cork based composites using polyolefin's as matrix: Morphology and mechanical performance. Compos Sci Technol. 2010;70:2310-8.

[104] Fernandes EM, Correlo VM, Chagas JAM, Mano JF, Reis RL. Properties of new cork–polymer composites: Advantages and drawbacks as compared with commercially available fibreboard materials. Compos Struct. 2011;93:3120-9.

[105] Pires RA, Aroso IM, Silva SP, Mano JF, Reis RL. Isolation of friedelin from black condensate of cork. Nat Prod Commun. 2011;6:1577-9.

[106] Li SH, Liu Q, DeWijn J, DeGroot K, Zhou BL. Biomimetic coating of bioactives ceramic on bamboo for biomedical applications. J Mater Sci Lett. 1996;15:1882-5.

[107] Li SH, Liu Q, deWijn JR, Zhou BL, deGroot K. In vitro calcium phosphate formation on a natural composite material, bamboo. Biomaterials. 1997;18:389-95.

[108] Klemm D, Schumann D, Kramer F, Heßler N, Hornung M, Schmauder H-P, Marsch S. Nanocelluloses as Innovative Polymers in Research and Application Polysaccharides II. Advances in Polymer Science; 2006; 205: 49-96.

[109] Millon LE, Wan WK. The polyvinyl alcohol-bacterial cellulose system as a new nanocomposite for biomedical applications. J Biomed Mater Res B. 2006;79B:245-53.

[110] Tahara N, Tabuchi M, Watanabe K, Yano H, Morinaga Y, Yoshinaga F. Degree of polymerization of cellulose from Acetobacter xylinum BPR2001 decreased by cellulase produced by the strain. Biosci Biotechnol Biochem. 1997;61:1862-5.

[111] Miyamoto T, Takahashi S-i, Ito H, Inagaki H, Noishiki Y. Tissue biocompatibility of cellulose and its derivatives. J Biomed Mater Res. 1989;23:125-33.

[112] Svensson A, Nicklasson E, Harrah T, Panilaitis B, Kaplan DL, Brittberg M, Gatenholm P. Bacterial cellulose as a potential scaffold for tissue engineering of cartilage. Biomaterials. 2005;26:419-31.

[113] Yano H, Sugiyama J, Nakagaito AN, Nogi M, Matsuura T, Hikita M, Handa K. Optically Transparent Composites Reinforced with Networks of Bacterial Nanofibers. Adv Mater. 2005;17:153-5.

[114] Wippermann J, Schumann D, Klemm D, Kosmehl H, Salehi-Gelani S, Wahlers T. Preliminary Results of Small Arterial Substitute Performed with a New Cylindrical Biomaterial Composed of Bacterial Cellulose. European Journal of Vascular and Endovascular Surgery. 2009;37:592-6.

[115] Backdahl H, Risberg B, Gatenholm P. Observations on bacterial cellulose tube formation for application as vascular graft. Mater Sci Eng C Mater Biol Appl. 2011;31:14-21.

[116] Helenius G, Backdahl H, Bodin A, Nannmark U, Gatenholm P, Risberg B. In vivo biocompatibility of bacterial cellulose. J Biomed Mater Res A. 2006;76A:431-8.

[117] Bodin A, Concaro S, Brittberg M, Gatenholm P. Bacterial cellulose as a potential meniscus implant. J Tissue Eng Regen M. 2007;1:406-8.

[118] Ciechanska D. Multifunctional bacterial cellulose/chitosan composite materials for medical applications. Fibres Text East Eur. 2004;12:69-72.

[119] Hutmacher DW. Scaffolds in tissue engineering bone and cartilage. Biomaterials. 2000;21:2529-43.

[120] Puppi D, Chiellini F, Piras AM, Chiellini E. Polymeric materials for bone and cartilage repair. Prog Polym Sci. 2010;35:403-40.

[121] Oksman K, Mathew AP, Bondeson D, Kvien I. Manufacturing process of cellulose whiskers/polylactic acid nanocomposites. Compos Sci Technol. 2006;66:2776-84.

[122] Vasita R, Katti DS. Nanofibers and their applications in tissue engineering. Int J Nanomedicine. 2006;1:15-30.

[123] Fang B, Wan Y-Z, Tang T-T, Gao C, Dai K-R. Proliferation and Osteoblastic Differentiation of Human Bone Marrow Stromal Cells on Hydroxyapatite/Bacterial Cellulose Nanocomposite Scaffolds. Tissue Eng Part A. 2009;15:1091-8.

[124] Wan YZ, Huang Y, Yuan CD, Raman S, Zhu Y, Jiang HJ, He F, Gao C. Biomimetic synthesis of hydroxyapatite/bacterial cellulose nanocomposites for biomedical applications. Mat Sci Eng C-Bio S. 2007;27:855-64.

[125] Saska S, Barud HS, Gaspar AMM, Marchetto R, Ribeiro SJL, Messaddeq Y. Bacterial cellulose-hydroxyapatite nanocomposites for bone regeneration. Int J Biomater. 2011;2011:175362.

[126] Mathew AP, Oksman K, Sain M. Mechanical properties of biodegradable composites from poly lactic acid (PLA) and microcrystalline cellulose (MCC). J Appl Polym Sci. 2005;97:2014-25.

[127] de Mesquita JP, Donnici CL, Pereira FV. Biobased Nanocomposites from Layer-by-Layer Assembly of Cellulose Nanowhiskers with Chitosan. Biomacromolecules. 2010;11:473-80.

[128] Wang Y, Chang C, Zhang L. Effects of Freezing/Thawing Cycles and Cellulose Nanowhiskers on Structure and Properties of Biocompatible Starch/PVA Sponges. Macromol Mater Eng. 2010;295:137-45.

[129] Bondeson D, Oksman K. Polylactic acid/cellulose whisker nanocomposites modified by polyvinyl alcohol. Composites Part A. 2007;38:2486-92.

[130] Goffin AL, Raquez JM, Duquesne E, Siqueira G, Habibi Y, Dufresne A, Dubois P. From Interfacial Ring-Opening Polymerization to Melt Processing of Cellulose Nanowhisker-Filled Polylactide-Based Nanocomposites. Biomacromolecules. 2011;12:2456-65.

[131] Dugan JM, Gough JE, Eichhorn SJ. Directing the Morphology and Differentiation of Skeletal Muscle Cells Using Oriented Cellulose Nanowhiskers. Biomacromolecules. 2010;11:2498-504.

[132] Samir M, Alloin F, Sanchez JY, El Kissi N, Dufresne A. Preparation of cellulose whiskers reinforced nanocomposites from an organic medium suspension. Macromolecules. 2004;37:1386-93.

[133] Garcia de Rodriguez NL, Thielemans W, Dufresne A. Sisal cellulose whiskers reinforced polyvinyl acetate nanocomposites. Cellulose. 2006;13:261-70.

[134] Fleming K, Gray D, Prasannan S, Matthews S. Cellulose crystallites: A new and robust liquid crystalline medium for the measurement of residual dipolar couplings. J Am Chem Soc. 2000;122:5224-5.

[135] Osorio-Madrazo A, Eder M, Rueggeberg M, Pandey JK, Harrington MJ, Nishiyama Y, Putaux JL, Rochas C, Burgert I. Reorientation of Cellulose Nanowhiskers in Agarose Hydrogels under Tensile Loading. Biomacromolecules. 2012;13:850-6.

[136] Eichhorn SJ, Young RJ. The Young's modulus of a microcrystalline cellulose. Cellulose. 2001;8:197-207.

[137] Kvien I, Tanem BS, Oksman K. Characterization of Cellulose Whiskers and Their Nanocomposites by Atomic Force and Electron Microscopy. Biomacromolecules. 2005;6:3160-5.

[138] Backdahl H, Helenius G, Bodin A, Nannmark U, Johansson BR, Risberg B, Gatenholm P. Mechanical properties of bacterial cellulose and interactions with smooth muscle cells. Biomaterials. 2006;27:2141-9.

[139] Czaja W, Krystynowicz A, Bielecki S, Brown Jr RM. Microbial cellulose - the natural power to heal wounds. Biomaterials. 2006;27:145-51.

[140] Hutchens SA, Benson RS, Evans BR, O'Neill HM, Rawn CJ. Biomimetic synthesis of calcium-deficient hydroxyapatite in a natural hydrogel. Biomaterials. 2006;27:4661-70.

[141] Wan YZ, Hong L, Jia SR, Huang Y, Zhu Y, Wang YL, Jiang HJ. Synthesis and characterization of hydroxyapatite–bacterial cellulose nanocomposites. Compos Sci Technol. 2006;66:1825-32.

[142] Wan WK, Hutter JL, Millon L, Guhados G. Bacterial cellulose and its nanocomposites for biomedical applications. In: Oksman K, Sain M, editors. Washington, DC: American Chemical Society; Cellulose Nanocomposites: Processing, Characterization, and Properties, 2006. 221-41.

[143] Grande CJ, Torres FG, Gomez CM, Carmen Bano M. Nanocomposites of bacterial cellulose/hydroxyapatite for biomedical applications. Acta Biomater. 2009;5:1605-15.

[144] Zhijiang C, Guang Y. Bacterial cellulose/collagen composite: Characterization and first evaluation of cytocompatibility. J Appl Polym Sci. 2011;120:2938-44.

[145] Lee H, Lin L, Liu H, Tsai C, Yu N. Preparation of PLA/Clay nanocomposites and its application. TW200819499-A: (Univ Vanung); 2008.

[146] Kalambur S, Rizvi SSH. Biodegradable and functionally superior starch-polyester nanocomposites from reactive extrusion. J Appl Polym Sci. 2005;96:1072-82.

[147] Paul M-A, Alexandre M, Degée P, Henrist C, Rulmont A, Dubois P. New nanocomposite materials based on plasticized poly(l-lactide) and organo-modified montmorillonites: thermal and morphological study. Polymer. 2003;44:443-50.

[148] Wambua P, Ivens J, Verpoest I. Natural fibres: can they replace glass in fibre reinforced plastics? Compos Sci Technol. 2003;63:1259-64.

[149] Lee J, Deng Y. Increased mechanical properties of aligned and isotropic electrospun PVA nanofiber webs by cellulose nanowhisker reinforcement. Macromol Res. 2012;20:76-83.

[150] Singh S, Ray SS. Polylactide based nanostructured Biomaterials and their applications. J Nanosci and Nanotechno. 2007;7:2596-615.

[151] Zhang X, Huang J, Chang PR, Li J, Chen Y, Wang D, Yu J, Chen J. Structure and properties of polysaccharide nanocrystal-doped supramolecular hydrogels based on Cyclodextrin inclusion. Polymer. 2010;51:4398-407.

[152] Laranjeira MCM, Fávere VTd. Quitosana: biopolímero funcional com potencial industrial biomédico. Quim Nova. 2009;32:672-8.

[153] Di Martino A, Sittinger M, Risbud MV. Chitosan: A versatile biopolymer for orthopaedic tissue-engineering. Biomaterials. 2005;26:5983-90.

[154] Suh JKF, Matthew HWT. Application of chitosan-based polysaccharide biomaterials in cartilage tissue engineering: a review. Biomaterials. 2000;21:2589-98.

[155] Kong J, Franklin NR, Zhou CW, Chapline MG, Peng S, Cho KJ, Dai HJ. Nanotube molecular wires as chemical sensors. Science. 2000;287:622-5.

[156] Alves NM, Saiz-Arroyo C, Rodriguez-Perez MA, Reis RL, Mano JF. Microhardness of starch based biomaterials in simulated physiological conditions. Acta Biomater. 2007;3:69-76.

[157] Marques AP, Reis RL. Hydroxyapatite reinforcement of different starch-based polymers affects osteoblast-like cells adhesion/spreading and proliferation. Mat Sci Eng C-Bio S. 2005;25:215-29.

[158] Marques AP, Cruz HR, Coutinho OP, Reis RL. Effect of starch-based biomaterials on the in vitro proliferation and viability of osteoblast-like cells. J Mater Sci - Mater Med. 2005;16:833-42.

[159] Leonor IB, Reis RL. An innovative auto-catalytic deposition route to produce calcium-phosphate coatings on polymeric biomaterials. J Mater Sci - Mater Med. 2003;14:435-41.

[160] Gouma P, Xue R, Goldbeck CP, Perrotta P, Balazsi C. Nano-hydroxyapatite-Cellulose acetate composites for growing of bone cells. Mater Sci Eng C Mater Biol Appl. 2012;32:607-12.

[161] Zhang K, Ma Y, Francis LF. Porous polymer/bioactive glass composites for soft-to-hard tissue interfaces. J Biomed Mater Res. 2002;61:551-63.

[162] Rodriguez K, Renneckar S, Gatenholm P. Biomimetic Calcium Phosphate Crystal Mineralization on Electrospun Cellulose-Based Scaffolds. ACS Appl Mater Interfaces. 2011;3:681-9.

[163] Kim EJ, Boehm CA, Fleischman AJ, Muschler GF, Kostov YV, Roy S. Modulating human connective tissue progenitor cell behavior on cellulose acetate scaffolds by surface microtextures. J Biomed Mater Res A. 2009;90A:1198-205.

[164] Ye H, Xia ZD, Ferguson DJP, Triffitt JT, Cui ZF. Studies on the use of hollow fibre membrane bioreactors for tissue generation by using rat bone marrow fibroblastic cells and a composite scaffold. J Mater Sci - Mater Med. 2007;18:641-8.

[165] Boesel LF, Mano JF, Reis RL. Optimization of the formulation and mechanical properties of starch based partially degradable bone cements. J Mater Sci - Mater Med. 2004;15:73-83.

[166] Boesel LF, Fernandes MHV, Reis RL. The behavior of novel hydrophilic composite bone cements in simulated body fluids. J Biomed Mater Res B. 2004;70B:368-77.

[167] Boesel LF, Cachinho SCP, Fernandes MHV, Reis RL. The in vitro bioactivity of two novel hydrophilic, partially degradable bone cements. Acta Biomater. 2007;3:175-82.

[168] Boesel LF, Reis RL. A review on the polymer properties of Hydrophilic, partially Degradable and Bioactive acrylic Cements (HDBC). Prog Polym Sci. 2008;33:180-90.

[169] Marques AP, Reis RL, Hunt JA. The biocompatibility of novel starch-based polymers and composites: in vitro studies. Biomaterials. 2002;23:1471-8.

[170] Jeon JH, Puleo DA. Formulations for Intermittent Release of Parathyroid Hormone (1-34) and Local Enhancement of Osteoblast Activities. Pharm Dev Technol. 2008;13:505-12.

[171] Jeon JH, Piepgrass WT, Lin YL, Thornas MV, Puleo DA. Localized intermittent delivery of simvastatin hydroxyacid stimulates bone formation in rats. J Periodontol. 2008;79:1457-64.
[172] Jeon JH, Thomas MV, Puleo DA. Bioerodible devices for intermittent release of simvastatin acid. Int J Pharm. 2007;340:6-12.
[173] Kitamura M, Nakashima K, Kowashi Y, Fujii T, Shimauchi H, Sasano T, Furuuchi T, Fukuda M, Noguchi T, Shibutani T, Iwayama Y, Takashiba S, Kurihara H, Ninomiya M, Kido JI, Nagata T, Hamachi T, Maeda K, Hara Y, Izumi Y, Hirofuji T, Imai E, Omae M, Watanuki M, Murakami S. Periodontal Tissue Regeneration Using Fibroblast Growth Factor-2: Randomized Controlled Phase II Clinical Trial. Plos One. 2008;3 e2611/1–e2611/11..
[174] Fukuyama T, Sato S, Fukase Y, Ito K. Effects of alpha-DT cement with hydroxypropyl cellulose on bone augmentation within a titanium cap in the rabbit calvarium. Dent Mater J. 2010;29:160-6.
[175] Kitamura M, Ohtsuki C, Iwasaki H, Ogata S, Tanihara M, Miyazaki T. The controlled resorption of porous alpha-tricalcium phosphate using a hydroxypropylcellulose coating. J Mater Sci - Mater Med. 2004;15:1153-8.
[176] Bohner M, Lemaitre J, VanLanduyt P, Zambelli PY, Merkle HP, Gander B. Gentamicin-loaded hydraulic calcium phosphate bone cement as antibiotic delivery system. J Pharm Sci. 1997;86:565-72.
[177] Bohic S, Weiss P, Roger P, Daculsi G. Light scattering experiments on aqueous solutions of selected cellulose ethers: contribution to the study of polymer-mineral interactions in a new injectable biomaterial. J Mater Sci - Mater Med. 2001;12:201-5.
[178] Turczyn R, Weiss P, Lapkowski M, Daculsi G. In situ self hardening bioactive composite for bone and dental surgery. J Biomat Sci-Polym E. 2000;11:217-23.
[179] Schmitt M, Weiss P, Bourges X, del Valle GA, Daculsi G. Crystallization at the polymer/calclum-phosphate interface in a sterilized injectable bone substitute IBS. Biomaterials. 2002;23:2789-94.
[180] Grimandi G, Weiss P, Millot F, Daculsi G. In vitro evaluation of a new injectable calcium phosphate material. J Biomed Mater Res. 1998;39:660-6.
[181] Struillou X, Boutigny H, Badran Z, Fellah BH, Gauthier O, Sourice S, Pilet P, Rouillon T, Layrolle P, Weiss P, Soueidan A. Treatment of periodontal defects in dogs using an injectable composite hydrogel/biphasic calcium phosphate. J Mater Sci - Mater Med. 2011;22:1707-17.
[182] Fatimi A, Axelos MAV, Tassin JF, Weiss P. Rheological characterization of self-hardening hydrogel for tissue engineering applications: Gel point determination and viscoelastic properties. Macromol Res. 2008;266:12-6.

[183] Bourges X, Weiss P, Daculsi G, Legeay G. Synthesis and general properties of silated-hydroxypropyl methylcellulose in prospect of biomedical use. Adv Colloid Interface Sci. 2002;99:215-28.

[184] Vinatier C, Magne D, Weiss P, Trojani C, Rochet N, Carle GF, Vignes-Colombeix C, Chadjichristos C, Galera P, Daculsi G, Guicheux J. A silanized hydroxypropyl methylcellulose hydrogel for the three-dimensional culture of chondrocytes. Biomaterials. 2005;26:6643-51.

[185] Krieger J. New coating increases efficiency of lamps. Chem Eng News. 1990;68:35.

[186] Zakharov NA, Ezhova ZA, Koval EM, Kalinnikov VT, Chalykh AE. Hydroxyapatite-carboxymethyl cellulose nanocomposite biomaterial. Inorg Mater. 2005;41:509-15.

[187] Jiang L, Li Y, Zhang L, Wang X. Preparation and characterization of a novel composite containing carboxymethyl cellulose used for bone repair. Mat Sci Eng C-Bio S. 2009;29:193-8.

[188] Jiang L, Li Y, Zhang L, Liao J. Preparation and properties of a novel bone repair composite: nano-hydroxyapatite/chitosan/carboxymethyl cellulose. J Mater Sci - Mater Med. 2008;19:981-7.

[189] Zimmermann KA, LeBlanc JM, Sheets KT, Fox RW, Gatenholm P. Biomimetic design of a bacterial cellulose/hydroxyapatite nanocomposite for bone healing applications. Mater Sci Eng C Mater Biol Appl. 2011;31:43-9.

[190] Wu HD, Ji DY, Chang WJ, Yang JC, Lee SY. Chitosan-based polyelectrolyte complex scaffolds with antibacterial properties for treating dental bone defects. Mater Sci Eng C Mater Biol Appl. 2012;32:207-14.

[191] Seifert M, Hesse S, Kabrelian V, Klemm D. Controlling the water content of never dried and reswollen bacterial cellulose by the addition of water-soluble polymers to the culture medium. J Polym Sci Pol Chem. 2004;42:463-70.

[192] Yun HS, Kim SE, Hyun YT, Heo SJ, Shin JW. Hierarchically Mesoporous-Macroporous Bioactive Glasses Scaffolds for Bone Tissue Regeneration. J Biomed Mater Res B. 2008;87B:374-80.

[193] Mansur HS, Mansur AAP, Bicallho S. Lignin-hydroxyapatite/tricalcium phosphate biocomposites: SEM/EDX and FTIR characterization. Bioceramics, Vol 172005. p. 745-8.[194] Liuyun J, Yubao L, Chengdong X. A novel composite membrane of chitosan-carboxymethyl cellulose polyelectrolyte complex membrane filled with nano-hydroxyapatite I. Preparation and properties. J Mater Sci - Mater Med. 2009;20:1645-52.

[195] Filpponen I, Kontturi E, Nummelin S, Rosilo H, Kolehmainen E, Ikkala O, Laine J. Generic Method for Modular Surface Modification of Cellulosic Materials in Aqueous Medium by Sequential "click" Reaction and Adsorption. Biomacromolecules. 2012;13(3):736-42.

[196] van den Berg O, Capadona JR, Weder C. Preparation of homogeneous dispersions of tunicate cellulose whiskers in organic solvents. Biomacromolecules. 2007;8:1353-7.

[197] Bondeson D, Oksman K. Dispersion and characteristics of surfactant modified cellulose whiskers nanocomposites. Compos Interfaces. 2007;14:617-30.

[198] Fink H, Ahrenstedt L, Bodin A, Brumer H, Gatenholm P, Krettek A, Risberg B. Bacterial cellulose modified with xyloglucan bearing the adhesion peptide RGD promotes endothelial cell adhesion and metabolism - a promising modification for vascular grafts. J Tissue Eng Regen M. 2011;5:454-63.

[199] Shankar S, Shikha. Laccase Production and Enzymatic Modification of Lignin by a Novel Peniophora sp. Appl Biochem Biotechnol. 2012;166:1082-94.

[200] Gizdavic-Nikolaidis M, Travas-Sejdic J, Bowmaker GA, Cooney RP, Kilmartin PA. Conducting polymers as free radical scavengers. Synth Met. 2004;140:225-32.

[201] de Arellano-López AR, Martínez-Fernández J, González P, Domínguez C, Fernández-Quero V, Singh M. Biomorphic SiC: A New Engineering Ceramic Material. Int J Appl Ceram Technol. 2004;1:56-67.

[202] Tampieri A, Sprio S, Ruffini A, Celotti G, Lesci IG, Roveri N. From wood to bone: multi-step process to convert wood hierarchical structures into biomimetic hydroxyapatite scaffolds for bone tissue engineering. J Mater Chem. 2009;19:4973-80.

[203] Gonzalez P, Serra J, Liste S, Chiussi S, Leon B, Perez-Amor M, Martinez-Fernandez J, de Arellano-Lopez AR, Varela-Feria FM. New biomorphic SiC ceramics coated with bioactive glass for biomedical applications. Biomaterials. 2003;24:4827-32.

[204] Rambo CR, Sieber H. Novel Synthetic Route to Biomorphic Al2O3 Ceramics. Adv Mater. 2005;17:1088-91.

[205] Cao J, Rambo CR, Sieber H. Preparation of porous Al2O3 -Ceramics by biotemplating of wood. J Porous Mat. 2004;11:163-72.

[206] Li Z, Shi T, Guo L. Preparation and morphology of porous SiO2 ceramics derived from fir flour templates. J Serb Chem Soc. 2010;75:385.

[207] Rambo CR, Cao J, Sieber H. Preparation and properties of highly porous, biomorphic YSZ ceramics. Mater Chem Phys. 2004;87:345-52.

[208] Li X, Fan T, Liu Z, Ding J, Guo Q, Zhang D. Synthesis and hierarchical pore structure of biomorphic manganese oxide derived from woods. J Eur Ceram Soc. 2006;26:3657-64.

[209] Lelli M, Foltran I, Foresti E, Martinez-Fernandez J, Torres-Raya C, Varela-Feria FM, Roveri N. Biomorphic Silicon Carbide Coated with an Electrodeposition of Nanostructured Hydroxyapatite/Collagen as Biomimetic Bone Filler and Scaffold. Adv Eng Mater. 2010;12:B348-B55.

[210] Zhu HX, Ding J, Deng CJ, Zhang SW. Low-temperature preparation of biomorphic TiC/C ceramic in molten salt media. In: Yin YS, Wang X, editors. Multi-Functional Materials and Structures Ii, Pts 1 and 22009. p. 1371-4.

[211] Sun BH, Fan TX, Zhang D, Okabe T. The synthesis and microstructure of morph-genetic TiC/C ceramics. Carbon. 2004;42:177-82.

[212] de Carlos A, Borrajo J, Serra J, González P, León B. Behaviour of MG-63 osteoblast-like cells on wood-based biomorphic SiC ceramics coated with bioactive glass. J Mater Sci - Mater Med. 2006;17:523-9.

[213] Gonzalez P, Borrajo JP, Serra J, Chiussi S, Leon B, Martinez-Fernandez J, Varela-Feria FM, de Arellano-Lopez AR, de Carlos A, Munoz FM, Lopez M, Singh M. A new generation of bio-derived ceramic materials for medical applications. J Biomed Mater Res A. 2009;88A:807-13.

[214] Slaughter BV, Khurshid SS, Fisher OZ, Khademhosseini A, Peppas NA. Hydrogels in Regenerative Medicine. Adv Mater. 2009;21:3307-29.

[215] Peppas NA, Hilt JZ, Khademhosseini A, Langer R. Hydrogels in Biology and Medicine: From Molecular Principles to Bionanotechnology. Adv Mater. 2006;18:1345-60.

[216] Allan S H. Hydrogels for biomedical applications. Adv Drug Deliver Rev. 2002;54:3-12.

[217] Eyholzer C, Borges de Couraça A, Duc F, Bourban PE, Tingaut P, Zimmermann T, Månson JAE, Oksman K. Biocomposite Hydrogels with Carboxymethylated, Nanofibrillated Cellulose Powder for Replacement of the Nucleus Pulposus. Biomacromolecules. 2011;12:1419-27.

[218] Elvira C, Abraham GA, Gallardo A, Román JS. Smart biodegradable hydrogels with applications in drug delivery and tissue engineering. In: Reis RL, Román JS, editors. Biodegradable systems in tissue engineering and regenerative medicine: CRC Press, Boca Raton; ISBN-0-8493-1936-6; 2005. p. 493-508.

[219] Malafaya PB, Silva GA, Reis RL. Natural-origin polymers as carriers and scaffolds for biomolecules and cell delivery in tissue engineering applications. Adv Drug Deliver Rev. 2007;59:207-33.

[220] Karaaslan AM, Tshabalala MA, Buschle-Diller G. Wood hemicellulose/chitosan-based semi-interpenetrating network hydrogels: mechanical, swelling and controlled drug release properties. Bioresources. 2010;5:1036-54.

[221] Pourjavadi A, Mahdavinia GR, Zohuriaan-Mehr MJ. Modified chitosan. II. H-ChitoPAN, a novel pH-responsive superabsorbent hydrogel. J Appl Polym Sci. 2003;90:3115-21.

[222] Kuang J, Yuk KY, Huh KM. Polysaccharide-based superporous hydrogels with fast swelling and superabsorbent properties. Carbohydr Polym. 2011;83:284-90.

[223] Zhang LM, Yang C, Yan L. Perspectives on: Strategies to fabricate starch-based hydrogels with potential biomedical applications. Journal of Bioactive and Compatible Polymers. 2005;20:297-314.

[224] Silva-Correia J, Oliveira JM, Caridade SG, Oliveira JT, Sousa RA, Mano JF, Reis RL. Gellan gum-based hydrogels for intervertebral disc tissue-engineering applications. J Tissue Eng Regen M. 2011;5:97-107.

[225] Oliveira JT, Martins L, Picciochi R, Malafaya IB, Sousa RA, Neves NM, Mano JF, Reis RL. Gellan gum: A new biomaterial for cartilage tissue engineering applications. J Biomed Mater Res A. 2010;93A:852-63.

[226] Sannino A, Madaghiele M, Conversano F, Mele G, Maffezzoli A, Netti PA, Ambrosio L, Nicolais L. Cellulose derivative-hyaluronic acid-based microporous hydrogels cross-linked through divinyl sulfone (DVS) to modulate equilibrium sorption capacity and network stability. Biomacromolecules. 2004;5:92-6.

[227] Crescenzi V, Cornelio L, Di Meo C, Nardecchia S, Lamanna R. Novel hydrogels via click chemistry: Synthesis and potential biomedical applications. Biomacromolecules. 2007;8:1844-50.

[228] Bulpitt P, Aeschlimann D. New strategy for chemical modification of hyaluronic acid: Preparation of functionalized derivatives and their use in the formation of novel biocompatible hydrogels. J Biomed Mater Res. 1999;47:152-69.

[229] Augst AD, Kong HJ, Mooney DJ. Alginate hydrogels as biomaterials. Macromol Biosci. 2006;6:623-33.

[230] Fricain JC, Granja PL, Barbosa MA, de Jéso B, Barthe N, Baquey C. Cellulose phosphates as biomaterials. In vivo biocompatibility studies. Biomaterials. 2002;23:971-80.

[231] Granja PL, Barbosa MA, Pouységu L, De Jéso B, Rouais F, Baquey C. Cellulose phosphates as biomaterials. Mineralization of chemically modified regenerated cellulose hydrogels. J Mater Sci. 2001;36:2163-72.

[232] Granja PL, Jéso BD, Bareille R, Rouais F, Baquey C, Barbosa M. Mineralization of regenerated cellulose hydrogels induced by human bone marrow stromal cells. Eur Cell Mater. 2005;10:31-9.

[233] Granja PL, Jéso BD, Bareille R, Rouais F, Baquey C, Barbosa MA. Cellulose phosphates as biomaterials. In vitro biocompatibility studies. React Funct Polym. 2006;66:728-39.

[234] Granja PL, Ribeiro CC, De Jéso B, Baquey C, Barbosa MA. Mineralization of regenerated cellulose hydrogels. J Mater Sci - Mater Med. 2001;12:785-91.

[235] Hutchens SA, Benson RS, Evans BR, O'Neill H. An Exopolysaccharide Nanofiber Composite for Biomedical Applications. Aatcc Rev. 2009;9:40-5.

[236] Ali AE-H, El-Rehim HAA, Kamal H, Hegazy DE-SA. Synthesis of carboxymethyl cellulose based drug carrier hydrogel using ionizing radiation for possible use as site specific delivery system. J Macromol Sci A. 2008;45:628-34.

[237] Sannino A, Pappadà S, Madaghiele M, Maffezzoli A, Ambrosio L, Nicolais L. Crosslinking of cellulose derivatives and hyaluronic acid with water-soluble carbodiimide. Polymer. 2005;46:11206-12.

[238] Sannino A, Madaghiele M, Demitri C, Scalera F, Esposito A, Esposito V, Maffezzoli A. Development and Characterization of Cellulose-Based Hydrogels for Use as Dietary Bulking Agents. J Appl Polym Sci. 2010;115:1438-44.

[239] Sannino A, Esposito A, De Rosa A, Cozzolino A, Ambrosio L, Nicolais L. Biomedical application of a superabsorbent hydrogel for body water elimination in the treatment of edemas. J Biomed Mater Res A. 2003;67A:1016-24.

[240] Zhang Z, Chen L, Deng MX, Bai YY, Chen XS, Jing XB. Biodegradable Thermo- and pH-Responsive Hydrogels for Oral Drug Delivery. J Polym Sci Pol Chem. 2011;49:2941-51.

[241] Vinatier C, Gauthier O, Fatimi A, Merceron C, Masson M, Moreau A, Moreau F, Fellah B, Weiss P, Guicheux J. An Injectable Cellulose-Based Hydrogel for the Transfer of Autologous Nasal Chondrocytes in Articular Cartilage Defects. Biotechnol Bioeng. 2009;102:1259-67.

[242] Fellah BH, Weiss P, Gauthier O, Rouillon T, Pilet P, Daculsi G, Layrolle P. Bone repair using a new injectable self-crosslinkable bone substitute. J Orthop Res. 2006;24:628-35.

[243] Bourgeois B, Laboux O, Obadia L, Gauthier O, Betti E, Aguado E, Daculsi G, Bouler JM. Calcium-deficient apatite: A first in vivo study concerning bone ingrowth. J Biomed Mater Res A. 2003;65A:402-8.

[244] Sa-Lima H, Tuzlakoglu K, Mano JF, Reis RL. Thermoresponsive poly(N-isopropylacrylamide)-g-methylcellulose hydrogel as a three-dimensional extracellular matrix for cartilage-engineered applications. J Biomed Mater Res A. 2011;98A:596-603.

[245] Million LE, Guhados G, Wan W. Anisotropic polyvinyl alcohol-bacterial cellulose nanocomposite for biomedical applications. J Biomed Mater Res B. 2008;86B:444-52.

[246] Mohammadi H. Nanocomposite biomaterial mimicking aortic heart valve leaflet mechanical behaviour. Proc Inst Mech Eng H J Eng Med. 2011;225:718-22.

[247] Wang J, Gao C, Zhang Y, Wan Y. Preparation and in vitro characterization of BC/PVA hydrogel composite for its potential use as artificial cornea biomaterial. Mater Sci Eng C Mater Biol Appl. 2010;30:214-8.

[248] Shi Z, Zang S, Jiang F, Huang L, Lu D, Ma Y, Yang G. In situ nano-assembly of bacterial cellulose-polyaniline composites. Rsc Advances. 2012;2:1040-6.

[249] Krawczyk H, Jonsson AS. Separation of dispersed substances and galactoglucomannan in thermomechanical pulp process water by microfiltration. Sep Purif Technol. 2011;79:43-9.

[250] Roos AA, Edlund U, Sjöberg J, Albertsson A-C, Stålbrand H. Protein Release from Galactoglucomannan Hydrogels: Influence of Substitutions and Enzymatic Hydrolysis by β-Mannanase. Biomacromolecules. 2008;9:2104-10.

[251] Albertsson A-C, Voepel J, Edlund U, Dahlman O, Söderqvist-Lindblad M. Design of Renewable Hydrogel Release Systems from Fiberboard Mill Wastewater. Biomacromolecules. 2010;11:1406-11.

[252] Yang JY, Zhou XS, Fang J. Synthesis and characterization of temperature sensitive hemicellulose-based hydrogels. Carbohydr Polym. 2011;86:1113-7.

[253] Raschip IE, Vasile C, Ciolacu D, Cazacu G. Semi-interpenetrating polymer networks containing polysaccharides. I xanthan/lignin networks. High Perform Polym. 2007;19:603-20.

[254] Nishida M, Uraki Y, Sano Y. Lignin gel with unique swelling property. Bioresour Technol. 2003;88:81-3.

[255] Feng QH, Chen FG, Wu HR. Preparation and Characterization of a Temperature-Sensitive Lignin-Based Hydrogel. Bioresources. 2011;6:4942-52.

[256] Tian H, Tang Z, Zhuang X, Chen X, Jing X. Biodegradable synthetic polymers: Preparation, functionalization and biomedical application. Prog Polym Sci. 2012;37:237-80.

[257] Guido K. Concepts for the incorporation of inorganic building blocks into organic polymers on a nanoscale. Prog Polym Sci. 2003;28:83-114.

[258] Ambrosio L, Demitri C, Sannino A. Superabsorbent cellulose-based hydrogels for biomedical applications. In: Steve R, editor. Biomedical hydrogels: Biochemistry, manufacture and medical applications: Cambridge, UK: Woodhead Publishing Limited; 2011. 25–46.

[259] Trojani C, Weiss P, Michiels JF, Vinatier C, Guicheux J, Daculsi G, Gaudray P, Carle GF, Rochet N. Three-dimensional culture and differentiation of human osteogenic cells in an injectable hydroxypropylmethylcellulose hydrogel. Biomaterials. 2005;26:5509-17.

[260] Kafienah W, Jakob M, Demarteau O, Frazer A, Barker MD, Martin I, Hollander AP. Three-dimensional tissue engineering of hyaline cartilage: Comparison of adult nasal and articular chondrocytes. Tissue Eng. 2002;8:817–26.

[261] Granja PL, Pouységu L, Deffieux D, Daudé G, De Jéso B, Labrug`ere C, Baquey C, Barbosa MA. Cellulose Phosphates as Biomaterials. II. Surface Chemical Modification of Regenerated Cellulose Hydrogels. J Appl Polym Sci. 2001;82:3354-65.

[262] Barbosa MA, Granja PL, Barrias CC, Amaral IF. Polysaccharides as scaffolds for bone regeneration. ITBM-RBM. 2005;26:212-7.

[263] Klouda L, Mikos AG. Thermoresponsive hydrogels in biomedical applications. Eur J Pharm Biopharm. 2008;68:34-45.

[264] Schönfelder U, Abel M, Wiegand C, Klemm D, Elsner P, Hipler U-C. Influence of selected wound dressings on PMN elastase in chronic wound fluid and their antioxidative potential in vitro. Biomaterials. 2005;26:6664-73.

[265] Nair LS, Laurencin CT. Biodegradable polymers as biomaterials. Prog Polym Sci. 2007;32:762-98.

[266] Lázaro Martínez JL, García Morales E, Aragón Sánchez FJ, Y. QM. Randomized comparative trial of a collagen/oxidided regenerated cellulose dressing in the treatment of the neuropathic diabetic foot ulcer Cir Esp. 2007;82:27-31.

[267] Batista EL, Novaes AB, Simonpietri JJ, Batista FC. Use of bovine-derived anorganic bone associated with guided tissue regeneration in intrabony defects. Six-month evaluation at re-entry. J Periodontol. 1999;70:1000-7.

[268] Simonpietri-C JJ, Novaes AB, Batista EL, Feres EJ. Guided tissue regeneration associated with bovine-derived anorganic bone in mandibular Class II furcation defects. 6-month results at re-entry. J Periodontol. 2000;71:904-11.

[269] Carrie S, Barbara B-J. Wound Care: A collaborative pratice manual for health professionals: Lippincott Williams & Wilkins; 2007.

[270] Ambrosio L, Nicolais L, Sannino A. Forming superabsorbent polymer hydrogel in biomedical devices involves cross-linking aqueous solution of carboxymethylcellulose salt precursor with citric acid

as cross-linking agent in presence of molecular spacer, washing and drying steps. WO2009022358-A1: (Ambrosio L; Nicolais L; Sannino A); 2009.

[271] Millon L, Wan W. Producing nanocomposite hydrogel comprises forming solution containing solvent, hydrogel-forming material and cellulose, crosslinking the material to give nanocomposite hydrogel and applying tensile force, and thermal cycling the hydrogel. US2009252800-A1: (Wan W; Millon L; Axcelon Biopolymers Corp); 2009.

[272] Guillot F, Domard A, Guillot FLH. A composition for wound dressings consists of a hydrogel of chitosan and is used alone or on a cellulose based adhesive support. WO2003068281-A1: (Octaris SA); 2003.

[273]http://www.ashland.com/Ashland/Static/Documents/ASI/PC_11607_Pharmaceutical_Applications.pdf. Accessed January 2013

[274]http://www.medline.com/wound-skin-care/xcell/lit/xcell%20N109.002-Press%20Ulcer%20Eval.pdf Accessed January 2013

[275] Jonas R, Farah LF. Production and application of microbial cellulose. Polym Degrad Stab. 1998;59:101-6.

[276] Millon LE, Oates CJ, Wan W. Compression Properties of Polyvinyl Alcohol - Bacterial Cellulose Nanocomposite. J Biomed Mater Res B. 2009;90B:922-9.

[277] Fernandes EM, Aroso I, Pires RA, Correlo VM, Pitkänen P, Koskimies S, Mano JF, Reis RL. Improvement on the mechanical properties of cork composites using suberin as coupling agent through a reactive extrusion process. ANTEC Conference Proceedings, Boston, 1, 2011, 611-5.

[278] Siepmann J, Peppas NA. Modeling of drug release from delivery systems based on hydroxypropyl methylcellulose (HPMC). Adv Drug Deliver Rev. 2001;48:139-57.

SECTION II – EXPERIMENTAL SECTION

Chapter 2.

Materials and methods

Materials and methods

The main focus of this chapter is to describe in more detail the materials used, the experimental techniques and the characterization methodologies employed that allowed to obtained results presented in this thesis. Along with Chapter I and to the introductions of each chapter, it aims to be a guideline of the rationale for this research, namely on the aspects related with the selection of the materials, on the processing routes used, and characterization methodologies adopted.

2.1 Materials

2.1.1 Cork and cork by-products

Cork oak produces three qualities of suberose tissue: "virgin cork", "secundaria" and "reproduction cork", corresponding to the first, second and subsequent debarks [1]. The first cork is used only for agglomerates, the second can be used to extract stoppers but with high production of disposals, the third and subsequent extractions produce regular cork tissue which is proper for stopper fabrication [2-4]. Industrial transformation of cork generates up to 25 wt.% of cork dust as by-product [2]. Figure 2.1, shows the four classes of cork-by products used in this thesis. It was used "amadia" cork in the powder and granulated cork. Moreover, different cork by-products obtained from the industrial cork process were also studied and the principal characteristics are provide below.

Figure 2.1. Cork oak tree and visual aspect of the different cork by-products resulting from the industrial process.

- **Cork**

The materials used in the thesis were cork granules, with an average particle size 0.5-1 mm and specific weight of 166 ± 21 kg.m^{-3}, moisture content of ~7.5 % and a cork powder, with an average particle size < 500 µm, a specific weight of 157 ± 2 kg.m^{-3} and moisture content of ~5.4% were both supplied by Amorim Revestimentos S.A. (S. Paio Oleiros, Portugal).

- **Cork by-products**

It was collected different cork powders obtained from the industrial cork process as a by-products being the qualities designed by grinding powder, sanding/external powder, Corkstyle® powder and floating powder provide from Amorim Revestimentos, S.A. (Portugal). These powders are present in Figure 2.1 and a small description of the principal characteristics is providing below. Since the sanding powder and the external powder are very similar, a mixture of the referred powders was used in the present thesis.

Grinding powder was the one with higher specific weight. This powder is characterized by presenting a dark brown colour due to the fact that it consists mainly of the outer bark, denser and very similar to wood. Moreover, this powder presents contaminations with silica from the sandpaper, resins, varnish and paint pigments due to the incorporation of materials for recycling. This waste was also the one with the highest moisture content.

Sanding/external powder is the powder with lowest specific weight and lower range of particle size. This kind of powder is mainly composed of cork particles of good quality and low density that can be obtained from the cork stopper waste. It may also present some contaminations with resins from the agglomeration glues and glue from the decorative process and some silica from the sandpaper but in very low amounts.

Corkstyle® powder is composed of high density fibreboard (HDF) formed during the machining process of the dock and cork, with a greater amount of HDF powder. The density is very similar compared with the floating powder.

Floating powder consists of cork and HDF particles. Polyvinyl chloride (PVC) particles are also presents in small amounts. Some varnish, paint pigments, resin and sinter bonding motifs may be present.

2.1.2 Natural fibre boards

Commercial well established underlayment materials used in this work such as, medium density fibreboard (MDF) and high density fibreboard (HDF) with 6 mm of thickness from Sonae Industria, were used as control to compare the advantages and disadvantages with the developed cork-polymer (50-50) wt.% composites.

MDF (brown) and HDF (green) is a dry-formed panel product manufactured from lignocellulosic fibres combined with a synthetic resin such as urea formaldehyde resin (UF), phenol formaldehyde resin (PF) or isocyanate binder under heat and pressure in the presence of moisture [5]. Formaldehyde is an organic compound and is part of the aldehyde family and is part of the volatile organic compound (VOC) family. The main source of formaldehyde inside of buildings is in wood agglomerates, used frequently as a construction material and in furniture. All these agglomerates containing formaldehyde are subject to European standards (EN 120, EN 312-1, EN 662-1) which aim to regulate and control the maximum concentration of formaldehyde.

2.1.3 Natural fibres

Biofibres offer several advantages over the traditional ones, the most important are low density and low cost, good specific strength properties, nonabrasive during processing, CO_2 neutral when burned and biodegradability [6-8]. The most efficient natural fibres have been considered those that have high cellulose content coupled with a low microfibrile angle, resulting in high mechanical properties of the fibre [8]. Depending of the natural origin there are six basic types of natural fibers. They are classified as follows: bast fibers (jute, flax, hemp, ramie and kenaf), leaf fibers (abaca, sisal and pineapple), seed fibers (coir, cotton and kapok), core fibers (kenaf, hemp and jute), grass and reed fibers (wheat, corn and rice) and all other types (wood and roots) [9].

In this thesis it was used coconut fibre (coir) from fruit and sisal from leaf origin. Moreover, it was also test short wood fibre and the results are reported in the appendix section, regarding the patent of the reinforce cork-polymer composites with natural fibres.

2.1.3.1 Sisal fibre

Sisal is a hard fibre is obtained from the leaves of an annually harvested plant, called *Agave sisalana* and is commercially produced in Brazil and East Africa [9, 10]. Chemically sisal is mainly composed by 65 wt.% of cellulose, 12 wt.% of hemicellulose, 9.9 wt.% of lignin and 2 wt.% of waxes [9]. Sisal fibre is one of the most widely used natural fibres and accounts for almost half the total production of natural fibres [11]. The hydroxyl groups which occur throughout the structure of natural fibres make them hydrophilic, but many polymer matrices are hydrophobic so that natural fibre-polymer composites have poor interfaces. Moreover, the hydrophilic sisal fibres absorb a large amount of water in the composite leading to failure by delamination. Adequate adhesion across the interface can be achieved at desirable levels by better wetting and chemical bonding between fibre and matrix [7, 10, 11]. To improve fibre-matrix adhesion chemical treatment of sisal fibre was employed and will be further indicated. The sisal fibre used in the thesis was from Madagascar, presents a diameter of 183 ± 35 μm and moisture content of ~11.3 %. The samples were randomly and gently isolated from the fibre bundles. All isolated fibres were re-conditioned at 20-22°C and 60% relative humidity before use.

2.1.3.2 Coconut fibre

Coir is a hard fiber found between the hard inner shell and the outer coat of coconuts, which grow extensively in tropic and subtropic regions of the world [7]. Chemically coir is mainly composed by 32 to 43 wt.% of cellulose, 0.15 to 0.25 wt.% of hemicellulose and 40 to 45 wt.% of lignin [9]. Coir is a cheap fiber, even cheaper than sisal [11, 12]. Coir as natural reinforcing in polymeric matrices presents inferior performance due to several factors such as its low cellulose content, high lignin content, high microfibrillar angle and large variable diameter [11]. There are two types of coir, a white fiber derived from harvesting coconuts before they are ripe, and a coarser brown fiber derived from harvesting coconuts after they have ripened. Between the two, coir fiber production worldwide is calculated to be roughly 250,000 tons. While the fiber is considered a poor reinforcing fibre because of its low strength and modulus, it has found interest due to its low density, low thermal conductivity and high elongation [7]. The brown coconut fibre used in the work was from Hayleys Exports PLC (Kotugoda, Srí Lanka) presented a diameter of 277.4 ± 38.8 μm, a humidity of 8.2 % and specific weight of 845.1 ± 46.6 Kg m^{-3}, was collected at Amorim Isolamentos S.A. (Vendas Novas, Portugal). The samples were randomly and gently isolated from the fibre bundles. All isolated fibres were re-conditioned at 20-22°C and 60%

relative humidity before use. No pre cleaning treatment was used to the fibres (e.g. soaked in distilled water for a period of time under a normal indoor environment).

2.1.4 Polyolefins

Polyolefins like polyethylene (PE) and polypropylene (PP) are two of the most commonly used polymers with wide range of applications. They are normally defined as polymers based on alkene-1 monomers or α-olefins, and are the most widely used group of thermoplastic polymers today. Based on their monomeric units and their chain structures, they can be divided into the following subgroups [13]:

Ethylene-based materials – polyethylenes (PEs) – produced under low pressure conditions with transition metal catalysts of various types and showing a predominantly linear chain structure. This subgroup includes high density PE (HDPE), medium density PE (MDPE), linear-low density PE (LLDPE) and other varieties, which are distinguished through the regulation of density and subsequently mechanical properties through the incorporation of higher α-olefins (mostly butene, hexene and octene) as comonomers.

Another subgroup is the propylene-based polymers produced with transition-metal catalysts - polypropylene (PP) and its copolymers - showing a linear chain structure with stereospecific arrangement of the propylene units. A wide variation of material properties can be achieved with the incorporation of ethylene and/or higher α-olefins in various fashions; single-phase and multiphase materials are possible.Table 2.1 presents the repeat structure and principal properties of both selected polyolefins used in the thesis.

Table 2.1. Structure and properties of commercial polyolefins used as matrix (Adapted from [14]).

Polymer matrix	T_m (°C)	T.M (MPa)	T.S. (MPa)	F.M. (MPa)	Density (g/cm³)	Chemical structure
High Density Polyethylene (HDPE)	130 - 137	800 - 1400	10 - 30	700 - 1700	0.941 – 0.967	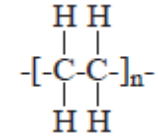
Polypropylene (PP)	164	1380	35.5	1690	0.903	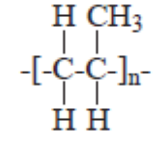

T_m: Melting point: T_g: glass transition temperature T.S.: Tensile strength; T.M.: Tensile Modulus; F.M. Flexural modulus.

Polyolefins are one of the preferred choices among the commercial polymers because of their excellent combination of chemical and physical properties along with the low cost, superior processability and good recyclability [15].

2.1.4.1 High-densitt polyethylene (HDPE)

Polyethylene (PE) is conventionally synthesized by following either low-pressure or high-pressure polymerization, the products of which differ markedly in properties. Polymerization at high pressure leads to branched chains and the polymer has a low density 0.915 – 0.935 $g.cm^{-3}$ with cristallinity between 40% and 50%. On the other hand, when ethylene is polymerized at low pressure, the chain branching is eliminated. The resulting material has a crystallinity of 60% - 80% and a density of 0.95 – 0.965 $g.cm^{-3}$ [16]. The density and modulus of polyethylene increase with crystallinity. The repeat structure of PE is written as $(– CH_2CH_2 –)_n$, and is shown in Table 2.1. Properties of PE depend on: molecular weight, molecular weight distribution, as well as on the degree and type of branching [17]. Polyethylene, like, polypropylene, has many good properties, which make it a material of choice for a number of applications and owing to this reason, the composites of polyethylene are continuously studied to expand the number of applications. High-density polyethylene (HDPE) exhibits good thermal stability, water vapour barrier (nonpolar), low glass transition temperature and high crystallinity, which make it suitable for instance in packaging frozen foods. Moreover is not is not attacked by most acids, bases, or solvents [16]. Since HDPE is relatively inert it is difficult to achieve good interfacial adhesion in composites. Often maleic anhydride grafted polyethylene is added to HDPE to improve interfacial adhesion to the reinforcing fibres [18]. In this thesis, it was used a high density polyethylene (HMA – 025), HDPE, with a MFI of 8.2 g.10min-1 (190 °C, 2.16 kg), supplied by ExxonMobil™ (Germany). The melt flow index was carried out according to ISO 1133 [19].

2.1.4.2 Polypropylene (PP)

Polypropylene is a linear hydrocarbon and the presence of a methyl group attached to alternate carbon atoms on the chain backbone can alter the properties of PP (see Table 2.1) as compared with the PE in different ways. The first effect leads to an increase in the crystalline melting point. Some aspects of chemical behaviour are also affected by the methyl group, for instance the ternary carbon atom provides a site for oxidation causing PP to be less stable than PE to the influence of oxygen. The most significant influence of the methyl group is its generation of different tacticity in the products, ranging

from the completely isotactic and syndiotactic structures to atactic molecules. The properties of the polymer depend on the size and type of crystal structure formed, which in turn is dependent on the size and type of crystal growth. The ratio of these two rates can be controlled by varying the rate of cooling and by incorporation of nucleating agents. In general, the smaller the crystal structures, the greater the transparency and flex resistance and lesser rigidity and heat resistance. PP has a number of advantages, such as low density (0.90 $g.cm^{-3}$) and low cost. It has a higher softening point and hence a maximum service temperature and dimensional stability [16]. Moreover and since polypropylene is nonpolar, it absorbs very little water. Due to its *Tg* below room temperature, it exhibits good impact strength [18]. In this thesis, it was selected a polypropylene homopolymer (1374 E2), PP, with a MFI of 20.8 $g.10min^{-1}$ (200 °C, 2.16 kg), supplied by Exxon Mobil (Germany). The melt flow index was carried out according to ISO 1133 [19].

2.1.4.3 Recycled polymer

Recycled and waste thermoplastics are some of the major components of global municipal solid waste (MSW) and they present a promising raw material source for lignocellulosic composites, especially because of the large volume and low cost of these materials [20]. High density polyethylene (HDPE), low density polyethylene (LDPE/LLDPE), polypropylene (PP), Polyethylene terephthalate (PET), polystyrene (PS) and polyvinyl chloride (PVC) are the primary constituents of plastics in MSW. Reutilizing the post-consumed polymeric materials reduces the environmental impact and the consumption of virgin plastics [21]. In this thesis, a mixture of recycled polyolefins in the grinding form with a MFI of 2.4 $g.10min^{-1}$ (190 °C, 2.16 kg), provided by Pallmann Maschinenfabrik GmbH & Co., Germany was used for the preparation of cork-polymer composites.

2.1.5 Bio-based aliphatic polyesters

Thermoplastics are having more environmental impact than thermosets because of its recyclability. Contributing to develop higher sustainable materials, bio-based products obtained from renewable resources maintain carbon dioxide neutrally [12]. Figure 2.2 shows the classification of the biodegradable polymers dived in four families and used in this work, adapted from Averous L. and Boquillon N. [22]. The family 1 to 3 are obtained from renewable resources. The first family is agro-polymers (e.g. polysaccharides such as starch and cellulose) obtained from biomass by fraction.

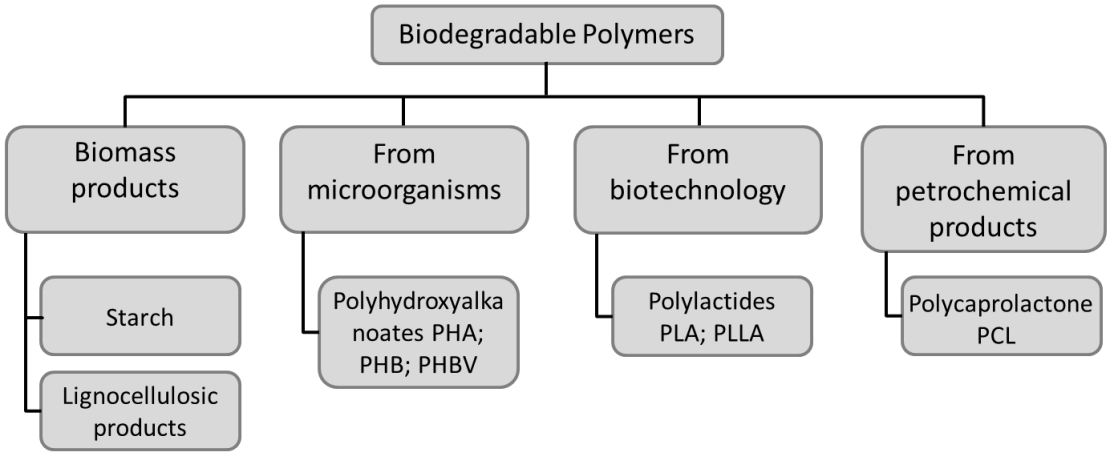

Figure 2.2. Classification of biodegradable polymers and their nomenclature (adapted from Averous L and Boquillon N. [22]).

The second and third families are polyesters, obtained respectively by fermentation from biomass or from genetically modified plants (e.g. polyhydroxyalkanoate, PHA) and by synthesis from monomers obtain from biomass (e.g. polylactic acid, PLA). The fourth family are polyesters, totally synthesized by the petrochemical process (e.g. polycaprolactone, PCL) [22, 23]. The selected bio-based matrices, physical properties and its chemical structure are presented in the Table 2.2:

Table 2.2. Physical, thermal properties and chemical structure of the bio-based polymers. Adopted from references [8, 24, 25].

Polymer matrix	T_m (°C)	T_g (°C)	T.M (MPa)	T.S. (MPa)	Elongation (%)	Density (g/cm³)	Chemical structure
Poly(lactic acid)	177-180	45	2800	45	3	1.21	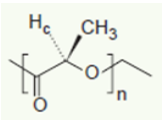
Polyhydroxybutyrate	168	5	4000	40	6	1.18	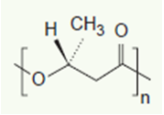
Poly(ε-caprolactone)	60	-60	386	4	300	1.15	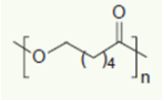

T_m: Melting point: T_g: glass transition temperature T.S.: Tensile strength; T.M.: Tensile Modulus.

2.1.5.1 Poly(lactic acid) (PLA)

Poly(lactic acid) (PLA), one of the promising biopolymers, is a linear aliphatic thermoplastic polyester, which can be synthesized using renewable agricultural resources, such as sugar feedstock and corn [6, 26]. They are composed of chains of lactic acid that are produced by converting starch into sugar which is then fermented. By removal of water lactide is formed which is then converted into PLA resins through solvent-free polymerization [6]. PLA have been the focus of attention because they are produced from renewable resources, they are biodegradable and compostable, and they have very low or no toxicity and high mechanical performance, comparable to those of commercial polymers [27]. However, the thermal stability of PLAs is generally not sufficiently high enough for them to be used as an alternative in many commercial polymers applications. PLA crystallinity, crystallization rate, transparency and degradation rate of finished products can be regulated by the copolymerization of the selected L- to D-isomer ratios of lactic acid [24]. For instance, the PLA homopolymer such as such as poly(L-lactic acid) (PLLA) is a hard, transparent and crystalline polymer having a melting point around 170 °C and a glass transition around 55 °C [25]. PLLA attracts much attention as matrix in biocomposites because of its easier processing and ecologically friendly nature [28]. Companies like Cargill Dow are confident that PLA polymers will compete on a cost-performance basis with certain polymers, like polyethylene, polypropylene and polyester [6]. The PLA used in this thesis was a PLLA with a L-lactide content of 99.6 % and a M_w of 69 000 g.mol^{-1}, and was obtained from Cargill Dow LLC.

2.1.5.2 Polyhydroxybutyrate (PHB)

Polyhydroxyallanoates (PHAs) are produced directly from renewable resources by microbes [22, 24]. Polyhydroxybutyrate (PHB) is a biotechnologically produced polyester that constitutes a carbon reserve in a wide variety of bacteria and has attracted much attention as a biodegradable thermoplastic polyester [23]. It can be degraded to water and carbon dioxide under environmental conditions through natural microbiological mineralization and has much potential for applications of environmental degradable plastics [25, 29]. The PHB presents some disadvantages compared with conventional plastics, such as, brittleness and a narrow processability window. To improve these properties it was developed the copolymer poly(3-hydroxybutyrate-co-3-hydroxyvalerate) (PHBV) that is highly crystalline with melting point and glass transition temperature similar to polypropylene [6].

The PHBV used in this thesis, presents 12% HV content and molecular weight (M_w) of approximately 425 692 g.mol^{-1} was provided by PHB Industrial, Serrana, Brazil.

2.1.5.3 Polyhy-ε-caprolactone (PCL)

Poly(ε-caprolactone) (PCL) is a petroleum-based linear polymer recognized as one of the few synthetic polymers that are completely biodegradable [24, 26]. PCL, is a partially crystalline linear polyester with a low glass transition temperature of -60 °C and a low melting temperature of 60 °C. PCL is a tough and a semi-rigid material at room temperature having a modulus between those of low-density and high-density polyethylene [6]. Moreover, PCL has good water, oil, solvent, and chlorine resistance, low viscosity, and is easily processed thermally [24]. It has been shown that PCL is degraded by enzymes, lipases, secreted from microorganisms [6].

The PCL used in this thesis was a PCL resin (commercially available as TONE® 787), with M_w of 125 000 $g.mol^{-1}$, was obtained from Union Carbide Chemicals and Plastics Division, New Jersey, USA.

2.1.5.4 Starch polyhy-ε-caprolactone (SPCL)

Starch is an expensive, annually renewable material from corn and other crops [24]. Starch converted to thermoplastic material (starch plastics) offers an interesting alternative for synthetic polymers where long-term durability is not needed and fast degradation is an advantage [6]. Starches exhibits poor melt processability, are highly water soluble, difficult to process, brittle, and hence need a plasticizer to make them suitable for engineering applications. Plasticizers such as water or glycols make starches flow and suitable for thermoplastic processing [25]. Under the Mater-Bi trademark, Novamont of Italy today produces four classes of biodegradable materials, all containing starch and differing in synthetic components [6]. In this sense, blending starch with synthetic biodegradable constituents such as PCL may also reduce the production cost [24]. The SPCL used in this thesis was a blend of corn starch with PCL 30/70 wt.% (SPCL) was supplied by Novamont, Italy. It contained about 63 wt.% of PCL, 27 wt.% of corn starch and 10 wt.% of natural plasticizers. The Mw of PCL present in this blend is about 118 000 $g.mol^{-1}$.

2.1.6 Chemical treatments

2.1.6.1 Coupling agents

Lignocellulosic composites using polyolefins (i.e. polyethylene and polypropylene) have gained increasing interest over the past two decades, both in the scientific community and in industry [30]. The main drawback with the use of natural based components such as natural fibres in polyolefin

composites is their hydrophilicity due to the high surface hydroxyl groups concentration which leads to poor interface and moisture resistance in composite materials [11]. The fibre–matrix interaction can be improved either via the fibre, usually by modifying its surface, or via the matrix, usually by employing additives called coupling agents [30]. Coupling is a common method of chemical modification. A coupling agent contains chemical groups which react with the fibre surface and the polymer matrix [7]. In such case, the interfacial bonding between the two components results in enhanced mechanical properties. Maleated polyolefins are the most widely used coupling agents [9, 31, 32]. They contain two functional domains: one a polyolefin typically high density polyethylene or polypropylene, which is able to form entanglements with the polymer matrix, and the second group, maleic anhydride, which is able to strongly interact with the fibre at extrusion temperatures, covalently (apparently), via hydrogen, or ionic bonds [32]. A schematic representation of the reaction between the lignocellulosic material surface and the coupling agent is provided in the Figure 2.3.

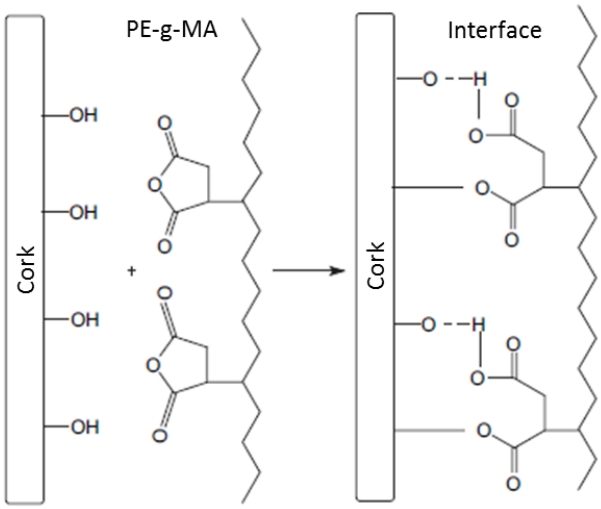

Figure 2.3. Representation of the interface reaction between the cork surface and the PE-g-MA (Adapted from Araújo J.R. *et al.* [33]).

Before compound, special care should be taken into account that maleated polyolefins since they can slowly react with air moisture during storage, and form free acid. As a result, chemical reactivity of the coupling agents decreases. Hence, it should be keep the maleated polyolefins dry, or heat them up before usage in order to regenerate the anhydride chemical structure [32]. In the composite formulation containing natural reinforcements or fillers, the maleated polyolefins are usually used at 1-5% by weight [32-35]. In the wood plastic composites the maleated coupling agent is the most expensive component

representing 4-20% of the total cost of the materials in the formulation, while the plastic represents 60-80% of the formulation [32].

In the work presented in this thesis, two different coupling agents based on maleic anhydride from ExxonMobil, Germany were used, to improve the interfacial bonding between cork and matrix and improved the mechanical properties of cork composites. The first coupling agent a HDPE functionalized with maleic anhydride (PE-g-MA), containing 0.5 to1.0 wt% of maleic anhydride, was Exxelor PE 1040, with MFI of 1.4 g.10min^{-1} (190 °C, 2.16 kg), and a melting point of 131.3 °C. The second one a PP grafted with maleic anhydride (PP-g-MA), containing 0.5 to 1.0 wt% of maleic anhydride (Exxelor PO 1020), with MFI of 110 g.10min^{-1} (190 °C, 1.2 kg), and a melting point of 156 °C.

2.1.6.2 Extraction of suberin and lignin

Suberin and lignin are the main chemical constituents from cork [2, 3]. Suberin is a natural biopolymer typically found in the cell walls of plants [36]. The structure of suberin in cork is not yet fully understood. It has been proposed that suberin consists of a polyester structure composed of long chain fatty acids, hydroxy fatty and phenolic acids, linked by ester groups [2, 37, 38]. Lignin is totally amorphous and hydrophobic in nature. It is the compound that gives rigidity to the plants. The main difficulty in lignin chemistry is that no method has been established by which it is possible to isolate lignin in its native state from the fibre [23].

The extraction of suberin and lignin from the cork powder was as follows: Extractive free cork powder was obtained after three consecutive 6 h soxhlet extractions with dichloromethane, ethanol and water. The resulting material was used to obtain the suberin and lignin fractions. Suberin extraction procedure was adapted from Ekman R et al. [39] and Pinto PCRO et al. [40]. The product (1g to 13ml) was refluxed in Ethanol:Water (25:1) containing 0.5M sodium hydroxide for a period of 6 h. After cooling, the resulting mixture was filtered and the liquid fraction was acidified to pH 5-6 with hydrochloric acid. After filtration, the solvent was removed in a vacuum evaporator. The resulting solid residue was suspended in water and extracted with 3 times the volume in chloroform. The organic fraction was recovered and the solvent removed in a vacuum evaporator, resulting in a brownish paste-like material.

The methodology for lignin extraction was adapted from Ekman et al. [39] and Browning BL [41]. The solid residue resulting from the suberin extraction was thoroughly washed with distilled water until neutral pH. 350 ml of a 72% sulfuric acid solution were added to 30 g of this residue and the mixture was maintained under agitation for 2 hours at room temperature, followed by the addition of 550 ml of distilled water and refluxing for 4 hours. After cooling to room temperature, the solid residue was

recovered through filtration and washed with distilled water until neutral pH, a dark powdery material being obtained.

2.1.6.3 Alkali treatment

Mercerization or alkali treatment with strong alkali bases was developed as a method for cotton fibre modification by John Mercerin 1850 [30]. Is a usual method to produce high quality natural fibres, by removing the natural and artificial impurities. The chemical treatment reduces the fibre diameter and thereby increases the aspect ratio [8]. Mercerization is usually performed applying aqueous solutions of NaOH, at reaction times of 30 min up to 3 hr. As a result of alkali treatment (use of sodium hydroxide), the following reaction (Equation 2.1) is presented [8].

$$Fiber - OH + NaOH \longrightarrow Fiber - O - Na^{+} + H_2O \qquad (2.1)$$

Theoretically, other alkali types can be used as well, but sodium atoms have been shown to provide the optimal diameter for cellulose swelling, meaning that the treatment with NaOH is most efficient [42]. In any case, excess alkali has to be removed by washing the modified fibres/fillers subsequently, followed by a drying step [30]. The aspect of the long sisal fibre is presented in Figure 2.4 a) and the cut sisal fibre after alkali treatment in Figure 2.4 b).

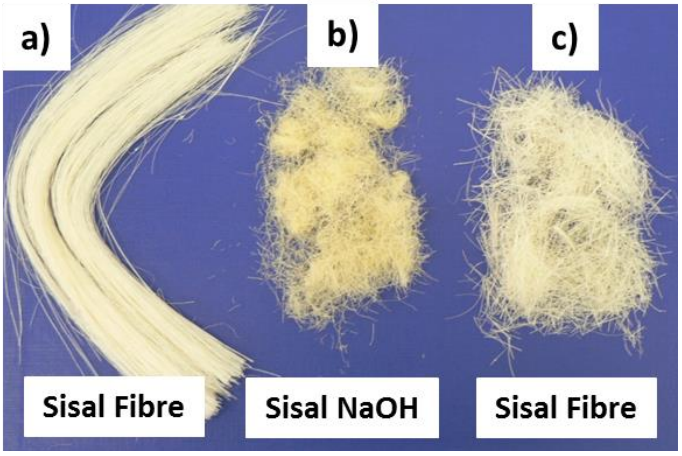

Figure 2.4. Natural fibre used to reinforce cork-polymer composites: (a) sisal fibre; (b) sisal after alkali treatment and (c) sisal cut fibre.

In this thesis, the preparation of alkali treated sisal (Sisal_NaOH) was as follows [43]: the sisal fibres were immersed in sodium hydroxide (NaOH) solution (5% w/v) for 2 h at room temperature. After that the fibres were washed with distilled water containing a few drops of acetic acid. Final washings were carried out with distilled water until neutrality (pH = 7), to remove the excess of NaOH present on the fibres, until this water no longer indicated any alkalinity reaction. Then, the fibres were air-dried at room temperature, followed by drying in a vacuum oven at 70 °C and after stabilise was stored in polyethylene bags for further characterization.

2.2 Composites processing

Composite material, is defined according to the standard ASTM D 3878 [44], as a substance consisting of two or more materials, insoluble in one another, which are combined to form a useful engineering material possessing certain properties not possessed by the constituents [44]. Composites using natural component such as the use of natural fibres to reinforce the polymeric matrix are manufactured using traditional manufacturing techniques that includes compounding, mixing, extrusion, injection moulding, compression moulding, and resin transfer moulding [9, 27]. In this work pultrusion, extrusion, injection moulding and compression moulding processes were used to proof their successability for producing cork-based composites and biocomposites with potential of application as sustainable products. The production of natural fibre composites is strongly limited by the temperature and processing times begin seeing significant thermal degradation around 180 - 210 °C, or over 175 °C for long periods with a significant decrease on the mechanical properties [7, 45]. Therefore, the processing of these composites must be limited to temperatures at the lower range of this degradation range and for limited processing times avoiding significant fibre damage and reduced composite performance [7]. The moisture content at a given relative humidity also can have a great effect on the biological performance of a composite made from natural fibers [9]. The low moisture of cork can be regarded as one of the advantages of cork to be selected as natural component in the composites, since is a hydrophobic material with low moisture content.

2.2.1 Pultrusion

Pultrusion is an automated process to produce continuous, constant-cross-section composites [7]. Long-fibre reinforced thermoplastic composites granules are usually produced with the pultrusion process. At the exit of this system the cross-section of the strand is calibrated by a nozzle, then cooled and granulated [46].

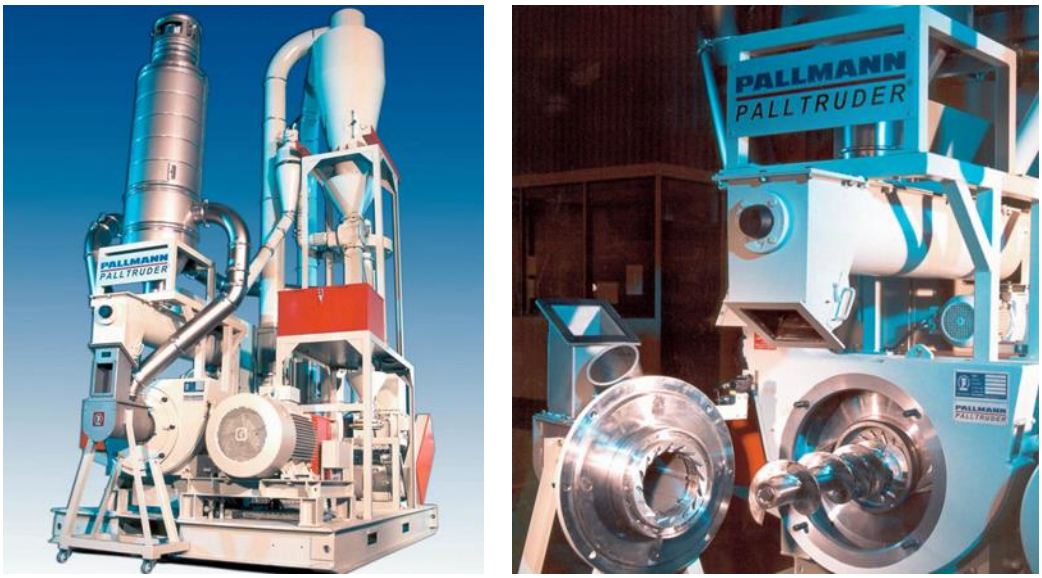

Figure 2.5. Pultrusion system used to compound the CPC pellets [47].

In this work the different cork powders were mixed with the thermoplastics (in 50-50 wt% ratio) in the dry form and further compounded in an industrial pultrusion system (Palltruder PFV 250, Germany) as shown in Figure 2.5, to obtain cork-polymer composite pellets (Pallmann Maschinenfabrik GmbH & Co., Germany). In this process the material mixture is equally plastified with frictional heat and pressure. Resulting steam is vacuumed off. The pultruded material is pneumatically transported into a granulator which produces a homogeneous and uniform granule [47].

2.2.2 Twin-screw extrusion

The extrusion process is used by the plastic industry for the production of granules and also in the continuous production of semi-finished products or components. Single screw as well as twin-screw extruders that run either co- or counter-rotating may be used for this process. Single screw extruders are used when the mixing effect does not have to be very high. The excellent mixing effect of twin-screw extruder the natural fibre materials can be homogenously distributed and wetted in the polymer melt [9, 46]. For instance, counter-rotating twin-screw extruders are mainly used in the processing of wood fibre reinforced thermoplastics (WPC), because the screws run in opposite directions, a secure material feed and a defined compacting of the material can be achieved [46]. The principal characteristics of both systems to process natural fibre composite systems are compared in Table 2.3.

Table 2.3. Counter-rotating versus co-rotating extruders (Adopted from [48]).

	Counter-rotating	Co-rotating
Advantages	Low screw speed suitable for very shear-sensitive products Positive pump – develops high pressures	Higher power – higher throughput potential Flexible screw design Excellent dispersive and distributive mixing
Disadvantages	Lower power – less throughput potential Screw design option limited Limited dispersive mixing: poor distributive mixing	Less positive pump – may require gear/screw pump to generate high pressure Higher screw speed not suitable for very shear-sensitive products

Downstream processing equipment these advantages and disadvantages must be considered and take into account to produce the novel cork-polymer composite pellets. In this thesis to produce cork-based composite pellets it was selected:

- Counter-rotating twin-screw extruder

This system was selected to produce cork-polymer composites materials with the highest cork content 50 wt.% and 70 wt.% respectively. Moreover the hybrid cork-based composite pellets reinforced with natural fibres were also compounding using this system due to the high complexity of the different components (i.e. cork, natural fibres, thermoplastic polymer and coupling agent).

In both cases, prior to compounding, all natural raw materials were dried at 80 °C during 24 h to stabilise the cork moisture content. These compositions were compound in a counter-rotating twin-screw extrusion machine (Carvex, Portugal), which had a screw diameter of 52 mm and an L/D ratio of 18 with a nonintermeshing, mixing mode screw configuration. The barrel temperature profile was in the range 150 up to 190 °C, and the screw speed was fixed at 30 rpm. The cork in the powder form and the grinding selected matrix (i.e. polyethylene or polypropylene) were pre-mixed and manually feed in the hopper system. No extrusion head was used in order to minimize the residence time and shear heat dissipation. The extruded material was cooled in air, granulated in a cutting mill to produce composite

pellets. The pellets were stored in plastic bags and sealed and further conditioned at room temperature for further investigation.

- Co-rotating twin-screw extruder

The co-rotating twin-screw extruder system was selected to produce several varieties of cork-polymer composites pellets for different purposes, being:

(a) To evaluate the effect of the cork addition to the polypropylene matrix, the effect of cork granulometry and addition of coupling agent on the properties of the composites. In this case, the compositions were compounded in a Leistriz LSM 30.34 intermeshing co-rotating twin-screw extruder with a screw diameter of 33.7 mm and a length to diameter ratio L/D of 29, coupled to a die with a two cylindrical outputs with 4 mm diameter each. The extruder was equipped with two automatic volumetric feeders, for the addition of grinding PP with or without coupling agent (i.e. volumetric (Moretto)) and the other for the cork in the granules or in the powder form (i.e. gravimetric (K-tron)) as shown in Figure 2.6. Generally, the polyolefin and the coupling agent were tumble-mixed and fed through the hopper. In all the experiments it was used a vacuum pump system and the feed rate was set for 2 kg/h.

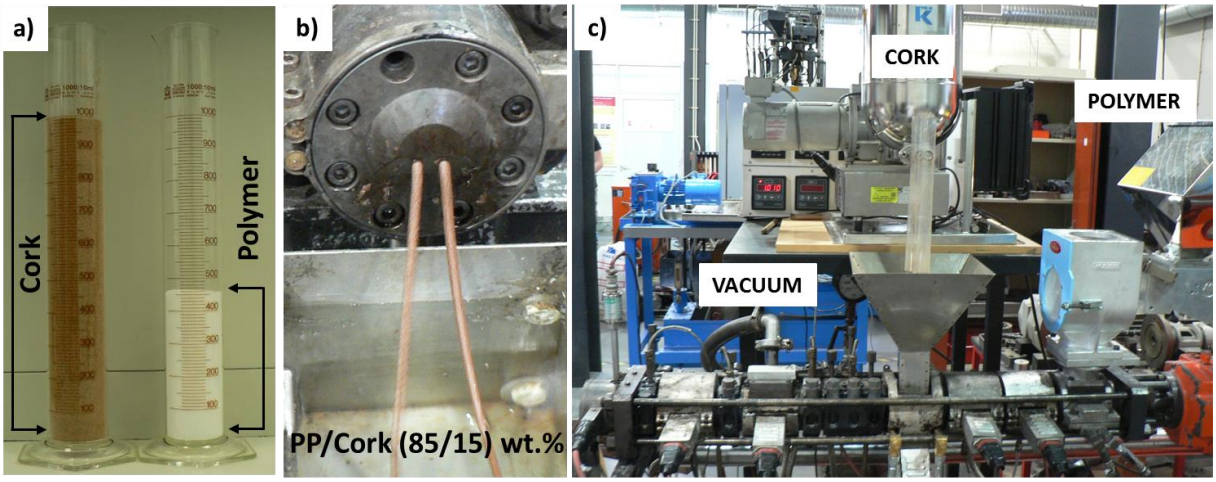

Figure 2.6. Extrusion of PP/cork composites using the extruder: (a) PP/Cork (70/30) wt.%; (b) extruder die and (c) Leistriz LSM 30.34 twin-screw extruder (TSE) with the two feeders and the vacumm system.

The temperature presents a decreasing at the end of the profile since it is compensated by the increased shearing which tends to increase the temperature of the composite. Part of the extrudate was cooled in water bath and subsequently ground by a Scheer (Germany) grinder in order to obtain pellets with length ≤ 5 mm. The pellets were dried in an oven at 80 °C and further packed and sealed in

plastic bags and conditioned at room temperature (23°C, 55% relative humidity) at least for 48 hours prior to further investigation.

(b) To evaluate the use of suberin and lignin as bio-based coupling agents through a reactive extrusion process. The extruder is an ideal reactor for polymer modification in that it serves as a pressure vessel equipped for intensive mixing, shear, control of temperature and residence time, venting of by-product and transport of molten polymer through the various sections of the extruder, each serving as a mini-reactor. It is an economically attractive process since the extrusion and the processing are done in a single stage and without chemical solvents emissions [49].

In this case, and before compounding, the cork powder was pre-dried at 80 °C in a vacuum oven until constant weight. The raw materials, including the pulverized polyethylene, the benzoyl peroxide (BPO) and the coupling agent PE-g-MA, were pre-mixed. Compounding was performed in a prototype modular laboratorial mini intermeshing co-rotating twin-screw extruder (TSE) as shown in Figure 2.7, with a screw diameter of 13 mm, and a length to diameter ratio (L/D) = 27, coupled to a rod die with a diameter of 3mm. The screw profile is built by sliding along a shaft conveying and kneading elements with a maximum channel depth of 1.5 mm.

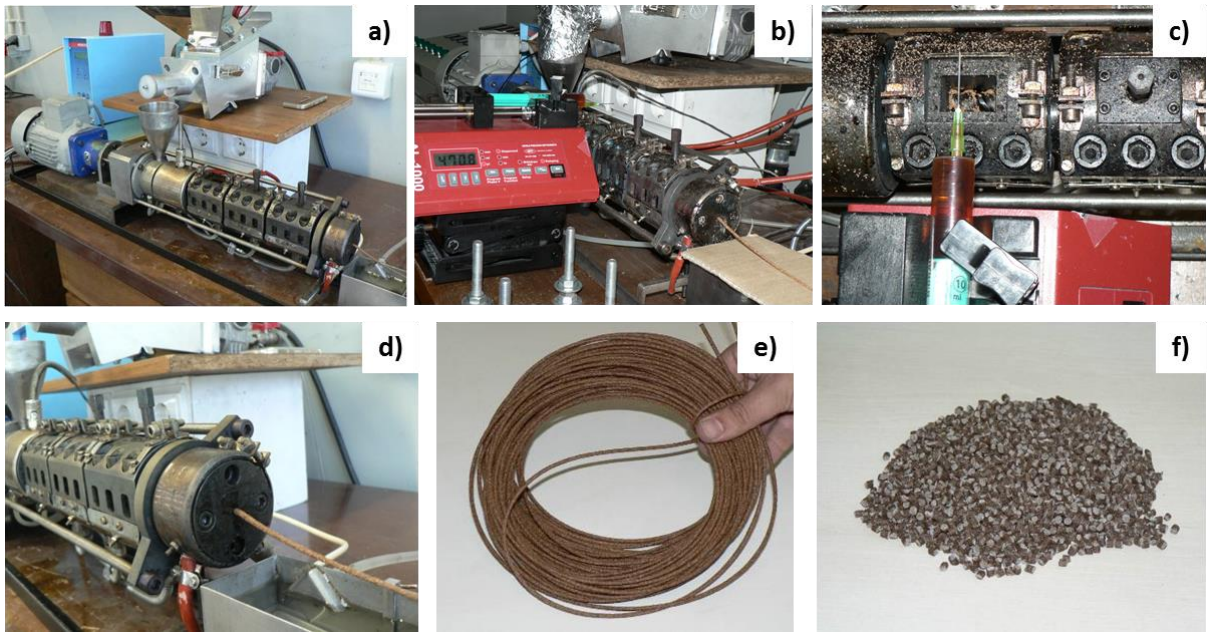

Figure 2.7. Reactive extrusion process: (a) and (d) represents the mini co-rotating twin-screw extruder (TSE) line used; (b) detail of the automatic syringe pump dispensing suberin; (c) detail of the suberin adition; (e) extruded of a functionalized cork composite with suberin and (f) functionalized cork composite pellets with lignin.

The temperature profile along the barrel and die was set to 165/180/185/185/175°C for all the experiments, the feed rate was kept at 130 g/h, and the screws rotating at 70 rpm. The pre-mixed polymer and cork were feed upstream by a miniaturized volumetric feeder (based on a Moretto DVM 18 L), together with the BPO initiator, or the PE-g-MA. Suberin and/or lignin were added as shown in Figure 2.7 b) and c), by means of an automatic syringe pump (AL-1000, from WPI, USA), or manually, respectively. After air-cooling, part of the extruded composite was pelletized.

(c) To produce biocomposite pellets with cork.

The raw materials were pre-mixed and then were compounded in a Rondol SCF modular co-rotating twin-screw extruder (TSE) as shown in Figure 2.8, with the screws diameter of 16 mm, a length to diameter ratio (L/D) = 25 and a single strand die of 3 mm.

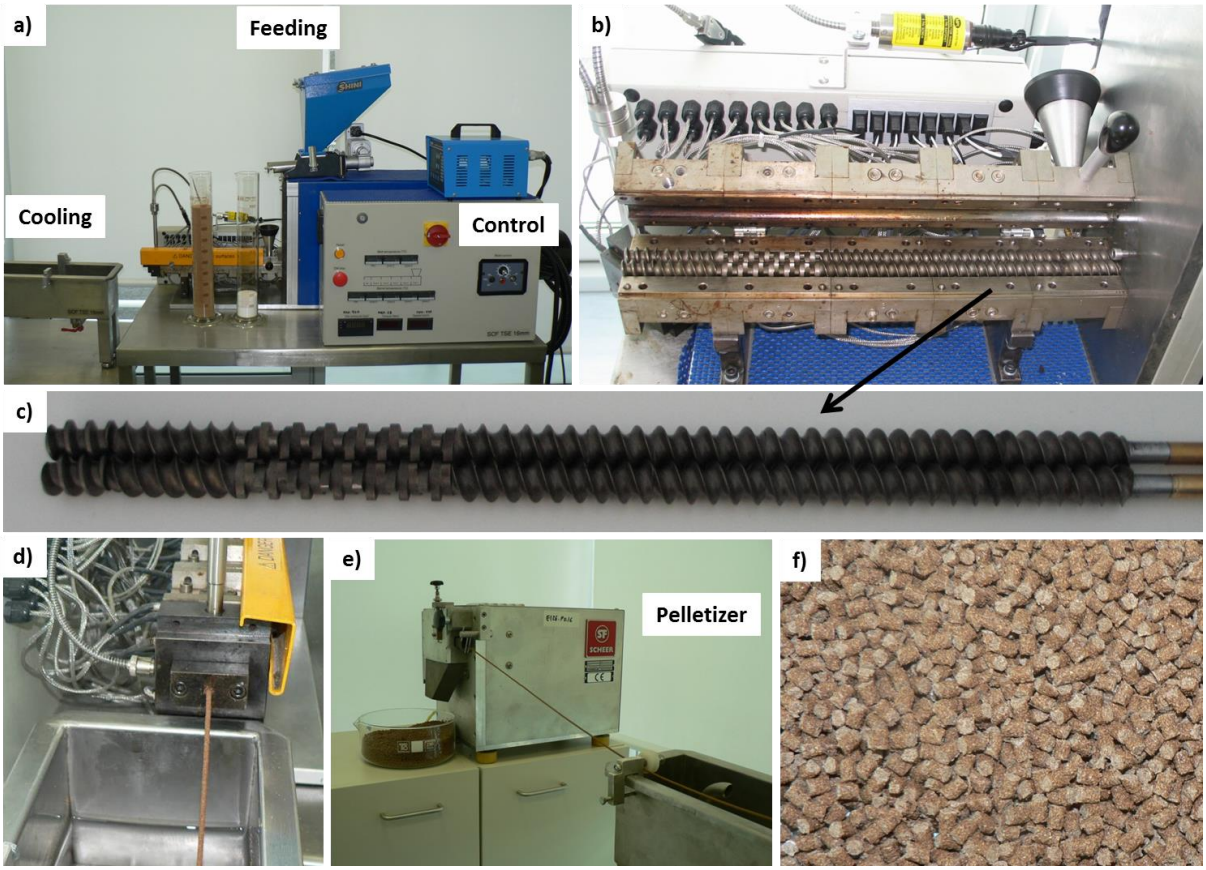

Figure 2.8. Extrusion of the cork biocomposites: (a) co-rotating twin-screw extruder (TSE); (b and c) detail of the screw configuration used (d) die of the extruder; (e) pelletizer system and (f) cork biocomposite pellets.

The mixture (i.e. granulated cork and bio-based polymer) was placed in the hopper and automatically feeded at a constant rate with a volumetric dosing unit from SHINI Plastics Technologies (Germany). Part of the extrudate was cooled in water bath and subsequently ground by a lab pelletizer SCHEER (Stuttgart) to produce composite pellets (see Figure 2.8 f) with length ≤ 5 mm for injection moulding.

2.2.3 Compression moulding

The pressure method is a common processing technique in the manufacture of natural fiber composites due to of its high reproducibility, simplicity and versatility [7, 9, 46]. Compression moulding materials combined with natural fibres are used in the automobile industry to produce car interior lining parts. The main reason for this application is the great strength and stiffness and the low composite density of the natural fibre composites [46].

In this work, compression moulding process of the obtained dry pellets after pultrusion or twin-screw extrusion were processed using a hydraulic press from (Moore, UK) or (Carver, USA) to produce boards with 3 and 6 mm of thickness from the different compositions (see Figure 2.9). A certain amount of pellets (approximately 70g) from each composition was collected and dispersed into a mold with a rectangular geometry (around 20x23cm^2) and 3mm of thickness, containing on the top and on the bottom two removal covers.

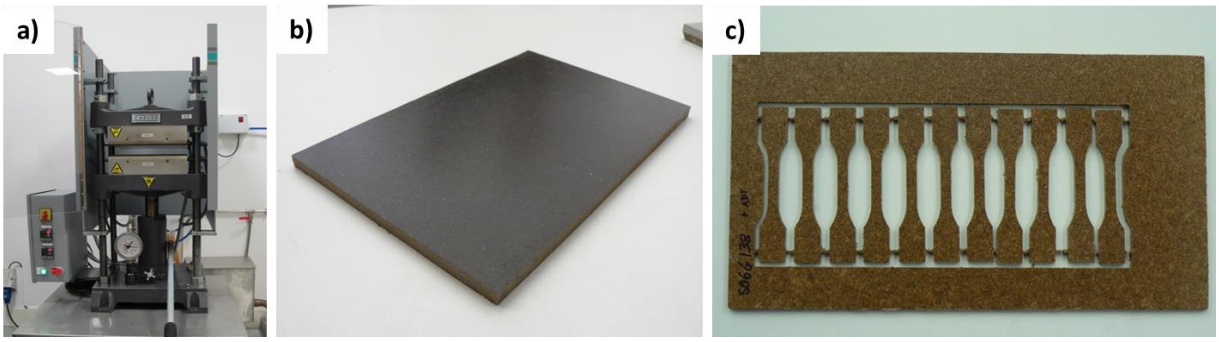

Figure 2.9. Compression moulding of cork-polymer composite: (a) The equipment used; (b) HDPE/Cork (50/50) wt.% board with 6mm thick and (c) Cork-polymer composite board after CNC process to obtain the tensile specimens.

Between the pellets and the top and bottom mold walls it was used two Teflon sheets to allow the unmolding. This system was placed in a hydraulic press at a temperature between 150-170 °C, depending on the thermoplastic matrix (PE or PP) used to produce the pellets, for a period of 8min to

allow the melting and homogenization of the pellets mass, and further pressed during 2min at a pressure of 11 ton followed by a cooling stage of 5 to 10min consisting on maintaining the pressure and using water to decrease the temperature aiming to decrease the temperature of the material inside the mold near to the room temperature. Finally, the pressure was removed and the small contraction that occurs on the board facilitates the unmolding of composite material.

To produce rectangular cork-polymer composite boards of 220×220×6 mm^3 it was applied similar conditions of temperature and pressure were the period of time was extended to 9-10 min followed by a period of 4-5 min under pressure before cooling and perform the mould release. Tensile bars in dog bone shape were obtained from these boards of 3mm thick using a computer numerical control CNC machine (Roland 3D Plotter MDX-20, UK). The specimens were produced according to ISO 527–2 [50, 51] and similar standard ASTM D 638 [52] as shown in Figure 2.9 c).

2.2.4 Injection moulding

It is possible to produce complex geometric components with functional elements fast and also in high volumes by this process [46]. Injection moulding is a major plastic forming process in which the components to obtain the final material passes through five stages: (1) mould closing, (2) filling, (3) packing–holding, (4) cooling and (5) mould opening are preceded repeatedly. The industry mostly adopted injection moulding for plastic processing since, as a cyclic process, it has rapid production rate on complex shape product with good dimensional accuracy and surface finishing [53]. It is a high-pressure process with machine capital costs and tooling costs generally high compared to other composites processing routes. However, these costs can be recovered through inherent short cycle times, automation, and low labour costs [54].

Prior to injection moulding, the produced pellets were dried in a vacuum oven at 50 °C until stabilize. It was used two different injection moulding machines to produce the tensile specimens as presented in Figure 2.10. The polypropylene and the PP/cork composite pellets were injection moulded in an ENGEL Spex Victory 50 (Austria GmbH) with 500 kN of clamping force.

The neat polymers and the biobased composite pellets were injection moulded in a Ferromatik-Milacron K85 (Germany) with 850 kN of clamping force. The mould temperature was controlled through a thermal regulator Piovan THN 6P (Piovan, Italy).

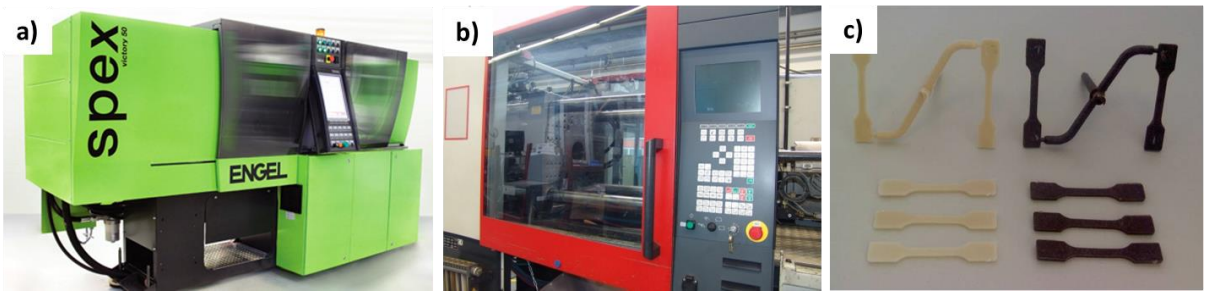

Figure 2.10. Injection moulded process: (a) ENGEL Spex Victory 50 unit [55]; (b) Ferromatik-Milacron K85 unit and (c) specimens of SPCL and respective biocomposite SPCL/Cork (70/30) wt.% tensile specimens.

In Both cases, the injection-moulded specimens were tensile bars produced according ASTM 638, with 60 mm length, a constant rectangular cross-section of 2×4 mm^2, and a neck length of 20 mm. The samples were placed in polyethylene plastic bags and conditioned at ambient temperature.

2.3 Characterization methods

2.3.1 Physical properties

2.3.1.1 Density of cork and cork composites

- Cork

The bulk density of the different cork powders was determined using a volumetric flask of 500ml were it was placed and compacted the material to minimise the possible empty spaces between the particles.

$$d = \frac{m}{v} \qquad (2.2)$$

The equation 2.2 was applied for density calculations were, d is the specific weight (Kg/m^3) of the cork raw material, m is the weight of the compact cork powder and v is the volume occupied by the cork powder into the volumetric flask. Three measurements were performed for each cork powder.

- Cork Composites

The density of the natural fibres and of the different composite specimens was determined according to the standard ASTM D 792 [56], using an analytical balance equipped with a stationary support for the

immersion vessel. Five specimens were weighted per each sample. It was used Propanol as immersion liquid and it was used the following equation:

$$\rho = \frac{W_{(a)}[\rho_{(liq)} - 0.0012]}{0.99983\ G} + 0.0012 \quad (2.3)$$

where ρ is the specific gravity of the solid (g/cm^3), G the Buoyancy of the plummet; ρ (liq) is the density of the liquid and ρ (liq. propanol) was 0,7982 g/cm^3 (being the experimental value). The density of the natural fibres (i.e. coir and sisal) was also determined using this method. Due to the reduced weight of a single fibre it was used a small number of fibres to determine the fibre density per condition.

2.3.1.2 Fibre diameter

Natural fibres are quite different from the synthetic fibres. Natural fibres often consists of a bundle of elementary fibres, which results in an irregular shape depending on the number of elementary fibres and the way by which they are packed together [57].

Figure 2.11 reveal a typical optical microscopic (OM) image of the morphology, showing the polished cross-section of a cork-polymer composite reinforced with the sisal after alkali treatment. The cross-section shows elementary fibres and we observed that is not perfectly round. Furthermore, the natural fibers also can present a hollow structure, called lumen, which looks like a small open channel in the centre of the cell and maybe affect the actual fibre area under a mechanical loading. Thus, the diameter observed under OM can vary a lot depending on the view it is observed.

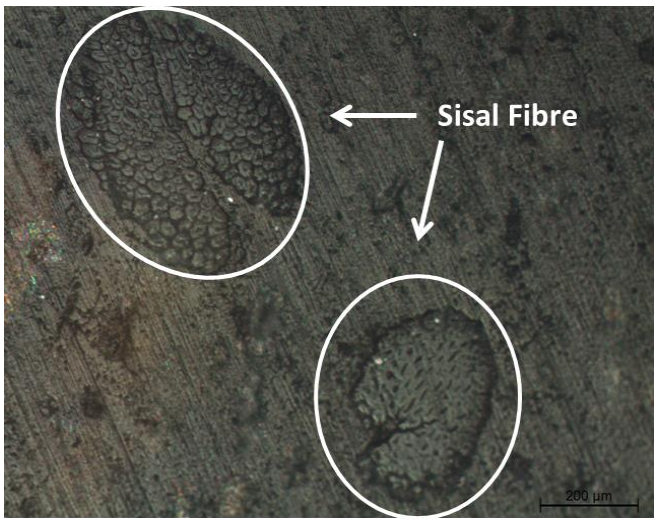

Figure 2.11. Optical image of a polished cork-polymer composite cross-section reinforced with sisal fibre after alkali treatment.

Since natural fibres presents irregular shape and are non-uniform along the fibre axis, it is difficult to obtain a good focus on the fibre image under OM to determine the fibre diameter. As shown in Figure 2.12, it is not easy to achieve a good focus of such stack of elementary fibre bundle.

Therefore, it is not surprised that this method often results in an inaccurate value of tensile strength with very high SD value for the natural fibres.

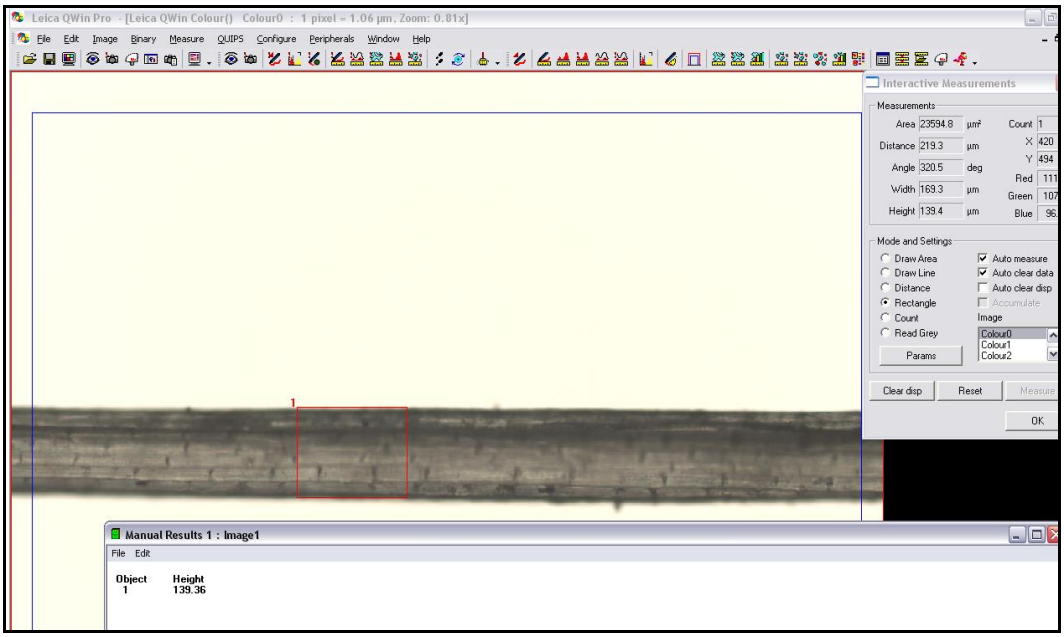

Figure 2.12. Partial view of the software used to determine the fibre diameter.

In this sense, and to reduce the variability of the experimental values, the diameter measurements of natural fibres were made in five spaced locations along the gauge length of 30 different specimens using an optical microscope Olympus BH-2 (Tokyo, Japan) equipped with an Olympus DP11, (Japan) digital camera. The measurements were performed used a software Leica Qwin Pro and a partial view of the program is shown in Figure 2.12, representing a sisal fibre.

2.3.1.3 Moisture content

The percentage of humidity of the different cork powders, or in the natural fibres was determined using a balance Sartorius (Sartorius AG, Germany) were the cork powder or the fibres were submitted to 105 °C during a period of 10min. This procedure was performed three times for each cork powder sample. The moisture content of the composite specimens was calculated as follows:

$$MC\ (\%) = [(W_w - W_d) / W_w] \times 100 \quad (2.4)$$

where W_w is the weight of the specimen before drying (g) and W_d is the weight of the sample after drying (g). Averages of five specimens were used for WA and MC measurements.

2.3.1.4 Water absorption

Aiming to study the dimensional stability of the developed cork composites the water absorption tests were conducted according the ASTM D 570 [58].

To determine the water absorption, specimens (measuring 6mm in thickness, 60mm wide and 90 mm long) from the different materials were immersed in distilled water, at 23 ± 1 °C and atmospheric pressure, for different time periods (up to 11 days). In the end of each time period, five specimens of each material were removed, gently blotted with tissue paper to remove the excess water on the surface and immediately weighed. The water absorption was calculated according to the equation (2.5):

$$Water\ absorption\ (\%) = \frac{W_a - W_b}{W_b} \times 100 \quad (2.5)$$

where W_a = weight of the specimen after being immersed for a certain period of time and W_b = weight of the same specimen before immersion (g).

2.3.1.5 Weight loss

The weight loss *(WL)* of the developed specimens was calculated as follows:

$$WL\ (\%) = [(W_i - W_d)/ W_i] \times 100 \quad (2.6)$$

where W_i is the initial weight of the specimen (g) and W_d is the weight of the sample after drying (g). For that purpose, the specimens were weighed using an analytical balance after being placed in a vacuum oven at 40 °C for 48 h, cooled and stabilized in a desiccator several days followed by reweighing of the specimens. Averages of five specimens in each time point were used for *WL* measurements.

2.3.1.6 Thickness swelling

The thickness swelling of the developed composite specimens was calculated as follows:

$$Thickness\ swelling\ (\%) = \frac{T_2 - T_1}{T_1} \times 100 \quad (2.7)$$

where T_2 = thickness of the specimen after immersion and T_1 = thickness of the same specimen before immersion. Moreover, the thickness of each immersed specimen was measured in two different points using a digital micrometer Mitutoyo (Japan), with a precision of ± 0.001 mm. Three to five specimens per each condition were measured.

2.3.1.7 Soil degradation tests

The soil burial test can be considered a realistic approach to the biodegradation process in a waste landfill. To demonstrate the potential of the biodegradable injection moulded matrices and the biocomposite cork-polymer specimens (i.e. PLLA/Cork; PHBV/Cork, PCL/Cork and SPCL/Cork) were placed in vessels of 5 L used as soil containers and buried in soil. The physical and chemical composition of the compost used, indicates an organic matter higher than 70%. The specimens were monitored and removed at predetermined intervals of time test up to 4320 days. The average room temperature was 19 – 21 °C and relative moisture was kept at least 50 % by pulverizing the soil with distilled water and allowing continuous aeration. Once removed, samples were withdrawn carefully, placed in small nets to avoid disintegration of the specimen and washed with distilled water. After that, the samples where dried at 40 °C in a vacuum oven to constant weight and kept in a desiccator, and then measured in terms of thickness variation and weight loss before undergo to further characterization. It was used averages of 5 independent specimens in each time point per condition.

2.3.1.8 Fibre crystallinity

To detect the crystalline structure of cellulose in sisal, Wide-angle X-ray diffraction (WAXRD) diffractograms were recorded using the Bruker-AXS D8 Discover diffractometer in θ–2θ geometry using Cu Kα1,2 lines collimated with a Gobël mirror, a divergent slit of 0.6 mm, a detector slit of 1 mm and 0.6 mm and a Ni filter. The data was collected from 6-50° with a step size of 0.04° and an acquisition

time of 1° sec per step. The percentage of crystallinity (%Cr), performed using a fitting program, was calculated based on:

$$\% Cr = (A_{cryst} / A_{total}) \times 100 \quad (2.8)$$

where, A_{cryst} is the area below the diffraction peak of the (002) plane, peak at 2θ = 22.5°, and from the (101) and ($10\bar{1}$) plane, peak at (13-18°), and A_{total} is the area below the whole region representing the amorphous material in the cellulosic fibres.

2.3.1.9 Acoustic tests

The building elements for acoustic tests consisted on a superior element from CPC or fibreboard with dimensions of 220X220X6 mm^3 and an agglomerated cork underlay with thickness of 1.8 mm thick as it is presented in Figure 2.13. Commercially available silicone glue (thickness of 0.5-0.6mm) was used to fix the agglomerated cork underlay to the previously produced boards (CPC, HDF and MDF boards) (Figure 2.13 a). The aim of including this agglomerated cork underlay was to avoid reverberation sound and fix the boards. The pavement was submitted to a uniformly distributed load (20 to 25 $kg.m^{-2}$). The tests were conduct in a reverberant chamber with a 7.25 m length, 5.88 m width, 4.65 m height and a volume of 202 m^3 as presented in the scheme of Figure 2.14. The tests were conducted at atmospheric conditions 22 °C and 66 % of humidity.

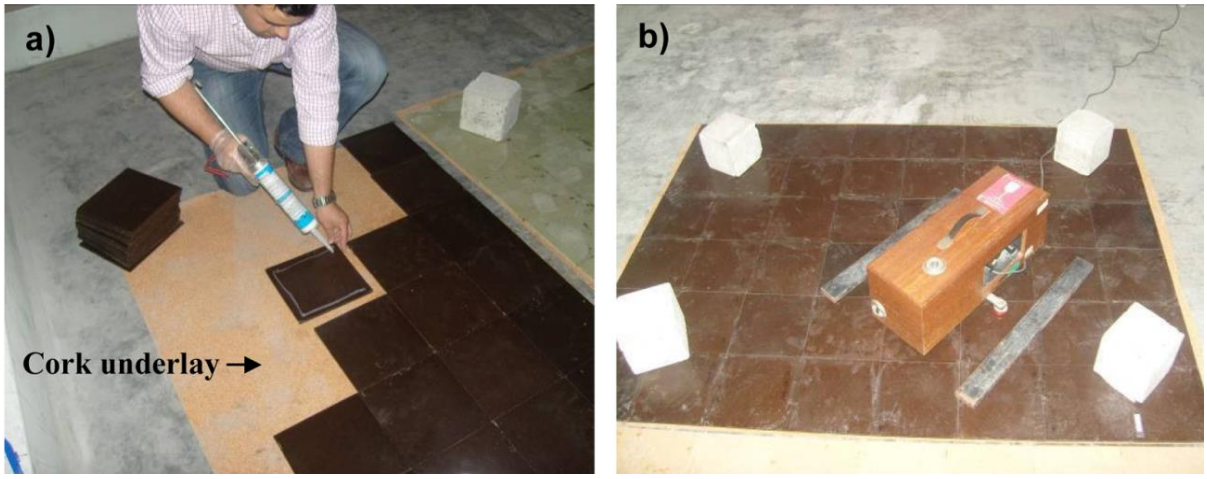

Figure 2.13. Detail of the installation of composite boards in the reverberation room for acoustic measurement testing: (a) silicone application on the CPC board b) normalized tapping machine on the floor system.

The equipment used for the measurements was a tapping machine Brüel & Kjaer (B&K, Germany) Type 3204; B&K *2260* dual channel real-time frequency analyser and B&K 13 mm microphone model 4189. The microphone height was about 1.4 m.

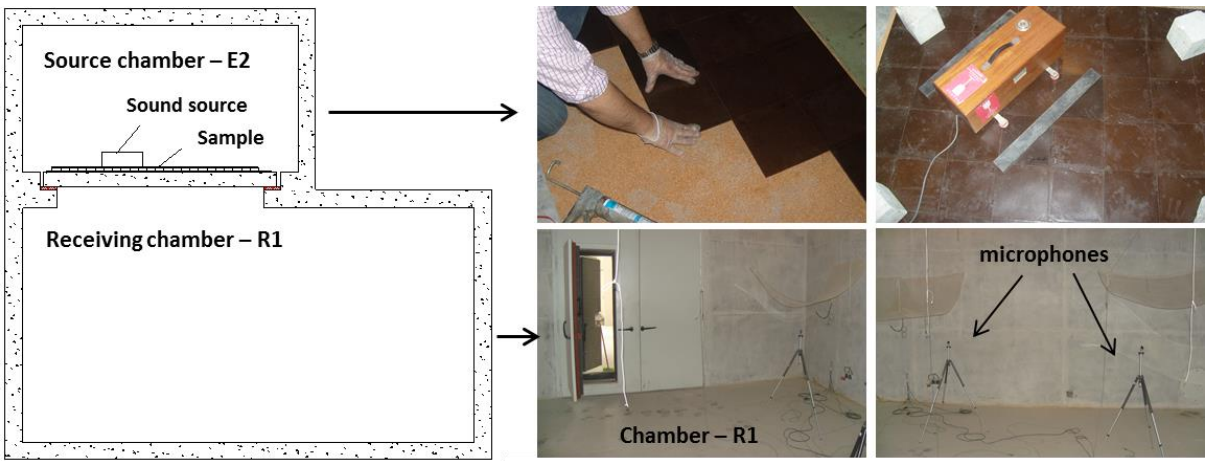

Figure 2.14. Scheme of the acoustic test performed in the reverberation chamber.

The measurements of sound insulation were performed according the standard EN ISO 140-8 [59] and 717-2 [60]. The measurements were taken at three locations of the tapping machine relative to the floor sample area of 2 m^2 and 5 positions of microphone with to different lectures using one-third-octave bands, 100 Hz to 4200 Hz. The reduction of impact noise by floor covering on standard floor was determined according the equation:

$$\Delta L = L_{n,0} - L_n \qquad (2.9)$$

where, ΔL is the reduction of impact sound pressure level, $L_{n,0}$ is the normalized impact sound pressure level in the absence of floor covering and L_n is the normalized impact sound pressure level with floor covering. The impact sound improvement index (ΔL_w) was determined according to the standard EN ISO 717-2 [60].

2.3.1.10 Warping

Warping can result from an inferior product construction, wrong choice of materials or inadequate processing routes. Other reason that can cause this effect is the high moisture content in the air. After

processing, CPC boards (220×220×6 mm^3) obtained by compression moulding were submitted to a specific test to access the possible occurrence of warping effect. The obtained results were compared with the commercial fibreboard composites cut with the same dimensions. In Figure 2.15 is shown a schematic illustration of the performed test.

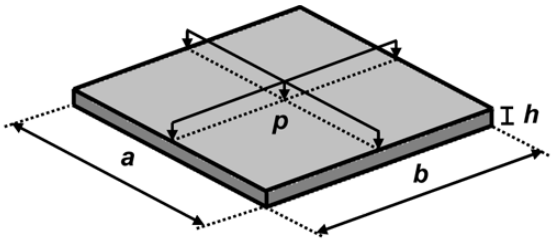

Figure 2.15. Scheme of the specimen's geometry with the measuring system for warping determination.

Figure 2.15 shows the used system with a pointer *p* with precision capability of 0.01 mm of displacement. Two perpendicular measurements in each board were performed according the indicated directions *a* and *b*. At least 15 boards (in dry state) of each condition were analysed to evaluate the warping effect.

2.3.1.11 Hardness

To infer eventual morphological variations of the cork-based composite materials and to characterize the developed materials after compression moulding, it was attempted microhardness measurements. However, due to the small indentations on the composite surface and due to the recovery properties of cork, this test was not indicated. The hardness of the materials was determined by Shore-D Hardness Tester (model bareiss – Prüfgeräte, Germany). The hardness test was performed according the standard ASTM D 2240-05 [61]. This test method is based on the penetration of a specific type of indentor when forced into the material under specified conditions. It is recommended that Durometer D tests be used when Durometer A results are greater than 90 [61]. Ten measurements were performed per condition.

2.3.2 Morphological properties

2.3.2.1 Scanning electron microscopy (SEM)

- **Morphology of the natural materials**

The different qualities of cork powder obtained from the industrial processing were analyzed using a Quanta 400 FEG model (FEI, USA) ambiental scanning electron microscope with low vacuum to avoid any possible desire effect in the natural raw material structure. Since the several cork powders presents low dimension, the objective was to confirm that the vacuum effect does not affect the observation of the cellular structure of the natural materials.

- **Morphology of the composites**

Scanning Electron Microscopy (SEM) of the developed cork-polymer composites fracture surface was performed using a Leica-Cambridge S-360 (UK) scanning electron microscope. All the samples were sputter-coated with gold before being analysed.

In addition, it was also used for examine the microstructure of the cork-polymer phases, fracture surfaces of the different specimens a NanoSEM 200 FEI (The Netherlands) scanning electron microscope (SEM). Before being analysed all the samples were coated by ion sputtering with an Au/Pd alloy (80-20 wt.%) in a high resolution sputter coater of Cressington 208HR (Watford, UK).

2.3.2.2 Optical microscopy (OM)

In order to understand the nucleating ability of cork on the matrix, a single cork powder was sandwiched between two thin PP films and heated at 200°C during 10min to erase the previous thermal history of the sample. Then, the sample was quickly shifted to a well-controlled temperature stage (Linkam, THMS-600) where the pre-determined crystallization temperature was maintained at 140 °C for 1h, to access to the crystallization process. A fast cooling was estimated to be 80°C.min^{-1} was used to reach the isothermal crystallization temperature. Dry nitrogen was introduced to eliminate any possible degradation in all cases. The crystallization of PP on the cork powder was observed on an optical microscope (Olympus B) connected to a Leica digital camera.

In addition, to observe the distribution of cork particles on the PP matrix, after injection moulding, was observed on a transmission optical microscope (Olympus BH-2) connected to a Leica DFC 280 digital camera and corresponding software. To prepare the samples for the analyses, one slice with a

thickness of 15 µm was cut, using a Leitz 1401 microtome equipped with a glass slicing knife, from the longitudinal section of the tensile specimen as presented in Figure 2.16. The images were obtained from the middle section of the tensile specimen.

Figure 2.16. Optical microscopy of a cross-section of a polypropylene/cork (70/30) wt.%: (a) scheme of the tensile specimen revealing the longitudinal section; (b) image observed from the microscope in bright field and (c) image with color treatment to evidence the distribution of cork particles in the polypropylene matrix.

Each sample slice was placed between a microscope glass slide and cover glass. To prevent them from curling up or corrugating, Canada balsam was used as a fixing resin. Special care was taken during the analysis to identify the cork particle distribution; the cork and the matrix domains as presented in Figure 2.16 b) and c). All samples were left to cure under a simple weight pressure during at least 12 h prior to analysis.

2.3.3 Chemical properties

2.3.3.1 Fourier transform infrared spectroscopy (FTIR)

To confirm the extraction of suberin and lignin extraction; the chemical groups attributed to the natural fibres including cork and to confirm the chemical modification in sisal, the fibres were analysed using Fourier transform infrared (FTIR) spectroscopy. All the spectra were acquired using a Shimadzu IR-Prestige 21. The attenuated total reflectance (ATR) methodology (PIKE Technologies) was used and the spectra were acquired between 4400 cm^{-1} to 800 cm^{-1} using a resolution of 4 cm^{-1}.

2.3.4 Mechanical properties

2.3.4.1 Tensile properties of the composites

- **Tensile properties of the composites**

All the tensile tests were conducted using a Universal tensile testing machine (Instron 4505 Universal Machine, USA) using a load cell of 1KN and a crosshead speed of 5mm min^{-1} was used up to a deformation at break. All the mechanical results were obtained with a minimum of five to ten tested specimens. The tensile tests were performed according the specifications of standard ISO 527 [50, 51] and ASTM 638 [52]. The test specimens were conditioned at 23 ± 2°C and 50 ± 5% relative humidity. The specimens with dog bone shape were obtained by compression moulding or by injection moulding. The specimen dimensions present 60 mm length, a constant rectangular cross-section of 2×4 mm^2, and a neck length of 20 mm. In the case of the compression moulded samples the thickness was slightly higher (3mm). In the tensile tests a force was taken as the maximum force in the force deformation curve. Tensile modulus was estimated by extending the initial linear portion of the load-extension curve and dividing the difference in stress corresponding to segment of section on this straight line by the corresponding difference in strain (average between 0.05% and 1%) using the linear regression method. According to the standard it can be also employed to determine the tensile modulus the secant method. The maximum tensile strength was determined by dividing the load at break or maximum load by the original minimum cross-sectional area. The result is expressed in (MPa). The percent elongation at break is calculated by dividing the elongation at the moment of rupture by the initial gauge length and multiplying by 100. Samples were conditioned at room temperature for at least 48 h before testing.

- **Tensile properties of the Single fibres**

After the observation and diameter measurement using optical microscopy, fibres with apparent defects were removed in this process, since such defects are not representative for the fibre. Single fibre tensile tests were performed with a Instron 4505 Universal Machine, (USA) using a 1 kN load cell, a crosshead speed of 1 mm min^{-1}, and a fibre gauge length of 30 mm. Prior to testing, fibres were mounted on sturdy paper frames using a high-strength hot melt glue and placed in a desiccators for a minimum period of 48 h. The tensile properties of the single sisal fibres were determined according to the standard ASTM C 1557 – 03 [62].

The observed fibres were temporarily fixed on the mounting card (see Figure 2.17) with thermal glue. The testing was then carried out as follows:

1) The prepared samples were subjected to optical microscopy to examine an accurate diameter of the test specimens. The diameter was measured in three different positions along the fibre and the mean values were used for data processing;
2) The samples were tested in a universal tensile test with mechanical grips;
3) Both sides of the card were cut in the middle before sating the test;
4) The test specimens were tested at a crosshead speed of 1mm/min with 30 mm gauge length;
5) The stress and strain of the loaded test specimens were tested automatically with Instron software;
6) Finally all the results (modulus, tensile strength and maximum deformation) were treated and recalculated using Microsoft Excel.

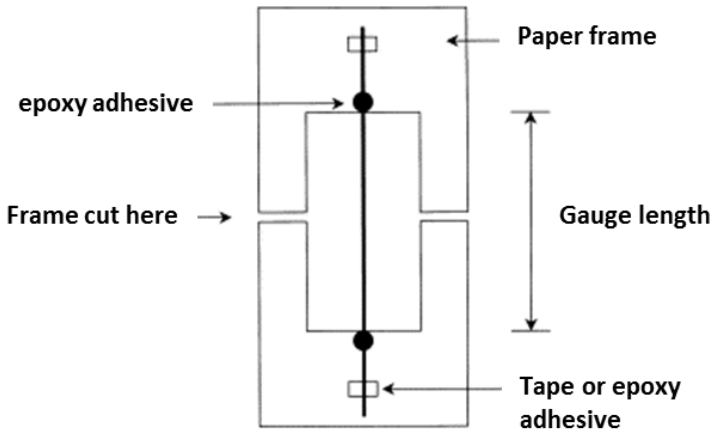

Figure 2.17. System used to test the natural fibres under tensile load.

2.3.4.2 Flexural testing

Three point static flexural tests were carried out using a Universal tensile testing machine (Instron 4505 Universal Machine, USA) with a load cell of 1KN in accordance with standard ISO 178 [63]. The dimensions of the specimens used were 120 mm length, 15 mm width and 6 mm thick as presented in Figure 2.18. The load was placed midway between the supports with a span (L) of 80 mm. The crosshead speed was 2.56 mm/min. For each condition, the specimens were loaded until the core break.

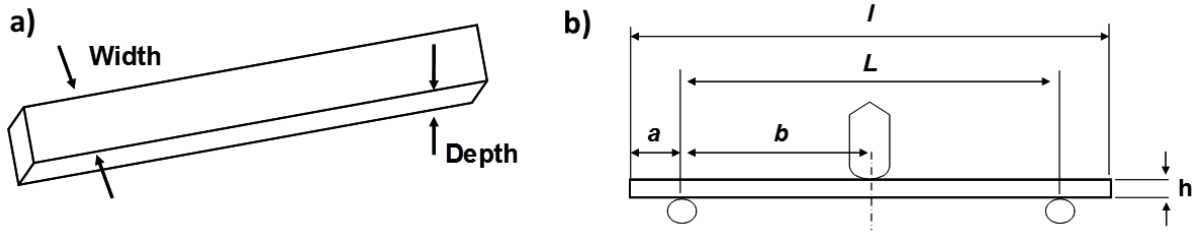

Figure 2.18. Geometry of the flexural specimen (a) and experimental scheme to perform the 3 point flexural tests.

The rectangular geometry of the specimens and the scheme of a 3 point flexural test is shown in Figure 2.18, being *L* the span length; b is the width of the specimen; h the thickness. Based on the geometry of the flexural specimens according the standard ISO 178 [63] and reported in the Table 2.4, we selected the dimensions for the specimens from the case 2.

Table 2.4. Dimensions of the specimens used in the flexural tests.

	Case 1	Case 2
Specimen thickness (mm)	6	6
Specimen width (mm)	10	15
Span *L* (mm)	80	120 *

* In the case 2 it was used a span of 80mm

The velocity of the flexural test (*V*) was determined according to the equation:

$$V = \frac{SrL^2}{6h} \quad with, L = 15h \; to \; 17h \tag{2.10}$$

being *h*= thickness, it was considered *h*=16.

V= (0,01*(16*6)^2)/(6*6) = 2.56 mm/min.

The flexural stress (σ_f) was determined according the following equation:

$$\sigma_f = \frac{3FL}{2bh^2} \quad (2.11)$$

being, F is the applied force in newtons; L is the span used in milimiters and h is the thickness of the specimen also in milimiters. The flexural strain (ε_f) in percentage was determined according:

$$\varepsilon_f = \frac{600\,sh}{L^2} \quad (2.12)$$

being, s the deflection in milimiters. The flexural modulus (E_f) expressed in megapascals, was determined using the following equation:

$$E_f = \frac{\sigma_{f2} - \sigma_{f1}}{\varepsilon_{f2} - \varepsilon_{f1}} \quad (2.13)$$

Being, σ_{f1} the flexural stress measured at the deflection S_1 and σ_{f2} the flexural stress measured at the deflection S_2, both in megapascal.

2.3.4.3 Impact testing

The Charpy impact tests were performed according the standard ISO 179-1 [64] and to ASTM 259-04 [65] on a Ceast Fractovis (Pianezza, Italy) instrumented falling weight impact tester with a pendulum energy of 2 J. The Charpy V-Notched specimens were rectangular bars with 120 mm length, 12 mm width and 6 mm thick. The V-Notched angle was 45°. The absorbed energy during the crack initiation process is given in kJ/m^2. It was tested a minimum of seven specimens per condition.

2.3.5 Statistical analysis

All results are provided as mean ± standard deviation (SD). The values obtained by tensile and flexural tests of the cork-polymer composites obtained by pultrusion followed by compression moulding were analysed in terms of the normality of the distribution of the mechanical results was evaluated using Shapiro-WilK test to evaluate their normal distribution at p <0.05. The results were compared using a Two-Sample t-Test and differences were considered significantly different at p<0.05.
Regarding the development of several injection moulded compositions of polypropylene with cork, the effect of cork loading, the coupling agent and in order to infer significant differences on the tensile

properties before and after water immersion tests, the data were statistically analysed using IBM SPSS software v. 23.0 (Release 23.0 for Windows). Firstly, a Shapiro-Wilk test was used to ascertain about the data normality. The normality was rejected, since as observed by the p value ($p < 0.05$). Therefore, nonparametric tests were used in further comparisons. Kruskal-Wallis nonparametric test was used to compare the medians of the tensile modulus, tensile strength and maximum strain for the composite specimens before and after immersion tests. Differences between groups were considered to be statistically significant at a confidence level of 95.0 %.

In the development of hybrid cork-polymer composites containing coconut fibre one-way analysis of variance (ANOVA) with post hoc Bonferroni multiple comparison tests was used to infer about significant differences between mean values of the mechanical properties in the developed cork composite materials. Assumptions of ANOVA such as normality were evaluated with Shapiro-Wilk test. A level of $\alpha = 0.05$ was used for statistical significance.

In addition, in the development of hybrid cork-polymer composites containing sisal fibre with and without coupling agents it was used Weibull to predict with more accuracy the tensile failure. In a first stage, the values obtained by tensile and flexural tests were analysed by the normality of the distribution of the mechanical results was evaluated using Shapiro-WilK test to evaluate their normal distribution at $p<0.05$. The means were compared using a Two-Sample t-Test or the non-parametric Kolmogorov-Smirnov test and differences were considered significantly different at $p<0.05$ (*). Additionally and in order to predict the failure probability of the developed hybrid cork composites the values obtained from the tensile tests were statistically analysed by using the two-parameter Weibull model, where the cumulative distribution function is given by the equation [66]:

$$F(x) = 1 - \exp^{-\left[\frac{x}{\alpha}\right]^{\beta}} \quad \text{, for } x > 0 \qquad (2.20)$$

where F(x) is the probability of failure of a composite material subjected to a stress level x. In equation (2), α and β are two constants to be determined, known as the “scale parameter” or “characteristic strength” and the “shaper parameter”, respectively. Finally the Kolmogorov-Smirnov test (K-S test) was employed to evaluate the goodness-of-fit to the data points.

2.3.6 Thermal properties

2.3.6.1 Thermogravimetric analysis (TGA)

The TGA involves weighing a small volume and weight of sample and exposing it to a heated chamber in the presence of nitrogen. The sample is suspended on a sensitive balance that measures the weight loss of the sample as the system is heated. Nitrogen or another gas (e.g. air), flows around the sample to remove the pyrolysis or combustion products. Weight loss is recorded as a function of time and temperature [67]. With the use of the computer software, the rate of weight loss as a function of time and temperature can also be measured. This is referred to as derivative thermogravimetric curve or DTG.

TGA was performed to understand the degradation characteristics of the cork and the natural fibres to test the thermal stability. In the case of sisal fibre was used to confirm the chemical modification. The thermal stability was determined using a TGA Q500 series thermogravimetric analyser (TA Instruments, USA). Experiments were performed in platinum pans, at a heating rate of 10 °C.min^{-1} from ambient temperature to 600 °C in nitrogen or in air atmosphere. In each chapter similar weight and geometry samples were tested. Analyses were performed in a minimum of two samples of each condition.

2.3.6.2 Differential scanning calorimetry (DSC)

- **Cork-polymer composite materials**

Differential scanning calorimetry (DSC) measurements were performed in a TA instrument DSC Q100 model (USA) equipment and using samples of 8–12 mg. DSC was conducted at a heating rate of 10 °C.min^{-1}, under nitrogen atmosphere (flux of ca. 50 ml min^{-1}). For all materials, the first scan is used for eliminating the thermal history of the material. The glass transition temperature (T_g) and melting temperature (T_m) are determined from the second heating scan. The crystallisation temperature (T_c) is obtained from the cooling scan because the samples are not quenched. T_g is determined at the mid-point of heat capacity changes, T_m at the onset peak of the endothermic and T_c at the onset peak of the exothermic. Two or three samples for each composite material were tested. By integration of the corresponding peaks, we have determined the different heats of melting and crystallization (ΔH_m and ΔH_c). These values (determined in J/g) can be corrected from a dilution effect linked to the fillers incorporation into the matrix e.g., see equation 2.14 where w is the cork fraction.

$$\Delta H'_m = \Delta H_m/(1-w) \quad (2.14)$$

The degree of crystallinity was calculated on the basis of a 100% crystalline polymer according to the equation:

$$\chi_c(\%) = \Delta H'_m/(\Delta H_m{}^0(1-w)) \times 100 \quad (2.15)$$

where $\Delta H'_m$ is the apparent enthalpy of fusion per gram of polymer and w is the weight fraction of cork in the composite. All the analysis were repeated at least once.

- **Bio-based composite materials**

Differential scanning calorimetry (DSC) measurements of the moulded specimens was assessed by DSC in a Perkin-Elmer, Pyris Diamond system at 20 °C min^{-1} under nitrogen atmosphere. The DSC scans were performed in bulk specimens cut from the central part of the rectangular cross-section of the tensile specimens. The glass transition temperature (T_g), cold-crystallization temperature (T_{cc}), melting temperature (T_m) and total enthalpy (ΔH) of all injection moulded materials were identified. The degree of crystallinity (χ_c) was calculated on the basis of a 100% crystalline a melting enthalpy of (ΔH_{m^0}) of the used polymer and according to the equation:

$$\chi_c(\%) = (\Delta H_{rec} + \Delta H_m)\ /\Delta H_m^0(1-w) \times 100 \quad (2.16)$$

where ΔH_{rec} is the enthalpy of recrystallization before melting; ΔH_m the enthalpy of melting and w is the weight fraction of cork in the composite. All the samples were repeated at least once.

2.3.6.3 Oxidation induction time (OIT)

The polymer is oxidizes in the atmosphere including Oxygen which deteriorates mechanical strength and electrical property. This decomposition by the oxidation starts from the low temperature than decomposition in an inert gas. For instance in polyethylene, the oxidation decomposition starts below than 200 °C in the air to the contrary of the thermal decomposition from the vicinity of 400 °C in the nitrogen atmosphere. For this reason, antioxidizing agents are employed to protect polyolefins such as

the polyethylene [68]. To determine if the addition of cork contributes to some positive effect the oxidation induction time (OIT) tests were concucted. OIT measurements were performed in a TA instrument DSC Q100 model (USA) equipment. Indium was used as calibration. The samples were heated at a rate of 20 °C.min-1 up to 200 °C under nitrogen atmosphere. After 4 min at 200 °C, the atmosphere was changed to oxygen (both gases at flux 50 ml.min-1) and oxidation induction time was measured during the isothermal period. The analyses were performed in three samples per each condition.

2.3.6.4 Melt flow index (MFI)

Melt Flow Index (MFI) also known as the Melt Flow Rate (MFR) is the output rate (flow) in grammes that occurs in 10 minutes through a standard die of 2.0955 mm diameter and 8.000 mm in length when a fixed pressure is applied to the melt via a piston and a load of total mass of 2.16 kg at a temperature of 190°C (some polymers are measured at a higher temperature, some use different weights). The higher a MFI, the more polymer flows under test conditions.

In the present work a Daventest (England) was used for obtaining data and allow determining melt flow index (MFI) of the neat polypropylene and of each composite material in the pellet form. Procedures were performed according to ISO 1133 [19] and ASTM D1238 [69], using 210 °C and 2.16 or 5 kg. Each condition was repeated once. For all the materials tested, the respective MFI was calculated according to:

$$MFI\ (T,L) = \frac{600 \times m}{t} \qquad (2.17)$$

In equation 2.17, T is the temperature, L is the load, m is the average weight of the extruded material and t is the time interval selected for the test.

2.3.6.5 Fire resistance tests

In designing building materials, fire resistance classification of the product is one of the most important features. Single flame fire tests were carried out according to the standard ISO 11925-2 [70]. The single flame source test was performed in specimens with dimensions of 188 x 119 mm^2 and 6 mm thick. The specimen was held vertically and a flame was applied from the bottom edge of the specimen becoming more aggressive effect on the materials. According to the standard a burning time of 15 to 20 seconds was applied and the burning dimensions after the test were registered. Three specimens

were tested for each composite during a period of 20 seconds. A filter paper is placed beneath the specimen holder to monitor the falling of flaming fragments as represented in Figure 2.19. The fire resistance classification was attributed according of the standard fire test of building materials EN ISO 13501-1 [71].

The classification for wall and ceiling products is based on the contribution to fire development the products will give in a scenario with a fire starting in a small room, by a single burning object. Classification for reaction to fire is in principle for products in their end-use application. The different classifications can be described as follows [72]:

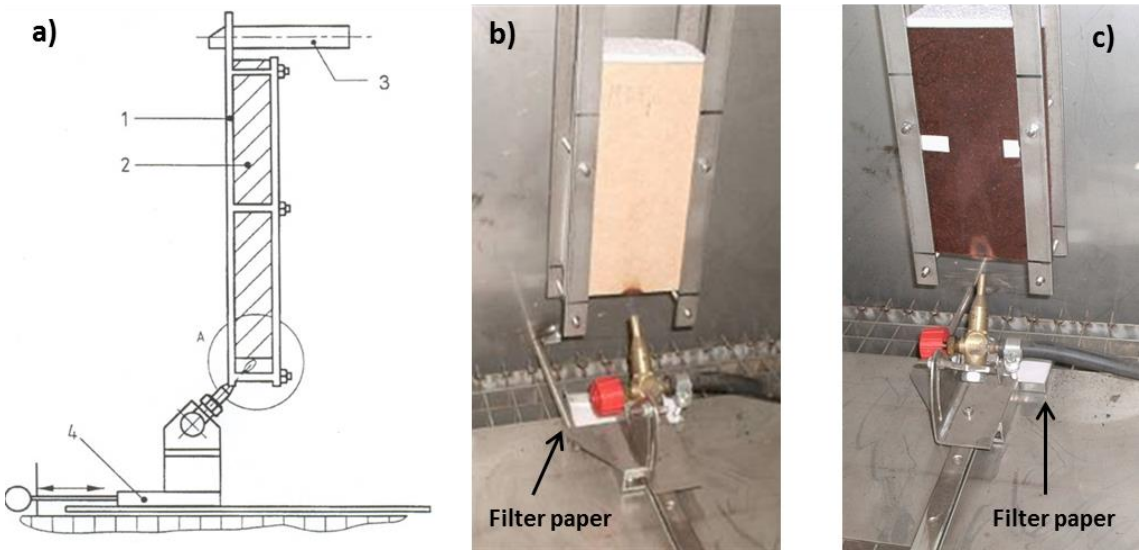

Figure 2.19. Scheme of the support type (a) presenting: 1) specimen holder; 2) specimen; 3) support; 4) base of the burner from the Standard ISO 11925-2 [70]; (b) presents the experimental test in a MDF board and (c) in a HDPE-Cork powder (50-50) wt.%.

Class A1 products will not contribute to the fire growth or to the fully developed fire;

Class A2 products will not significantly contribute to the fire growth and fire load in a fully developed fire; *Class B* products will not lead to a flashover situation, however they will contribute to the fully developed fire; *Class C* products may lead to a flashover situation, but only in the second part of the reference scenario test, i.e. after more than 10 minutes; *Class D* products may lead to a flashover situation, within the first part of the reference scenario test, i.e. within 10 minutes; *Class E* products may quickly lead to a flashover situation, possibly within the first two minutes of the reference scenario test; *Class F* no test is required.

In addition to the main classification for contribution to fire growth, additional classification parameters are assigned to a product, for smoke production and flaming droplets and particles.

2.3.6.6 Thermal conductivity and thermal resistance

The aim of this section is to analyse the differences in thermal insulation of the developed cork-polymer composites and additionally compare their properties with commercial products such as MDF and HDF.

The thermal conductivity and thermal resistance measurements were determined using the Fourier's Law that expresses the conductive heat transfer as:

$$Q = KA\,\frac{T_1 - T_2}{e} \times t \quad with\ T_1 > T_2 \qquad (2.18)$$

In equation 2.18, the amount of heat (Q) that passes through a certain sample area (*A*) in the time t is directly proportional to *A*, to the difference between the temperatures ($T_1 - T_2$) of the planes surfaces of the board and to time t and inversely to the thickness of the measured sample e [73]. *K* is the coefficient of thermal conductivity that is measured in watts per meter kelvin (*W/m.K)*.

In many construction materials are composed by several layers that are joint together by stitching or by fusion. In all cases, the way the individual layers are connected substantially affects the resulting thermal properties of the final construct. The total thermal resistance (R_t) is a thermal-property of a material to resist the flow of heat and is given by the equation [74]:

$$R_t = \frac{h_t}{\lambda}\ [m^2K/W] \qquad (2.19)$$

This parameter, calculated from the total thickness h_t and the resulting thermal conductivity, cannot always be considered as the algebraic sum of the thermic resistance of the individual layers.

The thermal conductivity (λ) of the processed board materials with 2 and 6mm of thickness were determined using the Alambeta instrument. In the present test the equipment was calibrated to use the following temperatures: T_1 = temperature of the plane surface at 32 °C and T_2 = temperature of the

plane surface at 20 °C. The sample thickness was automatically measured under constant pressure, which can be pre-set from 100 to 1000 Pa.
points.

2.4 References

[1] ISO/CD 633: Cork - Terms and definitions. 2004.

[2] Silva SP, Sabino MA, Fernandes EM, Correlo VM, Boesel LF, Reis RL. Cork: properties, capabilities and applications. Int Mater Rev. 2005;50(6):345-365.

[3] Pereira H. Cork: biology, production and uses. Amsterdam: Elsevier; 2007.

[4] Fortes MA, Rosa. ME, Pereira H. A Cortiça. Lisboa: IST Press; 2004.

[5] Halvarsson S, Edlund H, Norgren M. Properties of medium density fibreboard (MDF) based on wheat straw and melamine modified urea formaldehyde (UMF) resin. Ind Crop Prod. 2008;28:37-46.

[6] Mohanty AK, Misra M, Hinrichsen G. Biofibres, biodegradable polymers and biocomposites: An overview. Macromol Mater Eng. 2000;276-277(1):1-24.

[7] Fuqua MA, Huo SS, Ulven CA. Natural Fiber Reinforced Composites. Polym Rev. 2012;52(3-4):259-320.

[8] Bogoeva-Gaceva G, Avella M, Malinconico M, Buzarovska A, Grozdanov A, Gentile G, et al. Natural fiber eco-composites. Polym Compos. 2007;28(1):98-107.

[9] Faruk O, Bledzki AK, Fink H-P, Sain M. Biocomposites reinforced with natural fibers: 2000–2010. Prog Polym Sci. 2012;37(11):1552-1596.

[10] Li Y, Mai Y-W, Ye L. Effects of fibre surface treatment on fracture-mechanical properties of sisal-fibre composites. Compos Interface. 2005;12(1-2):141-163.

[11] Bismarck A, Mohanty AK, Aranberri-Askargorta I, Czapla S, Misra M, Hinrichsen G, et al. Surface characterization of natural fibers; surface properties and the water up-take behavior of modified sisal and coir fibers. Green Chem. 2001;3(2):100-107.

[12] Mohanty AK, Misra M, Drzal LT. Sustainable Bio-Composites from Renewable Resources: Opportunities and Challenges in the Green Materials World. J Polym Environ. 2002;10(1-2):19-26.

[13] Gahleitner M. Melt rheology of polyolefins. Prog Polym Sci. 2001;26(6):895-944.

[14] DeLassus PT, Whiteman NF. Physical and mechanical properties of some important polymers. In: Branddrup J, Immergut EH, Grulke EA, editors. Polymer Handbook. 4th Edition ed: John Wiley & Sons, Inc.; 2000. p. 59 - 68.

[15] Chung TC. Functionalization of Polyolefins. Academic Press; 2002.

[16] Mittal V. Polyolefin Nanocomposites Technology. In: Mittal V, editor. Advances in Polyolefin Nanocomposites: CRC Press Taylor & Francis Group; 2011. p. 1-21.

[17] Utracki LA. Introduction to Polymer Blends. In: Utracki LA, editor. Polymer Blends Handbook, vol. 1: Kluer Academic Publishers; 2002. p. 1-96.

[18] Muzzy JD. 2.02 - Thermoplastics—Properties. In: Kelly A, Zweben C, editors. Comprehensive Composite Materials, Oxford: Pergamon; 2000. p. 57-76.

[19] ISO 1133: Determination of the melt mass-flow rate (MFR) and the melt volume-flow rate (MVR) of thermoplastics. 1999.

[20] Ashori A. Municipal solid waste as a source of lignocellulosic fiber and plastic for composite industries. Polym-Plast Technol. 2008;47(8):741-744.

[21] Kazemi Najafi S. Use of recycled plastics in wood plastic composites – A review. Waste Manage. 2013;33(9):1898-1905.

[22] Averous L, Boquillon N. Biocomposites based on plasticized starch: thermal and mechanical behaviours. Carbohyd Polym. 2004;56(2):111-122.

[23] John MJ, Thomas S. Biofibres and biocomposites. Carbohyd Polym. 2008;71(3):343-364.

[24] Gross RA, Kalra B. Biodegradable polymers for the environment. Science. 2002;297(5582):803-807.

[25] Satyanarayana KG, Arizaga GGC, Wypych F. Biodegradable composites based on lignocellulosic fibers—An overview. Prog Polym Sci. 2009;34(9):982-1021.

[26] Wahit MU, Akos NI, Laftah WA. Influence of natural fibers on the mechanical properties and biodegradation of poly(lactic acid) and poly(ε-caprolactone) composites: A review. Polym Compos. 2012;33(7):1045-1053.

[27] Yu L, Dean K, Li L. Polymer blends and composites from renewable resources. Prog Polym Sci. 2006;31(6):576-602.

[28] Dobreva T, Perena JM, Perez E, Benavente R, Garcia M. Crystallization Behavior of Poly(L-lactic acid)-based Ecocomposites Prepared With Kenaf Fiber and Rice Straw. Polym Compos. 2010;31(6):974-984.

[29] Mohanty AK, Khan M, Sahoo S, Hinrichsen G. Effect of chemical modification on the performance of biodegradable jute yarn-Biopol® composites. J Mater Sci. 2000;35(10):2589-2595.

[30] Sobczak L, Brüggemann O, Putz RF. Polyolefin composites with natural fibers and wood-modification of the fiber/filler–matrix interaction. J Appl Polym Sci. 2013;127(1):1-17.

[31] Keener TJ, Stuart RK, Brown TK. Maleated coupling agents for natural fibre composites. Compos Part A-Appl S. 2004;35(3):357-362.

[32] Klyosov AA. Wood-Plastic Composites: John Wiley & Sons, Inc.; 2007.

[33] Araújo JR, Waldman WR, De Paoli MA. Thermal properties of high density polyethylene composites with natural fibres: Coupling agent effect. Polym Degrad Stab. 2008;93(10):1770-1775.

[34] Lei Y, Wu Q, Yao F, Xu Y. Preparation and properties of recycled HDPE/natural fiber composites. Compos Part A-Appl S. 2007;38(7):1664-1674.

[35] Adhikary KB, Pang S, Staiger MP. Long-term moisture absorption and thickness swelling behaviour of recycled thermoplastics reinforced with Pinus radiata sawdust. Chem Eng J. 2008;142(2):190-198.

[36] Koskimies S, Hulkko J, Pitkaenen P, Heiskanen N, Yli-Kauhaluoma J, Waehaelae K, et al. Method for the manufacture of oligo- and polyesters from a mixture of carboxylic acids obtained from suberin and/or cutin and the use thereof. WO2007045728-A1, Valtion Teknillinen Tutkimuskeskus, 2007.

[37] Cordeiro N, Belgacem MN, Silvestre AJD, Pascoal Neto C, Gandini A. Cork suberin as a new source of chemicals.: 1. Isolation and chemical characterization of its composition. Int J Biol Macromol. 1998;22(2):71-80.

[38] Pereira H. Química da cortiça IV. determinação da suberina em cortiça virgem e em cortiça de reprodução de Quercus suber L. Anais Instituto Superior Agronomia. 1981;40:17–25.

[39] Ekman R, Eckerman C. Aliphatic Carboxylic-Acids from Suberin in Birch Outer Bark by Hydrolysis, Methanolysis, and Alkali Fusion. Pap Puu-Pap Tim. 1985;67(4):255.

[40] Pinto PCRO, Sousa AF, Silvestre AJD, Neto CP, Gandini A, Eckerman C, et al. Quercus suber and Betula pendula outer barks as renewable sources of oleochemicals: A comparative study. Ind Crops Prod. 2009;29(1):126-132.

[41] Browning BL. Methods in Wood Chemistry. Interscience Publishers, New York.1967.

[42] John MJ, Anandjiwala RD. Recent developments in chemical modification and characterization of natural fiber-reinforced composites. Polym Compos. 2008;29(2):187-207.

[43] Huda MS, Drzal LT, Mohanty AK, Misra M. Effect of fiber surface-treatments on the properties of laminated biocomposites from poly(lactic acid) (PLA) and kenaf fibers. Compos Sci Technol. 2008;68(2):424-432.

[44] ASTM D 3878-04a: Standard terminology for composite materials. 2004.

[45] Dittenber DB, GangaRao HVS. Critical review of recent publications on use of natural composites in infrastructure. Compos Part A-Appl S. 2012;43(8):1419-1429.

[46] Bledzki AK, Jaszkiewicz A, Murr M, Sperber VE. Processing techniques for natural and wood-fibre composites. In: Pickering K, editor. Properties and performance of natural-fibre composites: Woodhead Publishing Series in Composites Science and Engineering N° 21; 2008.

[47] http://www.pallmannpulverizers.com/the_palltruder.htm. October 2013.

[48] Hanawalt K. Natural fibre extrusion. Plastics, Additives and Compounding 2002;4(11):22-25.

[49] Xanthos M. Reactive Extrusion: Principles and Practice. Hanser Publishers; 1992. p. 304.

[50] ISO 527-1: Plastics - Determination of tensile properties - Part 1: General principles. 1993.

[51] ISO 527-2: Plastics - Determination of tensile properties - Part 2: Test conditions for moulding and extrusion plastics. 1993.

[52] ASTM D638: Standard Test Method for Tensile Properties of Plastics. 2004.

[53] Injection Molding Handbook. In: Osswald TA, Turng LS, Gramann PJ, editors.: Hanser Publishers, Munich; 2001.

[54] Brooks R. 2.30 - Injection molding based techniques. In: Kelly A, Zweben C, editors. Comprehensive Composite Materials, Oxford: Pergamon; 2000. p. 999-1028.

[55] http://www.engelglobal.com/engel_web/global/en/2352.htm. November 2013.

[56] ASTM D 792 - 00: Standard Test Methods for Density and Specific Gravity (Relative Density) of Plastics by Displacement. 2000.

[57] Hu W, Ton-That M-T, Perrin-Sarazin F, Denault J. An improved method for single fiber tensile test of natural fibers. Polym Eng Sci. 2010;50(4):819-825.

[58] ASTM D570-98: Standard Test Method for Water Absorption of Plastics. Edited by ASTM International. West Conshohocken; 1998.

[59] ISO 140-8: Acoustics - Measurement of sound insulation in buildings and of building elements - Part 8: Laboratory measurements of the reduction of transmitted impact noise by floor coverings on a heavyweight standard floor. 1997.

[60] ISO 717-2: Acoustics - Rating of sound insulation in buildings and of building elements - Part 2: Impact sound insulation. 1996.

[61] ASTM D2240 - 05: Standard Test Method for Rubber Property—Durometer Hardness. 2005.

[62] ASTM C1557 - 03: "Standard Test Method for Tensile Strength and Young's Modulus of Fibers. Edited by ASTM International; 2008.

[63] ISO 178: Plastics - Determination of flexural properties. 2001.

[64] ISO 179-1: Determination of Charpy impact properties — Part 1: Non-instrumented impact test. 2000.

[65] ASTM D 256-04: Standard test methods for determining the Izod pendulum impact resistance of plastics. 2004.

[66] Caprino G, Giorleo G, Nele L, Squillace A. Pin-bearing strength of glass mat reinforced plastics. Compos Part A-Appl S. 2002;33(6):779-785.

[67] Hatakeyama T, Quinn FX. Thermal analysis: Fundamentals and applications to polymer science. Wiley; 1994. p. 1-190.

[68] High-Teck H. Oxidation Induction Time: Measurements by DSC 1988 (http://www.hitachi-hitec-science.com/en/documents/technology/thermal_analysis/application_TA_049e.pdf) accessed on October 2013.

[69] ASTM D1238: Standard Test Method for Melt Flow Rates of Thermoplastics by Extrusion Plastometer. 2004.

[70] ISO 11925-2: Reaction to fire tests - Ignitability of building products subjected to direct impingement of flame - Part 2: Single-flame source test. 2002.

[71] BS EN ISO 13501-1: Fire classification of construction products and building elements. Classification using test data from reaction to fire tests. 2002.

[72] EN 13501-1:2003 the European classification for thereaction to fire behaviour of building products. Efectis (Nederlands): Technical brochure; 2007.

[73] Pinto R, Melo B. Isolamento térmico: Aglomerados negros de cortiça e outros materiais isolantes. IPF. 1988;602:322-338.

[74] Hes L, Araújo Md, Djulay VV. Effect of mutual bonding of textile layers on thermal insulation and thermal contact properties of fabric assemblies. Textile Res J. 1996;66(4):245-250.

SECTION III – EXPERIMENTAL WORK

Chapter 3. Cork Based Composites using Polyolefin's as Matrix: Morphology and Mechanical Performance

Chapter 4. Properties of new cork-polymer composites: Advantages and drawbacks as compared with commercially available fibreboard materials

Chapter 5 – Polypropylene-based cork-polymer composites: Processing parameters and properties

Chapter 6. Functionalized cork-polymer composites (CPC) by reactive extrusion using suberin and lignin from cork as coupling agents

Chapter 7. Novel cork-polymer composites reinforced with short natural coconut fibres: Effect of fibre loading and coupling agent addition

Chapter 8. Hybrid cork-polymer composites containing sisal fibre: Morphology, effect of the fibre treatment on the mechanical properties and tensile failure prediction

Chapter 9. Cork-polymer biocomposites: assessment of biodegradability, mechanical, morphological and thermal properties

Cork based composites using polyolefins´s as matrix: morphology and mechanical performance[2]

Abstract

The cork industry produces high amounts of cork powders resulting from the final stages of cork processing or resulting from existing cork products. Usually these powders are burned and served to boilers in industrial processes. The main goal of this work is to transform this cork sub-product into a highly value composite product. The real value is dependent on the mechanical performance of this product. Thus the mixture between cork and thermoplastics, particularly the improvement of interfacial bonding, is an important topic, which needs to be developed. The interfacial affinity can be greatly increased, applying superficial modification of one of the components, or by the use of coupling agents. In this work, a high amount of cork powder (50wt.%) from different origins combined with different thermoplastic materials using melt based processes has been examined. Pultrusion was used to produce pellets and compression moulding to obtain boards to determine its properties. Coupling agents based on maleic anhydride (2wt.%) improved the tensile strength successfully, while the cork powder has an a important role in the stiffness. The morphology of the surface fractures indicated a good dispersion of the cork and a good adhesion between both phases. Thermal properties of the composites disclosed a nucleating effect promoted by cork.

[2] This chapter is based on the following publication:

Fernandes EM, Correlo VM, Chagas JA, Mano JF and Reis RL, 2010, Cork Based Composites using Polyolefin's as Matrix: Morphology and Mechanical Performance, Composites Science and Technology, 70: 2310-2318.

3.1 Introduction

Cork is the outer bark of an oak tree known botanically as *Quercus suber* L. which is periodically extracted from the tree, usually every nine to twelve years, depending on the culture region [1-3]. Cork presents a homogeneous tissue of thin-walled cells, regularly arranged without intercellular space [3, 4]. The cells are rectangular prisms, mostly pentagonal and hexagonal like a honeycomb structure (see Figure 3.1), with their axes along the tree's radial direction, stacked in columns [4, 5]. Like wood, cork is a lignocellulosic material were suberin an aliphatic polyester is the main chemical component of cork cell walls 30 - 50% [2, 6, 7] that is not present in wood cell walls. This anisotropic material has a unique combination of properties, such as a high coefficient of friction [8], resilience, imperviousness to liquids (excellent sealing ability), low thermal conductivity, low density [1], high energy absorption, excellent insulation properties, near-zero Poisson coefficient [9], fire resistant, among others, that makes it a adequate material for a variety of applications [3, 5, 10]. Every second, an area of rain forest corresponding to 19 tennis courts is lost [11], where the cork-tree offers the advantage of remain the only tree whose bark can regenerate itself after harvest, it is truly a renewable, environmentally friendly resource [2, 12].

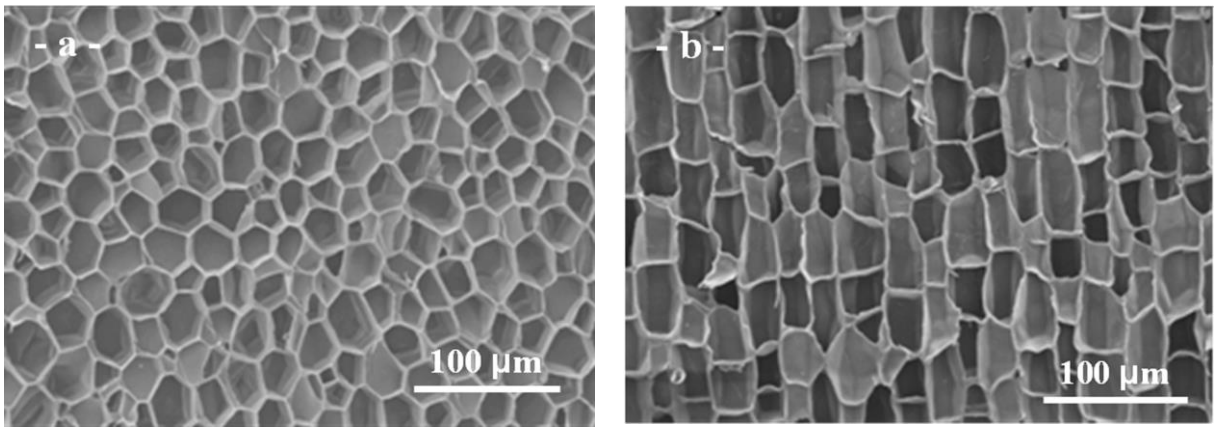

Figure 3.1. Cork morphology according a) radial direction and b) non-radial directions.

The most important sub-product provided from the different processes of cork industry is the cork powder, which possesses a high heating value, serving as raw material to feed the boilers in industrial processes [3, 13] but its commercial value is insignificant. There exist diverse types of cork powders that present different features. The most important are: the grinding powder, from granulation or pre-

grinding; the cleaning powder, without impurities; the finishing powder from cut and sanding operations or from cork disks and natural stoppers and finally the "burning powder" that comes from the mixture of these powders [13]. The degradation of cork is strongly dependent on temperature and mass losses become significant at 200 °C [14] and the colour start to change to dark brown and at 300 °C to black [15]. At lower temperatures 75 – 85 °C, only a phase transition was assigned to the melting of waxes present in cork obtained by DSC that was corroborated by dielectric spectroscopy [16, 17].

The aesthetical nature, the touch and the feeling of comfort promoted by the cork is also valued in several applications [18, 19] were its combination with other materials can improve their performance.

Cork combined with polymers leads to composites with novel properties and presents a new field of applications that contributes for the sustainability of the forestry sector. Cork-polymer composite (CPC) materials intend to combine the engineering properties of the thermoplastics with the unique described advantages of this natural origin material trough appropriated melt based technologies in order to develop products with new shapes from theses that cork can provide for acoustic, thermal insulation, energy absorbing or aesthetic applications. Earlier the industry saw in this natural material potential to be used in melt based technologies like extrusion [20-22] or to create a wood substitute material [22]. In a study performed by Barlow and Ashby [23], cork powders were mixed with different binding agents with a thermoplastic, a thermoset and a silicone rubber matrixes to create CPC. The mechanical performance of the composites decreases with the increase of cork content.

In the last years there was an increasing interest on the CPC materials [24-27] for different uses. Another study combines polypropylene with cork that was previously submitted to a surface modification to improve cork-matrix adhesion, based on a water treatment at room temperature during 1-3 h [28] and more recently some applications are looking to the valorisation of the cork powders [29-31]. The improvement of interfacial bonding, between the cork and the matrix is a field that needs to be further developed, for example by using superficial modification of one of the components or by the use of coupling agents. In other polymeric composites based on wood several studies propose different strategies to increase the interfacial adhesion between the different composite phases[32, 33]. The use of these kinds of methodologies has been scarce in materials containing cork.

In this study, cork powder with different qualities were mixed in high amounts (50wt.%), and were compounded with thermoplastic materials in a pultrusion system to create CPC pellets. These pellets were compressed moulded to obtain boards with a high dimensional stability. The effect of two coupling

agents based on a low percentage (2wt%) of maleic anhydride was analysed. The coupling agents were applied to promote adhesion between the cork-polyolefin phases, to improve tensile strength and the cork dispersion.

3.2 Experimental section

3.2.1 Cork materials

Several cork powders, from cork processing stages were collected at the Amorim Revestimentos S.A. (Portugal) industrial facilities. All of them are cork based powders coming from the processing industries namely, grinding powder, or sanding powder, external powder, cork style powder and floating powder, with density raging from 157 to 400kg.m^{-3}.

Grinding powder is mainly composed by the outer bark. This sub-product is characterized by having high density and dark brown colour (Figure 3.2), resembling the wood bark in its visual aspect. Moreover, this powder presents contaminations with silica from the sandpaper, resins, varnish and paint pigments due to the incorporation of materials for recycling.

Sanding/external powder is mainly composed of cork particles of good quality and low density. It may also present some contaminations with resins from the agglomeration glues and glue from the decorative process and some silica from the sandpaper but in very low amounts.

Corkstyle® powder is composed of high density fibreboard (HDF) formed during the machining process of the dock and cork, with a greater amount of HDF powder. The density is very similar compared with the floating powder.

Floating powder consists of cork and HDF particles. Polyvinyl chloride (PVC) particles are also presents in small amounts. Some varnish, paint pigments, resin and sinter bonding motifs may be present.

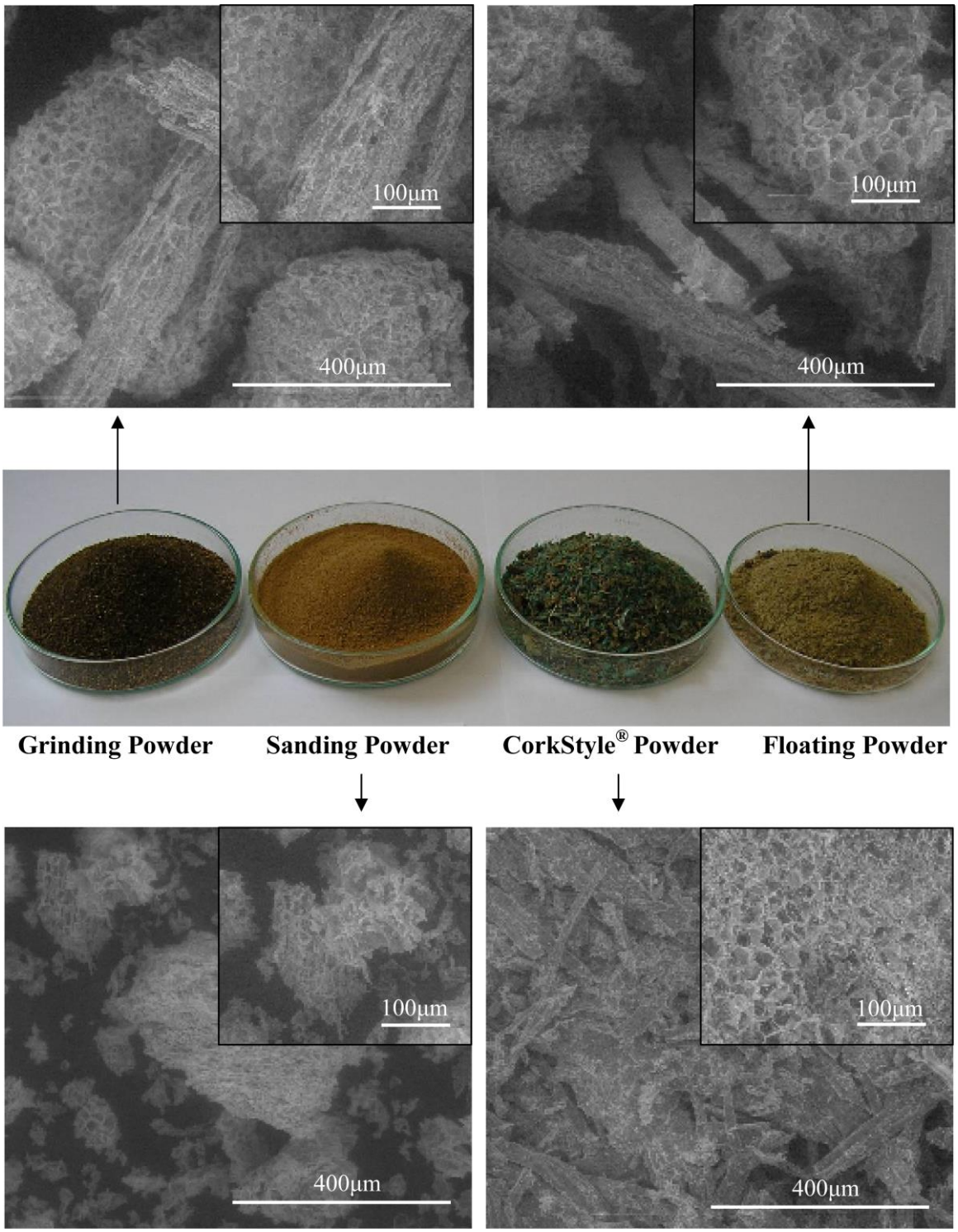

Figure 3.2. Ambiental scanning electron micrographs of each cork powder quality provide from the different steps of cork industrial process used to produce the CPC.

3.2.2 Polymer materials and coupling agents

A commercially available polyethylene (HMA – 025), PE, with a MFI of 8.2 g $10min^{-1}$ (190 °C, 2.16 kg). A polypropylene homopolymer (1374 E2), PP, with a MFI of 20.8 g $10min^{-1}$ (200 °C, 2.16 kg). Both polymers were supplied by Exxon Mobil (Germany).

A mixture of recycled polyolefins in the grinding form with a MFI of 2.4 g $10min^{-1}$ (190 °C, 2.16 kg), provided by Pallmann Maschinenfabrik GmbH and Co., Germany was also used for the preparation of composites. All tests of melt flow index were carried out according to ISO 1133.

Two different coupling agents based on maleic anhydride were used: 102 – 1 K1 MDEX for polyethylene and Po 1020 K1 for polypropylene respectively, supplied by A. Schulman GmbH, Germany.

3.2.3 Composites processing

The prepared compositions and processing conditions are summarized in Table 3.1. Before compounding all raw materials were pre-dried at 70 °C over night to stabilise the cork powders in terms of moisture content.

The different cork powders were mixed with the thermoplastics (in 50-50 wt.% ratio) in the dry form and further compounded in an industrial pultrusion system (Palltruder PFV 250, Germany) to obtain cork-polymer composite pellets (Pallmann Maschinenfabrik GmbH and Co., Germany).

In a further step, compression moulding of the obtained pellets using a hydraulic press from (Moore, UK) was applied to produce boards with 3mm of thickness from the different compositions. The mould temperature was around 150 – 170 °C depending on the thermoplastic matrix and the pressure was 1.42 MPa.

Tensile bars were obtained from these boards using a CNC machine (Roland 3D Plotter MDX-20, UK). The specimens had a neck cross-section area of 3 mm × 4 mm and a gage length of 20mm. The specimens were produced according ISO 527–2. Nevertheless, its thickness is slightly higher (3mm) than the standard.

Table 3.1. Processing conditions used for various blend and composite compositions studied

Code	Cork Powder	Polymer	Coupling Agent (wt %)	Composite (wt %)	Pultrusion Conditions		
					Temperature (°C)	Motor Current (A)	Pellets Humidity
PP-GP$_1$	Grinding	PP	—	50 – 50	160	150	0.90
PP-GP$_2$	Grinding		2	49 – 49	160	150	1.00
PP-SP$_1$	Sanding		—	50 – 50	170	120	0.20
PP-SP$_2$	Sanding		2	49 – 49	170	120	0.50
PP-EP$_1$	External		—	50 – 50	150	120	0.20
PP-EP$_2$	External		2	49 – 49	150	120	0.20
PP-CSP$_1$	Cork Style		—	50 – 50	160	130	0.50
PP-CSP$_2$	Cork Style		2	49 – 49	165	130	0.30
PP-FP$_1$	Floating		—	50 – 50	150	120	0.20
PP-FP$_2$	Floating		2	49 – 49	160	120	0.20
RP-SP$_1$	Sanding	Recycled	—	50 – 50	150	130	0.35
PE-SP$_1$	Sanding	HDPE	—	50 – 50	150	135	0.20
PE-SP$_2$	Sanding		2	49 – 49	140	120	0.20
PE-EP$_1$	External		—	50 – 50	135	130	1.01
PE-EP$_2$	External		2	49 – 49	135	130	0.35
PE-CSP$_1$	Cork Style		—	50 – 50	140	130	0.30
PE-CSP$_2$	Cork Style		2	49 – 49	130	125	0.30
PE-FP$_1$	Floating		—	50 – 50	130	130	0.35
PE-FP$_2$	Floating		2	49 – 49	130	125	0.40

3.2.4 Cork and pellets density and humidity

3.2.4.1 Cork density

The bulk density of the different cork powders was determined using a volumetric flask of 500ml were it was placed and compacted the material to minimise the possible empty spaces between the particles.

$$d = \frac{m}{v} \qquad (3.1)$$

The equation 3.1 was applied for density calculations were, d is the specific weight (Kg/m^3) of the cork raw material, m is the weight of the compact cork powder and v is the volume occupied by the cork powder into the volumetric flask. Three measurements were performed for each cork powder. The specific weight results and respective standard deviation are presented in Table 3.2.

3.2.4.2 Pellets apparent density

The apparent density of the different composite pellets, obtained after pultusion, was determined using the liquid displacement method based on the Archimedes principle. By this method, the volume of the sample is estimated by the mass of the volume that is displaced when the sample is submerged in a liquid. Thus, cork-polymer pellet samples weighting between 7 and 11g (the weight was determined with a precision nearest to 0.0001g) were it was added distillate water to fulfil the empty spaces between the pellets. Special care was taken to avoid the presence of air bubbles. This procedure was performed three times for each condition.

3.2.4.3 Moisture

The percentage of humidity of the different cork powders was determined using a balance Sartorius (Sartorius AG, Germany) were the cork powder was submitted to 105 °C during a period of 10min. This procedure was performed three times for each cork powder sample and the results are presented in Table 3.2.

3.2.5 Scanning electron microscopy

The morphological characterization of the developed cork-polymer composites fracture surface was performed using a Leica-Cambridge S-360 (UK) scanning electron microscope. All the samples were sputter-coated with gold before being analysed. The cork powders were analysed using a Quanta 400 FEG model (FEI, USA) ambiental scanning electron microscope with low vacuum to avoid any possible desire effect in the natural raw material structure.

3.2.6 Thermal properties

The differential scanning calorimetric experiments were performed in a TA instrument DSC Q100 model (USA), using a refrigerated cooling system and nitrogen as a purge gas (flux gas of ca. 50 ml min^{-1}). Both temperature and heat flux were calibrated with Indium at a scanning rate of 10 °$Cmin^{-1}$. The samples were obtained by cutting a small piece of material (with 5 to 5.5 mg weight) in the central region of the composite pellets parts. An effort was made to maintain the geometry of the different samples, in order to keep the same thermal resistance. All the experiments were performed at 10 °$Cmin^{-1}$, starting from room temperature. Only the second run was analyzed for melting temperature (T_m) and melting enthalpy (ΔH_m), which reflects the effect of the cork material contained in the composite avoiding the morphology effect developed during the processing. The crystallinity values of the polymeric phase were determined from the cooling cycle using the following equation:

$$\text{Degree of Crystallinity (\%)} = (\Delta H_m / \Delta H_{m^\circ}) \times 100 \qquad (3.2)$$

Where, ΔH_m is the melting enthalpy of the polymer and ΔH_{m° is the enthalpy of 100 % crystalline PP (ΔHm° = 209 J/g) [34].

3.2.7 Optical microscopy

To understand the nucleating ability of cork on the matrix, a single cork powder was sandwiched between two thin PP films and heated at 200 °C during 10 min to erase the previous thermal history of the sample. Then, the sample was quickly shifted to a well-controlled temperature stage (Linkam, THMS-600) where the pre-determined crystallization temperature was maintained at 140 °C for 1 h, to access to the crystallization process. A fast cooling was estimated to be 80 °C min^{-1} was used to reach the isothermal crystallization temperature. Dry nitrogen was introduced to eliminate any possible degradation in all cases. The crystallization of PP on the cork powder was observed on an optical microscope (Olympus B) connected to a Leica digital camera.

3.2.8 Mechanical properties and statistical analysis

The tensile properties were determined using a Universal tensile testing machine (Instron 4505 Universal Machine, USA) using a load cell of 1 KN. The tensile force was taken as the maximum force

in the force deformation curve. Tensile modulus was estimated from the initial slope of the stress–strain curve (between 0.05% and 1% strain) using the linear regression method. Samples were conditioned at room temperature for at least 48 h before testing. A crosshead speed of 5mm min^{-1} was used up to a deformation at break. The average and standard deviations were determined using seven specimens. The normality of the distribution of the mechanical results was evaluated using Shapiro-WilK test confirming their normal distribution at p <0.05. The results were compared using a two-sample t-test and differences were considered significantly different at p<0.05 (·).

3.3 Results and Discussion

3.3.1 Characterization of the cork powders

The different cork powders used on this study were physically and morphologically characterized before compounding. The used powders and some of their characteristics are presented in Table 3.2 and in Figure 3.2. Since the sanding powder and the external powder are very similar, a mixture of the referred powders was used in the work. Of the analysed cork powders, the grinding powder was the one with higher specific weight (409 ± 6 kg m^{-3}). This residual powder was also the one with the highest moisture content (18%) probably due to the presence of the wood present from the outer bark that is more hydrophilic than cork.

The sanding/external powder is the powder with lowest specific weight (157 ± 2 kg m^{-3}) and lower range of particle size distribution (60% of particle size less than 0.25mm). This material was also the one presenting the lowest humidity (around 5.4%).

The Corkstyle® powder and the floating powder presents a specific weight of 273 ± 6 kg m^{-3} and 256 ± 7 kg m^{-3} respectively. In terms of humidity the values are very similar and regarding the particle size distribution, the floating powder has a higher content of small particles (around 58%) less than 0.25 mm. Table 3.2 also reports the humidity present in the different powders before the preparation of the composite materials. Since the cork sub-products tend to absorb moisture, all the natural raw materials were pre-dried overnight in a vacuum oven to stabilize. The percentage of humidity present was around 2.65 - 4.18%.

Table 3.2. Type of cork powders and their characteristics in terms of distribution size, specific weight and the percentage of moisture, used for preparing cork based composites.

	Quality of cork residue			
Granulometry mesh (mm)	**Floating**	**Corkstyle**	**Grinding**	**Sanding/ External**
	%	**%**	**%**	**%**
> 4	1	0.4	0	0
2.8 – 4	1.9	2.6	0	0
2 – 2.8	4	8.1	0.2	0
1 – 2	10.2	2.2	0.3	0.7
0.5 – 1	10.3	**22.1**	**42.9**	7.6
0.25 – 0.5	**14.2**	13.1	**34.2**	3.5
< 0.25	**58.4**	**26.5**	**22.4**	**88.2**
Sum	100	100	100	100
Specific weight Kg/m³	256 ± 7	273 ± 6	409 ± 6	157 ± 2
Initial Humidity (%)	5.8 ± 0.4	6.4 ± 0.1	18.0 ± 0.3	5.4 ± 0.1
After Drying * Humidity (%)	2.7 ± 0.3	3.5 ± 0.2	4.2 ± 0.2	3.2 ± 0.1

* Humidity % present after dry in a vacuum oven during overnight at 70°C.

3.3.2 Composite morphology

Fracture surfaces after mechanical tests of the cork-polymer composites, obtained by scanning electron microscopy, are shown in Figure 3.3.

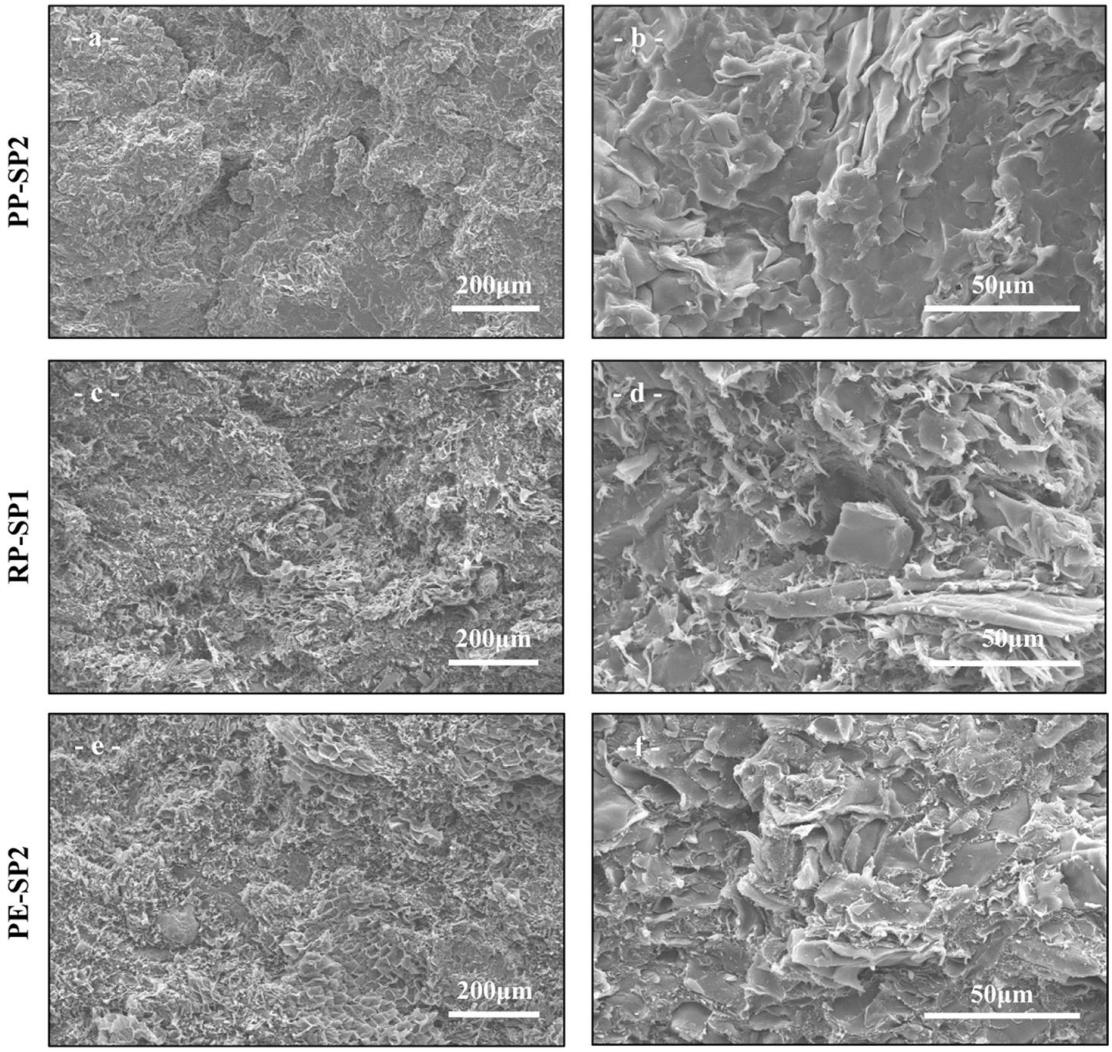

Figure 3.3. Morphology of the tensile-fracture surface of cork polymer composites. Figure a and b: PP-SP2; c and d: RP-SP1; e and f: PE-SP2.

In the micrographs is possible to observe the good dispersion of cork sanding powder in the different thermoplastic matrixes. At high magnifications the fracture surface of cork sanding powder with PP and 2wt% of coupling agent (Figure 3.3 b) indicates good adhesion between both phases of the composite. The same behaviour was observe for the PE matrix (Figure 3.3 e and f); while the cork sanding powder mixture with the recycled polymers at a high magnifications (Figure 3.3 d) demonstrate some pull out of the polymeric phase and some regions with gap between both phases. This may be due to the lower mechanical properties of this matrix since is a mixture of different grade of recycled plastics that could contain some impurities and due to the absence of coupling agent to improve the interface bonding.

3.3.3 Pellets density

Figure 3.4 indicates the apparent density of the cork-polymer composite pellets after the pultrusion process for all tested compositions presented in Table 3.1. The results indicate an important decrease in the density compared with the density of the matrix PE (964 kg m^{-3}) and PP (900 kg m^{-3}).

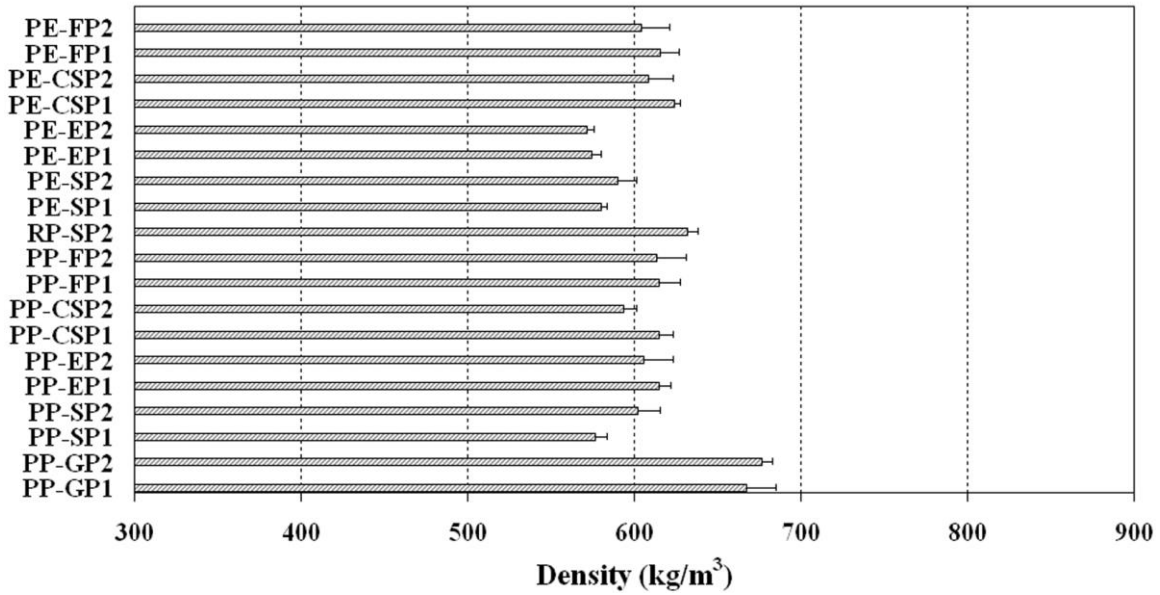

Figure 3.4. Density of the CPC pellets after the pultrusion process.

The pellets density is around 580-630 kg m^{-3} except for grinding cork powder with higher specific weight (see Table 3.2). The higher the density of the cork powder the superior is the density of the pellet composite. The production of composites by pultrusion process using high amounts of cork powder allows obtaining light weight composite materials. After compression moulding process of the pellets the final density of the composites is higher and very similar (1000 to 1060 kg m^{-3}) independently of the cork sub-product used.

3.3.4 Crystallization and melting properties

Thermal properties of all materials prepared were investigated by DSC. Representative DSC curves for the composites and pure PP are shown in Figure 3.5. The results are summarized in Table 3.3.

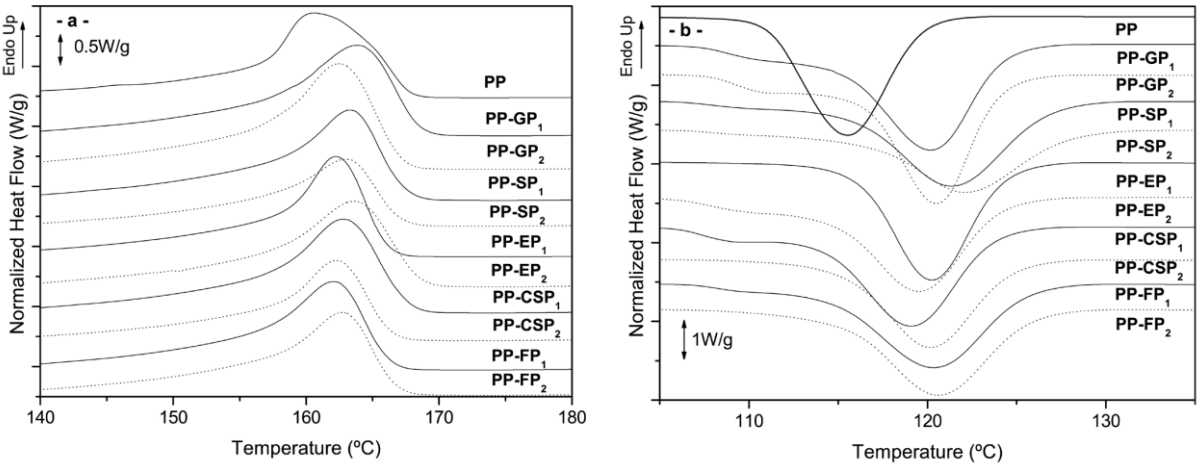

Figure 3.5. Representative DSC thermograms, obtained at 10°Cmin^{-1} of the CPC materials using PP as matrix of the composite (a) second heating step and (b) first cooling step.

Pure PP presents a onset crystallization temperature (Tc) of 119.7 °C. Comparing the pure PP with the cork-polymer composites, the T_c shifted to higher temperatures in the case of the composites. The increase of T_c could be considered to be due to the nucleation effect of cork present in the composites. Melting temperatures (T_m) of pure PP was 153.5 °C. The T_ms of the PP was not significantly affected by the addition of cork during the pultrusion process. Therefore, the addition of cork powders in PP does not have a significant influence on the thickness of the crystalline lamellar of the matrix. Values of ΔH_m provide important information about the crystallinity and shows significant variations in the composites. These results lead us to conclude that the addition of cork powder increases the crystallinity of the polymer in the most part of the compositions.

Table 3.3. Melting temperatures and enthalpies, crystallization temperatures and crystallinity degrees of CPC composites with PP as matrix.

Sample	T_c[a] (°C)	ΔH_c[a] (J/g)	χ_c[c] (%)	T_m[b] (°C)	ΔH_m[b] (J/g)	χ_c[c] (%)
PP	119.7	99.1	47.4	153.5	91.5	43.8
PP-GP$_1$	124.3	57.2 (114.4)	27.4 (54.7)	155.0	55.3 (110.6)	26.46 (52.9)
PP-GP$_2$	124.2	61.8 (126.1)	29.6 (58.0)	155.2	60.5 (123.5)	28.9 (56.8)
PP-SP$_1$	126.9	51.3 (102.6)	24.5 (49.1)	155.8	50.9 (101.8)	24.4 (48.7)
PP-SP$_2$	128.0	40.7 (83.1)	19.5 (38.2)	154.7	39.4 (80.4)	18.9 (37.0)
PP-EP$_1$	124.4	49.6 (99.2)	23.7 (47.5)	156.8	48.7 (97.4)	23.3 (46.6)
PP-EP$_2$	124.2	54.9 (112.0)	26.3 (51.5)	155.0	52.9 (108.0)	25.3 (49.6)
PP-CSP$_1$	124.0	55.7 (111.4)	26.7 (53.3)	155.3	53.7 (107.4)	25.7 (51.4)
PP-CSP$_2$	124.9	43.2 (88.2)	20.7 (40.5)	156.2	42.4 (86.5)	20.3 (39.8)
PP-FP$_1$	125.6	50.7 (101.4)	24.3 (48.5)	154.2	49.4 (98.8)	23.6 (47.3)
PP-FP$_2$	126.0	48.5 (99.0)	23.2 (45.5)	155.2	47.3 (96.5)	22.6 (44.4)

( ) Values divided by the weight proportion of polymer

[a] Crystallization temperature and enthalpy at second cooling from the melt at 10°C.mm^{-1}

[b] Melting temperature and enthalpy determined by DSC on the second heating at 10°C.mm^{-1}

[c] Crystallinity degree calculated on the basis of a ΔH_m value of 209 J/g for 100% crystalline PP [35].

3.3.5 Optical microscopy

Figure 3.6 presents the initial crystallization process of PP in the presence of the cork powder particle. The results suggest that this process takes place preferably at the surface sites of cork. Nevertheless once can observe simultaneously with this process the growth of individual of spherulites in the matrix. When cork is embedded into a thermoplastic melt it may act as a nucleating agent during the crystallization process. The result is more evident on Figure 3.6 c) in polarized light where it confirms the high number of spherulites around the cork. This nucleation effect is different from other fibres used in composites. In this case no transcrystalline layer on the cork usually found in semicrystalline thermoplastic composites with different synthetic or natural fibres [35-37] was observed. The present effect it is in accordance with the previous DSC results indicating the nucleation ability of cork.

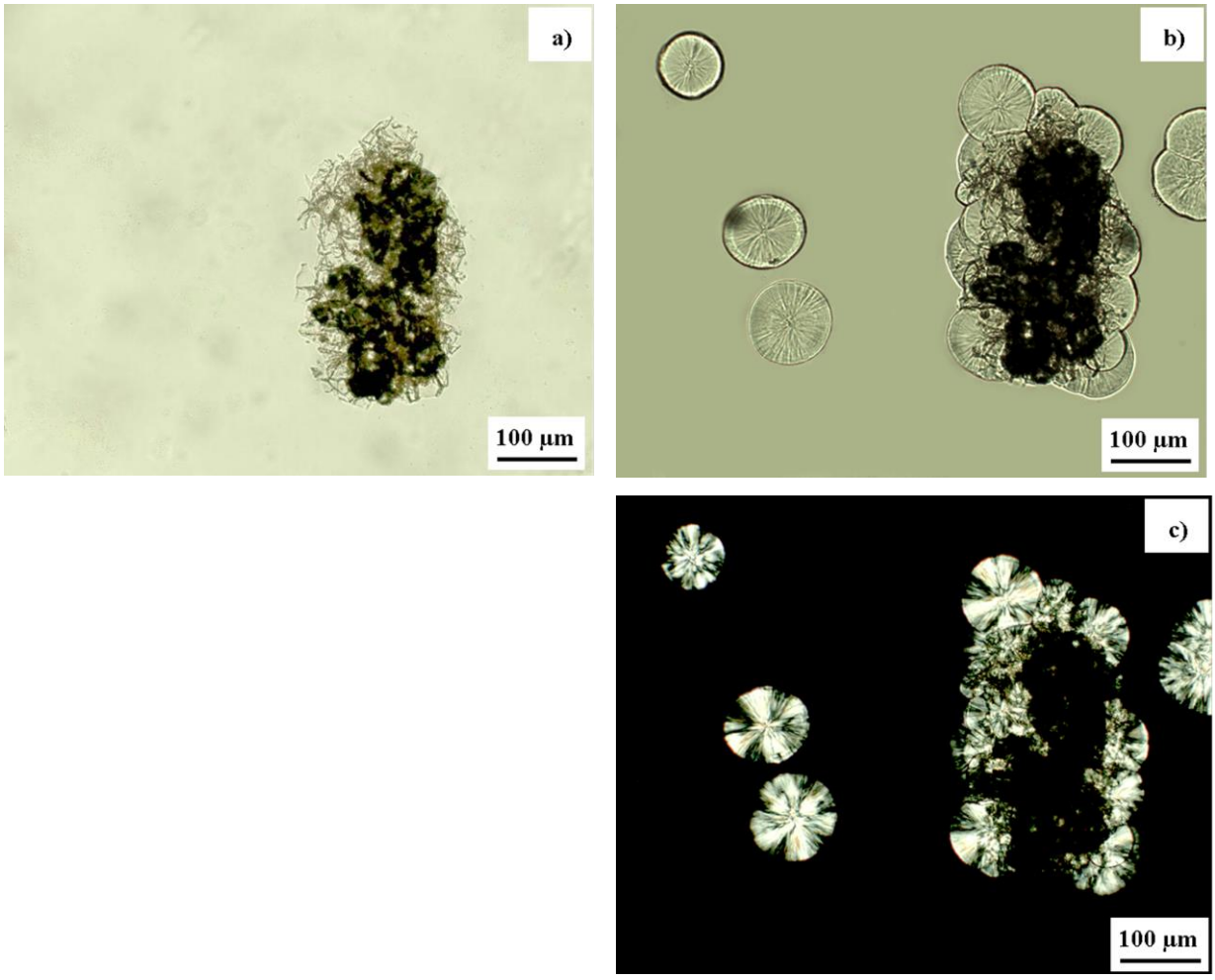

Figure 3.6. Optical micrographs showing the crystallization of PP in the presence of cork: figure a: 5min; b: 45min and c: 45min (Tc = 140°C, polarized light).

3.3.6 Mechanical properties of composites

In order to characterize the mechanical performance of the developed cork based composites, tensile tests were performed. Figure 3.7and Figure 3.8 summarizes the obtained results, in terms of tensile modulus and maximum tensile stress, for composites prepared with PP and PE matrices, respectively. One formulation consisting of recycled polyolefin's and cork sanding powder was also compounded and characterized (Figure 3.8). All results are expressed as means ± standard deviation.

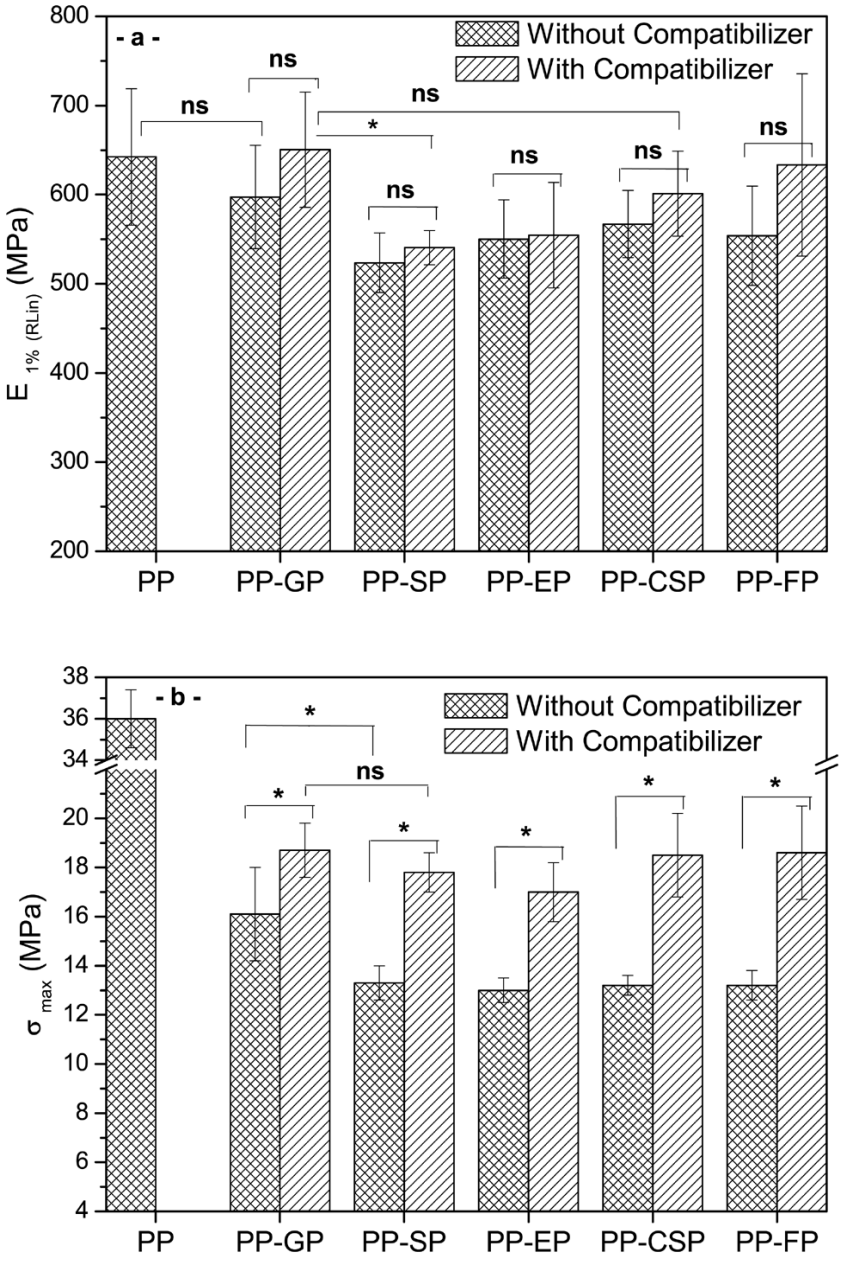

Figure 3.7. Tensile properties of various CPC materials using PP as matrix. (*) significant at 0.05; ns: non-significant at 0.05.

Considering the data from both Figure 3.7 and Figure 3.8, it is clear that composites prepared using PP as matrix are the ones with better mechanical performance, being the condition PP-GP1 the one with the highest stiffness and strength absolute values.

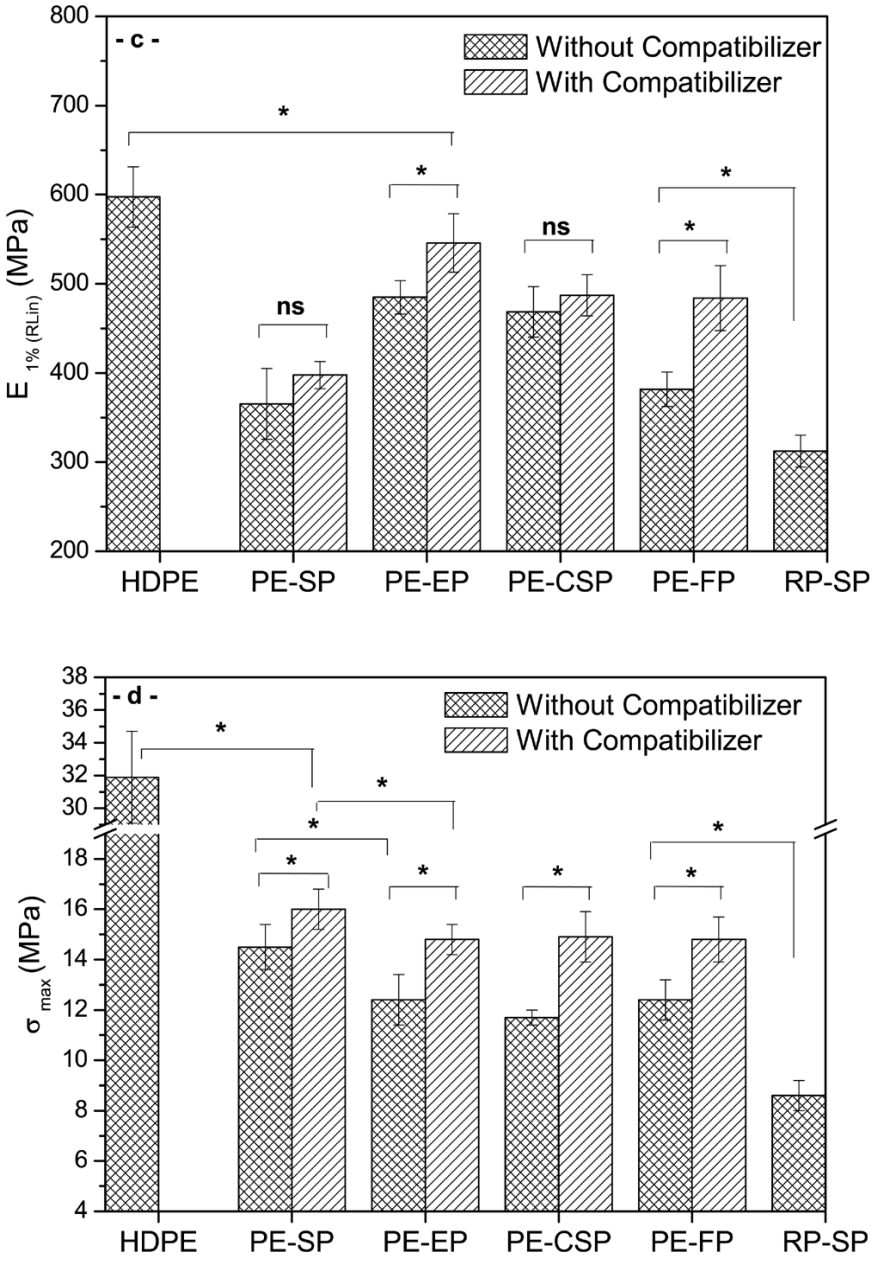

Figure 3.8. Tensile properties of various CPC materials using PE and recycled polymer as matrix. (*) significant at 0.05; ns: non-significant at 0.05.:

Two reasons can be used to explain the better performance of this composition: (i) pure PP has better mechanical properties than PE; (ii) the grinding powder (Fig. 2) is mainly composed of the outer bark that is denser and very similar to wood and could work as a more effective reinforcement. In general, composites from PP exhibited mean tensile modulus and maximum stress values respectively in the intervals [523.6 – 650.5] MPa and [13.0 – 18.7] MPa, depending on the type of cork powder used.

Composites prepared using PE as matrix and the different cork based powders displayed mean compressive modulus and maximum stress values respectively in the intervals [365.3 – 545.8] MPa and [12.4 – 16.0] MPa. Almost no correlation between the type of cork powders used and the final mechanical performance of the composites was observed.

Considering the formulation with best performance for each type of matrix used, the addition of 50 wt.% of cork powder in the most part of the compositions did not affect significantly ($p < 0.05$) the modulus of the final product, especially for the composites prepared with PP. Nevertheless, a decrease higher than ~50% on the strength was noticed.

As expected, the addition of a small amount (only 2 wt.%) of coupling agents (102 – 1 K1 MDEX for PE and Po 1020 K1 for PP) resulted in a significantly improvement ($p < 0.05$) of the mechanical performance in all the formulations studied. This effect is more pronounced on the strength of composites prepared using PP as matrix and increases up to 40.9 % (condition PP-FP_2) were achieved with the addition of Po 1020 K1 coupling agent. This is a clear indication that the use of a coupling agent improved the interfacial adhesion between the matrix (PP or PE) and the cork based powder used. Several studies on the literature report the positive effect of using coupling agents on the mechanical properties of composites [31, 33].

3.4 Conclusions

The following conclusions can be made base on the results presented in this work. SEM observation revealed well dispersed cork powders in the compression moulded samples after the pultrusion (pellets) and compression moulding processes. As expected, the tensile modulus and tensile strengths were significantly increased in the composites with the introduction low amounts (2 wt.%) of coupling agents to promote the adhesion between the cork-polymer phases. No significantly correlation between the type of cork powders used and the mechanical performance of the composites was observed. Cork powders that presents some wood particles induces similar stiffness only in the PP matrix, probably because the powder composition is based on outer bark and has higher density. The recycled polymer based on polyolefin's combined with the cork sanding powder reveal the lowest mechanical performance. The increase of the crystallinity on the composites occurred due to the addition of the cork powder, where cork presents a nucleation effect. By polarized optical microscopy it was confirmed that cork accelerates the crystallization process. The results of the present work clearly show that cork powders and polyolefin's can be successfully used to produce CPC with high cork content. In order to

obtain cork based composite materials with enhanced mechanical properties, reinforcement strategies must be taken in consideration.

3.5 References

[1] Gibson LJ. Cellular solids: structure and properties. 2nd ed.; Cambridge University Press: Cambridge, 1997.

[2] Gil L, Moiteiro C. Cork. Ullmann's Encyclopedia of Industrial Chemistry: Willey - VCH, Weinheim, 2002.

[3] Silva SP, Sabino MA, Fernandes EM, Correlo VM, Boesel LF, Reis RL. Cork: properties, capabilities and applications. Int Mater Rev 2005;50(6):345-365.

[4] Pereira H, Rosa ME, Fortes MA. The Cellular Structure of Cork from Quercus-Suber L. Iawa Bull 1987;8(3):213-218.

[5] Gibson LJ, Easterling KE, Ashby MF. The Structure and Mechanics of Cork. P Roy Soc Lond A Mat 1981;A 377:99-117.

[6] Pereira H. Chemical Composition and Variability of Cork from Quercus-Suber L. Wood Sci Technol 1988;22(3):211-218.

[7] Holloway PJ. Some variations in the composition of suberin from the cork layers of higher plants. Phytochemistry 1983;22:495-502.

[8] Vaz MF, Fortes MA. Friction properties of cork. J Mater Sci 1998;33(8):2087-2093.

[9] Fortes MA, Nogueira MT. The Poisson Effect in Cork. Mat Sci Eng A-Struct 1989;122(2):227-232.

[10] Pires RA, Mano JF, Reis RL. Surface properties of extracts from cork black condensate. Holzforschung 2010;64:217-222.

[11] Halada K. Progress of ecomaterials toward a sustainable society. Curr Opin Solid St M 2003;7(3):209-216.

[12] Pereira H. Cork: biology, production and uses. Amsterdam: Elsevier, 2007.

[13] Gil L. Cork powder waste: An overview. Biomass Bioenerg 1997;13(1-2):59-61.

[14] Pereira H. The Thermochemical Degradation of Cork. Wood Sci Technol 1992;26(4):259-269.

[15] Rosa ME, Fortes MA. Temperature-Induced Alterations of the Structure and Mechanical-Properties of Cork. Mater Sci Eng 1988;100:69-78.

[16] Mano JF. The viscoelastic properties of cork. J Mater Sci 2002;37(2):257-263.

[17] Mano JF, Correia NT, Ramos JJM, Saramago B. The Molecular Relaxation Mechanisms in Cork as Studied by Thermally Stimulated Discharge Currents. J Mater Sci 1995;30(8):2035-2041.

[18] Farag MM. Quantitative methods of materials substitution: Application to automotive components. Mater Design 2008;29(2):374-380.

[19] Matos MJ, Simplício MH. Innovation and sustainability in mechanical design through materials selection. Mater Design 2004;27:74-78.

[20] Improvements in or relating to extrudable compositions. GB 657 813 A, Armstrong Cork Co, 1951.

[21] Improvements in or relating to extrudable cork compositions. GB 646955 A, Armstrong Cork Co, 1950.

[22] Method of preparing wood substitute. GB 1395105 Idemitsui Kosan Co Ltd, 1975.

[23] Barlow CY, Ashby MF. Cork dust composites. in Proceedings of the Riso International Symposium on Metallurgy and Materials Science. 1989.

[24] Chong VC. Balls for use in baseball and softball. US 20040142779 A1, 2004.

[25] Cosby SA, Kelly M, VAN WB. Silicone-cork ablative material. EP 1482163 A2, United Technologies Corp., 2005.

[26] Antunes PJ, Dias GR, Coelho AT, Rebelo F, Pereira T. Hyperelastic Modelling of Cork-Polyurethane Gel Composites: Non-linear FEA Implementation in 3D Foot Model. 2008;587-588:700-705.

[27] Gil L. Cork Composites: A Review. Mater Design 2009;2:776-789.

[28] Abdallah FB, Cheikh RB, Baklouti M, Denchev Z, Cunha AM. Characterization of composite materials based on PP-cork blends. J Reinf Plast Comp 2006;25(14):1499-1506.

[29] Claro JCAR, Valente AJRP. Particle agglomeration process for wood and cork industrial sectors WO 2008/114103 (A1), WO 2008114103 A1, Universidade de Trás-os-Montes e Alto Douro, 2008.

[30] Fernandes EM, Silva VM, Chagas JAM, Reis RL. Cork-polymer composite (CPC) materials and processes to obtain the same. WO2009072914-A1, Amorim Revestimentos, S.A., 2009.

[31] Bledzki AK, Reihmane S, Gassan J. Thermoplastics reinforced with wood fillers: A literature review. Polym-Plast Technol Eng 1998;37(4):451-468.

[32] Bledzki AK, Faruk O. Creep and impact properties of wood fibre-polypropylene composites: influence of temperature and moisture content. Compos Sci Technol 2004;64(5):693-700.

[33] Bengtsson M, Stark NM, Oksman K. Durability and mechanical properties of silane cross-linked wood thermoplastic composites. Compos Sci Technol 2007;67(13):2728-2738.

[34] Yılser GD, Zakir MO, Rzaev EP. Functionalization of isotactic polypropylene with citraconic anhydride. Polym Bull 2007;59:447–456

[35] Wang C, Liu CR. Transcrystallization of polypropylene composites: nucleating ability of fibres. Polym 1999;40(2):289-298.

[36] Pompe G, Mäder E. Experimental detection of a transcrystalline interphase in glass-fibre/polypropylene composites. Compos Sci Technol 2000;60(11):2159-2167.

[37] Arbelaiz A, Fernández B, Ramos JA, Mondragon I. Thermal and crystallization studies of short flax fibre reinforced polypropylene matrix composites: Effect of treatments. Thermochim Acta 2006;440(2):111-121.

Properties of new cork-polymer composites: Advantages and drawbacks as compared with commercial available fibreboard materials[3]

Abstract

Cork powder (50 wt%) was mixed with polypropylene (PP) or polyethylene (PE) by pultrusion aiming to prepare cork-based composites. In a further step, samples were produced by compression moulding using the compounded composites. Bending strength, impact resistance, hardness, dimensional stability, thermal and acoustic properties of the developed cork-polymer composites (CPC) were determined and compared with commercially available products namely medium density fibreboard (MDF) and high density fibreboard (HDF). It was found that the CPC have good dimensional stability, lower water uptake, a better acoustic insulation performance and similar behaviour in terms of hardness and fire resistance when compared with both MDF and HDF. However, the mechanical strength is inferior comparing with both commercial materials based on fibres. It was also observed that addition of cork improved the flexural modulus, impact resistance and hardness on the developed CPC. Thus, the herein described CPC materials showed important characteristics to be considered as good candidates to be applied in the design of flooring and construction systems.

[3] This chapter is based on the following publication:

Fernandes EM, Correlo VM, Chagas JA, Mano JF and Reis RL, 2011, Properties of new cork-polymer composites: Advantages and drawbacks as compared with commercially available fibreboard materials, Composite Structures, 93: 3120-3129.

4.1 Introduction

Wood polymer composites (WPC), have successfully proven their applicability in several fields, particularly in the construction sector, due to their aesthetics (similar to wood), easy processability and low maintenance costs [1]. The use of lingocellulosics materials as fillers and reinforcement with thermoplastics has been gaining acceptance in commodity plastic applications [2]. Similar to wood, cork is a natural, renewable and sustainable raw material [3-5] with an unexploited potential to be used on the development of partially or completely natural based composites [6-9].

Cork is the bark of an Oak tree known botanically as *Quercus suber L.* [10] which is periodically extracted from the tree, usually every nine to twelve years, depending on the culture region and is of the highest importance for the forest economy of the Southern European countries and China [4, 10]. The cork-tree offers the advantage of being the only tree whose bark can regenerate itself after harvest, making it a truly renewable material. In terms of morphology, cork can be described as an anisotropic material with close cellular structure and thin-walled cells. Furthermore, cork presents a alveolar structure similar to a honeycomb according the radial direction and in the other directions (transversally) is a isotropic material where the cells are described as rectangular prisms packed base to base in columns parallel to the radial direction of the tree [11, 12]. A thickness of 1mm corresponds about thirty layers of cells [13].

Cork can be seen as a natural composite constituted by different groups of compounds. The chemical composition includes [4, 10]: suberin, an aliphatic polyester, usually present in high concentrations 33-50%; lignin, an aromatic polymer, corresponding to the second most abundant structure in cork with 13-29%; polysaccharides, including cellulose and hemicelluloses, that are usually present at concentrations in the range of 6-25%; and the extractable components at concentrations in the range 8.5-24%.

The structural properties of lingocellulosic materials like cork are strongly dependent on temperature. Thermal decomposition of cork has been studied by thermogravimetry [14] and the results have shown that the mass decreases about 30% upon heating at 300°C and less than 10% at 200°C [15]. It was also observed that the chemical degradation starts at about 250°C, in air, indicating that cork can be heated up to 250°C without inducing irreversible changes in its composition. Chemical methods [16, 17] and scanning electron microscopy [16] were also applied and the results demonstrated that waxes and other soluble components of cork begin to decompose at ca. 150°C and that cork is transformed

into ash for temperatures above 450°C. Polysaccharides are considered the most heat sensitive component of cork [18]. Mass spectroscopy [19] and ^{13}C solid-state NMR studies [17] reveal that at 400°C cork has been transformed into coke with traces of partially decomposed suberin.

The most important sub-products resulting from cork manufacturing are different types of cork powders. Part of these powders are used as fuel on industrial furnaces, while the remaining portions are usually disposed in landfills [20, 21]. The strategy of combining cork powder with polymeric matrixes [9, 21, 22], to produce composites, has received little attention by the research community. However, cork properties can provide several advantages in the development of composites containing bio-based components. Among other advantages, cork has a low density (120 – 240 kg m^{-3}), can be regarded as a hydrophobic and viscoelastic material, that possess high thermal and acoustic insulation properties, low thermal conductivity, fire resistance, aesthetic features and resistance to microbial activity [3, 4, 13, 23]. Moreover, cork powder is widely available, sustainable, recyclable and of low cost.

The development of appropriated methodologies for the valorisation of this bio-based resource is of high interest [9]. In this work two melt based technologies were used to produce cork-polymer composites (CPC) materials: pultrusion to compound and obtain pellets of two different composites (cork powder + PP and cork powder + PE, in both cases a 50/50 wt.% ratio was used) and compression moulding to produce boards with adequate characteristics to be applied as core in flooring systems, furniture and building applications. The use of a core based on CPC in alternative to the MDF could be regarded as a new type of flooring able to compete in the field of the floating floor coverings. For instance, wood-plastic composites have shown distinctly better behaviour than the MDF and natural wood after moisture exposure [24]. The growing of environmental awareness has resulted in a renewed interest in the use of natural materials with environmentally friendly characteristics [25]. Formaldehyde-based adhesives are currently used for fibreboard manufacture where the major drawback of using this resin is the presence of volatile organic compounds harmful to human health [26, 27].

In this study, different boards - produced using the CPC composites, the MDF and the HDF - were submitted to extensive characterization tests and the obtained results compared. The main goal was to prove and validate the potential of using the cork-based composites on the production of boards as core for floating floor coverings application. We selected to test MDF and HDF boards as control since they are the most widely used wood composites applied as building material, housing furniture and in laminated flooring [26-28].

4.2 Experimental section

4.2.1 Cork powder and fibre materials

The cork powder resulting from cork processing stages such as, sanding and external operations, was collected at Amorim Revestimentos S.A. (Oleiros, Portugal) industrial facilities. The cork powder presents a particle size of $\leq$ 250 μm, bulk density of 157 ± 2 kg m^{-3} and a humidity of ~5.4%. It was also used two different types of fibreboard materials as control: HDF with density of 920.3 ± 6.7 kg m^{-3} and MDF with density of 822.7 ± 2.7 kg m^{-3} both of them with a resin content of 8 wt.% and supplied by Sonae Industria SGPS, S.A (Maia, Portugal).

4.2.2 Polymeric materials

A commercially available high density polyethylene (HMA – 025), HDPE, containing a thermal stabilizer and with a MFI of 8 g 10 min^{-1} and a polypropylene homopolymer (1374 E2), PP, with a MFI of 21 g 10 min^{-1} were used on composites preparation. Both polymers were supplied by Exxon Mobil (Germany). More details on the properties of these polymers are reported in Table 4.1.

Table 4.1. Properties of the polymeric matrixes.

Polymer Matrix	Property	Value
HDPE	Melting temperature (°C) obtained by differential scanning calorimetry (DSC)	136.6
	Melt flow index (g 10 min^{-1}) at (T= 190 °C, load = 2.16 kg)	8.27
	Density* (kg m^{-3})	960.3
PP	Melting temperature (°C) obtained by differential scanning calorimetry (DSC)	153.5
	Melt flow index (g 10 min^{-1}) at (T= 200 °C, load = 2.16 kg)	20.86
	Density* (kg m^{-3})	900.9

* Density according to the standard ASTM D 792.

4.2.3 Composites processing

Before compounding all raw materials were dried (at 70 °C) over night in a vacuum oven (Binder, Germany). Before compounding the moisture content on the cork powder was ≤ 3 %. Two different cork-based composites – one consisting of cork powder with PE and other consisting of cork powder with PP (in both cases 50-50 wt.% ratio was maintained) – were compounded using an industrial pultrusion system (Palltruder PFV 250, Germany). The CPC consisting of HDPE with cork powder will be referred as PE/Cork and the one from PP and cork powder as PP/Cork.

The composites, as pellets, were further compression-moulded using a Moore hydraulic press (UK) to produce rectangular boards of 220×220×6 mm^3. The principal processing conditions are reported in Table 4.2 and are similar to the ones used in previous work [9]. Flexural, impact and tensile bars were cut from these boards using a CNC machine (Roland 3D Plotter MDX-20, UK).

Table 4.2. Processing conditions of the cork based composite boards of 6mm thickness.

Specimens	Pultrusion		Compression Moulding		
	Tempera-ture (°C)	Output (kg/h)	Temperature (°C)	Pressure (MPa)	Time (min)
PE/Cork (50 –50wt%)	150	350	150	1.42	14
PP/Cork (50–50wt%)	170	350	170	1.42	14

4.2.4 Dimensional stability tests

A Aiming to study the dimensional stability of the different materials, water absorption and thickness swelling tests were conducted according the ASTM D 570 [29]. To determine the water absorption, specimens (measuring 6mm in thickness, 60mm wide and 90 mm long) from the different materials were immersed in distilled water, at 23 ± 1 °C and atmospheric pressure, for different time periods (up to 11 days). In the end of each time period, five specimens of each material were removed, gently blotted with tissue paper to remove the excess water on the surface and immediately weighed. The water absorption was calculated according to the Eq. (4.1):

$$Water\ absorption\ (\%) = \frac{W_a - W_b}{W_b} \times 100 \qquad (4.1)$$

where W_a = weight of the specimen after being immersed for a certain period of time and W_b = weight of the same specimen before immersion (g).

To determine thickness swelling after immersion, the thickness of each immersed specimen was measured in two different points using a digital micrometer (± 0.01 mm). The thickness swelling was calculated as follows:

$$Thickness\ swelling\ (\%) = \frac{T_2 - T_1}{T_1} \times 100 \qquad (4.2)$$

where T_2 = thickness of the specimen after immersion and T_1 = thickness of the same specimen before immersion. Three specimens per each condition were measured..

4.2.5 Warping and density

Warping can result from an inferior product construction, wrong choice of materials or inadequate processing routes. Other reason that can cause this effect is the high moisture content in the air. After processing, CPC boards (220×220×6 mm³) obtained by compression moulding were submitted to a specific test to access the possible occurrence of warping effect. The obtained results were compared with the commercial fibreboard composites cut with the same dimensions. In Figure 4.1 is shown a schematic illustration of the performed test. Figure 4.1 a) shows the used system with a pointer *p* with precision capability of 0.01 mm of displacement.

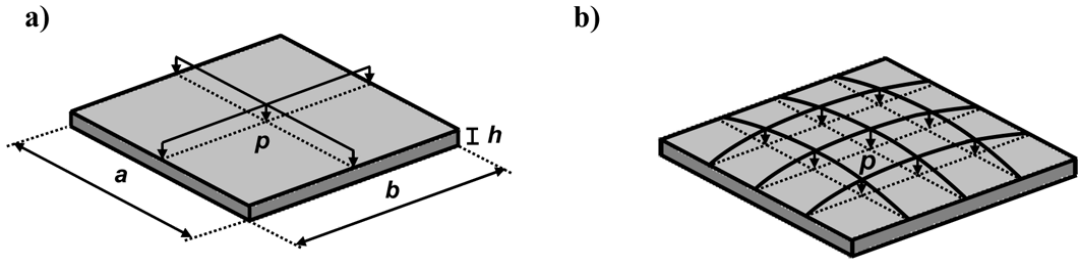

Figure 4.1. Scheme of the specimen's geometry: (a) with the measuring system and (b) board with warping

Two perpendicular measurements in each board were performed according the indicated directions *a* and *b*. At least 15 boards (in dry state) of each condition were analysed to evaluate the warping effect. The density of the materials was determined according the ASTM D 792 – 00 [30], using an analytical balance equipped with a stationary support for the immersion vessel. Five specimens were weighted per each sample.

4.2.6 Mechanical tests

The mechanical properties of the developed cork-based composites were determined performing flexural and impact tests. In more detail, three point static flexural tests were carried out in accordance with standard ISO 178 [31]. The dimensions of the specimens used were 120 mm length, 15 mm width and 6 mm thick. The load was placed midway between the supports with a span (L) of 80 mm. The crosshead speed was 2.56 mm/min. These tested were performed in an Instron 4505 Universal Machine (USA) equipped with a 1 kN cell load. For each condition, the specimens were loaded until the core break. The Charpy impact tests were performed according the standard ISO 179-1 [32] on a Ceast Fractovis (Pianezza, Italy) instrumented falling weight impact tester with a pendulum energy of 2 J. The notched specimens were rectangular bars with 120 mm length, 12 mm width and 6 mm thick. The hardness was determined by Shore-D Hardnes Tester (model bareiss – Prüfgeräte, Germany). For each sample, the value of Shore-D was calculated as the average of 10 indentations. All performed tests were carried out in a standard laboratory atmosphere of 23°C and 50% of relative humidity and seven specimens of each material were tested.

4.2.7 Morphology

To investigate cork distribution on the composite matrix and the fibreboard specimens, the fracture surface was analysed using a stereoscopic lens microscope Olympus SZ-PT (Tokyo, Japan) equipped with a light source Olympus Europe Highlight 2000, (Germany) and an Olympus DP11, (Japan) digital camera.

For more detailed analysis of the microstructure of the cork-polymer phases, fracture surfaces of the different specimens were examined using a NanoSEM 200 FEI (The Netherlands) scanning electron microscope (SEM). Before being analysed all the samples were coated by ion sputtering with an Au/Pd alloy (80-20 wt.%) in a high resolution sputter coater of Cressington 208HR (Watford, UK).

4.2.8 Thermal properties

The thermal stability studies, determined by thermogravimetric analysis (TGA) were performed to understand the degradation characteristics of the specimens using a TGA Q500 series thermogravimetric analyser (TA Instruments, USA). Experiments were performed in platinum pan, at a heating rate of 10 °C.min^{-1} from 50 °C to 600 °C in air atmosphere. Analyses were performed in two samples of each condition.

4.2.9 Fire resistance

In designing building materials, fire resistance classification of the product is one of the most important features. Single flame fire tests were carried out according to the standard ISO 11925-2 [33]. The single flame source test was performed in specimens with dimensions of 188 x 119 mm^2 and 6 mm thick. The specimen was held vertically and a flame was applied from the bottom edge of the specimen becoming more aggressive effect on the materials. According to the standard a burning time of 15 to 20 seconds was applied and the burning dimensions after the test were registered. Three specimens were tested for each composite. The fire resistance classification was attributed according of the standard fire test of building materials EN ISO 13501-1 [34].

4.2.10 Acoustic tests

The building elements for acoustic tests consisted on a superior element from CPC or fibreboard with dimensions of 220X220X6 mm^3 and an agglomerated cork underlay with thickness of 1.8 mm thick. Commercially available silicone glue (thickness of 0.5-0.6mm) was used to fix the agglomerated cork underlay to the previously produced boards (CPC, HDF and MDF boards).The aim of including this agglomerated cork underlay was to avoid reverberation sound and fix the boards. The pavement was submitted to a uniformly distributed load (20 to 25 kg m^{-2}). The tests were conduct in a reverberant chamber with a 7.25 m length, 5.88 m width, 4.65 m height and a volume of 202 m^3. The tests occur at atmospheric conditions 22 °C and 66 % of humidity. The equipment used for the measurements was a tapping machine Brüel & Kjaer (B&K, Germany) Type 3204; B&K *2260* dual channel real-time frequency analyser and B&K 13 mm microphone model 4189. The microphone height was about 1.4 m. The measurements of sound insulation were performed according the standard EN ISO 140-8 [35] and 717-2 [36]. The measurements were taken at three locations of the tapping machine relative to the

floor sample area of 2 m^2 and 5 positions of microphone with to different lectures using one-third-octave bands, 100 Hz to 4200 Hz. The reduction of impact noise by floor covering on standard floor was determined according the equation 4.3:

$$\Delta L = L_{n,0} - L_n \quad (4.3)$$

where, ΔL is the reduction of impact sound pressure level, $L_{n,0}$ is the normalized impact sound pressure level in the absence of floor covering and L_n is the normalized impact sound pressure level with floor covering. The impact sound improvement index (ΔL_w) was determined according to the standard EN ISO 717-2 [36].

4.3 Results and discussion

4.3.1 Dimensional stability tests

The results from the water absorption and thickness swelling tests are shown in Figure 4.2 and Figure 4.3 respectively. In the first 6h of immersion, the fibreboards samples absorbed 10.8 ± 0.4 % (HDF boards) and 14.8 ± 0.8 % (MDF boards). In the first 48 h of immersion the CPC samples absorbed less than 1% of water while the HDF and MDF ones absorbed 32.7 ± 1.5 % and 49.7 ± 0.7 % respectively. Moreover, after 11 days of immersion the maximum water absorption percentage of the developed CPC boards was 3.7 ± 0.6 % (for the PP/Cork) whereas the HDF and MDF boards absorbed, respectively, 77.9 ± 2.4 % and 125.6 ± 0.9 %. These differences (more than 70%) can be explained by the high amount of polyolefin (50 wt.%) present in the CPC composition since, the non-polar polyolefin absorbs no or little water amount [25, 37] and the inner volume accessible for water and oxygen is essentially zero [38].

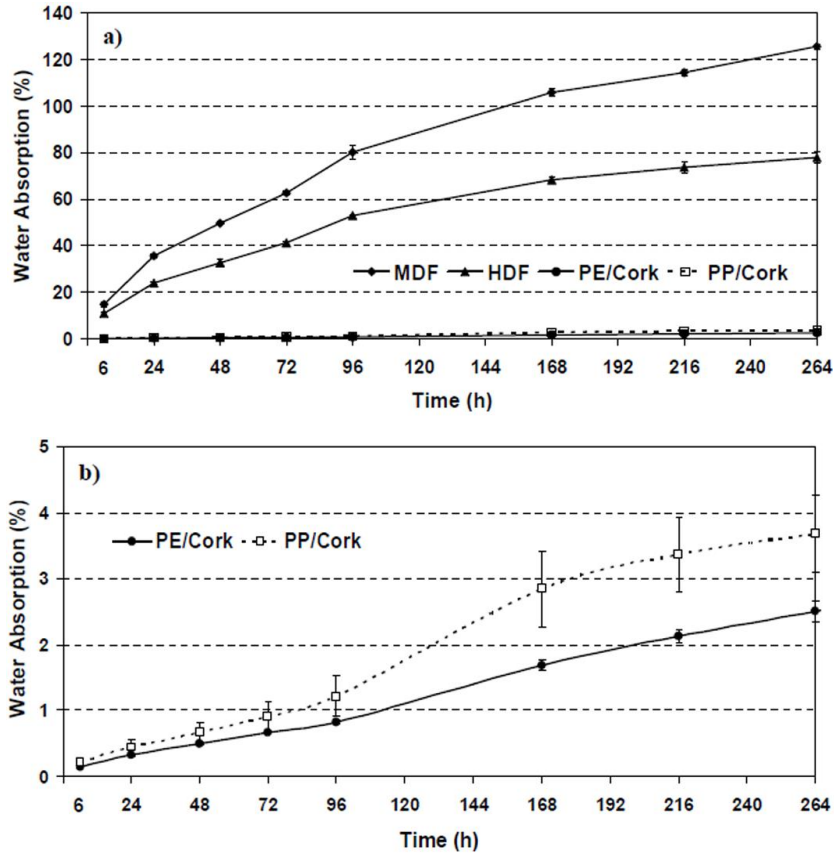

Figure 4.2. Water absorption behaviour for the tested specimens during the immersion time (a) and detail of the water absorption for the cork based composites (b).

Moreover, cork can also be considered a hydrophobic material. These results clearly indicate that CPC boards are more hydrophobic and absorb much less moisture than the hydrophilic MDF or HDF ones. These results also point out that CPC boards are more suitable to be used on environments where the materials are exposed to high moisture content than the control samples. Similar behaviour was observed for wood polyolefin composites developed using melt based technologies [39, 40]. Like in wood composites, the water absorption in CPC materials occurs due to the presence of fine pores or lenticels in the cork particles (capillary absorption) and hydrogen bonding sites, or by some micro-cracks or gaps in the interface between cork particles and the polymeric matrix.

The thickness swelling results are shown in Figure 4.3. The values observed for both fibreboards are considerably higher than the ones observed for the CPC boards. After an immersion period of 264 hours, the values of thickness swelling were, respectively, 0.5 ± 0.2 % and 0.8 ± 0.3 % for the PP/Cork and PE/Cork based composites, indicating good dimensional stability. On the contrary, for the same time period, the thickness swelling values of MDF and HDF were 85.3 ± 1.5 and 44.1 ± 1.0,

respectively. Moreover, for the fibreboard specimens, thickness swelling values followed a similar trend to water absorption behaviour: thickness swelling values increased with the immersion time (Figure 4.3).

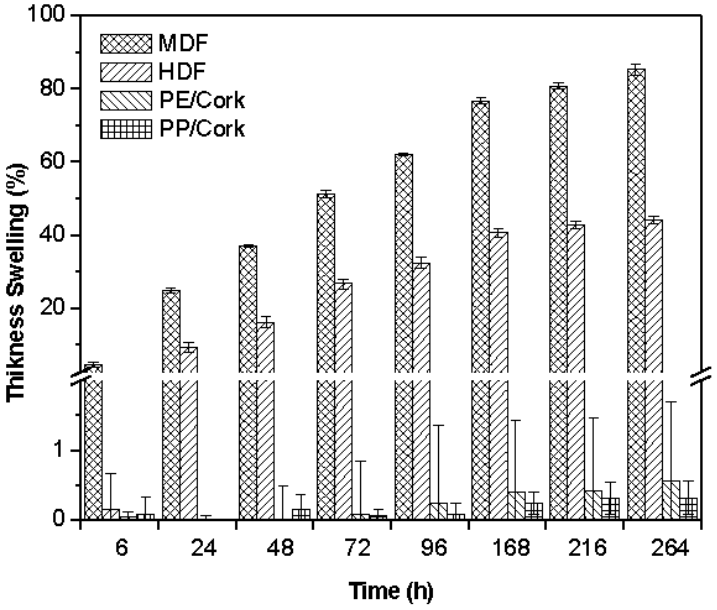

Figure 4.3. Thickness swelling of the fibreboard materials and the cork based composites during the immersion tests.

The CPC materials had a different behaviour: the thickness swelling was very low and the variation between the different immersion periods is almost insignificant. As in the water absorption behaviour, the low thickness swelling values of CPC materials can be an advantage for its application on the development and construction of several products, including its application as core material for laminated floor applications.

4.3.2 Warping and density

The density and warping values for the different materials are shown in Table 4.3. The warping of the control fibreboards was near zero, with the mean value of 0.14% for MDF and 0.18% for the HDF. The developed CPC materials registered warping values of 1.26% for PE/Cork and 1.44% for PP/Cork. These values, although higher than ones registered for the fibreboards, can be considered small enough to classify the developed composites of high dimensional stability. The warping values were reduced with the addition of cork powder and are probably related with the crystallinity of the polymeric matrices (PP and PE) [38] where the presence of 50 wt.% of cork powder noticeably reduced the warping when it

was applied the compression moulded process. Additionally, thicker areas cooled slower and part distortion could occur [41]. In this last case the warping can be reduced by increasing the cooling time during the compression moulding process.

Table 4.3. Density and warping measurements of the tested specimens.

Board	MDF	HDF	PE/Cork (50 - 50wt%)	PP/Cork (50 -50wt%)
Density* (kg m^{-3})	822.7 ± 2.7	920.3 ± 6.7	1060.6 ± 5.8	1017.5 ± 3.3
Warping mean (mm)	0.03 ± 0.02	0.04 ± 0.03	0.27 ± 0.16	0.31 ± 0.11
Board Warping (%)	0.14 ± 0.09	0.18 ± 0.14	1.26 ± 0.74	1.44 ± 0.51

* Density according to the standard ASTM D 792; ± Standard deviation values.

The density of the composites ranges from 1017.5 ± 3.3 Kg m^{-3} for the PP/Cork composites to 1060.6 ± 5.8 Kg m^{-3} for the PE/Cork composites. These values are higher than the ones observed for the fibreboards. To understand this effect is important to note that the cork cell wall density has been estimated to be 1200 kg m^{-3} [3, 4]. Previous work using similar cork-polyolefin formulations [9] indicates a bulk density of the CPC pellets after pultrusion of around 590 ± 11.4 Kg m^{-3} to 602 ± 13.4 Kg m^{-3}. The densification occurs in the compression moulding step due to the high applied compression force of 1.42MPa. Studies on wood-polyolefin (50-50 wt.%) composites regarding thermal and photo-oxidative stability indicate that the composite density controls the amount of air oxygen flowing into the pores of the composite matrix [38]. The higher density of a composite material blocks the access of oxygen and slows the oxidative degradation process.

4.3.3 Mechanical tests

Flexural, impact and hardness properties of the different materials were determined and the results are shown in Table 4.4. All results are expressed as means ± standard deviation. The flexural strength obtained for the fibreboard samples were higher than the results obtained with the CPC materials (Figure 4.4). The flexural strength and modulus of the control materials based on fibres where, respectively, ~58.9 MPa and ~5.3 GPa for the HDF and ~49.6 MPa and ~4.4 GPa for the MDF. The CPC materials presented modulus in the interval [1.8 – 1.3] GPa and strengths in the interval [19.1 –

17.1] MPa. The better mechanical performance of the CPC prepared with PP as matrix was expected since this polyolefin has better mechanical properties than the used PE. The lower values observed for the CPC samples can be related with the lack of interfacial adhesion and bonding between the matrix and the cork powder. Due to this, no stress transfer occurs during deformation resulting in low mechanical performance.

Table 4.4. Flexural, impact and hardness properties of the cork based composites (50wt% - 50wt%) and the commercial fibreboard materials.

Specimens	Flexural			Impact **	Hardness
	Strength * (MPa)	Modulus (GPa)	Strain at break * (%)	Strength (kJ/m²)	Shore D
MDF	49.6 ± 0.9	4.35 ± 0.10	2.30 ± 0.14	21.38 ± 2.71	50.8 ± 0.6
HDF	58.9 ± 3.7	5.27 ± 0.14	1.96 ± 0.20	9.73 ± 2.51	50.2 ± 0.6
PP	29.0 ± 1.0	1.03 ± 0.03	> 10	2.84 ± 0.21	45.9 ± 1.4
PP/Cork	19.1 ± 0.5	1.75 ± 0.10	1.68 ± 0.04	5.53 ± 0.24	49.5 ± 0.7
HDPE	19.5 ± 1.2	0.90 ± 0.08	> 10	4.44 ± 0.20	44.6 ± 2.1
PE/Cork	17.1 ± 0.7	1.29 ± 0.07	2.46 ± 0.10	6.49 ± 0.15	47.9 ± 1.3

± Standard deviation values; * Maximum stress; ** Notched Charpy impact strength (kJ/m²).

Regarding the flexural strain, the differences between the materials are not so evident. The samples from PE/Cork are the most ductile of the tested materials with 2.46% deformation, where the MDF presents a close value of 2.30%. The high capacity of deformation of polyolefin is well known from the literature [42]. However, the addition of high percentages of cork (50 wt.%) reduced the maximum strain to less than 3%. The results are in accordance with other composite materials like wood-thermoplastic composites, where the increase of wood content increases the flexural modulus and decreases the flexural strength and maximum strain values of the composites [1, 43].

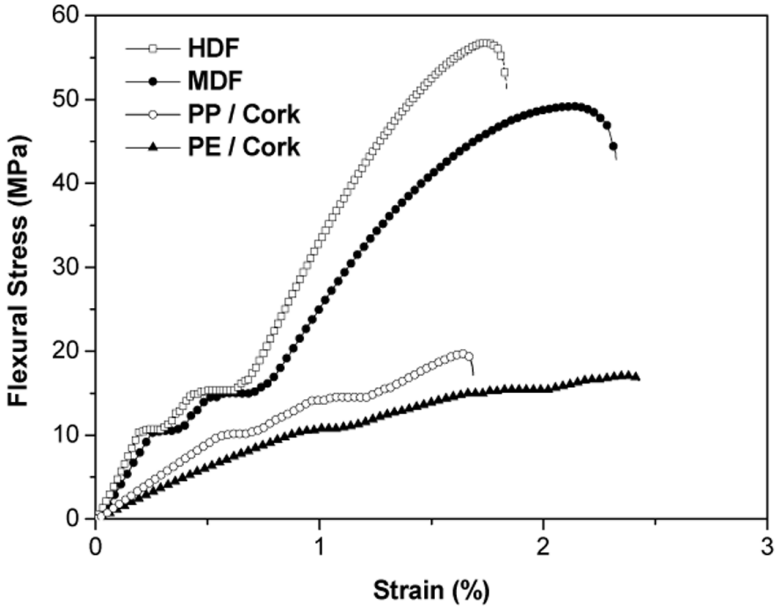

Figure 4.4. Flexural stress-strain curves of the developed cork based composites and the fibreboard materials.

The purpose of the impact tests was to measure and compare the resilience, i.e. the energy absorption capacity of the different materials. As expected, the Charpy notched impact strength of fibreboard samples, mainly the ones from MDF, exhibited better mechanical properties when compared with the developed CPC materials. The neat polymers present the lower value of impact strength of 4.4 kJ m^{-2} for HDPE and of 2.8 kJ m^{-2} for the PP. Nevertheless, the addition of 50 wt.% of cork powder to the HDPE and PP matrices increased, respectively, ~31% and ~51% the impact strength, indicating that the presence of cork in the composite reinforces the energy absorption capacity. The cellular and elastic structure of cork [3, 4] can be an explanation for these results. Regarding the CPC materials, the energy absorption capacity of PP/Cork composite was 20% higher than in the PE/Cork composite. Since it was used the same amount of cork powder (50 wt.%) and the processing conditions were similar, the higher MFI of PP contributed to a better dispersion of cork powder in the matrix and consequently increase in the absorption capacity. In terms of hardness, the specimens present similar values, around 49 to 51 Shore D, being the lower value corresponding to PE/cork and the high value to MDF material. When cork powder was added, hardness and the flexural modulus increased for both cases, probably due to the pultrusion process and the applied pressure of 1.42 MPa during the compression moulding process.

4.3.4 Morphology

The fracture surface, after Charpy notched impact tests, of the studied materials was analysed by optical microscopy and the results presented in Figure 4.5.

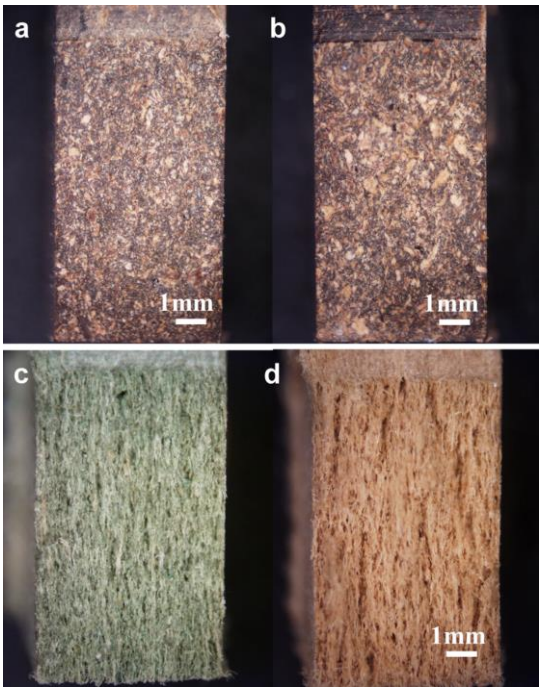

Figure 4.5. Fracture surfaces of the specimens after Charpy notched impact tests with a) PP/Cork (50–50wt%), b) PE/Cork (50–50wt%), c) HDF and d) MDF.

For both CPC materials, it was observed a good dispersion of the cork powder particles in the polymeric matrix. In the case of the CPC with PP matrix it seems that cork distribution is more homogeneous. A possible explanation is the higher MFI value of the PP when compared with the MFI of HDPE (see Table 4.1). The fibreboard materials illustrate the well known fibrous aspect where the fibres are stacked like rows. This fibrous morphology is consistent with the previously reported results, namely the higher flexural mechanical performance and the ability of water to penetrate on these structures, inducing higher thickness swelling variations.

SEM micrographs from the same fracture surfaces are presented in Figure 4.6. At low magnification (Figure 4.6 a and Figure 4.6 b) it is visible the high volume content of cork powder in the CPC materials.

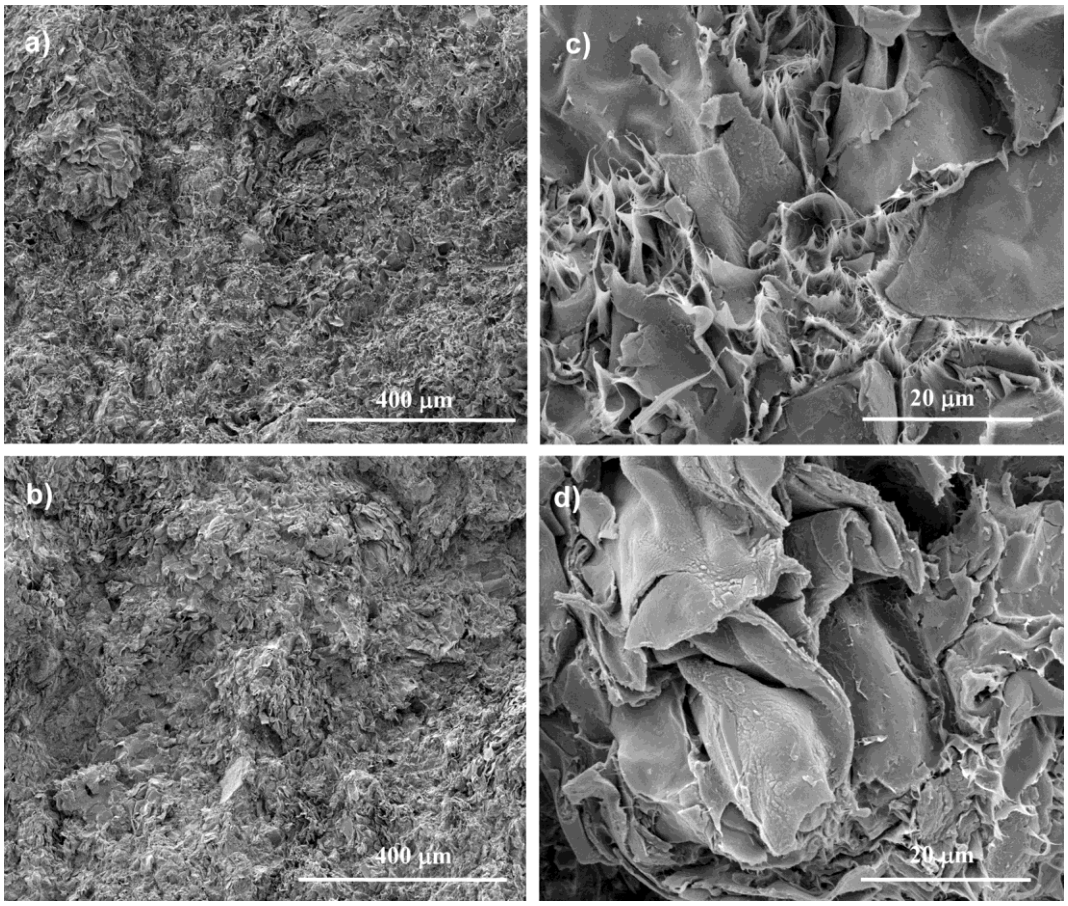

Figure 4.6. Micrographs of the impact fracture surfaces of the (a, c) PE/Cork (50–50wt%) and (b, d) PP/Cork (50–50wt%) composites.

The cork powder/polymer weight ratio used for the composites preparation was 50%, but the volume this ratio is respectively, 86 % - 14 %, respectively. In Figure 4.6 c is shown the morphology of the PE/Cork (50-50 wt.%) material, where is possible to see the stretching of the PE between the cork cell walls. The same effect was observed for the CPC with PP matrix (Figure 4.6 d). Both images suggest that the surface of the cork particles interacted well with the polymeric matrix since voids or empty spaces between the two phases were not detected.

4.3.5 Thermal properties

The results of the termogravimetric analysis (TGA), conducted under air atmosphere, and the respective derivate (DTG) are shown in Figure 4.7. Relevant data from all materials are summarized in Table 4.5.

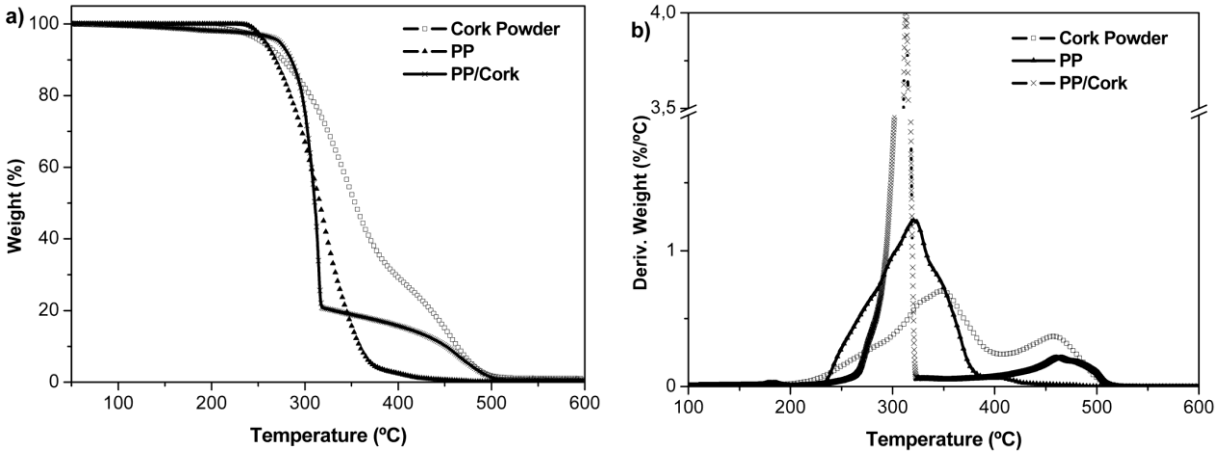

Figure 4.7. TGA thermograms of the CPC composites with PP matrix and their components (a) and DTG curves of the thermograms (b) under air atmosphere.

The cork powder showed an initial region of mass loss between room temperature and 100 °C that is more significant for the two fibreboard materials corresponding to the elimination of water. In the case of the fibreboards the moisture content was higher, presenting at 100°C values of around 6 % comparing with 3.4 % in cork. Nevertheless, as described in the literature, at 100 °C the moisture present in cork is not totally eliminated [14]. As expected, the current thermoplastics did not present residual moisture and, when combined with cork powder the CPC materials presented a weight loss in this region of 0.6 - 0.7 %.

Table 4.5. Thermal degradation characteristics of the tested specimens under air atmosphere.

Specimens	TGA			DTG	
	Onset Temp.(°C)	Weight loss (%)	Residual mass (%)	$T_{max\ 1}$ (°C)	$T_{max\ 2}$ (°C)
Cork Powder	258	5.71	1.04	348	458
PP	265	3.88	0.12	322	–
HDPE	274	0.76	0.11	358	451
HDF	275	13.80	0.59	318	455
MDF	265	10.29	0.23	319	446
PP/Cork	289	12.21	0.70	313	464
PE/Cork	282	5.81	0.70	341	416 / 482

Considering the data presented on Table 4.5, the chemical degradation of cork starts at 258 °C. This result suggests that the cork powder can be processed with polymers having melting temperatures lower than this value, such as the used polyolefin's. However, other effects like colour change of cork, promoted by the temperature and the processing time, must be considered. Additionally, results from Figure 4.7 have shown that when cork powder is mixed with PP through melt-based technologies the thermal stability of the polymer increases.

Analysing DTG curve from cork powder, two maximum peaks were detected, one at 348 °C and other at 458 °C, being the first one of large intensity. The first peak corresponds to the two major constituents of cork (lignin and suberin fractions) and the second one can be attributed to suberin, the most thermal resistant component in cork. The polysaccharides composed by cellulose and hemicellulose have degradation temperatures in the range between 300 °C to 400 °C [44].

The small values of weight loss (0.76 %) and the high onset temperature (274 °C) (see Table 4.5) obtained for HDPE are consistent with the presence of the thermal stabilizer. Other effect can be identified if the DTG values from both CPC are compared. In the case of PE/Cork the decomposition temperature peak (T_{max1}) occurred at 341 °C with a weight loss of 28 %. For PP/Cork the T_{max1} occurred earlier, at 313°C with higher weight loss of 59 %.

Both fibreboard materials showed multi-stepped degradation processes due to the presence of different species on their composition (data not shown). Literature described that the pyrolysis of wood begins with an early decomposition of hemicelluloses, followed by an early stage of pyrolysis of lignin, where the major decomposition temperature is normally attributed to the degradation of the cellulose [45].

Comparing all the tested materials, the most resistant is HDPE and PE/cork composite, since the used thermoplastic composition includes a thermal stabilizer. The fraction of the inorganic components, remaining from cork powder or from fibreboards, after exposed to 600 °C, is minimal being 1% for cork powder and less than 0.6 % for the fibreboards.

4.3.6 Fire resistance

The burning rates of the two different CPC and fibreboard materials were determined by single flame fire test (table 6). The set-up procedure for testing the fire resistance is illustrated in Figure 4.8 *a*. In this test the flame takes contact at the edges of the specimen and start to burn in the vertical direction. When the neat HDPE was submitted to the flame (Figure 4.8) the material started dripping after a few

seconds and the integrity of the material was completely lost. The addition of 50 wt.% of cork powder to the polymeric matrix improved such behaviour and the composites maintained the integrity during the whole test. The presence of cork powder sustained the polymeric phase and acted as a fire retardant improving the performance of the composites. This behaviour reinforces and agrees with the results obtained with the TGA analysis. The fire resistance tests conducted on the fibreboards revealed that these materials possess a self-extinguishing behaviour after removing the flame. This behaviour was not observed for the composite materials since the flame does not extinguish eventually (Figure 4.8c).

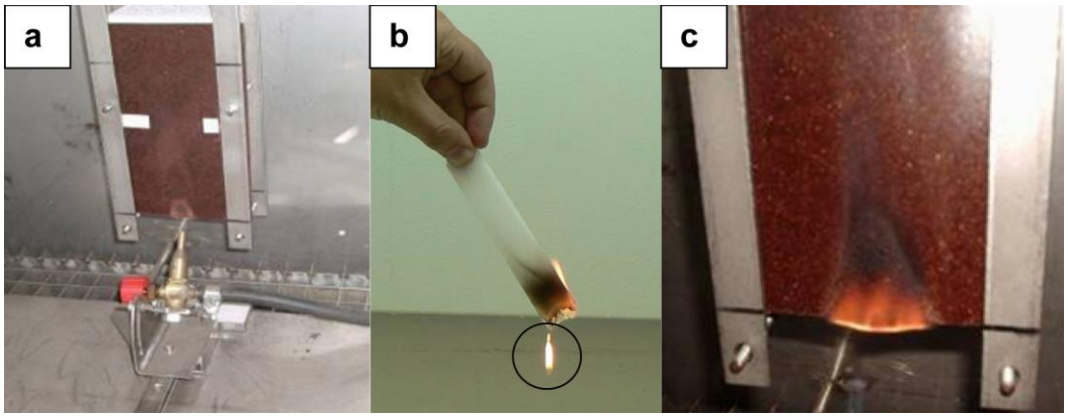

Figure 4.8. System for testing the fire resistance (a) behaviour of PE to the flame (b) and CPC behaviour after fire test of the PE/Cork (50–50wt%) specimen (c).

Table 4.6. Fire resistance test results for the tested specimens.

Specimen	Inflamability time (s)	Burning Dimensions			Fire Resistance Euroclasse *
		Lenght(mm)	Width(mm)	Depth(mm)	
MDF	15 - 20	17.0 ± 1.4	20.3 ± 0.5	0	**E**
HDF	15 - 20	20.0 ± 0.1	18.3 ± 0.5	0	**E**
PE/Cork	15 - 20	37.3 ± 4.0	38.3 ± 3.3	0	**E**
PP/Cork	15 - 20	39.3 ± 1.9	38.7 ± 3.5	0	**E**

* Fire resistance classification according the standard fire test of building materials BS EN 13501-1.

Small differences in the burnt area were found, being the fibreboard materials the ones with lower values. Between the two CPC composites no relevant differences were found. In our opinion, the effect of the cork powder is higher and overlaps with the thermal stabilizer in HDPE.

The results from the fire resistance tests (Table 4.6) indicated that all tested specimens possess a good behaviour regarding fire resistance since all the tested materials had a classification of *E*.

4.3.7 Acoustic tests

By measuring the impact sound pressure level reduction, ΔL, of the different board materials (Figure 4.9), it was possible to compare, as a function of the frequency, the behaviour of the different board systems. As expected, the sound pressure level reduction increased as the frequency increased. Moreover, it was found that, at high frequencies, the cork-based composite showed better behaviour when compared with the commercially fibreboard materials.

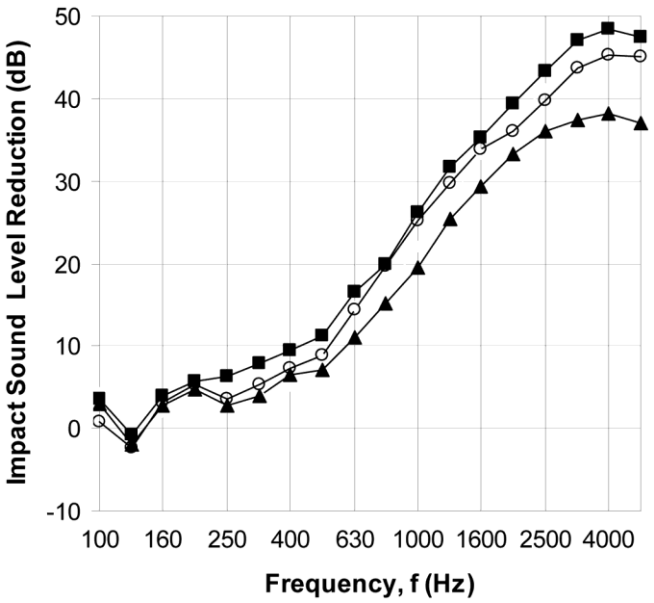

Figure 4.9. Impact sound reduction ΔL vs. frequency due to installation of the tested materials: (○) MDF; (▲) HDF and (■) PE/Cork (50 – 50 wt%). Experimental results in the 1/3 octave band frequency domain.

The impact sound attenuation index (ΔLw), is useful for a direct comparison of the reduction in impact noise transmission by the floor coverings. The ΔLw values ranged from 18 dB (for MDF and HDF floor covering) to 20 dB for the (PE/Cork) floor covering. The obtained values are in the same range of values in the literature [46, 47]. The cellular and corrugated structure of cork together with the high volume percentage of this natural material (~ 86%) can be the key for the superior ΔLw value of 20 dB.

The board density, which is described as a parameter affecting the sound transmission properties, can explain the improved behaviour of the MDF compared with HDF in terms of impact sound reduction especially for medium and high frequencies. In the literature is also pointed that the use of urea-formaldehyde (UF) resin in the fibre based materials can also contribute to additional improvement on the acoustic properties [28].

In the present work the ΔLw of the all tested floor coverings was influenced by the use of silicon glue to fix the cork underlay to the boards. The silicon might also improve the soundproof properties providing a small increase on the impact sound attenuation index values for all tested boards. The commercial fibreboard tested materials also present a small percentage of UF resin.

4.4 Conclusions

The purpose of this study was to compare two different CPC materials with two commercially available fibreboard materials and detect its advantages and drawbacks. The obtained results showed the potential of this natural-based product on the development of composites with improved characteristics namely, low water absorption, fire resistance, impact resistance and insulation properties.

Both CPC materials compounded by pultrusion and further processed by compression moulding presented a good dispersion and distribution of the cork powder particles in the thermoplastic matrix. Moreover, the CPCs reveal good dimensional stability with low water absorption in comparison with fibreboard materials.

The mechanical properties of the fibre-based materials were considerably superior compared with the ones from the CPCs. With the addition of cork (50 wt.%), the flexural strength and strain were considerably reduced and the modulus was improved in both cases. The impact resistance tests confirm that the addition of cork powder improved the energy absorption capacity of the used polyolefin's.

The presence of cork presents the advantage to act as fire retardant in the thermoplastic composite materials. The acoustic behaviour revealed that CPC materials possess improved impact sound insulation properties, low water absorption and reduced thickness swelling. These materials proved to be good candidates to be used as underlay materials on floor applications. The developed cork composite materials present some promising properties, although reinforcement strategies to reach to higher stiffness and strength could be needed for specific applications.

4.5 References

[1] Bledzki AK, Reihmane S, Gassan J. Thermoplastics reinforced with wood fillers: A literature review. Polym-Plast Technol Eng 1998;37(4):451-468.

[2] Rowell R. Challenges in Biomass–Thermoplastic Composites. J Polym Environ 2008;15(4):229-235.

[3] Gibson LJ. Cellular solids: structure and properties. 2nd ed.; Cambridge University Press: Cambridge, 1997.

[4] Silva SP, Sabino MA, Fernandes EM, Correlo VM, Boesel LF, Reis RL. Cork: properties, capabilities and applications. Int Mater Rev 2005;50(6):345-365.

[5] Matos MJ, Simplício MH. Innovation and sustainability in mechanical design through materials selection. Mater Design 2004;27(74-78.

[6] Fernandes EM, Silva VM, Chagas JAM, Reis RL. Cork-polymer composite (CPC) materials and processes to obtain the same. WO2009072914-A1, Amorim Revestimentos, S.A., 2009.

[7] Gil L. Cork Composites: A Review. Mater Design 2009;2(776-789.

[8] Cosby SA, Kelly M, VAN WB. Silicone-cork ablative material. EP 1482163 A2, United Technologies Corp., 2005.

[9] Fernandes EM, Correlo VM, Chagas JAM, Mano JF, Reis RL. Cork Based Composites using Polyolefin's as Matrix: Morphology and Mechanical Performance. Compos Sci Technol 2010;70(2310-2318.

[10] Pereira H. Cork: biology, production and uses. Amsterdam: Elsevier, 2007.

[11] Pereira H, Rosa ME, Fortes MA. The Cellular Structure of Cork from Quercus-Suber L. Iawa Bull 1987;8(3):213-218.

[12] Gibson LJ, Easterling KE, Ashby MF. The Structure and Mechanics of Cork. P Roy Soc Lond A Mat 1981;A 377):99-117.

[13] Gil L, Moiteiro C. Cork. Ullmann's Encyclopedia of Industrial Chemistry: Willey - VCH, Weinheim, 2002.

[14] Rosa ME, Fortes MA. Thermogravimetric Analysis of Cork. J Mater Sci Lett 1988;7(10):1064-1065.

[15] Rosa ME, Fortes MA. Temperature-Induced Alterations of the Structure and Mechanical-Properties of Cork. Mater Sci Eng 1988;100(69-78.

[16] Pereira H. The Thermochemical Degradation of Cork. Wood Sci Technol 1992;26(4):259-269.

[17] Neto CP, Rocha J, Gil A, Cordeiro NMA, Esculcas AP, Rocha S, Delgadillo I, Dejesus JDP, Correia AJF. C-13 solid-state nuclear-magnetic-resonance and Fourier-transform infrared studies of the thermal-decomposition of cork. Solid State Nucl Mag 1995;4(3):143-151.

[18] Varea S, García-Vallejo MC, Cadahía E, Simón BFd. Polyphenols susceptible to migrate from cork stoppers to wine. Eur Food Res Technol 2001;213(56–61.

[19] Bento MFS, Cunha MA, Moutinho AMC, Pereira H, Fortes MA. A mass-spectrometry study of thermal-dissociation of cork. Int. J. Mass Spectrom. Ion Process. 1992;112(2-3):191-204.

[20] Gil L. Cork powder waste: An overview. Biomass Bioenerg 1997;13(1-2):59-61.

[21] Barlow CY, Ashby MF. Cork dust composites. in Proceedings of the Riso International Symposium on Metallurgy and Materials Science. 1989.

[22] Abdallah FB, Cheikh RB, Baklouti M, Denchev Z, Cunha AM. Effect of surface treatment in cork reinforced composites. J Polym Res 2009;17(4):519-528.

[23] Mano JF. The viscoelastic properties of cork. J Mater Sci 2002;37(2):257-263.

[24] Bledzki AK, Gassan J, Theis S. Wood-filled thermoplastic composites. Mech Compos Mater 1998;34(6):563-568.

[25] Espert A, Vilaplana F, Karlsson S. Comparison of water absorption in natural cellulosic fibres from wood and one-year crops in polypropylene composites and its influence on their mechanical properties. Compos Part A - Appl S 2004;35(11):1267-1276.

[26] Li X, Li Y, Zhong Z, Wang D, Ratto JA, Sheng K, Sun XS. Mechanical and water soaking properties of medium density fiberboard with wood fiber and soybean protein adhesive. Bioresource Technol 2009;100(14):3556-3562.

[27] Singh B, Gupta M, Verma A. Mechanical behaviour of particulate hybrid composite laminates as potential building materials. Constr Build Mater 1995;9(1):39-44.

[28] Hashim R, Sulaiman O, Kumar RN, Tamyez PF, Murphy RJ, Ali Z. Physical and mechanical properties of flame retardant urea formaldehyde medium density fiberboard. J Mater Process Tech 2009;209(2):635-640.

[29] ASTM D570-98: Standard Test Method for Water Absorption of Plastics. 1998, Edited by ASTM International. West Conshohocken.

[30] ASTM D 792 – 00 Standard Test Methods for Density and Specific Gravity (Relative Density) of Plastics by Displacement. 2000.

[31] ISO 178: Plastics - Determination of flexural properties. 2001.

[32] ISO 179-1: Determination of Charpy impact properties — Part 1: Non-instrumented impact test. 2000.

[33] ISO 11925-2: Reaction to fire tests - Ignitability of building products subjected to direct impingement of flame - Part 2: Single-flame source test. 2002.

[34] BS EN ISO 13501-1: Fire classification of construction products and building elements. Classification using test data from reaction to fire tests. 2002.

[35] ISO 140-8: Acoustics - Measurement of sound insulation in buildings and of building elements - Part 8: Laboratory measurements of the reduction of transmitted impact noise by floor coverings on a heavyweight standard floor. 1997.

[36] ISO 717-2: Acoustics - Rating of sound insulation in buildings and of building elements - Part 2: Impact sound insulation. 1996.

[37] Shi SQ, Gardner DJ. Hygroscopic thickness swelling rate of compression molded wood fiberboard and wood fiber/polymer composites. Compos Part A - Appl S 2006;37(9):1276-1285.

[38] Klyosov AA. Wood-plastic composites. John Wiley & Sons, Inc., Hoboken, New Jersey, 2007.

[39] Ichazo MN, Albano C, Gonzalez J, Perera R, Candal MV. Polypropylene/wood flour composites: treatments and properties. Compos Struct 2001;54(2-3):207-214.

[40] Yang HS, Kim HJ, Park HJ, Lee BJ, Hwang TS. Water absorption behavior and mechanical properties of lignocellulosic filler-polyolefin bio-composites. Compos Struct 2006;72(4):429-437.

[41] Wakeman MD, Rudd CD, Anthony K, Carl Z, Compression Molding of Thermoplastic Composites, in Comprehensive Composite Materials. 2000, Pergamon: Oxford. p. 915-963.

[42] Mourad A-HI. Thermo-mechanical characteristics of thermally aged polyethylene/polypropylene blends. Mater Design 2010;31(2):918-929.

[43] Adhikary KB, Pang SS, Staiger MP. Dimensional stability and mechanical behaviour of wood-plastic composites based on recycled and virgin high-density polyethylene (HDPE). Compos Part B-Eng 2008;39(5):807-815.

[44] Averous L, Boquillon N. Biocomposites based on plasticized starch: thermal and mechanical behaviours. Carbohyd Polym 2004;56(2):111-122.

[45] Lee HL, Chen GC, Rowell RM. Thermal properties of wood reacted with a phosphorus pentoxide–amine system. J Appl Polym Sci 2004;91(4):2465-2481.

[46] Carvalho APO, Vafiadis C, Borrego H. The use of agglomerated cork as underlay for improvement of impact sound insulation in buildings. in 137th ASA Meeting & 2nd Forum Acusticum. 1999. Berlin.

[47] Rodrigues RC, Carvalho APO. Natural vegetal fibbers as a new resilient layer for floating floors. in Proceedings of 5th EuroNoise. 2003. Naples, Italy.

Polypropylene-based cork-polymer composites: Processing parameters and properties[4]

Abstract

Cork-polymer composites are one of the most promising fields of cork technology to create materials for a sustainable development. In this work, cork particles and powder were compounded with polypropylene (PP) by twin-screw extrusion and further processed by injection or compression moulding. The obtained PP/Cork injection moulded composites were used to investigate the tensile properties before and after water absorption (*WA*) tests. The addition of polypropylene-graft-maleic anhydride (PP-g-MA) and stearic acid was evaluated. The composites show good distribution and dispersion of cork with interesting aesthetic characteristics. Low cork content (5wt.%) reinforces the stiffness of the PP. The addition of PP-g-MA up to 8 wt.% promotes an increase on the tensile strength while the stearic acid contributes only with a slight increase on the tensile strain. The thermo-physical properties were investigated and the composites present low *WA*. In general the tensile properties of the composites were not significantly affected after the *WA* tests. Moreover, the *WA* was found to increase with an increase in cork content and was reduced with the PP-g-MA and stearic acid. It was also found, that cork act as nucleating agent and promotes antioxidant protection to PP. Both properties ameliorate with the increase of the cork content. Low cork content improves the thermal resistance while increasing the bio-based component increases the composite density and the thermal conductivity. The maximum incorporation of cork on the PP matrix through extrusion process was 93% in volume.

[4] This chapter is based on the following publication:

Fernandes EM, Correlo VM, Mano JF, Reis RL, 2013, Polypropylene-based cork-polymer composites: Processing parameters and properties, *submitted*.

5.1 Introduction

Polypropylene (PP) is a thermoplastic being widely applied in the industry and is usually combined with inorganic particles or fibres aiming to improve its mechanical properties and reduce cost [1]. The mostly used inorganic fillers includes talc [2, 3], mica [4], clay [5], calcium carbonate ($CaCO_3$) [6], carbon and glass fibres [7, 8]. Combining or replacing the inorganic part by lignocellulosic materials would be highly beneficial from the point of view of the environmental sustainability. The rational on using lignocellulosic materials as filler and reinforcement of thermoplastic composites relies on its advantageous intrinsic properties including low density, low cost, favourable strength/weight, high filling levels, renewable and sustainable source, non-toxic, low hardness, low energy consumption, and recyclability [9-11]. Potential applications of these eco-friendly composites include automotive, building and furniture industry [10].

Cork is the bark of the cork oak tree (*Quercus suber* L.) [12-14] and is a natural and complex polymeric composite material. Chemically, this plant tissue contains suberin (30-60 %), lignin (19-22 %), polysaccharides (12-20 %) and extractives (9-20 %) [13, 14]. Furthermore, cork presents closed cell structure and viscoelastic properties, exceptional insulation properties, is chemically inert, fire resistance and resistance to microbial decay [13, 15-17]. Nowadays, cork-polymer composites are one of the most promising fields under development in the cork industry aiming to create sustainable materials. Research involving cork and cork by-products combined with thermoplastics [15, 18, 19], thermosets [15, 20] and, more recently, with bio-based matrices [21, 22] can be found in the literature. As for other lignocellulosic composites, the final properties of these cork composites are highly dependent on the processing conditions. Thus, the final specifications of a cork composite can be tailored for a specific application by varying the compounding process, amount and cork particle size, chemical or surface treatment and type and amount of coupling agent [15, 23-25]. The ability to stress transfer from the thermoplastic matrix to the cork filler or reinforcement will depend essentially of the cork-polymer interactions that can be reduced due to the incompatibility between lignocellulosic materials and polymeric matrices. To overcome these limitations it is necessary to promote polymer modification with polar groups, such as maleic anhydride and their grafted polymers, stearic acid, silanes, zirconate, or titanate in order to enhance the adhesion between the polymeric matrix and the lignocellulosic component [26-29]. One of the most widely used coupling agents is polypropylene graft maleic anhydride (PP-g-MA). It is pointed that the interactions between anhydride groups of maleated coupling agents and the hydroxyl groups of natural fibres can overcome the problem of incompatibility,

increasing the interfacial adhesion between both components and, consequently, the mechanical performance of the composites [30-32]. One of the main concerns on the use of natural fibres in composites is their susceptibility to moisture absorption and the consequent effect on the physical and mechanical properties. The characteristics of that moisture absorption are influenced not only by the nature of the fibre and the matrix but also by the relative humidity and manufacturing process [33]. Despite these studies, the effect of cork on the mechanical behaviour of composites after water immersion has not been addressed. Thus, the main objectives of this research are (i) identify a proper processing design to avoid degradation of the natural component and particle agglomeration, (ii) study the effect of cork granulometry and the addition of coupling agent on the mechanical performance of the composites, (iii) study the effect of adding cork on the thermal properties of the developed materials and (iv) access the maximum incorporation of cork in the polypropylene matrix without compromising the processability of the final product.

5.2 Experimental section

5.2.1 Cork, polymer and coupling agents

Cork granules, with an average particle size 0.5-1 mm and specific weight of 166 ± 21 kg.m^{-3}, moisture content of ~7.5 % and a cork powder, with an average particle size < 500 μm, a specific weight of 157 ± 2 kg m^{-3} and moisture content of ~5.4% were both supplied by Amorim Revestimentos S.A. (S. Paio Oleiros, Portugal).

The matrix was a polypropylene (PP) homopolymer, (1374 E2 from ExxonMobil, Germany), with a MFI of 20.8 g.10min^{-1} (200 °C, 2.16 kg), and a melting point of 162 °C, supplied by Pallmann Maschinenfabrik GmbH & Co. (Germany) in the powder form. PP grafted with maleic anhydride (PP-g-MA), containing 0.5 to 1.0 wt% of maleic anhydride (Exxelor PO 1020), with MFI of 110 g.10min^{-1} (190 °C, 1.2 kg), and a melting point of 156 °C, was produced by ExxonMobil, Germany. Stearic acid in the powder form was supplied by Fluka.

5.2.2 Twin-screw extrusion compounding

Prior to compounding, all natural raw materials were dried at 80 °C during 24 h to stabilise the cork moisture content. After this step, the moisture content, determined by oven-dry weight before processing, was found to be less than 2.5%. The prepared formulations and processing conditions are summarized in Table 5.1.

Table 5.1. Compositions and processing conditions used on the preparation of the PP/Cork composites using PP-g-MA or stearic acid as coupling agent.

	Components				Processing conditions		
Code	PP	Cork		Coupling agent	Temperature profile	Screw speed	Extruder Type
		powder	granule				
	(wt.%)	(wt.%)		(wt%)	(°C)	(rpm)	
PP	100				160;180;180;185;185;190;180	150	1
CPC 1	95	5				150	
CPC 2	85	15				200	
CPC 3	70	30				300	
CPC 4	95		5			200	
CPC 5	85		15			200	
CPC6	70		30			300	
CPC 7	85	15		2		200	
CPC 8	85	15		4		200	
CPC 9	85	15		8		200	
CPC 10	85		15	2		200	
CPC 11	85		15	4		200	
CPC 12	85		15	8		200	
CPC 13	85	15		2 *		200	
CPC 14	50	50			155; 180; 190	30	2
CPC 15	30	70				30	

1 Co-rotating twin screw extruder (LEISTRITZ)

2 Counter-rotating twin screw extruder (CARVEX)

* Stearic acid as coupling agent

The compositions polypropylene, CPC 1 to CPC 13 were compounded in a Leistriz LSM 30.34 intermeshing co-rotating twin-screw extruder with a screw diameter of 33.7 mm and a length to diameter ratio L/D of 29, coupled to a die with a two cylindrical outputs with 4 mm diameter each. The scheme of cylinder and screw configuration used for the preparation of these composites is shown in Figure 5.1. The main screw profile includes conveying elements and different types of kneading blocks with staggering angles of -30°. Moreover, the extruder was equipped with two automatic volumetric

feeders, where the feeding 1, represents the addition of grinding PP with or without coupling agent. Generally, the polyolefin and the coupling agent were tumble-mixed and fed through the hopper. The feeding 2 indicates the location of the addition of cork powder or granules where the morphology and the volume relation of both are shown in Figure 5.2.

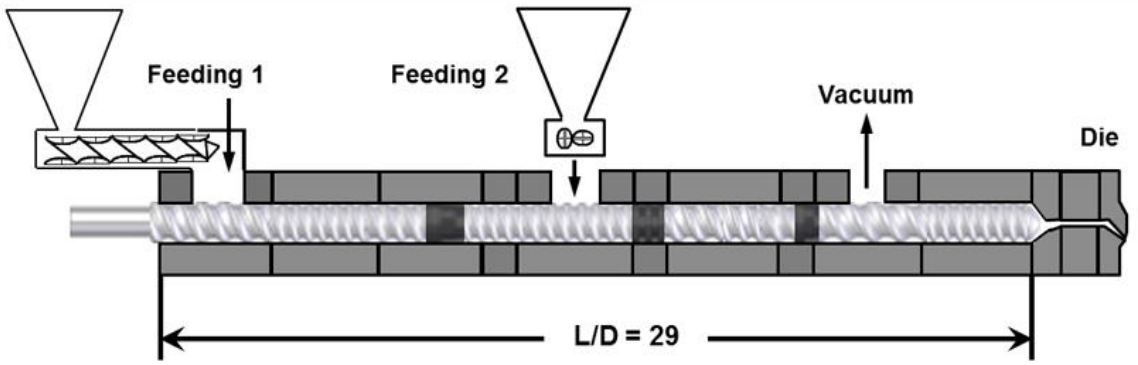

Screw element	1	2	3	KB -30	5	6	KB -30	8	9	10	KB -30	12	13	14	15
Length (mm)	120	120	60	30	60	120	30	60	60	30	22.5	120	30	60	60
Pitch (mm)	45	30	30	—	20	30	—	45	30	30	—	60	30	20	20

KB -30 denotes a block of left-handed kneading discs, with a staggering angle of 30°.

Figure 5.1. Extruder and screw profile configuration from the hopper to the die used to produce the PP/cork composites.

In all the experiments it was used a vacuum pump system and the feed rate was set for 2 kg/h. The temperature presents a decreasing at the end of the profile since it is compensated by the increased shearing which tends to increase the temperature of the composite. Part of the extrudate was cooled in water bath and subsequently ground by a Scheer (Germany) grinder in order to obtain pellets with length $\leq$ 5 mm. The pellets were dried in an oven at 80 °C and further packed and sealed in plastic bags and conditioned at room temperature (23°C, 55% relative humidity) at least for 48 hours prior to further investigation.

CPC 14 and CPC 15 compositions were compound in a counter-rotating twin-screw extrusion machine (Carvex, Portugal), which had a screw diameter of 52 mm and an L/D ratio of 18 with a nonintermeshing, mixing mode screw configuration. The barrel temperature profile was in the range 155-180-190 °C, and the screw speed was fixed at 30 rpm.

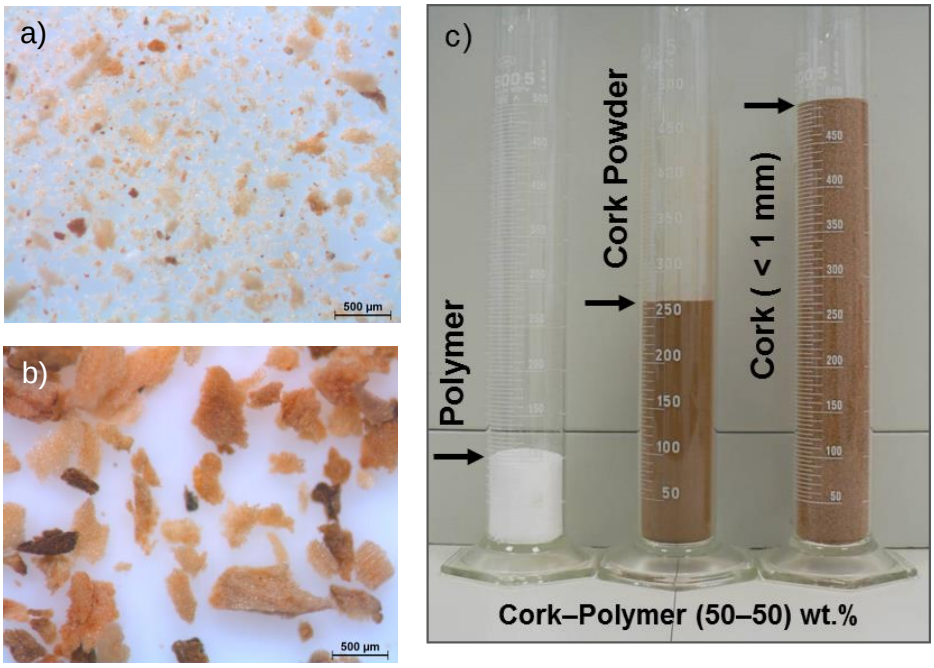

Figure 5.2. Representative micrographs from: a) cork powder and b) granulated cork. Image c) shows the differences (for the same weight) in volume between the three raw materials used.

The cork powder and the PP were pre-mixed and manually feed in the hopper system. No extrusion head was used in order to minimize the residence time and shear heat dissipation. The extruded material was cooled in air, granulated in a cutting mill to produce composite pellets. The pellets were stored in plastic bags and sealed and further conditioned at room temperature for further investigation.

5.2.3 Injection moulding

The polypropylene and the PP/cork composite pellets (PP, CPC 1 to CPC 13) were injection moulded in an ENGEL Spex Victory 50 (Austria GmbH). The processing conditions were optimized and the parameters described in Table 5.2 were used in all conditions. The injection-moulded specimens were tensile bars produced according ASTM 638, with 60 mm length, a constant rectangular cross-section of 2×4 mm^2, and a neck length of 20 mm.

Table 5.2. Processing injection moulding conditions of PP and PP/Cork composites.

	ENGEL
Injection speed (mm/s)	30
1st holding pressure (MPa)	28
1st holding pressure time (s)	0.33
2nd holding pressure (MPa)	1
2nd holding pressure time (s)	10
Moulding temperature (°C)	20
Cooling time (s)	20
Barrel temperature profile (°C)	190 / 180 / 170 / 160 / 30
Clamping force (kN)	500

5.2.4 Compression moulding

The PP/cork composite pellets were compression moulded using a hot press (Moore, UK) to produce plates with 186 × 118 mm^2 and 2 mm of thickness. The mould temperature was 180 °C and the material was kept 8 minutes in the mould without pressure followed by 2 minutes under 6 tones pressure followed by a cooling period with water under pressure.

5.2.5 Morphology

The distribution of cork particles on the PP matrix, after injection moulding, was observed on a transmission optical microscope (Olympus BH-2) connected to a Leica DFC 280 digital camera and corresponding software. To prepare the samples for the analyses, one slice with a thickness of 15 μm was cut, using a Leitz 1401 microtome equipped with a glass slicing knife, from the longitudinal section of the tensile specimen. Each sample slice was placed between a microscope glass slide and cover glass. To prevent them from curling up or corrugating, Canada balsam was used as a fixing resin. All samples were left to cure under a simple weight pressure during at least 12 h prior to analysis.

5.2.6 Physical testing

The physical tests involved accessing the dimensional stability by water absorption (*WA*), moisture content (*MC*) and density of the produced PP/Cork injection moulded composites and the plate

contraction after compression moulding. The *WA* was measured according to the ASTM D 570. The specimens, previously obtained by injection moulding, were dried at 70 °C oven night in a vacuum oven and stabilized in a desiccator before undergo the tests.

The *WA* was calculated by weighting the specimens before and after immersed in distilled water at room temperature (23 °C) and the tests were conducted up to 1344 h. The water absorption was calculated according to the Equation 1:

$$WA\ (\%) = [(W_a - W_b) / W_b] \times 100 \quad (5.1)$$

where W_a is the weight of the specimen after immersion (g) and W_b is the weight of the same specimen before immersion (g). Since cork is a natural material that presents some hygroscopic behavior, it was necessary to determine the moisture content before WA testing. For that purpose, the specimens were weighed using an analytical balance before being placed in a vacuum oven at 50 °C for 48 h. The specimens were then removed from the oven and cooled and stabilized in a desiccator several days followed by reweighing of the specimens. The moisture content of the specimens was calculated as follows:

$$MC\ (\%) = [(W_w - W_d) / W_w] \times 100 \quad (5.2)$$

where W_w is the weight of the specimen before drying (g) and W_d is the weight of the sample after drying (g). Averages of five specimens were used for WA and MC measurements.

The density of the PP matrix and PP/cork injection moulded composites was determined according to the standard ASTM D 792, using an analytical balance equipped with a stationary support for the immersion vessel using liquid propanol. Averages of five specimens were measured per condition.

The plate contraction was accessed after the compression moulding process by comparing the dimensions of the metallic mould frame with the final dimensions of the 2 mm thick produced plates.

5.2.7 Mechanical properties

Tensile properties of the polypropylene and PP/cork composites were measured using an Instron 4505 Universal Testing Machine, (USA) according to the standard ASTM D 638. The tests were conducted using a 1 kN load cell, with a gauge length of 20 mm and a crosshead speed of 5 $mm.min^{-1}$ until

rupture. The tensile force was taken as the maximum stress in the stress-strain curve. Tensile modulus was estimated from the initial slope of the stress–strain curve (between 0.5 and 1% strain) using the linear regression method. Samples were conditioned at room temperature for at least 48 h before testing. The average and standard deviations were determined using at least 5 specimens per condition. Data were statistically analysed using IBM SPSS software v. 23.0 (Release 23.0 for Windows) to infer about significant differences on the tensile properties of the developed composite materials. We first applied the Shapiro–Wilk test to test the assumption of Normality and the results showed that the data were not following a Normal distribution. Consequently, the Kruskal-Wallis nonparametric test was used to compare the medians of the tensile modulus, tensile strength and maximum strain for the composite specimens before and after immersion tests. Differences between groups were considered to be statistically significant at a confidence level of 95.0 %.

5.2.8 Thermal properties

A Daventest (England) was used for obtaining data and allow determining melt flow index (MFI) of the neat polypropylene and of each composite material in the pellet form. Procedures were performed according to ASTM D1238, using 210 °C and 2.16 or 5 kg. Each condition was repeated once.

Differential scanning calorimetry (DSC) and oxidation induction time (OIT) measurements were performed in a TA instrument DSC Q100 model (USA) equipment and using samples of 8–12 mg. DSC was conducted at a heating rate of 10 °C.min^{-1}, under nitrogen atmosphere (flux of ca. 50 ml min^{-1}). Only the second run was analysed for melting temperature (T_m) and melting enthalpy (ΔH_m). The degree of crystallinity was calculated on the basis of a 100% crystalline PP a melting enthalpy of ΔH_{m^0} = 209 J/g [34], according to the Eq. (3):

$$\chi_c(\%) = \Delta H_m / (\Delta H_m{}^0 (1 - w)) \times 100 \quad (5.3)$$

where ΔH_m is the apparent enthalpy of fusion per gram of composite and w is the weight fraction of cork in the composite. All the analysis were repeated at least once.

OIT is a method to measure the stability of material against oxidation. Indium was used as calibration. The samples were heated at a rate of 20 °C.min^{-1} up to 200 °C under nitrogen atmosphere. After 4 min at 200 °C, the atmosphere was changed to oxygen (both gases at flux 50 ml.min^{-1}) and oxidation

induction time was measured during the isothermal period. The analyses were performed in three samples per each condition.

Thermal conductivity, thermal resistance and sample thickness of the plates obtained by compression moulding were measured in an Alambeta, Sensora HDH (Czech Republic), at 21 °C. The principle of the equipment is described in the literature [35]. In more detail, the experimental procedure consisted on measuring the heat flow passing through the composite due to the difference of temperature where the bottom measuring plate was set at 20°C and the measuring head (upper plate) was constant heated at 34 °C. All the measurements were repeated 3 times. The composite ability to conduct heat through its internal structure is given by the thermal conductivity (λ) and is determined from the following equation [36]:

$$\lambda = Q/(F\tau(\Delta T/h))\ [Wm^{-1}K^{-1}] \quad (5.4)$$

where, Q is the amount of conducted heat, F is the area through which the heat is conducted, τ is the time of heat conducting, ΔT represents the drop of temperature and h the plate thickness obtained in this study by compression moulding.

The thermal resistance is a property of materials and indicates how well a material insulates and it is represented by [36]:

$$R_t = h/\lambda\ [m^2KW^{-1}] \quad (5.5)$$

where, R_t is the thermal resistance and depends on the composite thickness h.

5.3 Results and discussion

5.3.1 Physical properties

5.3.1.1 Water absorption and moisture content

The moisture content (*MC*) of the injection moulded specimens was determined before the water absorption (*WA*) tests and the results are presented in Table 5.3. The results show that, the highest *MC*

was 0.21 ± 0.02%, value obtained the CPC 3 composition containing 30 wt.% of cork powder. For all other compositions the *MC* value was less than 0.16 ± 0.02% being the reduced value of moisture obtain in the composites influenced by the processing methodology and the content of lignocellulosic material in the composite. The impermeability of cork to liquids and gases, derived from its closed cell walls that are made mainly of suberin, however it absorbs moisture at ambient relative humidity [12, 13].

The *WA* behaviour of the injection moulded specimens determined by equation 5.1 is shown in Figure 5.3. The obtained results suggest that the water uptake depends of several parameters, including cork amount and cork particle size as shown in Figure 5.3 a). The addition of cork particles increased the water uptake of the composites when compared with the neat polymer, being the composition CPC 3 containing cork powder the one with higher *WA*.

This behaviour was independent of the cork particle size. However, the influence of cork particle size was observed for the compositions prepared with higher cork content (30 wt.%), were the higher surface area of cork powder available to interact with water seems of significant importance. It was previously reported, that the contact angle of natural cork with water is around 84° and reduces with the time due to the *WA* [12]. We hypothesise that the hydrophilic polar hydroxyl and carboxylic groups present at the cork surface are responsible for the moisture uptake. Moreover, it was found that water absorption in lignocellulosic composites is mainly due to the presence of fine pores and hydrogen bonding sites in the bio-based component, gaps at the interfaces, and the micro-cracks in the matrix formed during the compounding process [37].

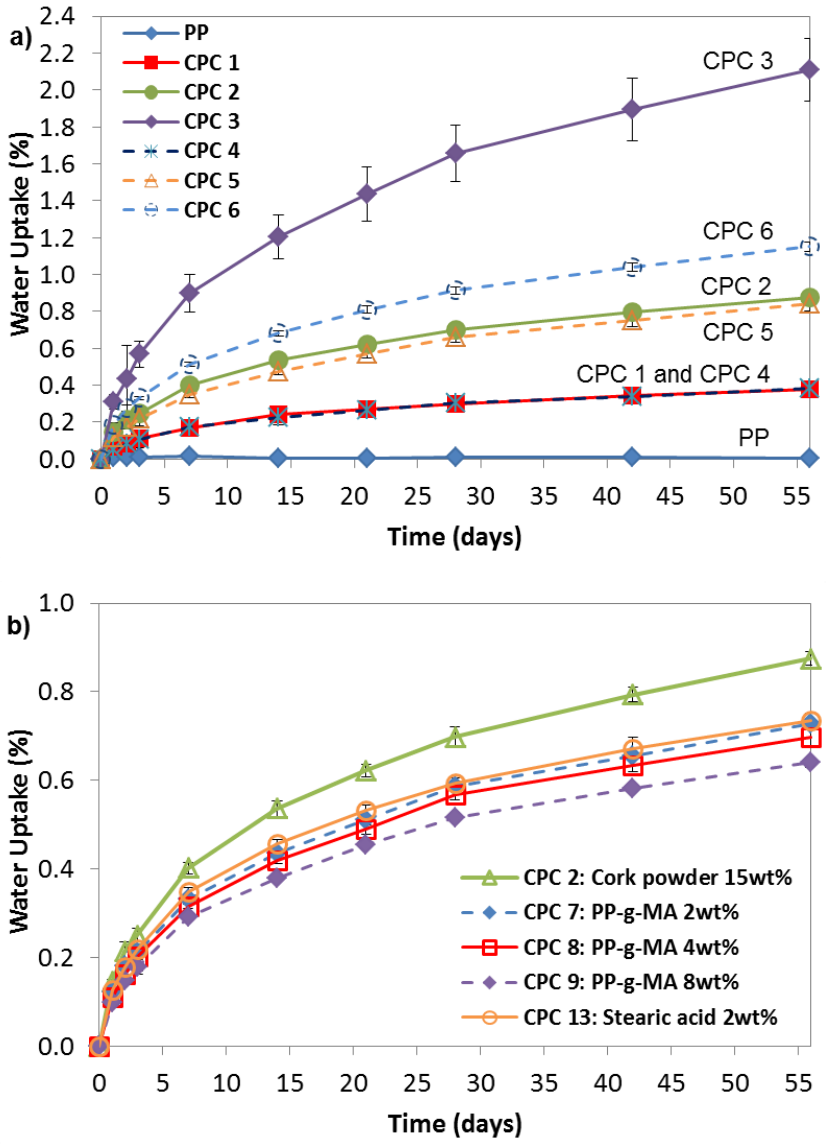

Figure 5.3. Water uptake of the different PP/cork formulations as function of the immersion time: a) effect of the amount and granulometry of cork particles; and (b) effect of the coupling agent (PP-g-MA or stearic acid).

Table 5.3. Physical and tensile properties of PP matrix and PP/cork composites after injection moulding.

	Injection moulding (tensile specimens with 2 mm of thickness)					
Composite Code	Density (kg/m^3)	Moisture Content (%)	Water uptake after 48h (%)	Tensile Strength (MPa)	Tensile Modulus (MPa)	Maximum Strain (%)
PP	896±0.3	-0.01±0.01	0.01±0.01	34.9±0.5	623.6±14.3	> 300
CPC 1	911±1.0	0.05±0.01	0.09±0.01	31.9±0.6	671.4±52.7	46.4±5.5
CPC 2	945±0.8	0.12±0.01	0.21±0.02	28.1±0.8	655.2±14.6	17.2±1.6
CPC 3	985±1.8	0.21±0.02	0.44±0.18	24.3±0.3	516.6±37.2	9.2±1.2
CPC 4	913±0.9	0.06±0.00	0.08±0.01	32.4±0.4	684.9±29.0	34.4±6.1
CPC 5	941±6.0	0.11±0.03	0.17±0.01	28.0±0.8	615.3±56.2	13.6±1.3
CPC6	967±2.6	0.16±0.01	0.28±0.02	25.8±0.5	617.7±19.8	11.7±1.2
CPC 7	939±1.7	0.08±0.01	0.18±0.02	33.1±1.0	618.7±66.2	17.3±2.1
CPC 8	937±1.9	0.13±0.00	0.16±0.02	33.6±0.4	588.4±47.6	20.4±0.9
CPC 9	932±1.4	0.12±0.00	0.15±0.01	33.9±0.4	670.0±32.9	21.1±3.2
CPC 10	941±3.2	0.15±0.01	0.18±0.01	31.6±0.2	664.9±25.6	12.2±1.0
CPC 11	939±1.3	0.15±0.01	0.16±0.01	32.6±0.4	646.4±40.5	14.9±0.7
CPC 12	933±0.6	0.14±0.01	0.13±0.01	32.9±0.4	634.9±38.0	15.1±1.9
CPC 13	935±0.3	0.10±0.01	0.18±0.01	27.7±0.5	595.4±20.5	19.4±2.3

± standard deviation.

The effect of adding a coupling agent, PP-g-MA or stearic acid, on the water absorption behaviour of the composites was also analysed (Figure 5.3 b). For that purpose, the compositions containing cork powder (15 wt.%) and different amounts of coupling agent were selected. From the obtained results is clear that the water uptake was reduced with the addition of coupling agent. In the case of PP-g-MA, the decrease of *WA* was more pronounced with the increase of the coupling agent content. The functional groups [-$(CO)_2$ O-] of maleic anhydride interact manly with the hydroxyl groups (-OH) [38] present in the lignocellulosic materials increasing the interfacial adhesion and reducing the available polar groups at the particle surface to absorb water. In the case of the stearic acid it is reported that the carboxyl group of stearic acid reacts with the hydrophilic hydroxyl groups of the natural fibre and improves water resistance properties [39]. The improvement on the compatibility between cork-polymer may result in a

reduction of possible micro voids resulting from the processing and consequently on a decrease on the *WA*. It should be highlighted that, even for the high cork content of 30 wt.%, the WA was very low being 2.11 ± 0.17 % the highest value after 1344 h of immersion.

5.3.1.2 Density of plates and of specimens

The effect of the processing method, type and amount of cork particles on the final density of the different compositions was analysed, see results in Figure 5.4.

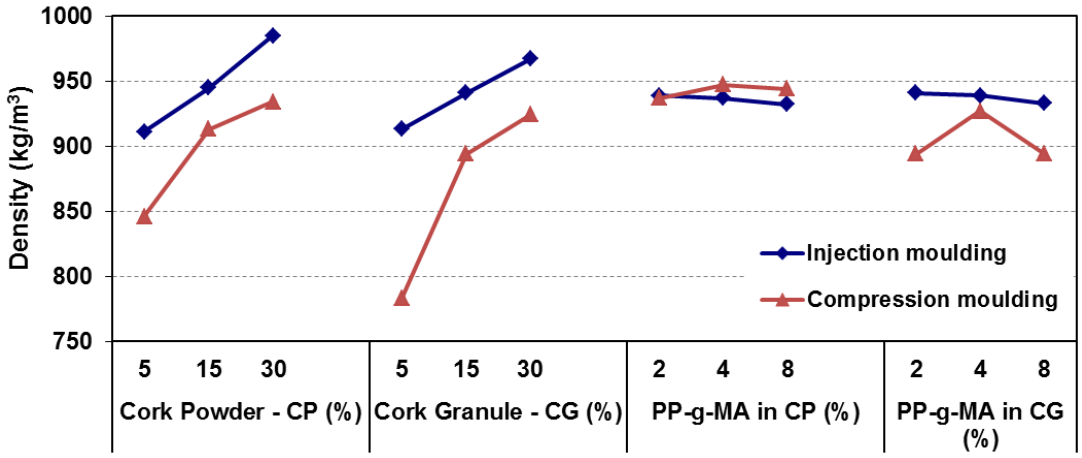

Figure 5.4. Density of the different PP/cork composites after injection and compression moulding processes.

Considering the density of the neat polypropylene 896 kg/m^3, it was observed that the injection moulded composite specimens exhibit higher density when compared with the compression moulded ones, probably due to the higher pressures (per unit of volume) involved during the injection moulding process (see Table 5.2). Unexpectedly, it was also observed that, for both processing methods, formulations containing higher amount of cork (30 wt.%) have shown higher density. For both cases, this behaviour was more evident on the composites prepared using cork powder (985 kg/m^3) than in the ones prepared with cork granules (967 kg/m^3), representing an increase on the density of 10 and 8% respectively. The presence and the amount of coupling agent during injection moulding promoted a small reduction on the composite density. This occurs probably due to the additional distributive capacity of the coupling agent that enhanced the dispersion of the cork particles during the extrusion process.

Applying compression moulding in the presence of coupling agent it was observed resulted in a small increasing on the composite plate's density, especially when using cork powder. As explained before, this could be due to a possible reduction of micro-voids that may occur during this static process. However the selected pressure applied in compression moulding enables to take some advantage of this natural cellular material in terms of final density of the composites as compared with the neat polypropylene. The increasing on density was also observed for the two additional formulations (CPC 14 and CPC 15) using higher cork amounts (50 and 70 wt.%) respectively. These compositions represent bio-based composites containing 85 and 93% of cork powder in volume. As presented in Table 5.4 using 70 wt.% of cork powder the final composite plate density was 1044 kg/m^3.

One possible explanation is the densification of the cork particles due to the high pressures involve in both processing methods. Cork is a light weight material (see Figure 5.2 c)) and it is composed by a closed cellular structure. The density of the cork cell wall was never experimentally measured but it was estimated by the density of the different polymeric components to be 1150 kg/m^3 [12, 17]. This may explain the effect of some densification that occurs using lignocellulosic materials such as cork combined with polyolefins after being processed by two melting processing steps.

Table 5.4. Properties of the matrix and of the cork composite materials after the indicated melt based processes.

Composite Code	Extrusion (pellets length < 5 mm)								Compression moulding (plates with 2 mm of thickness)				
	Melt Flow Index		T_c [1]	ΔH_c [1]	T_m [1]	ΔH_m [1]	χ_c [1]	OIT [1]	Thickness	Contraction	Density	Thermal conductivity [2]	Thermal resistance [2]
	Load	MFI											
	(kg)	(g/10min)	(°C)	(J/g)	(°C)	(J/g)	(%)	(min)	(mm)	(%)	(kg/m^3)	(Wm^{-1}K^{-1})	(m^{2}KW^{-1})
PP	2.16	23.1	119.9	100.1 (100.1)	155.6	99.4 (99.4)	47.6	2.7	2.0	4.0	879	0.082	0.030
CPC 1	2.16	11.4	122.0	99.6 (104.8)	156.6	96.8 (101.9)	48.8	20.0	2.0	3.4	846	0.072	0.033
CPC 2	2.16	4.3	122.1	87.8 (103.3)	156.4	86.2 (101.4)	48.5	33.0	2.0	3.5	913	0.096	0.024
CPC 3	5.00	7.8	123.1	71.3 (101.9)	156.4	69.4 (99.1)	47.4	37.4	2.3	2.9	934	0.108	0.023
CPC 4	2.16	12.5	121.9	99.6 (104.8)	156.5	97.5 (102.6)	49.1	13.5	2.1	2.9	783	0.082	0.030
CPC 5	2.16	4.9	122.7	86.1 (101.3)	156.4	85.2 (100.3)	48.0	26.1	2.1	2.7	894	0.092	0.027
CPC6	5.00	12.1	123.7	80.4 (114.3)	156.7	78.1 (111.5)	53.4	28.8	2.1	2.8	924	0.104	0.022
CPC 7	2.16	5.1	125.2	89.1 (104.9)	156.8	87.2 (102.6)	49.1	32.5	2.1	3.2	937	0.082	0.035
CPC 8	2.16	6.0	125.2	90.0 (106.0)	156.5	87.8 (103.3)	49.4	31.4	2.1	3.1	947	0.091	0.029
CPC 9	2.16	8.4	124.9	92.3 (108.6)	156.5	88.6 (104.3)	49.9	26.6	2.0	3.1	944	0.079	0.037
CPC 10	2.16	5.4	124.2	87.7 (103.2)	156.1	86.5 (101.8)	48.7	21.1	2.1	3.0	894	0.087	0.027
CPC 11	2.16	6.7	124.4	90.8 (106.9)	156.3	88.7 (104.5)	50.0	22.7	2.0	3.1	927	0.094	0.028
CPC 12	2.16	8.7	124.3	92.9 (109.4)	156.0	92.3 (108.1)	52.0	17.7	2.1	2.9	894	0.099	0.024
CPC 13	2.16	6.8	122.9	89.4 (107.7)	155.9	86.6 (104.3)	49.9	30.1	2.1	2.9	928	0.105	0.023
CPC 14	7.16	10.3	125.8	46.0 (92.0)	156.1	43.4 (88.9)	42.5	*	2.3	2.2	1012	0.140	0.018
CPC 15	21.6	*							2.3	1.8	1044	0.155	0.015

[1] Indicates the onset for crystallization temperature (T_c); crystallization enthalpy (ΔH_c); melting temperature (T_m); melting enthalpy (ΔH_m); crystallinity (χ_c) and oxidation induction time (OIT_{onset}) determined by DSC; [2] Thermal conductivity and thermal resistance determined at 34 °C; (*) not possible to determine; () values of apparent enthalpy of melting per gram of polymer $\Delta H'_m = \Delta H_m / (1 - w)$, where w is the cork fraction.

5.3.1.3 Plate contraction

The compression moulded plates were used to determine the contraction behaviour of the different compositions and the obtained results are indicated in Table 5.4. As expect, the 2 mm thickness plates prepared using only the neat polypropylene presented a high contraction of 4.0 % in the mould walls. By increasing cork concentration, the contraction was proportionally reduced, being 2.2% for the polymer-cork powder (50-50) wt.% composition CPC 14. Moreover, increasing the cork particle size reduced the contraction in the mould. This are an important results for the design of composite materials since the use of low amount of cork particles can contribute for increasing the dimensional stability of the final product.

5.3.1.4 Composite aesthetics

The aesthetic properties of the produced PP/cork composite plates with 5 wt.% of cork and 2 mm thickness, obtained by compression moulding, are presented in Figure 5.5.

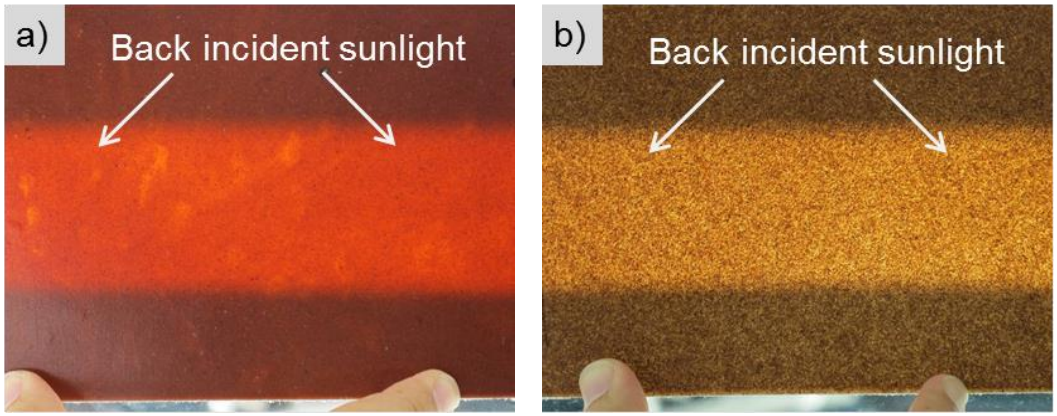

Figure 5.5. Visual aspect of 2 mm thick PP/cork composite plates formed by compression moulding: a) CPC 1 containing PP with 5 wt.% of cork powder and b) CPC 4 containing PP with 5 wt.% of granulated cork.

It was observed that both cork powder and granulated cork acts as a pigment promoting a brown colour (Figure 5.5 a). On the other hand, when granulated cork is used (Figure 5.5 b), it is possible to observe a homogeneous distribution of the cork granules promoting a better aesthetic on the final material. Taking aesthetics and environmental awareness as the main selection indices for a specific application, we can suggest that cork is one of the highest ranking candidates to be used in the development of sustainable materials.

5.3.2 Composite morphology

Transmission optical microscopy was employed to evaluate the cork particles distribution on the PP/cork composite specimens. Figure 5.6 shows the bright field micrographs from the longitudinal sections (flow direction) of injection moulded samples, revealing good dispersion and distribution of the cork particles, also promoted by the twin-screw extrusion process. A few dark particles were observed; however, the used cork particles also present some dark brown particles as shown in Figure 5.2 a) and b) that can be resulted from the wood bark of the tree and not resulted from a thermal degradation process of cork.

Increasing the cork bio-based content up to 30 wt% (Figure 5.6 d and g) no particle aggregation was observed, maintaining the homogeneous cork distribution and dispersion. It has been reported that one of the main problems in processing wood-thermoplastic composites is the tendency of untreated wood to form large aggregates, due to a high intramolecular bonding among the fibres [11]. Therefore, this may be a distinguishable feature of using cork if the proper extrusion conditions are used.

Since cork is a compressive foam material and PP matrix presents higher hardness, it was also expected to see some voids at the polymer-cork interface due to the cutting process during samples' preparation. On the contrary, the bright field microscopy micrographs showed a good cohesion of the cork particles in the structure film prepared for microscopy, revealing a good interfacial adhesion between cork and the PP matrix independently of the cork particle size or cork weight fraction or the use of coupling agent present in the composite. This absence of gaps or voids between cork-polymer without coupling agent may also be supported by the cellular structure at the cork surface allowing higher attachment of the PP during the melting compounding. The result also supports the low water absorption results of the composites containing cork. Several studies [11, 30, 31] using other lignocellulosic fibres or fillers without coupling agents showed lower interfacial adhesion with the presence of gaps between the matrix-fibre system at this magnification. Figure 5.6 b) and f) shows polarized light microscopic (PLM) micrographs of the PP/cork composites containing 5 wt%. of cork. These PLM images reveal a shell and a subshell that is formed due to a supercooling effect resulting from the low temperature of the mould during the injection moulding process. Moreover, in this region of the specimen were the composite material is in direct contact with the mould, it was found that cork particles are highly aligned in the longitudinal direction, though the flow direction, as indicated in Figure 5.6 b). No significant differences on the cork distribution were observed in the presence of the coupling agent PP-g-MA or with the stearic acid.

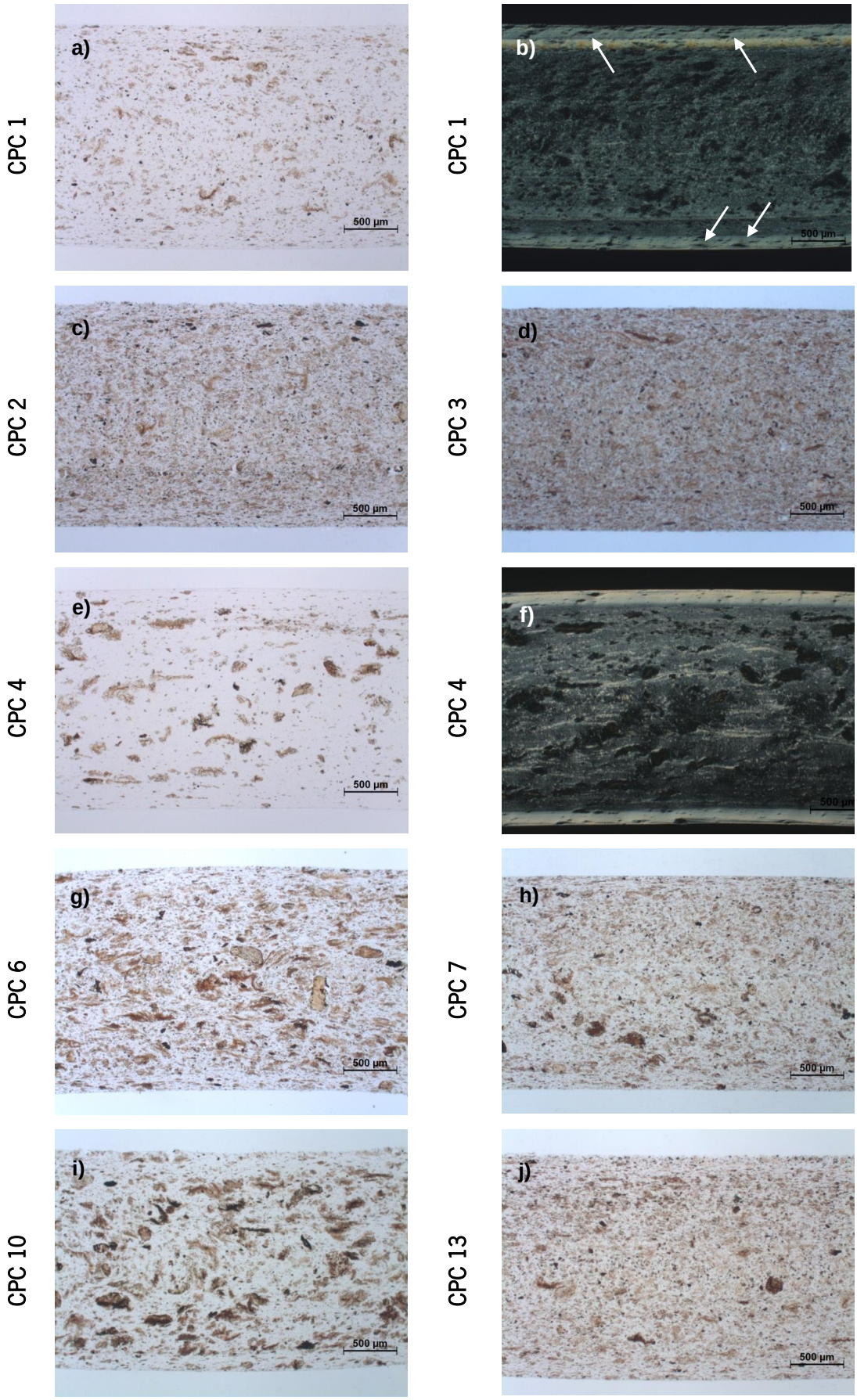
CPC 1
a)
500 µm
CPC 1
b)
500 µm
CPC 2
c)
500 µm
CPC 3
d)
500 µm
CPC 4
e)
500 µm
CPC 4
f)
500 µm
CPC 6
g)
500 µm
CPC 7
h)
500 µm
CPC 10
i)
500 µm
CPC 13
j)
500 µm

Figure 5.6. Transmission optical micrographs from the longitudinal section of injection moulded tensile bars of the different PP/cork composite specimens. Figure (b) and (f) are from polarized light microscope micrographs. Scale bar indicates 500 μm

5.3.3 Mechanical properties

Tensile strength, tensile modulus, and maximum strain are shown in Table 5.3. Representative stress–strain curves of the studied formulations are shown in Figure 5.7.

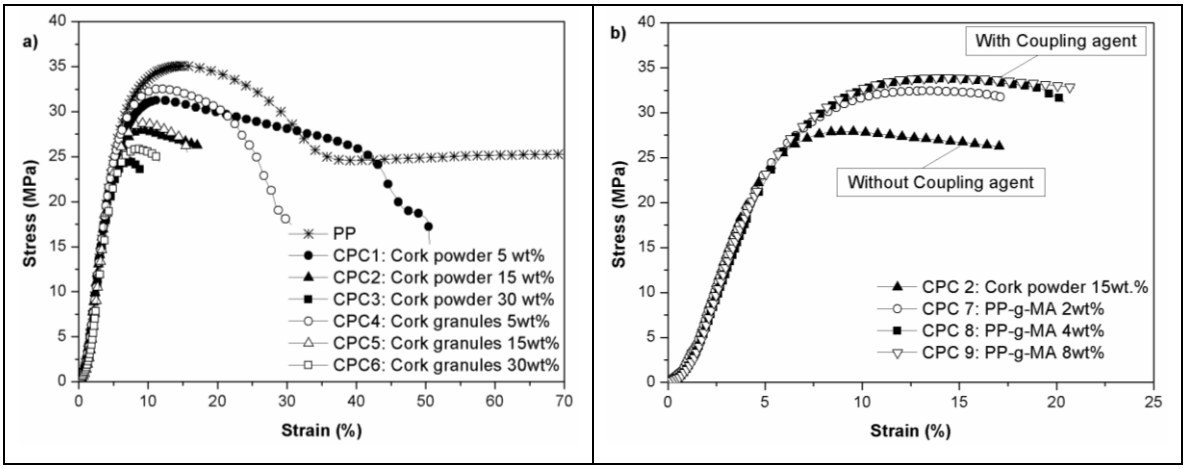

Figure 5.7. Representative tensile stress-strain curves of PP matrix and PP/Cork composites: a) effect of cork addition and its particle size and b) effect of the coupling agent on the composites containing cork powder.

5.3.3.1 Effect of cork addition

The effect of cork addition on the tensile properties of the composites was analysed and compared with the PP matrix in terms of percentage. The results are plotted on Figure 5.8 a, c and e). The addition of low amounts of cork (i.e. 5 wt.%) reinforced the stiffness of the polypropylene in 10%, while the use of cork up to 15 wt.% does not affect negatively the tensile modulus of the neat PP. When the cork content was increased to 30 wt.% an opposite effect was observed decreasing the composite stiffness.

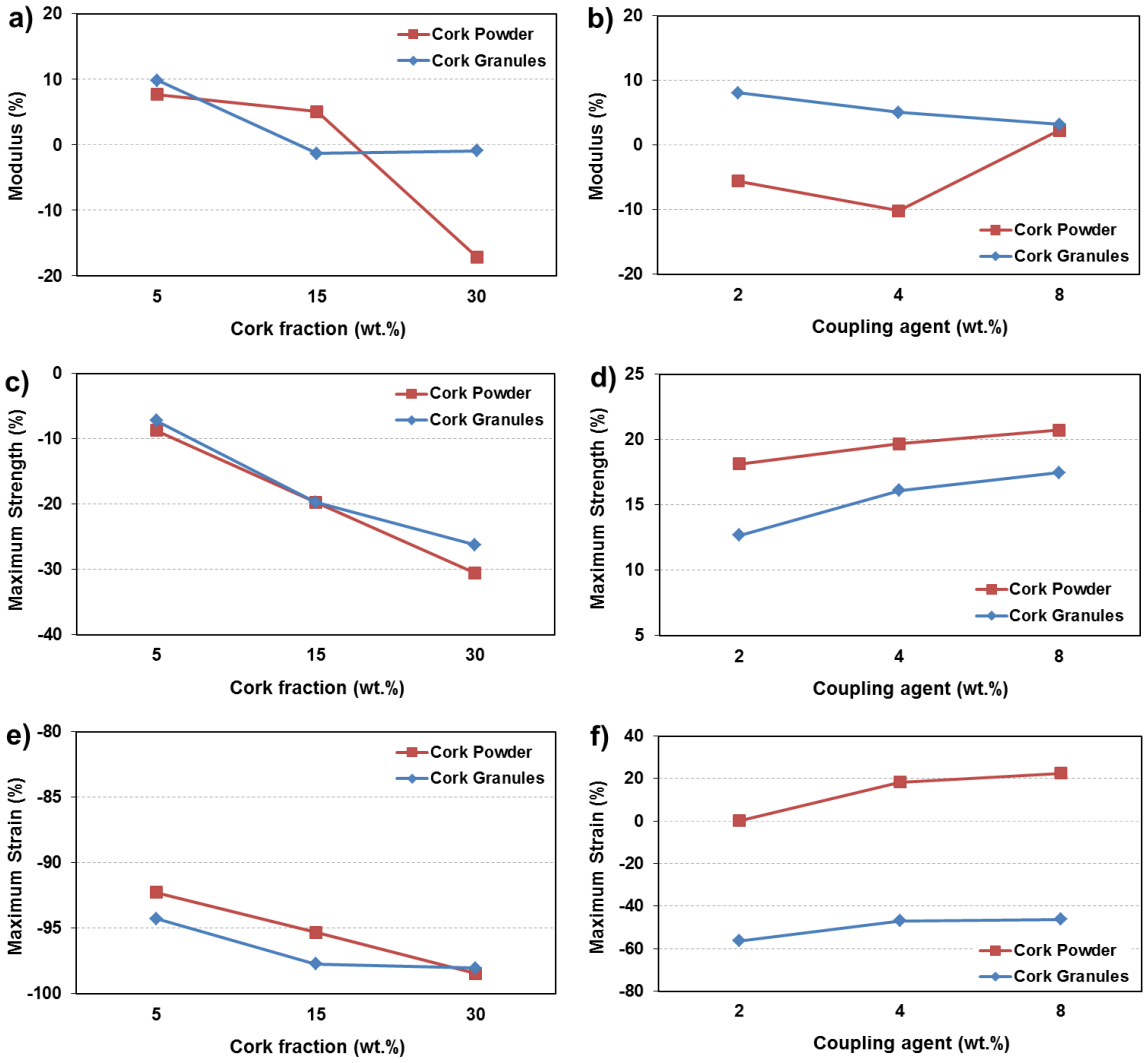

Figure 5.8. Effect of addition of cork (a, c, e) as compared with the PP matrix and the effect of the coupling agent (b, d, f) as compared with the PP/Cork composite with 15 wt.% of cork powder (CPC 2) or granules (CPC 5) on the tensile properties of the developed composites.

The tensile strength and the maximum strain were significantly reduced in all cases, where Figure 5.7 a) and Figure 5.8 e) show the clear decrease in the maximum strain with the addition of the bio-based component. The decrease in tensile strength is partially due to the inherent incompatibility between cork particles and PP matrix. As the load is applied to the composite material, the lack of interfacial adhesion between cork particles and the matrix will limit the load transfer process, thus, resulting in a decrease in the tensile properties. Additionally, the mechanical properties of cork under tensile load are lower when compared with the polypropylene matrix contributing to a diminishing of the tensile strength.

5.3.3.2 Effect of PP-g-MA and stearic acid

It is well known that the fibre–matrix interaction has a significant effect in the final mechanical properties of polymer composites. To improve the bonding strength between cork particles and the polymeric matrix, polypropylene graft maleic anhydride (PP-g-MA) and stearic acid were tested as coupling agents. The results are presented in Figure 5.7, Figure 5.8 and summarized in Table 5.3. The effect of PP-g-MA on the tensile modulus is shown in Figure 5.8 b). The stiffness of the composite presents a small improvement for the granulated cork while in the powder form a small decrease on the stiffness was obtained. Increasing the coupling agent up to 8 wt.% the composites exhibited similar stiffness when compared to the control specimens (CPC 2 and CPC 5) containing 15 wt.% of cork without coupling agent. Tensile strength of the composites was significantly improved with the addition of the PP-g-MA (Figure 5.7 b) and Figure 5.8 d)), resulting in a composites with higher strength and toughness. Additionally, the increase on tensile strength was not proportional to the increase of the amount of coupling agent used indicating that the use of PP-g-MA in 8 wt.% does not promoted a relevant increase on the tensile strength as compared with the composites using 4 wt.% of PP-g-MA. These results suggest that the addition of coupling agent based on maleic anhydride (MA) improves the interfacial adhesion between both components promoting the load transfer from the matrix trough the cork particles resulting in an increase of the tensile strength. As it was pointed before, the MA interact manly with the hydroxyl groups of the lignocellulosic materials increasing the interfacial bonding of PP-cork, which leads to a better stress transfer from the polymer to the cork resulting on the increase of the tensile properties. The maximum strain in PP/Cork (85/15) wt.% was also considerably improved with the addition of coupling agent (see Figure 5.8 d).

On the contrary, the use of stearic acid as presented in Table 5.3 does not influence the tensile strength, reduced the tensile modulus and promoted just a slight increase on the maximum strain at break. Similar effect has been reported on the properties of PP/wood flour composites [40], where the stearic acid slight increased the strain at break and promoted better homogeneity and processability. In this study, it was also observed that the addition of stearic acid acted as a release mould agent during the injection moulding. The use of solid lubricants is recommended to reduce the friction coefficient of the natural fibre materials [41].

5.3.3.3 Effect of cork particle size

The effect of cork particle size on the tensile properties of the PP/cork composites can be observed in Figure 5.8. In the absence of coupling agent and independently of the cork particle size, by increasing the cork content resulted in a reduction of the mechanical performance. Small differences were observed particularly the more pronounced reduction in the stiffness when it was used 30 wt.% of cork powder (Figure 5.8 a)). An opposite effect in the presence of PP-g-MA (Figure 5.8 b)) was observed. Higher content of coupling agent of 8 wt.% may contribute to reinforce the PP/Cork composite stiffness. The increase on tensile strength in the presence of coupling agent occurred independently of the cork particle size, however more significant in formulations prepared using cork powder. Furthermore, in the presence of 2 wt.% of coupling agent the maximum strain at break maintains (Figure 5.8 f) while the use of cork granules decreased the maximum strain in 60%. The result can be ascribed by the lower particle size of cork meaning a higher surface area of the bio-based fraction available to interact with the polypropylene matrix. It is expected that the use of coupling agent reduces the viscosity of the neat polypropylene increasing the contact of the thermoplastic with the cork particles and thus promoting higher tensile strength and strain at break in the final composite specimens.

5.3.3.4 Ashby diagram

The Figure 5.9 shows the Ashby plot presenting the specific maximum tensile strength against the specific tensile modulus of the PP and the PP/cork composites. It also includes the tensile properties reported for cork (good quality), being the tensile modulus of 30.8 MPa, the fracture stress of 1.05 MPa and the density ranging from 0.148 to 0.178 $g.cm^{-3}$ [42].

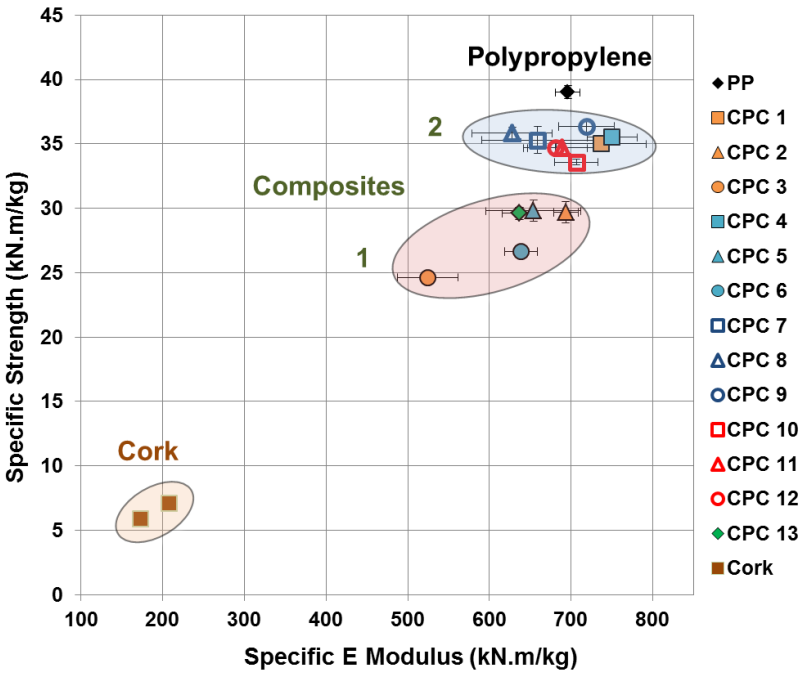

Figure 5.9. Ashby plot presenting the specific maximum tensile strength against the specific tensile modulus of the polypropylene (PP) and the PP/cork composites obtained by extrusion followed by injection moulding.

By normalizing the tensile properties by the density of each processed material two distinct regions were observed for the composites, being the region (1) containing the composites without coupling agent and with higher cork weight content (15 and 30 wt.%) and the region (2) the composites with coupling agent or with only 5 wt.% of cork. The addition of 5 wt.% of cork promotes a reinforcement on the PP matrix increasing the stiffness. Similar result was obtained using higher content of the coupling agent. The mechanical properties of the composites prepared with cork powder present higher variation as compared with the composites containing cork granules. However, higher tensile strength was achieved using cork powder with coupling agent. This result reinforces the idea of the lower the cork particle size, the higher the surface area and the interaction with the matrix due to the presence of PP-g-MA, resulting in higher mechanical properties.

5.3.3.5 Dry and wet tensile properties

Mechanical tests were performed for all the specimens before and after water absorption studies. Figure 5.10 compares the tensile properties in terms of modulus, maximum strength and maximum strain of the PP/Cork composites before and after immersion in water during 1344 hours. The used

Kruskal-Wallis statistical test compares the medians of tensile properties of the composites. *p* values less than 0.05, indicate statistically significant differences (*) between the medians at a confidence level of 95 %. In general, the mechanical properties are very similar before and after water saturation. This result is a clear advantage of cork composites since they can be used in wet conditions maintaining mechanical performance similar to dry environments. However, some statistical significant differences were observed and it is interesting to notice that, for several composite compositions, the ultimate tensile strength of wet samples is higher than that for dry samples, as shown in Figure 5.10. b).This could be due to the fact that high amounts of water causes swelling of the bio-based material, which could fill the spaces between the cork and the polymer matrix interface and eventually could lead to an increase in the mechanical properties of the composites, as reported in studies of natural fibre-matrix composites [33, 43].

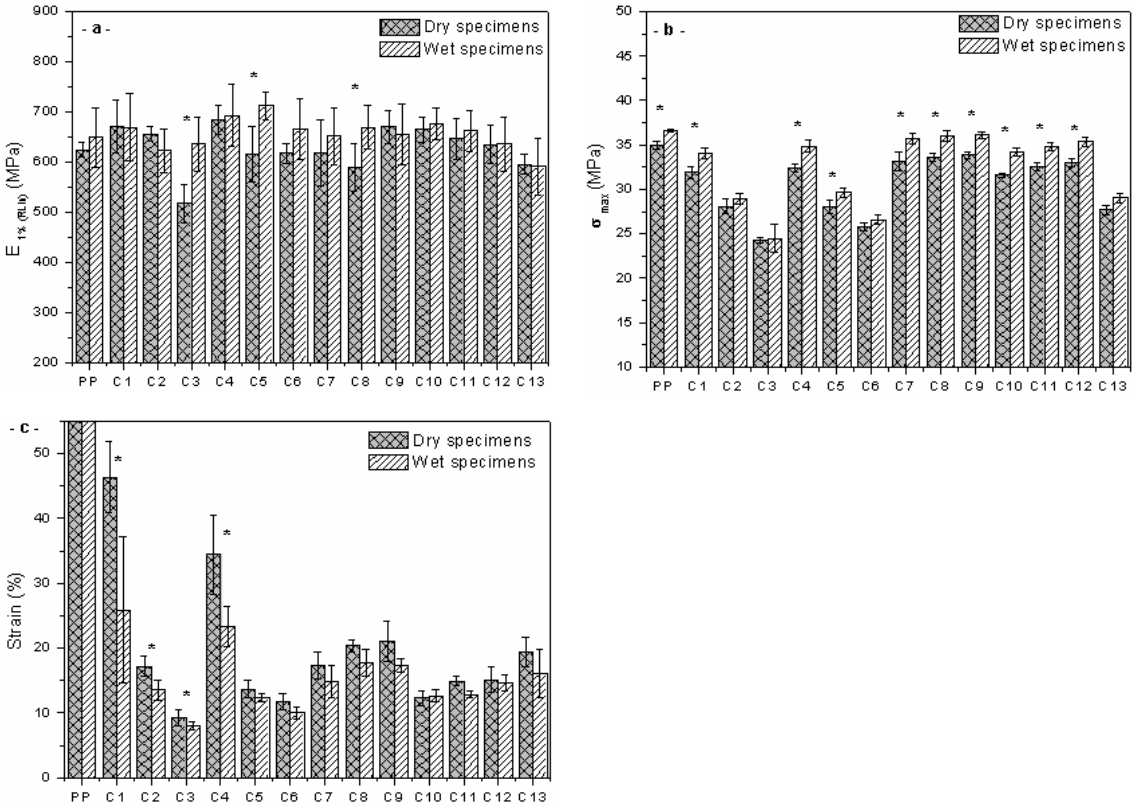

Figure 5.10. Tensile properties of the polypropylene (PP) and the PP/cork composites before and after water absorption tests. (*) denotes significant statistical differences for 0.05 of confidence in pairwise comparisons between dry and wet specimens.

On the contrary, it was observed a decrease on the tensile strain for the wet specimens (Figure 5.10 c). This effect is more evident for the composites containing low amounts of cork. Cork as a hydrophobic character with close cellular structure and is used as a sealant material [13, 14]; however it absorbs moisture, presenting low permeability to water. Once the moisture penetrates inside the cork particles tends to swell and after the saturation period it occurs an additional weakness of the cork-matrix interface which results in a clear loss on the maximum tensile strain.

5.3.4 Thermal Properties

5.3.4.1 Effect of the compounding method on the composite melt flow behaviour

The effect of cork addition on the properties of the extruded composite pellets was accessed by means of melt flow index (MFI) and the results are presented in Table 5.4. Effective mixing during compounding is important to achieve a good dispersion and distribution of cork and, consequently to optimize the composite properties. The addition of 5 wt.% of cork to the PP matrix exhibits a reduction around 50% of the MFI. As expected, this result indicates that by increasing the cork content the MFI tends to reduce, revealing the higher shear forces that occur during the extrusion process. However, for the same amount of cork, the presence of PP-g-MA and stearic acid reduces the viscosity promoting the mixability of the cork with the PP and the consequent increase on the MFI. Comparing all composition, it was observed a correlation between the cork particle size and the MFI values, being the lower the particle size the smaller is the MFI. For the same amount, there is higher number of cork particles in the powder form per volume as compared with the cork granules therefore, more interfaces between cork-matrix to restrict the flow during the extrusion and consequent reduction of the melt flow index. When a high content of cork (50 to 70 wt.%) is used the viscosity of the composite increases even more, resulting in processing difficulties justifying the option in this work to compound the CPC 14 and CPC 15 compositions without die. In addition, agglomeration of the cork as result of poor dispersion may also occur.

5.3.4.2 Crystallization and melting temperature

The thermal stability of composites was investigated by differential scanning calorimetry (DSC) and the obtained results are presented in Figure 5.11 and in the Table 5.4.

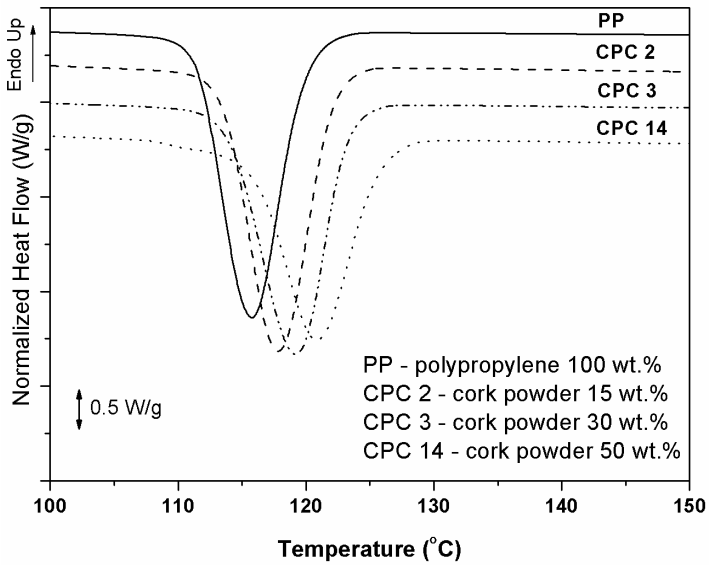

Figure 5.11. DSC curves obtained during cooling of PP and its PP/cork powder composites.

The differences to the neat PP were more relevant when the crystallization temperatures (T_c) were determined and compared from the first cooling cycling. The DSC curves show the effect of the cork powder on the crystallization of PP/cork composites. The PP/cork composites showed higher T_c than the neat PP being the increasing proportional to the cork weight fraction up to 50 wt.%. This result suggests that the crystallization process is favoured by the presence of cork particles. This effect is attributed to the nucleation effect of the cork: the particles act as sites for heterogeneous nucleation that induce the crystallization of the matrix. The nucleating ability of cork was also observed in a previous study [23] by optical microscopy and DSC using different cork powders, a by-product from cork industry, combined with polyolefins after pultrusion process. The addition of coupling agent based on maleic anhydride contributed also to increase the crystallization rate. This result implies that the coupling agent acted as a precursor increasing the crystallization. A previous study suggest that the crystallization of PP-g-MA is slightly hfaster than that of PP due to a possible chain branching of maleic anhydride and the better dispersion of the PP-g-MA in the polymer matrix [44]. Moreover, the results indicates that processing these PP/Cork composites needs less moulding time and energy than the neat PP. Table 5.4 also shows the melting temperature (T_m), melting enthalpy (ΔH_m) corrected by the cork content, and percentage of crystallinity (χ_c) that corresponds to the values obtained in the second heating scans of the neat PP and PP/Cork composites containing 5, 15 and 30 wt.% of cork. The addition of the natural cork to PP has no significant effect on the T_m, and no correlation of the results with the cork loading can be established. The increase on the cork content up to 30 wt.% on the PP matrix promoted a small increase on the crystallinity (χ_c) of the composites independently of the cork

particle size. A possible explanation for this observation is that, when cork is introduced into the PP matrix, the crystallinity of the polymer fraction increases, as a result new crystalline zones are formed around the cork particles through spherulitic crystallization on their surfaces. By increasing the cork content up to 50 wt.% the composite crystallinity (CPC 14) decreased to 42.5%. This result indicated that the crystallinity was reduced in 5.1% as compared to neat PP, probably due to the higher content of amorphous components that chemically constitute the cork. The presence of PP-g-MA in the composites seems to have influence on the enthalpy values: it was observed that the increase of coupling agent was followed by a slight increase on the crystallinity. This result was exhibited in all PP/Cork composites containing coupling agent. Thus, the increase on the crystallinity is also dependent of the degree of compatibility between the PP matrix and the cork. This behaviour was also observed in some different few natural fibres in the presence of polyolefin grafted with maleic anhydride [44-46] and supports the good interaction between the cork and the PP matrix in the presence of PP-g-MA as coupling agent observed in this study.

5.3.4.3 Oxidation induction time

Thermoplastics have points in its chain that are susceptible to the thermal oxidation during the processing and end use. On the other hand, lignocellulosic materials, such as cork, are sensitive to temperature and high shear rates during compounding that may cause degradation and consequent changes in the mechanical performance. The thermo-oxidative stability of the neat PP and the PP/cork composites in oxygen atmosphere was assessed by determining the oxidation induction time (OIT) at elevated temperatures, under isothermal conditions see results in Figure 5.12 and Table 5.4. The onset of oxidation on the matrix PP was detected immediately (after 2.7 min) as the atmosphere was changed from nitrogen to oxygen. Comparing with the matrix the increase in the OIT of the composites suggests that PP is stabilized by the addition of cork. The OIT values of the composites containing cork powder were considerably higher than the composites with granulated cork. It was found that increasing the cork content up to 30 wt.%, provides a higher antioxidative protection. The best results of OIT were obtained using cork powder (37.4 min), representing 12.9 times higher than the neat PP. This behaviour might be ascribed due to the higher surface area of the well dispersed cork particles available to interact with the matrix in combination with the higher composite density.

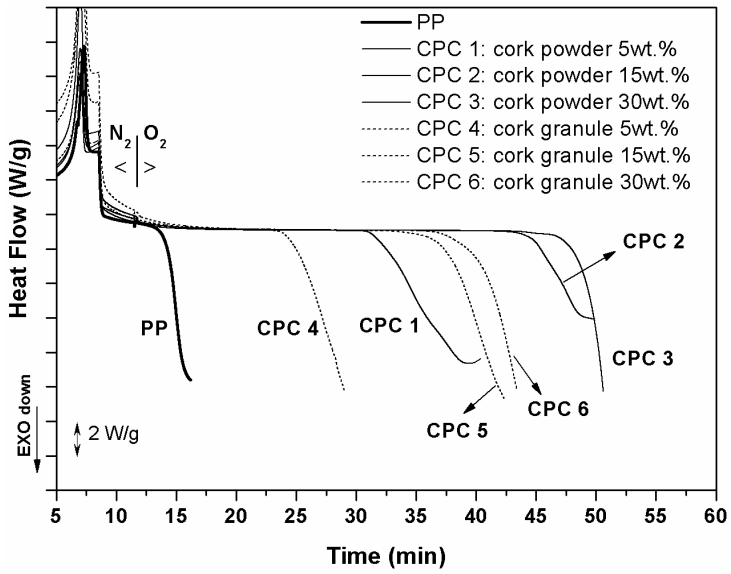

Figure 5.12. Thermal oxidative stability of the neat polypropylene (PP) and PP/cork composites at 200 °C revealing the onset of decomposition.

The higher density of the PP/cork composite material will block the access of oxygen and slows the oxidative degradation. The literature also point some studies were lignins, obtained from different processes, were added in low amounts to stabilize polypropylene against thermoxidation [47, 48] since they can impart antioxidant properties. Chemically, cork presents phenolic compounds that are present in the suberin and lignin that may also contribute for this antioxidant protection. In addition, cork extractives are non-structural organic components of the cork cell wall around up to 18 wt.% and among other components presents phenolic compounds [12] that might be released during the extrusion and mixed with the matrix contributing also to this result. It has been reported that the use of some natural fibres does not promote higher antioxidant effect in thermoplastics [26]. Nevertheless, this study shows that the two factors that are relevant to prolong the lifetime of the PP/cork composites are i) the presence of antioxidants that blocks the free radicals and ii) the composite density that may control the amount of oxygen into the composite. However, it is expected that the use of polymers containing antioxidant or thermal stabilizer compounds in their composition present higher oxidation stability than cork can provide. In that case, the stabilizer molecules are slowly released with time, thus, contributing to an extended stabilizer lifetime. It can be suggested that cork will affect positively the behaviour of the thermoplastic materials preventing the oxidative degradation of the polypropylene during compounding and subsequent service.

5.3.4.4 Thermal resistance and thermal conductivity

Thermal conductivity (*TC*) is a measure of the heat flux that will flow through the material if a certain temperature gradient exists over the material [49]. The small cells are an important feature of cork. The cells are much smaller than those in the polymeric foamed materials providing excellent insulating properties to the material [17]. The *TC* of the produced plates, as compared with the PP matrix, is presented in Table 5.4 and Figure 5.13. The results have shown that *TC* maintains or decreases only for the composites up to 5 wt.% of cork content. All the PP/cork composites present low *TC*, however, significant differences were observed in the composites. The results show that the *TC* increases with the increase of the cork weight fraction and the relationship being the stronger the smaller the filler particle size. The increase of *TC* of the PP/cork can be explained by the densification of cork on the composites after the two melt based processes. First, the higher shear forces during the extrusion and second due to the applied pressure in compression moulding.

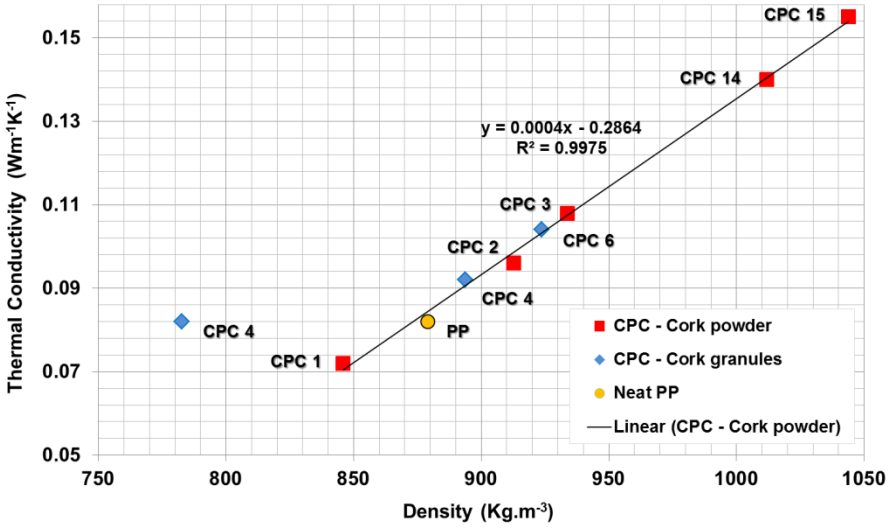

Figure 5.13. Thermal conductivity in function of the density of the plates obtained by compression moulding for the PP and PP/cork composites without coupling agent.

The plot of *TC* against the composite density shown in Figure 5.13 gave the regression value (R^2) to be 0.9975 for the cork powder composite plates, which indicated a good correlation between these two properties. Furthermore, the coefficient value was found to be positive indicating an increase in the *TC* with the increase of the composite density. Increasing the cork particle size (formulations CPC 4 to CPC 6) was not possible to infer significant differences between the cork particle size, since the compositions containing 15 and 30 wt.% tends to follow the same linear regression. The only outlier point was CPC 4

that contains only 5 wt.% of cork. In cellular materials different type of heat flow through the material can occur. The flow by conduction depends only on the amount of solid in the foam and not depends on the cell size. The flow by convection depends on the cell size, however for cells less than 1 mm in size, convection does not contribute significantly. Finally, the flow by radiation, also depends on the cell size: the smaller the cells, the more time the heat has to be absorbed and reradiated, and the lower is the rate of flow [17].

On the contrary, the thermal resistance (*TR*) shows an opposite effect as presented in Table 5.4 and is also dependent of the plate thickness as presented in the equation 5.5. For the CPC 15, condition containing 70 wt.% of cork powder the *TR* is half as compared with the neat polypropylene, due to a high densification of the cork powder in the matrix were the *TC* increased 89% as compared with the neat PP. This may be an advantage in applications were the material need to promote the heat transfer, such as in radiating floors where these PP/cork composites can be used as structural layer or in hardware for electronics. Being cork an excellent thermal insulator this result was not expected, however this study shows that by playing with the cork weight fraction it is possible to increase or decrease the *TR* of the composite material.

5.4 Conclusions

Polypropylene-cork (PP/cork) composites were produced using twin-screw extruder followed by injection or compression moulding process. The effect of cork fraction and particle size and the use of coupling agent on the mechanical and thermo-physical properties PP/cork composites were investigated. The important results are summarized as follows:

(1) The PP/cork composites exhibit reduced water uptake and the increase of cork fraction, increases the water absorption up to 2.3 wt.% after a period of 1344 hours. The increase of particle size of the cork tends to decrease the water uptake and the addition of coupling agent significantly reduces the composite water absorption.

(2) The morphology of the PP/cork composites evaluated by optical microscopy revealed good dispersion and distribution of cork due to the twin-screw extrusion process, promoting good aesthetic characteristics.

(3) The PP/cork composites exhibit higher density than the neat polypropylene and increases with the higher incorporation of cork. The use of coupling agent induces a slight decrease on the density due a better dispersion of the cork on the matrix.

(4) The tensile properties revealed a small reinforcement of around 10% in the stiffness provide by cork fraction 5 wt.%. For higher values an expected drop on the tensile properties was observed. The mechanical properties were enhanced by the addition of polypropylene graft maleic anhydride (PP-g-MA) preferably in terms of tensile strength and maximum strain, while the stearic acid promoted a slight increase on the maximum strain and acted as a release mould agent without significant negative effect on the mechanical performance.

(5) Regarding the thermal properties, the PP/Cork composites had higher crystallization temperatures than neat PP, and their thermal stability was similar that of PP. Cork and PP-g-MA acts as nucleating agent during the crystallization process and does not affect the thermal stability of the composites. Cork promoted a small increase on the composite crystallinity upto 30 wt.%, however the enhancement was also dependent of the degree of compatibility between the PP matrix and the cork.

(6) Cork promotes an antioxidant effect to the polypropylene increasing the time to oxidation. Reducing the cork particle size and consequently increasing the surface area of the particles and the composite density contributes to a higher thermal-oxidative protection. Using 30 wt.% of cork powder the oxidation was delayed 12.9 times as compared with the neat PP.

(7) The thermal conductivity of the plates increases with the increase of the cork weight fraction due to the increase of the density promoted by the addition of cork. This higher capacity for heat transfer may result in new potential applications for cork composites.

(8) The addition of cork to the thermoplastic reduces considerably the viscosity and consequently the melt flow index (MFI), while the addition of the coupling agent PP-g-MA to the polyolefin-cork system promotes opposite effect improving mixability.

(9) The maximum incorporation of cork to produce pellets was 70 wt.% (93% in volume) using cork powder compounded in a twin-screw extruder without die.

In areas were environmentally concern, aesthetics, reduced plastic touch and construction capability are required, the composites containing cork constitute a viable and interesting possibility. Regarding these properties, the applications for the developed cork composites may include furniture, flooring and insulation systems, hardware for electronics, toys for children, outdoor systems, in low content for automotive interior applications, among other sustainable applications.

5.5 References

[1] Vaidya UK, Chawla KK. Processing of fibre reinforced thermoplastic composites. Int Mater Rev. 2008;53(4):185-218.

[2] Velasco JI, De Saja JA, Martínez AB. Crystallization behavior of polypropylene filled with surface-modified talc. J Appl Polym Sci. 1996;61(1):125-132.

[3] Mehrjerdi AK, Adl-Zarrabi B, Cho S-W, Skrifvars M. Mechanical and thermo-physical properties of high-density polyethylene modified with talc. J Appl Polym Sci. 2013;129(4):2128-2138.

[4] Godlewski RE. Organosilicon chemical in mica filled polyolefins. Houston, TX, USA: SPI; 1983.

[5] Sharma SK, Nayak SK. Surface modified clay/polypropylene (PP) nanocomposites: Effect on physico-mechanical, thermal and morphological properties. Polym Degrad Stabil. 2009;94(1):132-138.

[6] Zhang S, Zhu A, Dai S. Coincorporation of nano-silica and nano-calcium carbonate in polypropylene. J Appl Polym Sci. 2011;121(5):3007-3013.

[7] Hartikainen J, Lindner M, Harmia T, Friedrich K. Mechanical properties of polypropylene composites reinforced with long glass fibres and mineral fillers. Plast Rubber Compos. 2004;33(2-3):77-84.

[8] Ravi Kumar BN, Suresha B, Venkataramareddy M. Effect of particulate fillers on mechanical and abrasive wear behaviour of polyamide 66/polypropylene nanocomposites. Mater Design. 2009;30(9):3852-3858.

[9] Rowell RM. Challenges in biomass-thermoplastic composites. J Polym Environ. 2007;15(4):229-235.

[10] Bledzki AK, Letman M, Viksne A, Rence L. A comparison of compounding processes and wood type for wood fibre—PP composites. Composites Part A. 2005;36(6):789-797.

[11] Bledzki AK, Reihmane S, Gassan J. Thermoplastics reinforced with wood fillers: A literature review. Polym-Plast Technol. 1998;37(4):451-468.

[12] Fortes MA, Rosa. ME, Pereira H. A Cortiça. Lisboa: IST Press; 2004.

[13] Silva SP, Sabino MA, Fernandes EM, Correlo VM, Boesel LF, Reis RL. Cork: properties, capabilities and applications. Int Mater Rev. 2005;50(6):345-365.

[14] Pereira H. Cork: biology, production and uses. Amsterdam: Elsevier; 2007.

[15] Barlow CY, Ashby MF. Cork dust composites. Proceedings of the Riso International Symposium on Metallurgy and Materials Science, 1989. p. 275-281.

[16] Mano JF. The viscoelastic properties of cork. J Mater Sci. 2002;37(2):257-263.

[17] Gibson LJ, Easterling KE, Ashby MF. The structure and mechanics of cork. 1981;377(1769):99-117.

[18] Abdallah FB, Cheikh RB, Baklouti M, Denchev Z, Cunha AM. Characterization of composite materials based on PP-cork blends. J Reinf Plast Comp. 2006;25(14):1499-1506.

[19] Fernandes EM, Correlo VM, Chagas JAM, Mano JF, Reis RL. Properties of new cork-polymer composites: Advantages and drawbacks as compared with commercially available fibreboard materials. Compos Struct. 2011;93(12):3120-3129.

[20] Antunes PJ, Dias GR, Coelho AT, Rebelo F, Pereira T. Hyperelastic Modelling of Cork-Polyurethane Gel Composites: Non-linear FEA Implementation in 3D Foot Model. Mater Sci Forum. 2008;587-588:700-705.

[21] Fernandes EM, Correlo VM, Mano JF, Reis RL. Innovative bio-based composites comprising cork and biodegradable polyester. In: Ferreira JAM, editor. 16th International Conference on Composite Structures (ICCS16), FEUP, Porto2011.

[22] Vilela C, Sousa AF, Freire CSR, Silvestre AJD, Pascoal Neto C. Novel sustainable composites prepared from cork residues and biopolymers. Biomass Bioenergy. 2013;55(0):148-155.

[23] Fernandes EM, Correlo VM, Chagas JAM, Mano JF, Reis RL. Cork based composites using polyolefin's as matrix: Morphology and mechanical performance. Compos Sci Technol. 2010;70(16):2310-2318.

[24] Abdallah FB, Cheikh RB, Baklouti M, Denchev Z, Cunha AM. Effect of surface treatment in cork reinforced composites. J Polym Res. 2010;17(4):519-528.

[25] Fernandes EM, Mano JF, Reis RL. Hybrid cork–polymer composites containing sisal fibre: Morphology, effect of the fibre treatment on the mechanical properties and tensile failure prediction. Compos Struct. 2013;105(0):153-162.

[26] Araújo JR, Waldman WR, De Paoli MA. Thermal properties of high density polyethylene composites with natural fibres: Coupling agent effect. Polym Degrad Stabil. 2008;93(10):1770-1775.

[27] Torres FG, Cubillas ML. Study of the interfacial properties of natural fibre reinforced polyethylene. Polym Test. 2005;24(6):694-698.

[28] Karnani R, Krishnan M, Narayan R. Biofiber-reinforced polypropylene composites. Polym Eng Sci. 1997;37(2):476-483.

[29] Saheb DN, Jog JP. Natural fiber polymer composites: A review. Adv Polym Tech. 1999;18(4):351-363.

[30] Keener TJ, Stuart RK, Brown TK. Maleated coupling agents for natural fibre composites. Composites Part A. 2004;35(3):357-362.

[31] Kazayawoko M, Balatinecz JJ, Matuana LM. Surface modification and adhesion mechanisms in woodfiber-polypropylene composites. J Mater Sci. 1999;34(24):6189-6199.

[32] Elkhaoulani A, Arrakhiz FZ, Benmoussa K, Bouhfid R, Qaiss A. Mechanical and thermal properties of polymer composite based on natural fibers: Moroccan hemp fibers/polypropylene. Mater Design. 2013;49:203-208.

[33] Dhakal HN, Zhang ZY, Richardson MOW. Effect of water absorption on the mechanical properties of hemp fibre reinforced unsaturated polyester composites. Compos Sci Technol. 2007;67(7–8):1674-1683.

[34] Wunderlich B. Macromolecular physics, Crystal melting. vol. 3: Academic Press, New York; 1980. p. 63.

[35] Hes L. Fast Determination of Surface Moisture Absorptivity of Smart Underwear Knits. International Textile Conference, Terrassa, 2001.

[36] Frydrych I, Dziworska G, Bilska J. Comparative analysis of the thermal insulation properties of fabrics made of natural and man-made cellulose fibres. Fibres Text East Eur. 2002;10(4):40-44.

[37] Bhaskar J, Haq S, Yadaw SB. Evaluation and testing of mechanical properties of wood plastic composite. J Thermoplast Compos. 2012;25(4):391-401.

[38] Bodirlau R, Teaca CA, Spiridon I. Preparation and characterization of composites comprising modified hardwood and wood polymers/poly(vinyl chloride). BioResources. 2009;4(4):1285-1304.

[39] Kabir MM, Wang H, Lau KT, Cardona F. Chemical treatments on plant-based natural fibre reinforced polymer composites: An overview. Composites Part B. 2012;43(7):2883-2892.

[40] Dányádi L, Móczó J, Pukánszky B. Effect of various surface modifications of wood flour on the properties of PP/wood composites. Composites Part A. 2010;41(2):199-206.

[41] Shalwan A, Yousif BF. In State of Art: Mechanical and tribological behaviour of polymeric composites based on natural fibres. Mater Design. 2013;48:14-24.

[42] Anjos O, Pereira H, Rosa ME. Tensile properties of cork in axial stress and influence of porosity, density, quality and radial position in the plank. 2011;69(1):85-91.

[43] Karmaker AC, Hoffmann A, Hinrichsen G. Influence of water uptake on the mechanical properties of jute fiber-reinforced polypropylene. J Appl Polym Sci. 1994;54(12):1803-1807.

[44] Pracella M, Chionna D, Anguillesi I, Kulinski Z, Piorkowska E. Functionalization, compatibilization and properties of polypropylene composites with Hemp fibres. 2006;66(13):2218-2230.

[45] Ndiaye D, Matuana LM, Morlat-Therias S, Vidal L, Tidjani A, Gardette J-L. Thermal and mechanical properties of polypropylene/wood-flour composites. 2011;119(6):3321-3328.

[46] Joseph PV, Joseph K, Thomas S, Pillai CKS, Prasad VS, Groeninckx G, et al. The thermal and crystallisation studies of short sisal fibre reinforced polypropylene composites. Compos Pt A-Appl Sci Manuf. 2003;34(3):253-266.

[47] Pouteau C, Dole P, Cathala B, Averous L, Boquillon N. Antioxidant properties of lignin in polypropylene. Polym Degrad Stabil. 2003;81(1):9-18.

[48] Košíková B, Demianová V, Kačuráková M. Sulfur-free lignins as composites of polypropylene films. J Appl Polym Sci. 1993;47(6):1065-1073.

[49] Annie Paul S, Boudenne A, Ibos L, Candau Y, Joseph K, Thomas S. Effect of fiber loading and chemical treatments on thermophysical properties of banana fiber/polypropylene commingled composite materials. Composites Part A. 2008;39(9):1582-1588.

Functionalized cork-polymer composites (CPC) by reactive extrusion using suberin and lignin from cork as coupling agents[5]

Abstract

High density polyethylene (HDPE) and cork powder were compounded in a co-rotating twin-screw extruder to obtain cork-polymer composites (CPC) with improved properties. Benzoyl peroxide (BPO) was used as initiator agent, and suberin or lignin isolated from cork enhanced filler-matrix bonding and promoted mechanical reinforcement with environmental benefits. The novel composites were characterized in terms of dimensional stability, evolution of morphology, thermal and mechanical properties and their performance was compared with that of composites containing polyethylene-grafted maleic anhydride (PE-g-MA) as coupling agent. As expected, composites with coupling agent present higher mechanical properties, lower water uptake and thickness swelling variation. Suberin acts as plasticizer with antioxidant benefits, while lignin works as a coupling agent, improving tensile modulus and maximum strength. Increasing lignin content does not improve the mechanical properties but improves thermal stability.

[5] This chapter is based on the following publication:

Fernandes EM, Aroso IM, Mano JF, Covas JA and Reis RL, 2013, Functionalized cork-polymer composites (CPC) by reactive extrusion using suberin and lignin from cork as coupling agents, *submitted*.

6.1 Introduction

The use of synthetic polymers combined with lignocellulosic materials has become a reliable alternative to develop new sustainable materials with good performance and reduced cost [1-3]. Cork is the outer bark of the Oak tree *Quercus suber* L. [4], where the harvesting of cork is a natural, renewable process that reduces subsequent carbon footprints. During industrial cork processing, up to 30 % results in sub-products such as cork powder, which is used in small amounts low value added applications. Cork-polymer composites (CPC) are usually prepared through melt based technologies. Increasing the percentage of cork in the composite without compromising the overall properties is seen as a desirable route towards sustainability. However, commodity thermoplastic matrices, such as polyethylene and polypropylene, are chemically incompatible with lignocellulosic materials, requiring the incorporation of coupling agents to improve interfacial adhesion. The addition of functionalized polymers containing maleic anhydride (MA) groups during compounding showed to be an effective method to improve interfacial bonding, even when using different cork qualities [5, 6]. The typical chemical composition of cork is about 40% of suberin, up to 22% of lignin, 18% of polysaccharides and up to 15% of other extractives [4, 7]. Suberin and lignin are thus the main constituents and in combination with a closed cellular morphology account for cork's unique properties, namely excellent insulation characteristics, low density and permeability, low thermal conductivity, high energy absorption, resilience, near-zero Poisson coefficient and high friction coefficient [7, 8]. Suberin is a natural biopolymer typically found in the cell walls of plants [9]. Cork suberin is constituted by a polyester structure of long chain fatty acids, hydroxyl and phenolic acids, linked by ester groups, with ferulic acid acting as a bridge between the aromatic and the aliphatic domains [10, 11]. Whether the aromatic domain is part of the suberin molecule is still a matter of debate [12]. The alkaline depolymerisation in an organic solvent results in the release of the aliphatic constituents through cleavage of the ester linkages and transesterification [11, 13, 14]. Full characterization of cork lignin is still incomplete because of the complex relation between true lignin and the aromatic fraction of suberin. Nevertheless, Marques et al. [15-17] found that cork is composed of a G type lignin with 94-96% guaiacyl, less than 3-5% syringyl and 2-3% hydroxyphenyl units [18]. In a previous study, the potential of suberin and chemically modified suberin to promote adhesion between low density polyethylene and cork was demonstrated [19]. Lignin has been proposed to reinforce the mechanical properties of composites [20, 21], to promote adhesion in natural fibre composites [22], or, in combination with a coupling agent, to improve mechanical

performance [21, 23]. In all cases, high amounts of lignin or the addition of a coupling agent were necessary to reinforce the composites.

This work focus on the development of cork-polymer composites (CPC) using suberin and lignin as bio-based coupling agents through a reactive extrusion (REX) process, in order to overcome with environmental benefits the insufficient adhesion between cork and a high density polyethylene (HDPE) matrix. REX has the capability of functionalize, prepare the composite and produce pellets in a single step. No environmental or health hazardous solvents are used, low investment costs and high production yields are obtained [18, 24]. Initiators are usually required, the most widely used in grafting reactions being organic peroxides, including benzoyl peroxide (BPO). The work investigates for the first time: (i) the evolution of morphology during the compounding process; (ii) the dimensional stability and thermal properties of the composites; (iii) the effect of suberin, lignin, and initiator agent on the tensile properties. These properties are compared with those of an equivalent system using a coupling agent based on maleic anhydride (PE-g-MA).

6.2 Experimental section

6.2.1 Materials

Cork powder, with an average particle size < 500 μm, a specific weight of 157 ± 2 kg m^{-3} and a humidity of ~5.4% was supplied by Amorim Revestimentos S.A. (Oleiros, Portugal).

The matrix was a high density polyethylene HDPE, (HMA – 025 from ExxonMobil, Germany), with a MFI of 8.2 g.10min^{-1} (190 °C, 2.16 kg), and a melting point of 136.6 °C, containing a thermal stabilizer.

HDPE grafted with maleic anhydride (PE-g-MA), containing 0.5 to 1.0 wt% of maleic anhydride (Exxelor PE 1040), with MFI of 1.4 g.10 min^{-1} (190 °C, 2.16 kg), and having a melting point of 131.3 °C, was produced by ExxonMobil, Germany.

Benzoyl peroxide (BPO, 75%), USP grade, Luperox®, was obtained from Atofina Chemicals.

The compositions prepared are presented in Table 6.1. The cork-polymer (20-80) wt.% ratio was maintained in all formulations.

Table 6.1. Compositions of the cork-polymer composites (CPC) using suberin and lignin and maleic anhydride as coupling agent.

	CPC Composition (wt.%)					
Sample	HDPE [a]	Cork	BPO [b]	Suberin	Lignin	PE-g-MA [c]
CPC1	80.0	20.0	–	–	–	–
CPC2	80.0	20.0	–	–	–	2
CPC3	77.6	19.4	1	2	–	–
CPC4	77.6	19.4	1	–	2	–
CPC5	76.0	19.0	1	–	4	–
CPC6	76.0	19.0	1	–	4	–
CPC7	79.2	19.8	1	–	–	–

[a] HDPE - high density polyethylene; [b] BPO - benzoyl peroxide; [c] PE-g-MA - coupling agent based on maleic anhydride, with a level content of 0.5–1.0 wt.%

6.2.2 Extraction of suberin and lignin

Extractive free cork powder was obtained after three consecutive 6 h soxhlet extractions with dichloromethane, ethanol and water. The resulting material was used to obtain the suberin and lignin fractions. Suberin extraction procedure was adapted from Ekman R et al. [25] and Pinto PCRO et al. [26]. The product (1g to 13ml) was refluxed in Ethanol:Water (25:1) containing 0.5M sodium hydroxide for a period of 6 h. After cooling, the resulting mixture was filtered and the liquid fraction was acidified to pH 5-6 with hydrochloric acid. After filtration, the solvent was removed in a vacuum evaporator. The resulting solid residue was suspended in water and extracted with 3 times the volume in chloroform. The organic fraction was recovered and the solvent removed in a vacuum evaporator, resulting in a brownish paste-like material.

The methodology for lignin extraction was adapted from Ekman et al. [25] and Browning BL [27]. The solid residue resulting from the suberin extraction was thoroughly washed with distilled water until neutral pH. 350 ml of a 72% sulfuric acid solution were added to 30 g of this residue and the mixture was maintained under agitation for 2 hours at room temperature, followed by the addition of 550 ml of distilled water and refluxing for 4 hours. After cooling to room temperature, the solid residue was

recovered through filtration and washed with distilled water until neutral pH, a dark powdery material being obtained.

6.2.3 Twin-screw compounding

Before compounding, the cork powder was pre-dried at 80 °C in a vacuum oven until constant weight. The raw materials, including the pulverized polyethylene, the benzoyl peroxide (BPO) and PE-g-MA, were pre-mixed. Compounding was performed in a prototype modular laboratorial mini intermeshing co-rotating twin-screw extruder (TSE), with a screw diameter of 13 mm, and a length to diameter ratio (L/D) = 27, coupled to a rod die with a diameter of 3mm. The screw profile is built by sliding along a shaft conveying and kneading elements with a maximum channel depth of 1.5 mm. As seen in Figure 6.1, the configuration used in the experiments induces polymer melting in the first restrictive block upstream and dispersive and distributive mixing in the second kneading block, which comprises 8 discs staggered at -30°. The extruder is provided with sampling devices along its length which are capable to collect in circa 1 second small amounts of material from within the screw channel [28].

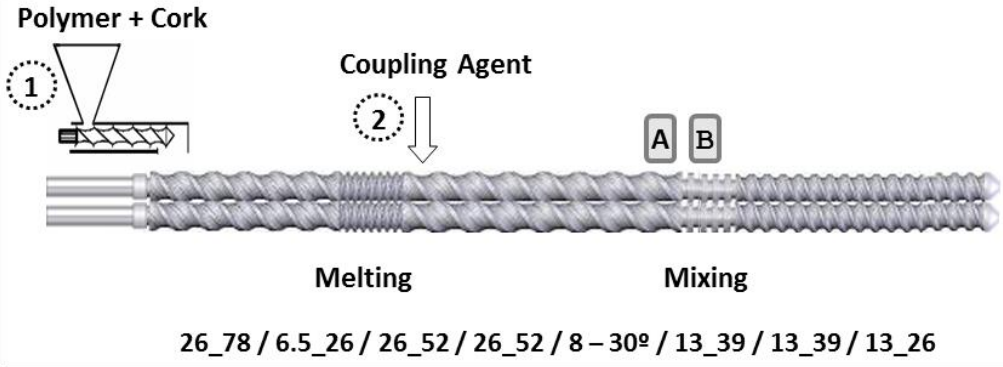

Figure 6.1. Twin-screw extruder set up. Screw profile is defined in terms of (pitch_length) of the various elements. A and B denote locations of material sampling.

This allowed to obtain cork-polymer samples at locations A and B identified in Figure 6.1, i.e., where most of the dispersive mixing action should take place. The temperature profile along the barrel and die was set to 165/180/185/185/175 °C for all the experiments, the feed rate was kept at 130 g/h, and the screws rotating at 70 rpm.

Figure 6.2 shows the compounding methodology adopted. The pre-mixed polymer and cork were feed upstream (position 1) by a miniaturized volumetric feeder (based on a Moretto DVM 18 L), together with the BPO initiator, or the PE-g-MA. Suberin and/or lignin were added in position 2, by means of an automatic syringe pump (AL-1000, from WPI, USA), or manually, respectively. After air-cooling, part of the extruded composite was pelletized.

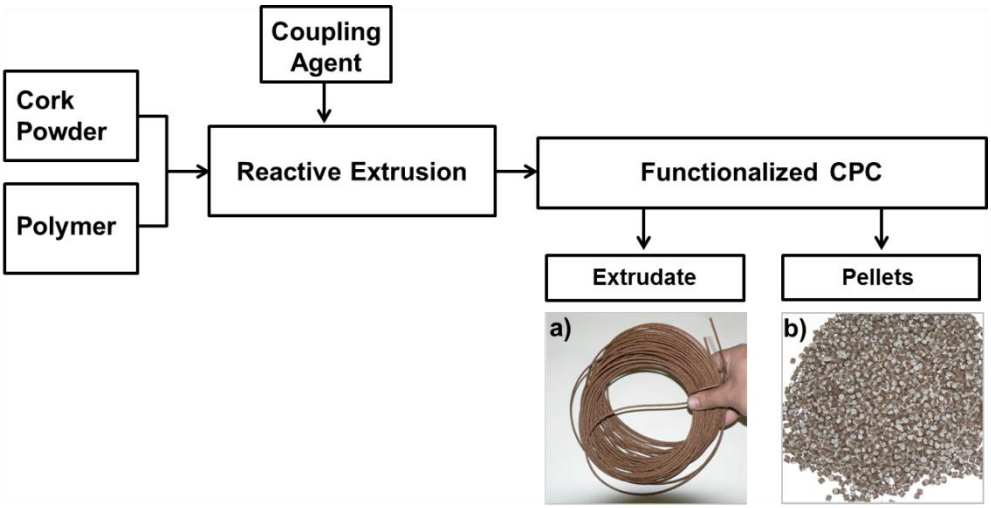

Figure 6.2. Scheme for the production of extruded functionalized cork-polymer composites (CPC) from a) CPC 3 composition with 2 wt.% of suberin and b) CPC 5 with 4 wt.% of lignin as coupling agent in the pellet form.

6.2.4 Chemical characterization

Suberin and lignin were analysed by Fourier transform infrared (FTIR) spectroscopy. The spectra were acquired between 4000 cm^{-1} and 500 cm^{-1} in a Shimadzu IR-Prestige 21 spectrometer, as the average of 32 scans with a resolution of 4 cm^{-1}. Suberin and Lignin spectra were obtained using the KBr pellet technique and cork spectra were recorded using the attenuated total reflectance (ATR) module (PIKE Technologies).

6.2.5 Thermal properties

The thermal stability of cork and of its major isolated chemical fractions was determined using a TGA Q500 Thermogravimetric Analyser (TA Instruments, USA). Experiments were performed at a heating rate of 10 °C.min^{-1} from 50 °C to 600 °C under air atmosphere. All tests were repeated once.

Differential scanning calorimetry (DSC) and oxidation induction time (OIT) measurements were performed in a TA instrument DSC Q100 model (USA) instrument on samples of 8–12 mg, at a heating rate of 10 °Cmin^{-1}, under nitrogen atmosphere (flux of ca. 50 ml min^{-1}). Only the second run was analysed for melting temperature (T_m) and melting enthalpy (ΔH_m). The degree of crystallinity was calculated on the basis of a 100% crystalline PE a melting enthalpy of ΔHm^o = 293 J/g [29]. The analyses were performed in two samples of each condition.

OIT measurements were conducted in the same equipment, with samples heated at a rate of 30 °C.min^{-1} up to 200 °C under nitrogen atmosphere. After 2 min at 200 °C the atmosphere was changed to oxygen (both gases at flux 50 ml.min^{-1}) and oxidation induction time was measured during the isothermal period. The analyses were performed in three samples of each condition.

6.2.6 Scanning electron microscopy

Fractured samples of the various composites were examined in a NanoSEM 200 FEI (The Netherlands) scanning electron microscope (SEM). Prior to the analysis, samples were coated with an Au/Pd alloy (80-20 wt. %) by ion sputtering in a high resolution sputter coater (Cressington 208HR, Watford, UK).

6.2.7 Mechanical properties

Three millimetre thick plaques were obtained by compression moulding in a hot press (Moore, UK) of the pellets of the various compositions at 150 °C under an applied pressure of 1.42 MPa. The pellets were kept during a period of 8 minutes without pressure and 2 minutes with pressure, followed by a cooling period under pressure. Tensile bars according to ISO 527–2 (with a cross-section of 3 × 4 mm^2 at the neck) were machined by a Roland 3D Plotter (MDX-20, UK).

The tensile properties were determined using a Universal tensile machine (Instron 4505 Universal Machine, USA) with a load cell of 1kN and a gauge length of 25 mm and a crosshead speed of 5mm min^{-1}. Samples were conditioned at room temperature for at least 48 h before testing and it was used 9 specimens per condition. The tensile force was taken as the maximum force in the force deformation

curve. Tensile modulus was estimated from the initial slope of the stress–strain curve (between 0.05 and 1% strain) using linear regression. The normality of the distribution of the mechanical results was evaluated using the Shapiro-WilK test confirming their normal distribution at p<0.05. The results were compared using one-way analysis of variance (ANOVA) with the post hoc Bonferroni multiple comparison tests to infer about the significant differences between mean values of the developed functionalized composites and the differences were considered significantly different at p<0.05 (*).

6.2.8 Dimensional stability

Measurements of water absorption and thickness swelling were made according to ASTM D 570 on the specimens used for tensile testing, after vacuum-drying at 70 °C and stabilization in a desiccator. Each specimen was immersed in distilled water, at ambient temperature, in falcon tubes of 14 ml for different time periods (up to 15 days). At the end of each period, five specimens of each condition were gently blotted with absorbent paper to remove the excess water on the surface, immediately reweighed and their thickness measured using a digital micrometer from Mitutoyo (Japan) (± 0.001 mm), and then re-immersed. Water absorption (*WA*) was calculated as:

$$WA\,(\%) = \frac{W_a - W_b}{W_b} \times 100 \qquad (6.1)$$

where W_a and W_b are the weights (g) after and before immersion, respectively. The thickness swelling (*TS*) is given by:

$$TS\,(\%) = \frac{T_2 - T_1}{T_1} \times 100 \qquad (6.2)$$

where T_2 is the thickness of the wetted specimen and T_1 is the initial thickness. Five specimens per condition were measured.

6.3 Results and Discussion

6.3.1 Chemical characterization

The FTIR spectrum of cork presented in Figure 6.3 is dominated by the presence of absorption bands for hydroxyl (3400 cm^{-1}), methylene (2920, 2850 and 1452 cm^{-1}) and ester (1736, 1240 and 1150 cm^{-1}) groups. The absorption band at 1508 cm^{-1} is associated with the vibration of the aromatic skeleton. This is consistent with the existence of highly suberized cell walls characteristic of cork.

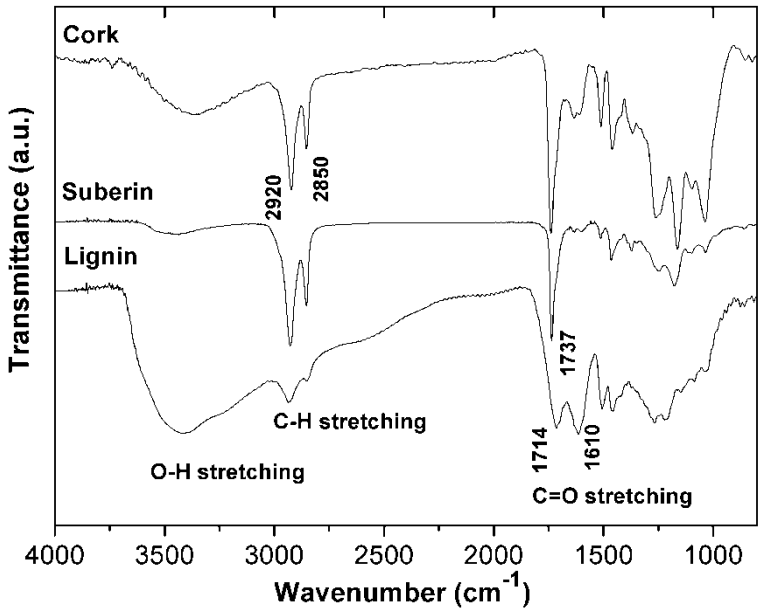

Figure 6.3. ATR-FTIR spectra of cork and its major chemical isolated components used as coupling agent.

The spectrum of suberin is similar to that of cork, retaining essentially the absorption bands related to the aliphatic ester moieties. Therefore, the suberin obtained by extraction probably has its constitutive aliphatic monomers transesterified or in oligomeric blocks arising from incomplete depolymerization. The lignin spectrum presents an intense band at 3400cm^{-1} due to hydroxyl groups, together with a shoulder at around 2570 cm^{-1}. This configuration, in combination with the absorption band at 1714 cm^{-1}, is consistent with the presence of carboxylic acid groups; the relatively intense 1610 and 1505 cm^{-1} bands are related to the presence of aromatic structures.

In summary, lignin and suberin partially retain the original cork structures. The aliphatic esterified domain is represented in suberin, whereas the aromatic domain in present in lignin.

6.3.2 Thermal properties

6.3.2.1 Cork, suberin and lignin

The thermogravimetric curves of cork and of its chemical fractions under air atmosphere are represented in Figure 6.4 in terms of weight loss and its derivative. A multi-step degradation process is evident. Cork and lignin show some weight reduction between room temperature and 150 °C, due to the loss of water molecules (suberin is hydrophobic).

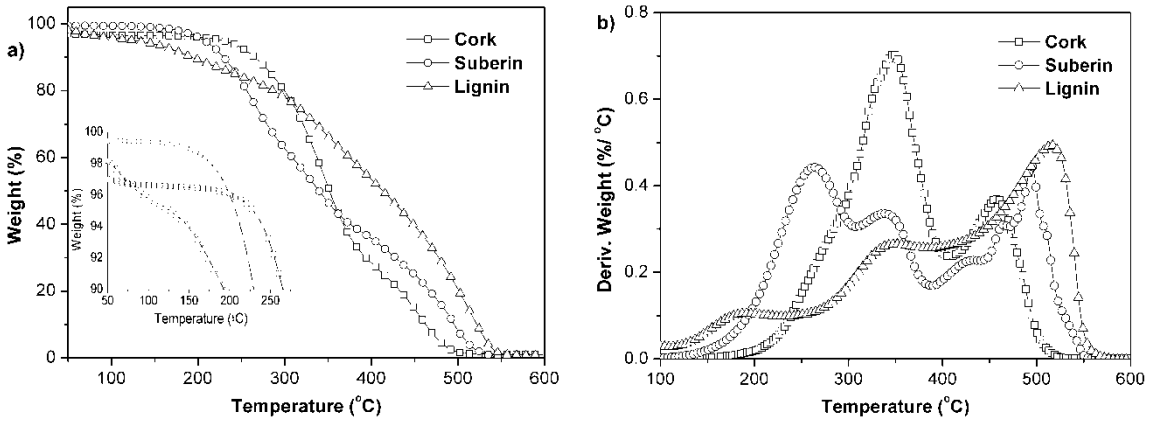

Figure 6.4. Thermogravimetric curves of cork and the principal chemical components under air atmosphere (a) and respective derivative curves (b).

The thermal degradation of cork starts at approximately at 270 °C, with the first intensive weight loss at ~ 348 °C and a second important region at circa 460 °C (Figure 6.4 b). This pattern should correspond to the degradation of the major cork components. The derivative curves of the isolated cork fractions demonstrate that the thermal decomposition of suberin and lignin occur independently. Suberin displays good thermal stability up to around 259 °C, followed by a progressive weight loss, reaching nearly 45% at 338 °C and 87% at 494 °C. Lignin shows a small shoulder at 193 °C, a low temperature when compared with cork and suberin, probably due to the monomeric structures of lignin resulting from extraction. Its maximum decomposition takes place at about 515 °C, confirming the higher thermal resistance as compared with suberin. At higher temperatures, the isolated cork fractions seem to present higher thermal stability. However, at 600 °C no char weight residue was detected.

6.3.2.2 Composites

The main features from the thermogravimetric analysis of the composites under air atmosphere are identified in Table 6.2. In all cases, the onset of degradation was higher than 265 °C and the ash content was less than 0.3% at 600 °C. Although the HDPE matrix contains a thermal stabilizer, the addition of PE-g-MA and of 4 wt.% of lignin seems to have acted as a thermal protective barrier to cork, enhancing the thermal stability up to temperatures as high as 387 - 395 °C. This characteristic agrees well with the curves of Figure 6.4, where lignin showed higher thermal resistance. Thus, lignin could be eventually used as a flame retardant.

Table 6.2. Initial degradation temperatures, obtained by TGA, of the CPC, in the presence and absence of suberin and lignin, and the coupling agent (PE-g-MA).

	TGA			DTG
Sample	T_{max1} (°C)	T_{max2} (°C)	Ash content (wt%) [a]	T_{max1} (°C)
CPC 1	273.7	387.2	0.25	399.8
CPC 2	276.1	391.1	0.29	404.3
CPC 3	272.3	384.0	0.25	389.7
CPC 4	267.0	386.0	0.26	391.0
CPC 5	268.6	394.7	0.29	396.8

T_{max1} (°C) - First weight loss process; [a] Ash weight content at 600 °C.

Table 6.3 lists the melting temperature (T_m), crystallization temperature (T_c), enthalpy (ΔH) and degree of crystallinity (X_c) of the neat polymer and composites, as determined from DSC curves. The results show a slight increment of T_c and degree of crystallinity for composites CPC 1 and CPC 2, indicating that the presence of cork promotes crystallization. This nucleating ability of cork has been previously observed [5]. No significant changes in the T_m of the composites were detected. The composites containing suberin and lignin revealed lower melting enthalpy and crystallinity, probably due to BPO modification, which induces the formation of macro-radicals that may produce branching and chain extensions [30].

Oxidative induction time (OIT) measurements were performed at 200°C to compare the oxidation of the composites and analyse the effect of the proposed eco-friendly coupling agents.

Table 6.3, shows high values of OIT for all tested composites due to the use of HDPE grade with thermal stabilizer. Significant differences in the onset decomposition time of the exothermic reactions were found, with the OIT varying from 54.2 to 74.6 min. It was found that the use of 2 wt.% of lignin CPC 4, does not influence significantly the thermal-oxidative stability of the composites under the isothermal conditions. However, the increase to 4 wt.% of lignin CPC 5, results in a reduction of the OIT. In despite of the reduction of the polymer %, the overall decrease of OIT is moderated by the presence of lignin.

Table 6.3. Melting temperatures and enthalpies, crystallization temperatures, crystallinity degrees and oxidation induction times of CPC composites with HDPE as matrix.

Sample	$T_{c\ onset}^{a}$ (°C)	ΔH_c^a (J/g)	$T_{m\ onset}^{b}$ (°C)	ΔH_m^b (J/g)	χ_c^c (%)	OIT (min)
HDPE	118.8	226.0	125.7	223.5	76.3	119.4 ± 0.5
CPC 1	121.9	188.3	126.2	185.7	79.2	60.4 ± 1.0
CPC 2	122.0	188.2	124.5	185.4	80.7	70.7 ± 1.2
CPC 3	123.2	173.9	125.5	172.0	75.6	74.4 ± 0.2
CPC 4	123.3	167.8	123.9	166.3	73.1	59.9 ± 1.6
CPC 5	123.2	163.0	124.2	161.6	72.6	54.9 ± 0.7
CPC 7	123.3	170.4	124.8	169.3	73.0	65.8 ± 0.5

[a] Crystallization temperature and enthalpy at second cooling from the melt at 10°C.mm^{-1}

[b] Melting temperature and variation of enthalpy determined by DSC on the second heating at 10°C.mm^{-1}

[c] Crystallinity degree calculated on the basis of a 100% crystalline PE a melting enthalpy of ΔH_{m^c} = 293 J/g [29].

OIT (min) - oxidation induction time determined under air atmosphere.

The phenolic groups in the lignin can impart antioxidant properties which provide stability to the polymer against thermal- and photo-oxidation [31]. The clear increase on the OIT for the compositions with PE-g-MA (CPC 2) and containing 2 wt.% of suberin (CPC 3), is an indication that both substances may act and can be used as antioxidant on the composites. It is speculated that the existing aromatic domains of suberin contain various substituted phenolic groups [32], that may function as antioxidant.

6.3.3 Morphology

6.3.3.1 Morphology evolution during compounding

The morphology evolution during the twin-screw extrusion (TSE) process of the principal compositions after cryogenic fracture is presented in Figure 6.5. The zone B location corresponds to the intensive mixing zone of the TSE. Composite samples were collected rapidly at specific barrel locations with a special sampling device. It can be observed the high distributive mixing capacity during the melting of the co-rotating TSE: the cork particles are well distributed and dispersed in the polymer matrix upstream the die zone, in particular for the CPC 2 to CPC 7 compositions. This result demonstrates: (a) the importance of intensive mixing zones in the screw configuration to promote the efficient mixing of the monomer with the polymer, in this case a block of 4 kneading disks with a staggering angle -30° and (b) highlights the importance of the coupling agent based on PE-g-MA, suberin or lignin to promote dispersion of the natural phase.

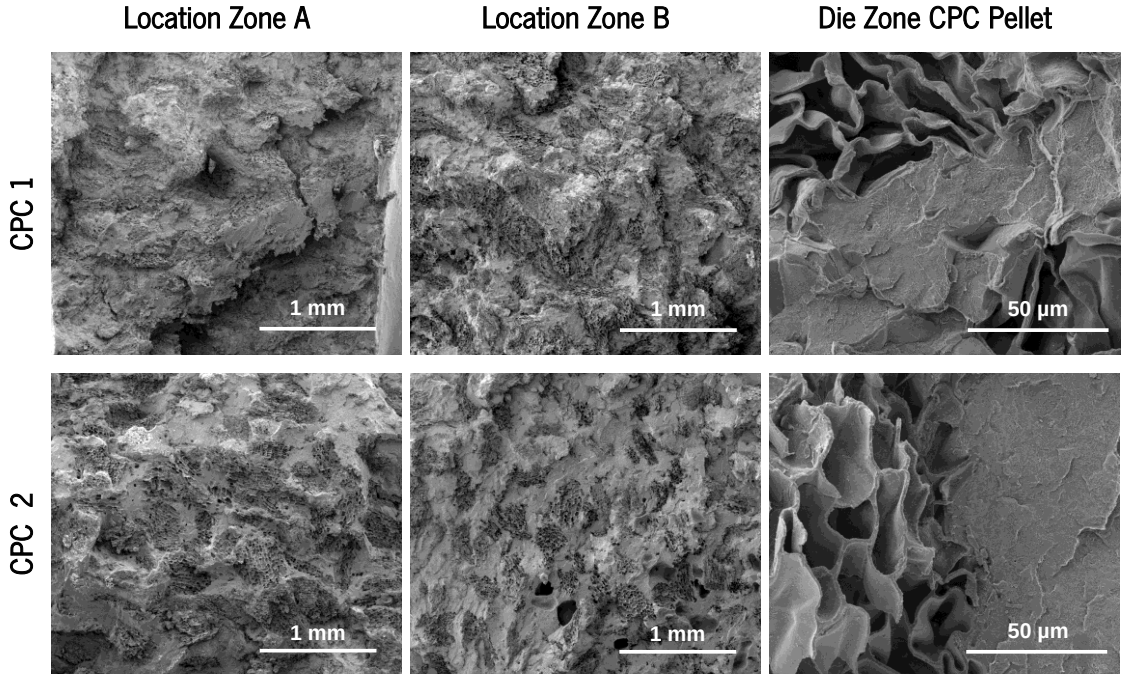

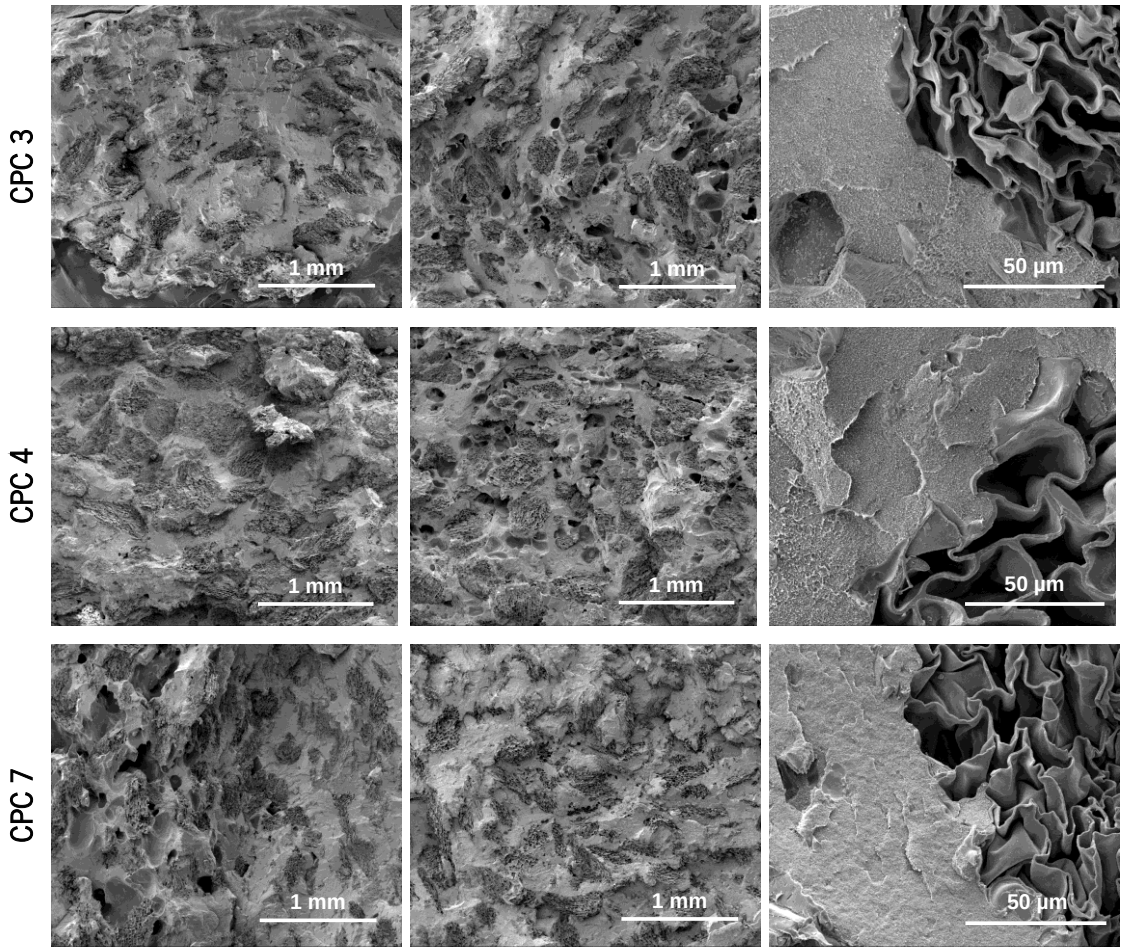

Figure 6.5. SEM micrographs after cryogenic fracture of the HDPE-cork composites removed from the extruder using the sampling device and collected after screw pulling in locations (A and B) and at the die at magnifications of ×100 and × 2400.

Moreover, micro voids on the morphology were observed, in particular in the compositions using BPO. A proper venting design with vacuum or an efficient devolatilization system on the extruder may be necessary to eliminate the entrapped gas and the residual products generated during the reactive extrusion process. In addition, at high magnification the obtained extruded CPC pellets present good linkage between the cork and the HDPE independently of the processed composition and the presence of micro pores in the structure was considerably reduced.

6.3.3.2 Morphology of composites

The composites present good aesthetic characteristics with a homogeneous visual distribution of cork. Figure 6.2 a) shows the visual aspect of a flexible extruded composition with 2 wt.% of suberin. The composite pellets containing lignin, presented in Figure 6.2 b), have a more intense brown colour with well dispersed lignin.

The fracture morphology of the composites after tensile tests is presented in Figure 6.6. The tensile fracture of the unreinforced CPC is presented in Figure 6.6 b) and reveals high stretched elements of HDPE between the cork particles. Figure 6.6 c and d) shows the influence of the addition of PE-g-MA with the fracture occurring at the same level of the cork and the polymeric matrix, supporting the indication of good adhesion.

Both results are in agreement with previous works using melt based technologies such as pultrusion and extrusion to produce cork based composites [6, 19]. The morphology of CPC 4 using 2wt.% of lignin presents similar fracture as compared with the composite using PE-g-MA. The composites with 2wt.% of suberin in Figure 6.6 f) two distinct zones of the polymeric phase can be observed: (i) a small portion of the polymeric matrix is stretched, probably due to the presence of suberin which is promoting additional ductility, also observed at lower magnification in Figure 6.6 e) and (ii) a fracture zone that occurs at the same level than cork phase due to the presence of the BPO. Moreover, during the extrusion process the visual aspect of the extruded composite surface containing suberin was smoother, reducing the shear during the extrusion. This effect may be related with a plasticizer capacity of suberin composed of esterified monomers and oligomers [9]. Additionally, we did not observe the presence of micro-voids on the different composites fracture, probably due to the temperature and pressure applied during the compression moulding to produce the composite boards.

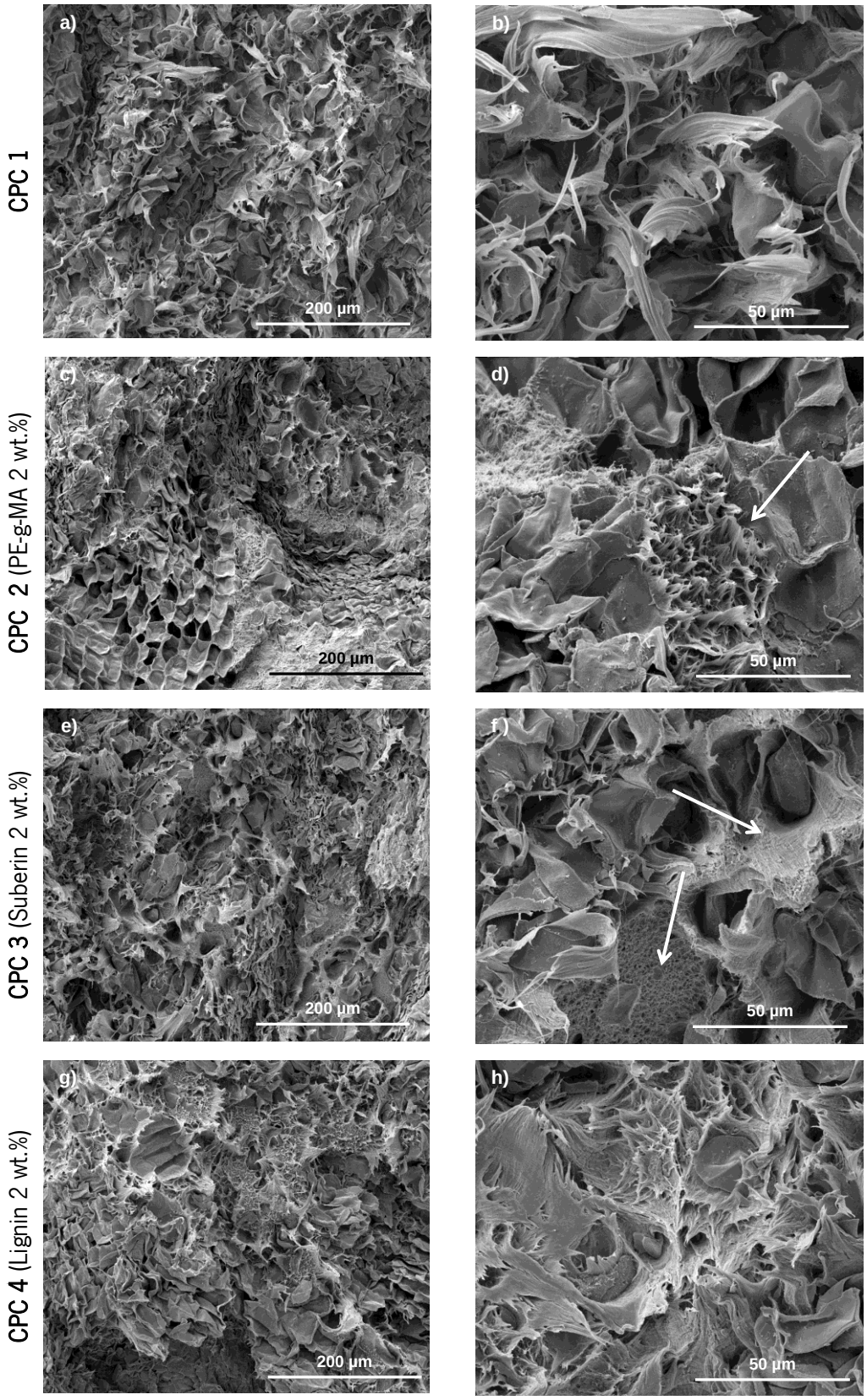

Figure 6.6. SEM pictures of cross-sectional fractured surfaces after tensile tests of the cork reinforced composites at magnifications ×600 and × 2400.

6.3.4 Mechanical properties

The maximum tensile strength and the tensile modulus of the developed cork-polymer composites are presented in Figure 6.7. The dashed line in the graphic represents the effect of BPO on the maximum tensile strength.

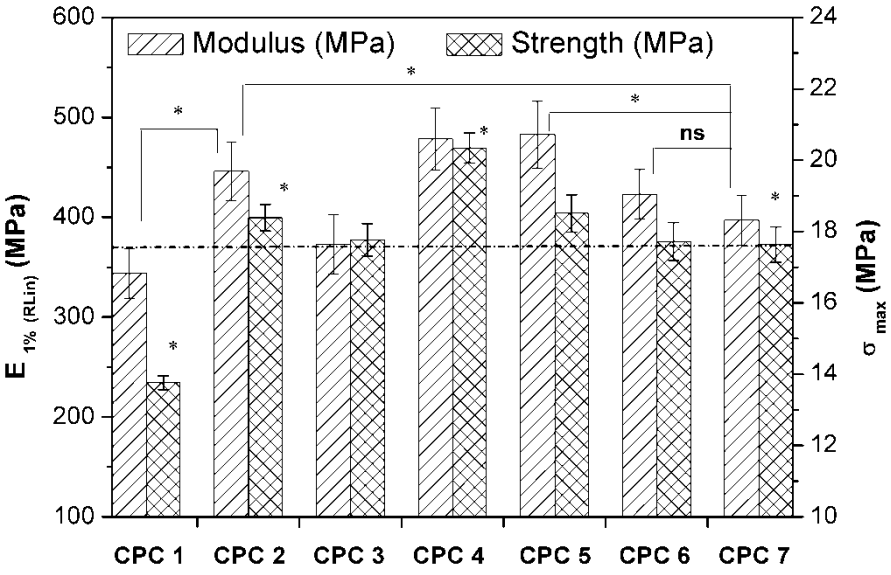

Figure 6.7. Tensile properties of the developed functionalized cork composites. (*) Significant at 0.05; ns: non-significant at 0.05.

Moreover, Figure 6.8 depicts summarized the mean variation (%) of the tensile properties, including the maximum strain, were the significant differences between samples are compared with the unreinforced cork-polymer composite CPC 1.

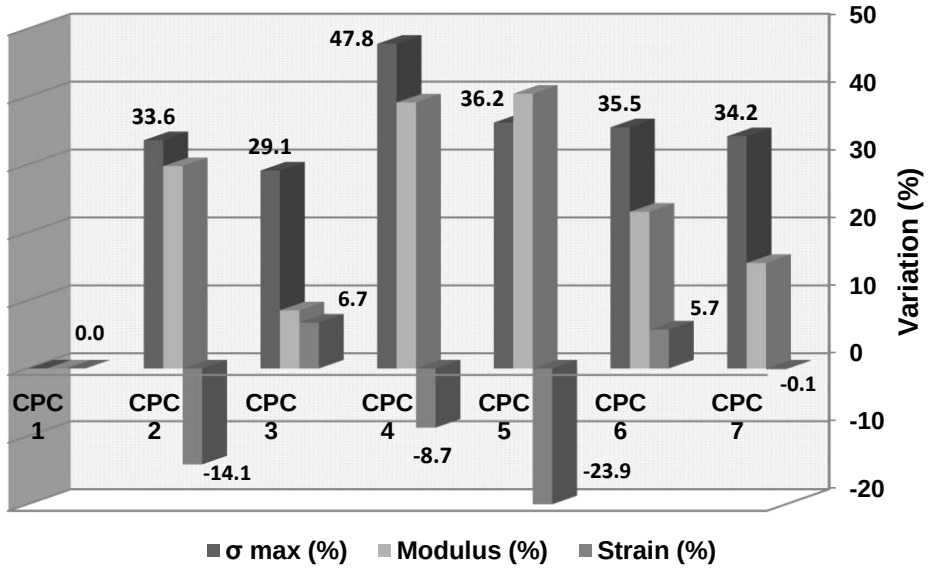

Figure 6.8. Variation of the tensile properties comparing with the control non-reinforced cork-polymer (20-80) wt.% composition (CPC 1).

It can be clearly observed that the use of a coupling agent based on maleic anhydride (MA) considerably increases both strength and modulus of the materials and reduces the maximum strain. The MA may interact with the polar groups of cork (mainly hydroxyl groups (-OH)) of lignin and hemicellulose to form covalent or hydrogen bonding, providing chemical affinity and strong adhesion at the interface. The use of the BPO is represented in CPC 7, showed to act as a coupling agent without a negative effect on the maximum strain. During the extrusion process, BPO may initiate radicals which react with the cork surface and the polymeric matrix, promoting chemical bonding between the two phases. In the literature [33], it is referred that the grafting of peroxide radicals onto polyethylene could take place though an attack on the tertiary carbons and on the few double bonds present in the backbone chain. Alternatively, the combination of peroxide groups and high temperatures could introduce polarity in the polymer, thereby increasing the adhesion at polymer-fibre contacts [33]. Due to the chemical nature of cork, it is speculated that a similar action process can occur during the processing of the developed composites, resulting in an enhancement on the mechanical performance. In the functionalized CPC, the addition of 2 wt% of suberin promoted an increase of the maximum tensile strength, modulus and maximum strain comparing with the unreinforced CPC 1. However and comparing with the CPC 7, the real effect of improvement was observed for the maximum strain with an increasing of 6.7%. It seems that suberin can act as plasticizer agent during the extrusion process, reducing the stiffness and contributing with some additional flexibility to the composite material. This

effect of suberin on the composites resembles in part its function on the cork material, being responsible for the elasticity on the cork material [7]. Moreover, glycerol is the principal monomer of suberin [13], which is used as plasticizer on composite systems [34, 35]. The challenge on the production of CPC with a high cork content using extrusion is the poor processability of the components, which may result in inadequate properties of the resulting composite. The use of suberin acting as bio-based plasticizer can reduce the high friction created by the cork, reducing the shear during the extrusion process.

Surprisingly, the introduction of 2 wt% of lignin in the presence of BPO (CPC 4) increased the maximum tensile strength in 48% and the tensile modulus in 39% and decreased the maximum strain. The result confirms the high effectiveness of lignin as coupling agent, improving the interfacial adhesion and providing stress transfer from the matrix to the natural filler. The function of lignin as coupling agent is enabled by the presence of both aliphatic and polar hydroxyl groups, which provide compatibility between nonpolar polymers and lignocellulosic materials [22, 23, 36], such as cork. The increase of the lignin content (CPC 5) does not contribute to an additional increase on the mechanical performance. On the contrary, it results on a reduction of the maximum tensile strength. On the other hand, we also found that the feeding of lignin in the hopper system of the extruder (CPC 6) is not so effective to promote strength but increases the maximum tensile strain. Probably, the higher residence time of the lignin in the extruder promoted a better dispersion of lignin and consequently of cork phase in the polyethylene matrix increasing the maximum strain in 5.7%.

6.3.5 Dimensional Stability

After processing, the moisture content of the developed composite specimens was determined, being the highest for CPC 1, with 0.313 ± 0.004 %, and the lowest for CPC 3, with 0.276 ± 0.011 %, corresponding to the functionalized composite with suberin. The functionalized CPC with the addition of lignin (CPC 4) presented 0.291 ± 0.009% of moisture content.

The water uptake behaviour of the different CPC was examined as a function of the time see in Figure 6.9. In the absence of coupling agent a faster water uptake was observed when compared with the functionalized composites due to the hydroxyl groups from cork which are available for interaction with water molecules.

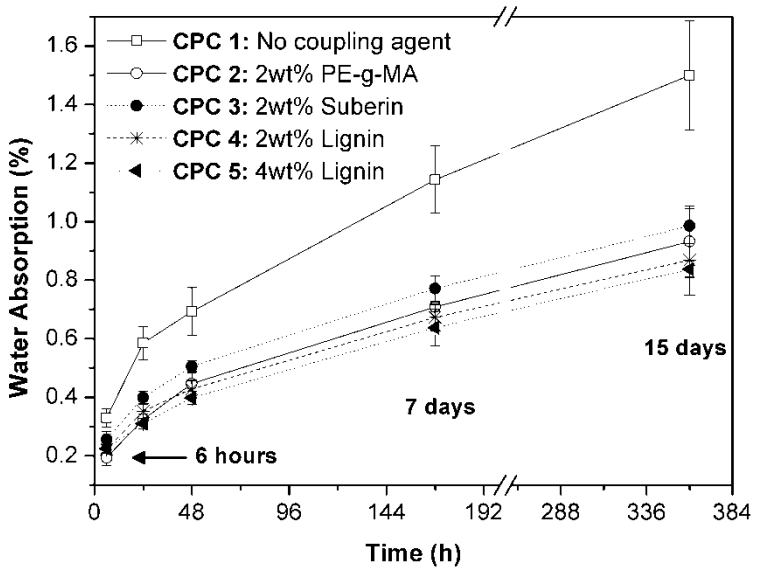

Figure 6.9. Water absorption behaviour of the HDPE-cork composites with and without coupling agent, being PE-g-MA the coupling agent based on maleic anhydride.

Even for the maximum period of immersion studied (360 h), the water uptake for the composites was inferior to 1.7%, which is a clear advantageous property for many applications. The use of coupling agent significantly reduces the water absorption of the developed composites. The specimens with suberin and lignin absorb less water comparing with the unreinforced cork-polymer composition. In the firsts 24h of immersion in water the CPC 1 absorbed 0.59 ± 0.06 wt.% of water while the CPC 3 containing 2 wt% of suberin only absorbs 0.40 ± 0.02 wt.%. This difference is more evident after the 7 days of immersion were the CPC 3 absorbs less 32.5% of water comparing with the condition of the CPC 1 and less 66.3% comparing with the composite containing 2wt% of lignin (CPC 4). This result supports the idea that suberin and lignin can act as coupling agent, reducing the moisture content and the water absorption of the CPC in a similar way to what was observed for the composite containing PE-g-MA. Moreover, suberin has a hydrophobic character that contributes to the low permeability of cork [4]. The addition of 1 wt.% of benzoyl peroxide could also be responsible to react with some hydroxyl groups from the cork structure, further contributing to reducing the water absorption.

The thickness swelling variation for all the composites was less than 0.4% as presented in Figure 6.10. It was observed that the coupling agent effect promotes less thickness variation. Increasing the lignin content (CPC 5), leads to a lower thickness variation. For the functionalized CPC and after the period of 15 days the thickness swelling variation tends to stabilize.

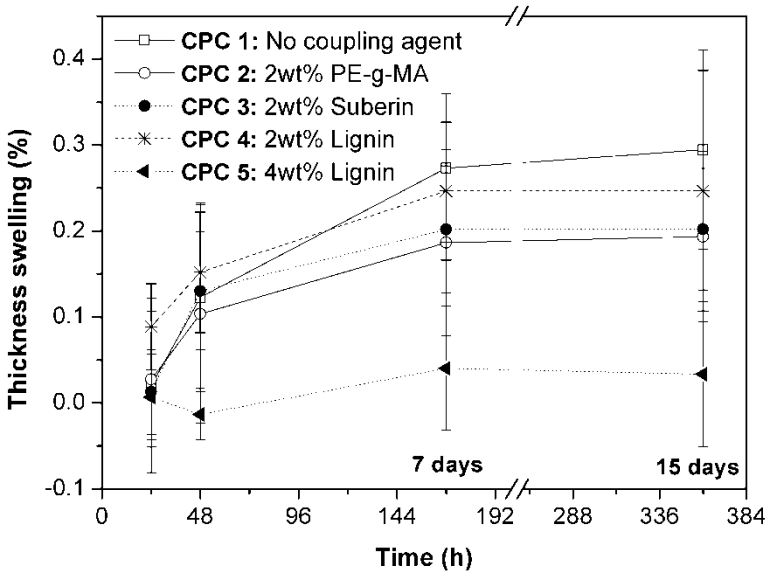

Figure 6.10. Thickness swelling variation of the functionalized CPC comparing with the control condition (CPC 1) with HDPE-cork (80-20) wt.%, being PE-g-MA the coupling agent based on maleic anhydride.

6.4 Conclusions

The following conclusions can be drawn base on the results presented in this work. Suberin and lignin fractions, isolated from cork, presents sufficient thermal stability to be applied in melt based technologies such as extrusion and compression moulding. A reactive twin-screw extrusion process was used to obtain the cork-polymer composites (CPC) in a continuous process. The mechanical tensile tests indicated that the suberin and lignin can be successfully used as bio-based coupling agents in the presence of benzoyl peroxide (BPO) to produce functionalized CPC with superior mechanical properties. Preferably, suberin acts as a plasticizer, improving the cork dispersion and reduces the composite stiffness, providing additional flexibility and formability to the composite. Lignin shows to act as a coupling agent and the use of 2wt% of lignin improved both maximum tensile strength and modulus in 48% and 39% respectively. Increasing the amount of lignin to 4 wt.% reduces the mechanical performance of the composites. The extrusion process shows that the addition of lignin in the feed hopper of the extruder is not advantageous and only increases the maximum tensile strain. The tensile tests also reveal that the use of 2 wt% of PE-g-MA increases 34% the maximum strength, 30% the tensile modulus and reduces the maximum strain. Coupling agents in CPCs play a very important role in improving compatibility and adhesion between the polar cork material and the non-polar polymer matrices. The CPCs present low water uptake and thickness swelling variation. The use of coupling

agent based on maleic anhydride or by adding suberin or lignin further reduces considerably the water uptake of the composites. The thermal properties showed that lignin can act as a thermal protective agent and suberin act as an antioxidant agent on the composites, while the PE-g-MA act as both. Coupling agents obtained from renewable resources may constitute a viable alternative to existing petroleum derivatives, contributing for a sustainable development of structural materials.

6.5 References

[1] Faruk O, Bledzki AK, Fink H-P, Sain M. Biocomposites reinforced with natural fibers: 2000 - 2010. Prog Polym Sci. 2012;37(11):1552-1596.

[2] Dittenber DB, GangaRao HVS. Critical review of recent publications on use of natural composites in infrastructure. Composites Part A. 2012;43(8):1419-1429.

[3] Bledzki AK, Gassan J. Composites reinforced with cellulose based fibres. Prog Polym Sci. 1999;24(2):221-274.

[4] Pereira H. Cork: biology, production and uses. Amsterdam: Elsevier; 2007.

[5] Fernandes EM, Correlo VM, Chagas JAM, Mano JF, Reis RL. Cork based composites using polyolefin's as matrix: Morphology and mechanical performance. Compos Sci Technol. 2010;70(16):2310-2318.

[6] Fernandes EM, Correlo VM, Mano JF, Reis RL. Novel cork-polymer composites reinforced with short natural coconut fibres: Effect of fibre loading and coupling agent addition. Compos Sci Technol. 2013(78):56-62.

[7] Silva SP, Sabino MA, Fernandes EM, Correlo VM, Boesel LF, Reis RL. Cork: properties, capabilities and applications. INT MATER REV. 2005;50(6):345-365.

[8] Mano JF. The viscoelastic properties of cork. J MATER SCI. 2002;37(2):257-263.

[9] Koskimies S, Hulkko J, Pitkaenen P, Heiskanen N, Yli-Kauhaluoma J, Waehaelae K, et al. Method for the manufacture of oligo- and polyesters from a mixture of carboxylic acids obtained from suberin and/or cutin and the use thereof. WO2007045728-A1, Valtion Teknillinen Tutkimuskeskus, 2007.

[10] Santos S, Graca J. Glycerol-omega-hydroxyacid-ferulic acid oligomers in cork suberin structure. Holzforschung. 2006;60(2):171-177.

[11] Graca J, Santos S. Linear aliphatic dimeric esters from cork suberin. Biomacromolecules. 2006;7(6):2003-2010.

[12] Bernards MA. Demystifying suberin. Can J Bot. 2002;80(3):227-240.

[13] Graca J, Pereira H. Methanolysis of bark suberins: Analysis of glycerol and acid monomers. Phytochem Anal. 2000;11(1):45-51.

[14] Graca J, Pereira H. Feruloyl esters of omega-hydroxyacids in cork suberin. J Wood Chem Technol. 1998;18(2):207-217.

[15] Marques AV, Pereira H, Meier D, Faix O. Quantitative-Analysis of Cork (Quercus-Suber L) and Milled Cork Lignin by Ftir Spectroscopy, Analytical Pyrolysis, and Total Hydrolysis. Holzforschung. 1994;48:43-50.

[16] Marques AV, Pereira H, Meier D. Isolation and characterization of a guaiacyl lignin from saponified cork of Quercus suber L. Holzforschung. 1996;50(5):393-400.

[17] Marques AV, Pereira H, Meier D, Faix O. Structural characterization of cork lignin by thioacidolysis and permanganate oxidation. Holzforschung. 1999;53(2):167-174.

[18] Xanthos M. Reactive Extrusion: Principles and Practice: Hanser Publishers - Oxford University Press; 1992.

[19] Fernandes EM, Aroso I, Pires RA, Correlo VM, Pitkänen P, Koskimies S, et al. Improvement on the mechanical properties of cork composites using suberin as coupling agent through a reactive extrusion process. ANTEC 2011, Annual Technical Conference of the Society of Plastics Engineeres (SPE) vol. 1 Boston, MA, 2011. p. 611-615.

[20] Sahoo S, Misra M, Mohanty AK. Enhanced properties of lignin-based biodegradable polymer composites using injection moulding process. Composites Part A. 2011;42(11):1710-1718.

[21] Kharade AY, Kale DD. Lignin-filled polyolefins. J Appl Polym Sci. 1999;72(10):1321-1326.

[22] Rozman HD, Tan KW, Kumar RN, Abubakar A, Mohd. Ishak ZA, Ismail H. The effect of lignin as a compatibilizer on the physical properties of coconut fiber–polypropylene composites. Eur Polym J. 2000;36(7):1483-1494.

[23] Morandim-Giannetti AA, Agnelli JAM, Lancas BZ, Magnabosco R, Casarin SA, Bettini SHP. Lignin as additive in polypropylene/coir composites: Thermal, mechanical and morphological properties. Carbohydr Polym. 2012;87(4):2563-2568.

[24] Moad G. The synthesis of polyolefin graft copolymers by reactive extrusion. Prog Polym Sci. 1999;24(1):81-142.

[25] Ekman R, Eckerman C. Aliphatic Carboxylic-Acids from Suberin in Birch Outer Bark by Hydrolysis, Methanolysis, and Alkali Fusion. Pap Puu-Pap Tim. 1985;67(4):255.

[26] Pinto PCRO, Sousa AF, Silvestre AJD, Neto CP, Gandini A, Eckerman C, et al. Quercus suber and Betula pendula outer barks as renewable sources of oleochemicals: A comparative study. Ind Crops Prod. 2009;29(1):126-132.

[27] Browning BL. Methods in Wood Chemistry. Interscience Publishers, New York.1967.

[28] Machado AV, Covas JA, Van Duin M. Evolution of morphology and of chemical conversion along the screw in a corotating twin-screw extruder. J Appl Polym Sci. 1999;71(1):135-141.

[29] Wunderlich B, Dole M. Specific heat of synthetic high polymers. VIII. Low pressure polyethylene. J Polym Sci. 1957;24(106):201-213.

[30] Pérez CJ, Cassano GA, Vallés EM, Failla MD, Quinzani LM. Rheological study of linear high density polyethylenes modified with organic peroxide. Polymer. 2002;43(9):2711-2720.

[31] Canetti M, Bertini F. Supermolecular structure and thermal properties of poly(ethylene terephthalate)/lignin composites. Compos Sci Technol. 2007;67(15-16):3151-3157.

[32] Gandini A, Pascoal Neto C, Silvestre AJD. Suberin: A promising renewable resource for novel macromolecular materials. Prog Polym Sci. 2006;31(10):878-892.

[33] Cousin P, Bataille P, Schreiber HP, Sapieha S. Cellulose-induced crosslinking of polyethylene. J Appl Polym Sci. 1989;37(10):3057-3060.

[34] Cunha AM, Liu ZQ, Feng Y, Yi XS, Bernardo CA. Preparation, processing and characterization of biodegradable wood flour/starch-cellulose acetate compounds. J MATER SCI. 2001;36(20):4903-4909.

[35] Fernandes EG, Cinelli P, Chiellini E. Thermal behavior of composites based on poly(vinyl alcohol) and sugar cane bagasse. Macromol Symp. 2004;218:231-239.

[36] Acha BA, Marcovich NE, Reboredo MM. Lignin in Jute Fabric-Polypropylene Composites. J Appl Polym Sci. 2009;113(3):1480-1487.

Novel cork-polymer composites reinforced with short natural coconut fibres: Effect of fibre loading and coupling agent addition[6]

Abstract

Composites from high density polyethylene filled with cork powder and coconut short fibres, in two different ratios, were prepared in a twin-screw extruder followed by compression moulding process. The main motivation of this work was to improve the mechanical performance without compromising the use of high weight percentage of natural component used in the preparation of cork-based composites. The morphology of the hybrid composites were more homogeneous in the presence of the coupling agent (CA) displaying enhanced fibre-matrix adhesion. Moreover, the use of CA based on maleic anhydride promotes a mechanical reinforcement effect on the tensile properties, including the elongation at break. The addition of coconut fibre resulted on an increase of 27% in elastic modulus and 47% in the tensile strength when compared with the unreinforced cork-based (50 – 50) wt.% composite. This work clearly shows that the addition of 10 wt.% of short-coconut fibres, randomly distributed, can be effectively used as reinforcing strategy of cork-based composite materials, preferably in the presence of 2 wt.% of CA.

[6] This chapter is based on the following publication:

Fernandes EM, Correlo VM, Mano JF, Reis RL, 2013, "Novel cork-polymer composites reinforced with short natural coconut fibres: Effect of fibre loading and coupling agent addition", Composites Science and Technology, 78, 56–62.

7.1 Introduction

Government regulations and a growing environmental consciousness throughout the world have generated a paradigm to move in the direction of designing materials compatible with the environment [1]. Over the past two decades, natural fibres have received considerable attention as a substitute for synthetic fibre reinforcements in polymeric materials. Natural fibres are increasingly used for reinforcement in thermoplastics over traditional reinforcing materials such as glass fibres and particle minerals (e.g. talc, $CaCO_3$ and mica) due to their low cost, lightweight, good thermal and acoustic insulation, acceptable specific strength, reduced tool wear, corrosion resistance, availability, renewable resource and recycling possible with lower environment impact [2, 3], promoting the concept of sustainability. As a result of these advantages some of the plant fibre based thermoplastic composites have already found applications in furniture manufacture, non-structural building applications and as interiors parts in automotive industry [4-6]. Cork is the suberous covering tissue of the species *Quercus Suber* L., commonly known as the cork oak and the unique properties arise from the closed cell structure [7, 8]. During the last years there has been an increasing interest concerning cork based materials and its potential to be used in composite applications [5, 9, 10]. However, natural materials are inherently incompatible with hydrophobic thermoplastics such as polyolefins reducing the mechanical performance. Major limitations of using natural materials as reinforcements in such matrices include poor interfacial adhesion between polar-hydrophilic fibre and nonpolar-hydrophobic matrix, and difficulties in mixing due to poor wetting of the fibre with the thermoplastic matrix [11]. Previous studies on cork-polymer composites (CPC) have demonstrate that increasing the cork content the tensile mechanical properties are compromised and reduced [12, 13]. Reinforcement strategies of cork composites, such as the use of low amounts of coupling agent (CA) [14], or the use of conventional chemical modification methods of the natural component [15], can be applied to improve the compatibility and interfacial bonding between polymeric matrix and dispersed component. The motivation of this work was to prepare high performance cork based composites, in order to support tensile stresses developed in complex geometries or when submitted to finishing operations such as lamination, by using natural fibres preferably in combination with a CA. Additionally, studies involving hybrid bio-fibre systems containing cork powder through melt based technologies have not been addressed so far. Therefore composites comprising these two kinds of natural materials (e.g. cork and coconut fibre) may exhibit the desirable properties of the individual constituents. Coconut fibre, or coir,

is a versatile lignocellulosic fibre obtained from coconut trees (*Cocos nucifera*), which grow extensively in tropical countries. Sri Lanka and India are considered to be the major coir fibre producers in the world. Coconut fibres may be decomposed in 20–30 years in the nature, and it may be regarded as an environmentally friendly material [16]. Chemical composition [7, 17-20] of both natural materials is presented in Table 7.1.

Table 7.1. Chemical constituents (wt.%) of the lignocellulosic materials used on the bio-based composites.

Chemical Composition (wt.%)	Origin	Cellulose	Hemicellulose	lignin	Suberin	Extractives	Ref.
Cork	Bark	12-25		21-29	33-45	8.5-19	[7, 19]
Coconut Fibre	Fruit	43	0.3	45	—	0.35-3.13	[17, 18, 20]

Coconut fibres as already been used to reinforce polyolefins [4, 21-23]. Both coconut fibres and cork are used as insulator material in thermal and acoustic applications [24, 25] and presents lower hydrophilic behaviour when compared with sisal fibre [26]. In this study, high density polyethylene (HDPE) was selected as the matrix to develop the hybrid cork-based composites because: HDPE presents a good balance property range, is easy to process through melt based technologies, such as extrusion and compression moulding, and is a high consumption industrial polymer that presents low price in the market which is of significant importance to the 'cost-performance' assessment. Additionally, it requires a relatively low processing temperature, which is essential because of the relatively low thermal stability of both natural components. In this work, we report the effect of using coconut fibre as a reinforcement material, preferably in the presence of 2 wt.% of CA, to promote higher mechanical performance of the cork-based composites.

7.2 Materials and Methods

7.2.1 Natural Materials

Cork sanding powder, with particle size < 500 μm and specific weight of 157 ± 2 kg m^{-3} and a humidity of ~5.4% was collected at the Amorim Revestimentos S.A. (S. Paio Oleiros, Portugal) industrial facilities.

The brown coconut fibre from Hayleys Exports PLC (Kotugoda, Srí Lanka) presented a diameter of 277.4 ± 38.8 μm, a humidity of 8.2 % and specific weight of 845.1 ± 46.6 Kg m^{-3}, was collected at Amorim Isolamentos S.A. (Vendas Novas, Portugal).

7.2.2 Polymer materials and coupling agent

A commercially available polyethylene (HMA – 025), HDPE, with a MFI of 8.2 g.10min^{-1} (190 °C, 2.16 kg), with a melting point of 132.5 °C from ExxonMobil (Germany) was supplied by Pallmann Maschinenfabrik GmbH & Co. (Germany) in the powder form with particle size between 125 μm and 1500 μm. The used coupling agent, a HDPE functionalized with maleic anhydride (PE-g-MA), containing 0.5 to1.0 wt% of maleic anhydride, was Exxelor PE 1040, with MFI of 1.4 g.10min^{-1} (190 °C, 2.16 kg), and a melting point of 131.3 °C, from ExxonMobil (Germany).

7.2.3 Fibre diameter and density

The diameter measurements of coconut fibres were made in five spaced locations along the gauge length of 30 different specimens using an optical microscope Olympus BH-2 (Tokyo, Japan) equipped with an Olympus DP11, (Japan) digital camera. A histogram for the coconut fibre was performed and a normal distribution to characterize the coconut fibre diameter. Regarding cork powder, the particle size was determined used an analytical sieve (Retsch. AS 200, Germany) after a sieving period of 5 min at a medium amplitude. The density of the coconut fibres and of the hybrid cork based composites were determined according to the standard ASTM D 792, using an analytical balance equipped with a stationary support for the immersion vessel using liquid propanol.

7.2.4 Chemical characterization

To confirm the existing differences in chemical composition, both natural materials were analysed using Fourier transform infrared (FTIR) spectroscopy. All the spectra were acquired using a Shimadzu IR-Prestige 21. The attenuated total reflectance (ATR) methodology (PIKE Technologies) was used and the spectra were acquired between 4400 cm^{-1} to 800 cm^{-1} using a resolution of 4 cm^{-1}.

7.2.5 Composites processing

Before compounding all natural raw materials were pre-dried at 80 °C during 24 h to stabilise the cork and the coconut fibres in terms of moisture content. The moisture content, determined by oven-dry weight before processing, was found to be 1.5-3%. The prepared compositions and processing conditions such as barrel temperature and screw speed are summarized in Table 7.2.

Table 7.2. Processing conditions used for the studied cork composite compositions.

Code	Cork (wt%)	HDPE (wt%)	Coco Fibre (wt%)	Coupling Agent (wt %)	Natural Component (wt %)	Extrusion	
						Temperature Profile (°C)	Motor (rpm)
CPC 1	50	50	0	0	50	130; 145; 155 [a]	30
CPC 2	49	49	0	2	49		
CPC 3	47.5	47.5	5	0	52.5	130; 150; 160 [b]	30
CPC 4	46.5	46.5	5	2	51.5		
CPC 5	45	45	10	0	55		
CPC 6	44	44	10	2	54		

[a] Temperature profile of CPC 1 and CPC 2 compositions.

[b] Temperature profile of CPC 3 to CPC 6 compositions.

The compounding was performed in a counter-rotating twin-screw extrusion machine (Carvex, Portugal), which had a screw diameter of 52 mm and an L/D ratio of 18 with a nonintermeshing, mixing mode screw configuration. The barrel temperature was in the range 130-160 °C, and the screw speed was fixed at 30 rpm. The cork powder and the grinding HDPE were pre-mixed and manually feed in the hopper system with the cut coconut fibres. No extrusion head was used in order to minimize the residence time and shear heat dissipation. The extruded material was cooled in air, granulated in a cutting mill to produce the composite pellets with dimensions $\leq$ 7 mm. In a further step, the obtained pellets were compression moulded using a hydraulic press (Moore, UK) to produce boards with 186 × 118 mm^2 and 3 mm of thickness from the different compositions. The mould temperature was 150 °C and the material was 8 minutes without pressure followed by 2 minutes under pressure of 1.42 MPa. Tensile bars in dog bone shape were obtained from these boards using a computer numerical control

CNC machine (Roland 3D Plotter MDX-20, UK). After cut the hybrid composites are compact and do not present macroscopic porous or voids. The specimens were produced according to ISO 527–2. Nonetheless, its thickness is slightly higher (3 mm) than the standard.

7.2.6 Scanning electron microscopy

The morphology of the natural fibres and the fracture surface of the tensile tested composite specimens were analysed using a NanoSEM 200 FEI (The Netherlands) scanning electron microscope (SEM). Before being analysed all the specimens were coated by ion sputtering with an Au/Pd alloy (80-20 wt.%) in a high resolution sputter coater of Cressington 208HR (Watford, UK).

7.2.7 Mechanical properties

Tensile properties of the bundle coconut fibres were measured with a Instron 4505 Universal Machine, (USA) using a 1 kN load cell, a crosshead speed of 1 $mm.min^{-1}$, and a fibre gauge length of 30 mm. Prior to testing, fibres were mounted on sturdy paper frames using a high-strength epoxy adhesive and placed in a desiccator for a minimum of 48 h.

The tensile properties of the developed cork based composites reinforced with coconut fibres were determined in the same equipment according the standard ISO 527–2, using a gauge length of 20 mm. The tensile force was taken as the maximum force in the force deformation curve. Tensile modulus was estimated from the initial slope of the stress–strain curve (between 0.05 and 1% strain) using the linear regression method. Samples were conditioned at room temperature for at least 48 h before testing. A crosshead speed of 5 $mm.min^{-1}$ was used until rupture. The average and standard deviations were determined using 8 specimens per condition. To allow for a comparison of the material property profiles in terms of the potential for reinforcement of the mechanical performance, the Ashby plots for the specific tensile modulus against the specific strength are illustrated for absolute property values with the respective standard deviations.

7.2.8 Statistical analysis

One-way analysis of variance (ANOVA) with post hoc Bonferroni multiple comparison tests was used to infer about significant differences between mean values of the mechanical properties in the developed

cork composite materials. Assumptions of ANOVA such as normality were evaluated with Shapiro-Wilk test. A level of $\alpha = 0.05$ was used for statistical significance.

7.3 Results and Discussion

7.3.1 Chemical characterization of the natural raw materials

The chemical composition of cork and coconut fibre was characterized using ATR-FTIR spectroscopy. Figure 7.1 shows the spectra region between 800 and 4000 cm^{-1}.

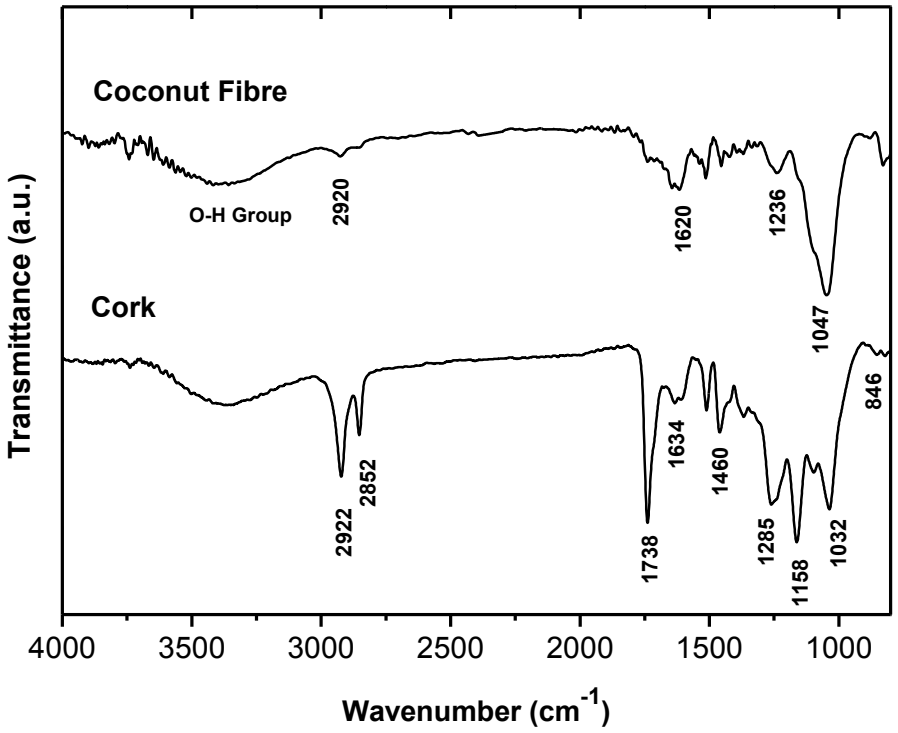

Figure 7.1. FTIR-ATR of the coconut fibre and the cork powder.

The main absorption bands are attributed to the presence of lignin, hemicellulose and cellulose, characteristic of natural fibres (Table 7.1), being cellulose (43 wt.%) the principal component of the coconut fibre and suberin (33 - 45 wt.%) the one for cork. In both native materials, the IR spectrum shows a large band in the 3200–3600 cm^{-1} range that is attributed to the axial deformation of the O–H group. The absorption spectrum on the infrared region of the coconut fibre presents a characteristic band at 2920 cm^{-1} that is related to the axial deformation of C–H group. The carbonyl group of the hemicelluloses appears at 1620 cm^{-1}, while the band at 1236 cm^{-1} is associated to the presence of C–

O–C in cellulose chain. The strong absorption band at 1047 cm^{-1} is related to the C–OH stretching vibration. Concerning to cork spectrum (Table 7.1) and, according to the literature [19], the bands at 2920 cm^{-1} and at 2852 cm^{-1} are related to suberin, cellulose, lignin, hemicellulose, low molecular weight compounds and polysaccharides. The C=O elongation at 1738 cm^{-1} is characteristic of the ester group present on the suberin chain.

7.3.2 Physical, morphological and mechanical properties of the natural component

The cork particle size distribution, the coconut fibre diameter variation and the morphology of the used natural components are reported in Figure 7.2.

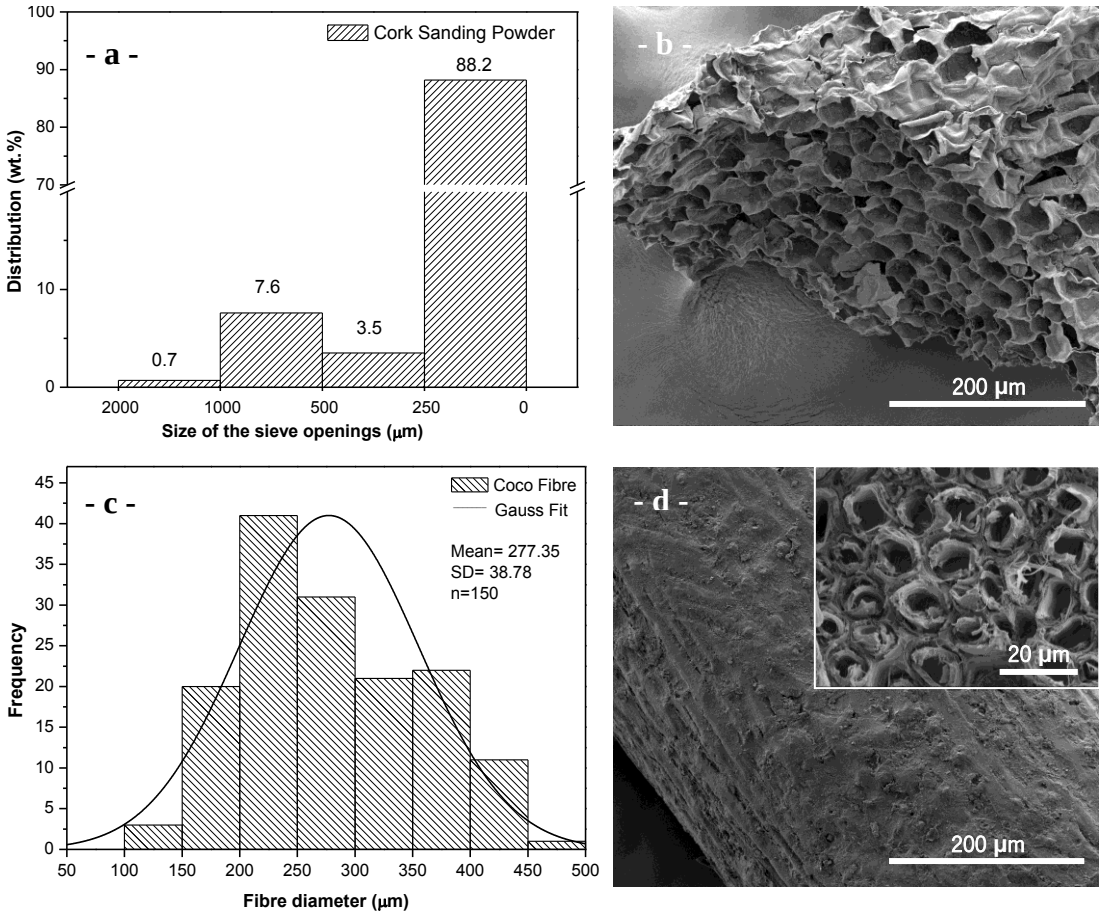

Figure 7.2. ATR-FTIR Particle size distribution of the cork powder and histogram of the coconut fibre diameter with the Gaussian fit curve (a, c) and respective morphology of the natural materials by scanning electron microscopy (b, d).

Cork powder, obtained from the sanding process, is composed of: a high percentage (88.2 wt.%) of particle with a size lower than 250 μm, a small fraction (11wt%) between 1 mm - 250 μm and a residual part (less than 1wt%) between 2-1mm (Figure 7.2 a). The histogram of Figure 7.2 c) shows the diameter distribution of coconut fibre, with the mean value of 277.4 μm and a gaussian fit distribution. The coconut fibre used to reinforce the cork-based composites presents a broad fibre diameter distribution of [71.8 – 465.6] μm for a confidence interval of 95%. Cork powder presents reduced density and lower initial moisture content when compared with the coconut fibre as presented in Table 7.3.

Table 7.3. Tensile properties of coconut fibre and the polyethylene matrix and respective density and moisture content of the used components to produce the composite materials.

Material	Max. Strength (MPa)	Modulus (GPa)	Maximum Strain (%)	Density (Kg/m^3)	Moisture Content (%)
Coconut Fibre	134.3±34.5	2.16±0.62	34.4±4.7	845±47	8.2
Cork	—	—	—	165±21	5.4
Polyethylene	26.8±0.4	0.63±0.04	> 200	956±1	0

The determined density of the used coconut fibres is similar to the HDPE matrix, although the literature typically reports higher values of 1150 kg/m^3 [17] for this natural fibre. The morphological analysis revealed that cork powder presents several cells despite its reduced particle size (Figure 7.2 b). This anisotropic foamed material presents a close cellular structure [7] where the section of the cork particle shows preferentially the radial direction. The morphology of the coconut fibres was also analysed and the results are shown in Figure 7.2 d). The obtained SEM image shows a representative top surface of the coconut fibre displaying many pinholes on the surface ('rotten wood'-like appearance) [26]. The inset image presents the cross-section of the coconut fibre, which can be more or less cylindrical, containing axially oriented cells/fibrils of around 10 μm diameter. These observations are in accordance with the results reported in literature [22, 26]. The mechanical tests of the coconut fibres revealed an higher mechanical performance than the thermoplastic matrix (Table 7.3 and Figure 7.3). The coconut fibres have a maximum tensile strength of 134.3 ± 34.5 MPa and tensile modulus of 2.16 ± 0.62 GPa. It was also observed that the tensile strength and elastic modulus of the fibres is inversely proportional to the fibre diameter: both properties decrease with increasing fibre diameter (Figure 7.3). According to

the linear regression analysis, this result was observed for 81% of the tested fibres. The strain at break for coconut fibres was 34.4 ± 4.7%. This higher failure strain capacity of the coconut fibres, as compared with other natural fibres, can also contribute for a better strain compatibility between the fibres and the polyethylene matrix, making them and interesting material to be used in short-fibre filled composites.

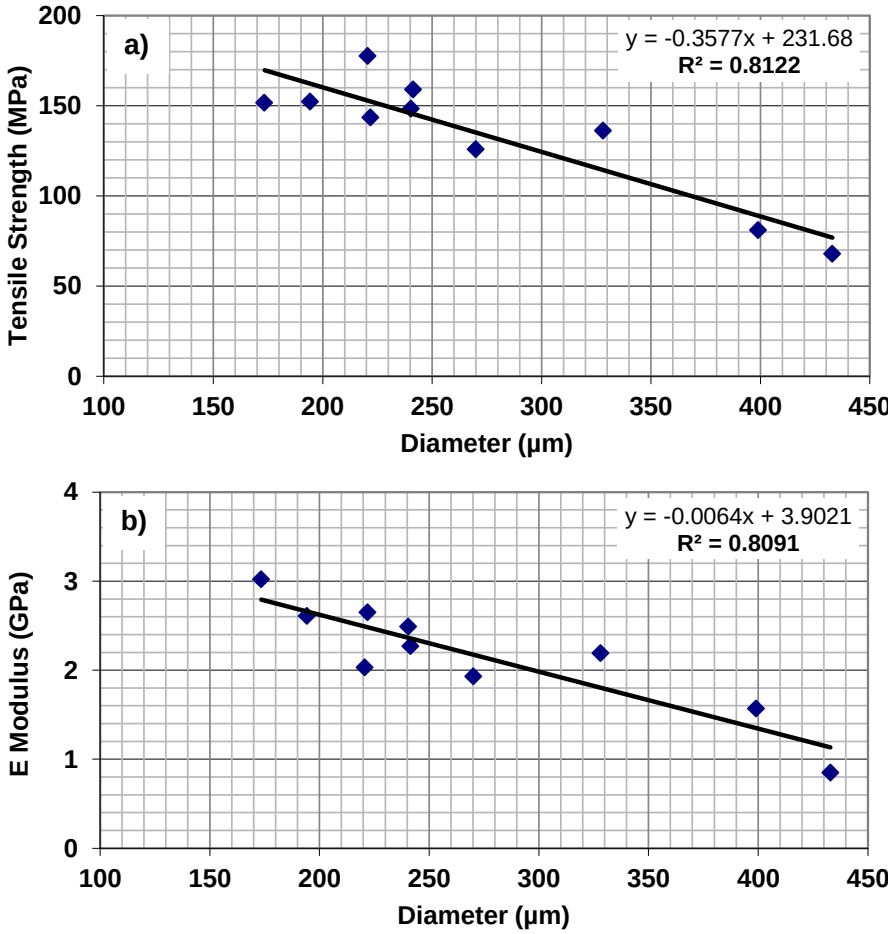

Figure 7.3. Mechanical properties of the coconut fibres as a function of the diameter: a) Tensile strength and b) E Modulus.

7.3.3 Composite morphology

Scanning electron microscopy (SEM) is a common method to analyse the level of fibre/matrix interfacial adhesion. The fracture surface morphology, after tensile tests, of the developed composites is shown in Figure 7.4.

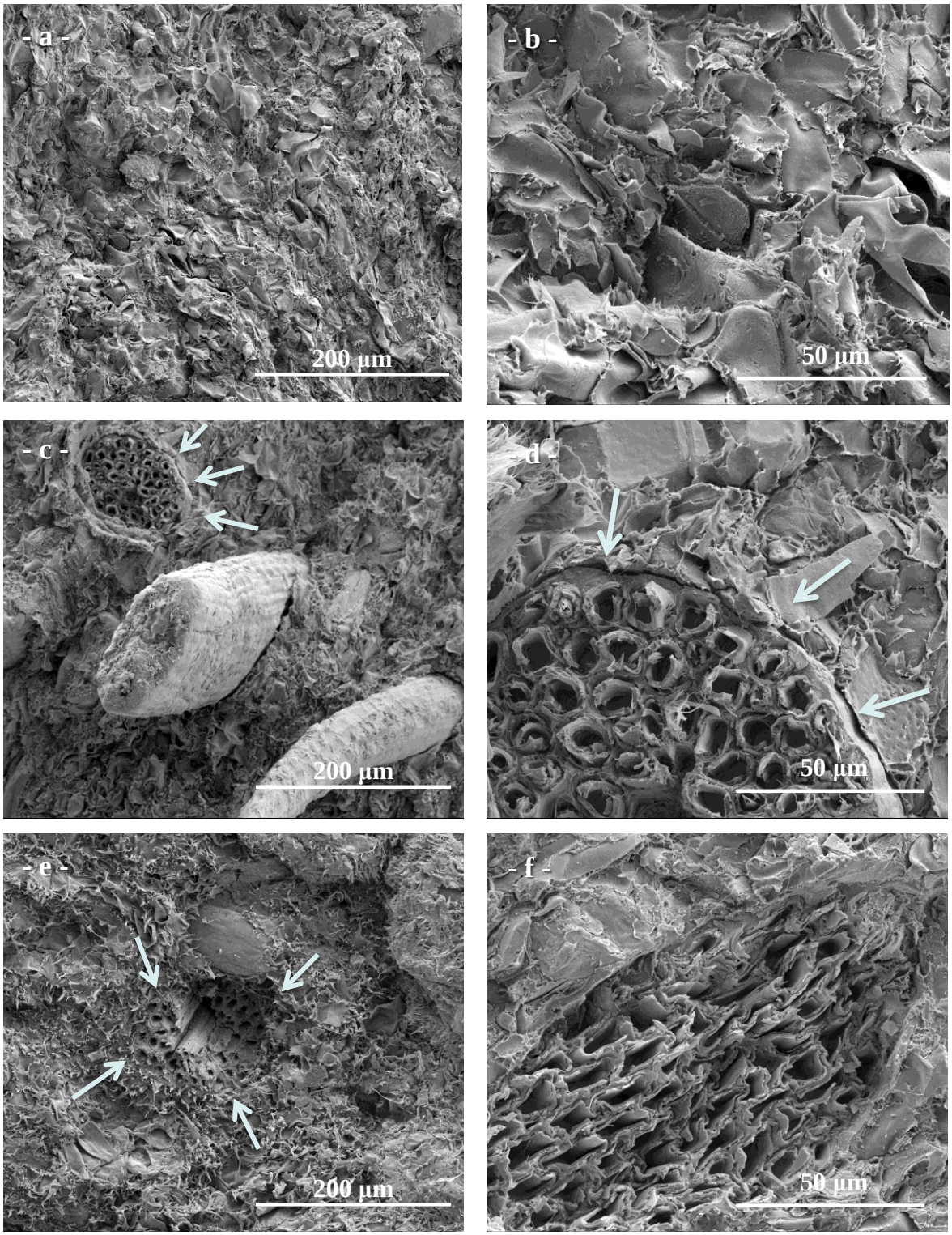

Figure 7.4. SEM micrographs of cork-polymer composite (CPC) fracture after tensile tests at magnifications of: (a) 600× and (b) 2400×; CPC reinforced with 10wt.% coconut fibre at magnifications of (c) 600× and (d) 2400×; CPC reinforced with 10wt.% coconut fibre with 2wt.% of coupling agent at magnifications of (e) 600× and (f) 2400×.

The micrographs of the cork-polymer composite (50 - 50) wt.% or CPC 1 composition (Figure 7.4 b) shows the cork powder cell walls in contact with the polyethylene matrix. This image reveals also a fragile fracture that is the result of the high volume content of cork powder. Moreover, the tensile fracture discloses that the cellular structure of cork powder is maintained but with a more compact morphology after the two processing steps of extrusion and compression moulding, explaining the densification that occurs on the lignocellulosic composites. The fracture surface of the composite prepared with the same cork/PE ratio and reinforced with 10 wt.% of short coconut fibre (CPC 5) was analysed and the results are shown in Figure 7.4 c) and d). From these images is possible to conclude that the interfacial adhesion between the fibres and the polymeric matrix is poor. The untreated fibres appear to be free of any matrix material adhering to them. It can be also observed the presence of cavities between the coconut fibre and the cork-polymer components. Additionally, significant coconut fibre breakage was observed during pelletization process after conventional melt mixing, reinforcing the idea of low adhesion between coconut fibres and the thermoplastic matrix. Nevertheless, the addition of 2% of maleic anhydride produced an opposite effect. The micrographs from the fracture surface of CPC 6 of (Figure 7.4 e and f) show a good interfacial adhesion between the coconut fibres (10 wt.%) and the polymeric matrix. In this last case, the fracture of the coconut fibre occurred preferentially at the same level of the composite fracture. Generally, chemical coupling agents are molecules pocessing two functions [6]: the first is to react with the hydroxyl groups of cork and of cellulosic fibres (OH groups) and the second is to react with functional groups of the matrix. The expected result is the reduction of these groups that contribute to the hydrophilic character, promoting the compatibility between the matrix and the natural component.

7.3.4 Composite mechanical properties

7.3.4.1 Tensile properties and density

Tensile tests were performed in order to evaluate the efficiency of the envisaged strategy aimed for improving the mechanical performance of the cork-polymer composites (CPC). Table 7.4 presents the experimental mean values with the standard deviation, the improvement on the mechanical properties in terms of variation (%) when compared with the CPC 1 cork-polymer (50 – 50) wt.%, the coefficient of variation (Cv) for each tested group and the density of the composite materials. In addition, Figure 7.5

shows the tensile properties of the developed composites with the statistical relevant differences for a confidence level of 95%.

The density of the cork based composites was in the range between 1032 to 1070 kg/m^3. The presence of 2 wt.% of coupling agent (CA), promotes a positive effect. This is shown by a slight decrease on the composite density, probably due to a better dispersion of the natural phase on the matrix.

Table 7.4. Mechanical properties of the cork-polymer composites reinforced with and without coconut fibres after tensile tests and respective density after two step processing.

Code	σ_{max} (MPa)	Variation (%)	C_v (%)	E1%(RLin) (MPa)	Variation (%)	C_v (%)	Deformation Max. (%)	CPC Density (Kg/m^3)
CPC 1	13.9±0.8	—	5.39	471.0±15.8	—	3.35	4.2±0.2	1049.2±2.4
CPC 2	15.7±0.4	12.5	2.08	431.8±24.4	-8.3	5.65	7.2±0.1	1037.0±5.4
CPC 3	13.4±0.3	-4.2	4.53	556.2±54.3	18.1	9.75	3.9±0.2	1058.8±8.0
CPC 4	17.7±1.1	26.8	6.19	488.9±42.7	3.8	8.74	5.4±0.4	1057.5±2.7
CPC 5	14.2±0.5	2.0	3.79	572.9±44.9	21.6	7.84	4.5±0.7	1066.1±4.4
CPC 6	20.4±0.3	46.2	1.56	598.7±19.5	27.1	3.25	6.4±0.4	1061.7±1.5

E1% (RLin) – Tensile modulus determined below 1% of deformation using linear regression (MPa);

σ_{max} – Maximum tensile strength (MPa);

Variation (%) – Variation of the mean value (%) of the mechanical property comparing with CPC1 (50-50) wt% condition;

C_v – Coefficient of variation (%);

± Standard Deviation.

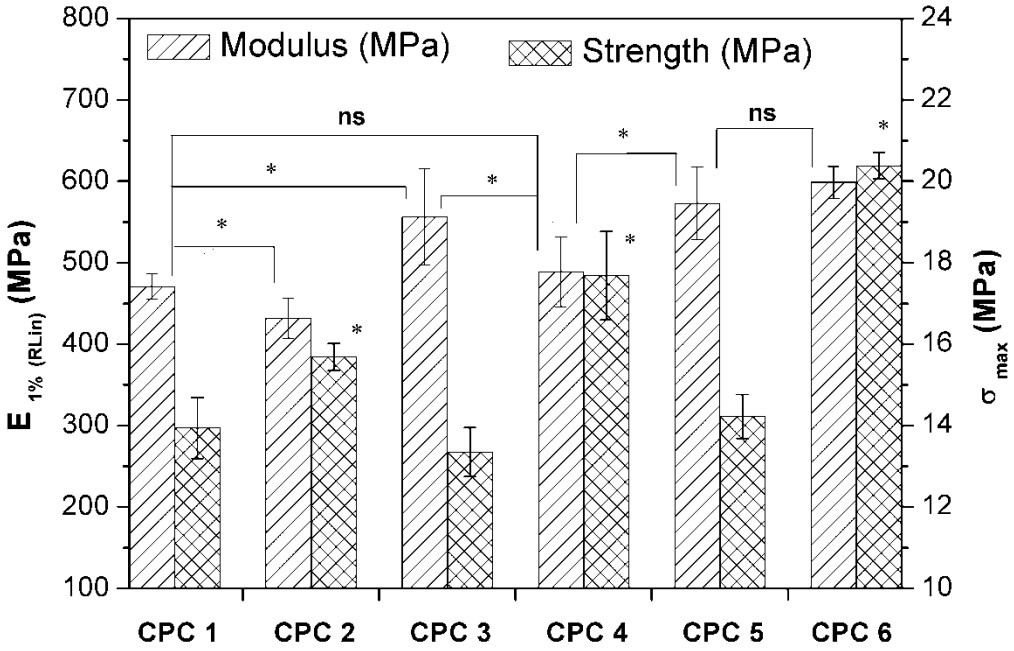

Figure 7.5. Mechanical Properties of the developed composites. Symbol (*) denote composite materials with statistical significant differences ($p<0.05$) and (ns) not significant, as using the one-way ANOVA method.

Comparing the CPC 1 and CPC 2 is possible to observe an increase of 12.5% in the maximum tensile strength promoted by the CA. The results are in accordance with the previous work using different qualities of cork powders with polyolefins processed by pultrusion [14]. When 5 to 10 wt.% of short coconut fibres (CPC 3 and CPC 5) were used an increase of 18.1 to 21.6% on the tensile modulus was achieve being the hybrid composites more stiffer. However, no significant differences were observed on maximum strength. Therefore, the use of fibres, without any additional physical or chemical treatment or additive, showed less efficiency than expected from their strength properties (see Table 7.3) due to the poor adhesive interaction between the matrix and coconut fibres. This was reflected on the almost insignificant increase on the tensile strength and reduction on ductility (Table 7.4). These results are in accordance with the morphological observations. On the other hand, the use of coconut fibres in combination with 2 wt.% of CA resulted in an significant increase of the tensile properties, independently of the amount of fibres used. These effect was more pronounced when it was used the higher fraction 10 wt.% of coconut fibre (CPC 6), resulting in an increase of 46% on maximum strength and 27% on tensile modulus and higher maximum strain at break when compared with the unreinforced cork-polymer composite (CPC 1). This considerable increment on the tensile properties is justified with the

enhancement of the interfacial adhesion between the matrix and the fibres promoted by the CA based on maleic anhydride that improves its ability to transfer stresses across the interface resulting on an increase of the mechanical properties of the final composite. The Cv percentages reported in Table 7.4, shows the weight of the standard deviation over the distribution. The maximum and minimum values registered were 6.2% and 1.6% for tensile strength and, 9.8% and 3.3% for tensile modulus. The lowest Cv values were obtained for the composite with higher mechanical performance (CPC 6). This is a clear indication that the produced boards had low variation on the mechanical properties, supporting the idea of homogeneous hybrid composites with good distribution of the natural component in the matrix.

7.3.4.2 Ashby diagram

The mechanical properties of the different formulations were additionally organized in an Ashby diagram by plotting maximum tensile strength *versus* tensile modulus of the CPC with the respective both standard deviations (Figure 7.6).

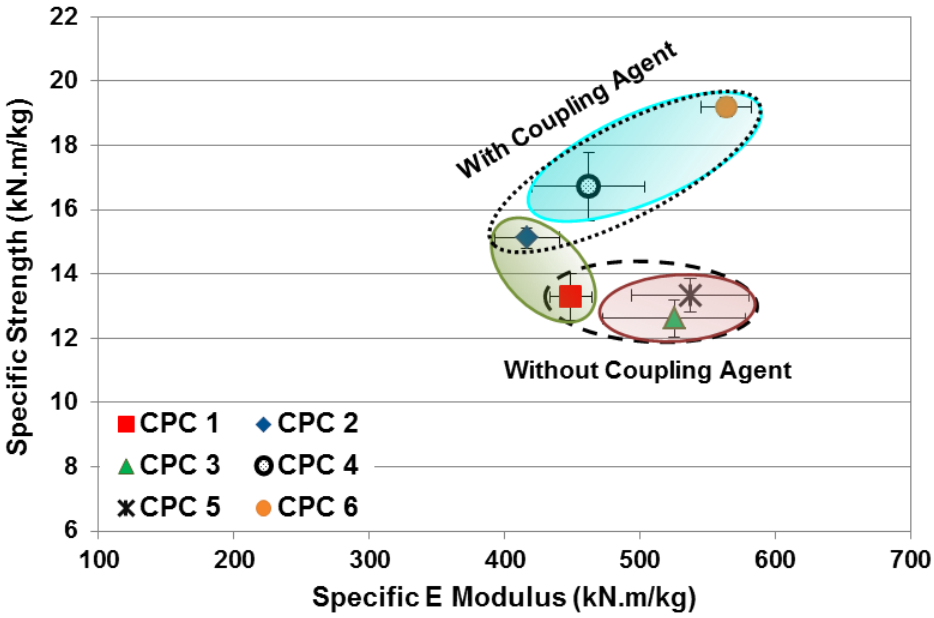

Figure 7.6. Ashby plot presenting the specific maximum tensile strength against specific tensile modulus of the cork-polymer composites (CPC) obtained by extrusion followed by compression moulding.

The results plotted in the graph can be divided in three distinct regions: a first region corresponding to the mechanical properties of the cork based composites with and without the CA (CPC 2 and CPC 1

respectively); a second region corresponding to the composites just reinforces with fibres (CPC 3 and CPC 5); and a third region corresponding to composites reinforced with fibres and treated with maleic anhydride - composites with higher tensile strength (CPC 4 and CPC 6). In Figure 7.6 the results were also divided just in two regions: a bottom region corresponding to the composites prepared without CA and presenting lowest values of tensile strength but similar tensile modulus; and a top region corresponding to the composites with highest values of tensile strength and tensile modulus. Interestingly, the diagram highlights the importance of the combine effect of CA based on maleic anhydride and the addition of coconut fibres as reinforcement strategy on cork-polymer composites.

7.4 Conclusions

The mechanical reinforcement strategy of cork powder composites using random discontinuous distributed coconut fibres through melt based technologies was investigated. The morphological observations were in accordance with the mechanical results, showing the improved effect of fibre-matrix adhesion in the presence of 2 wt.% of coupling agent (CA) based on maleic anhydride. The Ashby diagram supported to identify the best developed composite formulation and to visualize the improvement over the cork powder - polymer (50-50) wt.% composite. The incorporation of 10 wt.% of coconut fibre in the presence of 2 wt.% of CA on the cork-based composites presented an increase of 46% on the mechanical properties in terms of tensile maximum strength of and 27% in terms of tensile modulus comparing with the unreinforced cork-polymer composite solution. Additionally, the presence of CA increases the maximum strain values in all processed composites.

The maximum values registered in terms of coefficient of variation for this reinforced cork-based composite solution was 3.3% for the tensile modulus and 1.6% for the tensile strength properties. The lower coefficient variation supports the homogeneous properties in terms of short fibre distribution on the novel hybrid cork-based composites. With this strategy it was possible to both improve the mechanical performances of cork-based composites and to increase the natural component up to 54 wt.% on the novel hybrid cork-based composite materials.

7.5 References

[1] Mohanty AK, Misra M, Hinrichsen G. Biofibres, biodegradable polymers and biocomposites: An overview. Macromol Mater Eng. 2000;276(3-4):1-24.

[2] Bledzki AK, Gassan J. Composites reinforced with cellulose based fibres. Prog Polym Sci. 1999;24(2):221-274.

[3] Ku H, Wang H, Pattarachaiyakoop N, Trada M. A review on the tensile properties of natural fiber reinforced polymer composites. Compos Part B-Eng. 2011;42(4):856-873.

[4] Ayrilmis N, Jarusombuti S, Fueangvivat V, Bauchongkol P, White RH. Coir Fiber Reinforced Polypropylene Composite Panel for Automotive Interior Applications. Fiber Polym. 2011;12(7):919-926.

[5] Fernandes EM, Correlo VM, Chagas JAM, Mano JF, Reis RL. Properties of new cork-polymer composites: Advantages and drawbacks as compared with commercially available fibreboard materials. Compos Struct. 2011;93(12):3120-3129.

[6] Pandey JK, Ahn SH, Lee CS, Mohanty AK, Misra M. Recent Advances in the Application of Natural Fiber Based Composites. Macromol Mater Eng. 2010;295(11):975-989.

[7] Silva SP, Sabino MA, Fernandes EM, Correlo VM, Boesel LF, Reis RL. Cork: properties, capabilities and applications. Int Mater Rev. 2005;50(6):345-365.

[8] Gibson LJ, Easterling KE, Ashby MF. The Structure and Mechanics of Cork. P Roy Soc Lond A Mat. 1981(A 377):99-117.

[9] Gil L. Cork Composites: A Review. Mater Design. 2009;2(3):776-789.

[10] Fernandes EM, Silva VM, Chagas JAM, Reis RL. Fibre-reinforced cork-based composites. WO2011014085-A2, Amorim Revestimentos, S.A., 2011.

[11] Westerlind BS, Berg JC. Surface-energy of untreated and surface-modified cellulose fibers. J Appl Polym Sci. 1988;36(3):523-534.

[12] Barlow CY, Ashby MF. Cork dust composites. Proceedings of the Riso International Symposium on Metallurgy and Materials Science, 1989. p. 275-281.

[13] Moresco M, Leal Rosa SM, Santos EF, Bohrz Nachtigall SM. Agrofillers in Polypropylene Composites: A Relationship Between the Density and the Mechanical Properties. J Appl Polym Sci. 2010;117(1):400-408.

[14] Fernandes EM, Correlo VM, Chagas JAM, Mano JF, Reis RL. Cork based composites using polyolefin's as matrix: Morphology and mechanical performance. Compos Sci Technol. 2010;70(16):2310-2318.

[15] Abdallah FB, Cheikh RB, Baklouti M, Denchev Z, Cunha AM. Effect of surface treatment in cork reinforced composites. J Polym Res. 2009;17(4):519-528.

[16] Wei W, Gu H. Characterisation and utilization of natural coconut fibres composites. Mater Design. 2009;30(7):2741-2744.

[17] Bledzki AK, Reihmane S, Gassan J. Properties and modification methods for vegetable fibers for natural fiber composites. J Appl Polym Sci. 1996;59(8):1329-1336.

[18] Bilba K, Arsene M-A, Ouensanga A. Study of banana and coconut fibers - Botanical composition, thermal degradation and textural observations. Bioresour Technol. 2007;98(1):58-68.

[19] Pereira H. Chemical composition and variability of cork from Quercus suber L. Wood Sci Technol. 1988;22(3):211-218.

[20] Faruk O, Bledzki AK, Fink H-P, Sain M. Biocomposites reinforced with natural fibers: 2000–2010. Prog Polym Sci. 2012;37(11):1552-1596.

[21] Rozman HD, Tay GS, Kumar RN, Abubakar A, Ismail H, Ishak ZAM. Polypropylene hybrid composites: A preliminary study on the use of glass and coconut fiber as reinforcements in polypropylene composites. Polym-Plast Technol. 1999;38(5):997-1011.

[22] Brahmakumar M, Pavithran C, Pillai RM. Coconut fibre reinforced polyethylene composites: effect of natural waxy surface layer of the fibre on fibre/matrix interfacial bonding and strength of composites. Compos Sci Technol. 2005;65(3-4):563-569.

[23] Wambua P, Ivens J, Verpoest I. Natural fibres: can they replace glass in fibre reinforced plastics? Compos Sci Technol. 2003;63(9):1259-1264.

[24] Sampathrajan A, Vijayaraghavan NC, Swaminathan KR. Mechanical and thermal-properties of particle boards made from farm residues. Bioresour Technol. 1992;40(3):249-251.

[25] Lamazere JHA. Building boards from coconut husks using ground coconut shell filter with cement, sand and water for thermal and acoustic insulation. FR2666327-A1, Lamazere J H A, 1992.

[26] Bismarck A, Mohanty AK, Aranberri-Askargorta I, Czapla S, Misra M, Hinrichsen G, et al. Surface characterization of natural fibers; surface properties and the water up-take behavior of modified sisal and coir fibers. Green Chem. 2001;3(2):100-107.

Hybrid cork-polymer composites containing sisal fibre: Morphology, effect of the fibre treatment on the mechanical properties and tensile failure prediction[7]

Abstract

In this study, we investigated the use of short sisal fibre with and without polyethylene-graft-maleic anhydride (PE-g-MA) as a strategy to reinforce cork-polymer composite (CPC) materials. The use of alkali treatment of sisal to improve fibre-matrix adhesion was evaluated. High density polyethylene (HDPE) was used as matrix and the composites were produced in a two-step process using twin-screw extruder followed by compression moulding. FTIR, TGA and XRD were used to confirm the sisal fibre modification. Additionally, morphology, density, diameter and tensile properties of the fibres were evaluated before processing. The hybrid composites containing cork powder (40wt%) and randomly distributed sisal fibres were evaluated in terms of morphology and mechanical properties. The use of a 10 wt.% sisal fibre in the presence of a 2 wt.% coupling agent based on maleic anhydride, has shown to improve the tensile and flexural properties of the composites. The higher mechanical properties were achieved by using alkali treated sisal fibres and PE-g-MA. In the presence of the coupling agent the composite morphology revealed good interfacial adhesion between the natural components and the polypropylene matrix, being in accordance with the mechanical results. Weibull cumulative distribution was successfully used to accurately predict the tensile strength failure of the hybrid CPC materials.

[7] This chapter is based on the following publication:

Fernandes EM, Mano JF and Reis RL, 2013, Hybrid cork-polymer composites containing sisal fibre: Morphology, effect of the fibre treatment on the mechanical properties and tensile failure prediction, Composite Structures, 105: 153-162.

8.1 Introduction

In the last years, natural fibres reinforced composites have received high attention due to their low density, excellent thermal properties, low cost, biodegradability, availability, non-toxicity and absorbing CO_2 during their growth [1-4]. Although, certain drawbacks, like incompatibility with the hydrophobic polymer matrix, the tendency to form aggregates during processing and the low resistance to moisture, reduce the potential of using natural fibres as reinforcement in polymers [2, 3, 5]. The incompatibility may cause problems in the composite processing and in the material´s properties. The highly polar character of natural fibres has inherently low compatibility with nonpolar polymer matrices, especially hydrocarbon matrices such as polypropylene (PP) and polyethylene (PE) [5]. As a result, the polymer matrix is unable to transfer the stress to the filler through the interface when submitted to mechanical load, being the reinforcement efficiency reduced. Moreover moisture makes the use of natural fibre reinforced composites less attractive. Applying pre-treatments to the natural fibres can clean and chemically modify their surface, reduce the moisture absorption and increase surface roughness. These methods are able to ameliorate the fibre-matrix adhesion with a positive effect on the mechanical properties [4, 6-9]. A classic method of cellulose fibre modification is mercerization, which is an alkali treatment where the natural and artificial impurities are removed, leading to fibrillation of the fibre bundle to smaller fibres [6, 10, 11], meaning lower fibre diameter and increasing the aspect ratio [10] . The proper conditions of mercerization ensure the improvement of the tensile properties [3, 11, 12]. Cork is the bark of the oak (*Quercus suber* L.) which is periodically harvested each 9 to 12 years [13]. This lignocellulosic material holds environmental benefits to be applied on a new generation of composite materials [14-16]. Just a few studies were performed to improve the cork-matrix performance of cork based composites using different strategies, including: (i) chemical modification of cork [15], (ii) the use of coupling agents [15, 17] to promote cork-matrix bonding and (iii) the use of different natural or synthetic fibres to reinforce cork-polymer matrices [18-20]. The incorporation of different types of fibres into a single matrix has led to the development of hybrid composites. Hybrid composite materials that contain two or more types of fibre combine the advantages of one type of fibres with the lacking of properties in the other. As a consequence, a balance in cost and performance could be achieved through proper material design [21]. The properties of a hybrid composite depend on parameters such as fibre content, length and orientation of the fibres, fibre to matrix bonding and arrangement of the different fibres. The strength of the hybrid composite is also dependent on the

failure strain of individual fibres. Maximum mechanical performance results are obtained when the fibres are highly strain compatible [22]. Sisal fibre is a cellulosic fibre obtained from leaves of an annually harvasted plant, called *Agave sisalina* and is one of the strongest of all plant fibres [8, 23].
The aim of this work was to develop strategies to reinforce cork based composites with natural fibres, with and without chemical treatment, in the presence of low amounts of the coupling agent to ameliorate the mechanical properties. The production of hybrid composites was tested to obtain a composite with enhanced performance that could be used in complex geometries without failure, where cork cannot compete alone. Additionally one and two step extrusion processes were tested to evaluate the correct form to obtain the hybrid cork-polymer pellets reinforced with sisal fibres, to be applied in the compression moulding process in order to produce specimens of reinforced cork composites. The properties of the composites depend on the individual components and fibre-matrix interfacial compatibility. The Weibull distribution provides a reliable possibility to predict the tensile strength of a needed composite material, and this should be taken into account by the designer [24, 25]. Therefore, in this work we also consider the Weibull distribution to be a viable tool to predict the tensile strength failure of the novel hybrid composites under analysis.

8.2 Experimental section

8.2.1 Materials

Cork powder, with an average particle size < 500 μm a specific weight of 157 ± 2 kg m^{-3} and a humidity of ~5.4% was supplied by Amorim Revestimentos S.A. (S. Paio Oleiros, Portugal). The sisal fibre from Madagascar, presents a diameter of 183 ± 35 μm and moisture of ~11.3 %. The chemical composition of the used biofibres is present in Table 8.1 [7, 13, 26, 27].

Table 8.1. Chemical constituents of selected composite reinforcements (wt.%)

Chemical Composition	Cellulose	Hemicellulose	lignin	Suberin	Extractives	Ash	Literature Reference
Cork	12-13	12	21	42-45	13-19	1.2	[13, 27]
Sisal	67-74	10-14	8-11	–	2-6	1.0	[7, 26]

The matrix was a high density polyethylene, HDPE (HMA – 025) from ExxonMobil (Germany), with a MFI of 8.2 g.10min^{-1} (190 °C, 2.16 kg), and a melting point of 136.6 °C. The coupling agent, a HDPE grafted with maleic anhydride (PE-g-MA), containing 0.5 to1.0 wt% of maleic anhydride (Exxelor PE 1040) with MFI of 1.4 g.10min^{-1} (190 °C, 2.16 kg), and a melting point of 131.3 °C, produced by ExxonMobil (Germany). The polymer and the coupling agent were supplied by Pallmann Maschinenfabrik GmbH & Co. (Germany) after use a pulverizing system for plastics with particle size of 250 μm to 1.2mm.

8.2.2 Sisal fibre surface modification - Alkali treatment

The preparation of alkali treated sisal (Sisal_NaOH) was as follows [28]: the sisal fibres were immersed in sodium hydroxide (NaOH) solution (5% w/v) for 2 h at room temperature. After that the fibres were washed with distilled water containing a few drops of acetic acid. Final washings were carried out with distilled water until neutrality (pH = 7), to remove the excess of NaOH present on the fibres, until this water no longer indicated any alkalinity reaction. Then, the fibres were air-dried at room temperature, followed by drying in a vacuum oven at 70 °C and after stabilise was stored in polyethylene bags.

8.2.3 Composite production

Before compounding all raw materials were pre-dried at 80°C during 16h to stabilise the cork and the sisal fibres in terms of moisture content. After that the sisal fibres were cut in dimensions < 20 mm. The prepared compositions and processing conditions are summarized in Table 8.2. The compounding was performed in a counter-rotating twin-screw extrusion machine (Carvex, Portugal) which had a screw diameter of 52 mm and an L/D ratio of 18. The barrel temperature was in the range 130-160 °C, and the screw speed was fixed at 30 rpm. The cork powder and the grinding HDPE were pre-mixed and manually in small portions and feed in the hopper system with the sisal fibres. No extrusion head was used in order to minimize the residence time and shear heat dissipation. The extruded material was cooled in air, granulated in a cutting mill to produce hybrid composite pellets with dimensions $\leq$ 6 mm. In a further step, compression moulding of the obtained pellets using a hydraulic press (Moore, UK) was applied to produce boards with 3mm and 6mm of thickness for tensile and flexural tests respectively.

Table 8.2. Designation and processing conditions of the hybrid composite formulations based on polyethylene-cork (60-40) wt.%.

Code	HDPE (wt %)	Cork (wt %)	Sisal Fibre (wt %)	Coupling Agent (wt %)	Extrusion Conditions	
					Temperature Profile (°C)	Motor (rpm)
CPC $_1$	60.0	40.0	–	–	130; 145; 150	30
CPC $_2$	58.8	39.2	–	2	130; 145; 150	30
CPC $_3$	54.0	36.0	10	–	135; 150; 155	30
* CPC $_4$	54.0	36.0	10	–	135; 150; 155	30
CPC $_5$	52.8	35.2	10	2	135; 150; 155	30
CPC $_6$	52.8	35.2	10 **	2	135; 150; 155	30

* Pellets from CPC1 with 10 wt.% of sisal fibre (two extrusion steps); ** Sisal fibre modified with NaOH.

The mould conditions included temperature of 150 °C during 8 minutes and a pressure of 1.42 MPa was applied during the last 2 minutes. In the case of boards with thickness of 6mm the temperature was increased to 160 °C. The cooling with water occurs in the mould under pressure [19]. Tensile and flexural specimens were obtained from these boards (see Figure 8.1), using a computer numerical control CNC machine (Roland 3D Plotter MDX-20, UK).

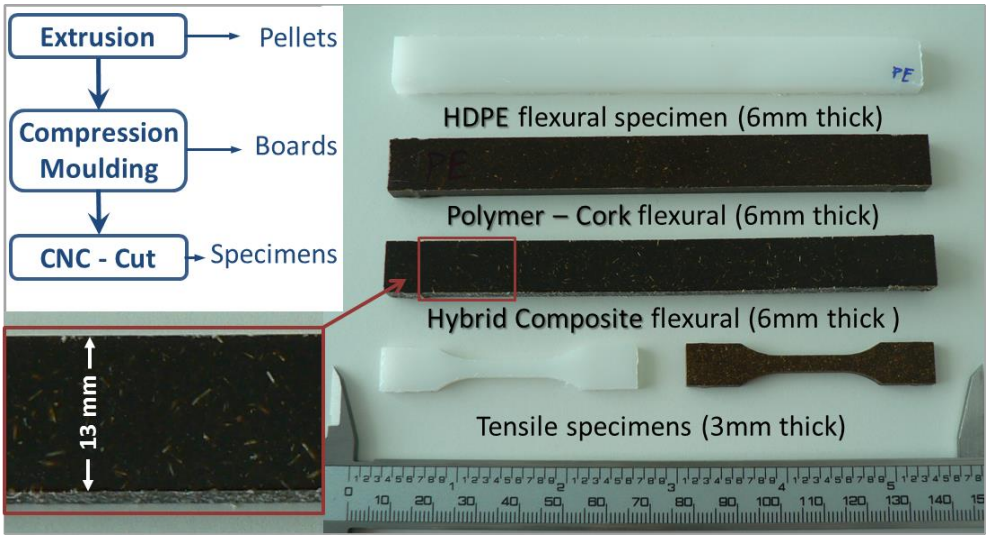

Figure 8.1. Scheme of the process to obtain the composites and geometry of the specimens used in the tensile and flexural tests.

8.2.4 Fibre characterization

8.2.4.1 Chemical characterization

To confirm the chemical treatment, the fibres were analysed using Fourier transform infrared (FTIR) spectroscopy. All the spectra were acquired using a Shimadzu IR-Prestige 21. The attenuated total reflectance (ATR) methodology (PIKE Technologies) was used and the spectra were acquired between 4400cm^{-1} to 800cm^{-1} using a resolution of 4cm^{-1}.

8.2.4.2 Crystallinity

To detect the crystalline structure of cellulose in sisal, Wide-angle X-ray diffraction (WAXRD) diffractograms were recorded using the Bruker-AXS D8 Discover diffractometer in θ–2θ geometry using Cu Kα1,2 lines collimated with a Gobël mirror, a divergent slit of 0.6 mm, a detector slit of 1 mm and 0.6 mm and a Ni filter. The data was collected from 6-50° with a step size of 0.04° and an acquisition time of 1° sec per step. The percentage of crystallinity (%Cr), performed using a fitting program, was calculated based on:

$$\%Cr = (A_{cryst} / A_{total}) \times 100 \qquad (8.1)$$

where A_{cryst} is the area below the diffraction peak of the (002) plane, peak at 2θ = 22.5°, and from the (101) and ($10\bar{1}$) plane, peak at (13-18°), and A_{total} is the area below the whole region in the XRD spectra representing the amorphous material in the cellulosic fibres.

8.2.4.3 Fibre diameter and density

The diameter measurements of sisal fibres with and without chemical treatment were made in five spaced locations along the gauge length of each specimen using an optical microscope Olympus BH-2 (Tokyo, Japan) equipped with an Olympus DP11, (Japan) digital camera. A histogram for each type of sisal fibre was performed and a normal distribution to characterize and compare the properties of the fibre with and without chemical treatment. The density of the sisal fibres was determined according to the standard ASTM D 792, using an analytical balance equipped with a stationary support for the immersion vessel. Five fibres were weighted per condition.

8.2.4.4 Thermal degradation

Thermogravimetric analyses (TGA) were performed to understand the degradation characteristics of the sisal fibres and confirm the chemical modification. The thermal stability was determined using a TGA Q500 series thermogravimetric analyser (TA Instruments, USA). Experiments were performed in platinum pans, at a heating rate of 10 °C.min^{-1} from 50 °C to 600 °C under nitrogen atmosphere. All tests were repeated once.

8.2.4.5 Mechanical properties of sisal fibres

Single fibre tensile tests were measured with a Instron 4505 Universal Machine, (USA) using a 1 kN load cell, a crosshead speed of 1 mm.min^{-1}, and a fibre gauge length of 30 mm. Prior to testing, fibres were mounted on sturdy paper frames using a high-strength hot melt glue and placed in a desiccators for a minimum period of 48 h. The tensile properties of the single sisal fibres were determined according to the standard ASTM C 1557.

8.2.5 Morphology of the fibres and the composites

The morphological characterization of the natural fibres and the developed reinforced cork polymer composites fracture surface were examined using a NanoSEM 200 FEI (The Netherlands) scanning electron microscope (SEM). Before being analysed all the samples were coated by ion sputtering with an Au/Pd alloy (80-20 wt. %) in a high resolution sputter coater of Cressington 208HR (Watford, UK).

8.2.6 Mechanical properties of composites

8.2.6.1 Tensile tests

The tensile properties of the developed cork based composites reinforced with sisal fibres were determined in the same machine according the standard ISO 527–2. The tensile bars had a neck cross-section area of 3 × 4 mm^2 and a neck length of 20 mm. The tensile force was taken as the maximum force in the force deformation curve. Tensile modulus was estimated from the initial slope of the stress–strain curve (between 0.05 and 1% strain) using the linear regression method. Samples were conditioned at room temperature for at least 48 h before testing. A crosshead speed of 5 mm.min^{-1} was

used up to a strain at break. The average and standard deviations were determined using eight specimens per condition.

8.2.6.2 Flexural tests

Three point static flexural tests were carried out in accordance with standard ISO 178. The dimensions of the specimens used were 132 mm length, 13 mm width and 6 mm depth. The load was placed midway between the supports with a span (L) of 80 mm. The crosshead speed was 2.56 mm/min. The tested specimens were performed in an Instron 4505 Universal Machine (USA) equipped with a 1 kN cell load. For each condition, the specimens were loaded until the core break. The average and standard deviations were determined using 7 specimens.

8.2.7 Statistical analysis

The values obtained by tensile and flexural tests were analysed by the normality of the distribution of the mechanical results was evaluated using Shapiro-WilK test to evaluate their normal distribution at $p<0.05$. The means were compared using a Two-Sample t-Test or the non-parametric Kolmogorov-Smirnov (K-S) test and differences were considered significantly different at $p<0.05$ (*). Additionally and in order to predict the failure probability of the developed hybrid cork composites the values obtained from the tensile tests were statistically analysed by using the two-parameter Weibull model, where the cumulative distribution function is given by [29]:

$$F(x) = 1 - \exp^{-\left[\frac{x}{\alpha}\right]^{\beta}} \quad \text{, for } x > 0 \qquad (8.2)$$

where F(x) is the probability of failure of a composite material subjected to a stress level x. In equation (2), α and β are two constants to be determined, known as the "scale parameter" or "characteristic strength" and the "shaper parameter", respectively. Finally the Kolmogorov-Smirnov test was employed to evaluate the goodness-of-fit to the data points.

8.3 Results and Discussion

8.3.1 Sisal fibre properties

8.3.1.1 Chemical characterization

Natural fibres are chemically treated to remove lignin, pectin and waxy substances covering the external surface of the fibre cell wall [30]. The chemical composition change at the sisal fibre surface structure by the chemical treatment was characterized using ATR-FTIR spectroscopy. Figure 8.2 shows the spectra region between 800 and 2000 cm^{-1} relative to unmodified fibre (Sisal), alkali treatment (Sisal_NaOH) which revealed that some changes did occur. In agreement with other previous works, the significant weight loss of sisal fibre after alkali treatment (see Table 8.3) can be attributed to the partial dissolution of hemicellulose [31], lignin and pectin [11]. The FTIR spectra confirm the disappearance of the carbonyl band (between 1660 and 1760 cm^{-1}), when the fibre was treated with NaOH.

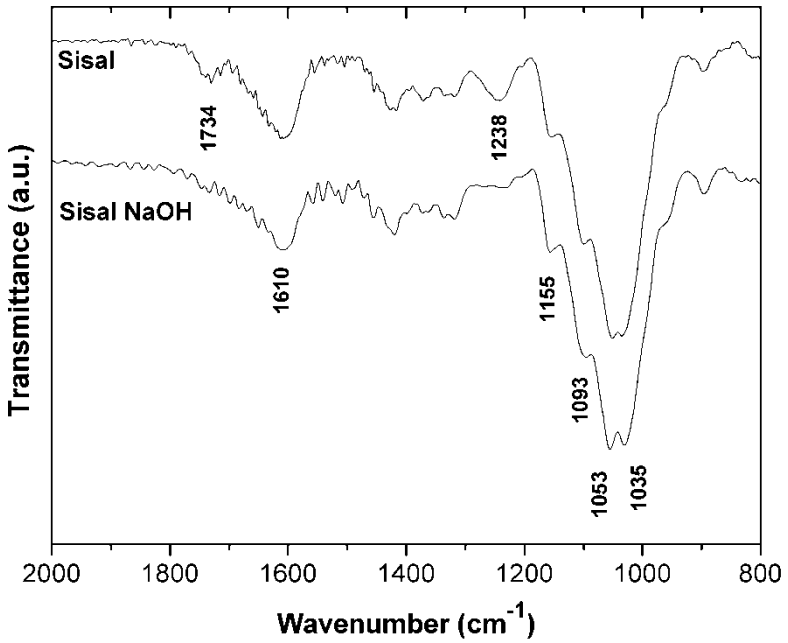

Figure 8.2. ATR-FTIR spectra of unmodified sisal fibre and sisal with alkali treatment (Sisal NaOH).

Table 8.3. Physical and crystallinity properties of the sisal fibres.

Fibre	Degree of crystallinity of cellulose (%)	Weight loss after treatment (%)	Density (kg/m³)		Diameter* (μm)	
					μ	σ
Sisal	24.1	—	770.0 62.2	±	175.9 ± 29.3	
Sisal_NaOH	29.6	14.2	840.9 96.8	±	141.5 ± 28.1	

* Values obtained using the Gauss fit curve with n = 150 measurements for each condition.

It was also reported before that alkali treatment reduces hydrogen bonding due to removal of the hydroxyl groups by reacting with sodium hydroxide [30]. The slightly diminished intensity of around 1610 cm^{-1} for the treated fibres could be attributed to the removal of some aromatic lignin-like impurities [31].

8.3.1.2 Crystallinity

The result of X-ray diffraction present in Figure 8.3 reflects the influence of the surface treatment on the sisal fibres between the amorphous and crystalline regions.

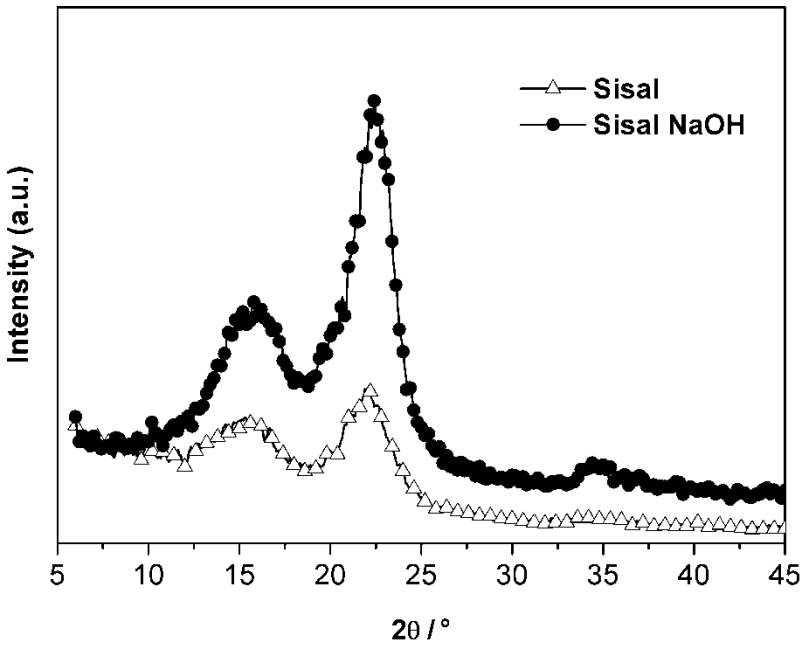

Figure 8.3. X-ray diffraction spectra of sisal untreated and alkali treated sisal fibres.

The spectra were almost similar; however, alkali-treated fibre peaks were more intense than untreated sisal peaks, which mean that the chemical treatment was able to remove part of the amorphous material covering the fibre, thus exposing the cellulose. Table 8.3 shows that a small increase on the cellulose crystallinity (% Cr) occurred when the sisal fibre was submitted to chemical treatment. The untreated sisal fibre has a %Cr of 24.1% that increases to 29.6% after chemical modification with NaOH. When the sisal fibre receives the alkali solution chemical treatment, the crystalline fraction of cellulose increased due to the partial elimination of lignin during alkaline treatment, losing part of its amorphous component [11]. This result is in accordance with the FTIR analysis. In the literature it is also indicated that thermal treatments on sisal fibres does not change significantly the chemical composition for temperatures below 200 °C and increases the degree of crystallinity [32], therefore it is also expected the occurrence of this phenomenon during the melt based processes of extrusion and compression moulding involving the use of sisal fibres.

8.3.1.3 Diameter, density and morphology

The fibre diameter variation and its morphology of both sisal fibres are present in Figure 8.4 and in Table 8.3. The Figure 8.4 refers to the diameter variation of the fibres in terms of mean and standard deviation, where the average fibre diameter decreases slightly with the surface treatment. Taking in consideration the Gaussian fit curve obtained from the histograms performed for the sisal fibres and presented in Figure 8.4a), the unmodified sisal fibre presents a diameter of [117.3 - 234.5] μm for a confidence interval of 95%. The diameter of the Sisal_NaOH fibre presented in Figure 8.4c) was smaller than the unmodified sisal ranging from [85.3 – 197.7] μm due to the alkali chemical treatment. The small increase on density was observed probably due to increase of the crystallinity after chemical treatment. In terms of morphology, the sisal fibre (Figure 8.4 b) consists of aligned fibrils with materials cementing the fibres together. After the chemical treatment a small reduction on the cell wall and fibre diameter (see Figure 8.4 d) was noticed. The alkali treatment leads to fibrillation of the fibre bundle into smaller fibres, reducing the diameter and increases the roughness [10]. After chemical treatment of the fibres, seems to be cleaner when compared with the unmodified sisal fibres.

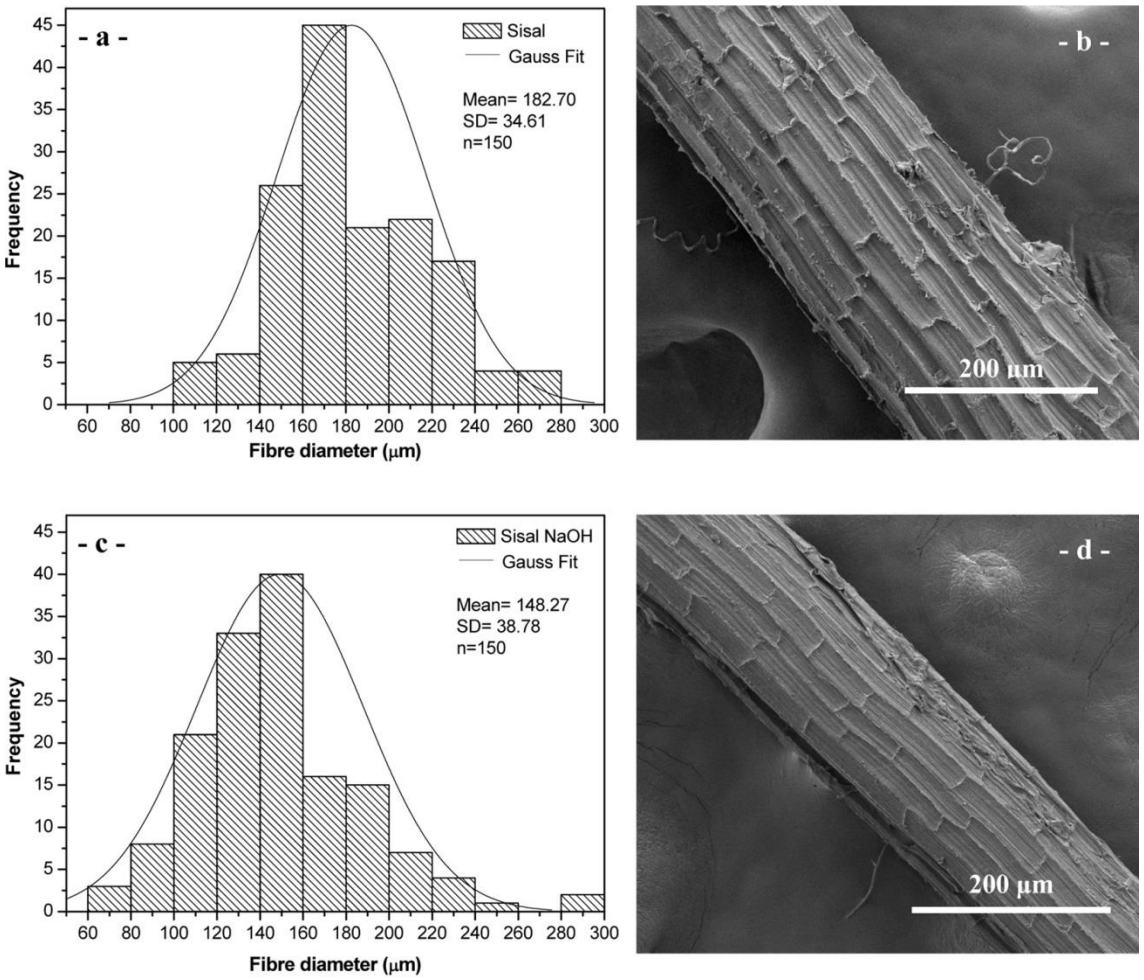

Figure 8.4. Histogram of the sisal single fibres diameter with the gaussian fit and its morphology (SEM micrographs) for: (a, b) sisal fibre; (c, d) sisal fibre with alkali treatment.

8.3.1.4 Thermal degradation

The TGA and DTG (first derivative of the TGA) curves of sisal fibres with and without chemical modification under nitrogen atmosphere are presented in Figure 8.5 a) and b) respectively. The TGA of the sisal fibre shows a two-step degradation process with a initial transition around 100°C is due to moisture evaporation. Cellulose is the main constituent of the cell wall of several lignocellulosic fibres such as wood and sisal. It is established in wood that the cellulose contains numerous hydroxyl groups that are strongly hydrophilic [33].

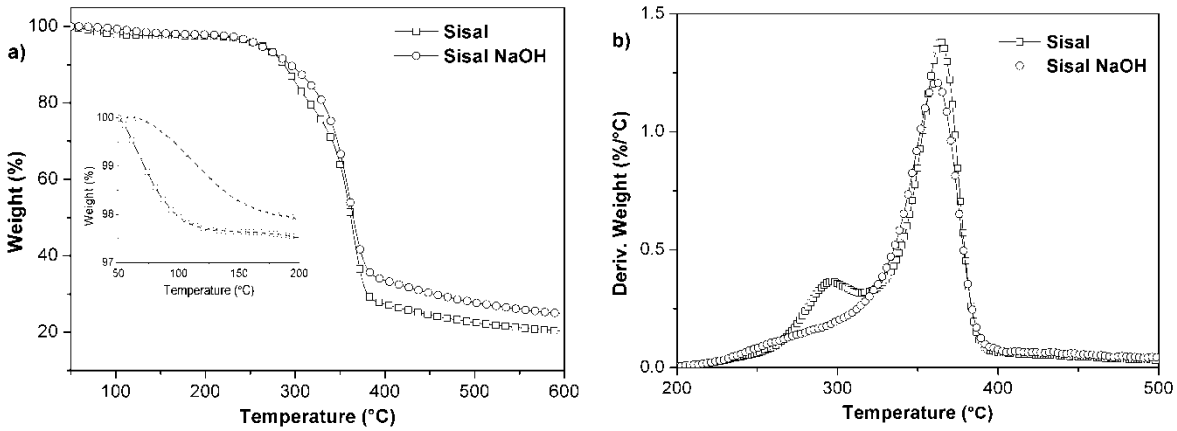

Figure 8.5. TGA curves of untreated and treated sisal fibres (a) and respective derivative curves (b).

In the inset graph of Figure 8.5 a) evidences the lower moisture content in the fibres after alkali treatment that induces the hydrophobicity of the fibre. The onset degradation temperature of the alkali treated fibre is very similar to the untreated sisal fibre. With the TGA was possible to confirm that the chemical modification does not induce a negative effect on the thermal resistance of the fibres. Figure 8.5 b) presents the derivative curve and was noticed in the fibre with alkali treatment the disappearing of the shoulder around 296 – 298 °C that is attributed to the removal the hemicellulose [34], while lignin decomposition extended to the whole range from 200 °C until 700 °C, due to different activities of the chemical bonds present on its structure [11, 35]. The more intense degradation peak around 351°C to 364 °C presented in both fibres could derive from the degradation of cellulosic components present on the sisal fibres. In terms of residual mass at 595 °C the sisal fibre presents 19.8% comparing with 24.2% for the alkali sisal treatment.

8.3.1.5 Mechanical properties of sisal fibres

The tensile properties of the single sisal fibre before and after chemical treatment are presented in Table 8.4. It is clear the higher tensile properties of the sisal fibre comparing to the thermoplastic polymers such polyethylene and polypropylene. Comparing the properties between the different fibres the mean values of maximum strength of the unmodified sisal is higher compared with the modified fibres. This may be related with the alkali chemical treatment that promoted the reduction of the fibre thickness and some removing of the hemicelluloses and lignin as discussed in the chemical characterization, promoting a more intense yellow colour to the sisal fibre.

Table 8.4. Mechanical properties of the single sisal fibres after uniaxial tensile tests.

Fibre	Tensile Modulus (GPa)	Tensile Maximum Strength (MPa)	Maximum Strain (%)
Sisal	12.93 ± 1.60	372.65 ± 125.86	3.05 ± 0.56
Sisal_NaOH	12.47 ± 1.42	298.35 ± 48.88	3.04 ± 0.50

The obtained high standard deviations values on the tensile test are in part related with the variation in the fibre diameter of the selected natural fibres.

8.3.2 Composite morphology

The properties of short fibre polymer composites are strongly dependent on the fibre volume fraction and on the orientation distribution. The fracture morphology of the cork based composites after tensile tests, obtained by scanning electron microscopy is presented in Figure 8.6. In the micrographs of Figure 8.6 a) and b) it is possible to observe the good adhesion between the cork and the polymeric matrix promoted by the use of the coupling agent. When the sisal fibres are added to the cork-polymer without the use of coupling agent (Figure 8.6 c and d), the fracture reveal voids from the pull-out of the sisal fibre indicating lower adhesion between the sisal fibres to the matrix. Additionally and at high magnification it was also observed the polymeric phase presents some stretching as compared with the previous composite CPC 2. Similar observation after mechanical tests was registered in a previous work using cork based composites obtained by pultrusion (pellets) follow by compression moulding [16]. Regarding the fibres with the alkali treatment we clearly observe at high magnification (Figure 8.6 f) particles of cork that are in contact along to the sisal fibre and there is a good linkage between the fibres and the matrix. The improvement of the adhesion was obtained by the combine effect of the low amount of coupling agent 2 wt% and the chemical modification of the sisal fibres.

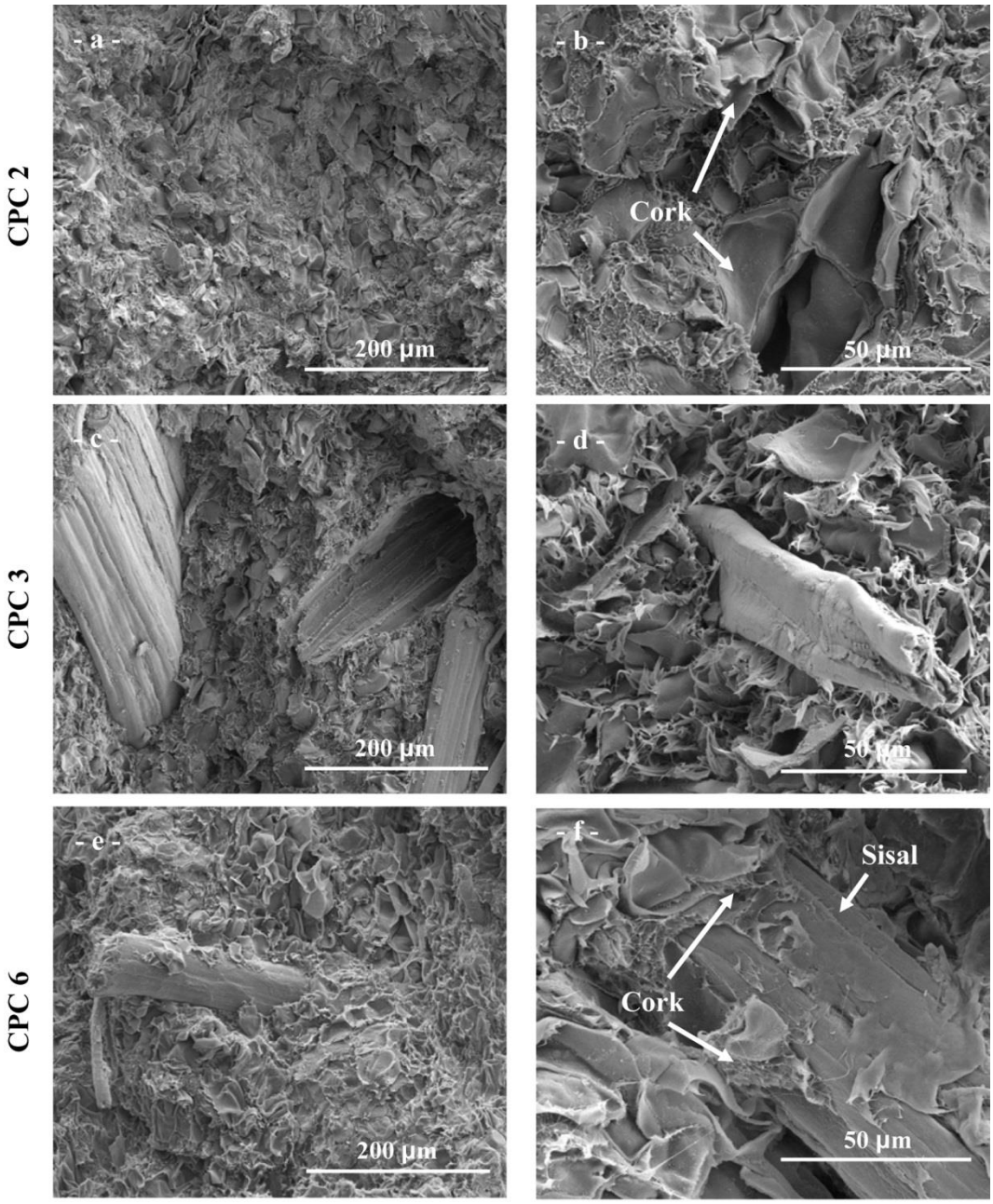

Figure 8.6. Fracture morphology at two different magnifications of the hybrid composite materials after tensile tests.

8.3.3 Mechanical properties of composites

8.3.3.1 Tensile tests

Tensile tests were performed in order to evaluate the mechanical performance of the novel hybrid cork composites. Figure 8.7 summarizes the obtained properties, in terms of tensile modulus and maximum strength for the composites with polyethylene matrix.

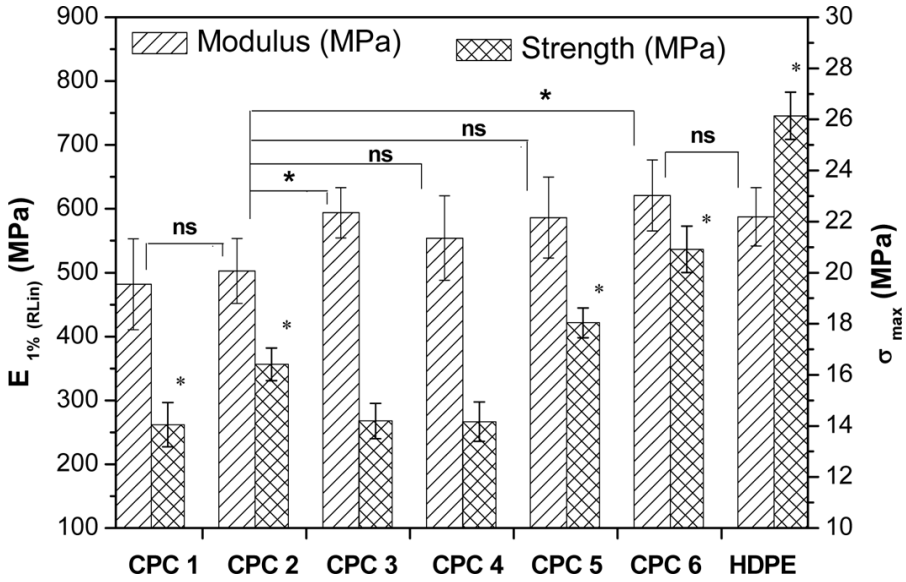

Figure 8.7. Mechanical properties of the reinforced cork-polymer composites with sisal fibres, when submitted to uniaxial tensile load. (*) Significant at 0.05; ns: non-significant at 0.05.

The statistical significance between samples with and without sisal fibre reinforcement was compared, being CPC 2 the cork-polymer composite reinforced with 2 wt.% of coupling agent. Considering the data of Figure 8.7, it is clear the effect of the coupling agent on the increase in terms of tensile strength (16.8%) for the composites CPC 1 and CPC 2 containing polymer and cork as main constituents. This result it is in agreement with a previous study [17] when it was used 50 wt.% of cork powder from different industrial processes by pultrusion and compression moulding on the development of composites. The addition of 10 wt.% of unmodified sisal fibre (CPC 3), leads to a significant reinforcement in terms of modulus of 23%. Additionally, the sisal fibres and the cork act as filler since it reduces the strength due to the increase of the natural component on the hybrid composite. CPC 4 presents the same composition as CPC 3 where the difference was the two extrusion step process to produce the composite pellets. The cork-polymer were first compounded into composite pellets and

then short sisal fibres were added in the cork-polymer composite pellets, to produce the hybrid reinforced composite. We observed that no improvements were noticed when we used a two-step extrusion process to produce the same hybrid composites. CPC 5 and CPC 6 are similar in terms of composition (see Table 8.2), where the important difference was the fibre treatment. Regarding the CPC 5 we can observe that the addition of 10 wt.% of sisal fibres in the presence of coupling agent 2 wt.% improved significantly both stiffness in 22% and the tensile strength in 28% of the hybrid composite. The improvement on the tensile properties was even higher by using the alkali treated sisal fibres, being 29 and 49% respectively due to the chemical surface modification and increase of surface roughness. Comparing with the polyethylene matrix, the developed hybrid cork based composites presents similar modulus values but a reduced strength performance. In the literature it is pointed that the use of coupling agents based on maleic anhydride (MA) increases the tensile strength of the composites due to the esterification reaction between sisal fibre hydroxyl groups and anhydride part which causes a reduction in interfacial tension and an increase in interfacial adhesion between thermoplastic and the fibre [36]. Similar hydroxyl groups are present in the chemical composition of cork and sisal fibres. The combined effect of the sisal fibre treatment with the presence of coupling agent based on MA for effective stress transfer across the interface enhances the adhesion between the interphases and consequently reinforces the tensile properties of the hybrid cork-polymer composites.

8.3.3.2 Flexural tests

Figure 8.8 displays representative stress-strain curves of the polyethylene matrix and the prepared cork composites with and without the reinforcement of sisal fibres after a three-point bending test. Figure 8.9 presents the corresponding flexural modulus and the maximum strength mean values with the respective standard deviation for comparison. Similar to the tensile behaviour results of the composites, the addition of 10 wt.% of sisal fibre without coupling agent (CPC 3) improves the stiffness; however it reduces significantly the flexural strength (see Figure 8.9) and reduces the strain at break as showing in Figure 8.8. The addition of coupling agent promotes mainly the flexural strength and the elongation at break (CPC 5). After chemical modification the resulting sisal fibres present a rough surface topography, with removal of surface impurities and removal of hydrophilic hydroxyl groups [30] improving the affinity with the thermoplastic matrix. The combined effect of the chemical modification of sisal and the use of 2 wt.% of coupling agent (CPC 6) result in hybrid composites with enhanced flexural performance. Comparing with the unreinforced composite CPC 1, it has higher stiffness 33%, higher flexural strength

98% and higher elongation at break due to the improvement on the interfacial adhesion between the matrix and the natural component.

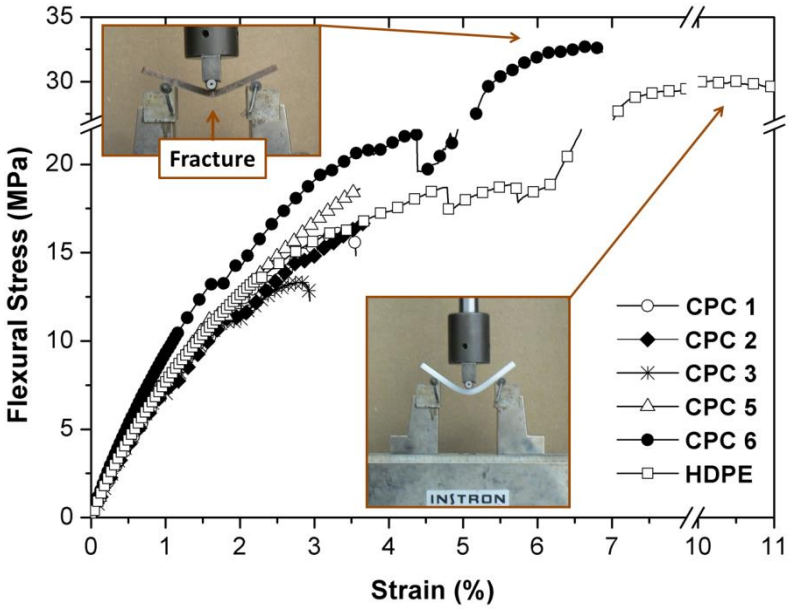

Figure 8.8. Representative flexural stress-strain curves of the developed cork-polymer composites (40-60 wt.%) reinforced, or not, with sisal fibres.

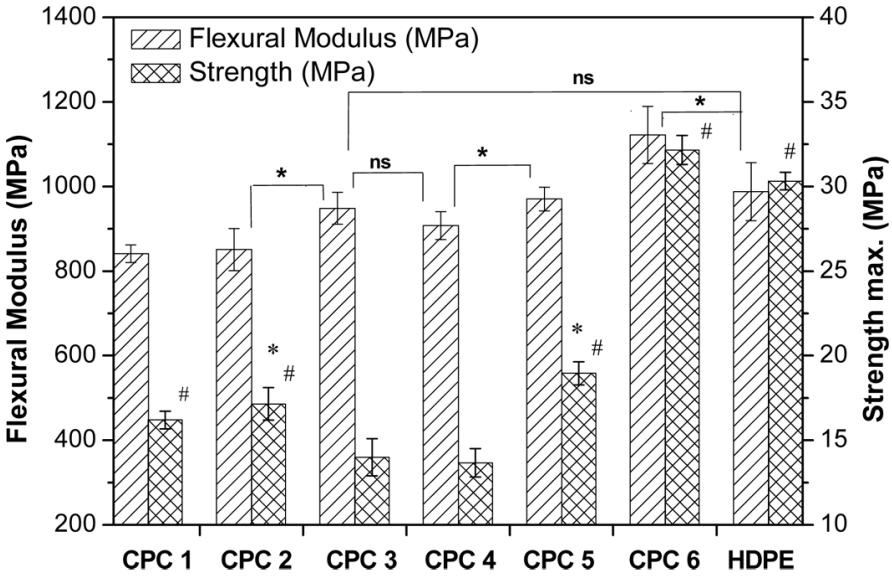

Figure 8.9. Flexural properties of the developed cork-polymer composites (40%-60%) reinforced, or not, with sisal fibres. (* and #) Significant at 0.05; ns: non-significant at 0.05.

Additionally, it was possible to reinforce the high density polyethylene matrix in terms of modulus (16%) and strength (11%) at flexural load mainly after the sisal fibres alkali treated. In the literature it was found that the sisal fibre after alkali modification improves the dispersion of the fibres but not their adhesion to the polymer matrix, due to a higher availability of OH groups in the particles surface [37]. Alkali treatment may leads to fibre fibrillation i.e. breaking down of fibre bundles into smaller fibres; which increases the surface area available for contact with the matrix [32]. The treatment is in accordance with the morphology results obtained, leading to a considerable enhancement on the mechanical properties. Higher improvements might be achieved by using higher amount of the natural fibre based in the presence of coupling agent. However, the high increase of the viscosity will make difficult the melt based processes of formulations riches in natural materials based on fibres and particles.

8.3.4 Weibull statistical analysis

Tensile strength life distribution diagrams have been obtained by using the cumulative Weibull distribution function (Eq. 2) for cork-polymer composite reinforced with sisal fibres. Figure 8.10 presents the reliability probability of survival (F) and can be found easily corresponding to any stress value from the diagram. The Weibull fit method was used to modelling the failure data of the hybrid composites when submitted to tensile load and compare the increase on the strength promoted by the sisal chemical modification. A very good agreement between the estimated strengths and experimental values is evident in Table 8.5, confirming the efficiency of the Weibull distribution in prediction the tensile strength failure properties of the developed hybrid composites. The tested composites present strength higher than 12.65 MPa see Figure 8.10. Comparing the estimated strength or probability of failure at 95% of confidence present in Table 8.5 for the cork-polymer composites (40-60) wt.%, the use of coupling agent improved in 20% the strength of the composite. The addition of the untreated sisal fibres with coupling agent (CPC 5) presents a higher improvement of 34% comparing with CPC 1 and an increase of 12% comparing with the CPC 2. The best results were obtained with sisal treated fibres, mostly using the sisal modified with NaOH that presents an increase of 55% and 30% comparing with the CPC 1 and CPC 2, respectively. Several methods, such as Chi-square, the Anderson–Darling test, allow to determine the goodness of fit of a probability distribution to a set of data [24, 38].

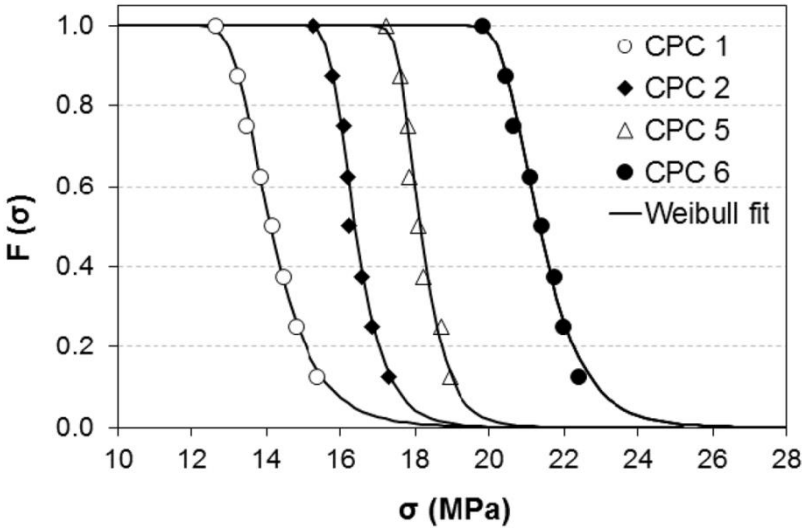

Figure 8.10. Tensile strength of the cork-polymer composites reinforced with sisal fibre. Lines show Weibull distribution with parameters values shown in Table 8.4.

In this study, the goodness-of-fit test was carried out by using the Kolmogorov-Smirnov (K-S) test that is used for statistical analysis of composites. The procedure was partially adapted from [39]:

(1) Since the K-S is a distance test, it was determined the maximum deviation $Dn = F_n - F_0$ and $D_n^- = F_0 - F_{n-1}$. Being F_n the cumulative observed values and F_0 the Weibull cumulative distribution function present in the equation 2.

(2) K-S tables of critical values (CV) are valid when the distribution parameters are known. Since the distribution parameters were estimated from the experimental data the CV will be $4 \times \alpha$ value [24], i.e. for a significance level of $\alpha = 0.05$ that means $\alpha' = 0.20$. For n=8 and a significance level of $\alpha = 0.05$, the $D_{nc} = 0.358$.

(3) If $D_n < D_{nc}$, the null hypothesis that the observed data follow the Weibull distribution is accepted.

The Weibull parameters and K-S goodness-of-fit test are listed in Table 8.5. The K-S statistic D_n values presented in Table 8.5 and obtained after the test are between 0.17 and 0.23, indicating that the tensile strength of the developed hybrid composites is strongly explained by the Weibull cumulative distribution because it departs significantly from the value of significance level $\alpha = 0.05$ and a sample size of n=8 for which the K-S of fit test was performed.

Table 8.5. Weibull distribution parameters, estimated tensile strength for the composites at 95% and 99% of confidence, obtained experimental results and K-S goodness-of-fit-test.

Composite	Distribution Parameters		Estimate Strength (MPa)		Experimental value (MPa)	K-S test	
	α	β	$p<0.05$	$p<0.001$	Max. Strength	Dn	Dnc
CPC $_1$	13.81	17.49	13.0	12.6	14.04 ± 0.87	0.17	0.358
CPC $_2$	16.19	29.60	15.6	15.4	16.41 ± 0.64	0.23	0.358
CPC $_5$	17.96	36.97	17.4	17.2	18.03 ± 0.58	0.23	0.358
CPC $_6$	21.05	26.76	20.2	19.8	20.92 ± 0.91	0.19	0.358

± Standard deviation values

8.4 Conclusions

Cork-polymer composites (CPC) reinforced with sisal discontinuous fibres has shown to be a viable strategy to obtaining structural materials with improved mechanical performances in terms of tensile and flexural properties. The improvement on the mechanical properties was effective when a 2 wt.% of coupling agent based on maleic anhydride (MA) was used, since the mechanical properties increased in terms of stiffness, strength and elongation at break. The improvement of the interfacial adhesion between the matrix, the cork and sisal fibres was also confirmed by the fracture morphology. In terms of processing to obtain the hybrid CPC pellets, there is no advantage in the use of two melt extrusion steps and add the sisal fibres only in the second step. This study demonstrates that the mechanical properties of CPC can be improved by: 1) the addition of a 2 wt.% of the coupling agent based on MA; 2) the sisal fibres addition (10 wt.%) without the use of a coupling agent, resulting in a hybrid CPC with similar modulus properties and with lower thermoplastic content and 3) by the combined effect of the addition of alkali treated sisal fibres with the use of the coupling agent resulting in composites with considerably higher mechanical properties. Under flexural load and using alkali treated sisal fibres with coupling agent in the new composites an increase of 33% in modulus and an increase of 98% in strength were obtained when compared with unreinforced cork composites. Comparing the improved mechanical properties of the hybrid CPC with the polyethylene matrix, it was possible to reinforce the matrix in terms of stiffness and strength at flexural load manly after the sisal fibres alkali treatment. In terms of tensile strength, they present similar stiffness and lower strength when compared to the

polyethylene matrix. The Weibull diagram was used to reliably identify the composites safety limits. The tensile strength of the hybrid reinforced CPC was found to be in agreement with the Weibull cumulative distribution, which can be used to accurately predict the mechanical performances in terms of strength of the developed hybrid cork composite materials.

8.5 References

[1] Kalia S, Kaith BS, Kaur I. Pretreatments of Natural Fibers and their Application as Reinforcing Material in Polymer Composites-A Review. Polym Eng Sci. 2009;49(7):1253-1272.

[2] Saheb DN, Jog JP. Natural fiber polymer composites: A review. Adv Polym Tech. 1999;18(4):351-363.

[3] Faruk O, Bledzki AK, Fink H-P, Sain M. Biocomposites reinforced with natural fibers: 2000–2010. Prog Polym Sci. 2012;37(11):1552-1596.

[4] Kabir MM, Wang H, Lau KT, Cardona F. Chemical treatments on plant-based natural fibre reinforced polymer composites: An overview. Composites Part B. 2012;43(7):2883-2892.

[5] Bledzki AK, Gassan J, Theis S. Wood-filled thermoplastic composites. Mech Compos Mater. 1998;34(6):563-568.

[6] George J, Sreekala MS, Thomas S. A review on interface modification and characterization of natural fiber reinforced plastic composites. Polym Eng Sci. 2001;41(9):1471-1485.

[7] Li X, Tabil LG, Panigrahi S. Chemical treatments of natural fiber for use in natural fiber-reinforced composites: A review. J Polym Environ. 2007;15(1):25-33.

[8] John MJ, Anandjiwala RD. Recent developments in chemical modification and characterization of natural fiber-reinforced composites. Polym Compos. 2008;29(2):187-207.

[9] Pandey JK, Ahn SH, Lee CS, Mohanty AK, Misra M. Recent Advances in the Application of Natural Fiber Based Composites. Macromol Mater Eng. 2010;295(11):975-989.

[10] Bogoeva-Gaceva G, Avella M, Malinconico M, Buzarovska A, Grozdanov A, Gentile G, et al. Natural fiber eco-composites. Polym Compos. 2007;28(1):98-107.

[11] Barreto ACH, Rosa DS, Fechine PBA, Mazzetto SE. Properties of sisal fibers treated by alkali solution and their application into cardanol-based biocomposites. Compos Part A-Appl S. 2011;42(5):492-500.

[12] Gassan J, Bledzki AK. Alkali treatment of jute fibers: Relationship between structure and mechanical properties. J Appl Polym Sci. 1999;71(4):623-629.

[13] Silva SP, Sabino MA, Fernandes EM, Correlo VM, Boesel LF, Reis RL. Cork: properties, capabilities and applications. Int Mater Rev. 2005;50(6):345-365.

[14] Gil L. Cork Composites: A Review. Mater Design. 2009;2:776-789.

[15] Abdallah FB, Cheikh RB, Baklouti M, Denchev Z, Cunha AM. Effect of surface treatment in cork reinforced composites. J Polym Res. 2009;17(4):519-528.

[16] Fernandes EM, Correlo VM, Chagas JAM, Mano JF, Reis RL. Properties of new cork-polymer composites: Advantages and drawbacks as compared with commercially available fibreboard materials. Compos Struct. 2011;93(12):3120-3129.

[17] Fernandes EM, Correlo VM, Chagas JAM, Mano JF, Reis RL. Cork based composites using polyolefin's as matrix: Morphology and mechanical performance. Compos Sci Technol. 2010;70(16):2310-2318.

[18] Brook G. Silicone-fiber-cork ablative insulation material. United Technologies Corporation, 2004.

[19] Fernandes EM, Silva VM, Chagas JAM, Reis RL. Fibre-reinforced cork-based composites. WO2011014085-A2, Amorim Revestimentos, S.A., 2011.

[20] Fernandes EM, Correlo VM, Mano JF, Reis RL. Novel cork–polymer composites reinforced with short natural coconut fibres: Effect of fibre loading and coupling agent addition. Compos Sci Technol. 2013;78(0):56-62.

[21] Thwe MM, Liao K. Durability of bamboo-glass fiber reinforced polymer matrix hybrid composites. Compos Sci Technol. 2003;63(3-4):375-387.

[22] Thomas S, Pothan L. Natural fibre reinforced polymer composites: from macro to nanoscale: Old City Publishing, Inc.; 2009.

[23] Li Y, Mai YW. Interfacial characteristics of sisal fiber and polymeric matrices. J Adhesion. 2006;82(5):527-554.

[24] Lawless JF. Statistical models and methods for lifetime data: John Wiley and Sons; 1982.

[25] Gañan P, Garbizu S, Llano-Ponte R, Mondragon I. Surface modification of sisal fibers: Effects on the mechanical and thermal properties of their epoxy composites. Polym Compos. 2005;26(2):121-127.

[26] Bledzki AK, Reihmane S, Gassan J. Properties and modification methods for vegetable fibers for natural fiber composites. J Appl Polym Sci. 1996;59(8):1329-1336.

[27] Gil L. Cortiça: produção, tecnologia e aplicação. Lisbon1998.

[28] Huda MS, Drzal LT, Mohanty AK, Misra M. Effect of fiber surface-treatments on the properties of laminated biocomposites from poly(lactic acid) (PLA) and kenaf fibers. Compos Sci Technol. 2008;68(2):424-432.

[29] Caprino G, Giorleo G, Nele L, Squillace A. Pin-bearing strength of glass mat reinforced plastics. Compos Part A-Appl S. 2002;33(6):779-785.

[30] Mwaikambo LY, Ansell MP. Chemical modification of hemp, sisal, jute, and kapok fibers by alkalization. J Appl Polym Sci 2002;84(12):2222–2234.

[31] Rong MZ, Zhang MQ, Liu Y, Yang GC, Zeng HM. The effect of fiber treatment on the mechanical properties of unidirectional sisal-reinforced epoxy composites. Compos Sci Technol. 2001;61(10):1437-1447.

[32] Li Y, Mai YW, Ye L. Sisal fibre and its composites: a review of recent developments. Compos Sci Technol. 2000;60(11):2037-2055.

[33] Ichazo MN, Albano C, Gonzalez J. Behavior of polyolefin blends with acetylated sisal fibers. Polym Int. 2000;49(11):1409-1416.

[34] Martins MA, Joekes I. Tire rubber–sisal composites: Effect of mercerization and acetylation on reinforcement. J Appl Polym Sci. 2003;89(9):2507-2515.

[35] Yang H, Yan R, Chen H, Lee DH, Zheng C. Characteristics of hemicellulose, cellulose and lignin pyrolysis. Fuel. 2007;86(12-13):1781-1788.

[36] Joseph PV, Joseph K, Thomas S. Short sisal fiber reinforced polypropylene composites: the role of interface modification on ultimate properties. Compos Interface 2002;9(2):171-205.

[37] Ichazo MN, Albano C, González J, Perera R, Candal MV. Polypropylene/wood flour composites: treatments and properties. Compos Struct. 2001;54(2-3):207-214.

[38] Alqam M, Bennett RM, Zureick A-H. Three-parameter vs. two-parameter Weibull distribution for pultruded composite material properties. Compos Struct. 2002;58(4):497-503.

[39] Zhang Y, Wang X, Pan N, Postle R. Weibull analysis of the tensile behavior of fibers with geometrical irregularities. J Mater Sci. 2002;37(7):1401-1406.

Cork-polymer biocomposites: assessment of biodegradability, mechanical, morphological and thermal properties[8]

Abstract

This work addresses to the preparation of biocomposites combining different biodegradable aliphatic polyesters with cork 30 wt.%. The lignocellulosic biomass was compounded with poly(L-lactic acid), (PLLA); polyhydroxybutyrate-co-hydroxyvalerate, (PHBV); poly-ε-caprolactone (PCL) and starch-poly-ε-caprolactone (SPCL) using twin-screw extruder prior to injection moulding into tensile samples. The cork biocomposites were engineered to satisfy acceptable stiffness, strength, and in-service durability while maintaining the tendency for rapid out-of-service biodegradation. The physico-mechanical and morphological properties and thermal stability of the matrices and the bio-based cork composites were investigated. Moreover, the biodegradability of the materials under static water immersion and in soil burial tests was also monitored. This study shows that cork contributes to lightweight composite materials using PLLA and PHBV matrices and promotes an increase on the stiffness of PCL. Cork increases the thermal stability and the crystallinity degree of the biocomposites. The weight loss, thickness variation and the reduction in tensile properties of biodegradable composite in soil are significantly greater than those in water. The materials present low water absorption and the highest values corresponded to the biocomposites. The presence of cork contributes for the initial degradation; however at long time it slows the biodegradation rate due to cork microbial resistance. As expected, the use of starch biomass accelerates the biodegradation rate of the materials. Composites using biodegradable polymers with cork will contribute to increasing their market acceptance and for the development of novel sustainable products.

[8] This chapter is based on the following publication:

Fernandes EM, Correlo VM, Mano JF, Reis RL, 2013, Cork-polymer biocomposites: assessment of biodegradability, mechanical, morphological and thermal properties, *submitted*.

9.1 Introduction

Lignocellulosic biomass represents a renewable, biodegradable, lightweight, abundant and cheap source of raw, making them attractive for the development of sustainable products [1-5]. Cork is the outer bark of an oak tree known botanically as *Quercus suber* L; being the major chemical constituents suberin (33-50%); lignin (13-29%); polysaccharides, (6-25%); and extractives (8.5-24%) [6, 7]. Cork reveals an anisotropic closed cellular structure as shown in Figure 9.1. It is composed of an aggregate of cells, about 42 million per cubic centimeter [8]. Cork is a lightweight material, elastic and impermeable to liquids or gases, good thermal, acoustic and electrical insulator, sound and vibration insulator and exhibits a near-zero Poisson coefficient, which found applications from the stoppers to aeronautics [6, 9-11].

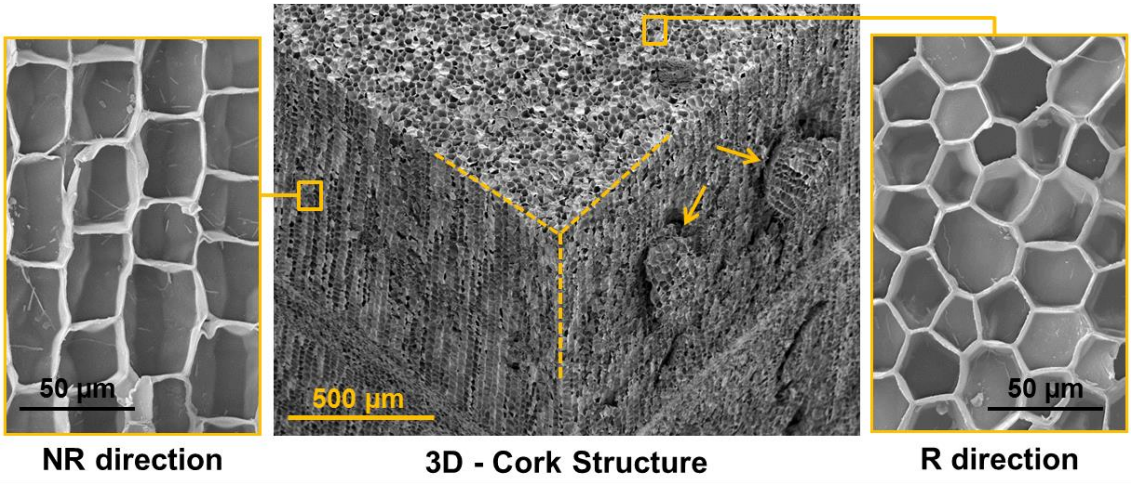

Figure 9.1. SEM micrographs of the 3D cork morphology showing in detail the non-radial direction (NR) and radial direction (R).

Furthermore, cork composites are one of the most promising fields of cork technology [9]. The combination of cork biomass with polymers trough melt based technologies brought added-value to cork based materials that can open a wide range of innovative applications. Studies can be found on the combination of cork and cork by-products with polyolefins such as polyethylene (PE) and polypropylene (PP) and the effect of coupling agent in the mechanical properties [12, 13], chemical surface modification to improve cork-polymer compatibility [14] and hybrid cork composite systems reinforced

with natural fibres [15-17]. Recently, the combination of the unique properties of cork with biodegradable matrices [18, 19] was also evolved to the production of more sustainable materials containing cork. A sustainable product is a product which will gives as little impact on the environment as possible during its life cycle [20]. One of the main drawbacks pointed to composites is the low sustainability due to the separation problems of the mixed materials [20]. One interesting approach is to consider the re-manufacturing of old products or the use of biodegradable polymers as matrices combined usually with biofibres as reinforcing element, to produce fully biodegradable materials, the so called biocomposites or green composites [1, 5, 21].

Biodegradable polymers and bio-based plastic products from renewal resources can form sustainable and eco-friendly products than can compete in the current market [4, 5, 22]. The worldwide capacity of bio-based plastics is expected to increase from 0.36 million metric ton (2007) to 2.33 million metric ton by 2013 and to 3.45 million metric ton in 2020 [2]. From the different biodegradable polymers it was defined 4 classes [23]: The agro-polymers (e.g. polysaccharides) obtained from biomass by fractionation such as starch and lignocellulosic products. The second and third are polyesters, obtained, respectively by fermentation from biomass or from genetically modified plants (e.g. polyhydroxyalkanoates (PHAs), including polyhydroxybutyrate (PHB)) and by synthesis from monomers obtained from biomass (e.g. polylactic acid (PLA)). The fourth family are polyesters, totally synthesized by the petrochemical process (e.g. polycaprolactone (PCL)) [1, 3, 23]. The interest of these polymers has grown, since they present similar mechanical and thermal properties as compared with synthetic thermoplastic such as polyethylene (PE) and polypropylene (PP) [24]. The PLA and PHB reveal higher mechanical properties, with a modulus around 2.8 to 3.4 GPa and 1.0 to 2.1 GPa respectively [2, 4, 25]. The aliphatic polyesters present proper mechanical and degradation properties that make them good candidates for several applications [21].

The aim of this study was to produce and characterize different renewable resource derived-biocomposites based on, poly(L-lactic acid), (PLLA); polyhydroxybutyrate-co-hydroxyvalerate, (PHBV); PCL and starch-poly-ε-caprolactone (SPCL) combined with granulated cork through twin-screw extrusion followed by injection moulding. We hypothesized that by combining proper melt based technologies this study can provide information for basic properties of several cork biocomposites, as well as their major characteristics and degradation behavior under static water and soil burial conditions.

9.2 Experimental section

9.2.1 Cork and polymer materials

Cork granules, with an average particle size 0.5-1mm and specific weight of 166 ± 21 kg m^{-3}, moisture of ~7.5 % was supplied by Amorim Revestimentos S.A. (S. Paio Oleiros, Portugal). The polymers used in the preparation of the cork based composites includes: i) PLLA used had L-lactide content of 99.6 % and a M_w of 69 000 $g.mol^{-1}$, and was obtained from Cargill Dow LLC, USA; ii) PHBV polymer with 12% HV content and molecular weight (M_w) of approximately 425 692 $g.mol^{-1}$ was provided by PHB Industrial, Serrana, Brazil; iii) PCL resin (commercially available as TONE® 787), with M_w of 125 000 $g.mol^{-1}$, was obtained from Union Carbide Chemicals and Plastics Division, New Jersey, USA and iv) A blend of corn starch with PCL 30/70 wt.% (SPCL) was supplied by Novamont, Italy. It contained about 63 wt.% of PCL, 27 wt.% of corn starch and 10 wt.% of natural plasticizers. The M_w of PCL present in this blend is about 118 000 $g.mol^{-1}$.

9.2.2 Twin-screw extrusion compounding

Prior to compounding all natural raw materials were pre-dried at 40 to 70 °C during 24 h to stabilise in terms of moisture content and the polymers were thereafter reduced to a grain size less than 0.5 mm in a Ultra centrifugal mill from Retsch. The prepared compositions and processing conditions are summarized in Table 9.1. The raw materials were pre-mixed and then were compounded in a Rondol SCF modular co-rotating twin-screw extruder (TSE) with the screws diameter of 16 mm, a length to diameter ratio (L/D) = 25 and a single strand die of 3 mm. The mixture was placed in the hopper and automatically feeded at a constant rate with a volumetric dosing unit from SHINI Plastics Technologies (Germany). The temperature profile along the barrel to the die and the rotation screws was set according to the information present in Table 9.1. Part of the extrudate was cooled in water bath and subsequently ground by a lab pelletizer SCHEER (Stuttgart) to produce composite pellets with length $\leq$ 5 mm suitable for injection moulding. Prior to this step, the produced pellets were dried in a vacuum oven at 50 °C until stabilize.

Table 9.1. Compositions and processing conditions of the polymer matrices and the respective bio-based cork-polymer composites.

	CPC Composition (wt.%)		Extrusion conditions	
Sample Code	Polymer	Cork	Temperature profile (°C)	Motor RPM
PLLA	100	0	110; 160; 175; 175; 170	50
PLLA/Cork	70	30		
PHBV	100	0	110; 150; 175; 175; 180	50
PHBV/Cork	70	30		
PCL	100	0	40; 60; 70; 75; 80	50
PCL/Cork	70	30		
SPCL	100	0	30; 60; 70; 75; 80	50
SPCL/Cork	70	30		

9.2.3 Injection moulding

The neat polymers and the biobased composite pellets were injection moulded in a Ferromatik-Milacron K85 (Germany) with 850 kN of clamping force. The injection-moulded specimens were tensile bars produced according ASTM 638, with 60 mm length, a constant rectangular cross-section of 2×4 mm^2, and a neck length of 20 mm. The samples were placed in polyethylene plastic bags and conditioned at ambient temperature.

9.2.4 Degradation testing

The degradation tests involved both water and soil degradation tests. The water degradation tests were performed to determine the dimensional stability of the injection moulded specimens and to access to some biodegradability and the soil degradation tests were performed to monitoring the evolution of biodegradability of the specimens under soil conditions.

9.2.4.1 Water degradation tests

The dimensional stability tests included measurements of water absorption *(WA)*, thickness swelling *(TS)*, weight loss *(WL)* and moisture content *(MC)*. The *WA*, *TS* and *MC* were measured according to the ASTM D 570. The specimens, previously obtained by injection moulding, were dried at 40 °C in a vacuum oven during 48 h, stabilized in desiccator and the *MC* of the specimens was calculated as follows:

$$MC\ (\%) = [(W_w - W_d) / W_w] \times 100 \qquad (1)$$

where W_w is the weight of the specimen before drying (g) and W_d is the weight of the sample after drying (g).

Figure 9.2 a) represents the scheme of the water degradation tests. Each individual specimen was placed in a falcon tube containing 14 ml of distilled water. The water absorption (WA) was calculated by weighting the samples before and after immersed in distilled water at room temperature (23 °C). The tests were conducted during 1440 h.

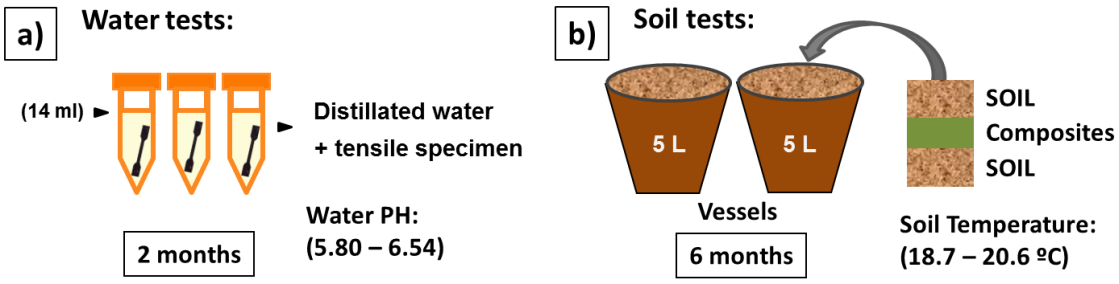

Figure 9.2. Schematic representation of the degradation tests under a) water and b) soil conditions.

The water absorption was calculated according to the Eq. (2):

$$WA\ (\%) = [(W_a - W_b) / W_b] \times 100 \qquad (2)$$

where W_a is the weight of the sample after immersion (g) and W_b is the weight of the same sample before immersion (g). The *TS* was determine by measured thickness of the sample before and after

immersed in distilled water at room temperature (23 °C) for different periods of time. The thickness swelling was calculated as follows:

$$TS\ (\%) = [(T_2 - T_1)/T_1] \times 100 \quad (3)$$

where T_2 is the thickness of the sample after immersion (g) and T_1 is the thickness of the same sample before immersion (g). The weight loss *(WL)* of the specimens was calculated as follows:

$$WL\ (\%) = [(W_i - W_d)/W_i] \times 100 \quad (4)$$

where W_i is the initial weight of the specimen (g) and W_d is the weight of the sample after drying (g). For that purpose, the specimens were weighed using an analytical balance after being placed in a vacuum oven at 40 °C for 48 h, cooled and stabilized in a desiccator several days followed by reweighing of the specimens. Averages of 5 specimens in each time point were used for *TS*, *WA, MC* and *WL* measurements.

9.2.4.2 Soil degradation tests

The injection moulded matrices and the biocomposite specimens were placed in vessels of 5 L used as soil containers and buried in soil. The physical and chemical composition of the compost is indicated in Table 9.2, indicating an organic matter higher than 70%.

The specimens were monitored and removed at predetermined intervals of time test up to 4320 days as depicted in the scheme of Figure 9.2 b). The average room temperature was 19 – 21 °C and relative humidity was kept at least 50 % by pulverizing the soil with distilled water and allowing continuous aeration. Once removed, samples were withdrawn carefully, placed in small nets to avoid disintegration of the specimen and washed with distilled water. After that, the samples where dried at 40 °C in a vacuum oven to constant weight and kept in a desiccator, and then measured in terms of thickness variation and weight loss before undergo to further characterization. It was used averages of 5 independent specimens in each time point per condition.

Table 9.2. Physical and chemical characteristics of the soil.

Property	Natural soil *
pH in $CaCl_2$	5.5 - 6.5
Moisture (%)	50 – 60
Conductivity (CE)	0.6 - 1.2
Nitrogen (N) (mg/l)	150 – 250
Phosphorus (P_2O_5) (mg/l)	150 – 250
Potassium (K_2O) (mg/l)	300 – 500
Organic matter (%)	>70

* Substrate from *SIRO-PLANT*

9.2.5 Composites density

The density of the bio-based injection moulded specimens was determined according to the standard ASTM D 792, using an analytical balance equipped with a stationary support for the immersion vessel using liquid propanol. Fives specimens were measured per condition.

9.2.6 Morphology

The morphological characterization of the developed bio-based composites surface before and after degradation tests were examined using a NanoSEM 200 FEI (The Netherlands) scanning electron microscope (SEM). Before being analysed all the samples were coated by ion sputtering with an Au/Pd alloy (80-20 wt. %) in a high resolution sputter coater of Cressington 208HR (Watford, UK).

9.2.7 Mechanical properties

Tensile properties of the injection moulded specimens before and after water and soil degradation tests were measured using an Instron 4505 Universal Machine, (USA) according to the standard ASTM D 638. The tests were conducted using a 1 kN load cell, with a gauge length of 20 mm and a crosshead speed of 5 $mm.min^{-1}$ until rupture. The tensile force was taken as the maximum stress in the stress-strain curve. Tensile modulus was estimated from the initial slope of the stress–strain curve (between

0.5 and 1% strain) using the linear regression method. Samples were conditioned at room temperature for at least 48 h before testing. The average and standard deviations were determined using 5 specimens per condition.

9.2.8 Thermal properties

Thermogravimetric analyses (TGA) were performed to understand the degradation characteristics of the developed composites and their matrices. The thermal stability was determined using a TGA Q500 series thermogravimetric analyser (TA Instruments, USA). Experiments were performed in platinum pans, at a heating rate of 10 °C.min^{-1} from 50 °C to 600 °C under nitrogen atmosphere. All tests were repeated once.

Differential scanning calorimetry (DSC) measurements of the moulded specimens was assessed by DSC in a Perkin-Elmer, Pyris Diamond system at 20 °C min^{-1} under nitrogen atmosphere. The DSC scans were performed in bulk specimens cut from the central part of the rectangular cross-section of the tensile specimens. The glass transition temperature (T_g), cold crystallization temperature (T_{cc}), melting temperature (T_m) and total enthalpy (ΔH) of all injection moulded materials were identified. The degree of crystallinity (χ_c) was calculated on the basis of a 100% crystalline a melting enthalpy of (ΔH^o_m) of the used polymer and according to the Eq. (5):

$$\chi_c(\%) = (\Delta H_{rec} + \Delta H_m) / \Delta H_m^0 (1 - w) \times 100 \qquad (5)$$

where ΔH_{cc} is the enthalpy of cold crystallization before melting; ΔH_m the enthalpy of melting and w is the weight fraction of the non-polymeric part in the composite. All the samples were repeated at least once.

9.3 Results and discussion

9.3.1 Degradation properties

The physical properties of the injection moulded specimens include the moisture content *(MC),* water absorption *(WA),* thickness swelling *(TS)* and weight loss *(WL)* after water degradation tests and the *WL*

and *TS* after soil degradation tests. Additionally, it was measure the density of the specimens to determine the effect of the presence of 30 wt.% of cork on the produced materials.

Figure 9.3 shows the schematic representation of the potential benefits of utilization renewable cork as forest biomass in bio-based products. In the scheme it is visualized the injection moulded specimens used in the tests.

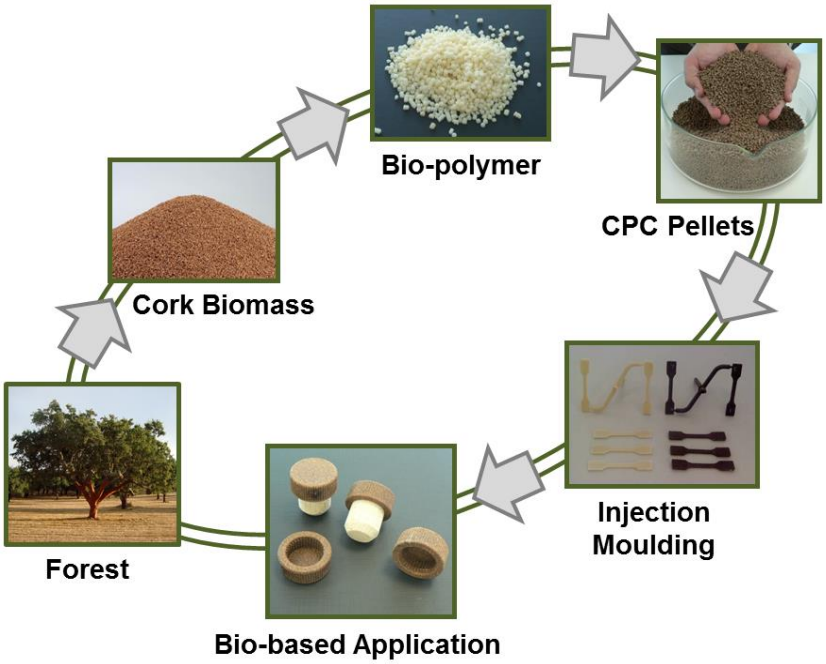

Figure 9.3. Schematic diagram of cycle from the cork bark to the biocomposite cap as prototype.

We also present a fully bio-based polyerter cap for wine sealing with 30 wt.% of granulated cork obtained by injection moulding as prof of concept and as one of the potential uses for the developed fully natural products.

9.3.1.1 Water degradation tests

The *MC* of injection moulded specimens is present in Figure 9.4. It was observed the presence of some moisture in the specimens preferably in the biocomposites with cork. In the case of the biocomposites containing PLLA, PHBV and PCL as matrices the *MC* varied between 0.37 ± 0.03 and 0.55 ± 0.12 %. The SPCL matrix presents the high *MC* since the biomass starch is sensitive to moisture. In this case,

the biocomposite containing SPCL as matrix showed a reduction in the *MC* of 0.25% where the hydrophobic character of cork promoted some stability to the material.

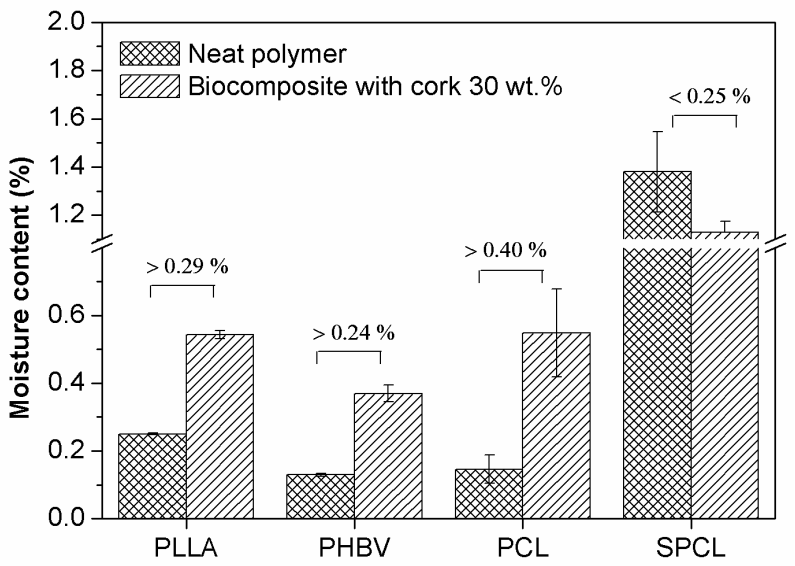

Figure 9.4. Moisture contentin the biodegradable polyesters and in the corresponding biocomposites after injection moulding.

The behaviour of the specimens after water immersion tests are presented in Figure 9.5, revealing the water absorption (*WA*), weight loss (*WL*) and the thickness swelling (*TS*) variation in function of immersion time. The *WA* of the specimens shown in Figure 9.5 a) and b) was more sharp for the biocomposites containing 30 wt.% of cork. Since cork is a cellular material with closed cell structure [6, 7], we suggest that the low water uptake up to 2 months is manly absorbed at the cork-polymer interface and in the available lenticular channels across the cells of cork. The lenticular channels constitute what is called the porosity of cork [7]. All the specimens tend to present higher values of water uptake in the first 15 days and after this period tend to reduce or approach to equilibrium. The lower sorption capacity of biocomposites seems to be related to the type of the biodegradable polyester used and with some possible cork-matrix interaction. Furthermore, the processing methodology may play an important role on the water absorption behaviour. In a recent study using PLA with 30 wt.% of cork powder compounding by melting mixing and followed by injection moulding, the materials exhibited *WA* values of 18% after 60 days [19]. In the present study, using a twin-screw extrusion followed by injection moulding, it *WA* was just 5.5 ± 0.1% . It is expected that the cork powder instead of the used granulated cork induced lower water resistance; however this difference of 3 times in the *WA*

should also be the result of the processing methodology, revealing the adequated mixing effect promoted by the twin-screw extrusion process.

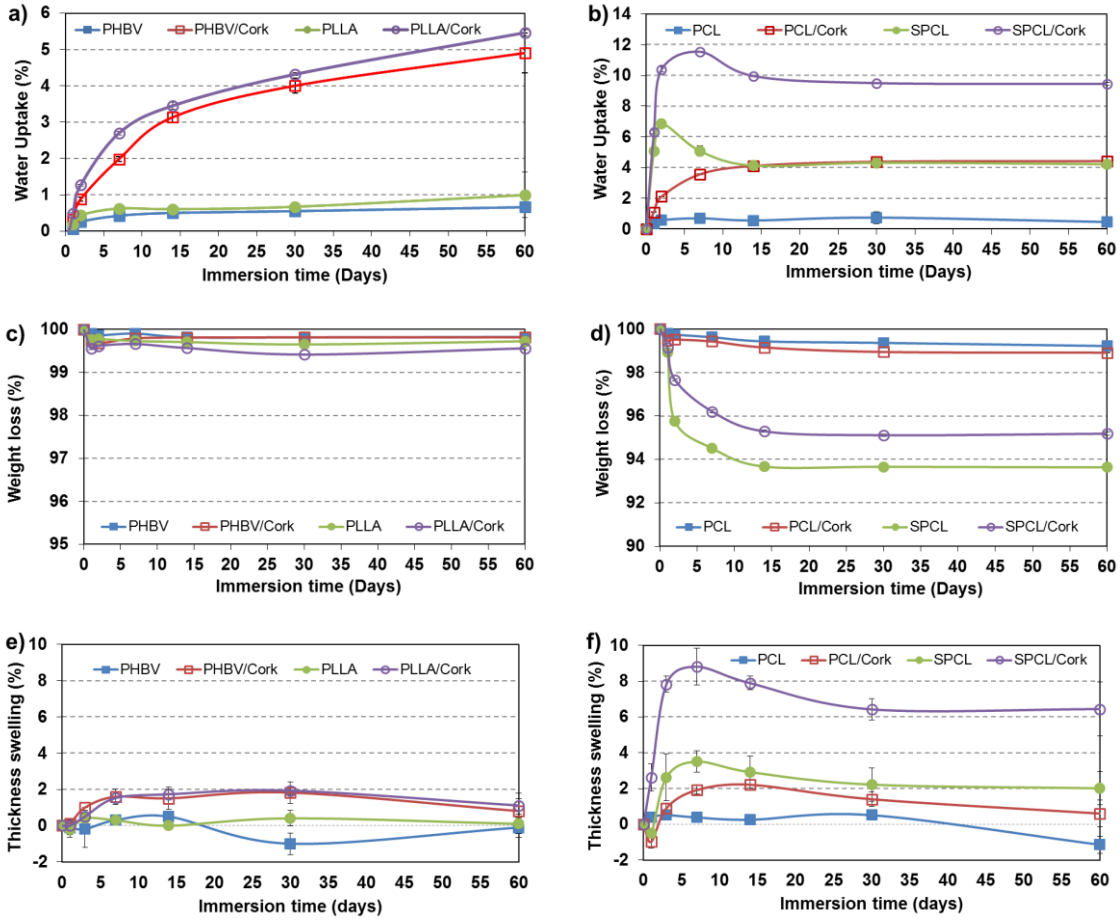

Figure 9.5. Physical behaviour of the bio-based materials under water immersion tests: (a, b) water uptake, (c, d) weight loss and (e, f) thickness swelling variation.

The SPCL blend contains around 30 wt.% of starch that is permeable to water, whereas the biocomposite PCL/Cork contains the same weight fraction in cork particles. Comparing in terms of water uptake in Figure 9.5 b), the absorption profile of the PCL/Cork biocomposite is more slowly in the first 7 days of immersion as compared with the SPCL. After a period of 2 weeks, they reach the maximum absorption with similar values and tend to stabilize. Furthermore, the weight loss graphic in Figure 9.5 d) displays that PCL/cork does not reveal a significant weight loss and follows the same trend as the PCL matrix, revealing a good physical interaction between cork and matrix. On the contrary, in the first 2 weeks of immersion, particles of starch are partially dissolved and released from the matrix surface due a lower interaction between starch and PCL and the weight loss occurs showing some

appetence to biodegradation in static conditions. In addition, the literature has evidenced that degradable synthetic polyesters, such as PCL are susceptible to hydrolytic degradation independently of the crystallinity fraction, because the ester groups are separated by CH_2 groups, which impart some flexibility to the chain [24]. This polymer is definitely biodegradable but only under outdoor conditions. For instance, in the human body, it is slowly hydrolytically degradable [26]. Concerning the thickness swelling variation *(TS)* reported in Figure 9.5 f) the presence of starch tends to increase considerably the *TS* since the starch swells when immersed in water expanding the biocomposite. After the first two weeks, the blend with starch showed lower *TS* due to the obtained *WL*. The starch is a water soluble material [4, 27] and its consumption or release from the biocomposite might contribute to the decrease and stabilization of *TS* after the 30 days of immersion. The PLA and PHBV and its biocomposites does not showed significant *WL* or *TS* variation after the 2 months of immersion.

9.3.1.2 Soil degradation tests

The soil burial test can be considered a realistic approach to the biodegradation process in a waste landfill. The biodegradability of the injection moulded specimens with 2 mm thick under indoor soil burial conditions was monitored during 6 months. The evolution of biodegradation at different periods of time is shown in Figure 9.6 and the result of injection moulded specimens under test in Figure 9.7. The biodegradation of a polymer is described as a process that comprises the deterioration of its physical and chemical properties and a reduction of its molecular mass due to its conversion into CO_2, H_2O, and CH_4 along with other low molecular weight products under the influence of microorganisms in both aerobic and anaerobic conditions [26]. The weight loss (*WL)* is one of is one of the most valuable data indicating the biodegradation of polymeric material after composting. Figure 9.6 a) and b) show that the *WL* of the specimens with PLLA and for the PLLA/Cork was negligible. Literature indicates that PLLA decomposes completely in proper compost environment to yield carbon dioxide and biomass [28]. In this work, the used soil and the temperature conditions may not be appropriated for the PLLA be decomposed by microorganisms such as fungi or bacteria. The soil temperatures were much lower (19–21 °C) than the minimum temperatures inducing biodegradation of PLA (30 °C, but better 40 °C and higher, i.e. 58 °C) simulating conditions at municipal and industrial composting facilities [29]. This explains why the rate of biodegradation of PLLA in burial soil conditions was rather low. After the period of 1 month the specimens containing PCL or SPCL as matrix starts to present a significant *WL,* around

11% up to 18.5%, being more intense for the blend containing starch. At this stage, the *WL* of the biocomposites was lower since cork was not degraded.

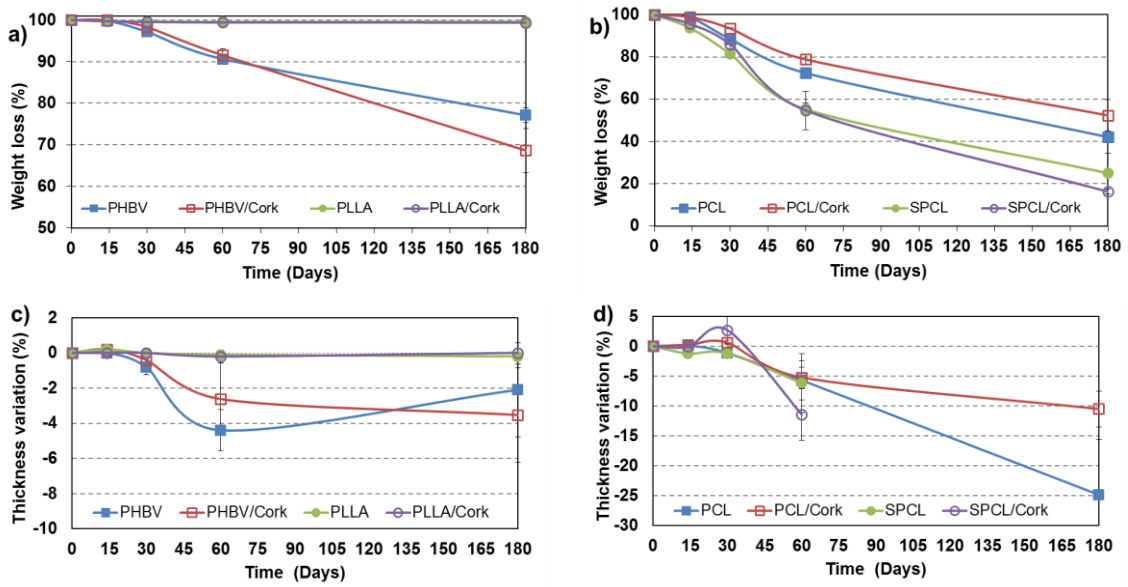

Figure 9.6. Physical behaviour of the bio-based materials under soil conditions: (a, b) weight loss and (c, d) thickness variation.

Increasing the biodegradation time (2 months) lead to a *WL* of 10% for the PHBV and 8.5% for the PHBV/Cork, where in the case of the SPCL and its biocomposite the loss was around 40% of the initial weight. After 6 months, the biodegradationof the specimens decreased in the following order: SPCL/Cork > SPCL > PCL > PCL/Cork > PHBV/Cork > PHBV > PLLA/Cork and PLLA. At this stage a considerable increase on the *WL* for the PHBV and PHBV/Cork of 20% and 30% respectively was obtained. The biodegradation process of the injection moulded specimens was higher for the biocomposites, where the only exception to this behaviour was the PCL and its biocomposite, probably due to a chemical surface affinity between the ester groups present in cork and in the PCL monomer structure. The biodegradation process of the specimens is ascribed to (a) the soil composition including pH and soil temperature, (b) the hydrolytic degradation that are in contact with the produced materials and (c) the erosion process resulting in the release of the cork particles to the soil and the consequent higher *WL* for the biocomposites as compared with the matrices. The literature comprises studies showing that biodegradable polymers whether natural or synthetic materials may be susceptible to

microbial and/or enzymatic degradation depending wish the repetitive unit, morphology (e.g. crystallinity and size of spherulites), hydrophilicity and surface area and presence of additives [30].

The evolution of the biodegradation is clearly observed in Figure 9.7 were the PCL, SPCL and its biocomposites loses the integrity accompanied by change in colour with the biodegradation process under soil conditions. In this sense, the thickness variation of the specimens was also affected, see Figure 9.6 c) and d). The obtained results are consistent with the *WL* observations. The PLLA and the respective biocomposite do not present reduction of thickness, whereas a small thickness reduction was observed for the PHBV and its biocomposite. As expected the higher thickness variation was observed for the PCL and SPCL compositions, where after the 60 days, it was not possible to obtain any measurements for the blend with starch due to a disintegration of the specimens. In addition, the small increase in the thickness variation obtained for the SPCL/Cork after 30 days can be ascribed by the swelling of the starch leading to a faster *WL* followed by the disintegration of the composite structure. In spite of the results it is expected for the biocomposites a significantly lower rate of degradation at compostable environmental conditions as compared with the neat polymers.

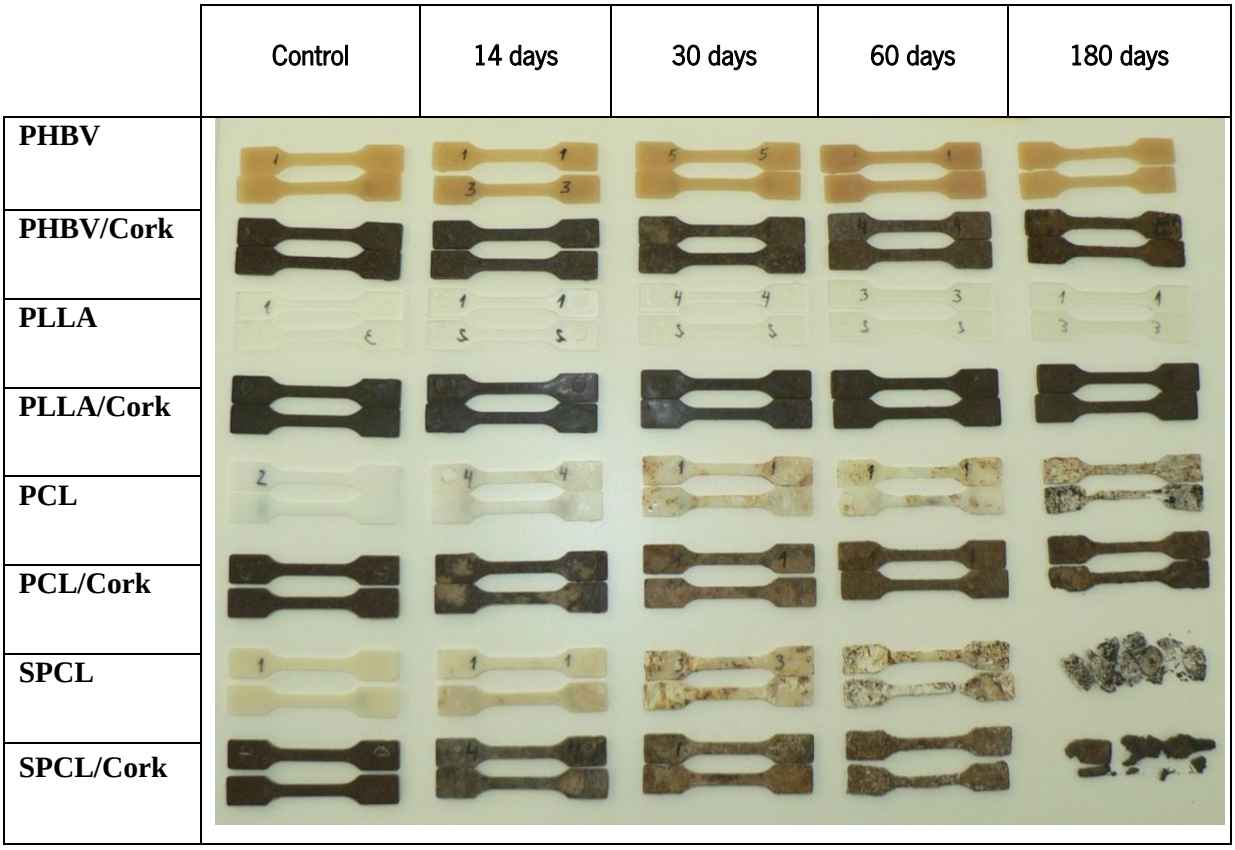

Figure 9.7. Tensile test specimens with 60 mm length after the diferent periods of time under soil burial degradation tests.

9.3.2 Density

The density of the injection moulded specimens, was determined in order to evaluate the effect of the 30 wt.% addition of granulated cork in the bio-based polymers.

Figure 9.8 shows that the density of the biocomposites containing cork with PLLA and PHBV is lower as compared with the neat polymers, in a range of 3.9 % and 1.7 % respectively. This behaviour is ascribed to the lower density of cork as compared with the used matrices. Lower density of the cork filled composites can result in increased specific mechanical properties (property/density). Moreover, features such as: reduced weight, increasing of the amount of renewable material, reduced material costs and the possibility to recycle are of considerable importance in the automotive industry. On the contrary, the PCL matrix presents a lower density value of 1110 $kg.m^{-3}$, where the addition of cork increased the density in 4.5%. Comparing the effect of adding around 30 wt.% of starch to the PCL (i.e. SPCL blend) and the same weight fraction of cork to the PCL (PCL/Cork composite) was obtained a reduction of 5.1%. This result reveals that the use of cork can be an environmental friendly approach to reduce the cost and promote aesthetic without compromise significantly the density of the PCL.

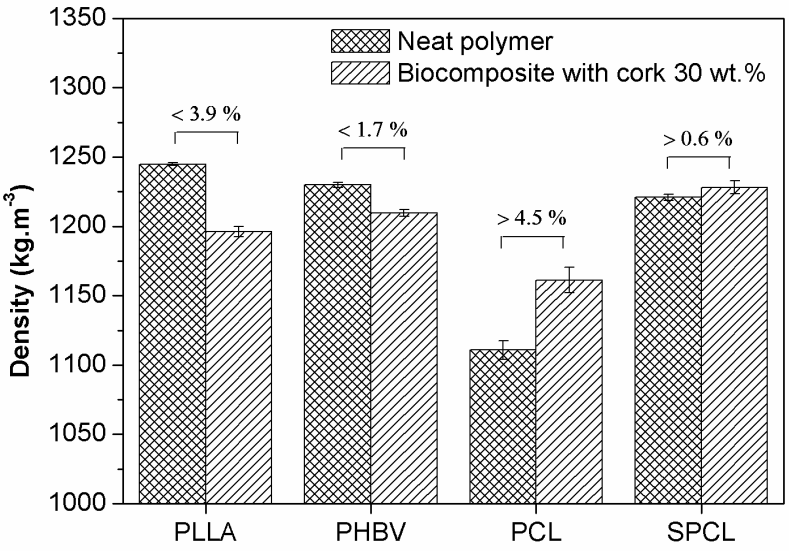

Figure 9.8. Density of the polymer matrices and the bio-based composites containing 30 wt.% of cork.

9.3.3 Morphology

Figure 9.9 and Figure 9.10 reveal the surface morphology before and after water and soil degradation tests of the biocomposites and the used matrices. The pristine morphology of the neat injection moulded polymers exhibited a smooth surface with similar irregularities due to processing. Furthermore, the roughness tends to be more pronounced in the biocomposites due to the presence of cork particles that are in contact to the surface.

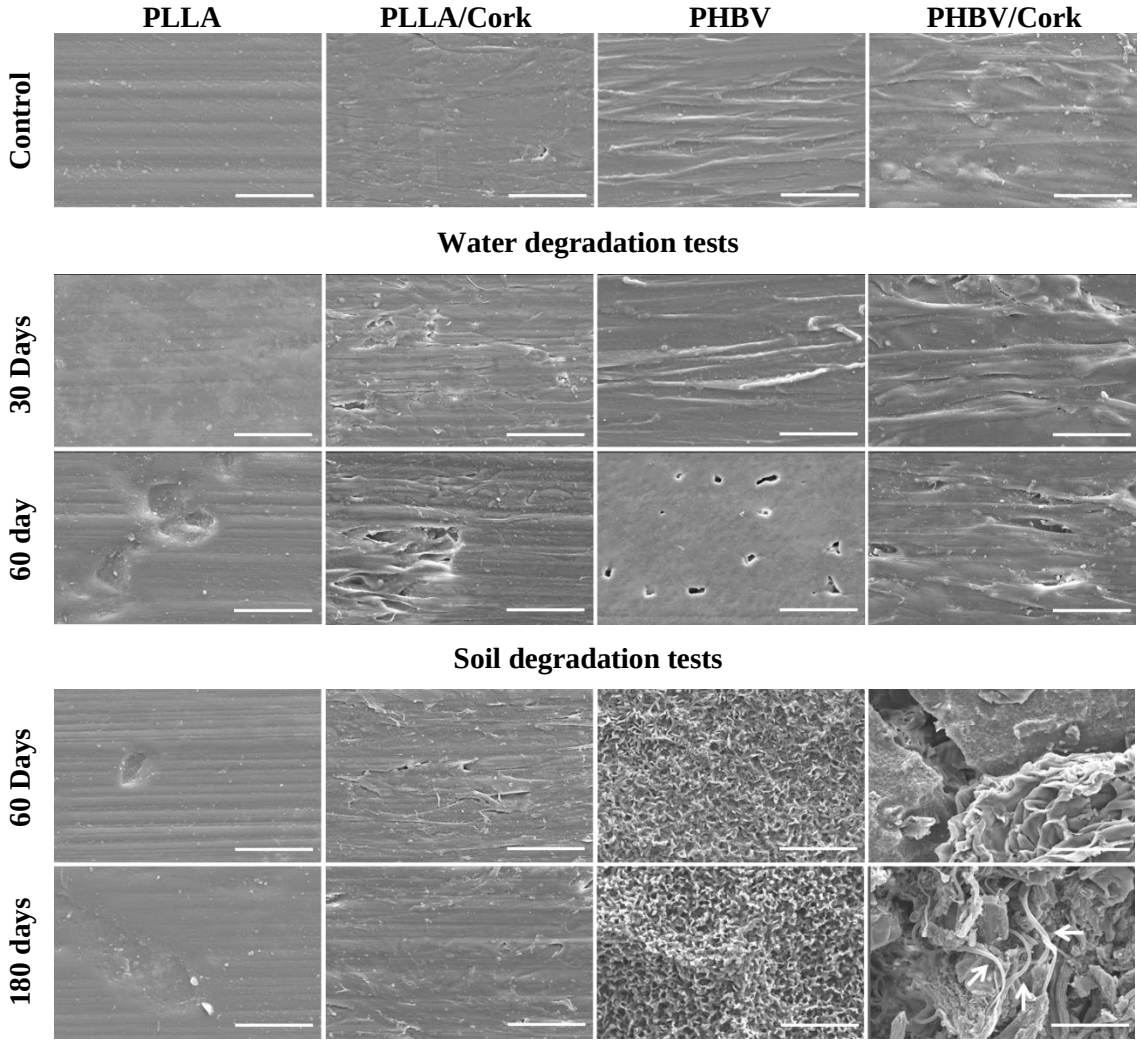

Figure 9.9. Morphology of the prystine surfaces of the injection moulding specimens using PLLA and PHBV matrices before and after the water and soil degradation tests, as seen by SEM. Scale bar indicates 50 μm.

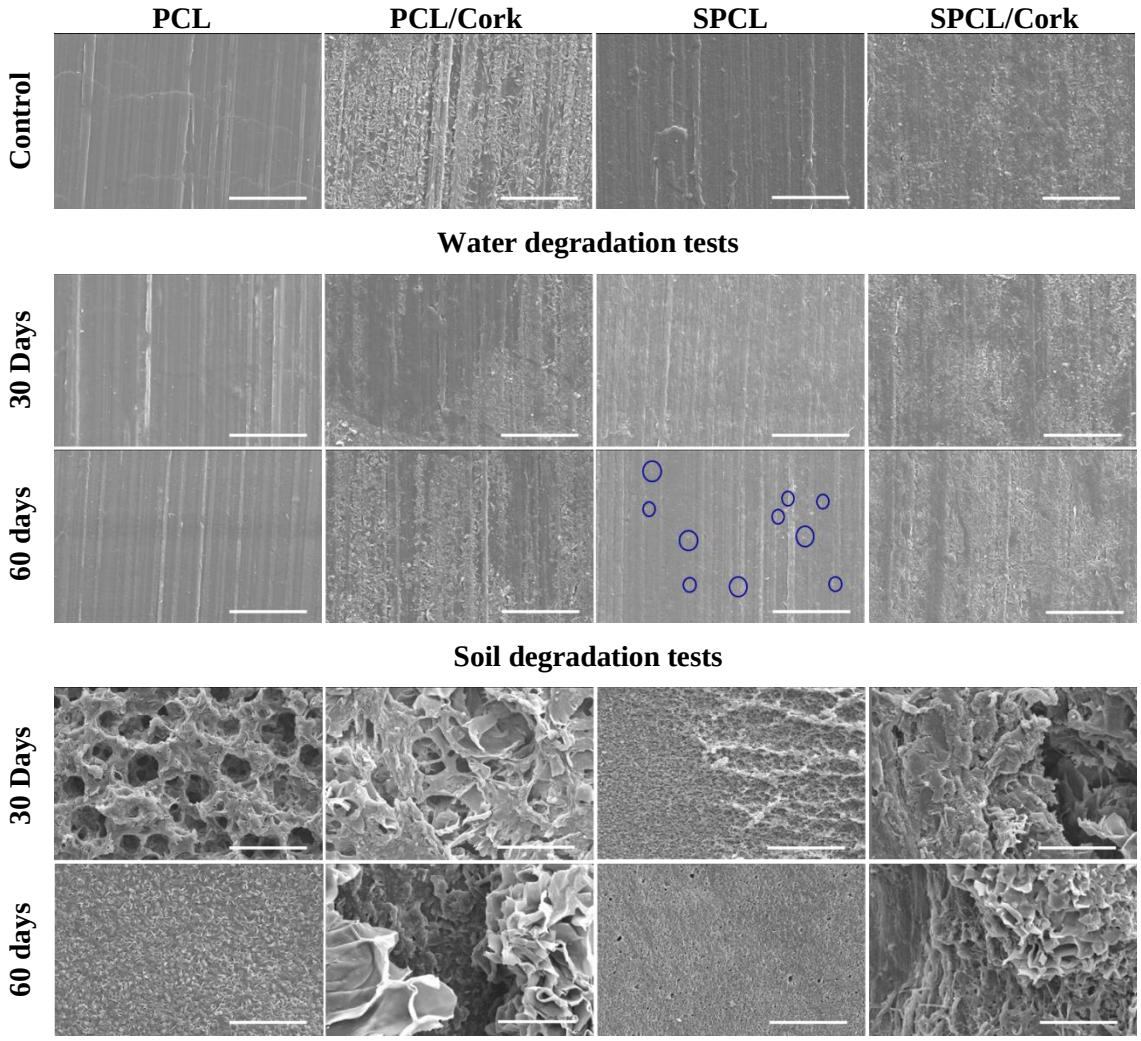

Figure 9.10. Morphology of the prystine surfaces of the injection moulding specimens using PCL and SPCL matrices before and after the water and soil degradation tests, as seen by SEM.. Scale bar indicates 50 μm.

The essays conducted under water just revealed two relevant conditions of biodegradation: (i) the micrograph of PHBV after 60 days, presents smoother surface and some micro holes that justifies the small higher water uptake as compared with the PHBV/Cork biocomposite ; (ii) the SPCL micrograph after the same 60 days of immersion presents some smaller micro holes (indicated with circles in the micrograph) probably due to swelling and release of the starch particles from the surface. Biodegradation was found to occur primarily at the polymer surface and was more pronounced for the

burial soil specimens. SEM micrographs of Figure 9.9 show that after 60 days under soil, PLLA was not affected and PHBV starts to loose thickness. For the fully bio-based PHBV composite deep cracks are observed, as well as cork exposure at the surface.

After 180 days the PLLA presents similar surface characteristics, suggesting that the enzymes from soil microbes had no significant effects on the degradation of the PLLA specimens. Moreover, it was clearly observed for the PHBV/Cork the typical random shape morphology evidencing microbial activity and the presence of living organisms such as fungi. After 180 days both surfaces were colonized by hyphae as indicated (with arrows) in the PHBV/Cork of Figure 9.9. In polymers, the crystalline part is more difficult to degrade than the amorphous regions that have higher mobility of the polymeric chains and, therefore, are more accessible to the microorganisms. The presence of lignocellulosic particles distributed in the polymer matrix may act as channels and facilitate the microbial attack in natural cork semi-crystalline matrix composites. Moreover, soil results as revealed in Figure 9.10, showed that cork presents high fungi resistance; however it is known that the structural components of cork (e.g. suberin, lignin and cellulose) also present in other plants can be degraded by specific enzymes or bacteria [31-34].

In addition, several authors point the idea that lignocellulose-based fibres are the most widely used, as biodegradable filler [21, 35, 36], indicating their potential to be used in biodegradable applications. Since both constituents are biodegradable, cork combined with bio-based matrices, also can potentially origin fully biodegradable composites. For example, the materials based on PCL and SPCL showed that the biodegradation process is clear observed after 30 days. In the PCL and SPCL biocompsites after 60 days, the cork particles are more visible.

For the SPCL/Cork these elements appear more exposed due to the selective loss of starch from the matrix. After this period and for 180 days the disintegration and erosion of the specimens occurs due to the high rate of biodegradation and not allowed the SEM observation. The decomposition sequence for the biocomposites under soil can be described as follows. The biodegradable polymer at the specimen surface first decomposes, followed by exposure of the internal cork granules stacked in the polymer matrix. At the same time, the biodegradable polymer in cork-matrix interface decomposes, resulting in the formation of interfacial gaps that increases with time exposing considerably more the cork particles. Finally, we suggest that substantial decomposition of the biodegradable polymer occurs and on cork starts to occur.

9.3.4 Mechanical Properties

9.3.4.1 Control and water degradation tests

The tensile properties of the injection moulded biodegradable aliphatic polyesters and the biocomposites before biodegradation essays are shown in Figure 9.11 a) for the tensile modulus and in Figure 9.11 b) for the maximum tensile strength. Table 9.3 indicates the values and standard deviations of the tensile properties including the maximum strain of the materials. Two distinct groups of materials could be identified from these data. PLLA and PHBV present considerable higher stiffness and tensile strength as compared with the PCL or SPCL specimens.

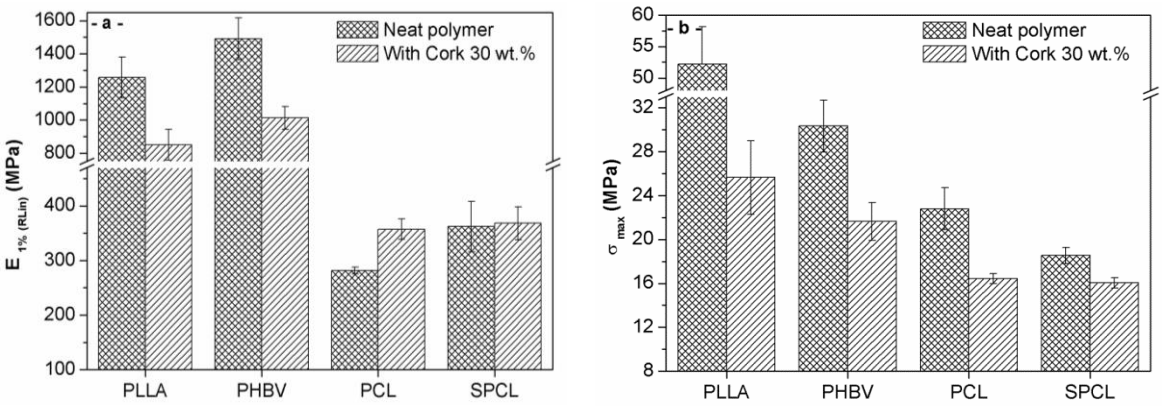

Figure 9.11. Mechanical properties of the neat polymers and the biocomposite materials under tensile load.

In opposite sides, PLLA has brittle properties, i.e. high strength and low maximum strain at break, while PCL reveals a ductile behaviour with low tensile modulus and higher strain at break. The addition of cork to PLLA and PHBV reduces the tensile modulus probably due to the higher elasticity of cork as compared with the neat polyesters, contributing to some ductility. The effect of the elasticity of cork particles was preferably observed in PHBV and its biocomposite were the reduction of stiffness it was followed by an increase of the strain at break. In general, the modulus of a composite material is also related with the density of the obtained material. This finding was also observed in the biocomposites, where the addition of 30 wt.% of cork increases the tensile modulus of PCL matrix in 33% and maintained the properties of the SPCL matrix as shown in Table 9.3. Moreover, cork promotes similar effect as the addition of starch to the PCL matrix. Regarding both PLLA and PHBV, the presence of cork

reduces the tensile modulus in 32%. Since cork is a foamed material, the modulus is much lower, that the used bio-based polyesters: around 23.9 to 31.7 MPa depending of the direction [6, 7]. Concerning the maximum tensile strength, the addition of cork promoted a reduction up to 50.1% for the PLLA; 28.7% for the PHBV; 28.1% for the PCL and only 13.5% for the SPCL matrix. Based on the mechanical properties of the control samples (matrices and its biocomposites), and in previous studies [12, 15, 16] using polyolefins as matrices, we observed that the tensile strength on cork-polymer composites is dependent preferably on the type of the matrix and on the compatibility between matrix and cork and its content, whereas the tensile modulus is influenced by the cork content and processing characteristics.

Table 9.3. Physical properties of the used biodegradable polyesters, and corresponding biocomposites with cork.

Property	PLLA	PLLA/ Cork	PHBV	PHBV/ Cork	PCL	PCL/ Cork	SPCL	SPCL/ Cork
Melting point (°C)	160.5	166.4	170.2	171.2	55.1	58.9	56.2	58.0
Tensile strength (MPa)	52.2 (5.9)	25.7 (3.3)	30.3 (2.4)	21.6 (1.7)	22.8 (1.9)	16.4 (0.4)	18.5 (0.7)	16.0 (0.5)
Tensile modulus (MPa)	1256.6 (123.2)	850.6 (92.6)	1490 (125.8)	1012.4 (68.8)	281.4 (6.0)	375.2 (18.6)	362.0 (46.4)	368.3 (30.1)
Strain at break (%)	5.5 (1.4)	3.4 (1.3)	2.9 (0.2)	3.8 (0.5)	> 200	9.10 (0.3)	10.3 (0.4)	7.0 (0.5)
Density (kg/m^3)	1244.9 (1.0)	1196.3 (3.7)	1229.9 (1.8)	1209.6 (2.5)	1110.8 (6.5)	1161.2 (9.2)	1221.0 (2.4)	1228.2 (4.6)

( ) standard deviation value.

It should be also highlighted that, when natural cork is under tensile load in radial direction, the fracture occurs at stress values of about 1.1 MPa, corresponding to a strain of about 8% [7]. Moreover, the reduced strength of cork contributes to an inferior stress transfer between the cork-matrix and consequent lower mechanical properties.

The tensile properties along the water degradation tests are shown in Figure 9.12, where it was observed in some cases a small reduction in the mechanical performance with time. Moreover, starch swells high water contents, so it was expected that both strength and stiffness tend to decline with the time. However in almost all conditions this was not significant due to the high standard deviations of the specimens indicating some variation on the materials surface as supported by the previous morphological results.

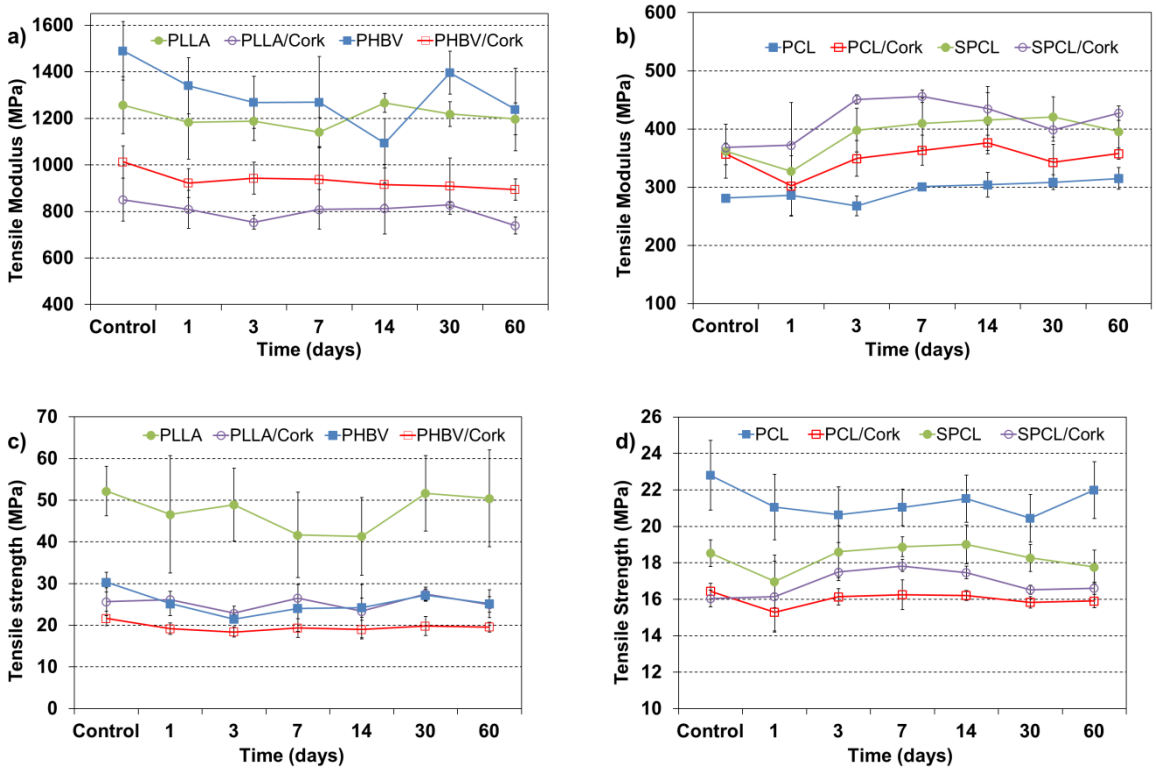

Figure 9.12. Mechanical behaviour of the biocomposites under water during 60 days.

Furthermore, it was found for a period up to 14 days an increase in the tensile modulus for the materials containing starch. This occurred probably due to a plasticizing effect promoted by the water absorbed by the starch and the presence of some plasticizers in the blend composition. Since the blend and its biocomposite were mechanically evaluated after drying we suggest the influence of sorption-desorption mechanism effect. The drying process of the biocomposites may cause the drying of some residual water-filled cellular lumia in cork that causes shrinkage, contributing to some minor variation on the composite stiffness.

9.3.4.2 Soil degradation tests

The loss of the mechanical properties of the injection moulded specimens was more pronounced under soil conditions. The relationship between tensile strength and burial period under soil is shown in Figure 9.13. According to the tensile modulus the bio-based materials gradually loses the mechanical properties with the time. Even PLLA presented higher standard deviation in function of time essay that may indicate some chemical degradation of the polyester structure.

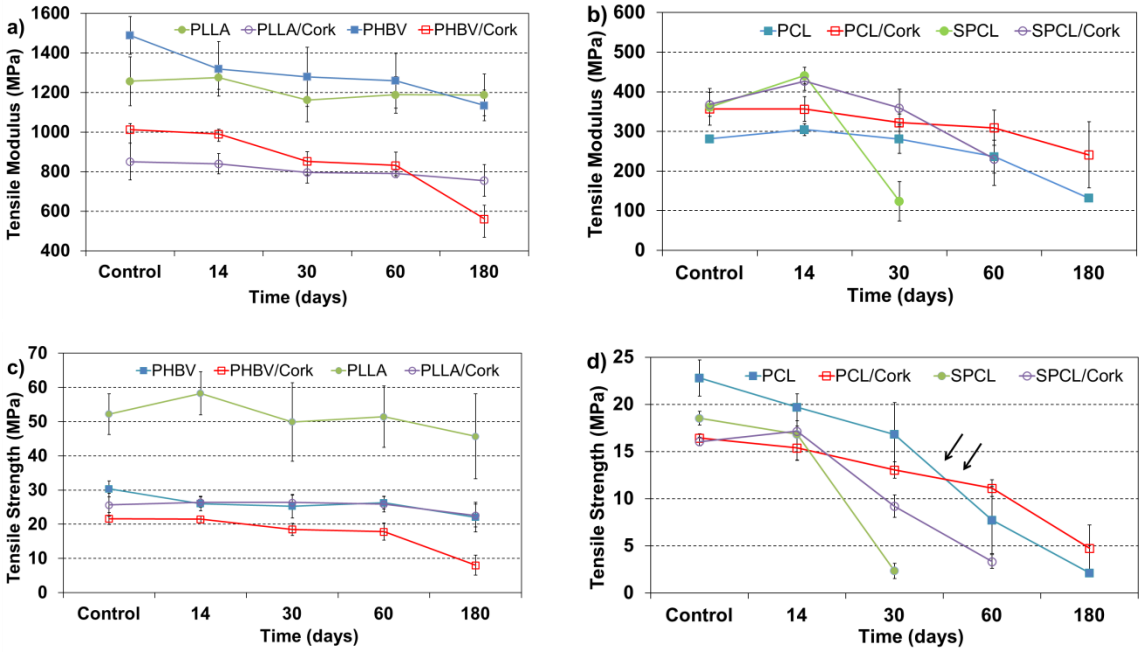

Figure 9.13. Mechanical behaviour of the biocomposites under soil during 180 days.

The mechanical properties were in agreement with the previous weight loss results and morphological observations, being the materials most affected the PCL and SPCL based materials. It was also observed after 14 days the increase in the tensile modulus for the SPCL materials around 20%. This occurred due to the high moisture content absorbed by the starch under soil conditions acting as plasticizer and by the presence of plasticizer in the SPCL blend composition. After the 14 days the drop on the mechanical properties was quite noticeable, especially in terms of maximum strength. It was possible to monitoring the behavior of the SPCL/cork biocomposite up to 60 days, while the SPCL blend after the 30 days loses the specimen integrity to be tested under tensile load. Furthermore, the mechanical response of the developed materials it confirmed that granulated cork decreases the biodegradation rate. This behaviour was also observed for the PCL matrix and its biocomposite as indicated in Figure 9.13 d), being evident the loss in the tensile strenght between 30 and 60 days,

where PCL starts to lose more properties due to biodegradation. This mechanical failure is consistent with the higher porosity of PCL surface as compared with the PCL/Cork observed by SEM micrographs after the 30 days of burial soil test, see Figure 9.10.

9.3.5 Thermal analysis

The influence of cork on the thermal stability of the injection moulded biocomposites and the stability of the polyesters was studied by thermogravimetric analysis (TGA) essays. TGA results and the respective derivative thermogravimetric curves (DTG) are shown in Figure 9.14.

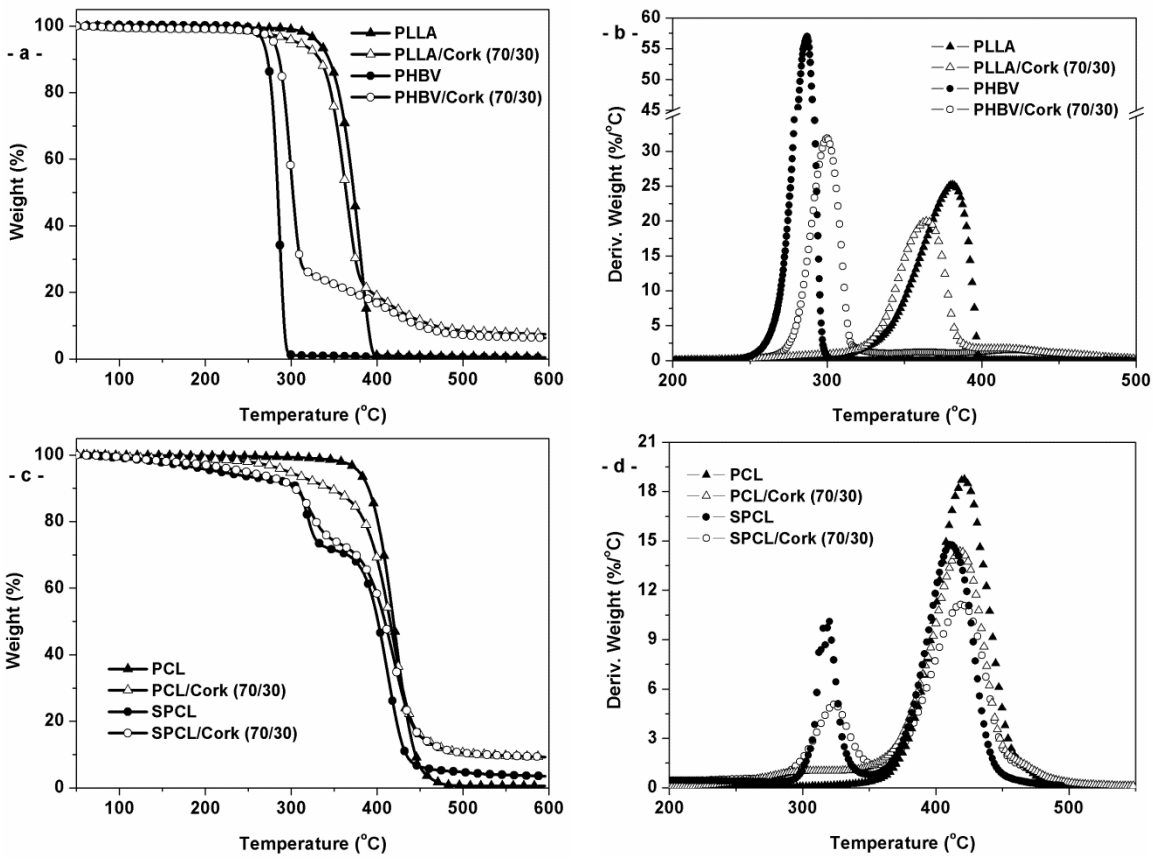

Figure 9.14. Thermogravimetric curves of the neat polymers and the biocomposites.

The initial degradation temperature (Tonset), maximum peaks obtained in the DTG curve and the ash content are shown in Table 9.4. The thermal degradation process of PLLA, PHBV and its biocomposites occurs in only one weight loss step, while for the PCL, SPCL and its biocomposites a multi-step degradation process was observed. In the presence of cork the curves are shifted to lower temperatures

indicating a small decreasing in thermal stability of biocomposite. The only exception was with PHBV, where the addition of cork improved the initial thermal stability. This small increase on the thermal stability occurred despite of cork presented the lower initial degradation temperature of 246.3°C as compared with the used polyester matrices (see Table 9.4). Some recent studies evidenced that the addition of nano-clay and natural fibres reduced or maintain, respectively, the thermal stability of PHBV [37, 38]. However in the present study cork promoted a slight and positive increase in 5.5% to the initial degradation temperature.

Table 9.4. The initial degradation temperatures, the peak temperatures, and the ash of the neat polymers and its biocomposites with cork obtained by TGA.

Sample	Tonset (°C)		DTG peak temperatures (°C)		Ash content (%)
PLLA	341.68		380.62		0.59
PLLA/Cork	335.80		364.39		7.40
PHBV	269.32		286.82		0.39
PHBV/Cork	284.20		299.81		6.28
PCL	387.74		420.99		0.50
PCL/Cork	266.87	386.99	293.75 *	418.62	9.34
SPCL	309.64	382.32	318.44	411.42	4.84
SPCL/Cork	303.71	386.63	323.63	418.94	9.25
Cork	246.33	379.96	292.88	414.33	19.81

* Very small intensity peak

Furthermore, during the injection moulding process it was observed that PHBV presents a slow crystallization rate, inducing some warping in the samples that was ameliorated by the addition of cork. The TGA curves and Table 9.4 showed that thermal decomposition of SPCL started at 309 °C with the decomposition of starch and continued at 411 °C with the degradation of the PCL fraction. Comparing the effect of cork and starch on the PCL matrix, Figure 9.14 c) shows that cork revealed higher thermal stability than starch. This result was also confirmed by the DTG curve of

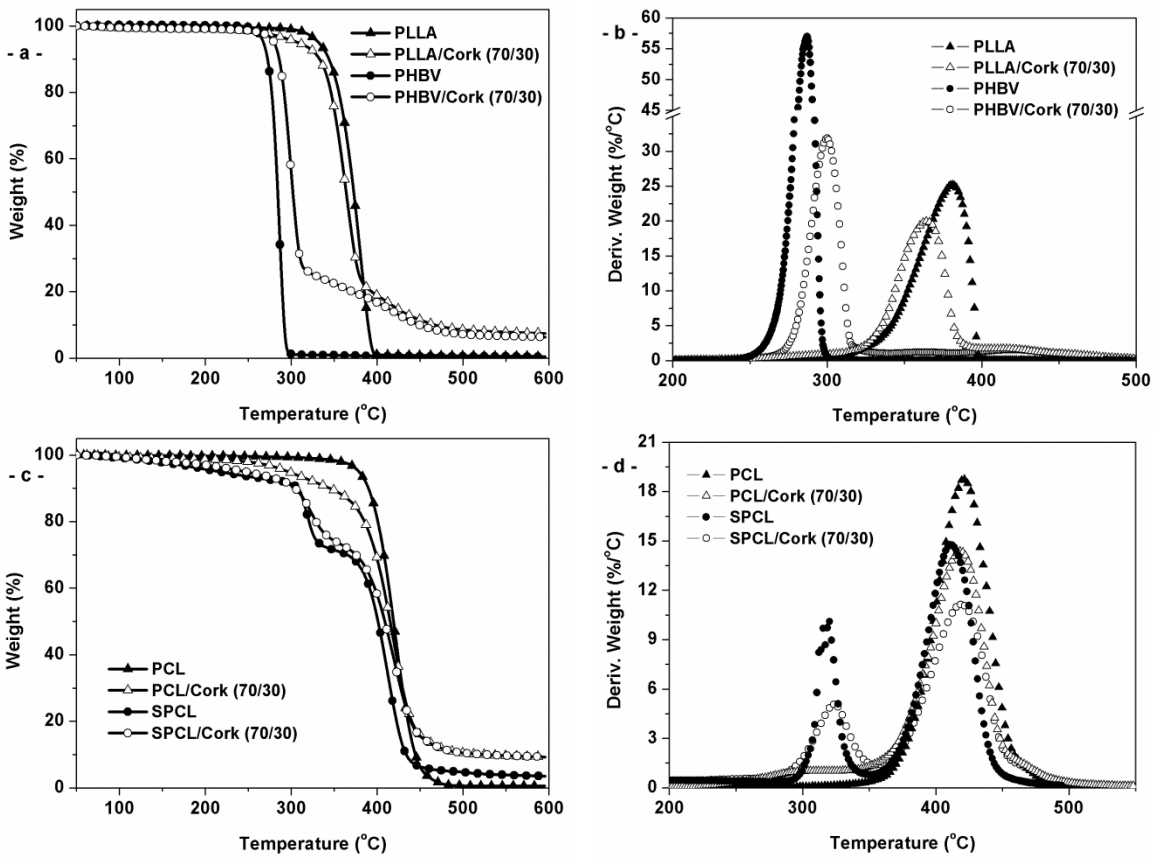

Figure 9.14. d) with the intense peaks appearing at 318.4 °C for SPCL and 323.6 °C for PCL/Cork.

The TGA curves and the results of Table 9.4 indicated that thermal degradation of biocomposites is a combined phenomenon of thermal degradation of each of the components; i.e., the selected matrix and the granulated cork. The TGA findings also point that cork was the last material to be degraded promoting a slower thermal degradation to the biocomposites at higher temperatures resulting in a lower weight loss rate and higher ash content, from 6.3% up to 9.3%.

Differential scanning calorimetry (DSC) also provides relevant information about the thermal and structural characteristics of materials. In this study, DSC was performed to understand the effect of the cork on the nucleation and crystallinity of the bio-based polyesters, using for that the second heating scan. Thus, we are erasing any previous thermal story through the first heating cycle. The onset values of phase transition temperatures (crystallization temperature T_c, cold crystallization temperature T_{cc} and melting temperature T_m), glass transition temperature T_g at the mid-point of heat capacity changes and enthalpies (ΔH_{cc}, cold crystallization enthalpy, ΔH_m, melting enthalpy and ΔH_c, crystallization enthalpy)

recorded by DSC of the injection moulded materials are summarized in Table 9.5. The thermograms are shown in Figure 9.15.

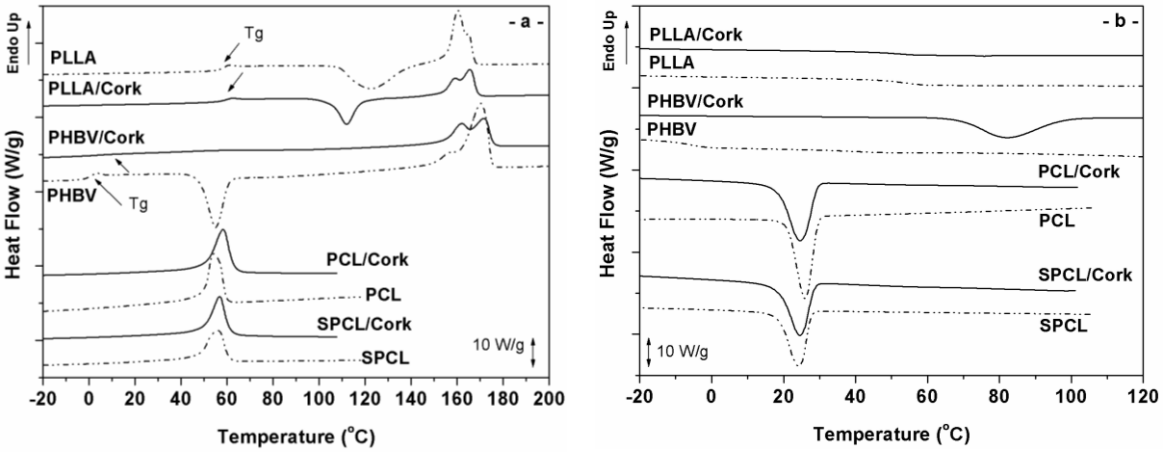

Figure 9.15. DSC termograms of the biobased composites with cork at 20 °C min^{-1} showing: a) the second heating and b) the first cooling.

In this study, we observed that the PLLA, PHBV and the respective biocomposites (Figure 9.15 a) displayed on heating three main transitions: glass transition, a cold crystallization exothermic followed by a melting endothermic event. We also observed the influence of cork on the *Tg* of the PLLA and PHBV polyesters. It has been found that *Tg* was slightly affected by the composition, with a small increase with the cork content, from 57.3 to 58.4 °C and -0.6 to 4.6 °C (see Table 9.5), suggesting confinement of the mobile amorphous phase. This finding, previously observed in the PHB using a different type of natural fibres [39], was explained by an intermolecular interaction between carbonyl (-C=O) groups of the PHBV and hydroxyl (-OH) groups of the natural fibre that decreases the molecular flexibility of the polymer chains involved in the glass transition.

The PLLA present an amorphous structure that might be related with the DSC cooling rate of 20 °C/min that could prevent crystallization of the material. In the case of the PLLA thermogram, the cold crystallization temperature peak was shifted to lower temperature with the addition of cork. This agrees with the finds in the literature [40] that the presence of some lignocellulosic materials such as wood can promote the initial cold crystallization temperature of the PLLA matrix. Moreover, the thermograms of the PLLA and PHBV show a single melting temperature peak event at 160.5 °C and 170 °C respectively.

Table 9.5. Melting temperatures and enthalpies, crystallization temperatures, and crystallinity degrees of the bio-based composites containing cork, obtained by DSC.

Sample	1st cooling		2nd heating					
	T_c (°C)	ΔH_c (J/g)	Tg (°C)	T_{cc} (°C)	ΔH_{cc} (J/g)	T_m (°C)	ΔH_m (J/g)	χ_c[a] (%)
PLLA			57.25	108.84	-42.37	155.31	44.55	2.3
PLLA/Cork			58.39	105.88	-40.79	154.15	47.49	7.2
PHBV			-0.64	47.05	-68.98	160.56	94.59	17.5
PHBV/Cork			4.55	98.22	-67.06	153.65	97.08	20.6
PCL	29.64	62.24				50.32	69.37	49.7
PCL/Cork	29.10	69.00				50.07	80.12	57.4
SPCL	27.45	64.12				49.24	61.18	43.9
SPCL/Cork	28.05	66.23				50.29	64.73	46.4

[a] Crystallinity degree calculated on the basis of a 100% crystalline polymer a melting enthalpy of ΔH_{m° = 93 J/g corresponding to poly(L-lactic acid) (PLLA) [42]; 146 J/g for polyhydroxybutyrate-co-hydroxyvalerate (PHBV) [43] and 139.5 J/g for poly-ε-caprolactone (PCL) [44].

For the biocomposites PLLA/Cork and PHBV/Cork the maximum melting peak occurs at a high temperature being 166.4 °C and 171.2 °C respectively. Moreover, for the biocomposites it was observed a second melting peak with smaller intensity and lower temperature. In different lignocellulosic biocomposites, the presence of two melting peaks almost completely overlapped were attributed to the presence and reorganization of a different type of crystals with higher order degree and stability [41]. Cork interferes in the crystal morphology of PLLA and PHBV during the melting as a result the nucleation growth of the bio-based polyester becomes more homogenised in presence of cork particles. The onset temperature of the crystallisation during the cooling tends to show a slight but not significant increase with the cork content in the semi-crystalline PCL and SPCL. In the PLC the T_c was found to occur at 29.6 °C and for PLC/Cork at 29.1°C, while the SPCL and SPCL/Cork showed it at 27.5 and 28.1°C, respectively. We observed that the heating of crystallization and the heating of melting of the bio-based matrices in all the biocomposites increased with the addition of cork indicating

an improvement in the degree of crystallinity (χ_c) as shown in Table 9.5. These findings suggest that cork may have the ability to modify the crystallisation by increasing the number of nucleating sites in the bio-based polyesters and enhancing its crystallinity degree. Moreover, the addition of starch to the PCL reduced the crystallinity in 5.8%, thus contributing to enhancing the biodegradation.

9.4 Conclusions

This study dealt with the effect of water immersion and soil degradation on the weight changes, tensile and morphological properties of biodegradable polyester biomposites containing granulated cork (30 wt.%) processed by extrusion followed by injection moulding. This environmental friendly approach of using a renewable material such as natural cork, promoted a reduction of PLLA and PHBV density resulting in lightweight biocomposites. All materials revealed low water absorption, being the higher values correspond to the biocomposites containing cork and preferably in the presence of the starch. Thermal properties by DSC have confirmed the positive effect on the use of cork that increases the crystallinity degree for all the used bio-based polyester matrices. Biodegradation of the specimens under burial soil during 6 months was significantly more severe than under static water conditions, as monitored from the loss of tensile modulus and maximum strength. As expected the use of starch accelerates the biodegradation rate also confirmed by morphological observation. Moreover, this study allowed comparing the contribution of cork and starch to the PCL polymer (i.e. SPCL and PCL/Cork). Cork contributes with higher hydrolytic and dimensional stability than starch. Both materials improved considerably the stiffness; however cork induces weight reduction and is less sensitive to moisture. TGA showed that cork presents higher thermal stability than starch. Regarding the degree of crystallinity, the DSC analysis revealed an opposite effect for both fillers were starch contributed to an increase of the amorphous phase supporting the higher biodegradation. This findings could demonstrate the benefits of combine cork with bio-based matrices that can origin fully biodegradable eco-friendly composites. Besides the cost reduction of bio-based matrices by adding cork, it is possible to provide aesthetic characteristics, or reduce matrix weight or even increase stiffness depending of the used biodegradable polymer. Cork biocomposites are good candidates for the production of sustainable products promoting added-value to cork biomass for a wide range of applications.

9.5 References

[1] John MJ, Thomas S. Biofibres and biocomposites. Carbohydr Polym. 2008;71(3):343-364.

[2] Faruk O, Bledzki AK, Fink H-P, Sain M. Biocomposites reinforced with natural fibers: 2000-2010. Prog Polym Sci. 2012;37(11):1552-1596.

[3] Yu L, Dean K, Li L. Polymer blends and composites from renewable resources. Prog Polym Sci. 2006;31(6):576-602.

[4] Satyanarayana KG, Arizaga GGC, Wypych F. Biodegradable composites based on lignocellulosic fibers-An overview. Prog Polym Sci. 2009;34(9):982-1021.

[5] Mohanty AK, Misra M, Drzal LT. Sustainable bio-composites from renewable resources: Opportunities and challenges in the green materials world. J Polym Environ. 2002;10(1-2):19-26.

[6] Silva SP, Sabino MA, Fernandes EM, Correlo VM, Boesel LF, Reis RL. Cork: properties, capabilities and applications. Int Mater Rev. 2005;50(6):345-365.

[7] Pereira H. Cork: biology, production and uses. Amsterdam: Elsevier; 2007.

[8] Gil L, Moiteiro C. Cork. Ullmann's Encyclopedia of Industrial Chemistry: Wiley-VCH Verlag GmbH & Co. KGaA; 2000.

[9] Gil L. Cork Composites: A Review. Materials. 2009;2(3):776-789.

[10] Gibson LJ. Cellular solids. MRS Bull. 2003;28(4):270-274.

[11] Gil L. Cork powder waste: An overview. Biomass Bioenerg. 1997;13(1-2):59-61.

[12] Fernandes EM, Correlo VM, Chagas JAM, Mano JF, Reis RL. Cork based composites using polyolefin's as matrix: Morphology and mechanical performance. Compos Sci Technol. 2010;70(16):2310-2318.

[13] Fernandes EM, Correlo VM, Chagas JAM, Mano JF, Reis RL. Properties of new cork-polymer composites: Advantages and drawbacks as compared with commercially available fibreboard materials. Compos Struct. 2011;93(12):3120-3129.

[14] Abdallah FB, Cheikh RB, Baklouti M, Denchev Z, Cunha AM. Effect of surface treatment in cork reinforced composites. J Polym Res. 2010;17(4):519-528.

[15] Fernandes EM, Correlo VM, Mano JF, Reis RL. Novel cork–polymer composites reinforced with short natural coconut fibres: Effect of fibre loading and coupling agent addition. Compos Sci Technol. 2013;78(0):56-62.

[16] Fernandes EM, Mano JF, Reis RL. Hybrid cork–polymer composites containing sisal fibre: Morphology, effect of the fibre treatment on the mechanical properties and tensile failure prediction. Compos Struct. 2013;105(0):153-162.

[17] Fernandes EM, Silva VMCD, Chagas JAMD, Reis RLGD. Fibre-reinforced cork-based composites. WO2011014085-A2; PT104704-A1; WO2011014085-A3, Amorim Revestimentos SA, 2011.

[18] Fernandes EM, Correlo VM, Mano JF, Reis RL. Innovative bio-based composites comprising cork and biodegradable polyester. In: Ferreira JAM, editor. 16th International Conference on Composite Structures (ICCS16), FEUP, Porto2011.

[19] Vilela C, Sousa AF, Freire CSR, Silvestre AJD, Pascoal Neto C. Novel sustainable composites prepared from cork residues and biopolymers. Biomass Bioenerg. 2013;55(0):148-155.

[20] Ljungberg LY. Materials selection and design for development of sustainable products. Mater Design. 2007;28(2):466-479.

[21] Mohanty AK, Misra M, Hinrichsen G. Biofibres, biodegradable polymers and biocomposites: An overview. Macromol Mater Eng. 2000;276-277(1):1-24.

[22] Fernandes EM, Pires RA, Mano JF, Reis RL. Bionanocomposites from lignocellulosic resources: Properties, applications and future trends for their use in the biomedical field. Prog Polym Sci. 2013;38(10–11):1415-1441.

[23] Avérous L. Biodegradable Multiphase Systems Based on Plasticized Starch: A Review. J Macromol Sci - Part C. 2004;44(3):231-274.

[24] Bogoeva-Gaceva G, Avella M, Malinconico M, Buzarovska A, Grozdanov A, Gentile G, et al. Natural fiber eco-composites. Polym Composite. 2007;28(1):98-107.

[25] Gross RA, Kalra B. Biodegradable polymers for the environment. Science. 2002;297(5582):803-807.

[26] Kaith BS, Mittal H, Jindal R, Maiti M, Kalia S. Environment Benevolent Biodegradable Polymers: Synthesis, Biodegradability, and Applications. In: Kalia S, Kaith BS, Kaur I, editors. Cellulose Fibers: Bio- and Nano-Polymer Composites: Springer; 2011. p. 426-446.

[27] Swift G. Requirements for biodegradable water-soluble polymers. Polym Degrad Stabil. 1998;59(1-3):19-24.

[28] Hakkarainen M, Karlsson S, Albertsson AC. Rapid (bio)degradation of polylactide by mixed culture of compost microorganisms—low molecular weight products and matrix changes. Polymer. 2000;41(7):2331-2338.

[29] Rudnik E, Briassoulis D. Comparative Biodegradation in Soil Behaviour of two Biodegradable Polymers Based on Renewable Resources. J Polym Environ. 2011;19(1):18-39.

[30] Karlsson S, Albertsson A-c. Biodegradable polymers and environmental interaction. Polym Eng Sci. 1998;38(8):1251-1253.

[31] Kolattukudy PE. Structure, Biosynthesis, and Biodegradation of Cutin and Suberin. Annu Rev Plant Phys. 1981;32:539-567.

[32] Crawford DL, Crawford RL. Microbial Degradation of Lignocellulose: the Lignin Component. Appl Environ Microb. 1976;31(5):714-717.

[33] de Boer W, Folman LB, Summerbell RC, Boddy L. Living in a fungal world: impact of fungi on soil bacterial niche development. Fems Microbiol Rev. 2005;29(4):795-811.

[34] Leschine SB. Cellulose degradation in anaerobic environments. Annu Rev Microbiol. 1995;49:399-426.

[35] Saheb DN, Jog JP. Natural fiber polymer composites: A review. Adv Polym Tech. 1999;18(4):351-363.

[36] Bledzki AK, Gassan J. Composites reinforced with cellulose based fibres. Prog Polym Sci. 1999;24(2):221-274.

[37] Thire R, Arruda LC, Barreto LS. Morphology and Thermal Properties of Poly(3-hydroxybutyrate-co-3-hydroxyvalerate)/Attapulgite Nanocomposites. Mater Res-Ibero-AMJ. 2011;14(3):340-344.

[38] Russo P, Carfagna C, Cimino F, Acierno D, Persico P. Biodegradable Composites Reinforced with Kenaf Fibers: Thermal, Mechanical, and Morphological Issues. Adv Polym Tech. 2013;32(S1):313-322.

[39] Avella M, Martuscelli E, Pascucci B, Raimo M, Focher B, Marzetti A. A new class of biodegradable materials: Poly-3-hydroxy-butyrate/steam exploded straw fiber composites. I. Thermal and impact behavior. J Appl Polym Sci. 1993;49(12):2091-2103.

[40] Pilla S, Gong S, O'Neill E, Yang L, Rowell RM. Polylactide-recycled wood fiber composites. J Appl Polym Sci. 2009;111(1):37-47.

[41] Masirek R, Kulinski Z, Chionna D, Piorkowska E, Pracella M. Composites of poly(L-lactide) with hemp fibers: Morphology and thermal and mechanical properties. J Appl Polym Sci. 2007;105(1):255-268.

[42] Fischer EW, Sterzel HJ, Wegner G. Investigation of structure of solution grown crystals of lactide copolymers by means of chemical-reactions. Colloid Polym Sci. 1973;251(11):980-990.

[43] Gogolewski S, Jovanovic M, Perren SM, Dillon JG, Hughes MK. The effect of melt-processing on the degradation of selected polyhydroxyacids: polylactides, polyhydroxybutyrate, and polyhydroxybutyrate-co-valerates. Polym Degrad Stabil. 1993;40(3):313-322.

[44] Crescenzi V, Manzini G, Calzolari G, Borri C. Thermodynamics of fusion of poly-β-propiolactone and poly-ϵ-caprolactone. comparative analysis of the melting of aliphatic polylactone and polyester chains. Eur Polym J. 1972;8(3):449-463.

SECTION IV – CONCLUDING REMARKS

General conclusions and future perspectives

The investment in academic research and innovation, in Portugal, is far from being exploited by national companies, as a tool for sustainable growth. This thesis is part of the result of a straightforward collaboration with the industry to develop knowledge and new applications based on cork-polymer composite (CPC) materials. The main objectives of this thesis were:

- to combine the engineering properties of the commodity thermoplastic matrices with the unique properties of cork trough melt based technologies and to create cork-based composites;
- to promote an added-value to different cork by-products obtained from finishing industrial operations and from end life products,
- to get the knowledge of compounding the lignocellulosic materials (i.e. cork and/or natural fibres) with thermoplastics, allowing high volumes of cork in the final material;
- to reinforce the developed cork-polymer composites (CPC) using the potential of coupling agents based on maleic anhydride with good distribution and dispersion of the particles in the polymer matrix;
- to isolate the major chemical components of cork powder (i.e. suberin and lignin) and use them as a coupling agent to promote the interfacial adhesion;
- to improve the mechanical response of CPC using natural fibres, creating novel hybrid composite systems;
- to engineering a class of cork biocomposites more sustainable with acceptable in-service performance and tendency for rapid out-of-service biodegradation.

Figure 10.1 shows an overall view of the integrating work performed with the CPC materials and their potential applications. The general conclusions of the research work produced in the present thesis, which extends from Chapter 3 to 9, are summarized as follows:

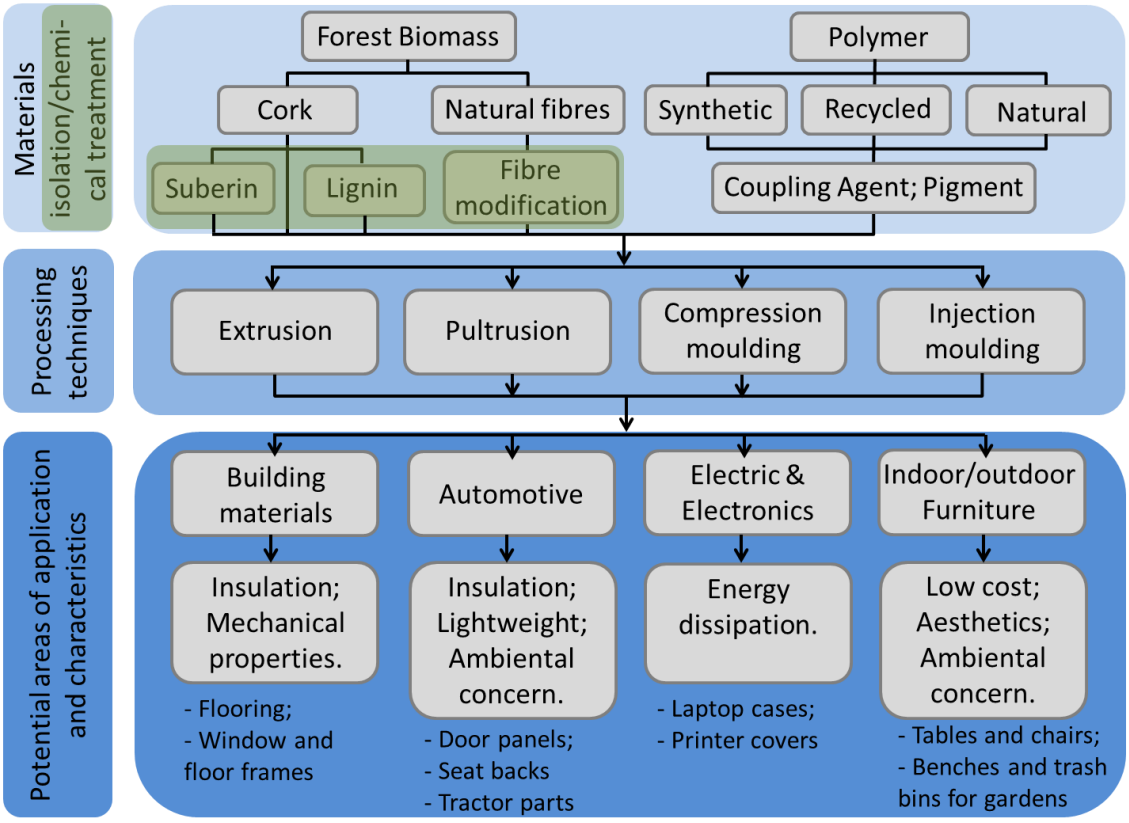

Figure 10.1. Global scheme of the work developed on cork-polymer composites (CPC) and potential areas of application.

Chapter 3 creates a viable and profitable alternative to storage or burn of cork by-products, such as powders from grinding, sanding, external industrial operations and from corkstyle or floating products. The moisture content of these by-products ranged from 5.4 up to 18.0%, being the lower values of moisture referents to the cork sanding/external powder. The moisture content on the natural component is an important issue during the compounding process. In this sense, a correct dry and stabilization of these components is fundamental, in order to avoid reduction of properties on the final product.

In this study, different classes of cork powders were combined with high-density polyethylene, recycled polymer and polypropylene by pultrusion to created CPC pellets of cork-polymer (50-50 wt.%) followed by compression moulding to produce boards. The reduced density of the cork-based composite pellets, shows the potential of the pultrusion technology to develop pultruded products taking the advantages of the cork low density.

Thermal analysis by DSC of the crystallization process, revealed the nucleating ability of cork, promoting an increase on the composite crystalinity. Microscopic optical observation confirmed a preferential

increasing of the spherulites around the cork particle in the thermoplastic matrix. Contrary to other lignocellulosic materials such as natural fibres, cork did not present evidence of the transcrystallinity phenomena.

The mechanical performance showed that, in a number of properties polypropylene is superior compared to polyethylene, since it is lighter, stronger and stiffer. The use of cork powder in 50 wt.% reduces the mechanical properties of the polyolefin matrix. The use of polyolefins as matrices in the production of lignocellulosic composites can be limited by the lower affinity between the components. The addition of 2 wt.% of functionalized polymers containing maleic anhydride (MA) groups during compounding (i.e.PE-g-MA or PP-g-MA) showed to be an effective method to improve interfacial bonding, even when using different cork qualities. The tensile properties of the different CPC were considerably enhanced in terms of tensile modulus and tensile strength.

The work shows that the use of recycled polymers combined with cork by-products from the cork industrial process revealed to be an interesting approach that contributes to higher sustainable products. However, the diminishing of the mechanical properties must be considered for the envisaged application.

CPC produced by pultrusion clearly show that cork powders and polyolefin's can be successfully used to produce CPC with high cork content. In order to obtain cork based composite materials with enhanced mechanical properties, reinforcement strategies must be taken in consideration.

Another possibility to be explored the cork by-products, is to produce CPC on a flat-press like the traditional wood-based panels. The advantage of this technology is that only a relatively low pressure level is required as compared to the extrusion and injection moulding.

Along with the previous Chapter 3, the work of **Chapter 4** potentiates the use of cork-polymer composite materials for building applications such as underlay material in flooring systems and we compared their characteristics with the well-established high-density fibreboard (HDF) and medium-density fibreboards (MDF) materials. On HDF and preferentially on MDF, moisture problem arises due to wood being a naturally hygroscopic material. In service these products can be exposed to a range of environmental conditions. The relationship between moisture content and strength properties is very important, if panel products are to be used as structural materials subjected to atmospheric moisture conditions as is the case of flooring systems. The CPC obtained by pultrusion followed by compression moulding can take advantage, since they show much lower water absorption and lower thickness swelling variation. They are also free from formaldehyde emission when compared to the HDF and MDF.

The morphological studies of cork based composites showed good dispersion and distribution or the cork along the matrix. Thus, the cork based composites presented reduced warping characteristics indicating good dimensional stability. Regarding the fibreboards, the fibrous morphology explains the superior mechanical properties obtained as compared with the CPC (50-50) wt.%. The addition of 50wt.% of cork improves the flexural modulus of the thermoplastic matrix, while considerably reduces the flexural strength.

The cork fraction represents around 86% in volume of the composite material. This fact supports the CPC good acoustic behaviour when compared with the commercial fibre boards. The CPC materials present similar acoustic performance to the fibreboards, however at high frequencies the behaviour of the CPC is superior, probably due to the cellular structure of cork.

Cork presents the advantage to act as fire retardant in the polyolefins. According to the fire resistance tests and to the stands, the developed cork based composites presents the same "fire class" as compared with the HDF and MDF. Thus, CPC materials proved to be good candidates to be used as underlay materials on floor applications. More information related with the CPC process is provided in the Appendix 1 (patent WO2009072914 (A1)) of this thesis. Figure 10.2 shows a prototype of a laminated flooring system using CPC (50-50) wt.% as underlay.

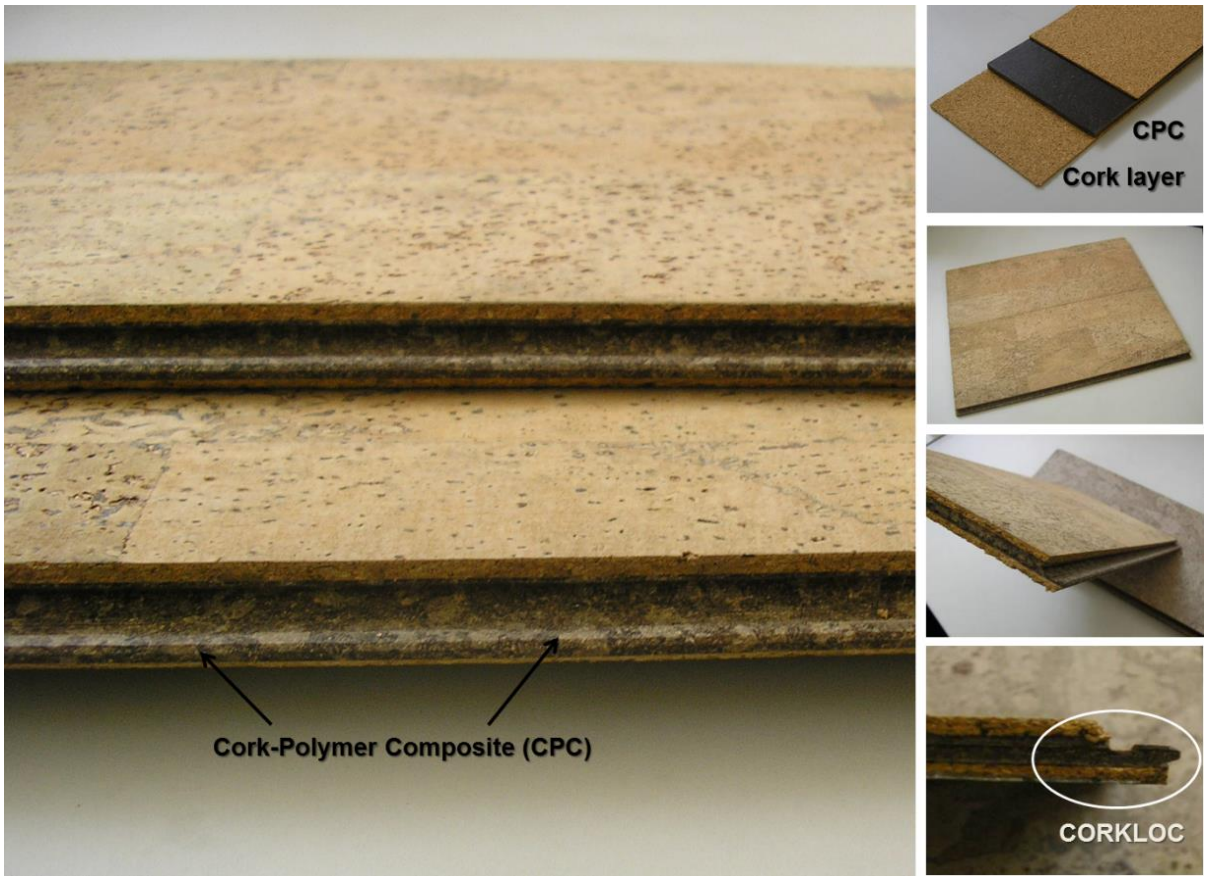

Figure 10.2. Prototype of a laminated flooring system using CPC as underlay.

Further work on the optimization of the compression moulding conditions of the CPC using a design of experiments (DOE) can be used to obtain the correct temperature, applied pressure and amount of coupling agent that are the principal parameters to optimize in order to obtain the appropriated mechanical response for the selected application. Furthermore, finishing operations in the prototypes, such as machining, lamination, cutting or gluing the CPC with other layer should be addressed.

As compared with other lignocellulosic composites, the final properties of the CPC are highly dependent on the processing conditions. Thus, the final specifications of a CPC material can be tailored for a specific application by varying the compounding process, amount and cork particle size, chemical or surface treatment and type and amount of coupling agent.

In **Chapter 5**, it was studied the polypropylene-cork (PP/cork) composites produced using co-rotating twin-screw extruder followed by injection or compression moulding process. During the extrusion process it was avoided an aggressive mixing configuration in the screw profile with several mixing zones, since this fact may increase the density of the cork particles during the compounding.

The effect of cork on the melt viscosity of the polypropylene was accessed by melt flow index (MFI). The addition of cork to the thermoplastic reduces considerably the viscosity and consequently the MFI. The addition of the coupling agent PP-g-MA to the composite promotes an opposite effect and improves the mixability.

The injection moulded PP/Cork composites exhibit low water uptake and the increase of cork fraction, increases the water absorption up to 2.3 wt.% after a period of 1344 hours. It seems that the hydrophobic nature of cork may take some advantage over other natural fibre materials such as wood. It was possible to reduce the water uptake by: (a) increasing the particle size of the cork and (b) by the addition of coupling agent that significantly reduces the water absorption of the CPC.

The morphology evaluated by optical microscopy revealed good dispersion and distribution of cork and a high good cohesion between cork and the polyolefin, even in the absence of coupling agent. No voids were observed in the different conditions.

The composites density is higher than the neat polypropylene and increases with the higher incorporation of cork. The use of coupling agent induces a slight decrease on the density due to a better dispersion of the cork along the matrix.

The mechanical properties under tensile load shows a small reinforcement of around 10% in the stiffness provided by incorporating cork at a 5 wt.%. For higher cork content (i.e. up to 30wt.%) the

tensile properties are reduced. The ability to transfer the stress from the thermoplastic matrix to the cork or reinforcement will depend essentially of the cork-polymer interactions that can be reduced due to the incompatibility between lignocellulosic materials and polymeric matrix. To overcome these limitations it is necessary to promote polymer modification, with the use of polar functional groups, such as maleic anhydride. The mechanical properties were enhanced by the addition of polypropylene graft maleic anhydride (PP-g-MA) in terms of tensile strength and maximum strain. A good balance of the mechanical properties was achieved by using 2 wt.% upt to 4 wt.% of coupling agent. The use of the stearic acid in 2 wt.% does not modify significantly the tensile properties, however a slight increase on the maximum strain was noticed. The stearic acid acts as plasticizer in the cork-polymer system.

One of the main concerns on the use of lignocellulosic in composites is their susceptibility to moisture absorption and the consequent effect on the physical and mechanical properties. The tensile properties of PP/cork composites were compared before and after water immersion tests and revealed to be very similar, which is a clear advantage of the CPC materials.

The use of DSC on the thermal properties of the PP/Cork composites revealed higher crystallization temperatures than neat PP, and their thermal stability was similar to that of PP. The results are according to the achieved in the cork composites obtained by pultrusion, where in this study cork and PP-g-MA acted as nucleating agents during the crystallization process. Cork promoted a small increase on the composite crystallinity up to 30 wt.%, however the enhancement was also dependent on the degree of compatibility between the PP and the cork.

Polypropylene is more susceptible to oxidation when compared with polyethylene due to its chemical structure, requiring higher amounts of antioxidants and stabilizers. Thermal analysis by DSC at 200°C revealed that the addition of cork promotes an antioxidant effect to the polypropylene increasing the time to oxidation. Reducing the cork particle size and consequently increasing the surface area of the particles contributes to a higher thermal-oxidative protection. By using 30 wt.% of cork powder the oxidation was delayed almost 13 times as compared with the neat PP.

Cork is well known to be a good thermal and acoustic insulator material. Unexpectedly, the thermal conductivity of the PP/cork composites increases with the increase of the cork weight fraction. This effect is related with the high pressures applied in the melt based processes increasing the density of the final cork composite and consequently reducing the thermal resistance. The higher capacity for heat transfer on the developed cork composites may result in new potential applications in electric and electronic cover systems.

The maximum incorporation of cork on the polypropylene matrix was 70 wt.% that represents 93% in volume of the cork based composite. This was achieved using cork powder compounded in a counter-rotating twin-screw extruder without die.

Figure 10.3 shows the potential to obtain 3D cork-based composite structures obtained by the injection moulding process, where cork cannot compete alone.

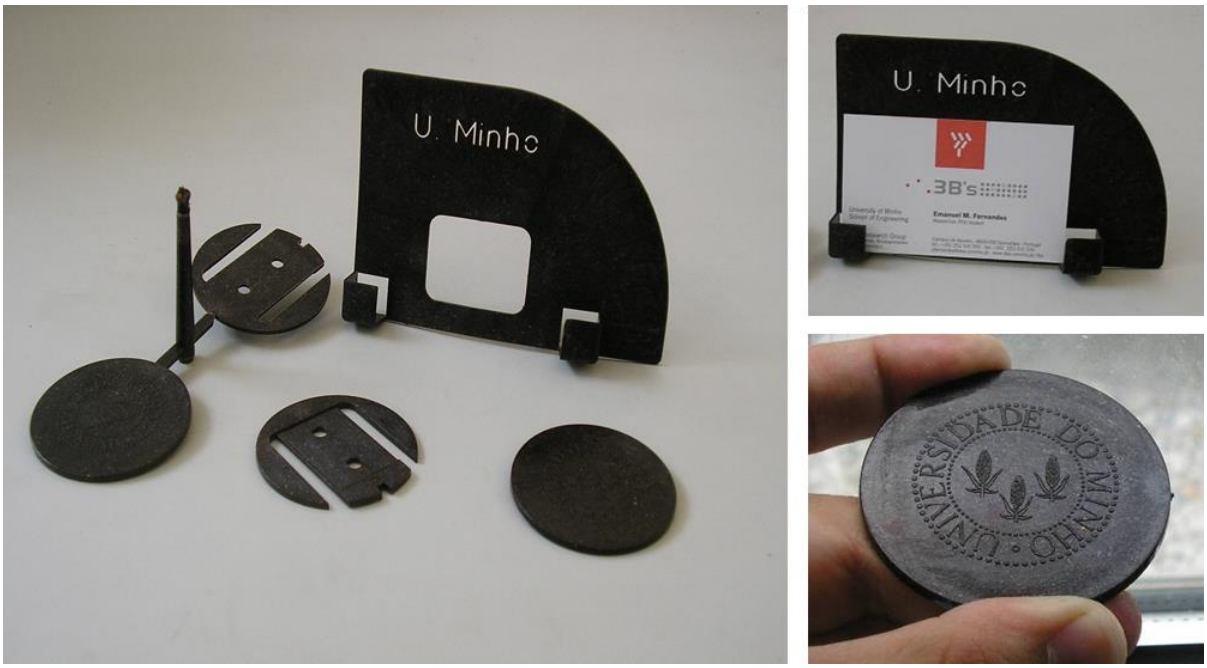

Figure 10.3. CPC materials (50-50) wt.% obtained by injection moulding.

As future work, a better understanding of the rheological behaviour of the developed CPC should be addressed to improve the compounding process. The production of cork-polymer composites materials in a single melt based technology step such as extrusion of a profile must be considered to obtain the final product. In the development of cork-based composite flooring application, the incorporation of substances with the capability to promote electromechanical properties, motion sensors embedded in the composite, or the improvement of conductivity for heating flooring systems will be of high relevance. The developed cork composites may include furniture, flooring and insulation systems, hardware for electronics, outdoor systems, among other sustainable applications.

The need to improve the interface between cork-polymer was previously achieved by the use of coupling agent and it is well known that compatibility between lignocellulosic materials and the polymer matrix plays an important role in determining the properties of a composite. Lignocellulosic materials such as

cork, which have polar hydroxyl groups on the surface, have difficulty to create bonded interfaces with a nonpolar polymer matrix such as polyethylene and polypropylene, limiting their use.

In **Chapter 6**, the used methods from the literature allowed isolating the major fractions from cork (i.e. suberin and lignin) that were confirmed by chemical FTIR analysis. However, it is also known that the structure of the major components of cork has not been fully established.

TGA analysis confirmed that suberin and lignin fractions, isolated from cork, present sufficient thermal stability to be applied in melt based technologies such as extrusion processes.

The research methodology of using a reactive extrusion (REX) process as a reactor, allowed using suberin and lignin as environmentally friendly coupling agents to improve interfacial adhesion of cork-polymer system. REX has the capability of functionalizing, preparing the composite and producing CPC pellets in a single step.

The mechanical tensile tests indicate that the suberin and lignin can be used as bio-based coupling agents in the presence of benzoyl peroxide (BPO) to produce functionalized CPC with superior mechanical properties. Suberin acts as a plasticizer, improving the cork dispersion and reduces the composite´s stiffness, providing additional flexibility and formability to the composite. Lignin shows to act as a coupling agent and the use of 2wt% of lignin improved both maximum tensile strength and modulus in 48% and 39% respectively. Increasing the amount of lignin to 4 wt.% reduces the mechanical performance of the composites. The use of 2wt% of PE-g-MA increases 34% the maximum strength, 30% the tensile modulus and reduces the maximum strain. Coupling agents in CPCs play a very important role in improving compatibility and adhesion between the polar cork material and the non-polar polymer matrices.

All the developed functionalized CPC present low water uptake and thickness swelling variation, displaying similar behavior as compared with coupling agents based on maleic anhydride.

Thermal properties by TGA and DSC reveal that lignin can act as a thermal protective agent and suberin act as an antioxidant agent on the composites, while the PE-g-MA act as both.

Further work should be conducted to deeper understanding this complex system and which of the chemical groups are responsible to contribute to this enhancement on the mechanical properties.

The research methodology present in **Chapter 7** and **Chapter 8**, allowed the production of hybrid cork based composite materials reinforced with short natural fibres (i.e. coconut and sisal fibre). In both chapters, hybrid cork based composites using high density polyethylene as matrix were obtained by twin-screw extrusion followed by compression moulding and presented a cork ratio of 40 wt.% up to 50

wt.%. This reinforcement strategy shows that the lignocellulosic–matrix interaction was improved either via the use of natural fiber, or by modifying the fibre surface, or via the matrix, by employing coupling agents resulting in composites with considerably higher mechanical properties.

The physical modification of the sisal fibres by using alkali treatment (or mercerization) was confirmed by FTIR, showing potential to dissolve some lignin and wax from the fibre surface promoting a cleaner fibre surface to interact with the matrix.

XRD results reflect the influence of the alkali treatment and show a small increase on the crystallinity, confirming the surface modification of the sisal fibres.

In terms of uniaxial tensile strength the mean values of maximum strength of the unmodified sisal is higher compared with the modified fibres. This may be related with the alkali chemical treatment that promoted the reduction of the fibre thickness and some removing of the hemicelluloses and lignin.

The fracture morphology of the hybrid cork based composites reinforced with the short natural fibres by SEM was in accordance with the mechanical results, showing the improved effect of fibre-matrix adhesion in the presence of coupling agent.

The improvement on the mechanical properties under tensile load of the hybrid composites with coconut and sisal was effective in the presence of coupling agent based on maleic anhydride (MA), revealing higher stiffness, strength and elongation at break.

The flexural properties using alkali treated sisal fibres with coupling agent presents an increase of 33% in flexural modulus and an increase of 98% in the strength when compared with unreinforced cork composites. This alkali treatment leads to higher mechanical properties of the composites since cellulose has higher mechanical properties compared to lignin and also increases specific surface area leading to better interaction with the matrix.

Comparing the properties of the hybrid CPC with the polyethylene matrix, it was shown that a reinforcement of the matrix in terms of stiffness and strength at flexural load is achieved mainly after the sisal fibres alkali treatment. In terms of tensile strength, they present similar stiffness and lower strength when compared to the polyethylene matrix. Higher mechanical properties where obtain using wood fibre with coupling agent based on maleic anhydride and the additional results related with this invention are provided in the Appendix (patent WO2011014085 (A3)) of this thesis.

The low values of coefficient of variation of the mechanical properties of the hybrid CPC solutions, supports the homogeneous properties in terms of cork and fibre distribution on the composites.

The Ashby diagram allowed to identify the best developed CPC composite formulation and to visualize the improvement over the CPC without fibre reinforcement.

Weibull diagram was used to reliably identify the composites safety limits. The tensile strength of the hybrid reinforced CPC was found to be in agreement with the Weibull cumulative distribution, which can be used to accurately predict the mechanical properties of the CPC composites.

This reinforcement strategy shows the potential to obtain CPC with superior mechanical performance. This knowledge can be applied in the flooring system to reinforce complex geometries or to improve resistance, to machining or to apply the CPC as structural materials.

Furthermore, different natural fibres should be tested and the cork surface modification attempted to promote cork-matrix compatibility. A deeper understanding of the complex nature of cork and natural fibers and their surface properties is still needed in order to optimize natural fiber surface modification processes. Using materials like natural based composites that reduce construction waste and increase energy efficiency would provide a solution to immediate infrastructure needs while promoting the concept of sustainability.

Chapter 9 shows injection moulded biocomposites combining different biodegradable aliphatic polyesters (i.e. PLLA, PHBV, PCL and SPCL) with cork 30 wt.%. Cork combined with bio-based matrices can originate fully biodegradable composites for sustainable applications. The cork biocomposites were engineered to satisfy acceptable stiffness, strength, and in-service durability while maintaining the tendency for rapid out-of-service biodegradation. A possible application is shown in Figure 10.4 as biodegradable caps for wine bottles.

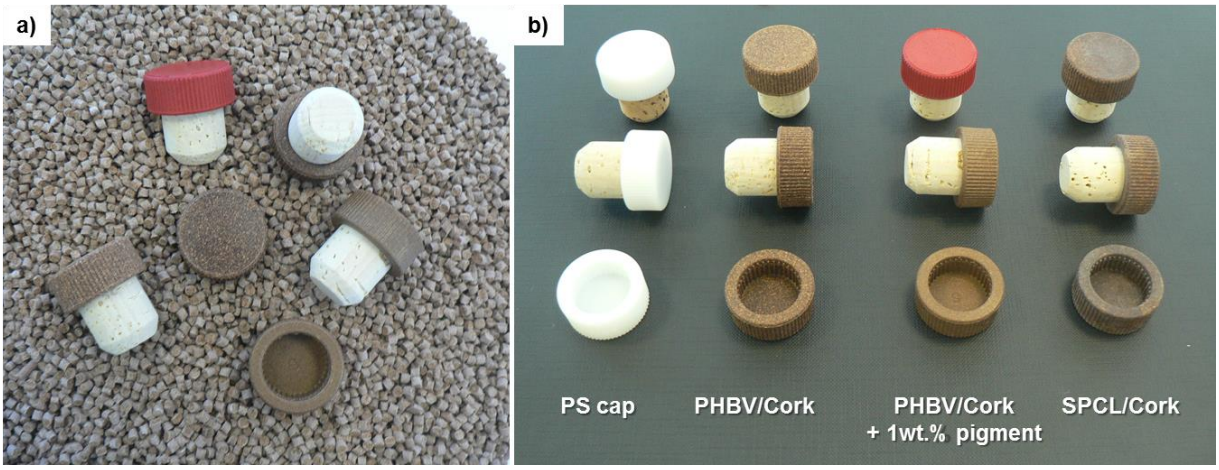

Figure 10.4. Cork biocomposites as cap for wine bottles: a) Prototype of the cap solution and CPC pellets and b) polystyrene (PS) cap and developed biodegradable solutions with cork.

The lower density obtained in the biocomposites is one potential advantage to create lightweight sustainable materials in the automotive area with improved insulation properties.

The injection moulded materials revealed low water absorption, being the higher values corresponding to the biocomposites containing cork and preferably in the presence of the starch.

Cork combined with PLLA and PHBV presents adequate mechanical properties, high dimensional stability under water and reduced density resulting in lightweight biocomposites.

SEM micrographs show that biodegradation was found to occur primarily at the polymer surface and was more pronounced for the materials under burial soil.

Biodegradation of the specimens under burial soil was significantly more severe than under static water with the loss of tensile modulus and maximum strength. After 6 months, the biodegradation of the biocomposites decreased in the following order: SPCL/Cork > SPCL > PCL > PCL/Cork > PHBV/Cork > PHBV > PLLA/Cork and PLLA. During soil burial tests, PCL, SPCL and its biocomposites revealed a sustained weight loss and diminishing on the mechanical properties in terms of tensile modulus and maximum strength with the time. On contrary, the durability of some biocomposites such as PLLA/Cork and PHBV/Cork, that shows lower rate of degradation, results in products that require less maintenance and a much longer life.

The thermal characterization by DSC has evidenced that the presence of cork increases the crystallinity degree for all the used bio-based polyester matrices. The presence of starch decreases considerably the biocomposite crystallinity contributing to an increase of the amorphous phase supporting the higher biodegradation rate. The melting temperature of the cork biocomposites is higher as compared with the aliphatic polyesters due to the thermal resistance of cork material. This behaviour should be taken into account during the melt based process.

TGA analysis confirmed that the biocomposites presented a multi-degradation process, where cork only was able to improve the thermal stability for the PHBV matrix. In the other polyester matrices the presence of cork reduces the initial degradation temperature, being the lower value of 266.9°C for the PCL/Cork biocomposite. Moreover, it was confirmed that cork starts to degrade at 246.3°C, however it contributes to a slower degradation rate of the biocomposites higher temperatures. TGA showed that cork presents higher thermal stability than starch.

The results show the benefits of combining cork with bio-based matrices that can originate fully biodegradable eco-friendly composites. Besides the cost reduction of bio-based matrices by adding cork, it was possible to increase the composite stiffness depending of the used biodegradable polymer, reduce the matrix weight and improve aesthetic characteristics.

Future work on innovative technologies and process solutions should be intensively researched to get the high strength engineering composites which are related to their new applications area. Strategies to reduce composite density, such as (i) the use of cork and (ii) the use of foaming agents in the matrix, without considerable loss on the mechanical performance, must be considered. Based on the literature review of this thesis, there is a great potential on nano structures obtained from lignocellulosic materials that present potential to reinforce these biocomposites, potentiating a new class of cork bionanocomposite materials.

As a final remark, we can say that this thesis allowed developing different classes of cork-polymer composite pellets for different areas of application. In areas where environmental concern, aesthetics, reduced plastic touch and construction capability are required, the composites containing forest based materials such as cork constitute a viable and interesting possibility. Regarding these properties, the applications for the developed cork composites may include furniture, flooring and insulation systems, hardware for electronics, toys for children, outdoor systems, automotive interior applications, among other sustainable applications.

APPENDIXES

Appendix 1. Patent entitled "Cork-Polymer composite (CPC) materials and processes to obtain the same"
WO2009072914 (A1)

Appendix 2. Patent entitled "Fibre-Reinforced cork-based composites"
WO2011014085 (A3)

(12) INTERNATIONAL APPLICATION PUBLISHED UNDER THE PATENT COOPERATION TREATY (PCT)

(19) World Intellectual Property Organization
International Bureau

(43) International Publication Date
11 June 2009 (11.06.2009)

PCT

(10) International Publication Number
WO 2009/072914 A1

(51) International Patent Classification:
C08L 97/00 (2006.01) *C08L 67/04* (2006.01)
C08L 23/12 (2006.01) *C08L 23/06* (2006.01)

(21) International Application Number:
PCT/PT2008/000051

(22) International Filing Date:
2 December 2008 (02.12.2008)

(25) Filing Language: English

(26) Publication Language: English

(30) Priority Data:
103898 4 December 2007 (04.12.2007) PT

(71) Applicant *(for all designated States except US)*: **AMORIM REVESTIMENTOS, S.A.** [PT/PT]; Rua do Ribeirinho, nº 202, P-4536-907 S. Paio De Oleiros (PT).

(72) Inventors; and

(75) Inventors/Applicants *(for US only)*: **FERNANDES, Emanuel Mouta** [PT/PT]; Rua da Senra, nº 309, Vilar do Pinheiro, P-4485-883 Vila Do Conde (PT). **SILVA, Vitor Manuel Correlo da** [PT/PT]; Travessa Doutor Francisco Machado Owen nº 30 Apartamento 33_____a, P-4710 Braga (PT). **CHAGAS, José António Marchão das** [PT/PT]; Urbanização do Formal, nº 10, P-4500-669 Silvade (PT). **REIS, Rui Luís Gonçalves dos** [PT/PT]; Rua João Andersen, 101 - Hab. 2.3, P-4250-242 Porto (PT).

(74) Agent: **MOREIRA, Pedro Alves**; Rua do Patrocínio, 94, P-1399 - 019 Lisboa (PT).

(81) Designated States *(unless otherwise indicated, for every kind of national protection available)*: AE, AG, AL, AM, AO, AT, AU, AZ, BA, BB, BG, BH, BR, BW, BY, BZ, CA, CH, CN, CO, CR, CU, CZ, DE, DK, DM, DO, DZ, EC, EE, EG, ES, FI, GB, GD, GE, GH, GM, GT, HN, HR, HU, ID, IL, IN, IS, JP, KE, KG, KM, KN, KP, KR, KZ, LA, LC, LK, LR, LS, LT, LU, LY, MA, MD, ME, MG, MK, MN, MW, MX, MY, MZ, NA, NG, NI, NO, NZ, OM, PG, PH, PL, PT, RO, RS, RU, SC, SD, SE, SG, SK, SL, SM, ST, SV, SY, TJ, TM, TN, TR, TT, TZ, UA, UG, US, UZ, VC, VN, ZA, ZM, ZW.

(84) Designated States *(unless otherwise indicated, for every kind of regional protection available)*: ARIPO (BW, GH, GM, KE, LS, MW, MZ, NA, SD, SL, SZ, TZ, UG, ZM, ZW), Eurasian (AM, AZ, BY, KG, KZ, MD, RU, TJ, TM), European (AT, BE, BG, CH, CY, CZ, DE, DK, EE, ES, FI, FR, GB, GR, HR, HU, IE, IS, IT, LT, LU, LV, MC, MT, NL, NO, PL, PT, RO, SE, SI, SK, TR), OAPI (BF, BJ, CF, CG, CI, CM, GA, GN, GQ, GW, ML, MR, NE, SN, TD, TG).

Published:
— *with international search report*

WO 2009/072914 A1

(54) Title: CORK-POLYMER COMPOSITE (CPC) MATERIALS AND PROCESSES TO OBTAIN THE SAME

(57) Abstract: The present invention refers to the processes for development of cork polymer composites (CPC) using synthetic, recycled or natural based polymers or blends of these with cork particles or cork waste from the industrial process, which can contain other elements, for example additives and/or compatibilizing agents and/or the raw materials being previously functionalized. The components are mixed in the solid form and further processed, for example in a twin-screw extruder, resulting in pellets that will be subject to a subsequent process, for example compression moulding, injection techniques, among others, in order to obtain materials with different properties comparing with current existent cork products, which could contain or not compatibilizing agents and/or other types of additives in order to facilitate the processing, promote better performance properties or give any additional characteristic.

"CORK-POLYMER COMPOSITE (CPC) MATERIALS AND PROCESSES TO OBTAIN THE SAME"

FIELD OF THE INVENTION

This invention relates to obtaining composite materials from cork with polymer and the methods to obtain the same. More specifically, the invention presents the mixture of at least two constituents, at least one of them being cork, the constituents allowing being pre-functionalized, resulting in cork with polymer composites called as CPC.

STATE OF THE ART

Cork is the outer bark from a tree, which name is cork oak, of the oak's family (Quercus suber L.) and presents an anisotropic structure, as shown in Figure 1, of low density, with a high coefficient of friction and impermeability. It presents excellent properties of thermal, acoustic and antivibrating insulation, has a Poisson coefficient around zero and low thermal conductivity, among others, that make it a material of choice for several applications like is described in Gibson L.J. and Ashby M.F., (2001) 2nd ed.: Cambridge University Press. 453-467, or more recently by Silva S.P. et al., (2005) International Materials Reviews, 50(6). 345-365.

On the other hand cork can be regarded as a composite material comprising a mixture of polymer constituents such as cellulose, lignin and suberin where each component has a specific function in the final performance of the material.

The cork industry gets a large amount of wastes from several ending stages of processing like the cutting, grinding and sanding, as well as wastes coming from existing products such as agglomerates, insulation, called cork dusts as referred by Gil L., (1997). Biomass and Bioenergy, 13(1-2): 59-61, having different particle size and densities with more or less content of impurities according to the quality and operations

to which cork was subjected and which final end is mostly the burning, serving as raw material to feed the boilers in industrial processes.

The mixture between cork and other polymeric materials, particularly the bonding thereof, it is a field with potential to be developed. These are two materials which affinity can be substantially increased, either by superficial modification of one of the components or by use of compatibilizing agents.

There are a small number of patented applications as well as studies related to cork composites. It should be highlighted the patent of Schmidt D., (1983), patent US4373718, reporting applications of thermoplastics with cork applied in hand grips for sport materials; in another patent a study with promising results related to morphological and thermal conductivity level of Barlow C.Y. et al., (1989) Proceedings of the tenth Rise International Symposium, relates to polymer composites with cork waste using only the technique of extrusion, by extrusion of the material to a mould, which is different of guideline presented in this invention; the international patent of Tesch G., (1993) patent WO9324719, describes cork granules forming the visual layer that are compacted with thermoplastic materials under the action of temperature and pressure for insulation applications; in building construction, in laminated floor where the cork of low density is agglomerated with wood particles through synthetic fibres or thermoplastic material (see Thierry M., et al. (2006) patent FR2873953); on furniture (see Jerome M., (1997) FR patent 2741005) where the agglomerated cork is reinforced during the processing with the addition, for example, of cellulose acetate fibres; in the footwear according to Gianfranco L. (1994) patent IT1244750, where the cork is combined with polyurethanes, or moreover in the area of agglomerated composites, according to Gil L. et al., (2005), international patent WO2005003216, which combines waste from the cork stoppers (after its life time) with recycled material from the tetrapak® packaging and the addition of compatibilizing agents or glue in materials for packaging; also in materials with potential for application to ceilings, coating for walls, doors or walls panels (see Gil L. et al. (1991), patent PT94133).

In the process of the cited document, the cork particles are compacted by the effect of temperature and pressure using thermoplastic materials. Besides the advances proposed in this patent to accomplish the process between 1h30m and 2h followed by air cooling during 24 h for dimensional stabilisation, such doesn't happen in the present invention.

Despite several differences comparing with previous process, the present invention uses, besides different processing methodologies, much less material processing and stabilization times when it is necessary use compression moulding, due to the achieving of cork pellets with polymer of natural or synthetic origin at an early stage of the process, which are further used in different processes. Another differentiator factor in the present invention and relating to the compression moulding process, it is that the cooling of the moulding occurs within the mould under the action of water or other refrigerant agent, the mould being or not under pressure, which reduces significantly the stabilization time and provides an excellent surface finishing.

In the field of composite materials, a more recent study proposes simple treatments of boiling cork to increase its thermal stability in order to reinforce the matrix of a thermoplastic material, (see Abdallah F.B. et al., (2006) Journal of Reinforced Plastics and Composites 25 (14), pp. 1499-1506) which is not the case in the method described here, or moreover in the patent of Marti J. et al., (2007) patent EP1803694A1, referring to the potential manufacturing of construction materials including in its base composition a complex mixture of non-recyclable materials with polyethylene, paper, polypropylene, among others, where cork could be present or not in a maximum value of 20%, differentiating itself from the purpose of this invention where the matrix from natural or synthetic origin is combined with cork that is regarded as the principal element of reinforcement due to its unique properties mentioned above.

The combination of cork dust from the industrial process, or the dust of end products with cork, or even of cork granulated, with other polymers from natural or synthetic origin presents a set of potentialities combined with the appropriate processing

technology, allowing obtaining structural products with more complex geometries resulting in new potential applications.

SUMMARY OF THE INVENTION

The present invention relates to a process of production of cork polymer composites, characterized by comprising the steps of:

- preparation and mixture of raw materials,
- composition,
- cooling and,

optionally, followed by

- drying,
- processing,
- obtaining the cork polymer composite,
- mould,
- cut and
- finishing,

wherein

in said step of preparation and mixture of raw materials, these are mixed together in the solid form, in a continuous mechanical mixer, producing an homogeneous mixture,

in said step of composition is used one of the techniques of

pultrusion, at a temperature lower than 200 °C, so as to obtain the half-finished, finished or in pellets form product; or

extrusion, at a temperature lower than 200 °C, so as to obtain the half-finished, finished or in pellets form product under mechanical action by at least a mono-screw or twin-screw extruder,

in said step of cooling, the material from said at least one extruder is cooled by exposure to an air stream, a water bath or a cooling liquid and the like,

in said step of drying, it is only removed the excess moisture from said composition step,

in said step of processing is used one of the techniques of

co-extrusion;

extrusion;

compression moulding, in which a mould is placed into a hydraulic arm press and heated up to a temperature lower than 200 °C for a time period lower than 20 minutes, followed of hot pressing for a time period lower than 20 minutes at a pressure between about 196 and 2950 Kpa, finishing with water cooling or other cooling liquid, inside the mould and for 1 - 10 minutes; or

injection moulding, in which pellets are collected in a reciprocating screw which produce the melting of pellets which molten material is injected into a mould and then cooled with water, cooling liquid or the like; by multimaterial injection; injection with pre-composition; or co-injection.

On an embodiment of present invention the process of production of cork polymer composites is characterized by said step of cooling comprises at least one area of conveying rolls.

On other embodiment the process of production of cork polymer composites is characterized by, in said compression moulding technique of said processing step, the hot pressing is accomplished at a pressure in the range of about 490 to 1770 Kpa.

On a further embodiment the process of production of cork polymer composites is characterized by, in said mould step, said composites with defect being recycled, sent to a granulator or, again, to said step of composition or to said step of pellets production.

On another embodiment of the invention the process of production of cork polymer composites is characterized by, in said cut step, the excess material is re-granulated and sent to the composition step or to the pellets production step.

Still on further embodiment the process of production of cork polymer composites is characterized by, in said processing step, the mould of said moulding technique has a shape similar to a rim and a thickness equal to that of a final board of said composite.

The present invention also relates to a composite of polymer with cork comprising cork dust, granulate or waste and the like, natural, synthetic recycled polymer or mixture thereof, compatibilizing agents and additives characterized by having a composition comprising about

a) 5%-95% by weight of cork dust, granulate or waste or the like;

b) 5%-95% by weight of natural, synthetic recycled polymer or mixture thereof;

c) 0%-20% by weight of at least one type of compatibilizing agent for improving bonding of phases of produced composite;

d) 0%-20% by weight of at least one additive for improving the processability, coloration and the like and for providing UV and/or thermal resistance against abrasion or flame.

On an embodiment the composite of polymer with cork is characterized by said cork constituent and/or said polymeric constituent are functionalized.

On other embodiment the composite of polymer with cork is characterized by comprising any external protection agent applied to other biocide, algaecide, fungicide and/or repellent to water type lenhocellulosic materials and the like.

On a further embodiment the composite of polymer with cork is characterized by its faces allow superficial finishing selected from the group comprising varnish and/or paint coating, adding glues, decorative materials, grinding, rolling, drilling and the like.

The process of the present invention is intended for production of finished products of polymer cork composites.

The process of the present invention is further intended for production of products of polymer cork composites comprising thicknesses of at least 0.5 mm.

The process of the present invention comprises applying compatibilizing agents and/or additives at the polymer cork composite surface either in depth or layered.

The polymer cork composite of the invention is intended for ceilings, floors, footers, doors, and partitions insulation applications, in the field of furniture, automobile engines, in the field of footwear, and the like.

BRIEF DESCRIPTION OF FIGURES

The description of present application is supported by following figures:

Figure 1: Cork morphology according the tangential cross section (a) and according the radial cross section (b) (magnification x 300)

Figure 2: Schematic description of the necessary stages to obtaining cork waste based composites, according to the polymer to be used and the envisaged application.

Figure 3: fracture surface using liquid nitrogen showing the adhesion between the two phases of a CPC composed by Cork + PVC (45-55%) after the process of compression moulding under action of temperature and pressure of the pellets. At low magnifications (of ×50 (figure a)) there is observed the two phases present in the composite and at higher magnifications (of ×700 (figure b)) there is found the adhesion between the two phases.

Figure 4: The table represents the behaviour of water absorption (%) of boards processed by extrusion, followed by compression moulding, of CPC samples: 1 - Sanding Powder + Recycled Polymer (50-50%), 2 - External Powder + PE (49-49%), 3 - External Powder + PP (49-49%), 4 - Board of PP, 5 - External Powder + PE (49-49%) + cork layer (0.5 - 1mm) without the addition of glue.

Figure 5: The table presents the composition of each CPC by weight as well as the tensile mechanical properties: each material modulus at 1% of strain using linear regression, as well as the maximum stress (σ Max) of the composites processed by compression moulding.

Figure 6: Fracture surface after tensile testing of the CPC: Sanding powder + PE (50-50%) (magnifications of ×50 and ×700).

Figure 7: The table presents the composition of several CPC by weight, with and without compatibilizing agent, and one mixture of pellets of grinding powder with polypropylene and compatibilizing agent (49-49%) mixed with sanding

powder with polypropylene (50-50%), as well as the tensile mechanical properties: modulus of each material at 1% of deformation using linear regression as well as maximum stress (σMax) of the composites processed by compression moulding.

DETAILED DESCRIPTION OF THE INVENTION

This invention aims the development of composites based on cork or cork waste resulting of the process of cork industry with polymers from natural, synthetic or recycled origin, allowing integrate the normal processes of transformation of several companies from the polymer and cork industry. The described method (based on Figure 2) can be developed in a continuous or discontinuous way and has the following stages:

Stage 1: Raw Materials

This stage consists on the selection of raw materials in accordance with the formulation and the stages required.

At this stage the raw materials from natural or synthetic origin can be submitted to a chemical modification by using alkaline or acid treatments, plasma treatments or corona discharge, to improve the surface characteristics. It can be submitted to functionalization processes, for example with amino groups, epoxy, isocyanates, acrylic acid, anhydrides, methacrylate, phenol, melanin, among others, to promote better adhesion between the cork-polymer constituents as it occurs with other lenhocellulosic materials, or further being submitted to simple operations of washing with one or more solvents, and drying of the cork wastes. As an alternate solution to the functionalization, it will be use previously functionalized polymers.

The composite formulation can include:

About 5%-95% by weight of powder or granulated cork with different densities or cork dust from the industrial process known as grinding powder, sanding powder, or from technical products such as the floating powder, among others, or from the mixture of more than one variety of cork waste.

About 5%-95% by weight of polymer from natural origin, synthetic or recycled in accordance with the intended application.

About 0%-20% by weight of compatibilizing agents.

Around 0%-20% by weight of other additives.

Stage 2: Mixture of raw materials

At this stage the raw materials are mixed in the solid form, together, in a continuous mechanical mixer, creating a homogeneous mixture that will feed the stage 3.

Stage 3: Composition

For compounding cork-polymer composites using raw materials, previously functionalized or not, two processing techniques can be used in order to obtain the pellets. Both allow, by effect of temperature and shear stress, to obtain a raw material in which the different constituents of the composite are mixed and bonded. In the process of pultrusion it is possible to obtain directly the product on its semi-final or final shape or in the form of pellets to be further used in other processing processes (extrusion, pultrusion, injection moulding and compression moulding). In the case of extrusion, there is a mono-screw or preferably twin-screw extruder and may be co-rotating or preferably counter-rotating disposed horizontally and/or vertically (one or more extrusion machines) in the

process. Moreover, during the extrusion process it will be possible to obtain directly the CPC in the semi-final or final shape, allowing in this case being a profile more or less complex according to the geometry of the extruder die, or in the form of pellets which will be used later in other transformation processes. The reactive extrusion can be used to functionalize the raw materials and simultaneously to allow obtaining the different CPC compositions in the form of pellets or in the form of final product.

Stage 4: Cooling

At this stage, the material only from the extruder , in the form of pellets or in the final form of product, is cooled at room temperature or with the use of a air stream and/or with a water bath and going directly to stage 5, followed or not by an area with rolls, preferably placed near to the extruder die.

Stage 5: Pellets Manufacturing

At this stage the extruded material from stage 4 is grained for obtaining CPC pellets, which will be further send directly to other equipment, for example, for an injection moulding machine.

Stage 6: Drying

At this discontinuous stage of the process, the drying of material (pellets) from the extrusion process is used only to remove the moisture in excess.

Stage 7-9: Processing

The stages mentioned here correspond to the use of different processing methodologies to transform the CPC in the final product, which means they are subsequent pellets achievement.

In this stage, extrusion or co-extrusion will be used. The extrusion process is described in stage 3 and can only be applied if the polymer selected in stage 1 allows it. Once again the processing temperatures must be lower than the 200°C. As in stage 3, the equipment allows the introduction of additives that can be added to confer a specific property to the final product, such as for example, better mechanical properties, fire resistance among others.

In the compression moulding process, a mould with geometry and thickness according to the intended application can be feed manually, by gravity or through a conveyor belt that is feed continuously. The mould may contain or not in one or both sides a release film, for example a Teflon sheet, comprising the pellets mass homogeneously distributed. The mould, with the amount of material needed in its interior, will be placed in a hydraulic arm press and heated to a temperature lower than 200 °C for a period of time lower than 20 minutes for melting and homogenization of pellets mass and subsequently hot pressed for a period lower than 20 minutes (preferably the pellets mass should be under pressure from the beginning), at a pressure between 196 and 2950 kPa, preferably between 490 and 1770 kPa, followed by cooling with water, or any other coolant liquid, inside the mould and under pressure during 1-10 min, this period of time allowing to reduce the temperature of the material so as to enable unmoulding it without any kind of damage. Finally the pressure is removed and the small contraction that occurs in the sample allows the easy unmoulding of the composite from the system.

During the placement of the pellets inside the mould, granulated cork without addition of glue can be added in one or both faces of the mould and preferably in a single step, before applying temperature for a short period of time on the mass of the pellets

(this mass can be pre-heated to promote an increment on thermal conductivity) followed by a small pressing, in order to create a CPC with one or both faces coated with a cork layer or a film without the addition of glue, the cork granules can be replaced by a decorative sheet, for example a sheet of wood, a sheet of agglomerated cork or natural cork among others.

In injection moulding, the pellets are collected through the feeder or hopper, then falling by gravity into a reciprocating screw that promotes, by action of temperature and shear stresses generated by drag, the melting of the pellets obtained in stage 3 or 5. Then the molten material is injected into a mould with the shape of the desired product, the mould allowing being cooled with water or other type of coolant liquid to quickly lower the temperature of the CPC. Also, could be used unconventional techniques such as multimaterial injection moulding, injection moulding with pre-composition, co-injection, where, in all cases, the processing temperatures should not exceed 200 °C, the equipments configuration, such as in the extrusion process, can be in vertical and/or in horizontal position.

Stage 10: CPC composite

In this stage is obtained a composite material with geometry and structural stability (rigid or more flexible), according to the intended application. The developed composites presents a good bonding between its constituents as shown in Figure 3, good corrosion resistance, reduced water absorption and low thermal and electrical conductivity.

Stage 11: Mould

At this stage and in the case of obtaining a CPC with defects resulting from one or more of the previous processing stages, and the constituents could be subjected to more than one thermal cycle, the latter could be sent to a granulator or to stage 3 or 5

and may be added to process in a certain percentage according to desired final mechanical properties.

Stage 12: Cut

At this stage the CPC is cut according to the desired dimensions and shape and in accordance with the processes of stage 7-9. The exceeded material will be re-granulated and sent to stage 3 or 5, which may be added in small amounts in the composition of new CPC.

Stage 13: Finishing

At this stage the composite can be submitted to several operations such as laminating, milling, sanding, drilling, application of a coating, paint, varnish or glue, in which can further be applied compounds that promote thermal, abrasion and ultraviolet (UV) resistance, once the constituents in their composition may have a higher or lower number of chromophore groups, and may suffer photo-oxidation. Although cork is a material with good thermal resistance it may be necessary to increase the resistance of the polymer phase. Still at the finishing stage and according to the final product it may be introduced, among others, a biocide, algaecide, fungicide or a repellent to water.

Stage 14: Product

The resulting product of process called CPC is characterized by presenting an excellent appearance, good chemical resistance, the physical properties includes a good dimensional stability, more or less resilience and low thermal and electrical conductivity, good acoustic properties according to the amount by weight of cork introduced in the initial composition, may have several 2D and 3D geometries, such as, for example, a

profile, board, among others, according to the stages of processing and final application. The method described in this invention also allow to obtain 100% natural CPC.

The product presents high potential either combined or not with other materials, can be applied as an insulate element in roofs, floors, footers, doors, partitions, in the field of furniture, in joints for automobile engines, in the field of footwear, among others, through the incorporation of cork in polymer materials. This invention is further explained by the following examples, but these should not be considered as limiting the scope of the present invention.

EXAMPLES

Example 1:

Experimentally, compositions were prepared using just two materials: polymer-residue. Of the tested residues, some of them are cork residues coming from the industrial process, namely sanding powder, or grinding powder residues, or floating powder residues with density of 150 - 400 kg/m^3. The polymer used was polyethylene with melting point of 136.6°C (determined by Differential Scanning Calorimetry). For all cases, the polymer/cork dust ratio was equally proportional by weight between the two materials (50/50 %). Before starting the compounding process, each composition was placed separately into a mechanical agitator, for 10 minutes, for mixing and homogenizes both constituents. Each composition was placed alternately into a counter-rotating twin-screw extruder with a die of circular geometry, which allowed the composition and posterior production of pellets thereof, obtaining by this way different formulations of cork powder residues composites with polyethylene (CPC) in the pellet shape.

Afterward, a mass of pellets (about 70g) from each composition was collected and placed into a similar mould with a rim of rectangular geometry (about 20x23 cm^2) and 3 mm of thickness, containing on its base a removable cover over which a Teflon

unmoulding sheet was placed in both faces comprising the pellets mass uniformly delivered. This system is placed in a hydraulic arm press at a temperature between 140-170 °C depending on the type of cork residue used in achievement of pellets, for a period of about 8 min to melting and homogenization of the pellets mass, and further pressed for a 2 min period at a pressure of 1.42 MPa followed by cooling with water inside the mould and under pressure for 5 min, this time allowing to take mass to temperatures near to the room temperature. Finally the pressure is removed and the small contraction that occurs on the board allows the easy unmoulding of composite material from the system.

The boards from the cork composites or CPC so obtained present a thickness of 3 ± 0.1 mm and show a brownish colour where the cork particles distributed in the entire surface can be seen, with higher or smaller size according to the type of cork residue used. The boards from the different CPC produced formulations are rigid and present a density of about 1 ± 0.1 g/cm^3, at room temperature present low water absorption as can be seen in Figure 4. Using these boards, tensile test pieces with standard dimensions were prepared and further submitted to traction at a 5 mm/min speed, obtaining the tensile mechanical properties described in Figure 5. The morphology presented in Figure 6 denotes a good adhesion between the CPC constituents.

Example 2:

The same type of cork residues from example 1 were used and mixed with another thermoplastic material, called polypropylene (PP) with a melting point of 153,2 °C (determined by Differential Scanning Calorimetry), in a ratio of 50-50%. The composites were processed according the methodology described on example 1. Boards from different formulations of CPC were obtained showing a surface appearance similar to the composites with polyethylene but with mechanical properties slightly different as shown in Figure 7 due to the use of a different thermoplastic material.

Example 3:

The same type of sanding powder residue from the previous example was used to compound in a 50-50% ratio by weight with a polymer made up of a blend of several recycled polymers, obtaining the pellets by the same extrusion process described above and subsequently the board by hot pressing at 150 °C followed by water cooling inside the mould as described on example 1. The CPC board is rigid and has a thickness of 3 ± 0.1 mm, presents a surface with a mixture of brownish colours combined with small coloured dots due to different recycled thermoplastic used and dispersed in all the board, also being characterized by possessing a density of about 1 ± 0.1 g/cm^3, presents a low water absorption at room temperature but a slightly higher comparing to the previous examples described on Figure 4. Regarding to mechanical properties, it presents a modulus at 1% of tensile deformation of 312.3 ± 17.8 MPa and an ultimate tensile strength of 8.6 ± 0.6 MPa, presenting a strain at break of 4.1 ± 0.3%.

Example 4:

The same materials from example 2 were used, but this time in a ratio of 49-49% by weight between both to allow the addition of 2% of a compatibilizing agent to facilitate the mixture and promote the adhesion of the polymeric phase with the cork, obtaining pellets and further boards from the different cork composites formulations (CPC), following the methodology described on example 1 process. The surface aspect of these composites is similar to the ones of examples 1 and 2 processed with PE and PP. The cork based composites (CPC) processed according to this methodology possess a density of 1 ± 0.1g/cm^3, present low water absorption at room temperature as presented in Figure 4, but have better tensile mechanical properties as shown in Figure 7.

Example 5:

After obtaining the pellets according to the example 1, 37.5 g of pellets from the grinding powder formulation with PP (49-49%) and 2% of compatibilizing agent were removed and mixed with 37.5 g of pellets from the sanding powder formulation with PP (50-50%), where were further processed by compression moulding as described on example 1. It was obtained a homogeneous and stiff board from composite material, presenting no significant visual differences and intermediate values of mechanical properties, namely tensile, were obtained relatively to the properties initially presented by each pellets quality, as shown in Figure 7.

Example 6:

A composition of cork granules (0.5-1 mm) and a polyhydroxybutyrate (PHB) with a melting point of 170 °C (determined by Differential Scanning Calorimetry) was used and a composite of 50-50% by weight was prepared by process described on example 1, obtaining a 100% natural CPC board of brownish colour showing at the surface only the agglomerate cork particles and very pleasant to touch. Moreover, the boards produced with this cork based composite (CPC) are stiff and present a density of about 0.95 g/cm^3. In terms of tensile mechanical properties, they present a modulus at 1% of strain of 313.3±32.0 MPa and an ultimate tensile strength of 9.5±0.5 MPa, presenting a strain at break of 5.5±0.6%.

CLAIMS

1. Process of production of cork polymer composites, characterized by comprising the steps of:

- preparation and mixture of raw materials,
- composition,
- cooling and,

optionally, followed by

- drying,
- processing,
- obtaining the cork polymer composite,
- mould,
- cut and
- finishing,

wherein

in said step of preparation and mixture of raw materials, these are mixed together in the solid form, in a continuous mechanical mixer, producing an homogeneous mixture,

in said step of composition is used one of the techniques of

pultrusion, at a temperature lower than 200 °C, so as to obtain the half-finished, finished or in pellets form product; or

extrusion, at a temperature lower than 200 °C, so as to obtain the half-finished, finished or in pellets form product under mechanical action by at least a mono-screw or twin-screw extruder,

in said step of cooling, the material from said at least one extruder is cooled by exposure to an air stream, a water bath or a cooling liquid and the like,

in said step of drying, it is only removed the excess moisture from said composition step,

in said step of processing is used one of the techniques of

co-extrusion;

extrusion;

compression moulding, in which a mould is placed into a hydraulic arm press and heated up to a temperature lower than 200 °C for a time period lower than 20 minutes, followed of hot pressing for a time period lower than 20 minutes at a pressure between about 196 and 2950 Kpa, finishing with water cooling or other cooling liquid, inside the mould and for 1 - 10 minutes; or

injection moulding, in which pellets are collected in a reciprocating screw which produce the melting of pellets which molten material is injected into a mould and then cooled with water, cooling liquid or the like; by multimaterial injection; injection with pre-composition; or co-injection.

2. Process of production of cork polymer composites, according to claim 1, characterized by said step of cooling comprises at least one area of conveying rolls.

3. Process of production of cork polymer composites, according to claim 1, characterized by, in said compression moulding technique of said processing step, the hot pressing is accomplished at a pressure in the range of about 490 to 1770 Kpa.

4. Process of production of cork polymer composites, according to claim 1, characterized by, in said mould step, said composites with defect being recycled, sent to a granulator or, again, to said step of composition or to said step of pellets production.

5. Process of production of cork polymer composites, according to claim 1, characterized by, in said cut step, the excess material is re-granulated and sent to the composition step or to the pellets production step.

6. Process of production of cork polymer composites, according to claim 1, characterized by, in said processing step, the mould of said moulding technique has a shape similar to a rim and a thickness equal to that of a final board of said composite.

7. Composite of polymer with cork comprising cork dust, granulate or waste and the like, natural, synthetic recycled polymer or mixture thereof, compatibilizing agents and additives characterized by having a composition comprising about

a) 5%-95% by weight of cork dust, granulate or waste or the like;

b) 5%-95% by weight of natural, synthetic recycled polymer or mixture thereof;

c) 0%-20% by weight of at least one type of compatibilizing agent for improving bonding of phases of produced composite;

d) 0%-20% by weight of at least one additive for improving the processability, coloration and the like and for providing UV and/or thermal resistance against abrasion or flame.

8. Composite of polymer with cork according to claim 7, characterized by said cork constituent and/or said polymeric constituent are functionalized.

9. Composite of polymer with cork according to claims 7 and 8, characterized by comprising any external protection agent applied to other biocide, algaecide, fungicide and/or repellent to water type lenhocellulosic materials and the like.

10. Composite of polymer with cork according to claims 7 to 9, characterized by its faces allow superficial finishing selected from the group comprising varnish and/or paint coating, adding glues, decorative materials, grinding, rolling, drilling and the like.

11. Use of process of claims 1 to 6, characterized by being intended for production of finished products of polymer cork composites.

12. Use of process according to claim 11, characterized by being intended for production of products of polymer cork composites comprising thickness of at least 0.5 mm.

13. Use of process according to claims 11 and 12, characterized by comprising applying compatibilizing agents and/or additives at the polymer cork composite surface either in depth or layered.

14. Use the polymer cork composite of claims 7 to 10, characterized by being intended for ceilings floors, footers, doors, and partitions insulation applications, in the field of furniture, automobile engines, in the field of footwear, and the like.

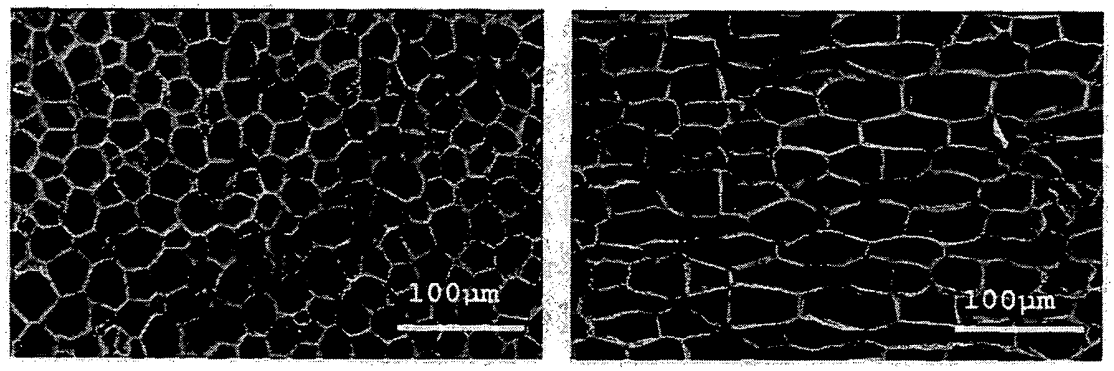

a) b)

Figure 1

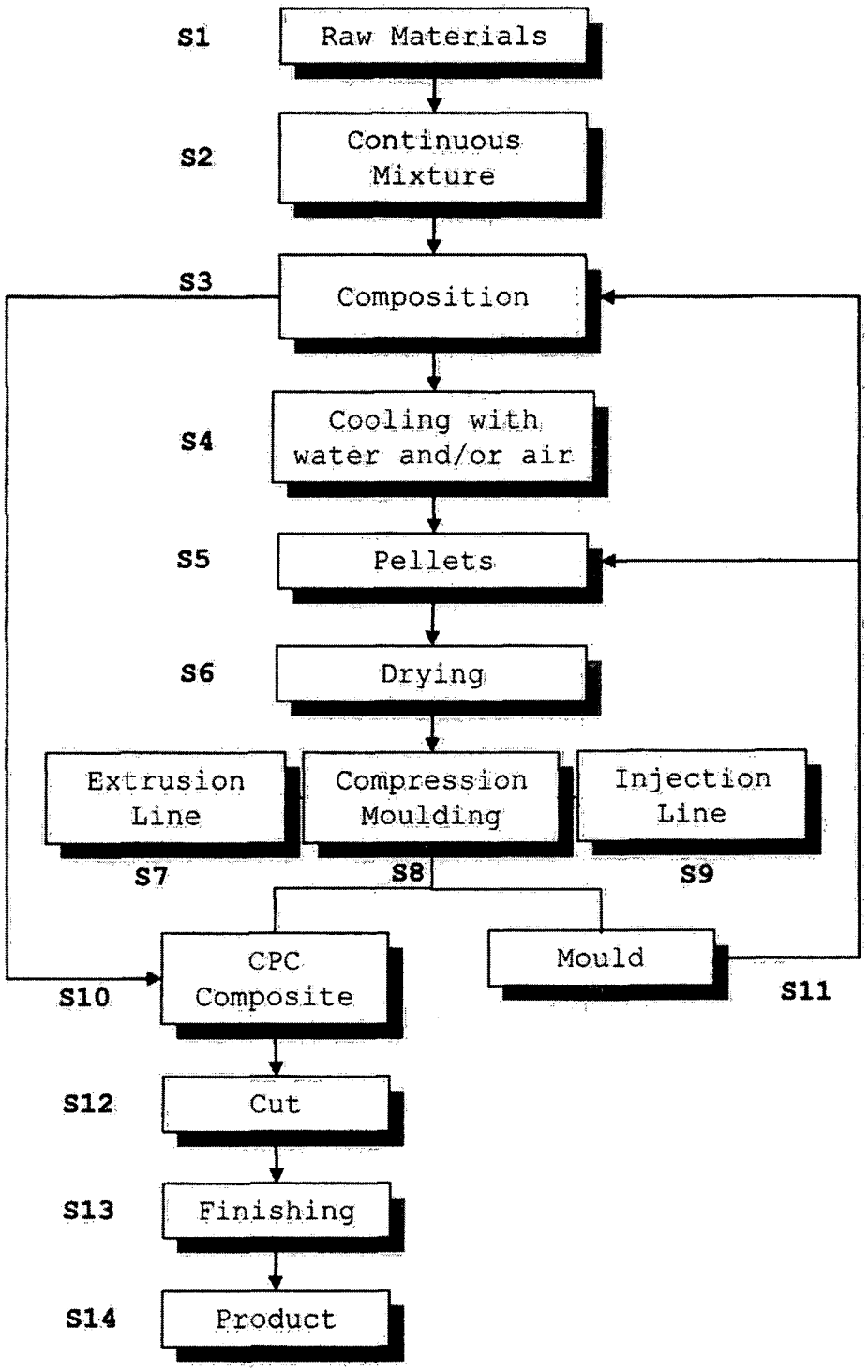
S1
Raw Materials
S2
Continuous Mixture
S3
Composition
S4
Cooling with water and/or air
S5
Pellets
S6
Drying
Extrusion Line
Compression Moulding
Injection Line
S7
S8
S9
CPC Composite
Mould
S10
S11
S12
Cut
S13
Finishing
S14
Product

Figure 2

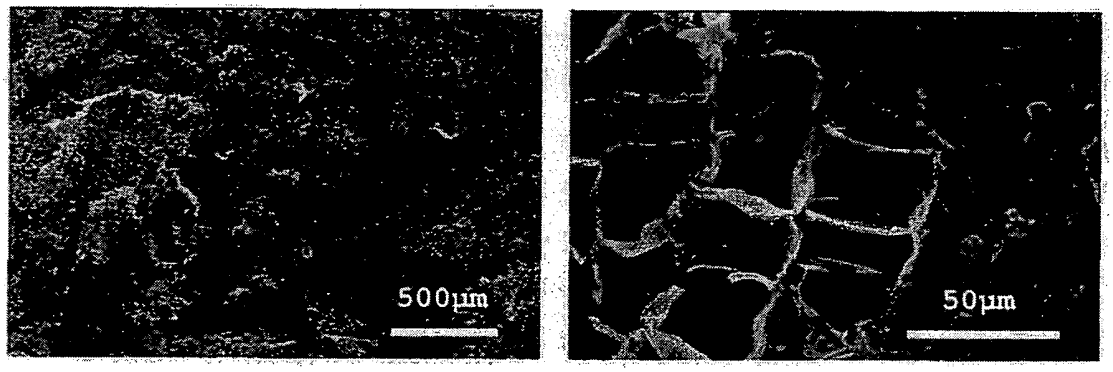

a) b)

Figure 3

	Water Absorption (%)			
Sample	**2h**	**24h**	**48h**	**192h**
1	0.32±0.01	1.06±0.08	1.53±0.13	3.17±0.35
2	0,21±0.02	0.69±0.02	0.92±0.02	1.81±0.04
3	0.12±0.02	0.48±0.02	0.73±0.04	1.38±0.04
4	0.00	0.00	0.00	0.00
5	3.75±0.33	8.70±0.62	10.56±0.80	14.40±1.03

Figure 4

Cork / Quality	Polymer	Composite	Modulus (MPa)	σ max (MPa)
Sanding Powder	PE	(50-50%)	365.3 ± 39.8	14.5 ± 0.9
External Powder		(50-50%)	484.9 ± 18.7	12.4 ± 1.0
Floating Powder		(50-50%)	381.7 ± 19.1	12.4 ± 0.8

Figure 5

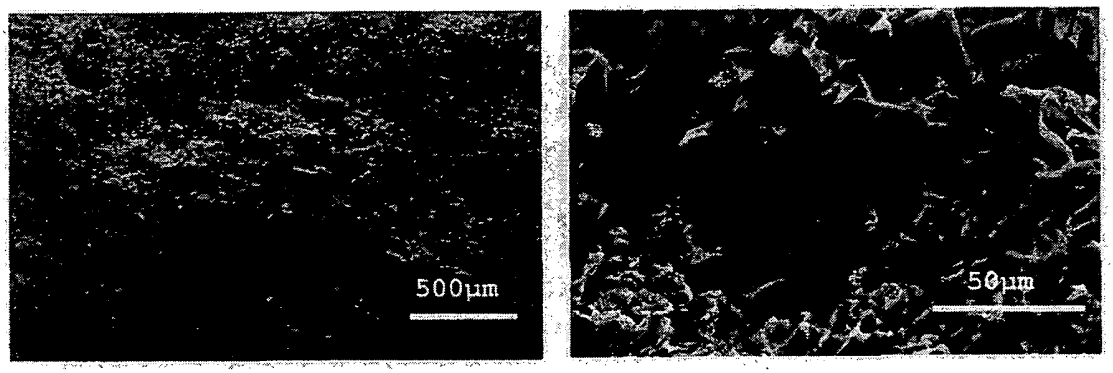

a) b)

Figure 6

Cork/Quality	Polymer	Composite	Modulus (MPa)	σ max (MPa)
Grinding Powder	PP	(50-50%)	597.4±58.0	16.1±1.9
Sanding Powder		(50-50%)	523.6±33.5	13.3±0.7
Grinding Powder	PP + Compatibilizing agent	(49-49%)	650.5±64.6	18.7±1.1
Sanding Powder		(49-49%)	540.7±19.3	17.8±0.8
Mixture	PP	(50-50%)	605.27±33.9	13.9±0.4

Figure 7

(12) INTERNATIONAL APPLICATION PUBLISHED UNDER THE PATENT COOPERATION TREATY (PCT)

(19) World Intellectual Property Organization
International Bureau

(43) International Publication Date
3 February 2011 (03.02.2011)

PCT

(10) International Publication Number
WO 2011/014085 A2

(51) **International Patent Classification**:
C08J 5/12 (2006.01)

(21) **International Application Number**:
PCT/PT2010/000033

(22) **International Filing Date**:
21 July 2010 (21.07.2010)

(25) **Filing Language**: English

(26) **Publication Language**: English

(30) **Priority Data**:
104704 31 July 2009 (31.07.2009) PT

(71) **Applicant** *(for all designated States except US)*: **AMORIM REVESTIMENTOS, S.A.** [PT/PT]; Rua do Ribeirinho, nº 202, P-4536-907 S. Paio de Oleiros (PT).

(72) **Inventors; and**

(75) **Inventors/Applicants** *(for US only)*: **FERNANDES, Emanuel Mouta** [PT/PT]; Rua da Senra, nº 309, Vilar do Pinheiro, P-4485-883 Vila do Conde (PT). **SILVA, Vitor Manuel Correlo da** [PT/PT]; Travessa Doutor Francisco Machado Owen nº30 Apartamento 33, P-4710 Braga (PT). **CHAGAS, José António Marchão das** [PT/PT]; Urbanização do Formal, nº 10, Silvade, P-4500-669 Espinho (PT). **REIS, Rui Luís Gonçalves dos** [PT/PT]; Rua João Andersen, 101 - Hab. 2.3, P-4250-242 Porto (PT).

(74) **Agent**: **MOREIRA, Pedro Alves**; Rua do Patrocínio, 94, P-1399 - 019 Lisboa (PT).

(81) **Designated States** *(unless otherwise indicated, for every kind of national protection available)*: AE, AG, AL, AM, AO, AT, AU, AZ, BA, BB, BG, BH, BR, BW, BY, BZ, CA, CH, CL, CN, CO, CR, CU, CZ, DE, DK, DM, DO, DZ, EC, EE, EG, ES, FI, GB, GD, GE, GH, GM, GT, HN, HR, HU, ID, IL, IN, IS, JP, KE, KG, KM, KN, KP, KR, KZ, LA, LC, LK, LR, LS, LT, LU, LY, MA, MD, ME, MG, MK, MN, MW, MX, MY, MZ, NA, NG, NI, NO, NZ, OM, PE, PG, PH, PL, PT, RO, RS, RU, SC, SD, SE, SG, SK, SL, SM, ST, SV, SY, TH, TJ, TM, TN, TR, TT, TZ, UA, UG, US, UZ, VC, VN, ZA, ZM, ZW.

(84) **Designated States** *(unless otherwise indicated, for every kind of regional protection available)*: ARIPO (BW, GH, GM, KE, LR, LS, MW, MZ, NA, SD, SL, SZ, TZ, UG, ZM, ZW), Eurasian (AM, AZ, BY, KG, KZ, MD, RU, TJ, TM), European (AL, AT, BE, BG, CH, CY, CZ, DE, DK, EE, ES, FI, FR, GB, GR, HR, HU, IE, IS, IT, LT, LU, LV, MC, MK, MT, NL, NO, PL, PT, RO, SE, SI, SK, SM, TR), OAPI (BF, BJ, CF, CG, CI, CM, GA, GN, GQ, GW, ML, MR, NE, SN, TD, TG).

Published:

— *without international search report and to be republished upon receipt of that report (Rule 48.2(g))*

WO 2011/014085 A2

(54) **Title**: FIBRE-REINFORCED CORK-BASED COMPOSITES

(57) **Abstract**: Composites produced from cork, reinforced with natural or synthetic fibres are disclosed. The polymeric matrix can be made of natural, synthetic or recycled polymers. In order to control the mechanical properties of the resulting composites, binders may be added or applied functionalizing technologies for improving binding between fibres and/or cork and the polymeric matrix. The composites of the invention can be prepared using several melting-based processing techniques. The resulting composites have improved thermal and acoustic insulation properties due to the inclusion of cork, being their mechanical characteristics significantly improved by the incorporation of natural and/or synthetic fibres, such that they can be used in the construction, inland transport, aeronautic, shipbuilding, furniture and automobile industries.

"FIBRE-REINFORCED CORK-BASED COMPOSITES"

FIELD OF THE INVENTION

The present invention relates to composites and biocomposites produced from different cork materials reinforced with natural or synthetic fibres. More specifically, it relates to cork composites with synthetic, recycled or natural derived polymers, or combinations thereof, reinforced with natural and/or synthetic fibres, preferably using at least one binder.

BACKGROUND OF THE INVENTION

Composite materials typically consist of a continuous matrix and of a dispersed, fibrous or discontinuous, second phase which can reinforce the material, function as filler, modify magnetic or electrical properties, and improve wear or erosion strength, such that its combination results in the product features.

In recent years there has been an increasing interest concerning cork raw material and its potential use in composite applications, by combining this natural raw material with polymers functioning as binders.

There are a few innovative applications dealing with realistic and cost-effective alternatives for industrial by-products derived from the cork industry which are mostly burned to produce energy for industrial processes or dumped in the ground.

FR 2741005 application discloses a composite material made of cork agglomerate which is reinforced with fibres during manufacture, which fibres can be of cellulose acetate and is potentially useful in furniture.

EP 1482163 A2 application discloses an insulation material formed from a mixture of cork particulate, having 40 to 120 mesh or less, with a plurality of synthetic fibres and a siloxane based binder (silicone), optionally using a primer and a binder, wherein components are mixed and sprayed onto a surface to be protected. The insulation material may have a homogeneous or non-homogeneous composition and can be used in rocket engines and airframe structures.

More recently, WO 2008/114103 application discloses the use of cork powder or residues, wood residues, fibre powder, wood shavings and wood dust in a particle agglomeration process using a pre-polymer with a di-isocyanate and possibly a catalyst, for use in wood and cork industrial sectors, often designated as the boards and veneers sub-sectors and in the cork agglomerates sub-sector, having a very long material stabilization stage.

WO 2007093521 A1 application discloses a process for producing mouldings from cork particles derived from bottle cork manufacturing, the cork particles being bonded with thermoplastic polymers. More specifically, WO 2007093521 A1 application provides a method where the thermoplastic polymer is used in the form of a water-soluble polymer powder, comprising one or more base polymers, protective colloids and, optionally, anticaking agents. Furthermore, the cork and synthetic polymer particles are mixed and then converted into mouldings under pressure. The material is useful in the footwear, clothing, furniture, sports, leisure and construction industry.

PCT WO 2009072914 A1 application relates to methods for obtaining composite materials from cork with polymers by mixing at least two components, at least one being selected from granulated cork or cork dust, wherein components can be pre-functionalized, resulting in pellets which are subsequently used in another process or directly converted into the final product by applying conventional or non-conventional melting technologies, for potential use in different fields and in applications requiring complex geometry as well.

Last two prior-art documents disclose thermoplastic composites having good mechanical characteristics. However, surprisingly, the composites of the present invention reinforced with natural or synthetic fibres, and preferably having a binder to provide a good chemical binding between different phases, considerably improve the tensile, bending and impact strength.

SUMMARY OF THE INVENTION

The present invention relates to a fibre-reinforced cork-based composite comprising at least three components, wherein a first component is a cork-based material, a second component is a thermoplastic material and a third component is reinforcing fibres.

In an embodiment, the fibre-reinforced cork-based composite comprises:

(a) 10% to 75% by weight of cork-based material;
(b) 20% to 80% by weight of thermoplastic material;
(c) 1% to 35% by weight of fibres, and

further comprises

(d) 0.5% to 12% by weight of binders.

In another embodiment, the fibre-reinforced cork-based composite comprises:

(a) 20% to 70% by weight of cork-based material;
(b) 40% to 60% by weight of thermoplastic material;
(c) 10% to 30% by weight of fibres;
(d) 1% to 10% by weight of binders.

In a further embodiment, the fibre-reinforced cork-based composite comprises:

(a) 25% to 60% by weight of cork-based material;
(b) 35% to 50% by weight of thermoplastic material;
(c) 10% to 25% by weight of fibres;
(d) 1% to 10% by weight of binders, and

further comprises

(e) 0.5% to 10% by weight of additives.

Still in a further embodiment, the fibre-reinforced cork-based composite comprises:

(a) 30% to 55% by weight of cork-based material;
(b) 35% to 45% by weight of thermoplastic material;
(c) 12% to 20% by weight of fibres;
(d) 1% to 9% de binders.

Yet in another embodiment, the fibre-reinforced cork-based composite comprises about:

40% by weight of cork-based material,
40% by weight of thermoplastic material,
15% by weight of fibres,
3% by weight of binders and
2% by weight of additives.

In another embodiment, said cork-based material is selected from the group comprising granulated cork, cork dust, cork residues and combinations thereof.

In another embodiment, said thermoplastic material is selected from the group comprising synthetic, recycled and natural materials, and combinations thereof.

Still in a further embodiment, said thermoplastic material is selected from the group comprising polyethylene, polypropylene, ethylene, alkyl or aryl anhydride, ethylene acrylate homo- or copolymer, polystyrene, polycarbonate, polymethylmethacrylate, polyvinyl chloride, polyamide, polyurethane, polyethylene terephthalate, poly(butylene succinate), polylactide, polycaprolactone, polyhydroxyalkanoate and the like, and combinations thereof.

Yet in a further embodiment, said reinforcing fibres are selected from the group comprising natural, artificial and synthetic fibres, and combinations thereof.

In a further embodiment, said reinforcing fibres are discontinuous fibres having a length of about 0.1 to 50 mm.

Yet in a further embodiment, said reinforcing fibres are selected from the group comprising coconut, sisal, flax, cotton, kenaf, hemp, sugar cane, bamboo, palm, jute, wood, wool, leather, silk, aramid, ceramic, metallic, glass, polymeric and carbon fibres and the like, and combinations thereof.

In a further embodiment, said reinforcing fibres are previously subjected to a physical or chemical modification in order to improve compatibility with distinct composite components.

In another embodiment, said binders are selected from the group comprising silane, glycerin, glycerol, epoxy groups, carboxylic acid and maleic anhydride based binders, and the like, and combinations thereof.

Still in another embodiment, said thermoplastic material is a mixture of at least two of said synthetic, recycled and natural thermoplastic materials.

In yet another embodiment, said thermoplastic material is functionalized.

The present invention also relates to the use of the fibre-reinforced cork-based composite designed for the construction, inland transport, aeronautic, shipbuilding, furniture and automobile industries, and the like.

BRIEF DESCRIPTION OF DRAWINGS

The present invention will be described in detail with reference to the accompanying drawings, wherein:

Fig. 1 is a board cross section view using a stereoscopic lens, showing a cork polymeric composite containing 10% of non-linearly dispersed sisal fibre, after the extrusion and compression moulding steps.

Figs. 2a and 2b are magnified photographs obtained by electron microscopy, showing cork polymeric composites reinforced with coconut fibres and 2% binder after a tensile test.

DETAILED DESCRIPTION OF THE INVENTION

The present invention relates to new high performance, mouldable, recyclable or biodegradable, cork-based composites reinforced with discontinuous, short or long, natural and/or synthetic fibres. Such composites can be fully or partially biodegradable according to the polymeric matrix type and reinforcing fibres used in their production. Specifically, the cork-based product of the invention comprises at least three components, such as a cork-based material, a synthetic, recycled or natural thermoplastic, or a mixture of at least two of these, and natural and/or synthetic fibres.

The present invention uses melting-based technologies in order to induce a better homogenization of the different phases, playing the addition of fibres a key role. The mechanical properties of the cork and polymer composites reinforced with fibres are dependent on the fibres length and diameter, fibres dispersion, interaction in the interface fibres/cork and polymeric matrix, the chemical nature of the fibres, the amount and type of binder and the process technology used, since fibres can have a different dispersion degree in the final product.

The composite material is obtained using melting-based conventional technologies, such as extrusion or injection moulding techniques, preferably extrusion or pultrusion techniques, to yield pellets reinforced with fibres of different lengths according to the intended application. The pellets, exhibiting better mechanical characteristics, may be subsequently used in a injection moulding, compression moulding, transfer moulding or thermoforming step, or other non-conventional techniques such as, *inter alia*, reaction injection moulding or overmoulding.

Surprisingly, the new composite product, having improved mechanical characteristics, also allows incorporation of high amounts of cork, exhibiting stiffness similar to that of the simple thermoplastic materials, due to fibre incorporation in the presence of a binder. Such new composite can be used in the construction, furniture, automobile, shipbuilding or aeronautic industry, and the like.

In the present disclosure, the term "composite" relates to materials typically consisting of at least 3 components; a continuous thermoplastic matrix and two dispersed phases, one of these being the cork granules, or cork dust or cork residues derived from the production process and the other a reinforcing fibre-based phase, one of the phases optionally functioning as a filler, optionally containing a new phase in order to modify the magnetic or electrical properties, improve the wear or erosion resistance, such that its association results in the product features.

The term "binder," also known as compatibilizer or compatibilizing agent, refers to an adhesion promoter which is involved and induces a chemical binding between the different composite phases, being also involved in the dispersion of the particles.

The term "additives" refers to one or more substances applied in small amounts, used to modify and/or improve several properties such as, inter alia, promoting processability, conferring thermal stability, colouring and improving antistatic properties, superficial hardness and fire resistance.

The expression "fully biodegradable" composite relates to a material consisting of cork embedded in a natural or synthetic, biodegradable polymeric matrix, reinforced with natural fibres. The expression "partially biodegradable" composite relates to materials made of cork and a non-biodegradable polymeric matrix, reinforced with natural fibres.

The composites of the invention are materials having unique properties and performance. Examples of such material characteristics comprise a high processing ability (using current machinery), making them useful for producing complex products for the final user multiple applications, better thermal and acoustic insulation and improved mechanical characteristics. The fibre-reinforced cork-based composite of the present invention, is suitable for use in construction, inland transport, aeronautic, shipbuilding, furniture, automobile parts and other structural applications.

Manufacturing of cork-based composites reinforced with fibres can be made by pultrusion or extrusion, either in a single- or multiple-step process, to provide a pellet or a material with any other final shape. Subsequently, the final product might be obtained by melting-based techniques, such as injection moulding, compression moulding, transfer moulding, thermoforming or a combination thereof, and non-conventional techniques, such as reaction injection moulding, overmoulding, in-mould decoration and the like, or a combination thereof.

Polymers, cork and fibres do not promptly combine, though some polymers are more suitable than others to provide a good binding interface. Accordingly, the mechanical properties of the cork and polymer composites improve with the addition of natural and/or synthetic fibres, preferably with a binder and/or a functionalized polymer.

The fibre-reinforced cork composites of the present invention comprise:

(a) 10% to 75% by weight of granulated cork, which may have different densities and granulometries, or cork residues derived from industrial processes, or a mixture comprising more than one cork residue type;

(b) 20% to 80% by weight of at least one thermoplastic matrix material, which may be synthetic, recycled or natural. Said thermoplastic material may be functionalized;

(c) 1% to 35% by weight of fibres selected from the group comprising natural, synthetic, organic, inorganic fibres and the like, and combinations thereof, which fibres can be of any discontinuous, short or long, fibres;

(d) 0.5% to 12% of binders selected from the group comprising silane, glycerin, glycerol, epoxy groups, carboxylic acid or maleic anhydride based binders, and the like and combinations thereof.

Other components, such as additives selected from the group comprising waxes, pigments, lubricants and the like, and combinations thereof, may be added to the initial composition or during blending process, such that better processing ability, aesthetic or other characteristics are conferred.

Therefore, in an embodiment of the present invention, the fibre-reinforced cork composites comprise:

(a) 20% to 70% by weight of said granulated cork;
(b) 40% to 60% of at least one said matrix material;
(c) 10% to 30% by weight of said fibres; and
(d) 1% to 10% of said binders.

In another embodiment, the fibre-reinforced cork composites comprise:

(a) 25% to 60% by weight of said granulated cork;
(b) 35% to 50% of at least one said matrix material;
(c) 10% to 25% by weight of said fibres; and
(d) 1% to 10% of said binders.

In a further embodiment, the fibre-reinforced cork composites comprise:

(a) 30% to 55% by weight of said granulated cork;
(b) 35% to 45% of at least one said matrix material;
(c) 12% to 20% by weight of said fibres; and
(d) 1% to 9% of said binders.

Still in a further embodiment, the fibre-reinforced cork composites comprise:

(a) 30% to 50% by weight of said granulated cork;
(b) 35% to 45% of at least one said matrix material;
(c) 12% to 18% by weight of said fibres; and
(d) 1% to 9% of said binders.

Yet in another embodiment, the fibre-reinforced cork composites comprise about 40% by weight of said granulated cork, about 40% by weight of said matrix material, about 12% by weight of said fibres, about 7% by weight of said binders and about 1% by weight of additives.

The cork material might be of any source and type, including granulated cork with different densities and/or granulometries and/or cork residues from industrial processes, such as grinding powder, sanding powder, or from technical products such as, *inter alia*, corkstyle®, floating powder, or a mixture of more than one type of cork residues.

Matrix material of the present invention comprises any polymeric thermoplastic material having a melting point lower than the cork or reinforcing fibres decomposition temperature. Examples of thermoplastic materials suitable as matrix include polyolefins, preferably polyethylene, polypropylene, propylene copolymers with other monomers including ethylene, alkyl or aryl anhydride, ethylene acrylate homo- or copolymer, or a combination thereof. Other thermoplastic materials are selected from the group comprising polystyrene, polycarbonate, polymethylmethacrylate, polyvinyl chloride, polyamides, polyurethane, polyethylene terephthalate, and mixtures of thermoplastic materials. The present invention allows for the use of any recycled thermoplastics from the above examples.

Fully biodegradable compositions may be prepared with biopolymers. Said biodegradable polymers comprise, biodegradable polyesters, preferably poly(butylene succinate), polylactides, polycaprolactones or polyhydroxyalkanoates.

The amount of matrix material depends on, for example, the product intended application, manufacturing process and/or product desired characteristics and properties. For example, as previously mentioned, the matrix material may be present in an amount of about 20 to 80% by weight, more preferably, of about 40 to 60% by weight.

According to the present invention, reinforcing fibres are selected from the group comprising organic, inorganic, natural and synthetic fibres and the like, and combinations thereof. Representative examples include cellulose, polymeric, metallic, ceramic and glass materials. The amount of fibres used is typically in the range of at least 1 to about 35% by weight of product, preferably between about 10 and about 30%

by weight. Fibres may be of any type of discontinuous, short or long, fibres, having a length of about 0.1 to 50 mm.

Natural fibres include any fibre type of any renewable source and selected from the group comprising coconut, sisal, flax, cotton, kenaf, hemp, sugar cane, bamboo, palm, jute and wood fibres present in the wood or paper pulp. Moreover, other natural materials may also be used as sources of natural fibres, such as, for example, wool, leather and or silk, and the like, and combinations thereof, to confer reinforcement and ecological and recycling features to the final product.

Synthetic fibres comprise any type of artificial or chemical fibres, such as, for example, aramid, ceramic, metal, glass, polymers and carbon fibres, or a combination thereof.

Representative polymeric fibres comprise, for example, polyester, nylon, acrylic, polyethers, polyamides, polyolefins, such as polyethylene and polypropylene based fibres.

According to the present invention, natural fibres may be admixed or combined with fibres of a different type, *e. g.*, aramid, ceramic, metal, glass, polymers and carbon fibres and/or other materials from natural fibres, to obtain a fibre useful as a reinforcing material for preparing the cork-based composites of the invention.

Alternatively, a mixture of separated fibres from identical or different sources may be used.

The composites of the present invention include binders selected from the group comprising silane, glycerin, glycerol, epoxy groups, carboxylic acid and maleic anhydride based binders, and the like and combinations thereof, which function as a binding agent for both cork particulate and reinforcing fibres. Binders may be added either in the solid or liquid state.

Furthermore, the composites of the invention may contain at least one additive, said additive being selected from the group comprising waxes, pigments, lubricants, antioxidant compounds, fire-resistant compounds, antibacterial compounds, UV absorbers and the like, and combinations thereof.

For a better understanding and practice of the invention, processes for improving adhesion in the interface between the matrix and the dispersed phase, namely cork granules and/or fibres, are disclosed.

Thus, compatibilizing methods can provide an adhesive binding between the cork material, polymeric material and fibres, improving the binding interface and, therefore, the mechanical properties of the final product. A suitable compatibilizing method comprises subjecting any of the raw materials to chemical treatments, such as alkaline or acid treatments, or providing chemical modification by using plasma or corona discharge treatments, to improve the surface characteristics.

Functionalization methods with reactive groups, such as, *inter alia*, amine, epoxy, isocyanates, acrylic acid, anhydrides, methacrylate, phenol and melanine groups, can be used to promote a better interface binding of the cork and reinforcing fibres with the polymeric matrix, as occurs with other lignocellulosic materials, or to subject the cork wastes and reinforcing fibres to a washing step with one or more solvents, and a drying step.

Previously functionalized polymers may be used as an alternative to functionalization.

Fibre distribution in the matrix depends on a manufacturing process disclosed bellow for a better understanding of the invention. The process allows for parameters adjustment in order to yield different levels of fibre distribution.

In the present invention, the reinforced cork-based composites can be produced using any of the standard techniques for producing composites including, *inter alia*, pultrusion, extrusion, injection moulding, compression moulding, transfer moulding and non-conventional techniques such as reaction injection moulding, overmoulding, and in-mould decoration.

The first illustrative process for producing a fibre-reinforced cork-based composite is pultrusion. In the pultrusion process, the product can be directly obtained in its semi-final or final shape, for example as pellets, which is subsequently used in other processing methods, such as extrusion, pultrusion, injection moulding and compression moulding.

A second illustrative process for preparing the reinforced product is extrusion. Any extrusion device suitable for carrying out the extrusion of the composition may be used. For example, the extrusion device can be a single screw or twin-screw extruder, the latter having co-rotating screws or, preferably, counter-rotating screws disposed horizontally and/or vertically (in one or more extruding machines) during processing. In this case, a plurality of fibres is combined with the matrix material before or during the extrusion step. The material fed to the extrusion device may contain all of the components of the extrusion composition, or the different components of the composition may be added in separate steps in the course of the extrusion process. Furthermore, the fibre-reinforced cork-based composites may be produced in one or more extrusion steps.

In a third example, the fibre-reinforced cork-based composites may be prepared in a step consisting of admixing all materials, including cork and fibres, in an extrusion or pultrusion process, or some of the composition components may be introduced in an extrusion or pultrusion device yielding a compound and then other components are combined therein, *e. g.* reinforcing fibres, in a supplementary extrusion or pultrusion step. Moreover, during extrusion, the reinforced cork-based composite can be obtained directly in its semi-final or final shape as, for example, a profile having a low or high geometrical complexity according to the extruder die, for example pellets, which may be

subsequently used in other transformation processes. Reactive extrusion can be used to functionalize raw materials and/or simultaneously produce distinct reinforced cork-based composites as pellets or products having a different final shape.

The invention also relates to the use of said reinforced cork-based composites in construction, inland transport, aeronautics, shipbuilding, furniture, automobile parts and other structural applications.

EXAMPLES

The following examples illustrate a cork-containing mouldable thermoplastic reinforced with fibres or a combination of fibres, and methods for producing thereof.

Example 1

Compositions were prepared using a thermoplastic material and a cork residue derived from an industrial process, namely sanding powder having a density of 120 – 160 kg/m3. The polymer used was a high density polyethylene having a melting point of 136.6 °C (measured by Differential Scanning Calorimetry). In all instances, the polymer/cork residues weight ratio was proportional between the two materials (50%-50%) or (49%-49%) when using a binder. Prior to the blending process, each composition was placed separately into a mechanical agitator for 10 minutes, for mixing and homogenizing the components. Each composition was placed alternately into a counter-rotating, twin-screw extruder having a die of circular geometry, allowing compounding and subsequent preparation of pellets from the cork and polymers composite (CPC). After this step, the CPC pellets were subjected to another extrusion step for reinforcement with different percentages of coconut fibres having a diameter less than 500 μm, according to Table 1 below, thus providing different pellets having a length less than 5 mm.

Subsequently, 70 g of pellets were collected for each composition (which could be applied to the injection moulding process for generating the intended geometries) and placed into a mould of rectangular geometry (about 20×23 cm^2) and 3 mm of thickness, containing on its base a removable cover which was covered with an unmoulding Teflon sheet on both surfaces comprising the evenly distributed pellets. This system was inserted into a hydraulic arm press at a temperature between 140 and 160 °C, for about 8 minutes for melting and homogenising the pellets and further compressed for 2 minutes at a pressure of 1.42 MPa, followed by cooling inside the mould with water and under pressure for 10 minutes, thus allowing cool down of the pellets to temperatures close to room temperature. Finally, the pressure was removed and the small contraction that occurred on the board allowed the easy unmoulding of the composite material from the system. Samples having standard dimensions, according to ASTM standards, were prepared from the boards of cork and polymer composites reinforced with coconut fibres, and submitted to tensile tests at a speed of 5 mm/minute, providing the tensile mechanical properties shown in Table 1. The data herein clearly show a great improvement of the mechanical properties, as the thermoplastic phase is reduced and the abovementioned natural fibre is added, especially in the presence of a binder. It was possible to obtain the same stiffness (see modulus values) for the thermoplastic material. The morphology of the composites shown in Fig. 2 denotes a good adhesion between the cork-polymer and the natural fibres reinforcement.

TABLE 1

Cork+HDPE (weight %)	Coconut Fibre (weight %)	Binder (weight %)	E 1% (RLin) (MPa)	σ_{max} (MPa)	Distortion Max. (%)
0 - 100	0	0	597.5±33.7	31.9±2.8	405.7±96.1
50 - 50	0	0	365.3±39.8	14.5±0.9	4.9±0.7
49 - 49	0	2	397.7±15.2	16.0±0.8	6.1±0.4
47.5- 47.5	5	2	488.9±42.7	17.7±1.1	5.4±0.4
45 - 45	10	0	572.9±44.9	14.2±0.5	4.5±0.7
44 - 44	10	2	598.7±19.5	20.4±0.3	6.4±0.4

Example 2

The same type of cork residue, as described in example 1, was used and admixed with the same thermoplastic material in a 40-60 cork-polymer weight% ratio for preparing different formulations reinforced with natural or synthetic fibres and further comprising, in some instances, a binder, as shown in Table 2.

Composites were processed according to the methodology described in example 1, but for an essential difference since pellets reinforced with fibres have been obtained after a single extrusion step. Boards were obtained from different formulations of cork and polymer composites reinforced with fibres, exhibiting a good superficial aspect, providing some aesthetic properties of the cork with dispersed fibres, as shown in Fig. 1. The mechanical properties are slightly different, as illustrated in Table 1, due to the fibre type and formulation used. As regards to tensile properties, incorporation of natural or synthetic fibres provides a significant improvement on the composite properties, conferring greater stiffness and higher fracture stress and impact resistance, preferably in the presence of a small amount of binder. Charpy impact strength was also measured in notched samples using a pendulum impact tester according to DIN EN ISO 179-1

standard, exhibiting the cork and polymer composites reinforced with fibres a higher stiffness, denoting a higher impact resistance.

TABLE 2

Cork - HDPE (weight %)	Fibres (weight %)	Binder (weight %)	Fibres Type
40 - 60	0	0	---
39.2 - 58.8	0	2	---
34 - 51	15	0	Wood
33.2 - 49.8	15	2	Wood
34.8 - 52.2	10+3	0	Wood – Glass
36 - 54	10	0	Sisal
35.2 - 52.8	10	2	Sisal

TABLE 2 (cont.)

Cork-HDPE (weight %)	E1% (RLin) (MPa)	σ_{max} (MPa)	Distortion Max. (%)	Charpy Impact (w/notches) (KJ/m^2)
40 - 60	492.0±75.9	14.0±0.8	3.8±0.3	1.47±0.05
39.2 - 58.8	502.5±51.0	16.4±0.6	4.6±0.2	2.40±0.10
34 - 51	702.3±52.3	15.1±0.8	3.1±0.3	2.03±0.20
33.2 - 49.8	603.7±49.3	21.9±1.3	5.7±0.5	2.78±0.19
34.8 - 52.2	612.8±68.5	14.8±1.2	3.4±0.4	1.72±0.03
36 - 54	593.9±39.4	14.2±0.7	3.4±0.2	2.29±0.25
35.2 - 52.8	594.3±69.9	18.1±0.5	4.4±0.3	2.53±0.21

CLAIMS

1. Fibre-reinforced cork-based composite comprising at least three components, wherein a first component is a cork-based material, a second component is a thermoplastic material and a third component is reinforcing fibres.

2. Fibre-reinforced cork-based composite according to claim 1, comprising:

(a) 10% to 75% by weight of cork-based material;
(b) 20% to 80% by weight of thermoplastic material;
(c) 1% to 35% by weight of fibres, and

further comprising

(d) 0.5% to 12% by weight of binders.

3. Fibre-reinforced cork-based composite according to claim 1 or 2, comprising:

(a) 20% to 70% by weight of cork-based material;
(b) 40% to 60% by weight of thermoplastic material;
(c) 10% to 30% by weight of fibres;
(d) 1% to 10% of binders.

4. Fibre-reinforced cork-based composite according to claim 1 or 2, comprising:

(a) 25% to 60% by weight of cork-based material;
(b) 35% to 50% by weight of thermoplastic material;
(c) 10% to 25% by weight of fibres;
(d) 1% to 10% by weight of binders; and

further comprising

(e) 0.5% to 10% by weight of additives.

5. Fibre-reinforced cork-based composite according to claim 1 or 2, comprising:

(a) 30% to 55% by weight of cork-based material;
(b) 35% to 45% by weight of thermoplastic material;
(c) 12% to 20% by weight of fibres;
(d) 1% to 9% of binders.

6. Fibre-reinforced cork-based composite according to claim 4, comprising about:

40% by weight of cork-based material,
40% by weight of thermoplastic material,
15% by weight of fibres,
3% by weight of binders and
2% by weight of additives.

7. Fibre-reinforced cork-based composite according to claim 1, wherein said cork-based material is selected from the group comprising granulated cork, cork dust, cork residues and combinations thereof.

8. Fibre-reinforced cork-based composite according to claim 1, wherein said thermoplastic material is selected from the group comprising synthetic, recycled and natural materials, and combinations thereof.

9. Fibre-reinforced cork-based composite according to claim 8, wherein said thermoplastic material is selected from the group comprising polyethylene, polypropylene, ethylene, alkyl or aryl anhydride, ethylene acrylate homo- or copolymer, polystyrene, polycarbonate, polymethylmethacrylate, polyvinyl chloride, polyamide, polyurethane,

polyethylene terephthalate, poly(butylene succinate), polylactide, polycaprolactone, polyhydroxyalkanoate and the like, and combinations thereof.

10. Fibre-reinforced cork-based composite according to claim 1, wherein said reinforcing fibres are selected from the group comprising natural, artificial and synthetic fibres, and combinations thereof.

11. Fibre-reinforced cork-based composite according to claim 10, wherein said reinforcing fibres are discontinuous fibres having a length of about 0.1 to 50 mm.

12. Fibre-reinforced cork-based composite according to claim 10, wherein said reinforcing fibres are selected from the group comprising coconut, sisal, flax, cotton, kenaf, hemp, sugar cane, bamboo, palm, jute, wood, wool, leather, silk, aramid, ceramic, metallic, glass, polymeric and carbon fibres, and the like and combinations thereof.

13. Fibre-reinforced cork-based composite according to claim 10, wherein said reinforcing fibres are previously subjected to a physical or chemical modification for improving the compatibility with the distinct composite components.

14. Fibre-reinforced cork-based composite according to claim 2, wherein said binders are selected from the group comprising silane, glycerin, glycerol, epoxy groups, carboxylic acid and maleic anhydride based binders, and the like and combinations thereof.

15. Fibre-reinforced cork-based composite according to claim 8, wherein said thermoplastic material is a mixture of at least two of said synthetic, recycled and natural thermoplastic materials.

16. Fibre-reinforced cork-based composite according to claim 8, wherein said thermoplastic material is functionalized.

17. Use of the fibre-reinforced cork-based composite of any of the preceding claims, intended for the construction, inland transport, aeronautic, shipbuilding, furniture and automobile industries, and the like.

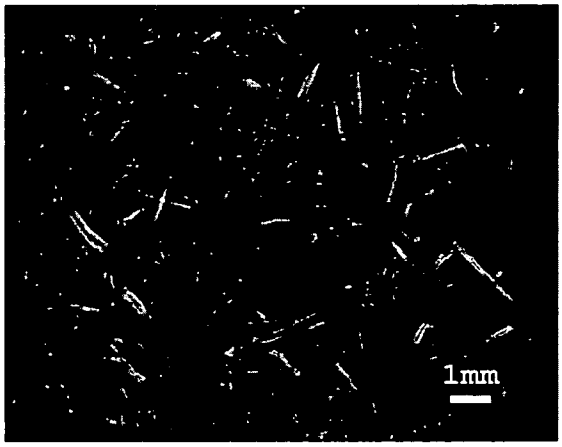

Fig. 1

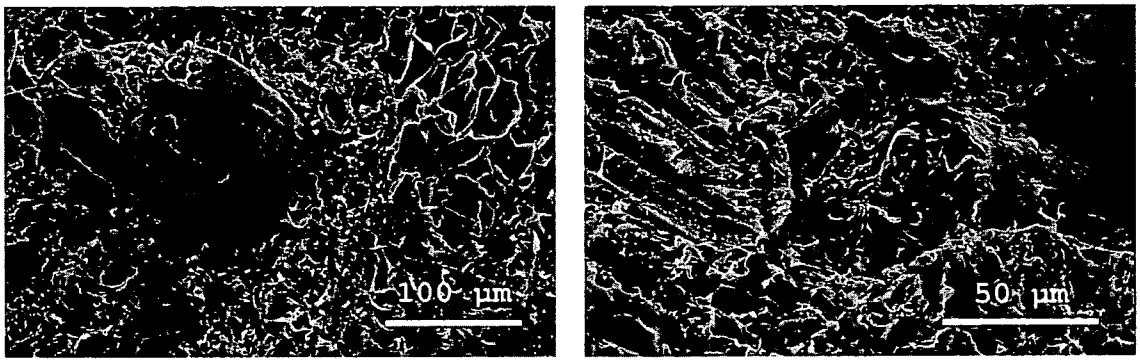

a) b)

Fig. 2